

3. THERMAL EVALUATION

The thermal evaluation in this addendum examines the incorporation of plutonium metal as a new payload for the PAT-1 package. The Pu metal is packed in an inner container (*T-Ampoule Assembly*,⁴ Drawing 2A0261, designated the T-Ampoule) that replaces the PC-1 inner container. The T-Ampoule and associated Pu metal contents packing configurations are described in Section 1.2.1 and Section 1.2.2 of this addendum, respectively.

The thermal evaluations documented in Chapter 3 of the Safety Analysis Report (SAR)¹ for the Plutonium Air Transportation Package, Model PAT-1, NUREG-0361¹ (SAR¹) apply to this PAT-1 Safety Analysis Report Addendum for the T-Ampoule and its contents. The thermal evaluation of the T-Ampoule contents addressed in this addendum assumes a bounding internal heating scenario where three plutonium metal samples (25 watts total) from a three-nested *Sample Container-1 (SC-1) Assembly* configuration, (Drawing 2A0268, designated SC-1) are collocated along the seal area of the T-Ampoule to present a concentrated heat source. The other configurations described in Section 1 of this addendum, which are the 831 g (1.83 lbm) Pu hollow cylinder, wrapped in tantalum foil or not wrapped based on operational determination, supported with crushed tantalum foil, and the two-nested sample container configuration (*Sample Container-2 [SC-2] Assembly*, Drawing 2A0265, designated SC-2) supported by a titanium *Inner Cradle* (Drawing 2A0385, designated Inner Cradle) present a less concentrated heat source against the seal area. Although the quantity of plutonium metal assumed for the bounding case has a lower decay heat energy (see Section 4 of this addendum) than the 25 watts (85.3 Btu/hr) the PAT-1 package is certified for, the 25-watt decay heat limit is conservatively used for this analysis. The heat absorbed by the components within the T-Ampoule is neglected also for conservatism. Results from thermal analyses presented in this section demonstrate that the thermal performance of the PAT-1 with the proposed metal payload will be acceptable under normal conditions of transport (NCT) as defined in 10 CFR 71.71,² under hypothetical accident conditions (HAC) as defined in 10 CFR 71.73,² and under the accident conditions for air transport of plutonium as defined in 10 CFR 71.74.² The results also demonstrate that the T-Ampoule will provide a eutectic barrier for the proposed metal payload under the accident conditions for air transport of plutonium, as defined in 10 CFR 71.74.² The components of the PAT-1 packaging not modified by this addendum perform as documented in the SAR.¹

3.1 Description of Thermal Design

The thermal design description provided in the SAR¹ remains valid for this addendum, as there are no alterations to the AQ-1 protective overpack (*Overpack AQ*, Drawing 1002, designated AQ-1) or the TB-1 stainless steel containment vessel (*Containment Vessel*, Drawing 1017, designated TB-1). The thermal effects of replacing the PC-1 inner container and aluminum spacer with the T-Ampoule inner container inside the TB-1, with the same 25 watts (85.3 Btu/hr) maximum heat generation, were conservatively bounded in the computer analyses, as explained in the next sections. Changing the content form inside the TB-1 has no negative effects on the thermal performance of the AQ-1 overpack thermal design features or the TB-1 containment vessel. The thermal performance of the PAT-1 package is adequate and will safely contain its

^A The drawing titles are in italics and are used interchangeably with the designated names in this addendum. See Section 1.3.2 in this addendum and Chapter 9 in the SAR¹ for drawing number, title, and revision.

contents as described in the SAR¹ under the test conditions specified in 10 CFR 71.71, 71.73, and 71.74.²

3.1.1 Design Features

The design features of the PAT-1, TB-1 stainless steel containment vessel, and the AQ-1 protective overpack assembly are unchanged and are described in Chapter 3 of the SAR¹. The *Ring, Filler* (Drawing 2A0262, designated Ring Filler) and the T-Ampoule inner container in the configurations depicted in Figures 1-3 through 1-5 of this addendum replace the PC-1 inner container and aluminum spacer documented in the SAR.¹ The effect of this change was captured in the thermal computer models described later in this section.

There are three basic configurations for plutonium metal contents within the T-Ampoule. One configuration consists of two titanium SC-2 sample containers supported and held in position inside the T-Ampoule by a titanium Inner Cradle (see Figure 1-3 in Section 1 of this addendum). The plutonium metal content within the SC-2 is a solid plutonium (Pu) cylinder of a diameter and length of 1.1 inches (0.0279 m). A second configuration consists of three SC-1 sample containers supported and held in position inside the T-Ampoule by a titanium Inner Cradle (see Figure 1-4). This configuration is similar to the two SC-2 configuration except it consists of three SC-1s and the plutonium metal sample packed in an SC-1 is a solid cylinder 0.88 inches (0.0224 m) in diameter and length. A third configuration consists of a single Pu hollow cylinder weighing from 731 to 831 grams (1.61 to 1.83 lbm) supported by crushed tantalum foil surrounding the cylinder (see Figure 1-5). The T-Ampoule, Ring Filler, SC-1, SC-2, Inner Cradle, and plutonium metal content all have melting temperatures above the 582°C (1080°F) temperature observed in the TB-1 during the plutonium air transport fire test described in SAR,¹ Section 3.6.1.2. Since the maximum total heat generation allowed in the TB-1 is limited to 25 watts (85.3 Btu/hr), a very conservative and bounding case for the application of the internal heating was used in the evaluation discussed in this section.

3.1.2 Decay Heat of the Contents

The PAT-1 package was assessed for a total decay heat load of its radioactive contents of 25 watts (85.3 Btu/hr). Sections 3.3 and 3.4 of this addendum demonstrate that with the 25 watt (85.3 Btu/hr) decay heat, the overall thermal performance of the PAT-1 package with the T-Ampoule and its plutonium metal payload is essentially the same as demonstrated in the SAR.¹ For the purpose of the analysis of the PAT-1 with the T-Ampoule and its plutonium metal content configurations addressed in this evaluation, the decay heat is conservatively assumed to be 25 watts. A bounding internal heating scenario was assumed in the analyses presented in this addendum. All 25 watts (85.3 Btu/hr) were assumed to be concentrated in a small region directly applying heat to the T-Ampoule elastomeric O-ring, as if all the solid plutonium metal cylinders were to group and transfer all their thermal energy to a small seal region. From the three basic configurations of plutonium metal contents discussed in Section 3.1.1 of this addendum, the hypothetical configuration that yields the smallest projected area for heat to flow through and therefore, provides maximum heat flux into the seal region is one where three plutonium metal cylinders are close together and aligned along the seal region as illustrated in Figure 3-1. Assuming the total 25 watts (85.3 Btu/hr) from these three plutonium cylinders are transferred to the seal region through the small projected area illustrated in Figure 3-2, the total concentrated heat flux q'' is:

$$q'' = \frac{25W}{(2.64'')(0.88'')} = \frac{25W}{(0.067056m)(0.022352m)} \cong 16,680 \frac{W}{m^2} \text{ or } 5,288 \frac{Btu}{hr - ft^2}. \quad (3-1)$$

Note that this scenario is extremely unlikely because the Pu cylinders will not come out of the sample containers during NCT or HAC, as documented in Section 2 of this addendum. In addition, if the three Pu cylinders were to align as described, a portion of the assumed 25 watts (85.3 Btu/hr) will be transferred by convection and radiation to other regions (and components) inside the T-Ampoule, and thereby reduce the actual quantity of energy available to be transferred by conduction through the hypothetical localized heating region described herein. Since this highly concentrated heat flux is understood to bound all plutonium metal loading configurations discussed in Section 3.1.1 of this addendum, only this heat flux was used to very conservatively represent the decay heat inside the T-Ampoule during the NCT and HAC evaluations.

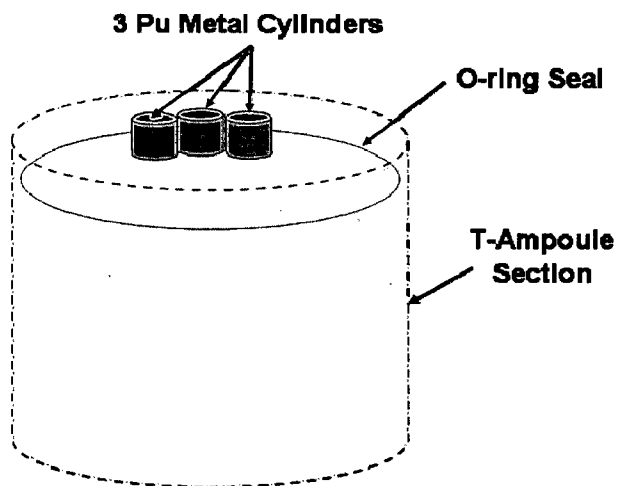


Figure 3-1. Schematic of Assumed Worst-Case Heating-to-the-Seal Scenario

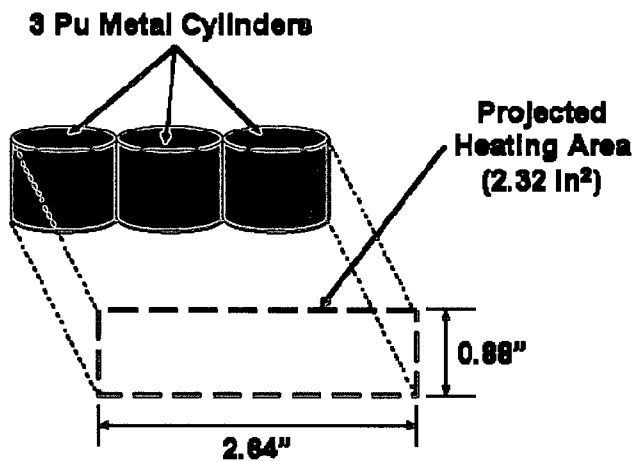


Figure 3-2. Schematic of Approximated Projected Heating Area
 $[m=0.0254 \cdot \text{in.}; m^2=6.45 \times 10^{-4} \cdot \text{in.}^2]$

3.1.3 Summary Tables of Temperatures

The SAR¹ describes how design features in the PAT-1 adequately contain the material inside the TB-1 even after the PAT-1 is exposed to the regulatory conditions specified in 10 CFR 71.71, 71.73, and 71.74.² The results from the thermal evaluation of the AQ-1, TB-1, and the T-Ampoule assuming the bounding concentrated internal heat described in Section 3.1.2 of this addendum are summarized in Table 3-1 of this addendum. These results show that the PAT-1 also protects the new components inside the TB-1 described in this addendum and adequately contains the material inside the TB-1, as the T-Ampoule seal temperatures are within the manufacturer's specifications and the T-Ampoule can withstand the pressure buildup during and after the regulatory specified heating.

Table 3-1. Summary of Temperatures Under NCT and HAC

| Component | NCT | | HAC |
|--|---------------|---------------|--|
| | Maximum | Minimum | Maximum |
| T-Ampoule (Seal) | 122°C (251°F) | -40°C (-40°F) | 153°C (308°F) @ 260 minutes after the fire |
| TB-1 (and TB-1 seal)* | 114°C (238°F) | -40°C (-40°F) | 147°C (296°F) @ 260 minutes after the 30-minute fire |
| Center of Redwood Between TB-1 and Load Spreader | 99°C (211°F) | -40°C (-40°F) | 132°C (270°F) @ 240 minutes after the 30-minute fire |
| <i>Aluminum Load Spreader</i> | 98°C (208°F) | -40°C (-40°F) | 131°C (267°F) @ 190 minutes after the 30-minute fire |
| Center of Redwood Between Load Spreader and Outer Skin | 95°C (203°F) | -40°C (-40°F) | 164°C (328°F) @ 30 minutes after the 30-minute fire |
| Stainless Steel Outer Drum | 93°C (200°F) | -40°C (-40°F) | 1003°C (1837°F) @ end of fire |

*Maximum seal temperature was conservatively taken as the TB-1 maximum temperature.

3.1.4 Summary Table of Maximum Pressures

Table 3-2 of this addendum summarizes the maximum pressures inside the T-Ampoule for the NCT, HAC and plutonium air transport accident conditions specified in 10 CFR 71.71,² 71.73,² and 71.74,² respectively. As demonstrated in Sections 2, 3.3.2, 3.4.3, 3.4.5, and 4 of this addendum, the pressures that arise in the container during NCT, HAC, and plutonium air transport accident conditions do not result in a loss of containment.

Table 3-2. Summary of Maximum Pressures inside the T-Ampoule for NCT and HAC

| Regulatory Condition | Maximum Pressure |
|-------------------------|------------------------|
| NCT (or MNOP) | 132.4 kPa (19.2 psig) |
| HAC | 152 kPa (22.1 psig) |
| Plutonium Air Transport | 6.547 MPa (949.5 psig) |

3.2 Material Properties and Component Specifications

3.2.1 Material Properties

A summary of the thermophysical properties of the materials used in PAT-1 is provided in the SAR,¹ Section 3.2, Table 3.2. To be consistent with the SAR¹ the same material properties for aluminum, ETC copper, stainless steel, and redwood (up to a certain temperature as described below) were used for the analyses presented in this addendum.

The following was considered for modeling the thermal response of redwood. Slow degradation (slow pyrolysis) of wood occurs in the temperature range of 200°C to 280°C (392°F to 536°F), until active pyrolysis begins in the 280°C to 500°C (536°F to 932°F) range. A temperature of 288°C (550°F) is used to locate the base of the char layer. Reference 3 (*Application of CMA Program to Wood Charring*) and the references cited therein contain additional information about temperature-dependent wood properties and wood charring. The thermal conductivity and specific heat provided in the SAR¹ are given in expressions that are a function of temperature. While these expressions are valid for the temperature range used for the determination, which was approximately 93°C (200°F) (see Section 3.2 and Appendix 3-A of the SAR¹), the same equations were used to determine properties up to the temperature at which wood starts to decompose (i.e., 200°C [392°F]). Given that the properties of redwood provided in the SAR¹ do not take degradation of wood into account, property values and mathematical expressions from Reference 3 were used at temperatures greater than 200°C (392°F). For thermal conductivity at temperatures above pyrolysis, a fixed value within the range in Reference 3 for charcoal was used. Therefore, the temperature-dependent thermal properties presented in Table 3-3 of this addendum were specified in the P/Thermal model to adequately represent the state and response of the redwood. In cases where wood reached pyrolysis temperatures, it was assumed that the properties would remain those of charred wood throughout the cool-down process. To corroborate the validity of these modeling assumptions, thermal models discussed in Sections 3.3 and 3.4 of this addendum were completed and results compared with tests of the PAT-1 under transient NCT and HAC documented in the SAR.¹ These comparisons showed acceptable agreement as demonstrated by the data presented in those sections. Thus, a computer model that was calibrated with the test and analysis data presented in the SAR¹ was developed and used.

Table 3-3. Thermophysical Properties Used to Represent Redwood

| Wood State | Temperature °C [°F] | Density kg/m ³ [lb/ft ³] | Specific Heat J/kg-K [Btu/lb-F] | Thermal Conductivity W/m-K [Btu/hr-ft-°F] | |
|--|------------------------|--|---------------------------------------|--|---------------------------|
| | | | | Parallel to Grain | Perpendicular to Grain |
| Before Pyrolysis | 16 [60] | 352 [22] | 1273 [0.30] | 0.330 [0.19] | 0.117 [0.07] |
| | 38 [100] | 352 [22] | 1591 [0.38] | 0.390 [0.22] | 0.136 [0.08] |
| | 93 [200] | 352 [22] | 2386 [0.57] | 0.533 [0.31] | 0.190 [0.11] |
| | 199 [390] | 352 [22] | 3898 [0.93] | 0.810 [0.47] | 0.290 [0.17] |
| During Slow and Active Pyrolysis | 200 [392] | 214 [13] | 1151 [0.28] | 0.073 [0.04] | 0.026 [0.02] |
| | 280 [536] | 214 [13] | 1314 [0.34] | 0.073 [0.04] | 0.026 [0.02] |
| | 500 [932] | 214 [13] | 1657 [0.44] | 0.073 [0.04] | 0.026 [0.02] |
| | 800 [1472] | 214 [13] | 1876 [0.45] | 0.073 [0.04] | 0.026 [0.02] |
| | 1000 [1832] | 214 [13] | 1861 [0.45] | 0.073 [0.04] | 0.026 [0.02] |

In addition to the material properties listed in the SAR¹ and in Table 3-3 of this addendum, the thermal properties for Ti-6Al-4V used in the computer analysis are presented in Table 3-4 of this addendum. These values were obtained from the MSC PATRAN Thermal (P/Thermal) computer code materials database,⁴ which lists References 5, 6, and 7 as the source. Materials inside the T-Ampoule were conservatively neglected for the thermal analysis (no credit was taken for heat absorbed by components inside the T-Ampoule); therefore, the thermal properties of those materials are not presented in this section.

Table 3-4. Thermophysical Properties of the Titanium Ampoule (Ti 6Al-4V)

| Temperature °C [°F] | Thermal Conductivity W/m-K [Btu/hr-ft-°F] | Specific Heat J/kg-K [Btu/lbm-°F] | Density Kg/m ³ [lbm/ft ³] |
|------------------------|--|--------------------------------------|---|
| -50 [-58] | – | 502 [0.120] | 4450 [277.8] |
| 0 [32] | 6.9 [3.99] | – | |
| 100 [212] | – | 561 [0.134] | |
| 200 [392] | 9.0 [5.20] | – | |
| 300 [572] | – | 615 [0.147] | |
| 400 [752] | 11.9 [6.89] | – | |

3.2.2 Component Specifications

The service temperature range for package components inside the TB-1 are presented in Table 3-5 of this addendum.

Table 3-5. Service Temperatures of Packaging Components and Content Inside the TB-1

| Component | Service Temperature Range °C [°F] | Reference |
|--|---------------------------------------|-----------------------------|
| TB-1 and T-Ampoule O-ring | -40°C to 204°C [-40°F to 400°F] | Appendix 3.5.2 ⁱ |
| TB-1 Copper Gasket | -40°C to >582°C [-40°F to >1080°F] | PAT-1 SAR ⁱⁱ |
| T-Ampoule (as eutectic barrier) ⁱⁱⁱ | -40°C to 625°C [-40°F to 1157°F] | [8] |
| Titanium Inner Cradle ⁱⁱⁱ | -40°C to 625°C [-40°F to 1157°F] | [8] |
| Ring, Filler ^{iv} | -40°C to >593°C [-40°F to >1100°F] | [9] |
| Copper Foam | -40°C to 626°C [-40°F to 1159°F] | [8] |
| Pu/Be Content ^{vi} | -40°C to 595°C [-40°F to 1103°F] | [8] |
| Tantalum Foil ^{vii} | -40°C to 640°C [-40°F to 1184°F] | [8] |

ⁱ Appendix 3.5.2 of this addendum provides the manufacturer's specifications, compound data sheet, and aging.

ⁱⁱ Based on thermal tests performed and documented in the PAT-1 SAR,¹ the TB-1 maintained containment after experiencing temperatures as high as 582°C (1080°F). Therefore, the copper gasket in the TB-1 can maintain seal at temperatures above these observed maximums.

- iii The melting point of the eutectic that may form when titanium is in contact with gallium is 625°C (1157°F).
- iv. Ti-6Al-4V has a yield strength of about 331 MPa (48 ksi) at 593°C (1100°F), which is approximately 40% of the nominal room temperature value of 827 MPa (120 ksi)⁸ and there are no forces other than gravitational acting on these components during and after the fire accident condition.
- v Copper-Plutonium eutectic melting point.
- vi The plutonium/beryllium eutectic represents the lowest melting point eutectic at 595°C (1103°F) in the system. The Pu/Be is a content, not a component within the TB-1.
- vii Upper temperature assumed to be the Plutonium-Tantalum eutectic melting point. From page 11 of Reference 8, there is insufficient gallium in the entire mass of plutonium metal for Tantalum-Gallium eutectic formation and melting to have a negative effect on the system.

3.3 Thermal Evaluation under NCT

The commercially available MSC Patran Thermal (P/Thermal) finite element (FE) computer code⁴ was used for the thermal evaluation of the PAT-1 package under NCT. P/Thermal is a well-respected FE code widely used to analyze a variety of thermal issues, including those related to nuclear transport packages. P/Thermal can solve one-, two-, and three-dimensional conduction, convection, and radiation heat transfer issues.

A three-dimensional model of the PAT-1 package was built using P/Thermal to demonstrate that containment is maintained by the TB-1 and that the temperature of the O-ring in the T-Ampoule does not exceed the manufacturer's recommended temperature range. The computational mesh of the PAT-1 model built using P/Thermal is shown in Figure 3-3. The model consists of 31,180 hexahedral finite elements and 34,697 nodes. Package features such as the different wood grain orientations and the respective anisotropic thermal properties of the redwood, the aluminum Load Spreader, the copper heat transfer tube, the stainless steel TB-1, and the titanium T-Ampoule were included in the model. The thin-walled outer drum was conservatively neglected. As mentioned in Section 3.1.2 of this addendum, the presence of components inside the T-Ampoule such as the sample containers (SC-1 and SC-2) and the titanium Inner Cradle were also conservatively neglected, and no other mass was assumed to absorb heat inside the T-Ampoule. Additionally, the 25-watt (85.3 Btu/hr) power from the Pu was conservatively applied to a small region on the inner surface of the T-Ampoule to maximize the thermal affect to the T-Ampoule seal, as explained in Section 3.1.2 of this addendum. The regions of the T-Ampoule, internal wall that did not receive this localized heat were conservatively assumed to be perfectly insulated (i.e., no heat transfer was allowed within the T-Ampoule, preventing the localized heated region from losing heat through convection or radiation to cooler T-Ampoule surface regions). Therefore, the small heated region was only allowed to transfer heat to the unheated (solid) regions through conduction.

The simplified temperature- and diameter-dependent correlation for a horizontal cylinder with laminar flow as employed in the TOPAZ heat transfer code⁹ was used for the determination of the natural convection coefficient during NCT. That is:

$$h_{\text{natural}} = 1.32 * [(T_{\text{surface}} - T_{\text{ambient}}) / \text{Diameter}_{\text{cylinder}}]^{0.25} \text{ W/m}^2\text{-K} \quad (3-2)$$

Assuming

$T_{\text{surface}} = 176^{\circ}\text{F}$ (80°C) (value obtained from NCT solution in the SAR¹)

$T_{\text{ambient}} = 100^{\circ}\text{F}$ (38°C) (ambient temperature in 10 CFR 71.71²)

$\text{Diameter}_{\text{cylinder}} = 20 \text{ in.}$ (0.5588 m) (PAT-1 approximate external diameter)

$$h_{\text{natural}} = 1.32 * [(80^{\circ}\text{C} - 38^{\circ}\text{C}) / 0.5588 \text{ m}]^{0.25} \text{ W/m}^2\text{-K} \quad (3-3)$$

$$h_{\text{natural}} = 3.9 \text{ W/m}^2\text{-K} \text{ or } 0.69 \text{ Btu/hr-ft}^2\text{-}^{\circ}\text{F} \quad (3-4)$$

This value of h_{natural} is on the low end of typical natural convection heat transfer coefficients for gases¹⁰. Ultimately, a more conservative value of $h_{\text{natural}} = 3.5 \text{ W/m}^2\text{-K}$ ($0.62 \text{ Btu/hr-ft}^2\text{-}^{\circ}\text{F}$) was used for the NCT calculation in this addendum.

The PAT-1 package model was subjected to the thermal conditions specified in 10 CFR 71.71² to evaluate if the TB-1 can maintain containment during NCT. It was assumed that the package will be transported horizontally as specified in Section 1 of this addendum. The boundary conditions used in the model to simulate the “heat” conditions specified in 10 CFR 71.71(c)(1)² are summarized in Table 3-6 of this addendum. Note that the temperature of the environment was increased to 54.4°C (130°F) as in the SAR.¹ Also note that the insolation data presented in this table represents a 24-hour average of the values as specified in 10 CFR 71.71,² as is typically assumed when a steady-state simulation is used to evaluate packages under the prescribed environment. For example, for curved surfaces, 10 CFR 71² specifies a 12-hour-period, total insolation energy of 400 g-cal/cm^2 ($16,747 \text{ kJ/m}^2$ or $1,475 \text{ Btu/ft}^2$). In order to more adequately model the NCT in a computer code running in steady-state mode, the total energy per unit area is spread over 24 hours:

$$\text{Insolation}_{\text{Curved_Surfaces}} = \frac{400 \text{ g-cal/cm}^2}{(24\text{hr})(3600\text{sec/hr})} \cong 4.63E^{-3} \frac{\text{g-cal}}{\text{cm}^2\text{-s}} \cong 193.8 \frac{\text{W}}{\text{m}^2} \text{ or } 61.4 \frac{\text{Btu}}{\text{hr-ft}^2} \quad (3-5)$$

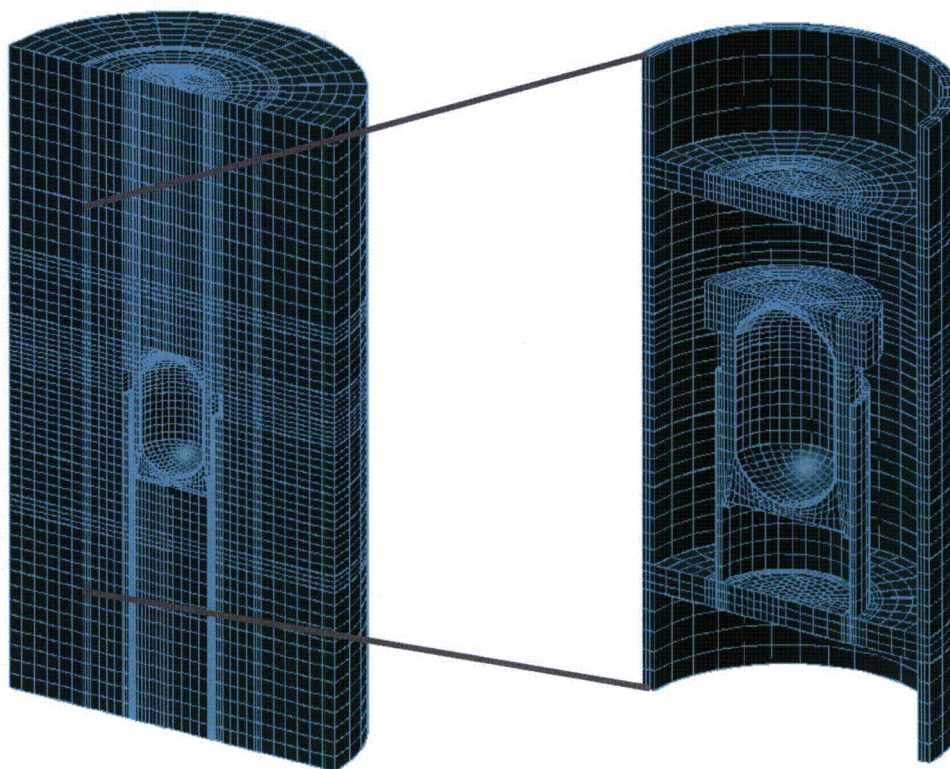


Figure 3-3. Finite Element Mesh of the PAT-1 Half-Symmetry Thermal Model and Enlarged Load Spreader, Copper Cylinder, TB-1, and T-Ampoule

Table 3-6. Boundary Conditions Used for the “Heat” NCT Thermal Evaluation

| Boundary Condition | Application Region | Value Used |
|--|--|--|
| Environment Temperature | External node representing environment | 54.4 °C (130°F) |
| Convection | Entire outer surface of the package | 3.5 W/m ² -K (0.62 Btu/hr-ft ² -°F) |
| Radiation | Entire outer surface of the package | Package surface emissivity of 0.2,* Environment emissivity of 1 |
| Insolation (Solar Flux averaged over 24 hours) | Curved surfaces | 193.83 W/m ² (61.44 Btu/hr-ft ²) |
| | Flat surfaces transported vertically (package ends) | 96.92 W/m ² (30.72 Btu/hr-ft ²) |
| Internal heat Flux (Decay heat) | Small region described in Section 3.1.2 of this addendum | 16,680 W/m ² (5287.5 Btu/hr-ft ²) |

* From Table 3.2 in the SAR¹

In addition to the “heat” NCT analysis, the package has to be able to maintain containment when exposed to an ambient temperature of -40°C (-40°F) in still air and shade as specified in 10 CFR 71.71(c)(2).² The results of exposing PAT-1 to these conditions are discussed in Section 3.3.1 of this addendum.

3.3.1 Heat and Cold

The finite element model described above was used for the NCT analysis. First, the model was verified by simulating both the steady-state test and the transient NCT analysis described in the SAR.¹ These models evenly distributed the 25W (85.3 Btu/hr) internal heat load and applied it to the inside wall of the TB-1. The results from this validation exercise are presented in Section 3.3.1.1 of this addendum. Once the model was verified against the results in the SAR,¹ the concentrated internal heat load described in Section 3.1.2 of this addendum was applied to the inner wall of the T-Ampoule. These results are presented in Section 3.3.1.2. of this addendum

3.3.1.1 Model Verification

The FE model described in Section 3.3 of this addendum was verified by simulating both the steady-state test and the transient NCT analysis described in the SAR.¹ The intent of this exercise was to verify the computer model against the data available in the SAR.¹ The validated model was then used to analyze the thermal response of the package with the plutonium metal content. These models evenly distributed the 25W (85.3 Btu/hr) internal heat load and applied it to the inside wall of the TB-1, as was the case for the models in the SAR.¹

First, the computer model was verified against a low-temperature thermal test that was performed and presented in the SAR.¹ This test was performed to empirically determine the effective thermal resistance values for PAT-1 components. While boundary conditions are not well known, it is understood that a PAT-1 package was placed in a temperature-controlled chamber maintained at approximately 93°C (200°F). An internal heater was maintained at 25 watts (85.3 Btu/hr) using a variable resistance power supply. Transient response was measured with thermocouples placed at key locations within and outside the package. These data are documented in Sections 3.4.1.2 and Appendix 3-A of the SAR.¹ The results of the verification analysis are presented in Figure 3-4. Temperature results after 50 hours favorably compare with those reported in Table 3-A.1 of Appendix 3-A in the SAR,¹ as illustrated in Table 3-7 of this addendum. Figure 3-4 also favorably compares with Figure 3.4 in the SAR.¹ The results from this validation exercise demonstrate that the geometry representation, material properties, and finite element representation are adequate to predict the performance of the PAT-1 package when exposed to similar thermal loads.

Second, the computer model was verified against the transient NCT analysis results presented in the SAR.¹ This included variable insolation heating (over time and position) as described in Section 3.4.1.2 in the SAR.¹ All boundary conditions were applied as described in that section of the SAR.¹ In order to model those conditions adequately, the half-symmetry model was mirror-copied to make a full three-dimensional model of the package. The results from this verification exercise, presented in Figures 3-5 and 3-6, compare favorably with the results presented in the SAR.¹ The data documented in Figure 3-6 is in agreement with the data shown in Figure 3.5 of the SAR.¹ This indicates proper three-dimensional modeling of the package. The three-dimensional temperature distribution of the package at the time just before sundown (the most severe case) is shown in Figure 3-7. This temperature distribution shows a peak outer skin temperature of 116°C (241°F), which is approximately 9°C (17°F) hotter than the maximum surface temperature reported in SAR,¹ Section 3.4.1.2.

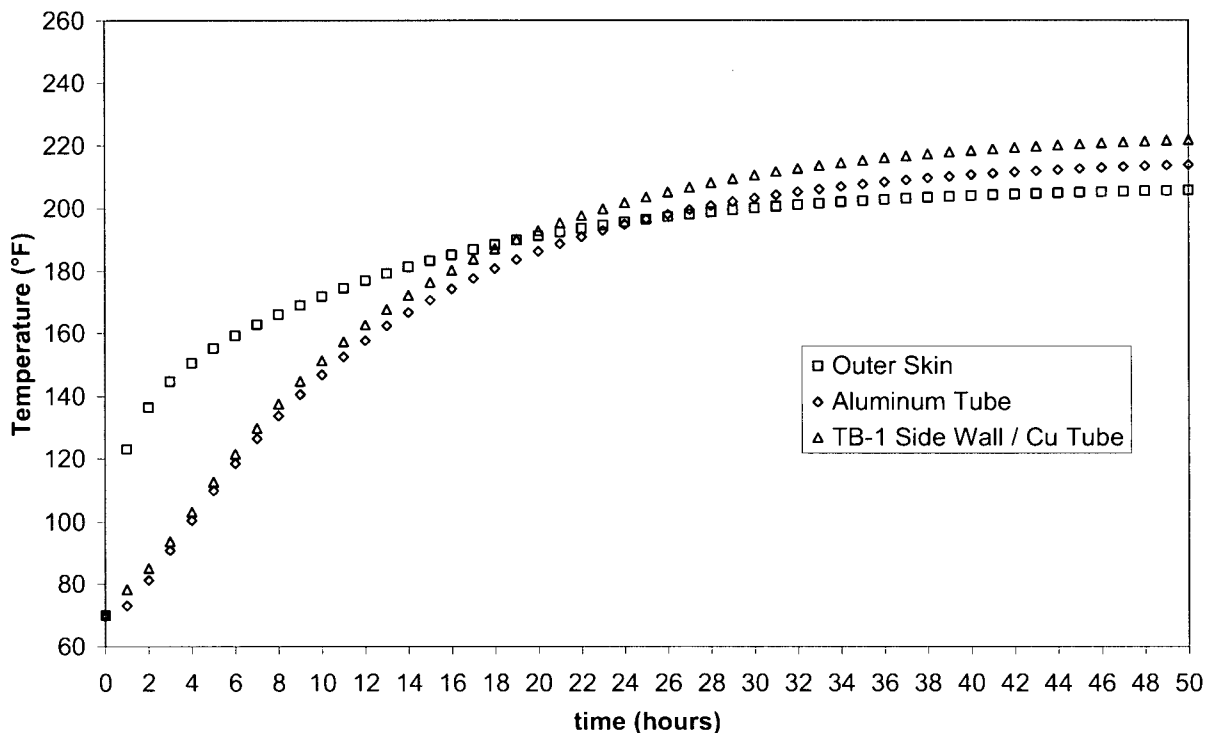


Figure 3-4. Low-Temperature Thermal Test Simulation Results. (°C=[°F-32]/1.8)

Table 3-7. Comparison of Test and Analysis Temperatures – Low Temperature Test

| Location | Steady-State Temperature – Test Data | Steady-State Temperature – Analysis Data at Package Mid-Height |
|------------|--------------------------------------|--|
| Cu Tube | 105°C (221°F) | 105.6°C (222°F) |
| Al Tube | 100°C (212°F) | 101°C (214°F) |
| Outer Skin | 93°C (200°F) | 96.6°C (206°F) |

Third, the boundary conditions in the computer model were changed to reflect those specified in 10 CFR 71.71² in a steady-state simulation and to verify how the package response under these conditions compares to the transient method used in the SAR.¹ The intent of this exercise was to determine if the new analysis for this addendum is still bounding when using the steady-state method. The results from this exercise are presented in Figures 3-7 and 3-8. A comparison of the results in these two figures with those obtained from the transient simulation described above indicate that while the outer temperatures (maximums and distributions) are different, the steady-state analysis thoroughly envelops the transient response of the TB-1 and its surrounding regions. Therefore, it was decided to run a steady-state NCT analysis of the PAT-1 with the new contents configuration. The results from the steady-state analysis for this addendum are presented in Section 3.3.1.2.

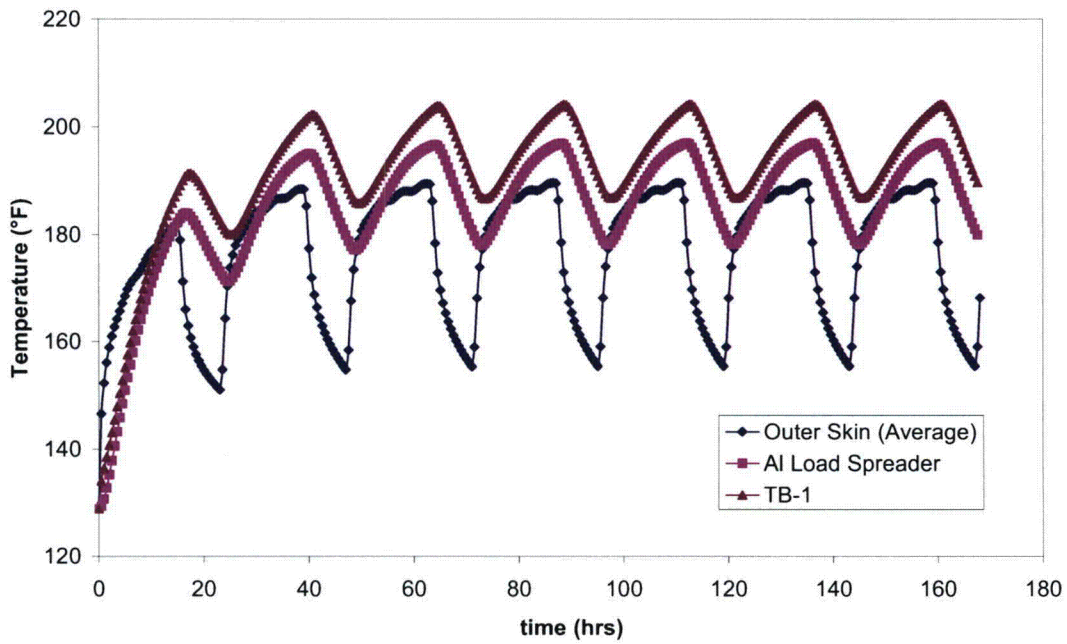


Figure 3-5. Seven-day Thermal Cycling for Quasi-Steady-State Analysis – Package Mid-Height Response ($^{\circ}\text{C}=[^{\circ}\text{F}-32]/1.8$)

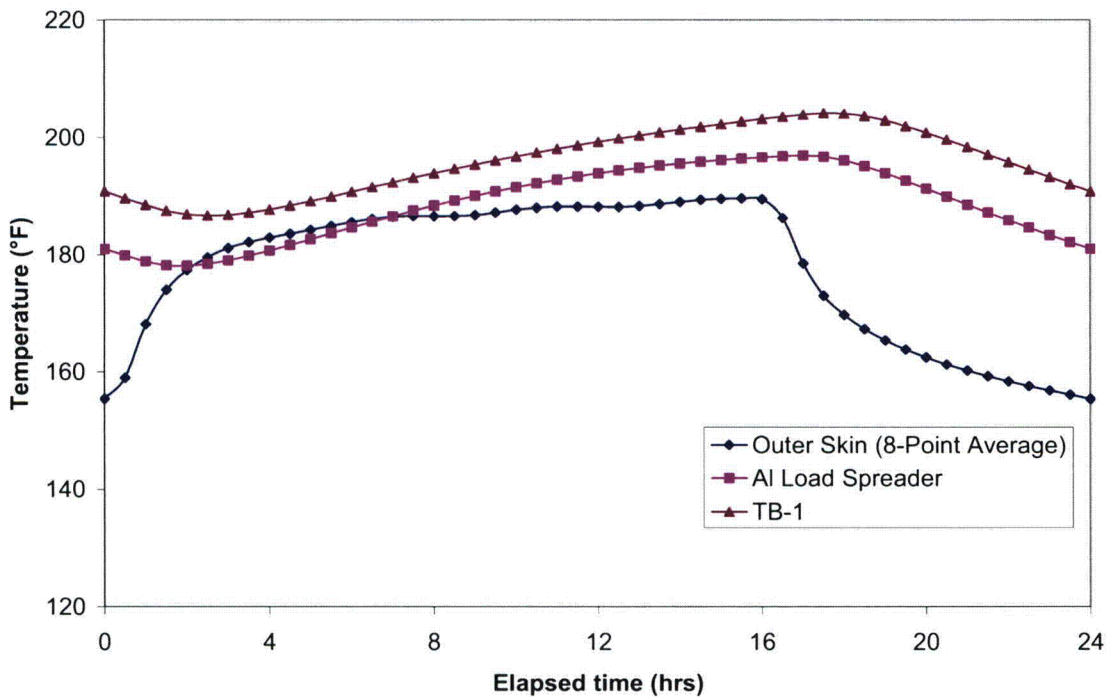


Figure 3-6. NCT Daily Thermal Cycle (Quasi-Steady-State NCT Solution) – Package Mid-Height Response ($^{\circ}\text{C}=[^{\circ}\text{F}-32]/1.8$)

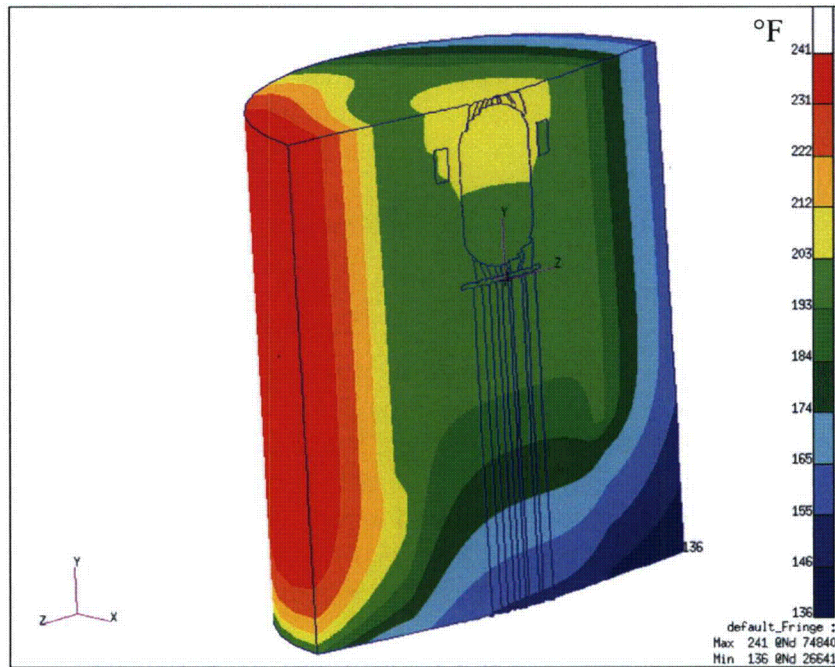


Figure 3-7. Temperature Distribution of PAT-1 Just Before Sundown – Most Severe Case of Transient NCT SAR¹ Analysis (Plot of ¼ of Package, °C=[°F-32]/1.8)

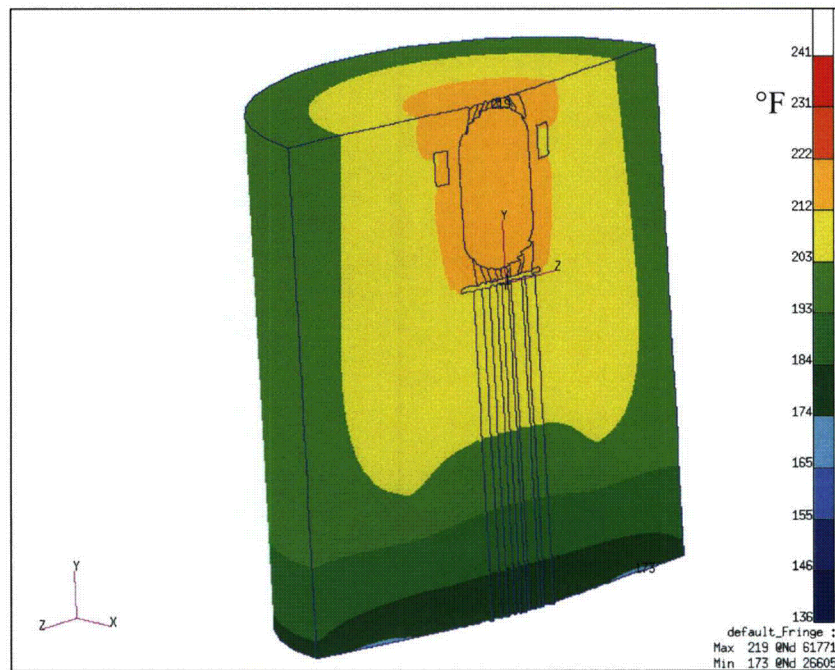


Figure 3-8. Temperature Distribution of PAT-1 – Steady-State NCT SAR¹ Analysis (Plot of ¼ of Package, °C=[°F-32]/1.8)

3.3.1.2 Addendum Analysis

The results from the NCT steady-state analysis of the package with the conservative internal heat load configuration of the new plutonium metal contents are presented in Figure 3-9. Note that the scale of the temperature distribution for this figure (and others in this section) is different from those previously shown. The temperature distribution shown in Figure 3-9 clearly illustrates the effect of the very concentrated heat applied to the seal region as described in Section 3.1.2 of this addendum. The T-Ampoule seal temperature was conservatively assumed to be the inside wall temperature of the T-Ampoule. This is conservative because the T-Ampoule closure was not explicitly modeled; instead the wall thickness of the T-Ampoule was assumed to be constant everywhere and therefore, that seal region had less thermal mass. This allows for more direct heating of the T-Ampoule seal, as energy that would be absorbed by the additional titanium in the vicinity of the seal is neglected and the heat path from the heated surface to the seal is shorter. The maximum T-Ampoule “seal” temperature is approximately 122°C (251°F) even in the very conservative internal heat load scenario. Therefore, the performance of the elastomeric O-ring in the T-Ampoule is not degraded and maintains product quality, as this temperature is within the operating range specified by the manufacturer. The maximum seal region temperature of the TB-1 was 114°C (238°F). This temperature is within the operating temperature range of both the elastomeric and the metallic seals. Therefore, the TB-1 is able to maintain containment.

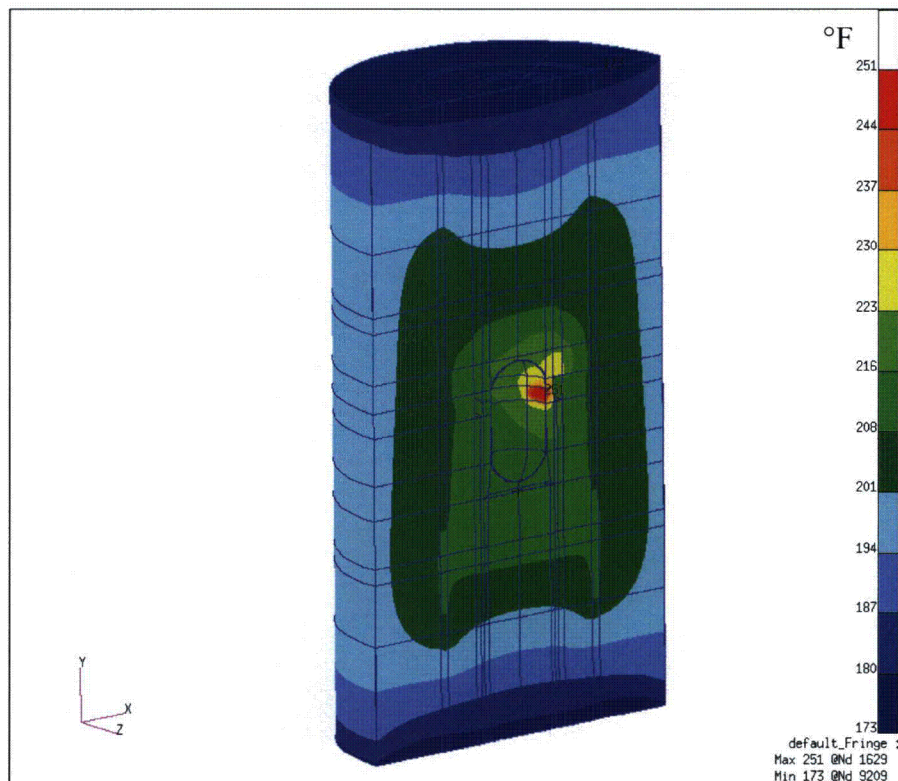
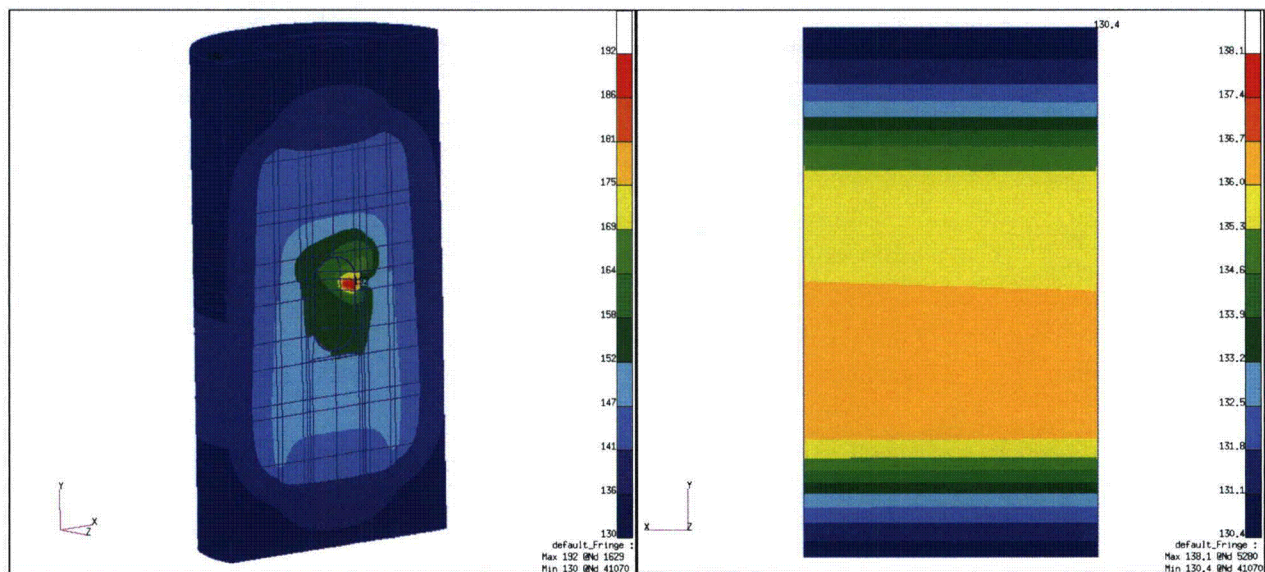


Figure 3-9. NCT Steady-State Temperature Distribution ($^{\circ}\text{C}=[^{\circ}\text{F}-32]/1.8$)

Regulatory requirements in 10 CFR 71.71(c)(2)² specify that the package must be capable of maintaining containment when it is exposed to an ambient temperature of -40°C (-40°F) in still air and shade. If one assumes no internal heating, the minimum temperature any PAT-1 package

component could reach is -40°C (-40°F). The specifications given by the manufacturer of the elastomeric seal of the TB-1 indicate an operating temperature range of -40°C to 248°C (-40°F to 400°F). Therefore, the PAT-1 can maintain containment at this low temperature extreme even without taking credit for any decay heat of the contents, which will definitely heat the seal region of the TB-1 to above -40°C (-40°F).

Since the results in Figure 3-9 show parts of the outer surface at temperatures above 85°C (185°F), an additional analysis was performed assuming the package is in the shade (no insolation), still air, and exposed to the conservative ambient temperature of 55°C (130°F). This was done to demonstrate compliance with 10 CFR 71.43(g),² which specifies that any accessible surface of a package must not exceed 85°C (185°F) in an exclusive use shipment. The results from this analysis are presented in Figure 3-10. Compliance with 10 CFR 71.43(g) is demonstrated, since the maximum outer surface temperature of the package is less than 58°C (137°F). The somewhat “skewed” temperature distribution seen in Figure 3-10(b) is the result of the concentrated internal heating of the package.



(a) Internal Temperatures

(b) Outer Surface Temperatures

Figure 3-10. Steady-State Analysis in the Shade – 10 CFR 71.43(g) ($^{\circ}\text{C}=[^{\circ}\text{F}-32]/1.8$)

3.3.2 Maximum Normal Operating Pressure

The maximum normal operating pressure (MNOP) that may occur within the TB-1 is estimated to be 132.4 kPa (19.2 psig) (see Section 4 of this addendum). This was calculated using the average internal surface temperature of the T-Ampoule as the average temperature of the gas inside the TB-1, which is 103.3°C (218°F) and the contribution to the internal pressure over time due to alpha decay. The MNOP was then estimated as $P_{\text{gauge}} = [1.801 \text{ atm} * (678^{\circ}\text{R} / 530^{\circ}\text{R}) - 1 \text{ atm}] = 1.304 \text{ atm}$ or $\sim 132.4 \text{ kPa}$ (19.2 psig), assuming initial fill of the TB-1 is done with gas at a room temperature of 21°C (70°F) and in an environment with an atmospheric pressure of one.

3.4 Thermal Evaluation under HAC

The P/Thermal FE model that was used for the NCT analysis was also used for the HAC analysis. Since the deformations shown in the SAR¹ after the package was dropped from 30 feet are minimal, the computer model used for the HAC thermal evaluation represents an undamaged package. Boundary conditions were modified to meet those specified in 10 CFR 71.73(c)(4).² In addition, the same model was used in a model verification exercise to simulate the 52-minute fire test documented in the SAR.¹

In the SAR,¹ a description of a longer-than-regulatory fire test and results are presented. The PAT-1 package used for the test did not have internal heating. The SAR¹ does not indicate the temperature distribution or overall temperature of the package prior to the test. For the purpose of model verification, an initial uniform temperature of 27°C (80°F) was assumed within the PAT-1 package and no internal heating was applied. The boundary conditions used are summarized in Table 3-8 of this addendum. The estimation for the convection heat transfer coefficients in this table is presented following the table. Note that for the purpose of this model verification exercise, the average temperature of 982°C (1800°F) on the thin-walled AQ-1 drum reported in Table 3.4 in the SAR¹ was used as the effective fire temperature.

Table 3-8. Boundary Conditions Used for the Transient Model Verification Exercise

| Boundary Condition | Application Region | Value Used During 52-Minute Fire | Value Used After Fire (Cool-down) |
|---------------------------------|--|---|--|
| Environment Temperature | External node representing environment | 982°C (1800°F)* | 27°C (80°F)** |
| Convection | Entire outer surface of the package | 11.5 W/m ² -K (2.03 Btu/hr-ft ² -°F) | 3.5 W/m ² -K (0.62 Btu/hr-ft ² -°F) |
| Radiation | Entire outer surface of the package (exchange with environment node) | Package surface emissivity of 0.8, Fire emissivity of 1 | Package surface emissivity of 0.2,*** Environment emissivity of 1 |
| Internal Heat Flux (Decay Heat) | N/A | 0 | 0 |

*From Table 3.4 in the SAR¹

**Assumed ambient temperature

***From Table 3.2 in the SAR¹

Values for convection heat transfer coefficients were estimated using correlations and verified with typically used values. For the convection heat transfer coefficient applied to the package surface during the fire (h_{fire}), a simplified temperature-only dependent correlation for a horizontal cylinder with turbulent flow as employed in the TOPAZ heat transfer code⁹ was used. That is,

$$h_{\text{fire}} = 1.24 \cdot (T_{\text{ambient}} - T_{\text{surface}})^{1/3} \text{ W/m}^2\text{-K}$$

where T_{ambient} is the temperature of the environment around the package and T_{surface} is the outer surface temperature of PAT-1, with both temperatures in °C or Kelvin.

Assuming

$T_{\text{ambient}} = 1475^{\circ}\text{F}$ (800°C) (fire temperature in 10 CFR 71.73)

$T_{\text{surface}} = 176^{\circ}\text{F}$ (80°C) (value obtained from NCT solution in the SAR¹)

$$h_{\text{fire}} = 1.24 \cdot (800^{\circ}\text{C} - 80^{\circ}\text{C})^{1/3} \text{ W/m}^2\text{-K}$$

$$h_{\text{fire}} = 11.11 \text{ W/m}^2\text{-K} \text{ or } 1.96 \text{ Btu/hr-ft}^2\text{-}^{\circ}\text{F}$$

This value of forced convection coefficient was corroborated using a more complex correlation proposed by Churchill and Bernstein¹¹ and experimental open-pool fire velocity measurements in Reference 12. In calm wind conditions for open-pool fires, vertical gas velocities are typically in the range of 5-10 m/s approximately 2 meters above the pool, but decrease to about 1 m/s near the surface of the pool.¹² Table 3-9 of this addendum presents typical values of the Grashof number (Gr_D) and the Reynolds number (Re_D) using a 5 m/s vertical gas velocity. To obtain these values, the temperature of the fire was assumed to be 800°C (1475°F) and air properties were used.

When $Gr_D/(Re_D)^2$ is less than 1, forced convection dominates. Therefore, the correlation suggested by Churchill and Bernstein for forced convection applies and was used to obtain an average convection coefficient:

$$\overline{Nu}_D = 0.3 + \frac{0.62 Re_D^{1/2} Pr^{1/3}}{[1 + (0.4/Pr)^{2/3}]^{1/4}} \left[1 + \left(\frac{Re_D}{282,000} \right)^{5/8} \right]^{4/5} \quad (3-6)$$

where \overline{Nu}_D is the Nusselt number and Pr is the Prandtl number. The convective coefficient, h, is equal to $\overline{Nu}_D k / D$, where k is the thermal conductivity of air and D is the diameter of the package. As demonstrated in Table 3-9 of this addendum the convection heat transfer coefficient is highest at the beginning of the fire when the temperature difference between the flame and the external wall of the cylinder is highest.

Table 3-9. Grashof, Reynolds, Nusselt Numbers for Calm Wind, Open-Pool Fire Conditions

| Surface Temperature, T_s | Gr_D | Re_D | Gr_D/Re_D^2 | Nu_D (Pr=0.7 for Air) | Convection Coefficient, h $\text{W/m}^2\text{-K}$ [$\text{Btu/hr-ft}^2\text{-}^{\circ}\text{F}$] |
|--|----------|--------|---------------|-------------------------|---|
| 80°C [176°F] | 2.39E+08 | 32870 | 0.22 | 106.1 | 10.0 [1.76] |
| 527°C [981°F] | 2.39E+07 | 21166 | 0.06 | 81.8 | 9.5 [1.67] |
| 800°C [1472°F] | 0 | 15102 | 0 | 67.4 | 8.7 [1.53] |

Given that the value of h_{fire} using the correlation suggested by Churchill and Bernstein is between 8.7 and 10 and the simplified correlation from Shapiro and Edwards⁹ is 11.11, a conservative heat transfer coefficient of $h_{\text{fire}} = 11.5 \text{ W/m}^2\text{-K}$ ($2.03 \text{ Btu/hr-ft}^2\text{-}^{\circ}\text{F}$) was used in the model.

The same simplified temperature- and diameter-dependent correlation for a horizontal cylinder with laminar flow that was used to calculate the natural convection coefficient for NCT in Section 3.3 of this addendum was used to estimate the natural convection coefficient for the modeling of the cool-down process after the fire. That is:

$$h_{\text{natural}} = 1.32 * [(T_{\text{surface}} - T_{\text{ambient}}) / \text{Diameter}_{\text{cylinder}}]^{0.25} \text{ W/m}^2\text{-K} \quad (3-7)$$

Assuming

$T_{\text{surface}} = 1475^{\circ}\text{F}$ (800°C) (assuming outer surface at prescribed regulatory fire temperature for bounding, maximum value calculation)

$T_{\text{ambient}} = 100^{\circ}\text{F}$ (38°C) (ambient temperature in 10 CFR 71.71²)

$\text{Diameter}_{\text{cylinder}} = 20 \text{ in.}$ (0.5588 m) (PAT-1 approximate external diameter)

$$h_{\text{natural}} = 1.32 * [(800^{\circ}\text{C} - 38^{\circ}\text{C}) / 0.5588 \text{ m}]^{0.25} \text{ W/m}^2\text{-K} \quad (3-8)$$

$$h_{\text{natural}} = 8 \text{ W/m}^2\text{-K} \text{ or } 1.4 \text{ Btu/hr-ft}^2\text{-}^{\circ}\text{F} \quad (3-9)$$

This estimated maximum value of h_{natural} is in the mid range of typical natural convection heat transfer coefficients for gases.¹⁰ However, a more conservative value of $h_{\text{natural}} = 3.5 \text{ W/m}^2\text{-K}$ ($0.62 \text{ Btu/hr-ft}^2\text{-}^{\circ}\text{F}$) (the same value used in the evaluation of NCT) was assumed for the cool-down calculation.

The results from the verification model are presented in Figures 3-11 through 3-15. Figures 3-11 and 3-12 show the temperature distribution of the overall package and the internal components at the end of the 52-minute fire. Figures 3-13 and 3-14 are similar to the previous two, but show the temperature distribution at the time when the internal temperature of the TB-1 peaked (300 minutes after the fire). The plot in Figure 3-15 illustrates the temperature history of the package at selected locations.

When the simulated temperature response was compared to the results of the 52-minute fire test discussed in the SAR,¹ it was found that the computer prediction overestimated the thermal response of the package. The spatial average temperature of the TB-1 at the time the peak temperature occurred was 100°C (212°F). This is 7°C (12°F) hotter than the average TB-1 temperature reported in the SAR.¹ Since the model in this verification exercise overestimated the TB-1 average temperature, the simulation of the package response to the HAC with the concentrated heat is also overestimated. Therefore, it is conservative to use this model to estimate the thermal response of the package configuration for this addendum. The results are presented in the following sections.

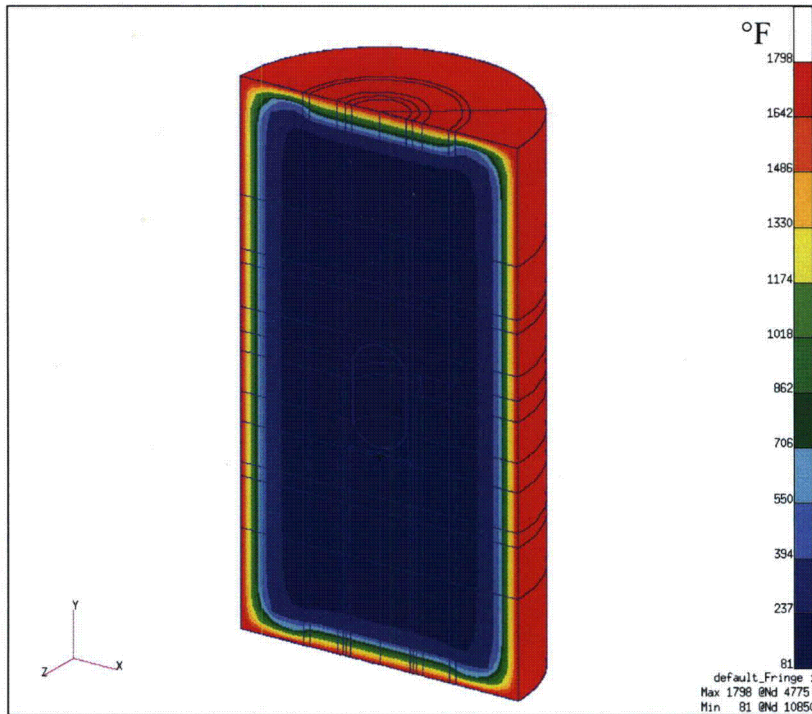


Figure 3-11. Temperature Distribution of the Verification Model at the End of the 52 Minute Fire — Complete Model ($^{\circ}\text{C}=[^{\circ}\text{F}-32]/1.8$)

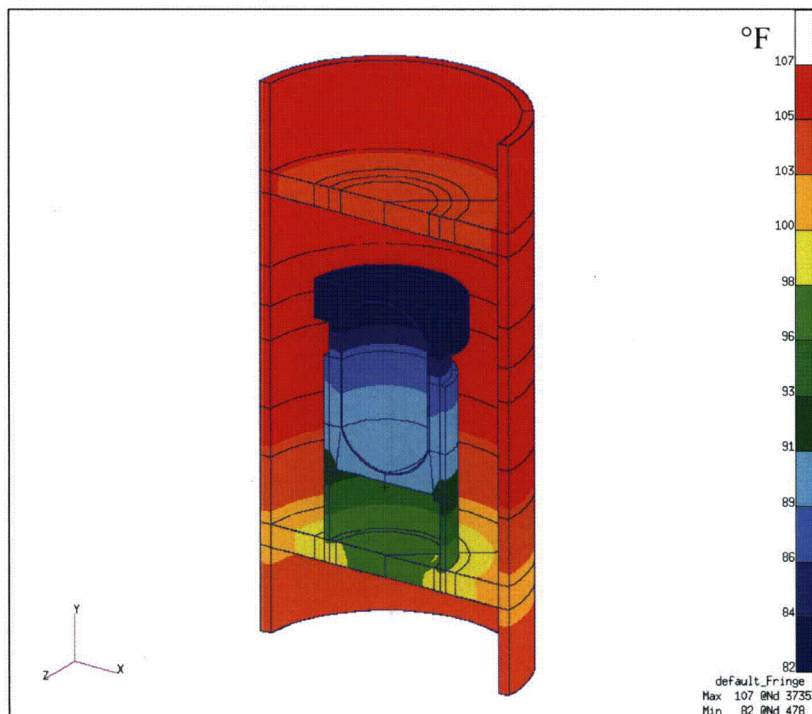


Figure 3-12. Temperature Distribution of the Verification Model at the End of the 52 Minute Fire — T-Ampoule, TB-1, Heat Transfer Cu Cylinder, and Aluminum Load Spreader ($^{\circ}\text{C}=[^{\circ}\text{F}-32]/1.8$)

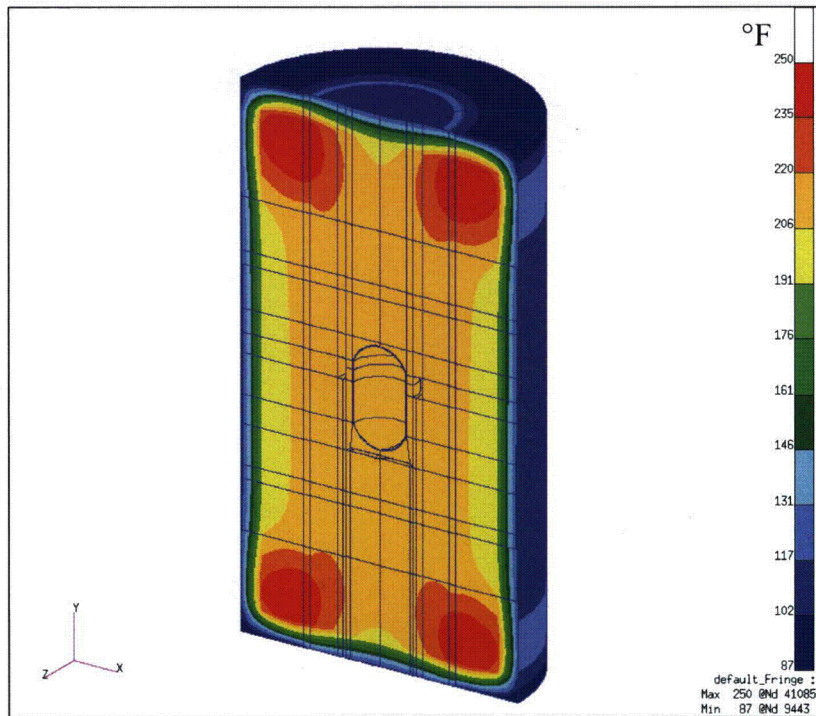


Figure 3-13. Temperature Distribution of the Verification Model at t=352 Minutes (300 Minutes after the 52 Minute Fire) — Complete Model ($^{\circ}\text{C}=[^{\circ}\text{F}-32]/1.8$)

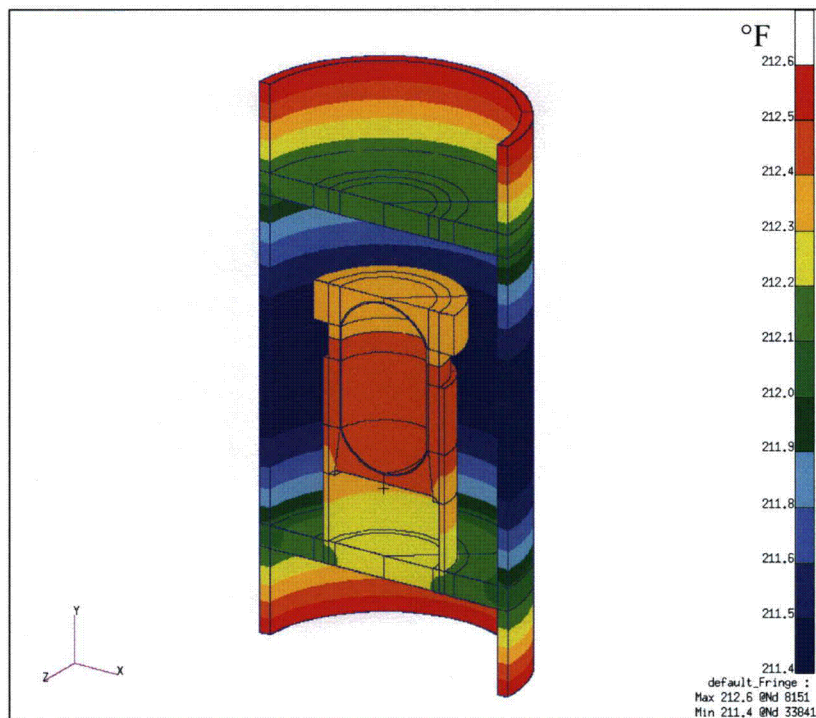


Figure 3-14. Temperature Distribution of the Verification Model at t=352 Minutes (300 Minutes after the 52 Minute Fire) — T-Ampoule, TB-1, Heat Transfer Cu Cylinder, and Aluminum Load Spreader ($^{\circ}\text{C}=[^{\circ}\text{F}-32]/1.8$)

3.4.1 Initial Conditions

The initial condition for the transient thermal analysis described in 10 CFR 71.73² is the temperature distribution calculated for the NCT. This initial temperature distribution is shown in Figure 3-9.

3.4.2 Hypothetical Accident Conditions (HAC)

The PAT-1 package model was subjected to the thermal transient conditions specified in 10 CFR 71.73² to evaluate whether the TB-1 can maintain containment and the T-Ampoule maintain seal (for product quality, not regulatory purpose) during and after a HAC fire event. The boundary conditions that were used in the model are summarized in Table 3-10 of this addendum. Note that only two boundary conditions were changed between this model and the one that was run for the 52-minute fire test verification exercise. That is, the fire duration was set to 30 minutes, and the same concentrated internal heat load applied to the NCT model was also used. As in the SAR,¹ the fire temperature was conservatively assumed to be 1010°C (1850°F) and the environment temperature for the cool-down period was conservatively assumed to be 54.4°C (130°F).

The results from the simulation of the 10 CFR 71.73(c)(4)² environment are presented in Figures 3-16 through 3-20. Figures 3-16 and 3-17 show the temperature distribution of the overall package and the internal components at the end of the 30-minute regulatory fire. Figures 3-18 and 3-19 are similar to the previous two but show the temperature distribution at the time when the internal temperature of the TB-1 peaked (260 minutes after the fire). The plot in Figure 3-20 illustrates the temperature history of the package at selected locations.

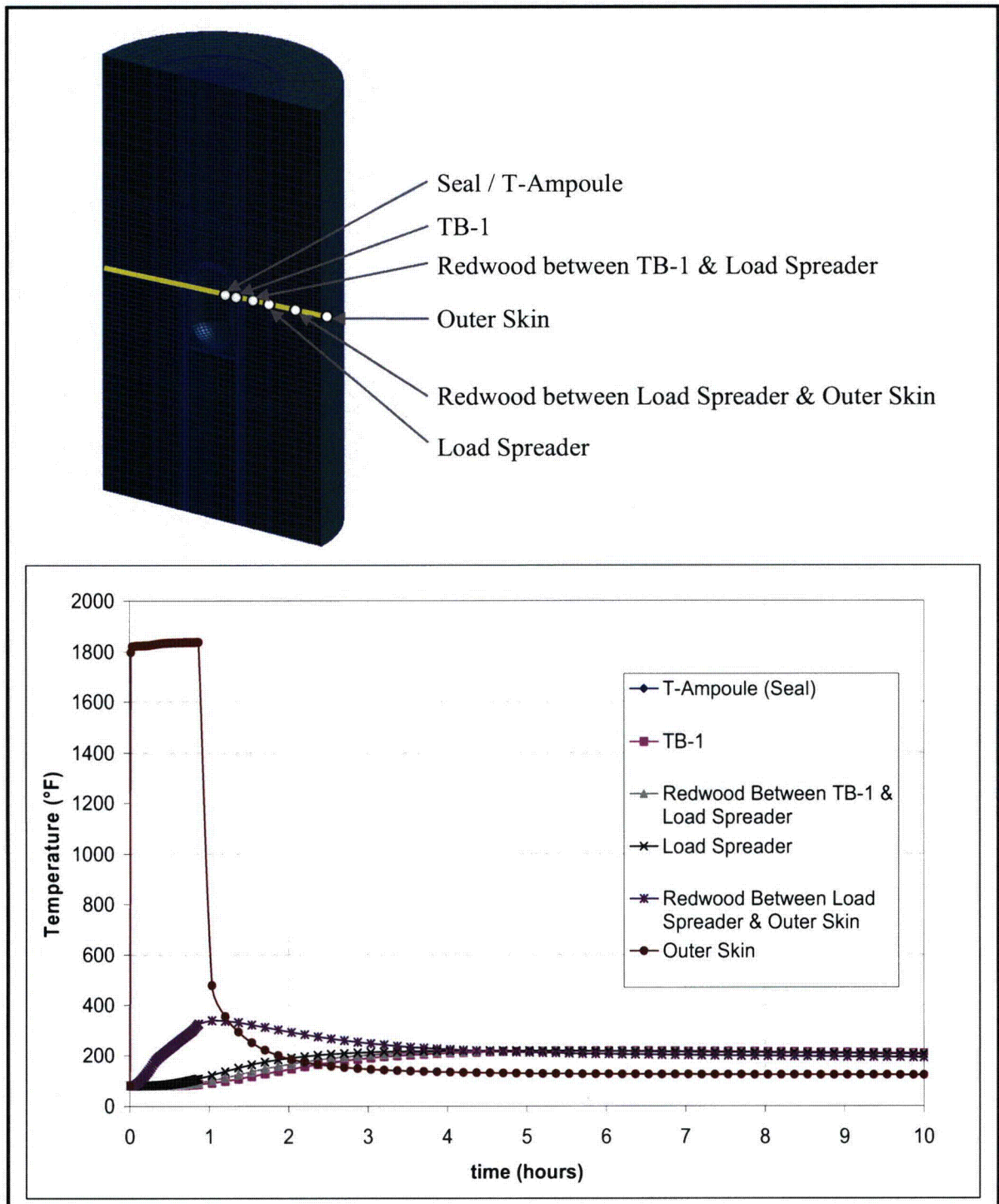


Figure 3-15. Temperature History at T-Ampoule Seal Height for the 52-Minute Fire Model Verification Exercise ($^{\circ}\text{C}=[^{\circ}\text{F}-32]/1.8$). Note: In the schematic above the plot, the reference yellow line crosses the cask at the T-Ampoule-seal height and the white dots are the approximate locations of the temperature history lines in the plot. The “T-Ampoule (Seal)” curve is completely covered by the “TB-1” curve.

Table 3-10. Boundary Conditions Used for the HAC Thermal Evaluation

| Boundary Condition | Application Region | Value Used During 30-minute Fire | Value Used After Fire (Cool-down) |
|---------------------------------|--|---|---|
| Environment Temperature | External node representing environment | 1010°C (1850°F) | 54°C (130°F) |
| Convection | Entire outer surface of the package | 11.5 W/m ² -K (2.03 Btu/hr-ft ² -°F) | 3.5 W/m ² -K (0.62 Btu/hr-ft ² -°F) |
| Radiation | Entire outer surface of the package | Package surface emissivity of 0.8, Fire emissivity of 1 | Package surface emissivity of 0.2,* Environment emissivity of 1 |
| Internal Heat Flux (Decay Heat) | Small region described in Section 3.1.2 of this addendum | 16,680 W/m ² (5287.5 Btu/hr-ft ²) | 16,680 W/m ² (5287.5 Btu/hr-ft ²) |

* From Table 3.2 in the SAR¹

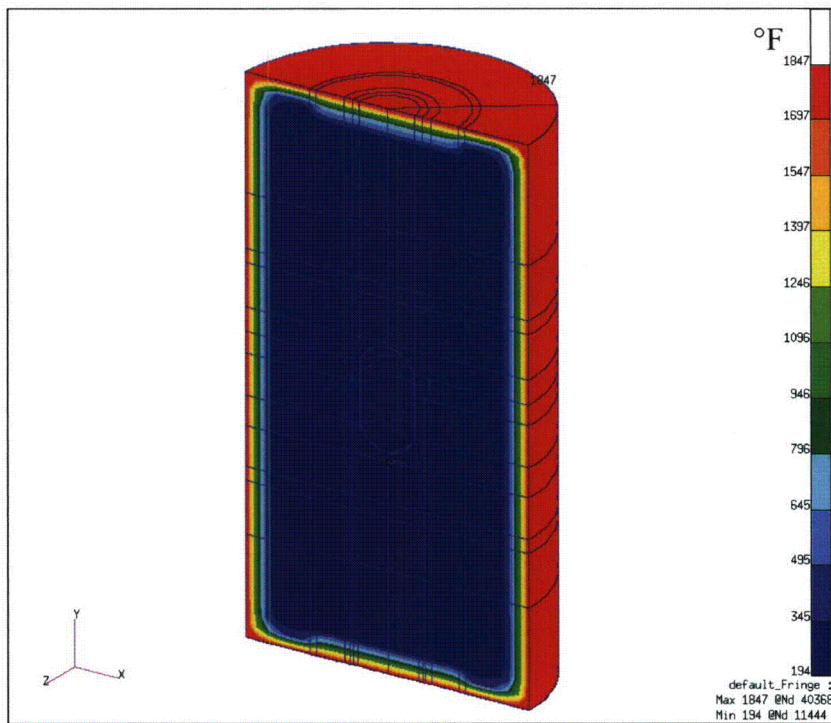


Figure 3-16. Temperature Distribution at the End of the 30-Minute Regulatory Fire — Complete Model (°C=[°F-32]/1.8)

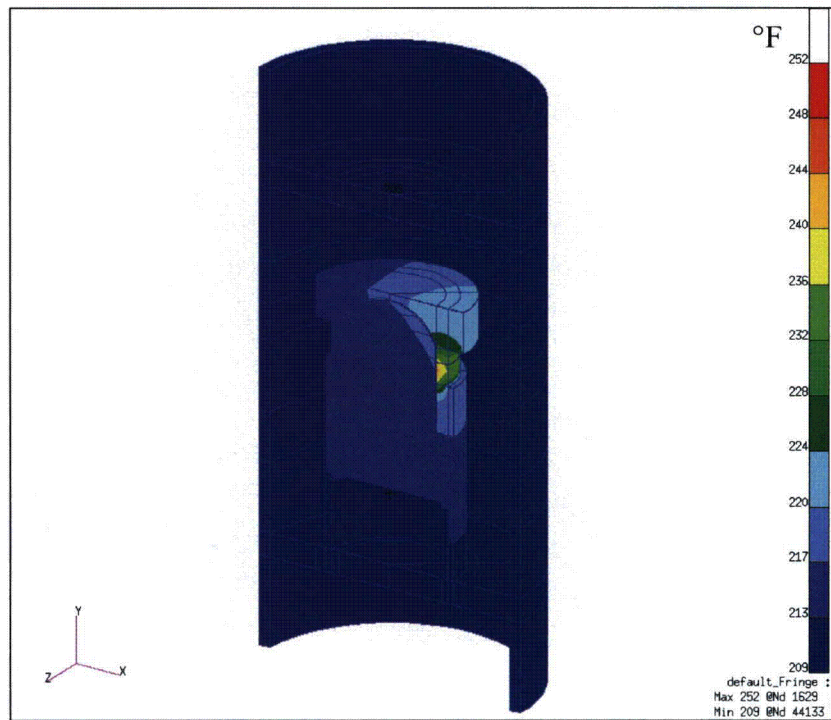


Figure 3-17. Temperature Distribution at the End of the 30-Minute Regulatory Fire — T-Ampoule, TB-1, Heat Transfer Cu Cylinder, and Aluminum Load Spreader ($^{\circ}\text{C}=[^{\circ}\text{F}-32]/1.8$)

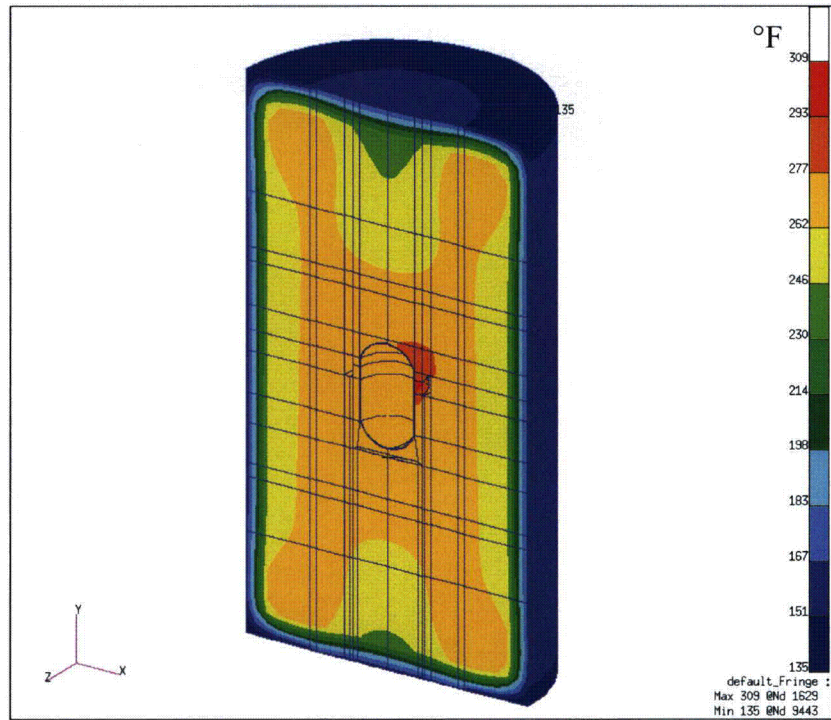


Figure 3-18. Temperature Distribution at t=290 Minutes (260 Minutes after the 30-Minute Fire) — Complete Model ($^{\circ}\text{C}=[^{\circ}\text{F}-32]/1.8$)

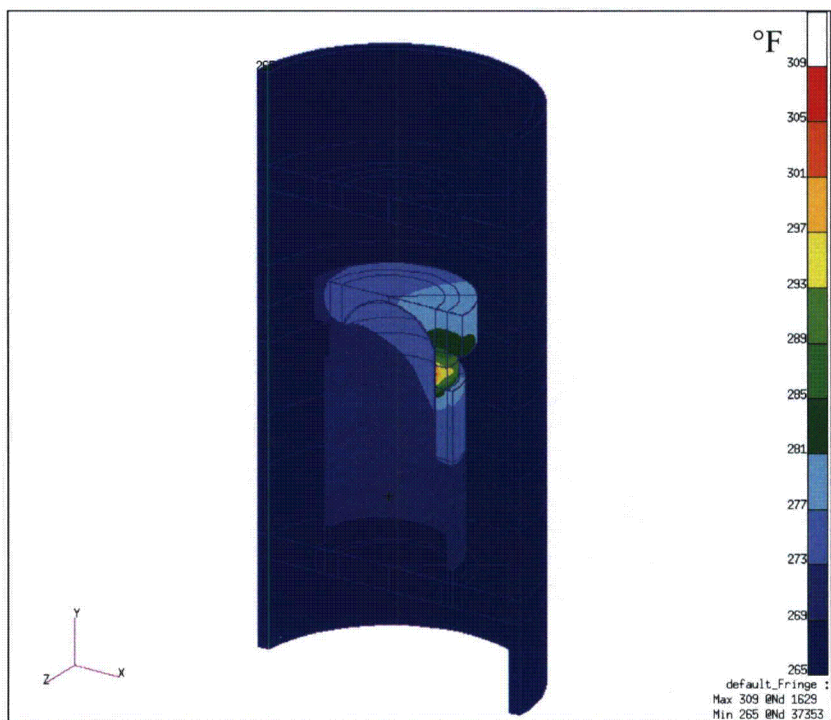


Figure 3-19. Temperature Distribution at t=290 Minutes (260 Minutes after the 30-Minute Fire) — T-Ampoule, TB-1, Heat Transfer Cu Cylinder, and Aluminum Load Spreader ($^{\circ}\text{C}=[^{\circ}\text{F}-32]/1.8$)

3.4.3 Maximum Temperatures and Pressure

Results from the hypothetical accident conditions evaluation of the AQ-1, TB-1, and the T-Ampoule, assuming the bounding concentrated internal heat described in Section 3.1.2 of this addendum and using the conservative transient computer model described in Section 3.4 of this addendum, are summarized in Table 3-11 of this addendum.

The components listed in this table did not reach temperatures of concern. Only the redwood regions closer to the outer skin of the package are expected to degrade as wood chars at temperatures above 288°C (550°F). Nevertheless, PAT-1 protects the package contents during and after the exposure to a severe fire environment, as required by 10 CFR 71.73.

The HAC evaluation indicated a peak T-Ampoule seal temperature of 153°C (308°F) and a peak TB-1 (and seal) temperature of 147°C (296°F). This TB-1 seal temperature is 38°C (69°F) higher than that reported as the TB-1 temperature in Section 3.5.1.1 of the PAT-1 SAR¹ and is, once again, considered to be overestimated (or conservative) due to the concentrated heat loading assumption. Nevertheless, this temperature does not exceed the manufacturer's specification for the elastomeric seal operating range in the TB-1 (-40°C to 204°C [-40°F to 400°F]) or the copper seal limit temperature. Therefore, the TB-1 is able to maintain containment. In addition, the T-Ampoule is also able to maintain a seal for product quality.

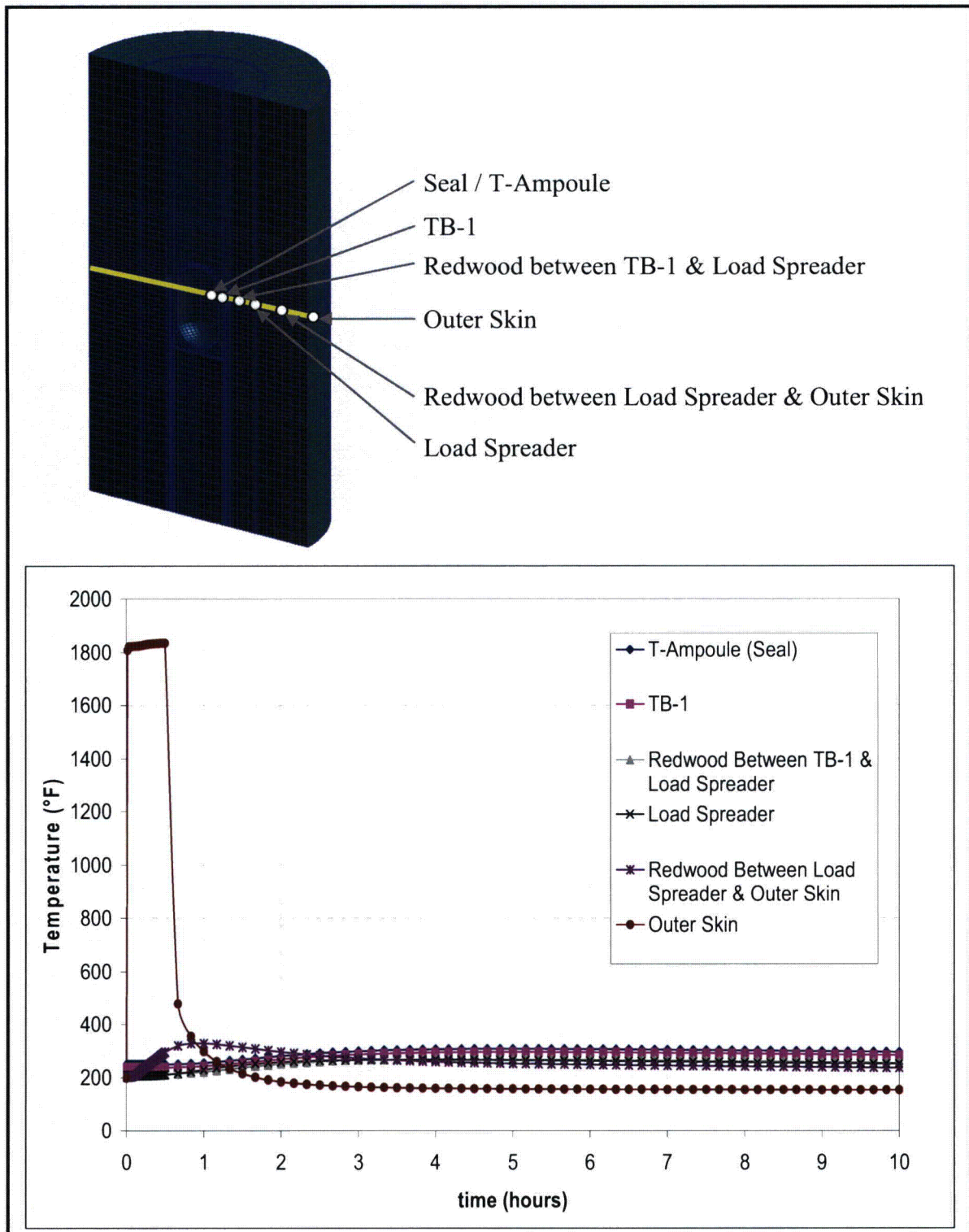


Figure 3-20. Temperature History at T-Ampoule Seal Height for the 30-Minute Regulatory Fire ($^{\circ}\text{C}=[^{\circ}\text{F}-32]/1.8$). Note: In the schematic above the plot, the reference yellow line crosses the cask at T-Ampoule-seal height and the white dots are the approximate locations of the temperature history lines in the plot.

Table 3-11. Summary of Maximum Temperatures and Times for the HAC

| Component | HAC Maximum Temperature and Time to Reach Temperature |
|--|---|
| T-Ampoule (Seal) | 153°C (308°F) @ 260 minutes after the fire |
| TB-1 (and TB-1 seal)* | 147°C (296°F) @ 260 minutes after the 30-minute fire |
| Center of Redwood between TB-1 and Load Spreader | 132°C (270°F) @ 240 minutes after the 30-minute fire |
| Aluminum Load Spreader | 131°C (267°F) @ 190 minutes after the 30-minute fire |
| Center of Redwood between Load Spreader and Outer Skin | 164°C (328°F) @ 30 minutes after the 30-minute fire |
| Stainless Steel Outer Drum | 1003°C (1837°F) @ end of fire |

*Maximum seal temperature was conservatively taken as the TB-1 maximum temperature.

The average T-Ampoule internal surface temperature was 136°C (276°F). Assuming the gas inside the TB-1 is at this average temperature, the maximum internal pressure that the TB-1 could experience under HAC can be estimated. When calculating this pressure, it was also assumed that the TB-1 was initially loaded at a room temperature of 21°C (70°F) and in a pressure environment of 1 atmosphere. Additionally, pressure generation due to alpha decay as calculated in Section 4 of this addendum was included in the total pressure calculation. Thus:

$$P_{TB-1@276^{\circ}\text{F-gaugc}} = (P_{\text{initial}} + P_{\text{alpha_decay}}) * (T_2/T_1) - 1\text{atm} = [1.801 \text{ atm} * (736^{\circ}\text{R}/530^{\circ}\text{R}) - 1\text{atm}]$$

$$= 1.5 \text{ atm or } \sim 152 \text{ kPa (22.1psig)} \quad (3-10)$$

In summary, these results show that the PAT-1 provides containment for the proposed new payload inside the TB-1 and adequately contains the material inside the T-Ampoule, as maximum seal temperatures are within manufacturer's specifications and the TB-1 can withstand the pressure that would arise during and after the HAC fire event. Additionally, the eutectic prevention barrier is retained because the T-Ampoule is constructed of titanium 6Al-4V alloy and can withstand the temperatures and pressures observed under the 10 CFR 71² HAC, as documented in Section 2 of this addendum.

3.4.4 Maximum Thermal Stresses

The maximum thermal stresses are determined from results of the differential thermal expansion analysis conducted and documented in Section 2.7.4.2 of this addendum. Since the American Society of Mechanical Engineers (ASME) Boiler and Pressure Vessel (B&PV) code does not provide the coefficient of thermal expansion (α) for Ti-6Al-4V, the value listed in the MIL-HDBK-5E¹³ ($9.18 \times 10^{-6} \text{ m/m}^{\circ}\text{C}$ [$5.1 \times 10^{-6} \text{ in/in}^{\circ}\text{F}$]) was used in this analysis.

A conservative estimate of the T-Ampoule maximum expansion can be calculated by assuming the T-Ampoule is a 0.2 m (7.418 in.) long cylinder (the actual T-Ampoule is capped) with a diameter of 0.11 m (4.22 in). Assuming a temperature increase of $(153^{\circ}\text{C} - 21.1^{\circ}\text{C}) = 132^{\circ}\text{C}$ ($[308^{\circ}\text{F} - 70^{\circ}\text{F}] = 238^{\circ}\text{F}$), the expansion produced equals $\alpha\Delta TL$, or 0.23 mm (0.009 in.) in the longitudinal direction and 0.41 mm (0.0161 in.) in circumference (or 0.13 mm [0.0051 in.] in

diameter). Since the gap between the T-Ampoule and the TB-1 is 0.381 mm (0.015 in.) around the entire perimeter, the T-Ampoule will not expand enough to induce any stress on the TB-1, even if thermal expansion of the TB-1 is ignored.

3.4.5 Hypothetical Accident Conditions for Fissile Material Packages for Air Transport

Thermal tests that meet the specifications in 10 CFR 71.64² were conducted on the PAT-1 and are documented in Chapter 3 of the SAR¹. Physical tests were the primary means used to demonstrate that the PAT-1 package met the requirements of the NRC Qualification Criteria (10 CFR 71.74²). The purpose of the assessment documented in Section 3.6 of the SAR¹ was to demonstrate that the maximum TB-1 temperature (reported in Section 3.6.3 of the SAR¹) used in Section 4.4.2 of the SAR¹ was a reasonable upper limit for bounding the results.

The package temperatures cited in Section 3.6.3 of the SAR¹ stated the following: “Based on the analysis and test results in Sections 3.6.1.1 and 3.6.1.2, the TB-1 is estimated to have attained a maximum temperature of approximately 582°C (1080°F) during the thermal test specified in the NRC Qualification Criteria.” This maximum temperature is not affected by any of the packing or content modifications presented in this addendum. That is, the maximum internal heat generation of the content remains the same [25 watts (85.3 Btu/hr)] and the package of the TB-1 and the rest of the packaging outward of the TB-1 is the same as evaluated in the SAR.¹ Therefore, the maximum temperature of the TB-1 used for this addendum, for the calculation of loads due to internal pressure and thermal expansion during the plutonium aircraft fire environment is 582°C (1080°F).

At the maximum temperature of the TB-1 after the plutonium aircraft accident fire, there is a potential for plutonium metal to form eutectics with certain metals such as iron in the TB-1. The materials that were selected for the components within the TB-1 were based on the resistance to eutectic formation with plutonium. The melting temperatures for different material combinations are presented in Section 3.5.3 of this addendum. Given that the melting point of the plutonium-iron eutectic is lower than the maximum TB-1 temperature in the plutonium air transport thermal evaluation, the titanium T-Ampoule is used as a barrier between the plutonium metal and the PH13-8Mo material in the TB-1. The structural analysis documented in Section 2 of this addendum demonstrates that the T-Ampoule wall will not be breached as a result of NCT, HAC, or the accident conditions for air transport of plutonium. Thus, the formation of a Pu-Fe eutectic as a result of the thermal conditions resulting from a 10 CFR 71.74 specified fire is not possible because of the separation between the Pu content and the Fe in the TB-1 provided by the T-Ampoule wall. The service temperatures of all components (T-Ampoule and its packing within the TB-1) shown in Table 3-5 in this addendum, which were derived in part from the eutectic evaluation in Section 3.5.3 in this addendum, are all above 582°C (1080°F).

In addition to the Pu-Fe eutectic potential discussed above, a plutonium-beryllium eutectic may also form. The melting point of this Pu-Be eutectic is 595°C (1103°F) (see Section 3.5.3 in this addendum). This is 13°C (23°F) higher than the highest temperature excursion that occurs in the system.

The maximum internal pressure that may occur within the TB-1 during the air transport thermal evaluation is estimated to be 6.547 MPa (949.5 psig) (see Section 4 of this addendum). This was

calculated adding the pressure generated from the decomposition of the O-rings in the SC-1 configuration, which includes the elastomeric seal of the TB-1, T-Ampoule, and three SC-1s (highest amount of elastomeric material), which yielded a pressure of 887.3 psi (from Section 4.5.4 of this addendum), the pressure generated due to the change in temperature $[(1540^{\circ}\text{R}/530^{\circ}\text{R}) * 14.7 \text{ psi} = 42.7 \text{ psi}]$, and the pressure from gas generation from alpha decay of plutonium $[(1540^{\circ}\text{R}/530^{\circ}\text{R}) * 11.78 \text{ psi} = 34.2 \text{ psi}]$, based on the largest plutonium content of 1300 grams in Section 4.5.3, Table 3-5 of this addendum for conservatism and corrected for the temperature change]. This maximum pressure of 6.547 MPa (949.5 psig) is lower than the maximum TB-1 pressure stipulated in the PAT-1 SAR¹ (1095.3 psig, see Section 4.4.2 of this addendum). Therefore, the TB-1 is capable of sustaining this maximum pressure observed during the plutonium air transport fire accident condition without rupturing. Note that the T-Ampoule will not retain any pressure because its elastomeric O-ring can extrude out of the O-ring groove and no longer maintain a seal at temperatures above its service temperature of 204°C (400°F).

The thermal expansion calculation in Section 2.8.6 of this addendum demonstrates that no stresses will be induced in the TB-1 by differential thermal expansion resulting from the air transport fire accident.

The analysis in this section demonstrates that the replacement of the PC-1 inner container (with its packing and contents) with the T-Ampoule inner container (with its packing and contents) does not alter the thermal performance of the PAT-1. Therefore, the discussion in Section 3.6 of the SAR¹ regarding the ability of the package to meet the requirements in the plutonium air transport regulations due to thermal loads remains valid. That is, the performance of the PAT-1 with the T-Ampoule (with its packing and contents) inside the TB-1 is bounded by the tests presented in the SAR¹ and therefore the TB-1 maintains containment.

3.5 Appendix

3.5.1 References

1. United States. Nuclear Regulatory Commission. NUREG-0361. "Safety Analysis Report for the Plutonium Air Transportable Package, Model PAT-1." Washington, D.C. 1978.
2. United States. Nuclear Regulatory Commission. Code of Federal Regulations, 10 CFR 64, 71, 73, and 74. January 1, 2009.
3. White, R.H., and E.L. Schaffer. "Application of CMA Program to Wood Charring," *Fire Technology*. Volume 14, Number 4 (1978): 279-290.
4. MSC Patran Thermal 2005 r2. MSC Software Corporation. <www.mssoftware.com.>
5. Touloukian, Y.S., "Thermophysical Properties of High-Temperature Solid Materials." (1967).
6. Schorsch, R.H., "Engineering Properties of Selected Materials." (1966).
7. Hodge, A.W. and D.J. Maykuth. "Properties of New High-Temperature Titanium Alloys," DMIC Memo 230, Defense Metals Information Center, Battelle Memorial Institute, Columbus Ohio. February 1968.
8. Mason, R.E. and S.P. Willson, "Eutectic Analysis of Ti-6Al-4V with Plutonium and Copper," LA-UR-08-07663. Los Alamos National Laboratory. Los Alamos, NM. 2008. (Presented in Appendix 3.5.3).
9. Shapiro, A.B. and A.L. Edwards. "TOPAZ2D Heat Transfer Code Users Manual and Property Data Base," UCRL-ID--104558. Lawrence Livermore National Laboratory. Livermore, CA. 1990.
10. Incropera, F.P. and D.P. DeWitt. "Fundamentals of Heat and Mass Transfer, 4th ed.," New Jersey: Wiley & Sons, Inc., 1996.
11. Churchill, S.W. and J. M. Bernstein. *Heat Transfer*. 99, 300. (1977).
12. Nakos, J.T., "Uncertainty Analysis of Steady-State Incident Heat Flux Measurements in Hydrocarbon Fuel Fires," SAND2005-7144. Sandia National Laboratories. Albuquerque, NM. December 2004.
13. Department of Defense. *Military Standardization Handbook: Metallic Materials and Elements for Aerospace Vehicle Structures*. MIL-HDBK-5E: May 1988.

3.5.2 Parker O-Ring Data Sheet



Compound Data Sheet
Parker O-Ring Division United States

MATERIAL REPORT

REPORT NUMBER: KJ0835
DATE: 10/10/89

TITLE: Evaluation of Parker Compound V0835-75 to MIL-R-83485
Type 1 Specifications
PURPOSE: To determine if V0835-75 meets the requirements.
CONCLUSION: Compound V0835-75 meets the specification requirements.

Recommended temperature limits: -40°F to 400°F

Recommended For

Low temperature
Petroleum, mineral, and vegetable oils
Silicone fluids
Aromatic hydrocarbons (benzene, toluene)
Chlorinated hydrocarbons
High vacuum
Ozone, weather, and aging resistance

Not Recommended For

Hot water and steam
Auto and aircraft brake fluids
Amines
Ketones
Low molecular weight esters and ethers

Parker O-Ring Division
2360 Palumbo Drive
Lexington, Kentucky 40509
(859) 269-2351



Compound Data Sheet
Parker O-Ring Division United States

REPORT DATA

Report Number: KJ0835

| <u>ORIGINAL</u> | <u>MIL-R-83485 TYPE 1, O-RINGS & COMPRESSION SEALS</u> | <u>V0835-75 ACTUAL VALUES</u> |
|---|--|-----------------------------------|
| Specific Gravity | As determined | 1.75 |
| Hardness points | 75 ± 5 | 78 |
| Tensile Strength, psi. min. | 1600 | 1708 |
| Elongation, % min. | 120 | 180 |
| Temperature Retraction, 10% (TR-10), °F, max. | -20 | -22 |
| <u>AFTER AIR AGING, 70 HRS. @ 75° ± 5°F. Compression Set</u> | | |
| % of original deflection, max. | 25 | -- (14) |
| <u>AFTER AGING, 70 HRS. @ 75°F IN TT-S-735, TYPE III</u> | | |
| Hardness Change, pts. | +5 | 77 (-1) |
| Tensile Strength decrease, % max. | 30 | 1662 (-3) |
| Elongation decrease, % max. | 20 | 165 (-8) |
| Volume change, % max. | 1 to 10 | -- (+2) |
| <u>AFTER AIR AGING, 70 HRS. @ 528° ± 5°F</u> | | |
| Hardness change, pts. | +5 | 78 (0) |
| Tensile Strength decrease, % max. | 35 | 1136 (-33) |
| Elongation decrease, % max. | 10 | 235 (+31) |
| Weight loss, % max. | 12 | -- (-7) |
| <u>AFTER AIR AGING, 166 HRS @ 347° ± 5°F. COMPRESSION SET</u> | | |
| % of original deflection, max. | 25 | -- (15) |
| 18 hrs. cooling | | -- (24) |
| <u>AFTER AIR AGING, 22 HRS @ 392° ± 5°F. COMPRESSION SET</u> | | |
| % of original deflection, max. | 20 | -- (11) |

Parker O-Ring Division
 2360 Palumbo Drive
 Lexington, Kentucky 40509
 (859) 269-2351



Compound Data Sheet
Parker O-Ring Division United States

| AFTER AGING, 70 HRS. @ 347°MIL-R-83485 ±5°F in AMS-3021 | MIL-R-83485 TYPE 1, O-RINGS % COMPRESSION SEALS | V0835-75 ACTUAL VALUES |
|---|---|---------------------------|
| Hardness change, pts | +0, -15 | 73 |
| Tensile Strength decrease, %, max. | 35 | 1406 (-18) |
| Elongation decrease, %, max. | 20 | 171 (-5) |
| Volume change, % | 1 to 20 | -- (+15) |
| Compression set, % of original deflection, max. | 10 | -- 7 |
| 18 hr. cooling | | -- 9 |

Parker O-Ring Division
 2360 Palumbo Drive
 Lexington, Kentucky 40509
 (859) 269-2351

3.5.3 Eutectic Analysis of Ti-6Al-4V with Plutonium and Copper

LA-UR 08-07663

Plutonium Metal Compatibility with Materials of the Ti-6Al-4V Packaging System

Prepared by:
Richard E. Mason, PMT-1
and
Stephen P. Willson, PMT-1

2 December 2008



Los Alamos National Laboratory, an affirmative action/equal opportunity employer, is operated by the Los Alamos National Security, LLC for the National Nuclear Security Administration of the U.S. Department of Energy under contract DE-AC52-06NA25396. By acceptance of this article, the publisher recognizes that the U.S. Government retains a nonexclusive, royalty-free license to publish or reproduce the published form of this contribution, or to allow others to do so, for U.S. Government purposes. Los Alamos National Laboratory requests that the publisher identify this article as work performed under the auspices of the U.S. Department of Energy. Los Alamos National Laboratory strongly supports academic freedom and a researcher's right to publish; as an institution, however, the Laboratory does not endorse the viewpoint of a publication or guarantee its technical correctness.

LA-UR-08-07663

Abstract

This technical basis report considers phase stability of plutonium metal encapsulated in a Ti-6Al-4V ampoule. The maximum temperature that these materials will be exposed to is 582°C. The plutonium metal may also be encapsulated in tantalum foil plus beryllium is potentially in contact with the plutonium. It is concluded by analysis of phase diagrams and composition of materials for all possible binary systems that no liquid phases are expected in this system at 582°C. Furthermore, it is anticipated that the lowest melting point phase that may form within this system is 595°C – the plutonium/beryllium eutectic temperature. This is 13°C higher than the highest temperature excursion considered for the system. This is not a large margin but the 595°C value is a conservative estimate, thus the system in a transient reaching 582°C is still considered safe. Review of the ternary phase diagrams available in the literature involving components of this system supports the conclusions drawn from the binary systems, however, the ternary systems are limited and this is a much more complex system than reviewed in the binary or ternary systems available in the literature.

LA-UR-08-07663

Table of Contents

| | |
|---|-----------|
| INTRODUCTION | 4 |
| INTERFACIAL REACTION ZONES | 6 |
| <i>Aluminum</i> | 6 |
| <i>Beryllium</i> | 8 |
| <i>Copper</i> | 10 |
| <i>Gallium</i> | 11 |
| <i>Plutonium</i> | 12 |
| <i>Tantalum, Titanium, and Vanadium</i> | 13 |
| <i>Binary interaction summary</i> | 13 |
| INVESTIGATION OF TERNARY SYSTEMS | 14 |
| ADDITIONAL CHEMICAL REACTION | 15 |
| CONCLUSIONS | 15 |
| REFERENCES | 15 |

LA-UR-08-07663

Introduction

The PAT-1 (Plutonium Air Transport) package was originally designed to transport plutonium oxide across the country and to other countries that process plutonium oxide. The TB-1 containment vessel was designed to contain this material. The TB-1 vessel is stainless steel. Because of the need to air transport alpha and delta-stabilized plutonium metal, the container or ampoule inside the TB-1 containment vessel is newly constructed of the Ti-6Al-4V alloy to protect the TB-1 vessel from attack by plutonium. This analysis focuses on binary eutectic compositions that could form in a hypothetical accident scenario in which the TB-1 vessel attains a maximum temperature of 582°C and is exposed to this temperature for up to four days. Within the liner is a copper foam support structure of $\geq 99.99\%$ copper, and an alpha or delta-stabilized plutonium metal sample. Plutonium metal is loaded into the copper foam and the combined package is loaded into the Ti-6Al-4V liner in an inert atmosphere glove box. The interior void space of the liner is flushed with helium, then sealed and leak-checked.

The melting points of pure metals considered for this analysis are presented in Table 1. [Lide 1991] A summary of the lowest melting points for the possible binary systems has been taken from the binary phase diagrams, and assembled in Table 2.

Table 1. Melting points of pure metals considered in this system.

| Element | Melt Temperature (°C) |
|-----------|-----------------------|
| Aluminum | 660 |
| Beryllium | 1287 |
| Copper | 1085 |
| Gallium | 30 |
| Plutonium | 640 |
| Tantalum | 3017 |
| Titanium | 1668 |
| Vanadium | 1910 |

LA-UR-08-07663

Table 2. Lowest melting points and compositions derived from binary phase diagrams.

| System | Lowest Melting Point (°C) |
|-----------------------|---|
| Ti6Al4V | 1604°C |
| Aluminum – Beryllium | 644°C eutectic |
| Aluminum – Copper | 548°C at compositions between pure aluminum and about 45 atom percent aluminum, 660C for copper alloying with aluminum up to about 3 weight percent Al, greater than 600°C for aluminum alloying with copper up to 25 weight percent Cu |
| Aluminum – Gallium | 26.3°C eutectic |
| Aluminum – Plutonium | 640°C for pure Pu |
| Aluminum – Tantalum | 660C for pure Al |
| Aluminum – Titanium | 660°C for pure Al |
| Aluminum – Vanadium | 660°C for pure Al |
| Aluminum – Beryllium | 644°C eutectic |
| Beryllium – Copper | The congruent melt temperature of 858°C is the lowest melt temperature in the binary system |
| Beryllium – Gallium | 30°C the gallium melt temperature. The gallium melts and there is minimal solution of the beryllium below 600°C |
| Beryllium – Plutonium | The additions of small amounts of beryllium may lower the plutonium rich metal to a melt temperature of 595°C |
| Beryllium – Tantalum | 1287°C as there was no binary phase diagram found |
| Beryllium – Titanium | 1287°C of pure Beryllium |
| Beryllium – Vanadium | 1287°C of pure Beryllium |
| Copper – Gallium | 625°C for phases containing greater than 55 atom percent gallium |
| Copper – Plutonium | 626°C for 6 atom% Cu, 1.7 wt% Cu |
| Copper – Tantalum | 1085°C of pure Cu |
| Copper – Titanium | 880°C for 27 atom% Ti, 22 wt% Ti |
| Copper – Vanadium | 1085°C for pure Cu |
| Titanium – Vanadium | >1600°C for 30 wt% V |
| Gallium – Aluminum | Compositions above 2 atom% (5 wt%) gallium are liquid at 625°C |
| Gallium – Copper | Compositions above 55 atom% gallium (57 wt%) are liquid at 625°C |
| Gallium – Plutonium | Compositions above 75 atom% gallium (47 wt%) are liquid at 625°C |
| Gallium – Titanium | Compositions above 99 atom% gallium (99 wt%) are liquid at 625°C |
| Gallium – Vanadium | Compositions above 97 atom% gallium (98 wt%) are liquid at 625°C |
| Plutonium – Tantalum | 640°C of pure Pu |
| Plutonium – Titanium | 640°C of pure Pu |
| Plutonium – Vanadium | 625°C for < 2 wt% V |
| Tantalum – Titanium | 1668°C for pure Ti |
| Tantalum – Vanadium | 1910°C for pure V |
| Titanium – Vanadium | 1668°C for pure Ti |

LA-UR-08-07663

Interfacial Reaction Zones

Reactions between metals of the Ti-6Al-4V alloy with the contents it will hold are restricted to contact zones between different metal compositions. Because none of the major individual starting materials reach their melting points during a 582°C temperature excursion, formation of new phases must depend upon solid state transport of material from one of the original phases into another. The original starting materials are not pure materials. Gallium is never in the system as a metal but is dissolved in plutonium and the gallium-plutonium alloy has a melting point well above 582°C. Redistribution of the gallium into a pure metal will not be an issue. Gallium can only influence the performance of the materials in this system if it diffuses to another metal or alloy. Material transport will only occur between phases that are in mechanical contact. Transport will be substantially impeded by the presence of thin surface oxide layers, which will be present on the titanium alloy, the copper, the beryllium and the plutonium. Formation of any new phases in the container, eutectic or otherwise, is explicitly dependent upon sufficient solid state mass transport, which depends on solid state solubility of the components, intimacy of contact between the components, and the time the system is held at the elevated temperature. The kinetic data that would be required to quantitatively address solid state diffusion between the plutonium, the beryllium, the copper, and the titanium ampoule is not available. Qualitative conclusions are drawn based on the available phase diagrams, which capture the thermodynamically stable compositions of binary systems, at a given temperature.

When an alloy is in contact with another metal composition, solid state transport will be different for the different components of the alloy, resulting in preferential reaction with one component, and changing the resultant concentrations of both phases by enriching one and depleting the other with respect to the most mobile component. Contact reaction zones are discussed by reference to binary phase diagrams. At the low temperature of 582°C diffusion will be slow and the integrity of the ampoule alloy will only be compromised if a liquid was to form. As long as all component combinations do not form a liquid, the ampoule will remain intact and contain the material shipped.

Aluminum

Aluminum contact with components of the Ti-6Al-4V packaging system

Aluminum is initially present at only 10 atom percent in the titanium alloy. Although aluminum binaries with the elements of this system are considered, it is improbable that interactions with aluminum alone and the other components would ever occur. The aluminum is alloyed with titanium and vanadium and all three form high temperature alloys with all of the components expected in a shipment of plutonium metal.

Aluminum contact with beryllium

The aluminum-beryllium system forms a eutectic at 644°C, 16°C below the melt temperature of pure aluminum. There are no intermediate phases thus liquid aluminum

LA-UR-08-07663

will exist above this temperature. This temperature is higher than the maximum temperature considered for safe operation of this system..[Landolt-Bornstein 1992]

Aluminum contact with copper

The aluminum-copper system is complex with a eutectic melt temperature of 548°C at 66.8 weight percent aluminum.[Landolt-Bornstein 1992] The 548°C solidus extends from about 5.6 weight percent aluminum to about 45 weight percent aluminum. The solidus temperatures between pure copper and 45 weight percent aluminum are much higher temperatures and with five intermediate phases in the system. Aluminum is an alloying element in copper is solid at 600C up to about 25 weight percent aluminum. This is not an issue because the aluminum is a minor alloy constituent and as titanium content increases the melt temperature of the copper-titanium-aluminum will likely increase. For alloy compositions with aluminum content greater than 45 weight percent aluminum, the melt temperature is much greater than 600°C and more than 5 weight percent aluminum would have to diffuse into the copper for the melt temperature to be lower than 600°C. Significant aluminum would have to diffuse out of the ampoule alloy into the copper or aluminum into the copper. Both are impractical at the maximum temperature that these materials could be exposed to.

Aluminum contact with gallium

Gallium metal melts at 29°C and the aluminum-gallium binary is a eutectic binary system. There are no intermediate phases in this system. This binary system is a simple eutectic system with eutectic temperature at 26.6°.[Landolt-Bornstein 1992] The liquidus is well known but the boundaries of the solid phases are not well known. The solubility of aluminum in gallium metal is very low. The maximum solubility of gallium in aluminum metal is approximately 9 atom percent and the aluminum is solid at 600C up to about 7 atom percent gallium. The formation of a separate gallium-aluminum phase is not credible because both gallium and aluminum are soluble in plutonium at the compositions present and at temperatures below the melting point of plutonium. It is impractical for an alloy composition to form that would be liquid because it would simultaneously require local concentration of the aluminum to 98 atom percent. This phase is highly unlikely.

Aluminum contact with plutonium

Aluminum forms five intermediate phases with plutonium with PuAl_2 being the dominant intermediate phase melting at $1540 \pm 50^\circ\text{C}$. The compound Pu_3Al of the plutonium rich compositions is formed by a very sluggish peritectoid reaction between the plutonium delta phase and PuAl . [Wick 1980] Aluminum goes into solid solution with plutonium up to 10 atom percent aluminum. As the content of aluminum increases the melt temperature increases up to the PuAl_2 solidus at 801°C . [Wick 1980] In this binary system the combination of the two elements increases the melt temperature.

Aluminum contact with tantalum

Aluminum and tantalum form four intermediate phases. With the addition of a small amount of tantalum to the aluminum the melt temperature of aluminum metal is raised about eight degrees and the solidus exists to 25 atom percent aluminum. At 25 atom percent aluminum Al_3Ta is the solid and it melts at about 1629°C . On the tantalum rich

LA-UR-08-07663

side of Al_3Ta the solidus temperature is a bit lower but remains close to 1629°C until the intermittent phase Al_3Ta_2 is reached where the solidus temperature is a few degrees lower. Thereafter, as the concentration of tantalum increased the solidus temperature increases.[Landolt-Bornstein 1992] Again the melting temperatures of the intermediate phases are much above the maximum temperature this system will be exposed to thus the combination of these two elements will not negatively affect the safe operation of this system but will more likely decrease the likelihood of liquid formation.

Aluminum contact with titanium

At aluminum concentrations between pure and 25 atom percent aluminum the solidus is 665°C . That is, with the addition of a small amount of titanium to the aluminum the melt temperature of aluminum metal is raised about five degrees and remains the solidus to 25 atom percent aluminum. The Al_3Ti melts at about 1387°C . [Landolt-Bornstein 1992] Again the melt temperatures of the intermediate phases are much above the maximum temperature this system will be exposed to thus the combination of these two elements will not affect the safe operation of this system.

Aluminum contact with Vanadium

Aluminum and Vanadium form five intermediate phases. With the addition of a small amount of tantalum to the aluminum the melt temperature of aluminum metal is raised about two degrees and remains the solidus to about 8 atom percent aluminum. As each intermediate phase is reached the solidus temperature is increased as the concentration of Vanadium increases.[Landolt-Bornstein 1992] Again the melting temperatures of the intermediate phases are much above the maximum temperature this system will be exposed to thus the combination of these two elements will not affect the safe operation of this system.

Beryllium

Beryllium and plutonium may contact the Ti-6Al-4V container if they are not wrapped with tantalum foil and either metal penetrates the copper foam. Tantalum may also be wrapped around the beryllium and/or plutonium pieces and in this case these materials would have to penetrate the tantalum wrapping material and then the copper foam before reaching the ampoule alloy.

Beryllium contact with copper

Beryllium and copper alloys are commonly used alloying elements. An alloy of beryllium and copper with 24 atom percent copper melts at 966°C . [Landolt-Bornstein 1992] This is the lowest melting alloy in this binary system with all other compositions and phases melting at higher temperatures. The combination of beryllium and copper will not compromise the safe use of this system.

LA-UR-08-07663

Beryllium contact with gallium

Beryllium and gallium do not form intermediate phases, consequently, at temperatures above gallium's melting point of 30°C and below 600°C there is minimal mixing of the two materials.[Landolt-Bornstein 1992] If the two materials were to interact, then above 30°C the gallium will be liquid at the grain boundaries causing a decrease in mechanical strength of the beryllium. Interaction of these two components of the system is an improbable scenario because the gallium in the plutonium is in solid solution and only at quantities less than 10 atom percent.

Beryllium contact with plutonium

The main feature of the beryllium-plutonium system is one intermediate compound PuBe_{13} which has a higher melt temperature than either pure constituent at $1950 \pm 50^\circ\text{C}$. The eutectic at 96 atom percent plutonium probably lowers the melt temperature only 10°C. [Wick 1980] However, one experimenter reported the eutectic melt temperature lowered by as much as 45°C. Although, Wick et al. report that a melt temperature drop of 10°C is most accurate the worse case would be the 45°C decrease from 640°C of plutonium metal or a melt temperature of 595°C. At 582°C the components are still solid but close to a potential melt temperature.[Wick 1980] This is the lowest melting material or alloy of the systems considered. It is a combination of material that could be present in an accident.

Beryllium contact with tantalum

The phase equilibria are not known.[Landolt-Bornstein 1992] In a sample containing 0.05 atom percent tantalum after solidification from the melt the solidified microstructure indicated a eutectic phase and several intermediate phases with one having a melting temperature of Be_{12}Ta at 1850°C and for $\text{Be}_{17}\text{Ta}_2$ a melting temperature of 1980°C.

Beryllium contact with titanium

There are four or more intermediate compounds in this system with an eutectic at 70 atom percent titanium and at a temperature of 980°C. [Murray 1987 & Ohnuma 2004] Should the beryllium penetrate the copper, the beryllium could be mechanically mixed with the titanium at the surfaces of the pieces. Even mixed the eutectic temperature is not reached and the containment not affected.

Beryllium contact with vanadium

There are three or more intermediate compounds in this system. The solidus temperature is raised more than 230°C when the vanadium content exceeds about 7 atom percent.[Landolt-Bornstein 1992] Vanadium is only 4 atom percent in the ampoule alloy but its contribution to any alloy of these systems would be to increase the melt temperature. Should the beryllium penetrate the copper beryllium could be mechanically mixed with the titanium at the surfaces of the pieces. Even mixed the eutectic temperature is not reached and the containment not affected.

LA-UR-08-07663

Copper

It is not expected that a liquid phase will form at this interface at the highest temperature of any hypothetical accident (582°C). Because the copper surrounds the metal as the structural matrix to hold the plutonium metal in favored positions within the ampoule, it is the first to interact with the plutonium, beryllium or tantalum that the plutonium metal is wrapped in. At 582°C, both copper and the titanium alloy ampoule are solid and 582°C is well below their respective melting points. Aluminum-copper compositions with more than 64 atom percent (43 weight percent) aluminum will melt at 625°C, which is also the melting point of the plutonium-vanadium eutectic, considered later in this report. Aluminum is present in the titanium alloy at a concentration of 10 atom percent. In order to form a melting composition with copper at 625°C, it needs to attain a concentration within the copper of 64 atom percent or greater. Solid state transport on the scale required for formation of a low melting phase (below 625°C) at this boundary in four days is not expected.

Copper contact with gallium

Gallium is in solid solution in copper up to about 19 to 20 atomic percent gallium with the alloying of these two metals lowering the melt temperature to about 900°C at 20 percent gallium.[Landolt-Bornstein 1992] Solid state transport of gallium from a 10 atom percent gallium-plutonium alloy into pure copper sufficient to form a 20 atom percent gallium-copper alloy is improbable. Incorporation of enough gallium into the copper at 582°C to form a liquid phase requires passage through five successive solid state phases. Formation of each of these phases requires a microstructure rearrangement before more gallium atoms can be incorporated, thus reduction of melting temperatures due to the combination of these two metals is very unlikely.

Copper contact with Plutonium

The plutonium rich component of the binary phase has a eutectic at about 6 atom percent copper and a temperature of 625°C. [Wick 1980 & Copper 2000] It is not expected that a liquid phase will form at this interface at a temperature of 582°C. First consider possible reaction of copper with alpha plutonium. Due to the softening of plutonium metal near its melting point, 640°C, and the roughly 5% expansion of alpha plutonium upon conversion to epsilon plutonium it is possible that alpha plutonium samples will tightly contact the copper foam, and reaction will occur at the interface. The progression of the reaction will be limited by the temperature actually reached, and by the time held at that temperature. The plutonium-copper eutectic composition will not melt at 582°C.

Copper contact with Tantalum

The mutual solubility of copper and tantalum is negligibly small and intermediate phases do not exist.[Landolt-Bornstein 1992] Copper and tantalum are immiscible at temperatures lower than 1083°C. Even the solubility of tantalum in liquid copper above the melting point is small. The solubility of Ta in liquid copper amounts to 0.0088 atom percent tantalum at 1200°C. Combining these two materials in this storage system will not lower the melting temperatures of the materials and are of no consequence to the safety of the system but may enhance the safety margin.

LA-UR-08-07663

Copper contact with titanium

The copper-titanium system is also a complex binary system with five intermediate phases and a eutectic at 860°C and 27 atom percent titanium.[Landolt-Bornstein 1992] Combining these two materials in this storage system will not lower the melting temperatures of the materials and are of no consequence to the safety of the system but may enhance the safety margin.

Copper contact with vanadium

The copper vanadium system is a simple eutectic system. The eutectic is on the vanadium rich side at about 15 atom percent copper and a eutectic temperature of 1530°C.[Landolt-Bornstein 1992] Combining these two materials in this storage system will not lower the melting temperatures of the materials and are of no consequence to the safety of the system but may enhance the safety margin.

Gallium

Gallium has an extremely low melting temperature when compared to the other metals in the ampoule material and the material to be shipped. The gallium is soluble in the plutonium and is a component of the plutonium up to 10 atom percent. The only thermodynamic driver of this conversion is the leaching ability of other metals from the plutonium-gallium alloy. Gallium is soluble in the plutonium epsilon phase and will not segregate to the interface and is consequently not easily leachable from the plutonium should one of the other elements have a higher affinity to alloy gallium than plutonium.

Gallium contact with Plutonium

The gallium is soluble in the plutonium up to about 10 atom percent gallium in the plutonium. The delta phase of plutonium is stabilized at room temperature by the addition of less than 10 atom% gallium. [Wick 1980] Because delta plutonium contracts upon conversion to epsilon, it will not experience increased pressure at the interface upon heating. Up to 20 atom percent gallium is soluble in the plutonium epsilon phase, so there will be no segregation of gallium upon transition to epsilon plutonium. A liquid phase will not form in the plutonium rich material until the melt temperature of plutonium is reached. There is also no driver for the gallium to segregate since it is already in solid solution

Gallium in contact with tantalum

There are four intermediate phases in this binary system and with increasing tantalum the solidus increases with each intermediate phase. The liquidus remains at 29°C until the intermediate Ga_3Ta is reached.[Landolt-Bornstein 1992] The phase relations in this system are not sufficient to give additional detail. Given sufficient gallium in the system this combination could compromise the safety of the system but there is simply insufficient gallium in the entire mass of plutonium metal to compromise the container.

Gallium in contact with titanium

LA-UR-08-07663

The gallium-titanium system requires more than 99 atom percent gallium in order to form a phase that melts at 625°C.[Landolt-Bornstein 1992] Because the gallium is soluble and stable at lower concentrations, formation of a phase with such high gallium content, nearly pure gallium is not expected to occur. Formation of a molten phase of either gallium-titanium or gallium-vanadium is unlikely given the available quantity of gallium and the thermodynamic stability of lower concentration solid phases.

Gallium in contact with Vanadium

There are four intermediate phases in this binary system and with increasing vanadium the solidus increases with each intermediate phase. The solidus remains at 29°C until the intermediate Ga_4V_8 is reached where the solidus on the vanadium rich side of this intermediate compound is 500°C. The gallium-vanadium compositions require more than 84 atom percent of gallium in order to form a phase that melts at 625°C.[Landolt-Bornstein 1992] Given sufficient gallium in the system this combination could compromise the safety of the system but there is simply insufficient gallium in the entire mass of plutonium metal to compromise the container.

Plutonium

It is not expected that a liquid phase will form at this interface. In the event that plutonium is sheared from the bulk and contacts the Ti-6Al-4V liner, consideration must be given to the interfacial reaction zone. The possible binary compositions of interest for contact between the liner and alpha plutonium include plutonium-aluminum, plutonium-titanium, and plutonium-vanadium. In the case of both plutonium-aluminum and plutonium-titanium, the melting point is increased relative to that of pure plutonium for all concentrations.

Plutonium contact with tantalum

This combination of materials is very stable and will not negatively impact the safe operation of the system. Tantalum and plutonium form a eutectic very close to pure plutonium. The eutectic reduces the melt temperature by only a degree or two. At temperatures above the 640°C solid tantalum can contain increasing plutonium up to about 25% plutonium near 2550°C.[Boxi 1991] There is also significant solubility of plutonium in the tantalum metal at temperatures above the plutonium melt temperature but limited solubility of plutonium in tantalum at temperatures below 640°C. [Wick 1980] Consequently, pure plutonium stored in pure tantalum foil is compatible at temperatures below plutonium's melting temperature. Above plutonium's melt temperature there is little reaction except that as the temperature rises an increasing amount of plutonium will diffuse into the tantalum metal matrix.

Plutonium contact with titanium

There are no intermediate phases in the binary system. A peritectoid composition at 6.5 atom percent titanium increases the solubility of titanium in the plutonium metal to a maximum of 25 atom percent at 770°C. Above the melting temperature of plutonium the liquid plutonium will combine with the tantalum to form a solid mixture up to 770°C, the highest solidus temperature in the system.[Landolt-Bornstein 1992] This reaction would stabilize the system in a high temperature transient situation.

LA-UR-08-07663

Plutonium contact with vanadium

The plutonium-vanadium eutectic composition forms with less than 2 weight percent vanadium resulting in a solidus temperature of 625°C from 2 to 100 weight percent vanadium. At all concentrations of more than 2 wt% vanadium in plutonium, and at a temperature of 625°C or higher, the plutonium-vanadium system exhibits a liquid phase.[Landolt-Bornstein 1992] At all compositions, at temperatures less than 625°C, only solid phases are present. If mobility into the solid plutonium metal leaves the ampoule alloy depleted in one of its other constituents, the melting point of the liner in the depleted zone will be increased.

Tantalum, Titanium, and Vanadium

Vanadium and aluminum are the minor constituents of the alloy of the ampoule at 10 atom percent or less. Consequently, titanium will probably dominate the interactions of the container with the packaged material. When tantalum is used to wrap the plutonium metal it too will be a major contributor to the performance of the shipping container during the transient. Interaction between or alloying of these four components aluminum, tantalum, titanium and vanadium produce material that will probably not form lower melt temperature

Tantalum contact with titanium

The Ti-Ta binary phase diagram is characterized by an isomorphous body centered cubic phase field extending from pure titanium at elevated temperatures to pure tantalum with limited mutual solubilities.[Landolt-Bornstein 1992] Since there are no intermediate phases and the solidus is essentially linear between the melt temperature of titanium (1670°C) and tantalum (3017°C), a combination of these metals with other compound will probably increase the melt temperature of the system.

Tantalum contact with Vanadium

There are no intermediate phases and the solidus and liquidus increase from the 1910°C melt temperature to the 3017°C melt temperature of tantalum. Addition of any of these two metals will likely increase the melt temperature of the resulting mixture.

Titanium contact with Vanadium

There are three intermediate phases and the solidus and liquidus increase from the 1668°C titanium melt temperature to the 1910°C melt temperature of vanadium.[Landolt-Bornstein 1992] Addition of any of these two metals will likely increase the melt temperature of the resulting mixture of container and package materials.

Binary interaction summary

The lowest melt temperature is 595°C between the plutonium and beryllium with the next lowest between the plutonium-vanadium eutectic at 625°C. The 595°C temperature may be a low estimate because of impurities in the material tested with the melt temperature of the beryllium-plutonium probably closer to 630°C. However, for safety evaluations this is the worst case temperature.

LA-UR-08-07663

The lowest melting phase with plutonium/vanadium liner contact is 625°C, and is unlikely to form based on the absence of a clean contact surface under pressure between the plutonium and the liner. The melting temperature of this eutectic is 43°C higher than that of the proposed high temperature excursion.

Addition of the beryllium to the system brings the melt temperature close to the maximum temperature that the ampoule may be exposed to. If all the components internal to the titanium ampoule are combined and intimately mixed, that is, plutonium, beryllium, gallium, tantalum, and copper are completely alloyed, the melt temperature could be lower than 582°C. There is no data to show otherwise and 595°C is close to this temperature. However, it is unlikely and impractical to intimately mix these components together by mechanical impact and then expose them to temperatures above the binary melting points. Significant work on this complex metal alloy system would be required if a mechanism could be hypothesized to form such an alloy by impact of separate alloys and metals but it is not considered plausible.

Investigation of Ternary Systems

Published information was available for eleven of the possible ternary systems considered. [Petzow 1992 & Villars 1995] The Ti-6Al-4V alloy was designed to be solid to 1604°C. The tantalum-titanium-aluminum system is solid above 1100°C. [Weaver 1995] It is generally true that for the ternary phase diagrams reviewed, there was little new information with respect to melting temperatures that was not captured by the binary diagrams. Expected compositions are those that do not require achieving large concentrations of a particular element in a phase against a strong concentration gradient. For example, given that aluminum begins at 10 atom percent in the titanium alloy used, it is considered unlikely that it would achieve concentrations of 20 atom percent or more in another phase. The same rule is applied with respect to the vanadium and gallium components, both of which begin at low concentrations in their respective thermodynamically stable alloys.

Reviewed binary and ternary systems that possess a liquid component at temperatures below 625°C are those with high concentrations of aluminum and gallium (greater than 50 atom percent combined aluminum and gallium content). It is considered improbable that with less than 9 atom percent gallium in the plutonium and 10 atom percent aluminum in the titanium alloy, any phases will form containing more than 50 atom percent combined gallium and aluminum.

In both titanium and plutonium, aluminum and gallium may substitute for each other, partially or completely, without altering the observed phase. Several of the ternary systems reviewed show no ternary phases, only mixtures of binary phases, all of which have already been captured by the preceding review of binary phase diagrams. The only ternary diagram available that contained plutonium was the aluminum-gallium-plutonium diagram.

LA-UR-08-07663

Conclusions drawn by reference to the binary phase diagrams are consistent with the information present in the ten available ternary phase diagrams.

Additional Chemical Reaction

Finely divided metals tend to oxidize rapidly in air due to the high surface area relative to mass of metal present. The oxidation reaction for a metal is generally exothermic, and in the event of finely divided powders in air, can often result in pyrophoricity. During the proposed accident scenario for this analysis, the system containment is not mechanically breached, and an inert environment is maintained. The small amount of oxygen in the system will exist as oxide on the various system components, rather than as gaseous oxygen. In the event that small particles are generated within the titanium alloy ampoule, they will not ignite due to an absence of oxygen necessary for the reaction. The initial system components are bulk metal materials. These are not pyrophoric.

Conclusions

All of the expected phases formed from the original materials at a temperature of 582°C are solid. The lowest probable binary phase melting point is 595°C (plutonium-Beryllium). The second lowest probable binary phase melting point is 625°C (plutonium-vanadium) and the third lowest melting point is 626°C (plutonium-copper). The lowest is possible if other impurities not considered in this technical basis were present. It is anticipated that the second and third lowest compositions will not form due to the presence of surface oxide layers on the initial components of the system. A review of available ternary phase diagrams supports the conclusions drawn from the binary phase diagrams. However, the many combinations of the product materials and the container materials make it impossible to absolutely rule out a lowering of the melting point due to mechanical mixing that could occur in a severe impact and post impact fire until some testing verification on the materials are conducted.

References

- Boxi, H.C., Massalski, T.B., and Rizzo, H.F., 1991, *The Pu-Ta (Plutonium-Tantalum) System*, Journal of Phase Equilibria, 12 No. 5 pp 593
- Brandes, E. A., ed. 1983. *Smithells Metals Reference Book*, Sixth Edition. Ch. 11.
- Kaufmann, A.R., Gordon, P., Lillie, D.W. 1950, *ASM Trans. Q.* **42** p 801.
- Cooper, N. G., ed. 2000. *Challenges in Plutonium Science, Volume II. Plutonium and Its Alloys*. pp. 291-335.
- Landolt-Bornstein – Group IV Physical Chemistry Volumes 5b and 5j (1992)
- Lide, D. R., ed. 1991. *CRC Handbook of Chemistry and Physics*, pp. 4-122, 4-123.

LA-UR-08-07663

Murray, J.L., 1987, The Be-Ti (Beryllium-Titanium) System, *Phase Diagrams of Binary Titanium Alloys*, J.L. Murray, Ed., ASM International, p 40-43

Ohnuma, I.; Kainuma, R.; Uda, M.; Iwadachi, T.; Uchida, M., Kawamura, H., and Ishida, K., 2003 "Phase Equilibria in the Be-V and Be-Ti Binary Systems," *Proc. Sixth International Workshop on Beryllium Technology for Fusion, 2003*, Japan. Atom. Energy Res. Inst.,

Petzow, G., Effenberg, G., ed., 1992, *Ternary Alloys*. VCH Publishers, NY, NY: ASM International.

Villars, P.; Prince, A.; Okamoto, H., 1995. *Handbook of Ternary Alloy Phase Diagrams*. Materials Park, OH: ASM International.

Weaver, M.L. and Kaufman, M.J., 1995 "Phase Relationships and Transformations in the Ternary Aluminum-Titanium-Tantalum system," *Acta metall, mater.* Vol. 43, No. 7, pp. 2625-2640.

Wick, O. J., ed. 1980. *Plutonium Handbook*. Chaps. 7 and 12-3. La Grange Park, IL: American Nuclear Society

4. CONTAINMENT

The Plutonium Air Transportable Package, Model PAT-1, is certified under Title 10 Code of Federal Regulations, Part 71,¹ by the U.S. Nuclear Regulatory Commission (NRC) per Certificate of Compliance (CoC) USA/0361/B(U)F-96 (current Revision 9).² The current authorized contents are plutonium oxide (PuO_2) and its daughter products, or a mixture of PuO_2 and uranium oxide (UO_2) and its daughter products. The (-96) in the certificate of compliance number indicates that the NRC has evaluated the PAT-1 against the current regulations (including 10 CFR 71.63) and determined that the package satisfies the current regulations.

The purpose of this addendum is to incorporate plutonium metal as a new payload for the PAT-1 package and to demonstrate that the package with the new *T-Ampoule Assembly*^A (Drawing 2A0261, designated the T-Ampoule) and packing within the TB-1 *Containment Vessel* (Drawing 1017, designated TB-1) meet the current containment requirements in 10 CFR 71.³ The 71.63 requirement is satisfied for the PAT-1 with the T-Ampoule and its packing material configuration because the plutonium metal payload contents are solid, pure or alloyed plutonium metal contents or Pu/Be composite samples.

The CoC² describes the TB-1 as a stainless steel containment vessel surrounded by a stainless steel and redwood overpack (*Overpack, AQ*, Drawing 1002, designated AQ-1). The plutonium oxide contents are sealed within a stainless steel product can (designated PC-1). The CoC does not identify the PC-1 as a “containment vessel,” but as a “sealed ... product can.” For the plutonium metal content packaging configuration described in this addendum, the PC-1, aluminum honeycomb top spacer and packing material is replaced with a T-Ampoule, *Ring, Filler* (Drawing 2A0262, designated Ring Filler) and packing material which provides a eutectic prevention barrier between the TB-1 and the plutonium metal content. The T-Ampoule provides the following:

- A eutectic prevention barrier between the stainless steel TB-1 and the plutonium metal payload for NCT, HAC, and air transport accident conditions.
- A T-Ampoule seal area that is not significantly deformed (see Sections 2 and 3 of this addendum) nor a seal temperature that exceeds the allowable temperature of the gasket material during NCT or HAC. The T-Ampoule is expected to remain sealed during NCT and HAC, like the PC-1.
- A retained eutectic prevention barrier function following the air transport accident condition drops and fire. Although the O-ring in the T-Ampoule would be expected to fail in the 10 CFR 71.74 air transport of plutonium fire test, the T-Ampoule is shown in Sections 2 and 3 of this addendum to remain intact (no significant deformation in the seal area and no breaches). The T-Ampoule is more robust than the PC-1.

The documentation and analysis in this section and other sections of this addendum demonstrate that the replacing the PC-1 with oxide content and associated packing material with

^A The drawing titles are in italics and are used interchangeably with the designated names in this addendum. See Section 1.3.2 in this addendum and Chapter 9 in the SAR⁴ for drawing number, title, and revision.

the T-Ampoule with plutonium metal content and associated packing material satisfies the requirements specified in 10 CFR 71.19(d). That is, the modifications of the PAT-1 described in this addendum are not significant with respect to the design, operating characteristics, safe performance of the containment system, or prevention of criticality when the package is subjected to the tests specified in 10 CFR 71.71, 71.73, and 71.74.

4.1 Description of the Containment System

The CoC USA/0361/B(U)F-96² defines the TB-1 as the containment vessel for the PAT-1 for the current PuO₂ and its daughter products and UO₂ and its daughter products as authorized contents. The description of the TB-1 containment vessel is provided in Sections 1 and 9 of the SAR.⁴ For this plutonium metals addendum, the TB-1 containment vessel (see Figure 4-1) provides the containment boundary for the proposed metal contents as it did for the oxide contents. The T-Ampoule replaces the PC-1.

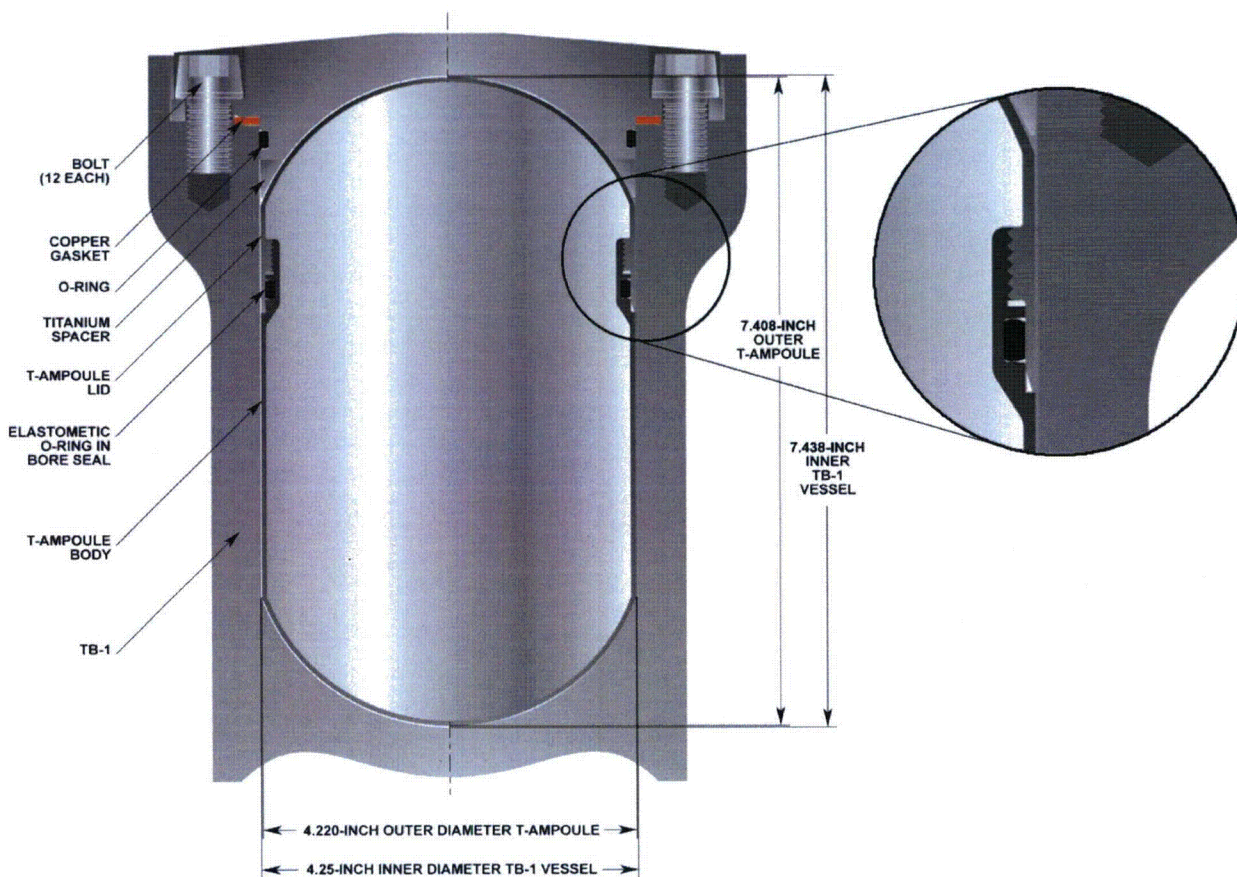


Figure 4-1. TB-1 Containment Vessel and T-Ampoule Contents Container

Table 4-1 of the SAR⁴ summarizes the results of the post-test assessment of PAT-1 containment of its surrogate PuO₂ powder contents during the three transport tests (10 CFR 71.71, 10 CFR 71.73, and 10 CFR 71.74) and demonstrates that the containment criteria are met.

Table 4-1. PAT-1 Package Post-Test Containment

| Component | Test Condition | Regulatory Acceptance Standard | Post Test Results | |
|-----------|---------------------------------|-----------------------------------|--------------------------------|--|
| | | | Helium Leak-Rate (atm-cc/sec) | Maximum Mass of Powder Release ^b (mg) |
| TB-1 | NCT (71.71) | 10^{-6} A ₂ /hr | Less than 1×10^{-10} | 0 |
| | HAC (71.73) | A ₂ /week | Less than 1×10^{-10} | 0 |
| | Plutonium Air Transport (71.74) | A ₂ /week ^a | Less than 4.5×10^{-5} | 0.17 |

^a For a typical mixture of plutonium oxide (PuO₂) powder, an A₂ quantity is approximately 2.55 mg.

^b Depleted uranium oxide powder was used as the surrogate for plutonium oxide powder during PAT-1 testing. From the SAR, the bounding magnitude of potential PuO₂ powder leakage from the TB-1 vessel would be less than 0.17 mg in one week.

4.1.1 Special Requirements for Plutonium

The proposed plutonium metal contents meet the current requirements set forth in 10 CFR 71.³ In 10 CFR 71.63, "Shipments containing plutonium must be made with contents in solid form, if the contents contain greater than 0.74 TBq (20 Ci) of plutonium." This requirement is satisfied for the PAT-1 with the T-Ampoule and its packing because the proposed plutonium metal payload contents are solid, pure or alloyed plutonium metal or Pu/Be composite samples.

The PAT-1 Certificate of Compliance² (CoC) (USA/0361/B(U)F-96) (current Revision 9) in Item 5. (a) Packaging, (2) includes the description of the PAT-1,

"A stainless steel containment vessel (designated TB-1) surrounded by a stainless steel and redwood overpack (designated AQ-1). The contents are sealed within a stainless steel product can (designated PC-1) inside the containment vessel."

The "-96" in the certificate of compliance number indicates that the NRC has evaluated the PAT-1 against the current regulations (including 10 CFR 71.63) and determined that the package satisfies the current regulations. The CoC² identifies the TB-1 as the containment vessel.

For this addendum, the PAT-1 is unchanged from the inside surface of the TB-1 containment vessel to the outside surface of the AQ-1 overpack. The only change to the PAT-1 package is replacement of the PC-1 and its contents, top spacer and packing material with the T-Ampoule and its contents, Ring Filler and packing material. The T-Ampoule, a titanium container, provides eutectic prevention for the metal payload.

The proposed contents include plutonium metal in the form of hollow cylinders, disks, plates, solid cylinders and test samples. The plutonium metal contents are typically loaded into the T-Ampoule in a glove box* containing a limited quantity of oxygen (0.5%). Prior to loading, the contents are brushed clean to remove any oxide present on the surface. The quantity of oxide

* Standard glove box line atmosphere: Nitrogen/Argon/Helium (N/Ar/He) with an oxygen (O) content not exceeding 0.5% and a water content not exceeding 20 ppm.

that could form in the T-Ampoule during transport is limited by the 0.5% concentration of oxygen in the glove box atmosphere. The estimate of oxide formation due to this atmosphere is provided in Section 4.5.2 and is approximately 0.08 g (0.00018 lb). If the atmosphere is assumed to be air and because this is an oxygen-limited system, the estimated quantity of oxide formed on the metal contents is 3.46 g, the activity of PuO₂ formed is 3.74 Ci if no decay is assumed (100% Pu-241), and 0.397 Ci if 100% decay is assumed (100% Am-241). If the metal contents are not cleaned sufficiently, conservative estimates that double the quantity of oxide could be present on the metal, 6.92 g, which is less than 8 Ci.

The function of the T-Ampoule is to provide a safety barrier that prevents the formation of a eutectic between the plutonium metal contents and the iron in the TB-1 containment vessel. The structural analyses in Section 2 of this addendum demonstrate that the bore seal area (see Figure 4-1) of the T-Ampoule is not significantly deformed and is expected to remain intact for all accident conditions analyzed. It can be concluded from these analyses that the T-Ampoule is more robust than the PC-1.

The PC-1 Product Can used for the oxide shipment must not be used for the metal shipment since the iron in the can could possibly form a eutectic with the plutonium metal contents. The titanium material for the T-Ampoule was selected to provide a eutectic prevention barrier between the metallic Pu contents and the TB-1 containment vessel. The *Body, T-Ampoule* (Drawing 2A0259, designated T-Ampoule Body) and *Lid, T-Ampoule* (Drawing 2A0260, designated T-Ampoule Lid) are fabricated from a solid block of Ti-6Al-4V Grade 5 alloy. There are no welds, penetrations, valves, or pressure relief devices in the T-Ampoule. Once placed within the TB-1, the T-Ampoule cannot be opened unintentionally. The clearance between the T-Ampoule and the TB-1 is 0.038 cm (0.015 in.) all around; thus, both walls have immediate contact to resist the impact forces created by the deceleration of the internal Pu contents during the impact accident environment. The sample containers (*Sample Container-1 [SC-1] Assembly*, Drawing 2A0268, designated SC-1, and *Sample Container-2 [SC-2] Assembly*, Drawing 2A0265, designated SC-2) and structure (*Inner Cradle*, Drawing 2A0385, designated Inner Cradle) are also constructed of Ti-6Al-4V Grade 5 alloy that is resistant to the formation of eutectics with the plutonium metal content. Tantalum foil, which may be used to wrap and protect the samples from contamination, and the copper foam, which may be used as packing material, were selected for their resistance to eutectic formation.

The shielding evaluation in Section 5 of this addendum demonstrates that the package with plutonium metal contents complies with the dose rate limits of 10 CFR 71.47(a) (non-exclusive use) for the normal conditions of transport (NCT) and 10 CFR 71.51(a)(2) for hypothetical accident conditions (HAC). The criticality evaluation in Section 6 of this addendum demonstrates that the package with plutonium metal contents remains subcritical under NCT and HAC and has a CSI value of 0.1 per 10 CFR 71.59.

The modifications to the PAT-1 package are not significant with respect to design, operating characteristics, or safe operation of the PAT-1 package when subjected to the tests specified in 10 CFR 71.71 and 10 CFR 71.73:

- The PAT-1 package is unchanged from the inside surface of the TB-1 containment vessel to the outside surface of the AQ-1 overpack.

- The T-Ampoule and its contents, Ring Filler and packing material replace the PC-1 and its contents, top spacer and packing material and provide protection for its metal contents.
- The T-Ampoule is a eutectic prevention barrier between the plutonium metal contents and the stainless steel TB-1 containment vessel. The structural analysis in Section 2 of this addendum demonstrates that the T-Ampoule does not breach during the 10 CFR 71.71, 10 CFR 71.73, and 10 CFR 71.74 structural evaluations, thus maintaining its eutectic function.
- The structural analyses in Section 2 demonstrated that the TB-1 met containment requirements. The TB-1's containment capability will be unaffected by the addition of metals contents through the plutonium air transport tests.
- The packing materials within the T-Ampoule are also not susceptible to eutectic formation with plutonium metal.
- The structural analysis in Section 2, the thermal analysis in Section 3, the shielding analysis in Section 5, and the criticality analysis in Section 6 of this addendum show that the requirements of 10 CFR 71.19(d) are met because the modifications to PAT-1 package are not significant with respect to the design, operating characteristics, or safe performance of the package design when subjected to the tests specified in 10 CFR 71.71 and 10 CFR 71.73.

4.1.2 Plutonium Metal Contents

The proposed plutonium metal contents (see Section 4.5.2 for estimate of oxides formed within the T-Ampoule) include:

- Electro-Refined (ER) Pu (Purity $\geq 99.8\%$ Pu 239) with up to 0.08 g (0.00018 lb) of surface oxide (0.5% oxygen in a limited inert atmosphere).
- Pu of various ages containing stabilization alloys such as gallium (Ga) with up to 0.08 g (0.00018 lb) of surface oxide (0.5% oxygen in a limited inert atmosphere).
- Composite samples consisting of Pu with up to 0.08 g (0.00018 lb) of surface oxide (0.5% oxygen in a limited inert atmosphere) and beryllium (Be) separated by an alpha barrier (Ti) to preclude neutron generation.

The forms of the metal include hollow cylinders, cylinders, discs, strips, etc.

The container configurations within the TB-1 containment vessel are:

- T-Ampoule for bulk metal hollow cylinders and sample containers; and
- Sample containers (SC-1 and SC-2) carried within the Inner Cradle of the T-Ampoule for smaller metal samples.

The isotopic compositions, masses, A_2 values, decay heat, activities, and impurities for ER plutonium metal, alloyed plutonium metal, and bonded plutonium metal are presented below.

4.1.2.1 ER Plutonium Metal¹

The maximum ER content is 831 g (1.83 lb) for an isotopic composition that excludes Pu-241 decay (see Table 4-2). ER metal mass estimates for 3000 A_2 range from 831 g (1.83 lb)

assuming no Pu-241 decay (Table 4-2), and 707 g (1.56 lb) assuming 100% Pu-241 decay (see Table 4-3). Note that Table 4-3 is used for comparative purposes only to determine the effect of assuming 100% Pu-241 decay. The ER metal will be manufactured and shipped prior to significant Pu-241 decay. The minimum ER cylinder weight as documented in Table 1-1 of Section 1 is 731 g.

Table 4-2. 831 g (1.83 lb): 3,000 A₂ Quantity of ER Plutonium Metal Assuming No Pu-241 Decay

| 831 grams: 3,000 A ₂ quantity of ER Pu metal assuming no Pu241 decay | | | | | | | | | |
|---|---------------------|---------------------|-------------------------------|-----------------|---------------------|----------------------|----------------|---------------|----------------|
| Metal Mass (g) (max) | Mass % (max) | Grams (max) | LANL Specification 55Y-638728 | Isotope | Pu Isotopic % (max) | Pu Isotopic mass (g) | Decay Heat (W) | Activity (Ci) | A ² |
| 831.00 | Plutonium 99.84% | Plutonium 829.67 | | Pu238 | 0.05% | 0.41 | 2.35E-01 | 7.05E+00 | 2.61E+02 |
| | | | | Pu239* | 92.35% | 766.20 | 1.46E+00 | 4.75E+01 | 1.76E+03 |
| | | | | Pu240 | 6.50% | 53.93 | 3.83E-01 | 1.24E+01 | 4.59E+02 |
| | | | | Pu241 | 1.00% | 8.30 | 1.04E-01 | 8.30E+02 | 5.19E+02 |
| | | | | Pu242 | 0.10% | 0.83 | 8.30E-05 | 3.24E-03 | 1.20E-01 |
| | | | | Am241 | 0.00% | 0.00 | 0.00E+00 | 0.00E+00 | 0.00E+00 |
| Impurities | 0.16% | Impurities 1.33 | | Impurities: N/A | | | | | |
| * stated as % balance | | | | | | Total: | 2.18E+00 | 8.97E+02 | 3.00E+03 |

Table 4-3. 707 g (1.56 lb): 3,000 A₂ Quantity of ER Plutonium Metal Assuming 100% Pu-241 Decay

| 707 grams: 3,000 A ₂ quantity of ER Pu metal assuming 100% Pu241 decay | | | | | | | | | |
|---|---------------------|---------------------|-------------------------------|-----------------|---------------------|----------------------|----------------|---------------|----------------|
| Metal Mass (g) (max) | Mass % (max) | Grams (max) | LANL Specification 55Y-638728 | Isotope | Pu Isotopic % (max) | Pu Isotopic mass (g) | Decay Heat (W) | Activity (Ci) | A ² |
| 707.00 | Plutonium 99.84% | Plutonium 705.87 | | Pu238 | 0.05% | 0.35 | 2.00E-01 | 6.00E+00 | 2.22E+02 |
| | | | | Pu239* | 92.35% | 651.87 | 1.24E+00 | 4.04E+01 | 1.50E+03 |
| | | | | Pu240 | 6.50% | 45.86 | 3.26E-01 | 1.06E+01 | 3.91E+02 |
| | | | | Pu241 | 0.00% | 0.00 | 0.00E+00 | 0.00E+00 | 0.00E+00 |
| | | | | Pu242 | 0.10% | 0.71 | 7.06E-05 | 2.75E-03 | 1.02E-01 |
| | | | | Am241 | 1.00% | 7.06 | 8.10E-01 | 2.40E+01 | 8.89E+02 |
| Impurities | 0.16% | Impurities 1.13 | | Impurities: N/A | | | | | |
| * stated as % balance | | | | | | Total: | 2.57E+00 | 8.10E+01 | 3.00E+03 |
| Note: Table shown for comparative purposes only. ER metal will be manufactured and shipped prior to significant Pu241 decay | | | | | | | | | |

4.1.2.2 Alloyed Plutonium Metal^A

The maximum contents in two SC-2 sample containers within the T-Ampoule is 676 g (1.49 lb). A₂ calculations were performed assuming no Pu-241 decay (2410 A₂) (see Table 4-4) and Pu-241 decay (2840 A₂) (see Table 4-5). Alloyed plutonium metal may be shipped in a hollow log form in the T-Ampoule if the requirements in Table 1-1 of this addendum and the shipper are met.

Table 4-4. 676 g (1.49 lb): Alloyed Plutonium Metal Assuming 100% Pu-241 Decay

| 676 grams: Alloyed Pu metal assuming 100% Pu241 decay | | | | | | | | | |
|---|---------------------|---------------------|-------------------------------|---------|---------------------|----------------------|----------------|---------------|----------------|
| Metal Mass (g) (max) | Mass % (max) | Grams (max) | LANL Specification 55Y-638728 | Isotope | Pu Isotopic % (max) | Pu Isotopic mass (g) | Decay Heat (W) | Activity (Ci) | A ² |
| 676.00 | Plutonium 98.84% | Plutonium 668.16 | | Pu238 | 0.05% | 0.33 | 1.89E-01 | 5.68E+00 | 2.10E+02 |
| | | | | Pu239* | 92.35% | 617.04 | 1.17E+00 | 3.83E+01 | 1.42E+03 |
| | | | | Pu240 | 6.50% | 43.43 | 3.08E-01 | 9.99E+00 | 3.70E+02 |
| | | | | Pu241 | 0.00% | 0.00 | 0.00E+00 | 0.00E+00 | 0.00E+00 |
| | | | | Pu242 | 0.10% | 0.67 | 6.68E-05 | 2.61E-03 | 9.65E-02 |
| | | | | Am241 | 1.00% | 6.68 | 7.67E-01 | 2.27E+01 | 8.41E+02 |
| Impurities | Impurities | Impurities: N/A | | | | | | | |
| 0.16% | 1.08 | | | | | | | | |
| Gallium | Gallium | Gallium: N/A | | | | | | | |
| 1.00% | 6.76 | | | | | | | | |
| * stated as % balance | | | | | | Total: | 2.44E+00 | 7.66E+01 | 2.84E+03 |

Table 4-5. 676 g (1.49 lb): Alloyed Plutonium Metal Assuming No Pu-241 Decay

| 676 grams: Alloyed Pu metal assuming no Pu241 decay | | | | | | | | | |
|---|---------------------|---------------------|-------------------------------|---------|---------------------|----------------------|----------------|---------------|----------------|
| Metal Mass (g) (max) | Mass % (max) | Grams (max) | LANL Specification 55Y-638728 | Isotope | Pu Isotopic % (max) | Pu Isotopic mass (g) | Decay Heat (W) | Activity (Ci) | A ² |
| 676.00 | Plutonium 98.84% | Plutonium 668.16 | | Pu238 | 0.05% | 0.33 | 1.89E-01 | 5.68E+00 | 2.10E+02 |
| | | | | Pu239* | 92.35% | 617.04 | 1.17E+00 | 3.83E+01 | 1.42E+03 |
| | | | | Pu240 | 6.50% | 43.43 | 3.08E-01 | 9.99E+00 | 3.70E+02 |
| | | | | Pu241 | 1.00% | 6.68 | 8.35E-02 | 6.68E+02 | 4.18E+02 |
| | | | | Pu242 | 0.10% | 0.67 | 6.68E-05 | 2.61E-03 | 9.65E-02 |
| | | | | Am241 | 0.00% | 0.00 | 0.00E+00 | 0.00E+00 | 0.00E+00 |
| Impurities | Impurities | Impurities: N/A | | | | | | | |
| 0.16% | 1.08 | | | | | | | | |
| Gallium | Gallium | Gallium: N/A | | | | | | | |
| 1.00% | 6.76 | | | | | | | | |
| * stated as % balance | | | | | | Total: | 1.75E+00 | 7.22E+02 | 2.41E+03 |

4.1.2.3 Bonded Plutonium Metal⁴

A 60 g (0.13 lb) bonded 16.85 mm diameter x 16.85 mm height Pu/Be metal cylinder (or a number of smaller cylinders [up to 25 5.1 mm diameter x 5.1 mm height cylinders] as described in Table 1.1, Section 1 of this addendum) may each be shipped in the SC-1 sample container for a total payload weight of 180 g (0.39 lb) (657 A₂) or in the SC-2 sample container for a total payload weight of 120 g (0.26 lb) within the T-Ampoule. The composite payload weight is limited to 60 grams or less in each sample container. See Table 4-6 for estimate of curies, number of A₂, decay heat, weight, and isotopic composition of the Pu/Be material based upon a disk configuration.

Table 4-6. 60 g (0.13 lb): Bonded Pu/Be Metal Disk Assuming 100% Pu-241 Decay

| 60 grams: Bonded Pu/Be metal disc assuming 100% Pu241 decay | | | | | | | | | | |
|---|----------------------|-----------------------------|----------------------------|--|-----------------|---------------------|----------------------|----------------|---------------|----------------|
| Composite % | Metal Mass (g) (max) | Mass % (max) | Grams (max) | LANL Specification 55Y-638728 | Isotope | Pu Isotopic % (max) | Pu Isotopic mass (g) | Decay Heat (W) | Activity (Ci) | A ² |
| Pu metal 87.00% | 52.20 | MT52 Plutonium 98.84% | MT52 Plutonium 51.59 | | Pu238 | 0.05% | 0.03 | 1.46E-02 | 4.39E-01 | 1.62E+01 |
| | | | | | Pu239* | 92.35% | 47.65 | 9.05E-02 | 2.95E+00 | 1.09E+02 |
| | | | | | Pu240 | 6.50% | 3.35 | 2.38E-02 | 7.71E-01 | 2.86E+01 |
| | | | | | Pu241 | 0.00% | 0.00 | 0.00E+00 | 0.00E+00 | 0.00E+00 |
| | | | | | Pu242 | 0.10% | 0.05 | 5.16E-06 | 2.01E-04 | 7.45E-03 |
| | | | | | Am241 | 1.00% | 0.52 | 5.92E-02 | 1.75E+00 | 6.50E+01 |
| | | Impurities 0.16% | Impurities 0.08 | | Impurities: N/A | | | | | |
| | | Gallium 1.00% | Gallium 0.52 | | Gallium: N/A | | | | | |
| Beryllium 13.00% | 7.80 | Beryllium 13.00% | Beryllium 7.80 | | Beryllium: N/A | | | | | |
| Alpha Barrier 0.00% | 0.00 | Alpha Barrier 0.00% | Alpha Barrier 0.00 | Assumes no alpha barrier to yield maximum dose | | | | | | |
| 100.00% | 60.00 | ◀ ◀ ◀ Totals ▶ ▶ ▶ | | | | | 1.88E-01 | 5.92E+00 | 2.19E+02 | |
| *stated as % balance | | | | | | | | | | |

4.2 Containment under Normal Conditions of Transport (NCT)

The TB-1 containment vessel meets the regulatory acceptance standard for NCT of 10⁻⁶ A₂/hr as demonstrated in Table 4-1. The T-Ampoule is not a containment vessel under NCT.

The thermal analysis in Section 3.3 of this addendum, which analyzed a localized 25-watt (85.3 Btu/hr) thermal source against the O-ring seal of the T-Ampoule, indicated an average temperature of 103.3°C (218°F).

The internal pressure within the TB-1 during NCT with an internal heat generation of 25 watts (85.3 Btu/hr) from the plutonium metal contents indicated a maximum pressure of 18.8 psia, due to the temperature difference. The calculation assumes an initial room temperature of 20°C (70°F), then:

$$P_2 = 1\text{atm} * (678/530R) = 1.28 \text{ atm or } \sim 18.8 \text{ psia}$$

To determine the pressure generated from the alpha decay of plutonium, the TB-1 was assumed to be filled at ambient temperature and to reach the NCT temperature quickly (see Section 4.5.3). The helium pressure, shown below, is thus:

$$P_{\text{He}} = n_{\text{He}} * (RT/V)$$

where $n_{\text{He}} = gm_{\text{He}}/4$

T = the NCT average temperature in Kelvin (absolute)

V = 1.252 liters

R = 0.082 l-atm/mole-K, the gas constant

Pressure in psi = 14.7*Pressure in atmospheres

The pressure from helium (He) generation for 1300 g Pu (for conservatism) at NCT temperature via alpha decay is 15.1 psia.

The total pressure as the result of internal heat generation and alpha decay is 33.9 psia, or 19.2 psig, which defines the maximum normal operating pressure (MNOP) for the TB-1.

The MNOP of 19.2 psig (33.9 psia) calculated above is slightly less than that calculated for the PuO₂ contents in the SAR (34.3 psia) since a small quantity of moisture was assumed to be present in the PuO₂ within the TB-1.

4.3 Containment under Hypothetical Accident Conditions (HAC)

The TB-1 meets the regulatory acceptance standard for HAC of A₂ in a week as documented in Table 4-1. The T-Ampoule is not a containment vessel under HAC.

The thermal analysis in Section 3.4 of this addendum includes localized heating produced by the plutonium metal contents, and the HAC evaluation indicated that the average temperature is 136°C (276°F) in the T-Ampoule. The temperature of the T-Ampoule seal does not exceed the manufacturer's specification for the operating range of the seal material (204°C [400°F]).

The pressure calculated within the TB-1 as the result of internal heat generation of 25 watts from the plutonium metal contents and the HAC indicated that the maximum pressure is 20.4 psi. The calculation assumes an initial room temperature of 21°C (70°F), then:

$$P_2 = 1\text{atm} * (736\text{R}/530\text{R}) = 1.39\text{ atm or } \sim 20.4\text{ psia}$$

Pressure from He generation for 1300 g of Pu metal (for conservatism) via alpha decay is 16.4 psia from Section 4.5.3 of this addendum.

The total pressure as a result of internal heat generation and alpha decay is 36.8 psia. The pressure of 36.8 psia is less than the HAC pressure reported in the SAR⁴ (38.7 psia [Section 3.5.4 of the SAR⁴]).

4.3.1 Containment under Plutonium Air Transport Fire Test

The TB-1 meets the regulatory acceptance standard for the plutonium air transport tests of A₂ in a week as documented in Table 4-1. The T-Ampoule is not a containment vessel under the plutonium air transport conditions.

In LA-UR-08-07810, *Thermal Decomposition of Viton® O-rings for PAT-1 Accident Scenario*,⁶ the calculation (see Section 4.5.4) was performed to examine the rise in pressure from decomposition of the elastomeric O-rings within the TB-1, T-Ampoule, and two SC-2 or three SC-1 sample containers. The three SC-1 configuration yielded the highest pressure rise. The pressure rise assuming that the O-rings char was 443.17 psi, and with no char (complete decomposition which is very conservative) was 887.28 psi. Including the rise in pressure from ambient temperature to 582°C (1080°F) of 42.7 psia and the helium pressure generation from 1300 g of plutonium (for conservatism) from alpha decay of 34.2 psia, the total pressure within the TB-1 is 964.2 psia. The PAT-1 SAR,⁴ Section 4.4.2 stipulates that the maximum allowable TB-1 pressure during the post-fire plutonium air transport accident condition was 1,110 psia.

The results of the highly conservative calculation of the thermal degradation of *Viton A*® *O-rings* in LA-UR-08-07810 show that this maximum internal pressure is not exceeded.

In summary, the TB-1 structure is unaffected by the impact and thermal environments and maintains its containment integrity for HAC.

4.4 Leakage Rate Tests for Type B Packages

The leakage rate tests for the TB-1, which is the primary containment vessel, remain unchanged from the SAR.⁴

4.5 *Appendix*

4.5.1 References

1. United States. Nuclear Regulatory Commission. Code of Federal Regulations. 10 CFR 71. "Packaging and Transportation of Radioactive Material." January 1, 2009.
2. United States. Nuclear Regulatory Commission. "Certificate of Compliance for Radioactive Material Packages." Certificate Number 0361, Revision Number 9, Docket Number 71-0361, Package Identification Number USA/0361/B(U)F-96. March 4, 2009.
3. United States. Nuclear Regulatory Commission. Code of Federal Regulations. 10 CFR 71.63. "Special requirements for plutonium shipments," as published in 69 FR 3795. January 26, 2004.
4. United States. Nuclear Regulatory Commission. NUREG-0361, "Safety Analysis Report for the Plutonium Air Transportable Package, Model PAT-1." Washington, D.C. 1978.
5. Caviness, M. L., and J.B. Rubin. "Authorized Contents Proposed for the Plutonium Air Transporter (PAT-1) Packaging (U)," LA-UR-08-05154. Los Alamos National Laboratory. Los Alamos, NM: August 7, 2008.
6. Rubin, J. B. "Thermal Decomposition of Viton® O-rings for the PAT-1 Packaging Accident Scenario," LA-UR-09-05112. Los Alamos National Laboratory. Los Alamos, NM: December 10, 2008.

4.5.2 PAT-1 Contents

LA-UR-08-05154

*Approved for public release;
distribution is unlimited*

| | |
|---------------|--|
| Title: | Authorized Contents Proposed for the Plutonium Air Transporter (PAT-1) Packaging (U) |
| Author(s): | Michael L. Caviness, PMT-3 Jim B. Rubin, PMT-2 |
| Intended for: | Development of an application to the US Nuclear Regulatory Commission for the transport of plutonium metal by air in the Plutonium Air Transporter (PAT-1) packaging |



Los Alamos National Laboratory, an affirmative action/equal opportunity employer, is operated by the Los Alamos National Security, LLC for the National Nuclear Security Administration of the U.S. Department of Energy under contract DE-AC52-06NA25398. By acceptance of this article, the publisher recognizes that the U.S. Government retains a nonexclusive, royalty-free license to publish or reproduce the published form of this contribution, or to allow others to do so, for U.S. Governmental purposes. Los Alamos National Laboratory requests that the publisher identify this article as work performed under the auspices of the U.S. Department of Energy. Los Alamos National Laboratory strongly supports academic freedom and a researcher's right to publish; as an institution, however, the Laboratory does not endorse the viewpoint of a publication or guarantee its technical correctness.

Form BSO (7/08)

Authorized Contents Proposed for the Plutonium Air Transporter (PAT-1) Packaging

Authors: Michael Caviness, PMT-3, Nuclear Materials Management

Jim Rubin, PMT-2, Actinide Process Chemistry



PAT-1 Packaging Assembly

ELECTRO-REFINED PLUTONIUM METAL

1,300 grams: Maximum quantity of Electro-refined (ER) Pu metal excluding Pu241 decay

| Metal Mass (g) (max) | Mass % (max) | Grade (max) | Isotope | Pu Isotope % (max) | Pu Isotope mass (g) | Decay Heat (W) | Activity (Ci) | A ² | |
|----------------------|--------------|-------------|-----------------|--------------------|---------------------|----------------|---------------|----------------|----------|
| 1,300.00 | 99.94% | 1257.20 | Pu-233 | 0.05% | 0.65 | 1.62E-01 | 1.92E+01 | 4.05E+02 | |
| | | | Pu-239 | 22.35% | 1103.63 | 2.26E+00 | 7.43E+01 | 2.75E+03 | |
| | | | Pu-240 | 6.50% | 84.35 | 5.20E-01 | 1.24E+01 | 7.15E+02 | |
| | | | Pu-241 | 1.00% | 12.95 | 1.03E-01 | 1.30E+03 | 0.41E+02 | |
| | | | Pu-242 | 0.10% | 1.30 | 1.30E-04 | 5.00E-03 | 1.07E-01 | |
| | | | Am-241 | 0.00% | 0.00 | 0.00E+00 | 0.00E+00 | 0.00E+00 | |
| | | | Impurities: N/A | | | | | | |
| * based on % balance | | | | | | Total | 3.41E+00 | 1.40E+03 | 4.05E+03 |

Reference Values
Decay Heat

| Isotope | Watt/gram |
|---------|-----------|
| Pu-233 | 5.67E-01 |
| Pu-239 | 1.20E-02 |
| Pu-240 | 7.19E-03 |
| Pu-241 | 1.25E-02 |
| Pu-242 | 1.00E-04 |
| Am-241 | 1.15E-01 |

831 grams: 3,000 A² quantity of ER Pu metal assuming no Pu241 decay

| Metal Mass (g) (max) | Mass % (max) | Grade (max) | Isotope | Pu Isotope % (max) | Pu Isotope mass (g) | Decay Heat (W) | Activity (Ci) | A ² | |
|----------------------|--------------|-------------|-----------------|--------------------|---------------------|----------------|---------------|----------------|----------|
| 831.00 | 99.94% | 639.67 | Pu-233 | 0.05% | 0.41 | 2.35E-01 | 7.02E+00 | 2.61E+02 | |
| | | | Pu-239 | 22.35% | 716.20 | 1.46E+00 | 4.25E+01 | 1.76E+03 | |
| | | | Pu-240 | 6.50% | 53.55 | 3.03E-01 | 1.24E+01 | 4.59E+02 | |
| | | | Pu-241 | 1.00% | 8.30 | 1.04E-01 | 0.32E+02 | 5.42E+02 | |
| | | | Pu-242 | 0.10% | 0.83 | 8.30E-05 | 3.24E-03 | 1.20E-01 | |
| | | | Am-241 | 0.00% | 0.00 | 0.00E+00 | 0.00E+00 | 0.00E+00 | |
| | | | Impurities: N/A | | | | | | |
| * based on % balance | | | | | | Total | 2.10E+00 | 0.87E+02 | 3.05E+03 |

Reference Values
A² value of radioisotopes

| Isotope | A ² (Ci) | CF ₂ |
|---------|---------------------|-----------------|
| Pu-233 | 2.73E-02 | 1.70E+01 |
| Pu-239 | 2.73E-02 | 0.20E-02 |
| Pu-240 | 2.73E-02 | 2.30E-01 |
| Pu-241 | 1.00E+00 | 1.00E+02 |
| Pu-242 | 2.73E-02 | 3.00E-03 |
| Am-241 | 2.73E-02 | 3.40E+02 |

cf: CFR 101.454, Table of A² and CF Values for Radioisotopes

707 grams: 3,000 A² quantity of ER Pu metal assuming 100% Pu241 decay

| Metal Mass (g) (max) | Mass % (max) | Grade (max) | Isotope | Pu Isotope % (max) | Pu Isotope mass (g) | Decay Heat (W) | Activity (Ci) | A ² | |
|----------------------|--------------|-------------|-----------------|--------------------|---------------------|----------------|---------------|----------------|----------|
| 707.00 | 99.94% | 716.07 | Pu-233 | 0.05% | 0.35 | 1.00E-01 | 6.00E+00 | 2.21E+02 | |
| | | | Pu-239 | 22.35% | 621.07 | 1.24E+00 | 4.04E+01 | 1.50E+03 | |
| | | | Pu-240 | 6.50% | 45.54 | 1.24E-01 | 1.59E+01 | 1.21E+02 | |
| | | | Pu-241 | 0.00% | 0.00 | 0.00E+00 | 0.00E+00 | 0.00E+00 | |
| | | | Pu-242 | 0.10% | 0.71 | 7.00E-05 | 2.70E-03 | 1.02E-01 | |
| | | | Am-241 | 1.00% | 7.00 | 8.10E-01 | 2.40E+01 | 0.85E+02 | |
| | | | Impurities: N/A | | | | | | |
| * based on % balance | | | | | | Total | 2.27E+00 | 0.15E+01 | 3.05E+03 |

Note: Table shown for comparative purposes only. Pu metal will be manufactured and shipped prior to significant Pu241 decay.

Impurity Limits (max)

| Volume in parts per million (ppm) | | |
|-----------------------------------|---------|---------|
| As: 500 | Fe: 200 | Ti: 100 |
| Ar: 200 | Ge: 300 | Th: 100 |
| B: 50 | Mg: 500 | Tl: 500 |
| Bi: 3 | Ni: 500 | U: 100 |
| C: 200 | Nb: 100 | V: 200 |
| Ca: 500 | Na: 100 | Zr: 100 |
| Cd: 10 | Pb: 100 | |
| Cr: 500 | Se: 100 | |
| Cu: 100 | Sr: 100 | |

U.S. Specification 857-04879

ALLOYED PLUTONIUM METAL

| 676 grams: Alloyed Pu metal assuming no Pu241 decay | | | | | | |
|---|----------------------|----------------------|----------------|---------------|----------------|--|
| Isotope | Pu Isotopic % (mass) | Pu Isotopic mass (g) | Decay Heat (W) | Activity (Ci) | A ² | |
| Pu-238 | 0.05% | 0.33 | 1.62E-01 | 5.03E+00 | 2.92E+02 | |
| Pu-239P | 22.35% | 617.04 | 1.17E+00 | 3.03E+01 | 1.42E+03 | |
| Pu-240 | 0.50% | 43.43 | 3.06E-01 | 9.36E+00 | 3.73E+02 | |
| Pu-241 | 1.00% | 6.60 | 3.36E-02 | 6.03E+02 | 4.18E+02 | |
| Pu-242 | 0.10% | 6.67 | 6.62E-05 | 2.61E-03 | 9.65E-02 | |
| Am-241 | 0.00% | 0.00 | 0.00E+00 | 0.00E+00 | 0.00E+00 | |
| Impurities: N/A | | | | | | |
| Gallium: N/A | | | | | | |
| Total | | | 1.75E+00 | 7.22E+02 | 2.41E+03 | |

| 676 grams: Alloyed Pu metal assuming 100% Pu241 decay | | | | | | |
|---|----------------------|----------------------|----------------|---------------|----------------|--|
| Isotope | Pu Isotopic % (mass) | Pu Isotopic mass (g) | Decay Heat (W) | Activity (Ci) | A ² | |
| Pu-238 | 0.05% | 0.33 | 1.62E-01 | 5.03E+00 | 2.92E+02 | |
| Pu-239P | 22.35% | 617.04 | 1.17E+00 | 3.03E+01 | 1.42E+03 | |
| Pu-240 | 0.50% | 43.43 | 3.06E-01 | 9.36E+00 | 3.73E+02 | |
| Pu-241 | 0.00% | 0.00 | 0.00E+00 | 0.00E+00 | 0.00E+00 | |
| Pu-242 | 0.10% | 6.67 | 6.62E-05 | 2.61E-03 | 9.65E-02 | |
| Am-241 | 1.00% | 6.60 | 7.67E-01 | 2.27E+01 | 0.41E+02 | |
| Impurities: N/A | | | | | | |
| Gallium: N/A | | | | | | |
| Total | | | 2.46E+00 | 7.02E+01 | 2.84E+03 | |

| Reference Values | |
|------------------|-----------|
| Decay Heat | |
| Isotope | Watt/gram |
| Pu-238 | 5.67E-01 |
| Pu-239 | 1.20E-02 |
| Pu-240 | 7.10E-03 |
| Pu-241 | 1.25E-02 |
| Pu-242 | 1.00E-04 |
| Am-241 | 1.15E-01 |

| Reference Values | | |
|--|---------------------|----------|
| A ² values of radioisotopes | | |
| Isotope | A ² (Ci) | C/kg |
| Pu-238 | 2.92E+02 | 1.70E+01 |
| Pu-239 | 2.70E+02 | 6.20E+00 |
| Pu-240 | 2.70E+02 | 2.30E+01 |
| Pu-241 | 1.60E+00 | 1.00E+02 |
| Pu-242 | 2.70E+02 | 3.90E+03 |
| Am-241 | 2.70E+02 | 1.40E+00 |

| Impurity Limits (mass) | | |
|-----------------------------------|---------|---------|
| Values in parts per million (ppm) | | |
| As: 500 | Fe: 200 | Ti: 100 |
| Ar: 200 | Ga: N/A | Th: 100 |
| B: 50 | Mg: 500 | Tr: N/A |
| Be: N/A | Mn: 100 | U: 100 |
| C: 200 | Ni: 100 | V: 200 |
| Ca: 500 | Np: 100 | Zr: 100 |
| Co: 10 | Pb: 500 | |
| Cr: 500 | Se: 100 | |
| Cu: 100 | Sn: 500 | |

BONDED PLUTONIUM METAL

| 60 grams Bonded Pu/Be metal disc assuming 100% Pu241 decay | | | | | | | | | | Reference Values | | |
|--|----------------------|------------------------|-----------------------|--|---------------------|----------------------|----------------|---------------|-------------------------|-------------------------|------------------|--|
| Compound % | Metal Mass (g) (max) | Mass % (max) | Quantity (max) | Isotope | Pu isotopic % (max) | Pu isotopic mass (g) | Decay Heat (W) | Activity (Ci) | A' | Isotope | Weight (g) | |
| Pu metal 67.00% | 52.20 | Pu241 90.84% | Pu241 51.52 | Pu238 | 0.05% | 0.03 | 1.45E-02 | 4.30E-01 | 1.62E+01 | Pu238 | 5.67E-01 | |
| | | | | Pu239 | 92.35% | 47.25 | 2.05E-02 | 2.25E+00 | 1.09E+02 | Pu239 | 1.90E+00 | |
| | | | | Pu240 | 0.50% | 3.35 | 2.38E-02 | 7.79E-01 | 2.06E+01 | Pu240 | 7.10E-01 | |
| | | | | Pu241 | 0.00% | 0.00 | 0.00E+00 | 0.00E+00 | 0.00E+00 | Pu241 | 1.25E-02 | |
| | | | | Pu242 | 0.10% | 0.05 | 5.15E-06 | 2.01E-04 | 7.45E-03 | Pu242 | 1.00E-04 | |
| | | | | Am241 | 1.00% | 0.52 | 2.20E-02 | 1.75E+00 | 5.50E+01 | Am241 | 1.15E-01 | |
| | | | | Impurities: N/A | | | | | | | | |
| Beryllium 13.00% | 7.00 | Beryllium 13.00% | Beryllium 7.00 | Beryllium: N/A | | | | | | | Reference Values | |
| | | | | A' values of reconstruction | | | | | | | | |
| Alpha Barrier 0.50% | 0.00 | Alpha Barrier 0.00% | Alpha Barrier 0.00 | Assumes no alpha barrier to yield maximum dose | | | | | | | Isotope | |
| | | | | A' (Ci) | | | | | | | | |
| 92C-00% | 60.00 | ←←← Totals →→→ | | | | | | | Ci/g | | | |
| | | | | | | | | | Pu238 2.70E-02 1.70E+01 | | | |
| Dose rate calculations: | | | | | | | | | | Pu239 2.70E-02 6.20E-02 | | |
| Total (max) dose (Sv) | | | | | | | | | | Pu240 2.70E-02 2.30E-01 | | |
| Surface | | | | | | | | | | Pu241 1.00E+00 1.00E+02 | | |
| 0.3m (1ft) | | | | | | | | | | Pu242 2.70E-02 3.00E-03 | | |
| 1.0m (3.3ft) | | | | | | | | | | Am241 3.70E-02 3.40E+00 | | |
| The maximum dose rates stated above assumes the following: 1) three bonded Pu/Be disks are assumed to preferentially stack during NAC conditions (see layout at right); 2) the alpha barrier between the 3 bonded Pu/Be disks is conservatively ignored; 3) the 3 bonded Pu/Be disks without alpha barrier yield 5 instances of Pu/Be contact surfaces, and 4) the dose rate is calculated for 5X a given Pu/Be surface area of an unconfined disk diameter (max) ^{***} . | | | | | | | | | | Pu238 2.70E-02 1.70E+01 | | |
| *** The bonded Pu/Be disk diameter is not stated due to a security classified determination. The information (disk diameter) is available through classified communication. | | | | | | | | | | Pu239 2.70E-02 6.20E-02 | | |
| Unit dose (mrem/hr/cm ²) provided in LAMH Memorandum, RP-0-06-37, Crewport to Crewport, Subject: M750-Be Interface Disc Dose Calculations | | | | | | | | | | Pu240 2.70E-02 2.30E-01 | | |
| Configuration Layout | | | | | | | | | | Pu241 1.00E+00 1.00E+02 | | |
| The following configuration shows 3 bonded Pu/Be disks preferentially stacked with the alpha barrier conservatively removed to yield 5 instances of Pu/Be contact surfaces. | | | | | | | | | | Pu242 2.70E-02 3.00E-03 | | |
| Surface contact 1 W | | | | | | | | | | Am241 3.70E-02 3.40E+00 | | |
| Surface contact 2 W | | | | | | | | | | Pu238 2.70E-02 1.70E+01 | | |
| Surface contact 3 W | | | | | | | | | | Pu239 2.70E-02 6.20E-02 | | |
| Surface contact 4 W | | | | | | | | | | Pu240 2.70E-02 2.30E-01 | | |
| Surface contact 5 W | | | | | | | | | | Pu241 1.00E+00 1.00E+02 | | |
| Disk 1 | | | | | | | | | | Pu242 2.70E-02 3.00E-03 | | |
| Disk 2 | | | | | | | | | | Am241 3.70E-02 3.40E+00 | | |
| Disk 3 | | | | | | | | | | Pu238 2.70E-02 1.70E+01 | | |
| Impurity Limits (max) | | | | | | | | | | Pu239 2.70E-02 6.20E-02 | | |
| Value in parts per million (ppm) | | | | | | | | | | Pu240 2.70E-02 2.30E-01 | | |
| As: 100 | | | | | | | | | | Pu241 1.00E+00 1.00E+02 | | |
| Ar: 200 | | | | | | | | | | Pu242 2.70E-02 3.00E-03 | | |
| Br: 50 | | | | | | | | | | Am241 3.70E-02 3.40E+00 | | |
| Ca: N/A | | | | | | | | | | Pu238 2.70E-02 1.70E+01 | | |
| C: 200 | | | | | | | | | | Pu239 2.70E-02 6.20E-02 | | |
| Ce: 500 | | | | | | | | | | Pu240 2.70E-02 2.30E-01 | | |
| Cl: 10 | | | | | | | | | | Pu241 1.00E+00 1.00E+02 | | |
| Co: 100 | | | | | | | | | | Pu242 2.70E-02 3.00E-03 | | |
| Cu: 100 | | | | | | | | | | Am241 3.70E-02 3.40E+00 | | |
| G: 100 | | | | | | | | | | Pu238 2.70E-02 1.70E+01 | | |
| H: 100 | | | | | | | | | | Pu239 2.70E-02 6.20E-02 | | |
| I: 100 | | | | | | | | | | Pu240 2.70E-02 2.30E-01 | | |
| K: 100 | | | | | | | | | | Pu241 1.00E+00 1.00E+02 | | |
| L: 100 | | | | | | | | | | Pu242 2.70E-02 3.00E-03 | | |
| M: 100 | | | | | | | | | | Am241 3.70E-02 3.40E+00 | | |
| N: 100 | | | | | | | | | | Pu238 2.70E-02 1.70E+01 | | |
| O: 100 | | | | | | | | | | Pu239 2.70E-02 6.20E-02 | | |
| P: 100 | | | | | | | | | | Pu240 2.70E-02 2.30E-01 | | |
| Q: 100 | | | | | | | | | | Pu241 1.00E+00 1.00E+02 | | |
| R: 100 | | | | | | | | | | Pu242 2.70E-02 3.00E-03 | | |
| S: 100 | | | | | | | | | | Am241 3.70E-02 3.40E+00 | | |
| T: 100 | | | | | | | | | | Pu238 2.70E-02 1.70E+01 | | |
| U: 100 | | | | | | | | | | Pu239 2.70E-02 6.20E-02 | | |
| V: 200 | | | | | | | | | | Pu240 2.70E-02 2.30E-01 | | |
| W: 100 | | | | | | | | | | Pu241 1.00E+00 1.00E+02 | | |
| X: 100 | | | | | | | | | | Pu242 2.70E-02 3.00E-03 | | |
| Y: 100 | | | | | | | | | | Am241 3.70E-02 3.40E+00 | | |
| Z: 100 | | | | | | | | | | Pu238 2.70E-02 1.70E+01 | | |
| Lamh Specification 507-04873a | | | | | | | | | | | | |

Maximum Pu Oxide and Curies (Ci) formed in the TB-1 with a 21% Oxygen

| Oxide and Curie Values | | | | | |
|------------------------|-----------|----------|-------------------------|-----------|----------|
| No decay (100% Pu241) | | | 100% decay (100% Am241) | | |
| Isotope | Oxide (g) | Curie | Isotope | Oxide (g) | Curie |
| Pu238 | 1.73E-03 | 2.94E-02 | Pu238 | 1.73E-03 | 2.94E-02 |
| Pu239 | 3.20E+00 | 1.90E-01 | Pu239 | 3.20E+00 | 1.90E-01 |
| Pu240 | 2.75E-01 | 5.17E-02 | Pu240 | 2.25E-01 | 5.17E-02 |
| Pu241 | 3.45E-02 | 3.45E+00 | Pu241 | 0.00E+00 | 0.00E+00 |
| Pu242 | 3.45E-02 | 1.25E-05 | Pu242 | 3.50E-03 | 1.37E-05 |
| Am241 | 0.00E+00 | 0.00E+00 | Am241 | 3.45E-02 | 1.10E-01 |
| Total: | 3.45E+00 | 3.74E+00 | Total: | 3.45E+00 | 3.97E-01 |

| Isotopic % (241) | |
|------------------|--------|
| Pu238 | 0.02% |
| Pu239 | 82.25% |
| Pu240 | 6.53% |
| Pu241 | 1.00% |
| Pu242 | 0.10% |
| Am241 | 0.00% |

| Reference Values | | |
|------------------|---------------------|-----------------|
| Reference Values | | |
| Isotope | A ^o (Ci) | Q ₁₀ |
| Pu238 | 2.70E-07 | 1.70E+01 |
| Pu239 | 2.70E-03 | 6.20E-02 |
| Pu240 | 2.70E-03 | 2.30E-01 |
| Pu241 | 1.00E+00 | 1.00E+00 |
| Pu242 | 2.70E-03 | 3.90E-03 |
| Am241 | 2.70E-03 | 3.40E+00 |

LANL Specification 55Y-638728

49 (25) 178 (2), Table 2 (1) and (2) values by Radiochemical

| Data of Calculated Values | | | |
|--|--------------------------------------|----------|---|
| Variable: | Variable Unit: | Value | Definition of value |
| pressure inside of TB-1, P | atmosphere (atm) | 0.21 | 1 atmosphere pressure at 21% O ₂ in TB-1 |
| Internal volume of TB-1, V | cubic centimeters (cm ³) | 1,460.00 | Internal volume of TB-1 without contents as stated in the PAT-1 IAR |
| universal gas constant, R | constant | 82.00 | gas constant values based on pressure and volume units |
| temperature, T | kelvin (K) | 293.00 | assumes room temperature of 20C |
| O ₂ in TB-1 internal volume, n | moles | 0.013 | n = PV/RT (ideal gas law is suitable given the compressibility factor (Z) for air at 1.01 bar and 15°C(59°F) is 0.9999) |
| PuO ₂ formed from O ₂ in the TB-1, m | moles | 0.013 | Pu(m) + O ₂ (n) = PuO ₂ (m) |
| Molar mass PuO ₂ , M | constant | 276 | grams per mole (assuming molar mass of Pu = 244) |
| PuO ₂ formed, g | grams (g) | 3.46 | grams of PuO ₂ formed when all of the O ₂ reacts completely in the sealed TB-1 |

Summary of Maximum Pu Oxide and Curies (Ci) Formed in the TB-1 with 21% Oxygen:

An analysis⁴ was performed to determine the maximum quantity of PuO₂ that would form on the plutonium metal content contained within the TB-1 containment vessel. The table on Page 5 of 5 in LA-UR-08-05154 in this appendix presents the analysis methodology for calculating the quantities of oxides formed. The TB-1, which is normally filled with glove box atmosphere, was assumed to contain 1 atmosphere of air at 21% O₂. Using a TB-1 conservative internal empty volume of 1460 cm³ (89.19 in³) and the Ideal Gas Law, there are 0.013 moles of O₂ in the internal volume and 0.013 moles of PuO₂ in the TB-1. The molar mass of PuO₂ is 276 g/mole assuming a molar mass of Pu = 244. The quantity of PuO₂ formed is 3.46 g when all of the O₂ reacts completely inside of a sealed TB-1. Because this is an oxygen-limited system, no more than 3.46 g (0.0076 lb) of PuO₂ are formed when all of the O₂ completely reacts inside of a sealed TB-1 containment vessel.

To determine the isotopic composition of the PuO₂ that was formed, Los Alamos National Laboratory (LANL) Specification 55Y-638728⁴ on Page 5 of 5 in LA-UR-08-0515 in this appendix presents the maximum isotopic composition for the Pu contents. Included in the table are oxide and curie values assuming no decay (100% Pu-241) and 100% decay (100% Am-241).

For 3.46 g of oxide, the activity of PuO_2 is 3.74 Ci if no decay is assumed (100% Pu-241), and 0.397 Ci if 100% decay is assumed (100% Am-241). 3.46 g of oxide would be the maximum quantity, since the process of packing the plutonium metal includes brushing the plutonium metal with a stiff bristle brush just before transfer into an inert glove box. The brushing removes the majority of the surface oxide and any remaining oxide would be of minimal mass. For conservatism, in addition to the process knowledge provided, even if the quantity of oxide evaluated in the TB-1 volume calculation (3.46 g) was doubled, the total yield would be 6.92 g with an activity of 7.76 Ci.

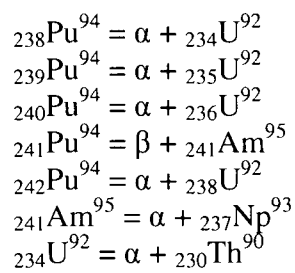
If a glove box atmosphere (0.5% oxygen in a limited inert atmosphere) is assumed within the TB-1, the quantity of PuO_2 formed on the surface of the plutonium metal content is 0.08 g (0.00018 lb).

4.5.3 Helium Generation

PAT-1 Analyses for Helium Generation Ruth F. Weiner

Sandia National Laboratories

Alpha particles are helium nuclei and, when emitted during alpha decay, pick up two electrons to form helium, a chemically inert gas that exists as helium atoms. In the present case, the relevant nuclear reactions are:



Helium is an ideal gas and at the temperatures considered behaves in accordance with the ideal gas law

$$PV = nRT \quad (1)$$

where P = pressure

V = volume

n = moles of gas

R = the gas constant, 0.082 liter-atmospheres per mole K.

T = temperature in absolute Kelvin

Air also behaves like an ideal gas. An assumption is made in this analysis that air makes up the internal free volume of the containers evaluated. The pressure in a sealed container will be the sum of the partial pressures of gases in the container: helium and air in the present case. For fixed values of V and T, pressure is directly proportional to the total moles of gas generated, so that the partial pressure of helium is directly proportional to the moles of helium generated by alpha decay. The atomic weight of helium is 4 grams per gram-atom (4 grams per mole).

The TB-1 and the TB-1 internal configurations were considered. From Table 1, the SC-1 and SC-2 quantities were less the 831 g Electro-Refined (ER) Pu hollow cylinder. The 1300 gram Pu metal hollow cylinder represents an upper limit of the quantity of Pu metal considered for the PAT-1 and is presented for reference. Consequently, pressure calculations for alpha decay were only performed for the 831 and 1300 gram amounts. The temperatures considered were the "normal" extremes, -40°C (-40°F) NCT temperature (104°C) and a temperature of 136°C in a HAC fire. A calculation at room temperature (21°C) was provided for reference.

Containments were assumed to be loaded at 1 atmosphere pressure (14.7 psi). Table 1 presents RT/V at these temperatures and volumes.

A 1300 g evaluation is provided for reference in Tables 1, 3, and 5; 831 g is the maximum plutonium content for this addendum. Helium generation was calculated from the mass loss of the Pu isotopic mixture. Table 2 shows the helium generation, per g of plutonium isotopic mixture, for the first year.

Table 1. RT/V for TB-1 Containment

| | Maximum Plutonium Mass (g) | 676 g SC-2 | 523 g SC-1 | 831 g Pu Hollow Cylinder | 1300 g Pu Hollow Cylinder |
|--------------|----------------------------|---|---------------|-----------------------------|------------------------------|
| | | Void Volume TB-1 Containment Boundary (liters) | | | |
| | | 1.103 | 1.112 | 1.275 | 1.252 |
| Deg C | K | P=RT/V(atm/mole)^a | | | |
| 104.00 | 377.00 | 27.80 | 27.84 | 24.25 | 24.69 |
| -40.00 | 233.00 | 17.18 | 17.21 | 14.99 | 15.26 |
| 136.00 | 409.00 | 30.16 | 30.21 | 26.31 | 26.79 |
| 20.00 | 294.00 | 21.64 | 21.62 | 18.85 | 19.19 |

^aR=0.082 liter-atm/mole-deg

Table 2. Helium Generation Per Gram of Pu Isotopic Mixture for One Year

| Time (weeks) | gm Pu | gm He | moles He | Time (weeks) | gm Pu | gm He | moles He |
|--------------|----------|----------|----------|--------------|----------|----------|----------|
| 0 | 1.00E+00 | 0.00E+00 | 0.00E+00 | 28 | 1.00E+00 | 6.92E-05 | 1.73E-05 |
| 2 | 1.00E+00 | 5.01E-06 | 1.25E-06 | 30 | 1.00E+00 | 7.41E-05 | 1.85E-05 |
| 4 | 1.00E+00 | 1.00E-05 | 2.50E-06 | 32 | 1.00E+00 | 7.90E-05 | 1.97E-05 |
| 6 | 1.00E+00 | 1.50E-05 | 3.75E-06 | 34 | 1.00E+00 | 8.39E-05 | 2.10E-05 |
| 8 | 1.00E+00 | 2.00E-05 | 5.00E-06 | 36 | 1.00E+00 | 8.88E-05 | 2.22E-05 |
| 10 | 1.00E+00 | 2.50E-05 | 6.25E-06 | 38 | 1.00E+00 | 9.37E-05 | 2.34E-05 |
| 12 | 1.00E+00 | 3.00E-05 | 7.49E-06 | 40 | 1.00E+00 | 9.85E-05 | 2.46E-05 |
| 14 | 1.00E+00 | 3.49E-05 | 8.73E-06 | 42 | 1.00E+00 | 1.03E-04 | 2.59E-05 |
| 16 | 1.00E+00 | 3.99E-05 | 9.97E-06 | 44 | 1.00E+00 | 1.08E-04 | 2.71E-05 |
| 18 | 1.00E+00 | 4.48E-05 | 1.12E-05 | 46 | 1.00E+00 | 1.13E-04 | 2.83E-05 |
| 20 | 1.00E+00 | 4.98E-05 | 1.24E-05 | 48 | 1.00E+00 | 1.18E-04 | 2.95E-05 |
| 22 | 1.00E+00 | 5.47E-05 | 1.37E-05 | 50 | 1.00E+00 | 1.23E-04 | 3.08E-05 |
| 24 | 1.00E+00 | 5.93E-05 | 1.48E-05 | 52 | 1.00E+00 | 1.28E-04 | 3.20E-05 |
| 26 | 1.00E+00 | 6.42E-05 | 1.61E-05 | | | | |

The partial pressure of helium and the total pressure in the containment depend on the containment volume and on the temperature. The total pressure is the sum of the partial pressure of helium and the air pressure at which the containment was loaded; the latter is assumed to be one atmosphere (14.7 psi).

The container was assumed to be filled at ambient temperature (294 K or 21 deg. C) and to reach the indicated temperature quickly. At two weeks the indicated temperature would have been reached. The helium pressure, shown in Table 1, is thus:

$$P_{\text{He}} = n_{\text{He}} \cdot (RT/V)$$

where $n_{\text{He}} = \text{gm}_{\text{He}}/4$

T= the final average temperature in Kelvin (absolute)

V = 1.252 liters

R = 0.082 l-atm/mole K, the gas constant.

Pressure in psi= 14.7*Pressure in atmospheres

Table 3 shows helium pressure in atm and psi in the TB-1 in weeks up to one year assuming 1300 g Pu content.

Table 3. Helium Pressure Generation in TB-1, Void Volume 1.252 Liters, for 1300 g Pu

| | deg C | 104 | -40 | 136 | 104 | -40 | 136 |
|-------|------------|-------------|---------|---------|---------|---------|---------|
| | K | 377 | 233 | 409 | 377 | 233 | 409 |
| | RT/V | 24.69 | 15.26 | 26.79 | 24.69 | 15.26 | 26.79 |
| | gm Pu | 1300.00 | 1300.00 | 1300.00 | 1300.00 | 1300.00 | 1300.00 |
| weeks | mole He/gm | Atmospheres | | | PSI | | |
| 0 | 0.00E+00 | 0.000 | 0.000 | 0.000 | 0.000 | 0.000 | 0.000 |
| 2 | 1.25E-06 | 0.040 | 0.025 | 0.044 | 0.591 | 0.365 | 0.641 |
| 4 | 2.50E-06 | 0.080 | 0.050 | 0.087 | 1.181 | 0.730 | 1.282 |
| 6 | 3.75E-06 | 0.120 | 0.074 | 0.131 | 1.771 | 1.094 | 1.921 |
| 8 | 5.00E-06 | 0.161 | 0.099 | 0.174 | 2.359 | 1.458 | 2.560 |
| 10 | 6.25E-06 | 0.200 | 0.124 | 0.218 | 2.947 | 1.821 | 3.197 |
| 12 | 7.49E-06 | 0.240 | 0.149 | 0.261 | 3.534 | 2.184 | 3.834 |
| 14 | 8.73E-06 | 0.280 | 0.173 | 0.304 | 4.120 | 2.547 | 4.470 |
| 16 | 9.97E-06 | 0.320 | 0.198 | 0.347 | 4.706 | 2.908 | 5.105 |
| 18 | 1.12E-05 | 0.360 | 0.222 | 0.390 | 5.291 | 3.270 | 5.740 |
| 20 | 1.24E-05 | 0.400 | 0.247 | 0.434 | 5.874 | 3.631 | 6.373 |
| 22 | 1.37E-05 | 0.439 | 0.271 | 0.477 | 6.457 | 3.991 | 7.006 |
| 24 | 1.48E-05 | 0.476 | 0.294 | 0.516 | 6.997 | 4.324 | 7.591 |
| 26 | 1.61E-05 | 0.516 | 0.319 | 0.559 | 7.578 | 4.684 | 8.221 |
| 28 | 1.73E-05 | 0.555 | 0.343 | 0.602 | 8.159 | 5.042 | 8.851 |
| 30 | 1.85E-05 | 0.594 | 0.367 | 0.645 | 8.739 | 5.401 | 9.481 |
| 32 | 1.97E-05 | 0.634 | 0.392 | 0.688 | 9.318 | 5.759 | 10.109 |
| 34 | 2.10E-05 | 0.673 | 0.416 | 0.730 | 9.896 | 6.116 | 10.736 |
| 36 | 2.22E-05 | 0.712 | 0.440 | 0.773 | 10.474 | 6.473 | 11.363 |
| 38 | 2.34E-05 | 0.752 | 0.465 | 0.816 | 11.050 | 6.830 | 11.988 |
| 40 | 2.46E-05 | 0.791 | 0.489 | 0.858 | 11.626 | 7.186 | 12.613 |
| 42 | 2.59E-05 | 0.830 | 0.513 | 0.900 | 12.202 | 7.541 | 13.237 |
| 44 | 2.71E-05 | 0.869 | 0.537 | 0.943 | 12.776 | 7.896 | 13.860 |
| 46 | 2.83E-05 | 0.908 | 0.561 | 0.985 | 13.350 | 8.251 | 14.483 |
| 48 | 2.95E-05 | 0.947 | 0.585 | 1.027 | 13.922 | 8.605 | 15.104 |

| | | | | | | | |
|----|----------|-------|-------|-------|--------|-------|--------|
| 50 | 3.08E-05 | 0.989 | 0.611 | 1.073 | 14.534 | 8.982 | 15.767 |
| 52 | 3.20E-05 | 1.028 | 0.635 | 1.115 | 15.105 | 9.336 | 16.387 |

Table 4 shows the helium pressure in atm and psi in the TB-1, in weeks up to one year assuming an 831 g Pu content.

Table 4. Helium Pressure Generation in TB-1, Void Volume 1.275 Liters, for 831 g Pu

| | deg C | 104 | -40 | 136 | 104 | -40 | 136 |
|-------|------------|-------------|-------|-------|-------|-------|--------|
| | K | 377 | 233 | 409 | 377 | 233 | 409 |
| | RT/V | 24.25 | 14.99 | 26.31 | 24.25 | 14.99 | 26.31 |
| | gm Pu | 831 | 831 | 831 | 831 | 831 | 831 |
| weeks | mole He/gm | Atmospheres | | | PSI | | |
| 0 | 0.00E+00 | 0.000 | 0.000 | 0.000 | 0.000 | 0.000 | 0.000 |
| 2 | 1.25E-06 | 0.025 | 0.016 | 0.027 | 0.371 | 0.229 | 0.402 |
| 4 | 2.50E-06 | 0.050 | 0.031 | 0.055 | 0.741 | 0.458 | 0.804 |
| 6 | 3.75E-06 | 0.076 | 0.047 | 0.082 | 1.111 | 0.687 | 1.206 |
| 8 | 5.00E-06 | 0.101 | 0.062 | 0.109 | 1.481 | 0.915 | 1.607 |
| 10 | 6.25E-06 | 0.126 | 0.078 | 0.137 | 1.850 | 1.143 | 2.007 |
| 12 | 7.49E-06 | 0.151 | 0.093 | 0.164 | 2.218 | 1.371 | 2.407 |
| 14 | 8.73E-06 | 0.176 | 0.109 | 0.191 | 2.586 | 1.598 | 2.806 |
| 16 | 9.97E-06 | 0.201 | 0.124 | 0.218 | 2.954 | 1.826 | 3.204 |
| 18 | 1.12E-05 | 0.226 | 0.140 | 0.245 | 3.321 | 2.052 | 3.603 |
| 20 | 1.24E-05 | 0.251 | 0.155 | 0.272 | 3.687 | 2.279 | 4.000 |
| 22 | 1.37E-05 | 0.276 | 0.170 | 0.299 | 4.053 | 2.505 | 4.397 |
| 24 | 1.48E-05 | 0.299 | 0.185 | 0.324 | 4.392 | 2.714 | 4.764 |
| 26 | 1.61E-05 | 0.324 | 0.200 | 0.351 | 4.757 | 2.940 | 5.160 |
| 28 | 1.73E-05 | 0.348 | 0.215 | 0.378 | 5.121 | 3.165 | 5.556 |
| 30 | 1.85E-05 | 0.373 | 0.231 | 0.405 | 5.485 | 3.390 | 5.951 |
| 32 | 1.97E-05 | 0.398 | 0.246 | 0.432 | 5.849 | 3.615 | 6.345 |
| 34 | 2.10E-05 | 0.423 | 0.261 | 0.458 | 6.212 | 3.839 | 6.739 |
| 36 | 2.22E-05 | 0.447 | 0.276 | 0.485 | 6.574 | 4.063 | 7.132 |
| 38 | 2.34E-05 | 0.472 | 0.292 | 0.512 | 6.936 | 4.287 | 7.525 |
| 40 | 2.46E-05 | 0.496 | 0.307 | 0.539 | 7.298 | 4.510 | 7.917 |
| 42 | 2.59E-05 | 0.521 | 0.322 | 0.565 | 7.659 | 4.733 | 8.309 |
| 44 | 2.71E-05 | 0.546 | 0.337 | 0.592 | 8.019 | 4.956 | 8.700 |
| 46 | 2.83E-05 | 0.570 | 0.352 | 0.618 | 8.379 | 5.179 | 9.090 |
| 48 | 2.95E-05 | 0.594 | 0.367 | 0.645 | 8.739 | 5.401 | 9.481 |
| 50 | 3.08E-05 | 0.621 | 0.384 | 0.673 | 9.122 | 5.638 | 9.897 |
| 52 | 3.20E-05 | 0.645 | 0.399 | 0.700 | 9.481 | 5.860 | 10.286 |

Table 5 presents helium pressure for all four masses of Pu at ambient temperature (21°C; 294 K) with their respective void volumes.

Table 5. Helium Pressure Generation in TB-1, Void Volume at 21 degrees C (294 K)

| | V (liters) | 1.103 | 1.112 | 1.275 | 1.252 | 1.103 | 1.112 | 1.275 | 1.252 |
|-------|------------|-------------|--------|--------|---------|--------|--------|--------|--------|
| | RT/V | 21.71 | 21.70 | 18.91 | 19.26 | 21.71 | 21.70 | 18.91 | 19.26 |
| | gm Pu | 676.00 | 523.00 | 831.00 | 1300.00 | 676.00 | 523.00 | 831.00 | 1300.0 |
| Weeks | mole He/gm | Atmospheres | | | | PSI | | | |
| 0 | 0.00E+00 | 0.00 | 0.00 | 0.00 | 0.00 | 0.000 | 0.000 | 0.000 | 0.000 |
| 2 | 1.25E-06 | 0.018 | 0.014 | 0.020 | 0.031 | 0.270 | 0.209 | 0.289 | 0.461 |
| 4 | 2.50E-06 | 0.037 | 0.028 | 0.039 | 0.063 | 0.540 | 0.418 | 0.578 | 0.921 |
| 6 | 3.75E-06 | 0.055 | 0.043 | 0.059 | 0.094 | 0.810 | 0.626 | 0.867 | 1.381 |
| 8 | 5.00E-06 | 0.073 | 0.057 | 0.079 | 0.125 | 1.079 | 0.834 | 1.155 | 1.840 |
| 10 | 6.25E-06 | 0.092 | 0.071 | 0.098 | 0.156 | 1.348 | 1.042 | 1.443 | 2.298 |
| 12 | 7.49E-06 | 0.110 | 0.085 | 0.118 | 0.187 | 1.616 | 1.249 | 1.730 | 2.756 |
| 14 | 8.73E-06 | 0.128 | 0.099 | 0.137 | 0.219 | 1.884 | 1.456 | 2.017 | 3.213 |
| 16 | 9.97E-06 | 0.146 | 0.113 | 0.157 | 0.250 | 2.152 | 1.663 | 2.303 | 3.670 |
| 18 | 1.12E-05 | 0.165 | 0.127 | 0.176 | 0.281 | 2.419 | 1.870 | 2.590 | 4.126 |
| 20 | 1.24E-05 | 0.183 | 0.141 | 0.196 | 0.312 | 2.686 | 2.076 | 2.875 | 4.581 |
| 22 | 1.37E-05 | 0.201 | 0.155 | 0.215 | 0.343 | 2.952 | 2.282 | 3.161 | 5.036 |
| 24 | 1.48E-05 | 0.218 | 0.168 | 0.233 | 0.371 | 3.199 | 2.473 | 3.425 | 5.456 |
| 26 | 1.61E-05 | 0.236 | 0.182 | 0.252 | 0.402 | 3.465 | 2.678 | 3.709 | 5.910 |
| 28 | 1.73E-05 | 0.254 | 0.196 | 0.272 | 0.433 | 3.730 | 2.884 | 3.994 | 6.363 |
| 30 | 1.85E-05 | 0.272 | 0.210 | 0.291 | 0.464 | 3.995 | 3.089 | 4.277 | 6.815 |
| 32 | 1.97E-05 | 0.290 | 0.224 | 0.310 | 0.494 | 4.260 | 3.293 | 4.561 | 7.266 |
| 34 | 2.10E-05 | 0.308 | 0.238 | 0.330 | 0.525 | 4.525 | 3.498 | 4.844 | 7.717 |
| 36 | 2.22E-05 | 0.326 | 0.252 | 0.349 | 0.556 | 4.789 | 3.702 | 5.127 | 8.168 |
| 38 | 2.34E-05 | 0.344 | 0.266 | 0.368 | 0.586 | 5.052 | 3.906 | 5.409 | 8.618 |
| 40 | 2.46E-05 | 0.362 | 0.280 | 0.387 | 0.617 | 5.316 | 4.109 | 5.691 | 9.067 |
| 42 | 2.59E-05 | 0.380 | 0.293 | 0.406 | 0.647 | 5.579 | 4.313 | 5.973 | 9.515 |
| 44 | 2.71E-05 | 0.397 | 0.307 | 0.425 | 0.678 | 5.841 | 4.516 | 6.254 | 9.963 |
| 46 | 2.83E-05 | 0.415 | 0.321 | 0.445 | 0.708 | 6.104 | 4.718 | 6.534 | 10.411 |
| 48 | 2.95E-05 | 0.433 | 0.335 | 0.464 | 0.739 | 6.366 | 4.921 | 6.815 | 10.857 |
| 50 | 3.08E-05 | 0.452 | 0.349 | 0.484 | 0.771 | 6.645 | 5.137 | 7.114 | 11.334 |
| 52 | 3.20E-05 | 0.470 | 0.363 | 0.503 | 0.801 | 6.906 | 5.339 | 7.394 | 11.780 |

4.5.4 O-Ring Decomposition

LA-UR- 09-05112

*Approved for public release;
distribution is unlimited.*

Title: Thermal Decomposition of Viton® O-rings for the PAT-1 Packaging Accident Scenario

Author(s): J.B. Rubin

Intended for: Support an amendment application to the US Nuclear Regulatory Commission for the PAT-1 packaging



Los Alamos National Laboratory, an affirmative action/equal opportunity employer, is operated by the Los Alamos National Security, LLC for the National Nuclear Security Administration of the U.S. Department of Energy under contract DE-AC92-06NA25396. By acceptance of this article, the publisher recognizes that the U.S. Government retains a nonexclusive, royalty-free license to publish or reproduce the published form of this contribution, or to allow others to do so, for U.S. Government purposes. Los Alamos National Laboratory requests that the publisher identify this article as work performed under the auspices of the U.S. Department of Energy. Los Alamos National Laboratory strongly supports academic freedom and a researcher's right to publish; as an institution, however, the Laboratory does not endorse the viewpoint of a publication or guarantee its technical correctness.

Form 836 (7/06)

Abstract

As part of the submission package to the NRC to amend the approved contents for the PAT-1 container, a calculation was necessary to determine the theoretical pressure rise in the PAT-1 containment vessel (TB-1) due to the thermal decomposition of o-rings within the container. These o-rings are composed of Viton A[®], whose number and mass are determined by the internal packing configuration. This report contains the calculations of the decomposition of these o-rings, in the theoretical accident conditions defined by the PAT-1 SARP, assuming both oxygen-deficient and oxygen-available environments. The results show that even for the case of complete thermal decomposition to gaseous products, the total pressure rise inside of the TB-1 containment vessel is less than the maximum allowable, as defined in the PAT-1 SARP.

The o-rings are treated as tori, with a volume given by

$$V = (2\pi R)(\pi r^2) \quad (1)$$

where r is the radius of the cross-sectional area of the torus and R is the distance from the center of the torus to the center of the cross sectional area, Figure 1 :

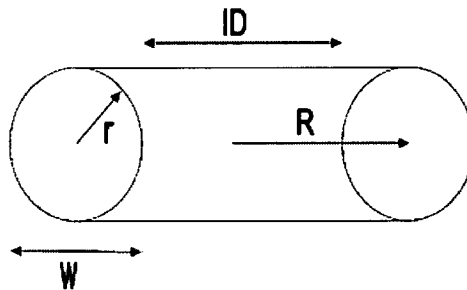


Figure 1. Cross section of a torus, showing the dimensional relations to Eq. (1).

Table 1. Dimensions and volumes of Viton A[®] o-rings contained within the TB-1 for the Packing Configurations described in Table 3 and shown schematically in Figure 2.

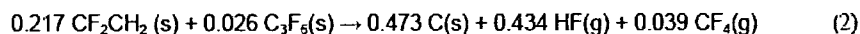
| o-ring location | o-ring designation | w (in) | r (in) | ID (in) | R (in) | Volume (in ³) | Volume (cm ³) |
|---------------------------------|--------------------|--------|--------|---------|--------|---------------------------|---------------------------|
| T-ampoule | Parker 2-241 | 0.139 | 0.070 | 3.859 | 3.929 | 0.1906 | 3.1233 |
| TB-1 | Parker 2-242 | 0.139 | 0.070 | 3.984 | 2.062 | 0.1966 | 3.2209 |
| SC-1/2 | Parker 2-147 | 0.103 | 0.052 | 2.675 | 1.389 | 0.0727 | 1.1916 |
| Packing Configuration #1 | | | | | | | |
| TB-1 | Parker 2-242 | 0.139 | 0.070 | 3.984 | 2.062 | 0.1966 | 3.2209 |
| T-ampoule | Parker 2-241 | 0.139 | 0.070 | 3.859 | 3.929 | 0.1906 | 3.1233 |
| | | | | | Total | 0.3872 | 6.3442 |
| Packing Configuration #2 | | | | | | | |
| TB-1 | Parker 2-242 | 0.139 | 0.070 | 3.984 | 2.062 | 0.1966 | 3.2209 |
| T-ampoule | Parker 2-241 | 0.139 | 0.070 | 3.859 | 3.929 | 0.1906 | 3.1233 |
| SC-2 | Parker 2-147 | 0.103 | 0.052 | 2.675 | 1.389 | 0.0727 | 1.1916 |
| SC-2 | Parker 2-147 | 0.103 | 0.052 | 2.675 | 1.389 | 0.0727 | 1.1916 |
| | | | | | Total | 0.5326 | 8.7275 |
| Packing Configuration #3 | | | | | | | |
| TB-1 | Parker 2-242 | 0.139 | 0.070 | 3.984 | 2.062 | 0.1966 | 3.2209 |
| T-ampoule | Parker 2-241 | 0.139 | 0.070 | 3.859 | 3.929 | 0.1906 | 3.1233 |
| SC-1 | Parker 2-147 | 0.103 | 0.052 | 2.675 | 1.389 | 0.0727 | 1.1916 |
| SC-1 | Parker 2-147 | 0.103 | 0.052 | 2.675 | 1.389 | 0.0727 | 1.1916 |
| | | | | | Total | 0.6053 | 9.9192 |

Table 1 gives the relevant dimensions (w, r and R as defined in Figure 1) of the o-rings, taken from the o-ring supplier's (Parker) catalog. From these dimensions, the volume of each o-ring is calculated using Eq. (1) and compared to the values given in the supplier's product catalog (as verification that the volume of each o-ring is accurate). From these individual o-ring volumes, the total o-ring (volume) inventory in the TB-1, for each of the three packing configurations, is obtained.

Based on literature review, the reaction products produced by pyrolysis of Viton A[®] in air is similar to that of pyrolysis of PTFE in air, namely, CO, CO₂, HF, CF₄, C₂F₄, C₃F₆, C₃F₈, C₄F₈. Therefore, for gas generation calculations, we will assume that the maximum amount of HF (g) is formed, since this specie would form the greatest amount of product, on a molar basis, from the degradation products, and therefore represents the maximum pressure contribution of any (single) pyrolysis product. Then, it is assumed that any fluorine in excess of that taken up in the formation of HF(g) will react with carbon to form the maximum amount of CF₄(g).

In the following section, a calculation will be given of the pressure rise due to o-ring degradation for Packing Configuration #3, which includes five o-rings, as shown in Table 1.

Viton A[®] is a vinylidene fluoride/hexafluoropropylene copolymer, manufactured by DuPont Corporation, with a nominal composition of 78 wt% CF₂CH₂ and 22 wt% C₃F₆. [1]. For packing configuration #3, the total elastomer volume is 9.9192 cm³ (Table 1). Assuming an elastomer specific gravity of 1.8 g/cm³, we have 17.855 g of elastomer material, or 13.927 g (0.217 moles) CF₂CH₂ and 3.928 g (0.026 moles) C₃F₆. The overall decomposition reaction, based on the assumed decomposition products is therefore



For the elastomer inventory in Packing Configuration #3, we have

$$13.927 \text{ g CF}_2\text{CH}_2 \left(\frac{37.996 \text{ g F}}{64.034 \text{ g CF}_2\text{CH}_2} \right) = 8.264 \text{ g F} \quad (3)$$

$$13.927 \text{ g CF}_2\text{CH}_2 \left(\frac{2.016 \text{ g H}}{64.034 \text{ g CF}_2\text{CH}_2} \right) = 0.438 \text{ g H} \quad (4)$$

$$13.927 \text{ g CF}_2\text{CH}_2 \left(\frac{24.022 \text{ g C}}{64.034 \text{ g CF}_2\text{CH}_2} \right) = 5.225 \text{ g C} \quad (5)$$

plus

$$3.928 \text{ g C}_3\text{F}_6 \left(\frac{113.988 \text{ g F}}{150.021 \text{ g C}_3\text{F}_6} \right) = 2.985 \text{ g F} \quad (6)$$

$$3.928 \text{ g C}_3\text{F}_6 \left(\frac{36.033 \text{ g C}}{150.021 \text{ g C}_3\text{F}_6} \right) = 0.943 \text{ g C} \quad (7)$$

or

$$11.249 \text{ g F} \quad (8)$$

$$6.168 \text{ g C} \quad (9)$$

$$0.438 \text{ g H} \quad (10)$$

If we assume that all available hydrogen and fluorine are liberated and form the maximum moles of gaseous products, we would have

$$\left(\frac{0.438 \text{ g H}}{1.008 \text{ g/mole H}} \right) = 0.435 \text{ moles hydrogen available for HF generation, and}$$

$$\left(\frac{11.249 \text{ g F}}{18.998 \text{ g/mole F}} \right) = 0.592 \text{ moles total fluorine minus the 0.435 moles of fluorine in HF, leaving,}$$

0.157 moles of fluorine available for $\text{CF}_4(\text{g})$ generation, or 0.039 moles $\text{CF}_4(\text{g})$. If these reaction products add incrementally, and ideally, then we would have 0.435 mole $\text{HF}(\text{g}) + 0.039$ mole $\text{CF}_4(\text{g})$, or a total of 0.474 moles of gaseous [$\text{HF}(\text{g}) + \text{CF}_4(\text{g})$] reaction products. For an unoccupied internal TB-1 volume of 1103.01 cm^3 (see Packing Configuration #3 in Table 3), and $T = 1080^\circ\text{F}$ (582.2°C , 855.4 K) for the PAT-1 hypothetical accident condition, there would be a pressure increment of

$$P = \frac{(0.474 \text{ mole}) \left(82.056 \text{ atm cm}^3 / \text{mole K} \right) (855.4 \text{ K})}{1103.01 \text{ cm}^3} = 30.16 \text{ atm} \quad (11)$$

or 443.23 psi due to the assumed o-ring degradation products. Once the hydrogen and fluorine are consumed in the formation of $\text{HF}(\text{g})$ and $\text{CF}_4(\text{g})$, there is a theoretical excess of

$$\left(\frac{6.168 \text{ g C}}{12.011 \text{ g/mole}} \right) = 0.514 \text{ moles of carbon in the virgin elastomer minus 0.039 moles carbon in}$$

CF_4 , or 0.475 moles.

At this point we could assume that (1) the theoretical excess of carbon will remain as solid, unreactive char, or that (2) the excess carbon can be further reacted with oxygen to form $\text{CO}(\text{g})$ or $\text{CO}_2(\text{g})$ (the formation of either $\text{CO}(\text{g})$ or $\text{CO}_2(\text{g})$ would produce the same number of moles of gaseous reaction products).

The formation of residual carbon char, as opposed to the formation of $\text{CO}(\text{g})$ or $\text{CO}_2(\text{g})$, would be supported based on (a) any oxygen present at the time of initial packaging is scavenged completely by the formation of plutonium oxide, and (b) the TB-1 remains intact at the theoretical accident conditions. Solid char is experimentally observed, even in the oxidative thermal decomposition of fluoroelastomers.^{v, vi, vii} Further, for studies of the thermal degradation of Viton A[®] in non-oxidizing environments, an incomplete volatilization of the polymer, as evidenced by a low yield of fluorine with respect to the theoretical quantity^v The calculated amount of char represents 32% of the original elastomer mass and 93% of the carbon contained in the original elastomer.

However, for the purposes of a conservative estimate, we assume the case where additional oxygen were to be made available in the TB-1 and sample containers, in a quantity sufficient to react completely with the excess carbon from the elastomer, to produce CO(g) or CO₂(g). Such a reaction would increase the overall moles of gaseous reaction products to 0.474 moles (HF(g) + CF₄(g)) + 0.475 (moles CO(g) or CO₂(g)), thereby doubling the overall pressure rise from 30.16 atm to 60.32 atm, or 887.28 psi.

Table 2 summarizes the calculation given above, which, again, represents the elastomer inventory in Packaging Configuration #3, along with a similar calculation of the remaining two Packaging Configurations, which have a reduced elastomer loading.

Table 2. Calculation of elastomer degradation products for the three Packaging Configurations described in Table 1 and shown schematically in Figure 2. The top summation in the right-hand part of each row represents the total number of moles assuming that the excess carbon forms a solid char (i.e., no CO(g) or CO₂(g) formation), while the bottom summation in each row is the total number of moles assuming that the excess carbon reacts completely to form gaseous product, either CO(g) or CO₂(g).

| | | | |
|---|---|---|---|
| Packing Configuration #1 (6.3442 cm ³ of Viton A [®]) | 8.907 g (0.139 moles) CF ₂ CH ₂ 2.512 g (0.017 moles) C ₃ F ₆ | 0.280 g (0.278 moles) H 7.194 g (0.379 moles) F 3.945 g (0.328 moles) C | 0.278 moles HF(g) 0.025 moles CF ₄ (g) $\Sigma = 0.303 \text{ moles}$ 0.303 moles CO(g) $\Sigma = 0.606 \text{ moles}$ |
| Packing Configuration #2 (8.7277 cm ³ of Viton A [®]) | 12.254 g (0.191 moles) CF ₂ CH ₂ 3.456 g (0.023 moles) C ₃ F ₆ | 0.386 g (0.383 moles) H 9.897 g (0.521 moles) F 5.427 g (0.452 moles) C | 0.383 moles HF(g) 0.035 moles CF ₄ (g) $\Sigma = 0.418 \text{ moles}$ 0.417 moles CO(g) $\Sigma = 0.835 \text{ moles}$ |
| Packing Configuration #3 (9.9192 cm ³ of Viton A [®]) | 13.927 g (0.217 moles) CF ₂ CH ₂ 3.928 g (0.026 moles) C ₃ F ₆ | 0.438 g (0.435 moles) H 11.249 g (0.592 moles) F 6.168 g (0.514 moles) C | 0.435 moles HF(g) 0.039 moles CF ₄ (g) $\Sigma = 0.474 \text{ moles}$ 0.475 moles CO(g) $\Sigma = 0.949 \text{ moles}$ |

Table 3 gives the overall pressure rise calculation for the three Packing Configurations, using the appropriate o-ring inventory (Table 1) and unoccupied TB-1 volume (Table 3) for each Configuration.

Table 3. Internal volume of the TB-1 container (top line), and solid volumes of T-ampoule, filler ring, sample containers (SC-1 or SC-2) and Pu metal payloads for each Packing Configuration (volume of optional tantalum foil and copper foam were neglected). Column 4 gives the resulting pressure rise for the case of char formation, while column 5 gives the result for the case of no char formation. Column 6 is a summation of the pressure rise from Column 5 plus an additional 2.9 atmospheres (42.62 psi), assumed originally present in the TB-1.

| components | Volume (in ³) | Volume (cm ³) | Pressure rise (psi) – with char | Pressure rise (psi) – no char | Pressure rise (psia) – no char |
|---------------------------------|---------------------------|---------------------------|---------------------------------|-------------------------------|--------------------------------|
| Empty TB-1 | 89.10 | 1460.09 | | | |
| Packing Configuration #1 | | | | | |
| T-ampoule | 7.83 | 128.31 | | | |
| Filler ring | 0.90 | 14.75 | | | |
| Pu cylinder 831 g | 2.57 | 42.11 | | | |
| <i>Unoccupied TB-1 volume</i> | 77.80 | 1274.91 | 245.10 | 490.20 | 532.83 |
| Packing Configuration #2 | | | | | |
| T-ampoule | 7.83 | 128.31 | | | |
| Filler ring | 0.90 | 14.75 | | | |
| SC-2 | 2.75 | 45.06 | | | |
| SC-2 | 2.75 | 45.06 | | | |
| SC-2 Cradle Assembly | 4.90 | 80.30 | | | |
| Pu cylinder 1.1" Ø x 1.1" h | 1.05 | 17.21 | | | |
| Pu cylinder 1.1" Ø x 1.1" h | 1.05 | 17.21 | | | |
| <i>Unoccupied TB-1 volume</i> | 67.87 | 1112.19 | 387.59 | 774.26 | 816.89 |
| Packing Configuration #3 | | | | | |
| T-ampoule | 7.83 | 128.31 | | | |
| Filler ring | 0.90 | 14.75 | | | |
| SC-1 | 2.15 | 35.23 | | | |
| SC-1 | 2.15 | 35.23 | | | |
| SC-1 | 2.15 | 35.23 | | | |
| SC-1 Cradle Assembly | 5.02 | 82.26 | | | |
| Pu cylinder 0.88"Ø x 0.88" h | 0.53 | 8.69 | | | |
| Pu cylinder 0.88"Ø x 0.88" h | 0.53 | 8.69 | | | |
| Pu cylinder 0.88"Ø x 0.88" h | 0.53 | 8.69 | | | |
| <i>Unoccupied TB-1 volume</i> | 67.31 | 1103.01 | 443.17 | 887.28 | 929.91 |

ⁱ. A.K. Burnham and R.K. Weese, "Kinetics of thermal degradation of explosive binders Viton A, Estane, and Kel-F", *Thermochemica Acta* 426 (2005) pp. 85-92.

ⁱⁱ. *Analytical Pyrolysis of Synthetic Organic Polymers*, ed. by Șerban Moldoveanu (2005) p.289.

ⁱⁱⁱ. I. Lee, R.R. Reed, V.L. Brady, and S.A. Finnegan, "Energy release in the reaction of metal powders with fluorine containing polymers", *J. Thermal Anal.* 49 (1997) pp. 1699-1705.

^{iv}. A.E. Venger, et al., "Thermogravimetric Study of the Thermal Decomposition of poly(tetrafluoroethylene) under Nonisothermal Conditions", *Vestsi Akademii Navuk BSSR, Seryya Fizika-Energetychnykh Navuk* 2 (1976) pp. 65.

^v. G. J. Knight and W. W. Wright, "The Thermal Degradation of Hydrofluoro Polymers", *J. Appl. Polym. Sci.* 16 (1972) pp. 683-693.

5. SHIELDING EVALUATION

This section describes the shielding evaluation for incorporating plutonium (Pu) metal contents as a new payload into the PAT-1 package. The Pu metal is packed in an inner container (*T-Ampoule Assembly*,^A Drawing 2A0261, designated the T-Ampoule) that replaces the PC-1 inner container. The T-Ampoule and associated Pu metal content packing configurations are described in Section 1.2.1 and Section 1.2.2 of this addendum, respectively.

To demonstrate compliance with the dose rate limits of 10 CFR 71.47(a) (non-exclusive use) for normal conditions of transport (NCT) and 10 CFR 71.51(a)(2) for hypothetical accident conditions (HAC), an evaluation of the shielding performance of the Plutonium Air Transportation (PAT-1) package has been completed. The evaluation assumes a package loaded with up to 1.3 kg* of Pu metal or plutonium/beryllium (Pu/Be) sources with a total mass of 200 g* or less of Pu; a combined Pu/Be contact surface area of 91 cm² or less; and an isotopic Pu composition, including allowance for decay, such that the total neutron source from the (α ,n) reaction with beryllium (Be) metal does not exceed 363 n/s/cm² (see Table 5-13). A detailed description of the shielding characteristics of the PAT-1 packaging is provided in Section 5.4 of the SAR.¹

5.1 Description of Shielding Design

5.1.1 Design Features

The shielding design features of the PAT-1 include the stainless steel overpack drum (*Overpack, AQ*,^A Drawing 1002 in the SAR,¹ designated the AQ-1); the stainless steel (PH13-8Mo) TB-1 *Containment Vessel* (Drawing 1017, designated the TB-1); and the titanium ampoule (*T-Ampoule Assembly*, Drawing 2A0261, designated the T-Ampoule), which secures the contents inside the containment vessel. In addition, the aluminum (Al) load spreader assembly, the copper heat conductor tube, and the redwood assemblies (both inner and outer) provide minimal additional shielding. While these additional features are largely designed for other purposes, they perform a dual role as shielding features. The lid and the bottom of the overpack drum, the containment vessel, and the T-Ampoule provide shielding in the axial direction. Shielding credit is not taken for the T-Ampoule (or for packing materials contained therein), the inner redwood assembly, or the thicker portions of the TB-1 vessel.

The stainless steel 304 materials are fabricated with a density of 7.9 g/cm³ with the exception of the TB-1 containment vessel, which is fabricated with a PH13-8Mo material² with a density of 7.5 g/cm³. The copper tube is fabricated from pure copper metal with a density of 8.94 g/cm³, and the Al load spreader is fabricated from Al 6061 with a density of 2.6989 g/cm³. The redwood is assumed to be cellulose (C₆H₁₀O₅)^{3,4} with a density of 0.36 g/cm³.

^A The drawing titles are in italics and are used interchangeably with the designated names in this addendum. See Section 1.3.2 in this addendum and Chapter 9 of the SAR¹ for drawing number, title, and revision.

* The plutonium quantities analyzed in this shielding section represent a conservative upper bound for analysis and are higher than the payload quantities shown in Table 1-1 of Section 1 of this addendum.

The shielding design requirements for these packages are minimal due to high purification and relatively low specific activity of the desired contents. Thus, with generous bounding assumptions on the source magnitude, the dose rates are still demonstrated to be small fractions of the regulatory limits.

5.1.2 Summary Table of Maximum Radiation Levels

The dose rates shown in Table 5-1 indicate that the PAT-1 meets regulatory dose limits as specified in the respective 10 CFR sections under NCT and HAC for nonexclusive use. The analysis for the limiting contents is based on the natural radioactivity produced from the decay of 1300 g of plutonium metal under bounding conditions that include peak dose rates due to decay (Pu shelf-life after separation), worst-case scenario for the various isotopes of Pu, and (α,n) production from an oxide matrix instead of a metal matrix. Details of the source generation and shielding analyses for the limiting contents are described in Sections 5.2 and 5.3, respectively. Description of an alternate content of Pu/Be sources is described in Section 5.5.3. It is shown in this section that Pu/Be is not the limiting content.

Table 5-1. Summary Table of External Radiation Levels (Non-Exclusive Use)

| NCT | Package Surface mSv/h (mrem/h) | | | 1 Meter from Package Surface mSv/h (mrem/h) | | |
|--------------------------|-----------------------------------|--------------|--------------------------|--|--------------------------|--------------------------|
| | Top | Side | Bottom | Top | Side | Bottom |
| Gamma | 0.060 (6.0) ^a | 0.277 (27.7) | 0.055 (5.5) ^a | 0.006 (0.6) ^a | 0.015 (1.5) | 0.006 (0.6) ^a |
| Neutron | 0.036 (3.6) ^a | 0.319 (31.9) | 0.038 (3.8) ^a | 0.003 (0.3) ^a | 0.014 (1.4) ^a | 0.003 (0.3) ^a |
| Total | 0.096 (9.6) ^a | 0.596 (59.6) | 0.093 (9.3) ^a | 0.009 (0.9) ^a | 0.029 (2.9) | 0.009 (0.9) ^a |
| 10 CFR 71.47(a) Limit | 2 (200) | 2 (200) | 2 (200) | 0.1 (10) ^b | 0.1 (10) ^b | 0.1 (10) ^b |

^a Monte Carlo statistics of 5% or less; all others 1% or less.

^b Transport index may not exceed 10.

| HAC | 1 Meter from Package Surface mSv/h (mrem/h) | | |
|--------------------------|--|-------------|-------------|
| | Top | Side | Bottom |
| Gamma | 0.024 (2.4) | 0.035 (3.5) | 0.021 (2.1) |
| Neutron | 0.015 (1.5) | 0.018 (1.8) | 0.014 (1.4) |
| Total | 0.039 (3.9) | 0.053 (5.3) | 0.035 (3.5) |
| 10 CFR 71.51(a)(2) Limit | 10 (1000) | 10 (1000) | 10 (1000) |

5.2 Source Specification

Because of the variety of contents envisioned for the PAT-1, a procedure to determine and generate bounding sources was developed that allows for a great deal of flexibility of allowed package contents. The gamma and neutron sources are based on a limiting Pu isotopic vector (see Table 5-2) that should allow for almost any form of plutonium metal to be loaded into the package, subject only to the mass and heat constraints of 1300 g of Pu and 25 watts, respectively.

The Pu isotopic distribution (Pu isotope versus mass fraction seen in Table 5-2) was generated through simulation of all conceivable routes of Pu production from different reactor types. The package was limited to 1300 g and a heat load of 25 watts although the isotopes for the radiation source are based on 2197 g with a heat load of 40 watts. For each isotope, the largest weight percent was selected across all the reactor types; taking the largest weight percent for each isotope regardless of other restrictions results in a total that exceeds 100 weight percent (wt %). The source definition is the upper bound of the actual source and therefore, yields an overestimate of the expected package doses. The analysis to support these Pu isotopic values is further described in Section 5.5.2.

Table 5-2. Plutonium Isotopics Used for Source Generation

| Isotope | Mass Fraction | Mass (g) |
|---------|-------------------|-------------------|
| Pu-236 | 2.0E-07 | 0.00026 |
| Pu-238 | 0.04 | 52 |
| Pu-239 | 1.00 | 1300 |
| Pu-240 | 0.40 | 520 |
| Pu-241 | 0.15 | <195 ^a |
| Pu-242 | 0.10 | 130 |
| Am-241 | 0.15 ^a | <195 ^a |
| Total | 1.69 ^b | 2197 |

^a The initial Am-241 is assumed to be zero, with 195 g of Pu-241. The time-varying source is optimized such that the maximum dose is computed with respect to the decay of Pu-241 to Am-241.

^b As a conservative assumption, the mass fractions used to generate the radiation source are allowed to exceed unity. The package is limited to 831 g (1300 g was used as an upper bound), although the isotopics for the radiation source are based on 2197 g. In addition, the allowed heat load is limited to 25 watts, while the radiation source used in this analysis is based on isotopics that would generate about 40 watts of heat.

5.2.1 Gamma Source

The gamma source arises from the beta and gamma decay of the Pu isotopes, each of which has distinct time and energy characteristics. The specific radiation characteristics of each of these isotopes are discussed further in Section 5.5.2. From this analysis, a gamma source is derived that bounds all realistic forms of plutonium metal. This source is given in Table 5-3 in the SCALE 18 group structure. This source corresponds to 2197 g of Pu (1300 g of Pu with the mass fractions specified in Table 5-2) and a decay time since Pu separation of 18.0 years (referred to as the shelf-life). While this decay time does not represent the peak source, it does represent the peak dose rate due to the dominance of the high-energy photons from the decay of Pu-236, which peaks at 18.0 years. In contrast, the lower-energy photons from predominately Pu/Am-241 have a very broad peak of about 75 years (see Figure 5-3).

5.2.2 Neutron Source

The neutron source consists of spontaneous fission and (α ,n) components, as shown in Table 5-4. The spontaneous fission component is invariant relative to the Pu matrix material (oxide or metal), is uniquely defined for each isotope, and decreases slightly with decay time. The (α ,n) component is a function of the impurities in the Pu matrix and exhibits a broad peak with decay

due to the variation of the Pu/Am-241 concentrations (see Figure 5-3). The (α ,n) component of the neutron spectrum, shown in Table 5-4, is based on an oxide matrix and represents a bound of the contents for a metal matrix (see Section 5.5.2). Both components of the neutron source shown are for a Pu decay time of 30 years, which corresponds to the peak source and dose with respect to the decay time.

Table 5-3. Gamma-Ray Source Used in the Shielding Analysis (2197 g Pu)

| Energy Group | Energy Boundaries (MeV) | Photons/s |
|--------------|-------------------------|-----------|
| 1 | 10 | 6.691E+02 |
| 2 | 8 | 3.182E+03 |
| 3 | 6.5 | 1.645E+04 |
| 4 | 5 | 4.162E+04 |
| 5 | 4 | 1.255E+05 |
| 6 | 3 | 6.089E+07 |
| 7 | 2.5 | 2.481E+05 |
| 8 | 2 | 7.277E+05 |
| 9 | 1.66 | 3.519E+06 |
| 10 | 1.33 | 2.546E+06 |
| 11 | 1 | 1.201E+07 |
| 12 | 0.8 | 1.396E+08 |
| 13 | 0.6 | 1.404E+08 |
| 14 | 0.4 | 4.397E+08 |
| 15 | 0.3 | 1.636E+09 |
| 16 | 0.2 | 7.217E+09 |
| 17 | 0.1 | 4.048E+12 |
| 18 | 0.05 | 5.459E+12 |
| | | |
| Total | | 9.517E+12 |

5.3 *Shielding Model*

5.3.1 Configuration of Source and Shielding

A slice of the three-dimensional shielding model used for the NCT evaluation is shown in Figure 5-1. This model is constructed with the dimensions given in Table 5-5 and contains the materials as described in Table 5-6. The dimensions correspond to those from the reference drawings with nominal dimensions used where given. The use of nominal dimensions is appropriate for this analysis since the package materials are not designed as shielding bodies and, therefore, produce minimal shielding effects. In addition, the inner redwood assembly, inner can assembly, T-Ampoule, and thicker regions along the side of the TB-1 containment vessel are assumed to be void in the shielding model. Since the geometry of the source material is variable, analyses were

performed to conservatively bound the configuration and magnitude of the source. The bounding of the source magnitude was previously discussed in Section 5.2.

Table 5-4. Neutron Source Used in the Shielding Analysis (2197 g Pu)

| Energy Group | Energy Boundaries (eV) | Spontaneous Fission (neutrons/s) | (α,n) Source (neutrons/s) | Total (neutrons/s) |
|--------------|------------------------|----------------------------------|------------------------------------|--------------------|
| 1 | 2.000E+7 | 1.161E+04 | 0.0 | 1.161E+04 |
| 2 | 6.434E+6 | 1.632E+05 | 2.658E+05 | 4.290E+05 |
| 3 | 3.000E+6 | 2.024E+05 | 5.305E+05 | 7.330E+05 |
| 4 | 1.850E+6 | 1.154E+05 | 1.185E+05 | 2.340E+05 |
| 5 | 1.400E+6 | 1.486E+05 | 7.443E+04 | 2.231E+05 |
| 6 | 9.000E+5 | 1.517E+05 | 5.428E+04 | 2.060E+05 |
| 7 | 4.000E+5 | 7.012E+04 | 2.719E+04 | 9.731E+04 |
| 8 | 1.000E+5 | 1.034E+04 | 4.798E+03 | 1.513E+04 |
| 9 | 1.700E+4 | 7.403E+02 | 3.497E+02 | 1.090E+03 |
| 10 | 3.000E+3 | 5.486E+01 | 2.255E+01 | 7.740E+01 |
| 11 | 5.500E+2 | 4.314E+00 | 1.855E+00 | 6.169E+00 |
| 12 | 1.000E+2 | 3.031E-01 | 1.385E-01 | 4.415E-01 |
| 13 | 3.000E+1 | 4.813E-02 | 2.516E-03 | 5.065E-02 |
| 14 | 1.000E+1 | 9.546E-03 | 8.739E-04 | 1.042E-02 |
| 15 | 3.05 | 1.081E-03 | 1.607E-04 | 1.242E-03 |
| 16 | 1.77 | 3.179E-04 | 5.900E-05 | 3.769E-04 |
| 17 | 1.30 | 1.025E-04 | 2.134E-05 | 1.238E-04 |
| 18 | 1.13 | 7.345E-05 | 1.632E-05 | 8.976E-05 |
| 19 | 1.00 | 1.040E-04 | 2.510E-05 | 1.291E-04 |
| 20 | 0.80 | 1.698E-04 | 5.021E-05 | 2.200E-04 |
| 21 | 0.40 | 2.504E-05 | 9.414E-06 | 3.445E-05 |
| 22 | 0.33 | 2.923E-05 | 1.255E-05 | 4.179E-05 |
| 23 | 0.23 | 2.847E-05 | 8.945E-06 | 3.742E-05 |
| 24 | 0.10 | 8.138E-06 | 0.0 | 8.138E-06 |
| 25 | 0.05 | 2.565E-06 | 0.0 | 2.565E-06 |
| 26 | 0.03 | 2.095E-06 | 0.0 | 2.095E-06 |
| 27 | 0.01 | 1.121E-06 | 0.0 | 1.121E-06 |
| | | | | |
| Total | | 8.743E+05 | 1.076E+06 | 1.950E+06 |

The shape of the source in this scenario determines the (1) degree to which the source particles are self-shielded for gamma emissions and (2) the magnitude of the neutron source multiplication due to fission. The bounding source geometry is determined from a series of three assumed source geometries (see Section 5.4.4):

- A full-density, solid sphere with a radius of 2.63 cm
- A reduced-density, smeared source that completely fills the central region shown in Figure 5-1
- A full-density, thin, hollow cylinder with inner and outer radii of 5.249 and 5.4 cm, respectively, and a height of 15.11 cm (the central cylindrical region shown in Figure 5-1).

Each of these three geometries is assumed to contain 1300 g of plutonium metal. The full-density models assume the use of plutonium metal with a density of 17.0 g/cm^3 (see Table 5-6 for material reference and discussion below). The bounding source geometry for the neutron dose is the solid, maximum-density sphere with the sphere moved outward so that it touches the inside surface of the TB-1 vessel. The bounding source geometry for the gamma doses is the smeared geometry, which minimizes the self-shielding effect and also moves the source material closer to the detector locations. The maximum total side dose (neutron plus gamma components) is simulated using the smeared geometry model for the gamma contribution and an intermediate full-density off-center sphere (density of 17 g/cm^3) for the neutron contribution; the predicted total doses using this hybrid approach are some 20% greater than those using consistent neutron/gamma contributions for the various geometry/density models. The top and bottom dose values reported in Table 5-1 are based on the reduced-density, smeared Pu source model only since these values are not limiting.

Spot checks were completed for the top and bottom geometries to ensure that the peak source geometries were evaluated. The shielding source model for the HAC is the same as the NCT reduced-density smeared source model with only the central Pu region and the TB-1 containment vessel remaining.

5.3.2 Material Properties

The constituents of the materials used in the shielding calculations are shown in Table 5-6. All materials are used at their stated densities, although the plutonium metal density is modified by the ratio of the full-density volume to the smeared-density volume used in the reduced-density source model that bounds the shielding results. The density for this case follows.

The volume of the bottom curved region (204.2 cm^3) is taken from Section 6.9.2. The cylindrical volume is given below and differs from that in Section 6.9.2 since a minimum thickness of the TB-1 lid is assumed here.

$$\text{Smeared-plutonium-source density} = 1300 \text{ g} / ([\pi * 5.4^2 * 15.11] + 204.2) \text{ cm}^3 = 0.818 \text{ g/cm}^3$$

The non-Pu materials use the SCALE standard definitions for the isotopic compositions, while selecting the minimal density from other sources, if available. The references used for each material are also presented in Table 5-6.

5.4 Shielding Evaluation

5.4.1 Methods

The shielding evaluation is performed by calculating the dose rates at the top, bottom, and radial directions of the PAT-1 package to verify compliance with the 10 CFR Part 71 nonexclusive dose rates during NCT. The dose rates are 2 mSv/h (200 mrem/h) at the package surface and 0.01mSv/h (10 mrem/h) at 1m from the accessible package surface under NCT, and 10 mSv/h (1000 mrem/h) at 1m, the 10 CFR Part 71 dose rate limit, under HAC.

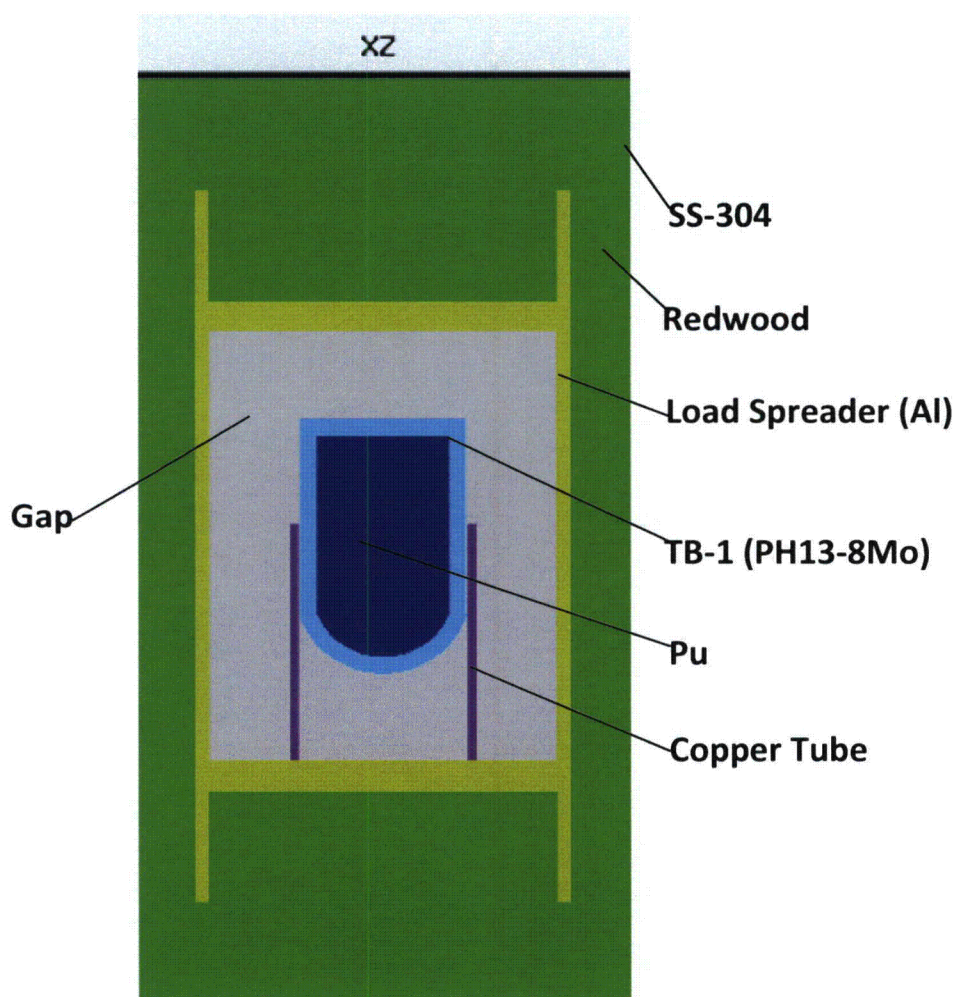


Figure 5-1. Cylindrical Shielding Model of PAT-1 Used in This Analysis (see Table 5-6 for Dimensional Information)

The evaluation has been performed for the PAT-1 package containing up to 1300g of plutonium metal. The Shielding Analysis Sequence #4 (SAS4)³ code was utilized to determine the dose rate at the surface and at 1 m from the surface, in both the axial and radial directions, for

bounding gamma and neutron sources. The dose locations evaluated in this scenario are shown in Figure 5-2. As shown in Table 5-1, the surface side dose is the most restrictive and is composed almost equally of gamma and neutron dose components.

The spatial distribution for each source used in these analyses was uniform within each of the defining cylindrical or spherical volumes (i.e., reduced-density, smeared cylinder; full-density annular cylinder; full-density sphere), as described in Section 5.3.1.

Table 5-5. Dimensions of Materials Regions Used in Shielding Analyses

| Body | Radius (cm) | Bottom location (cm) | Height (cm) | Description |
|---------------|-------------|----------------------|-------------|-------------------------------|
| 1 – cylinder | 5.40 | -5.64 | 15.11 | cylindrical inside of TB-1 |
| 2 – sphere | 5.72 | -3.74 ^a | — | curved inside of TB-1 |
| 3 – cylinder | 6.795 | -5.64 | 16.71 | outside of TB-1 |
| 4 – sphere | 7.12 | -3.74 ^a | — | curved outside of TB-1 |
| 5 – cylinder | 10.0 | -5.64 | 16.71 | dummy piece for geometry |
| 6 – cylinder | 6.875 | -10.86 | 21.93 | void outside TB-1 |
| 7 – cylinder | 6.875 | -18.25 | 7.39 | wood block below TB-1 |
| 8 – cylinder | 7.52 | -18.25 | 20.32 | copper tube |
| 9 – cylinder | 8.74 | 2.07 | 9.00 | void for thicker TB-1 region |
| 10 – cylinder | 13.97 | -18.25 | 36.79 | wood inside Al spreader |
| 11 – cylinder | 13.97 | -20.79 | 41.87 | upper and lower Al spreader |
| 12 – cylinder | 13.97 | -30.35 | 60.81 | top and bottom wood inside Al |
| 13 – cylinder | 15.24 | -30.35 | 60.81 | Al on outside of spreader |
| 14 – cylinder | 28.58 | -48.69 | 99.13 | wood inside drum |
| 15 – cylinder | 28.73 | -48.84 | 99.43 | steel drum |

^a For spherical bodies, this value is the z location of the sphere; all bodies shown are centered at x and y = 0.

All shielding calculations were performed with the SCALE 5.1 version of the SAS4. This sequence consists of multiple codes executed from a single input stream. The individual modules used are the:

- BONAMI and NITAWL codes, which process the cross sections into formats the subsequent shielding codes can utilize.
- XSDRNPM one-dimensional discrete ordinates code, which is run in the adjoint mode to automatically generate biasing parameters for the final shielding analysis.
- MORSE-SGC, which is the Monte Carlo shielding code that quantifies the fluxes and dose rates at desired locations in the geometry.

Unless otherwise noted, all results reported in Table 5-1 are converged to a Monte Carlo statistical value of 1% or less at the 1 sigma level, indicating that the results are well converged.

This degree of convergence is aided by the automated bias generation built into the SAS4 sequence. Automated biasing as implemented in SAS4 gives rise to some inherent geometry limitations (e.g., axially symmetric models). Section 5.5.4 contains a discussion of how these limitations were overcome.

Table 5-6. Elemental Compositions Used in Shielding Analysis

| Material | Density (g/cm ³) | Composition, wt % (atoms/barn-cm) | | |
|------------------------------------|---------------------------------|--------------------------------------|--------|-----------------|
| | | Element | wt % | (atoms/barn-cm) |
| PH13-8Mo ² | 7.74 (7.5 used) | Cr | 12.75 | (1.10753E-02) |
| | | Ni | 8.00 | (6.15690E-03) |
| | | Al | 1.13 | (1.88319E-03) |
| | | Mo | 2.25 | (1.05924E-03) |
| | | Fe | 75.88 | (6.13662E-02) |
| Redwood ^{3,4} | 0.36 | H | 6.2 | (1.33725E-02) |
| | | C | 44.4 | (8.02350E-03) |
| | | O | 49.4 | (6.68625E-02) |
| Aluminum ^{3,5} | 2.6989 | Al | 100.0 | (6.02375E-02) |
| 304 Stainless Steel ^{3,5} | 7.9 | C | 0.080 | (3.16873E-04) |
| | | Si | 1.000 | (1.69394E-03) |
| | | Cr | 19.000 | (1.73846E-02) |
| | | Mn | 2.000 | (1.73195E-03) |
| | | Fe | 68.375 | (5.82497E-02) |
| | | Ni | 9.500 | (7.70121E-03) |
| | | P | 0.045 | (6.91181E-05) |
| Copper ⁵ | 8.94 | Cu | 100.0 | (8.47233E-02) |
| Plutonium metal ⁶ | 15-19.7 (17.0 used) | Pu-239 | 100.0 | (4.28259E-02) |

The following is a complete list of the conservative assumptions and techniques used in this analysis to ensure that the results generated bound those of the actual contents under any circumstances.

1. The source is generated based on an extremely pessimistic representation of the Pu isotopes. The use of a burned reactor-grade Pu vector allows for isotopes other than Pu-239 to contribute significantly to the total source. The expected use of components more in line with weapons-grade Pu (higher Pu-239; lower for other isotopes) should produce radiation levels much lower than those assumed in this analysis. See estimates of this effect in Section 5.5.2.
2. The metal matrix anticipated for shipments using this package should have a neutron source that is significantly lower than the oxide matrix that was used for all source calculations (see Section 5.5.2).

3. The source generation scenario is based on a Pu mass 60% greater than allowed and a heat generation rate also 60% greater than the allowed rate, ensuring that doses are bounding. However, the actual mass of Pu in the package for self-shielding purposes is only 1300 g.
4. The shape of the source was varied to determine the configuration that produced the maximum dose for the bounding source spectrum described above and in Section 5.2.
5. The time variation of the source spectrum and magnitude was analyzed to select a decay time that produced bounding dose rates over any possible decay time.
6. The shielding analysis assumed the minimum Pu density expected for the various forms of plutonium metal.
7. The T-Ampoule, the thicker steel portions of the TB-1 containment vessel, and the inner redwood assembly were omitted from the shielding analysis. The structural material densities were the minimum values found in the literature.

In the model, the dose at a given location is obtained by assuming “point detectors,” which allow the dose at a specific point in space to be tabulated. Dose estimation via point detectors is less efficient than that based on radiation tracking across a specified surface length or area, but it allows for greater detail in the reported results. In each case, a series of point detectors were placed side-by-side to determine the location of the peak dose. In most cases, the peak dose was at the location corresponding to or in alignment with the center of the source region. The point locations shown in Figure 5-2 indicate where the point detectors were placed for the various locations reported in Table 5-1. The use of point detectors directly on the outermost shielding surface is limited; standard practice is to move the point detectors about 1 cm off the surface. The 1-m detectors are located precisely 1 m from the outermost shielding surface. For the HAC cases, only the contents and the TB-1 containment vessel were modeled, with the 1-m detectors placed at a distance of precisely 1 m from the outermost surface of the TB-1 body.

The cross section set used for all analyses was the SCALE 27N-18COUPLE library. This is the recommended library for all shielding calculations using the SCALE system.

5.4.2 Input and Output Data

A listing of the input data for the ORIGEN-S source generation is shown in Section 5.5.4. The output of this source generation calculation is automatically written onto a file named *fi71f001* and subsequently read in by the shielding analysis modules. SAS4 inputs for the shielding study of the radial neutron and gamma doses are also given in Section 5.5.4. SAS4 utilizes an automated bias parameter generator, which typically allows for both neutron and gamma problems to converge rapidly. In all cases, the results given in Table 5-1 are converged to 1% or less unless otherwise noted.

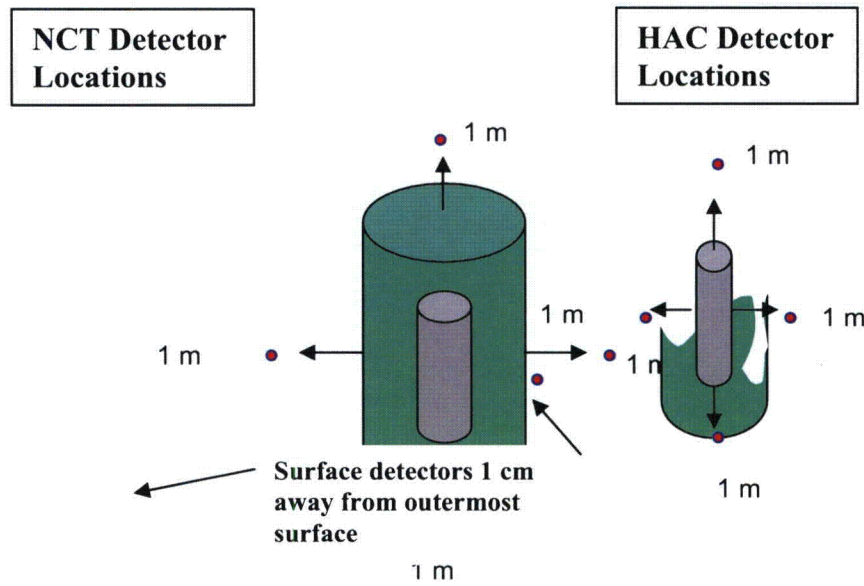


Figure 5-2. Dose Locations Analyzed for the PAT-1 Package

5.4.3 Flux-to-Dose-Rate Conversion

ANSI/ANS-6.1.1-1977 flux-to-dose-rate conversion factors are used in the SAS4 shielding calculations. These factors are provided in Tables 5-7 and 5-8 for neutrons in the SCALE 27 neutron group structure and gamma radiation in the SCALE 18 group gamma structure.

5.4.4 External Radiation Levels

Radiation levels corresponding to up to 1300 g of plutonium metal loaded in the PAT-1 package have been predicted in this section. The methods and techniques are based on current-generation, well-known, and approved codes and procedures and should be accurate to within 10–20%. A number of bounding approximations included in each phase of the analysis should ensure that the predicted results are larger than any actual radiation levels and, therefore, allow a high level of assurance that an actual shipment should pass the dose-measurement tests at the time approved contents are shipped. While no measurements of sufficient quality exist to serve as benchmarks for expected dose rates near plutonium metal components, the results reported herein are consistent with previous analyses⁷ performed prior to certification of Pu oxide contents in the same PAT-1 package. The sources and final dose predictions from that study differ only within a factor of 2 from those in this study, even though the techniques and underlying data sets have been updated since the previous study.

A comparison of dose predictions at the top, side, and bottom package locations (both at the surface and at 1 m) indicates very consistent relative dose values: the package surface values are a factor of 5 greater along the side than those along the top and bottom. At 1 m, this factor of 5 is reduced to approximately 3 (as expected), as the distributed Pu source will begin to approximate a point source as the distance from the package increases. The top and bottom doses are also consistent with each other as expected from a visual examination of Figure 5-1, which shows similar top and bottom geometries and similar distances from the package contents to the exterior surface locations.

Although not included in the analyses, the effect of ground scatter during the loading process should only be approximately 10–20%, which is readily bounded by the conservatism included in the analysis.

The bounding source configuration was found to be the reduced-density, smeared Pu source that completely filled the inside of the TB-1 containment vessel volume. This conclusion is based on the analysis of five other source configurations described as follows:

Table 5-7. Neutron Flux-to-Dose Conversion Factors Used in Shielding Analysis

| Group Number | Energy Bounds (eV) | Dose Factor (rem/h/neutrons/cm ² /s) |
|--------------|--------------------|---|
| 1 | 2.000E+07 | 1.492E-04 |
| 2 | 6.434E+06 | 1.446E-04 |
| 3 | 3.000E+06 | 1.270E-04 |
| 4 | 1.850E+06 | 1.281E-04 |
| 5 | 1.400E+06 | 1.298E-04 |
| 6 | 9.000E+05 | 1.028E-04 |
| 7 | 4.000E+05 | 5.118E-05 |
| 8 | 1.000E+05 | 1.232E-05 |
| 9 | 1.700E+04 | 3.837E-06 |
| 10 | 3.000E+03 | 3.725E-06 |
| 11 | 5.500E+02 | 4.015E-06 |
| 12 | 1.000E+02 | 4.293E-06 |
| 13 | 3.000E+01 | 4.474E-06 |
| 14 | 1.000E+01 | 4.568E-06 |
| 15 | 3.050E+00 | 4.558E-06 |
| 16 | 1.770E+00 | 4.519E-06 |
| 17 | 1.300E+00 | 4.488E-06 |
| 18 | 1.130E+00 | 4.466E-06 |
| 19 | 1.000E+00 | 4.435E-06 |
| 20 | 8.000E-01 | 4.327E-06 |
| 21 | 4.000E-01 | 4.197E-06 |
| 22 | 3.250E-01 | 4.098E-06 |
| 23 | 2.250E-01 | 3.839E-06 |
| 24 | 1.000E-01 | 3.675E-06 |
| 25 | 5.000E-02 | 3.675E-06 |
| 26 | 3.000E-02 | 3.675E-06 |
| 27 | 1.000E-02 | 3.675E-06 |

- A full-density, solid sphere of radius 2.63 cm located at the center of the TB-1 volume
- A solid sphere moved to the TB-1 vessel inner wall
- Three hollow cylindrical configurations with various radii and heights

The three hollow cylindrical sources are described as a small cylinder; a large cylinder; and a large, thin cylinder. The first two are actual components under consideration for loading. The

third is a hypothetical cylinder with an outer radius of 5.4 cm, which coincides with the inner radius of the TB-1 vessel, and a height of 15.11 cm, which is the complete height of the cylindrical section inside the TB-1 vessel. The inner radius was calculated to be 5.249 cm, which corresponds to 1300 g of plutonium metal at a density of 17.0 g/cm³. The complete set of results for the side surface of the package is shown in Table 5-9. These results show that the reduced-density, smeared cylinder is the bounding source geometry; however, the results also show very little sensitivity of the total dose to the source configuration. Hence, for the top and bottom dose locations, only the reduced-density, smeared cylinder source configuration was analyzed.

Table 5-8. Gamma Flux-to-Dose Conversion Factors Used in Shielding Analysis

| Group Number | Energy Bounds (eV) | Dose Factor (rem/h/photon/cm ² /s) |
|--------------|--------------------|---|
| 1 | 1.000E+07 | 8.772E-06 |
| 2 | 8.000E+06 | 7.478E-06 |
| 3 | 6.500E+06 | 6.375E-06 |
| 4 | 5.000E+06 | 5.414E-06 |
| 5 | 4.000E+06 | 4.622E-06 |
| 6 | 3.000E+06 | 3.960E-06 |
| 7 | 2.500E+06 | 3.469E-06 |
| 8 | 2.000E+06 | 3.019E-06 |
| 9 | 1.660E+06 | 2.628E-06 |
| 10 | 1.330E+06 | 2.205E-06 |
| 11 | 1.000E+06 | 1.833E-06 |
| 12 | 8.000E+05 | 1.523E-06 |
| 13 | 6.000E+05 | 1.172E-06 |
| 14 | 4.000E+05 | 8.759E-07 |
| 15 | 3.000E+05 | 6.306E-07 |
| 16 | 2.000E+05 | 3.834E-07 |
| 17 | 1.000E+05 | 2.669E-07 |
| 18 | 5.000E+04 | 9.347E-07 |

Table 5-9. Source Geometry Optimization Dose Results (at PAT-1 Side Surface)

| Source Configuration | Neutron Dose (mrem/h) | Gamma Dose (mrem/h) | Total Dose (mrem/h) |
|-----------------------------------|----------------------------------|--------------------------------|--------------------------------|
| reduced-density, smeared cylinder | 18.9 | 27.7 | 46.6 |
| centered sphere | 26.1 | 10.3 | 36.4 |
| off-center sphere | 31.9 | 11.1 | 43.0 |
| large cylinder | 20.3 | 20.5 | 40.8 |
| small cylinder | 20.3 | 16.9 | 37.2 |
| Large, thin cylinder | 20.2 | 25.6 | 45.8 |

Dose profiles were generated for each separate analysis. In all cases the peak dose occurs at the center point of the source region or just off the center point (due to the influence of the copper pipe in the radial calculations). These are the expected results for a uniformly distributed source and indicate no streaming through various regions of the PAT-1 geometry.

5.5 Appendix

5.5.1 References

1. United States. Nuclear Regulatory Commission. NUREG-0361, "Safety Analysis Report for the Plutonium Air Transportable Package, Model PAT-1." Washington, D.C. 1978.
2. Brown, Jr., W. F. and S. J. Setlak. *Aerospace Structural Metals Handbook, 37th Edition*, CINDAS/USAF CRDA Handbooks Operation, Purdue University, West Lafayette, IN. 2001.
3. SCALE-5.1, "A Modular Code System for Performing Standardized Computer Analyses for Licensing Evaluation for Workstations and Personal Computers, CCC-545," Oak Ridge National Laboratory. Oak Ridge, TN.
4. United States. Dept. of Agriculture. Alden, H. A., "Softwoods of North America," September 1997.
5. Davis, J.R., ed. *ASM Specialty Handbook: Copper and Copper Alloys*. p. 446-452, ASM International, 2001.
6. "LANL Content Description for PAT-1 Packaging," Los Alamos National Laboratory. Los Alamos, NM: August 9, 2007.
7. United States. Nuclear Regulatory Commission. NUREG/CR-0030 (SAND76-0587), "PARC (Plutonium Accident Resistant Container) Program Research, Design, and Development." Reprinted January 1983.
8. PAT-1 Content impurity description transmitted from SNL to ORNL on October 18, 2007.
9. Wilson, W.B., et al. "SOURCES 4C: A Code for Calculating (α ,n), Spontaneous Fission, and Delayed Neutron Sources and Spectra," LA-UR-02-1839: Los Alamos National Laboratory. Los Alamos, NM: April 2002.
10. Caviness, M. L., and J.B. Rubin. "Authorized Contents Proposed for the Plutonium Air Transporter (PAT-1) Packaging (U)," LA-UR-08-05154. Los Alamos National Laboratory. Los Alamos, NM: August 7, 2008.

5.5.2 Summary of Source Bounding Analyses

The isotopes of concern in generating a radioactive source for Pu are Pu-236, Pu-238, Pu-239, Pu-240, Pu-241, and Pu-242. Each of these have very different behaviors with respect to neutron and photon emissions and their variation over time since purification of the Pu product (referred to as either decay time or shelf-life). The key parameters of the neutron source, photon source, and decay heat per gram of each of these isotopes are given in Figures 5-3 through 5-5.

These values indicate that the primary contributors (per unit mass) to the photon source are, in order, Pu-236, Pu-238, and Pu-241. Of these, Pu-241 is typically the most abundant isotope. The primary contributors to the neutron source are the same three isotopes. The specific decay heat values from Figure 5-5 are 18.2, 0.57, 1.9E-3, 7.1E-3, 0.10, and 1.2E-4 watts/g for Pu-236,

Pu-238, Pu-239, Pu-240, Pu-241, and Pu-242, respectively. The value for Pu-241 corresponds to the peak time-varying value and can be used per gram of both Pu-241 and Am-241.

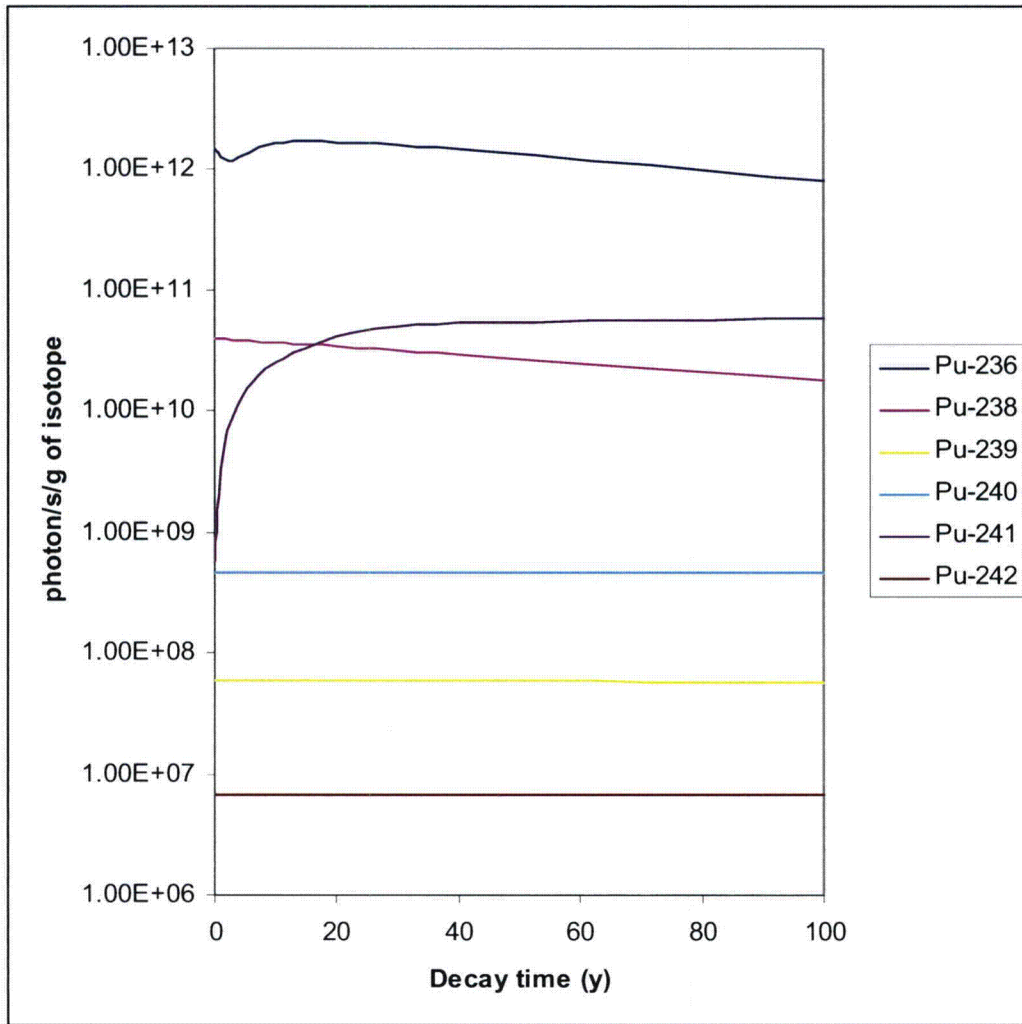


Figure 5-3. Photon Source per Gram of Each Isotope of Pu Initially Present (Note That Pu-241 Data Includes Buildup of Am-241)

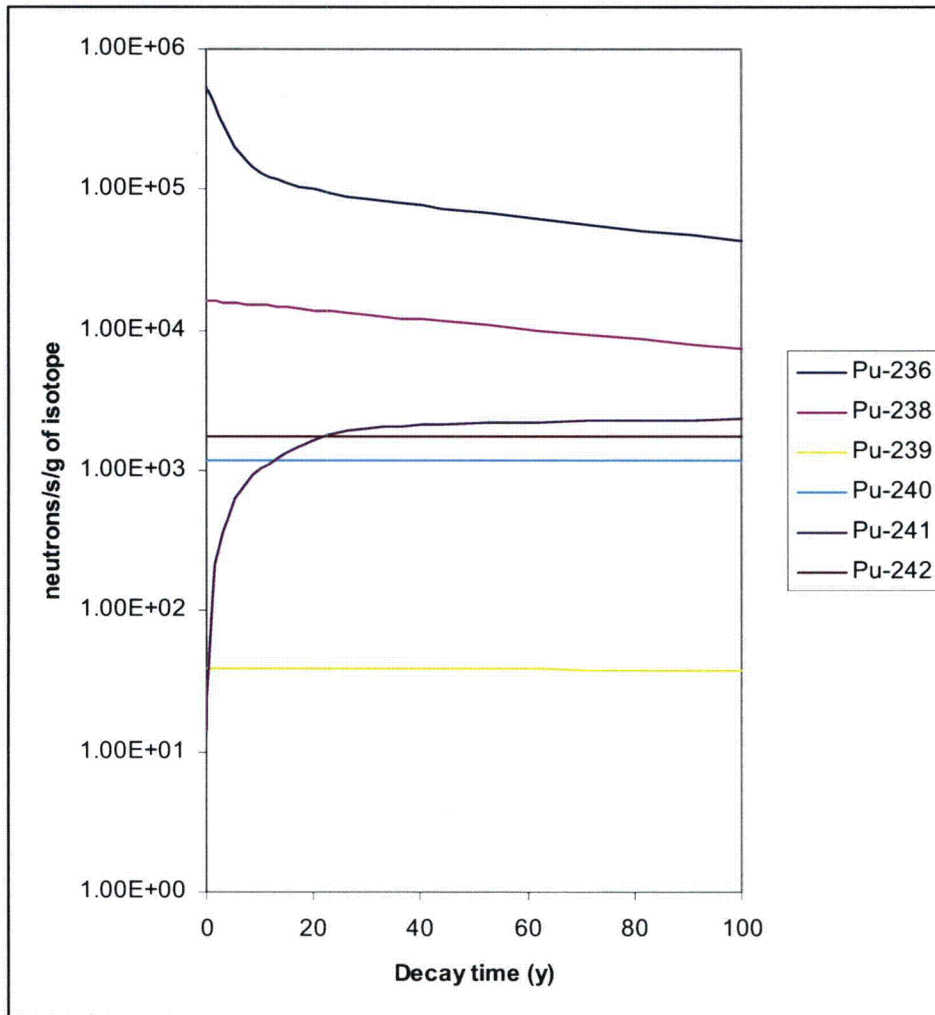
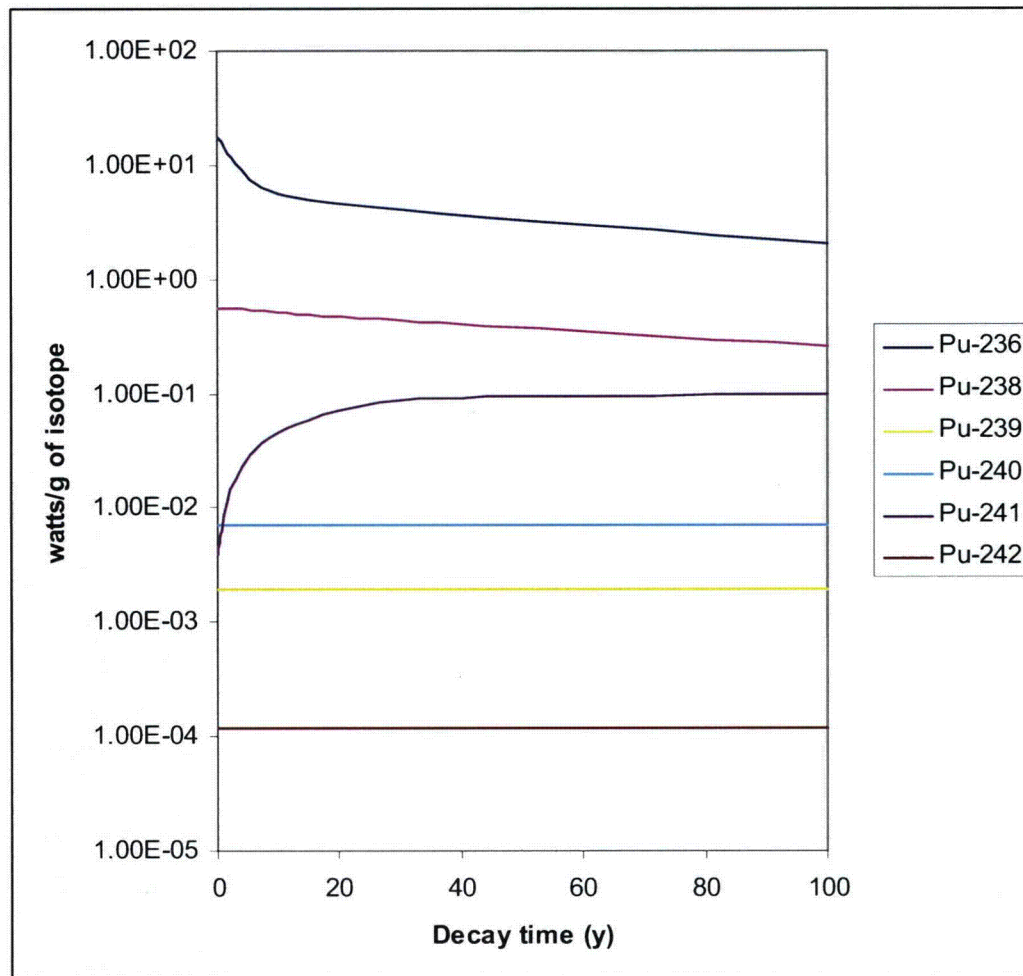


Figure 5-4. Neutron Source per Gram of Each Isotope of Pu Initially Present (Includes Both Spontaneous Fission and (α,n) Components with an Oxide Matrix; Also Note That Pu-241 Data Includes Buildup of Am-241)



**Figure 5-5. Watts per Gram of Each Isotope of Pu Initially Present
(Note That Pu-241 Data Includes Buildup of Am-241)**

In order to bound the Pu sources in this study, a series of seven depletion calculations were performed using the SCALE depletion code ORIGEN-ARP.³ The ORIGEN-ARP code uses the same ORIGEN-S code used to generate the neutron, photon, and decay heat values presented in Figures 5-3 to 5-5. The ARP portion of ORIGEN-ARP takes reactor-based cross sections tabulated for each reactor system and automatically interpolates to the desired burnup and enrichment values appropriate for a given level of depletion. Three reactor systems were selected for this study: a pressurized water reactor (PWR, Westinghouse 17×17 lattice), a CANDU (Canadian design power reactor), and the Hanford N Reactor (a government reactor primarily designed for Pu production). A total of seven depletion scenarios were performed for these systems as defined in Table 5-10, corresponding to medium and high burnups for the PWR and CANDU designs and to a low, medium, and high burnup for the N reactor. The goal of these studies is to predict the full range of Pu isotopes that would result from these scenarios. The resulting Pu isotope values are given in Table 5-10 for each scenario.

Table 5-10. Pu Isotope Wt % Under Various Depletion Scenarios

| Isotope | PWR (35 GWd/t) | PWR (60 GWd/t) | CANDU (5 GWd/t) | CANDU (10 GWd/t) | N_Reactor (2 GWd/t) | N_Reactor (5 GWd/t) | N_Reactor (10 GWd/t) |
|--------------|-------------------|-------------------|--------------------|---------------------|------------------------|------------------------|-------------------------|
| Pu-236 | 2.4E-6 | 1.6E-5 | 8.5E-8 | 2.5E-7 | 2.0E-8 | 1.0E-7 | 2.2E-7 |
| Pu-238 | 0.49 | 3.6 | 0.05 | 0.15 | 0.01 | 0.05 | 0.12 |
| Pu-239 | 74.9 | 49.3 | 75.4 | 59.5 | 93.6 | 83.9 | 76.7 |
| Pu-240 | 15.2 | 23.7 | 20.2 | 30.7 | 5.8 | 12.8 | 17.6 |
| Pu-241 | 8.4 | 15.2 | 3.7 | 6.9 | 0.6 | 3.0 | 5.0 |
| Pu-242 | 1.1 | 8.2 | 0.6 | 2.8 | 0.02 | 0.2 | 0.6 |
| Total | 100 | 100 | 100 | 100 | 100 | 100 | 100 |

From these individual results, the following Pu isotope definition is generated that bounds all the above scenarios. The maximum weight percent from each isotope in Table 5-10 is used to define the mass fractions given in Table 5-11 (for Pu-236, the value of 1.6E-5 is divided by 100 and rounded to 2E-7). The use of this Pu isotope definition should allow any realistic Pu production scenario to be accounted for.

In order to estimate the amount of overprediction for the bounding radiation sources, the bounding neutron and gamma sources are presented in Table 5-12 along with predicted sources based on the "N_Reactor 2 GWd/t" case shown in Table 5-10. The Pu isotopic distributions from this case correspond closely with typical weapons-grade plutonium metal along with corresponding impurities.^{6,8}

5.5.3 Analysis of Pu/Be Source Contents

An alternate content of Pu/Be sources is desired for the PAT-1 package. This section separately analyzes the shielding concerns related to this content.

The radiation emitted from a Pu/Be source, both neutron source magnitude and energy spectrum, is estimated using the SOURCE4C⁹ code. The source configuration used in this study is an interface source, where α particles emitted from the Pu and americium (Am) materials produce neutrons via interaction with the Be material along a common interface. The source from such a calculation is tabulated as n/s/cm², with the source directly proportional to the contact surface area between the two materials. For the materials expected to be shipped in this package, there is also an alpha barrier, which places another material between the Pu and Be, effectively making the neutron source much smaller. The influence of alpha barriers is conservatively ignored in these source estimates.

The neutron source used in the Pu/Be source study is given in Tables 5-13 and 5-14. The assumed Pu and Am isotopes are taken from Reference 10 and correspond to the expected material to be shipped; as a bound on the source magnitude, the Pu-241 is assumed to be completely decayed to Am-241. The neutron source spectrum is shown in Table 5-14.

The impurity content of the plutonium metal used for the Pu/Be sources is given in Reference 10; however, for this study the impurities were replaced with plutonium metal to maximize the quantity of α -producing material present in the calculations.

Table 5-11. Bounding Pu Isotope Mass Fraction Used in This Study

| Isotope | Mass Fraction | Mass (g) |
|---------|-------------------|-------------------|
| Pu-236 | 2E-7 | 0.00026 |
| Pu-238 | 0.04 | 52 |
| Pu-239 | 1.00 | 1300 |
| Pu-240 | 0.40 | 520 |
| Pu-241 | 0.15 | <195 ^a |
| Pu-242 | 0.10 | 130 |
| Am-241 | 0.15 ^a | <195 ^a |
| Total | 1.69 ^b | 2197 |

^a The initial Am-241 is assumed to be zero, with 195 g of Pu-241. The time-varying source is optimized such that the maximum dose is computed with respect to the decay of Pu-241 to Am-241.

^b As a conservative assumption, the mass fractions are allowed to exceed unity. The package is limited to 1300 g, although the source is based on 2197 g. In addition, the heat load is limited to 25 watts, while the source is based on a heating of about 40 watts.

Table 5-12. Estimation of Degree of Overprediction in Bounding Pu Source Used in This Study

| Case | Neutron Source (neutrons/s) | Gamma Source (photons/s) |
|-----------------------------|--------------------------------|-----------------------------|
| Bounding source | 1.950E+6 | 9.517E+12 |
| Typical source ^a | 3.241E+5 | 2.623E+11 |
| Ratio bounding/typical | 6.0 | 36.3 |

^a Case based on 1300 g of Pu with isotopic distribution corresponding to source scenario "N_Reactor 2 GWd/t" in Table 5-12 with the following impurities: 200 ppm each of Be, Li, B, F, Al, and Si; 300 ppm of Na; 500 ppm each of C and Mg.

In order to arrive at the total neutron source to be used in these shielding studies, the per-unit-area sources given in Table 5-13 require a bounding contact surface area. The value used in this study assumes that the diameter of the TB-1 container (a radius of 5.4 cm is given in Table 5-5) provides a bounding surface area of 91 cm². Thus, the sources loaded into the PAT-1 package under this analysis must have total contact surface areas equal to or less than this area.

Table 5-13. Pu/Be Source Specification Used in This Study

| Isotope | Mass Fraction | Atom Fraction | Neutron Source for Pure Isotope (n/s/cm ²) |
|---------|---------------------|---------------|--|
| Pu-238 | 0.0005 | 0.0005 | 65,000 |
| Pu-239 | 0.9235 | 0.9238 | 171.85 |
| Pu-240 | 0.0650 | 0.0648 | 637.58 |
| Pu-241 | 0.0000 ^a | 0.0000 | 5.36 |
| Pu-242 | 0.0010 | 0.0010 | 8.53 |
| Am-241 | 0.0100 | 0.0099 | 13,000 |
| Total | 1.0000 | 1.0000 | 363 ^b |

^a The Pu-241 is assumed to be completely decayed to Am-241 to bound the source for the typical material isotopes expected to be shipped.

^b This neutron source value is the basis for the Pu/Be source shielding calculations in this section. The value is obtained by multiplying the mass fraction values in column 2 by the neutron source for pure isotope values in column 4 and summing over all isotopes. A source with mass fractions that differ from those in this table can be shipped if the estimated source is less than this value with allowance for decay. Typical Pu/Be source materials should fit this specification provided the Pu-238 content is 0.4 wt % or less.

The mass of Pu material loaded into the package must also be bounded: the same value used in the criticality analysis, 200 g of plutonium metal, is assumed. Using a mass of 200 g and the default full density of α -phase plutonium metal (Reference 2 gives a density of 19.84 g/cc), the dimensions of this sphere can be calculated for use in the shielding studies: a sphere of full-density, α -phase plutonium metal with a mass of 200 g will have a radius of 1.34 cm. A spherical source of this dimension with offset distances corresponding to the package surface and 1 m from the package surface was used in the shielding analyses.

As described above, the shielding model for the Pu/Be source study was a sphere with radius of 1.34 cm containing full-density, α -phase plutonium metal. The rest of the PAT-1 package is conservatively omitted from the analysis. The offset distances used for the package surface and 1-m dose values were determined from the values in Table 5-5; the minimum distance from a source to the surface detector along the cask side is specified as the difference in radii for bodies 15 and 1 ($28.73 - 5.4 = 23.33$ cm). Along the cask bottom, the minimum source-to-detector distance is specified as the difference in bottom locations for bodies 11 and 15 ($48.84 - 20.79 = 28.05$ cm). Along the cask top, the minimum source-to-detector distance is specified as the differences in the top boundaries for bodies 11 and 15 ($99.43 - 48.84 - 41.87 + 20.79 = 29.51$ cm). These top and bottom distances assume that the source rests on the Al spacer material, which is conservative. In addition, because the side detector locations are closer to the source than the top and bottom locations, the side locations are used for side, top, and bottom dose estimates. The 1-m dose location for side, top, and bottom locations is therefore 123.33 cm. These locations are actually minimum distances from the outer surface of the spherical source touching these named bodies, but for conservatism, the code input assumes these distances are from the source center, not the edge.

Table 5-14. Neutron Source Spectrum Used in the Pu/Be Source Shielding Analysis

| Energy Group | Energy Boundaries (eV) | (α ,n) Source Spectrum |
|--------------|------------------------|--------------------------------|
| 1 | 2.000E+7 | 2.90211E-01 |
| 2 | 6.434E+6 | 4.11765E-01 |
| 3 | 3.000E+6 | 2.26912E-01 |
| 4 | 1.850E+6 | 1.91999E-02 |
| 5 | 1.400E+6 | 2.54550E-02 |
| 6 | 9.000E+5 | 2.39615E-02 |
| 7 | 4.000E+5 | 2.58964E-03 |
| 8 | 1.000E+5 | 8.56173E-05 |
| 9 | 1.700E+4 | 3.16844E-06 |
| 10 | 3.000E+3 | 4.29906E-08 |
| 11 | 5.500E+2 | 0.0 |
| 12 | 1.000E+2 | 0.0 |
| 13 | 3.000E+1 | 0.0 |
| 14 | 1.000E+1 | 0.0 |
| 15 | 3.05 | 0.0 |
| 16 | 1.77 | 0.0 |
| 17 | 1.30 | 0.0 |
| 18 | 1.13 | 0.0 |
| 19 | 1.00 | 0.0 |
| 20 | 0.80 | 0.0 |
| 21 | 0.40 | 0.0 |
| 22 | 0.33 | 0.0 |
| 23 | 0.23 | 0.0 |
| 24 | 0.10 | 0.0 |
| 25 | 0.05 | 0.0 |
| 26 | 0.03 | 0.0 |
| 27 | 0.01 | 0.0 |
| | 0.00001 | |
| Total | | 1.000E+00 |

The SAS1 module of the SCALE system, version 5.1³ was used to quantify the dose rates from a Pu/Be source using the source and geometry described above. Briefly, the SAS1 shielding model for both NCT and HAC consisted of an unshielded Pu sphere with a mass of 200 g. The NCT and HAC dose locations were specified as the minimum source-to-detector locations possible. The SAS1 code explicitly accounts for both secondary gamma radiation and subcritical source multiplication. The cross section library was the same SCALE 27N-18COUPLE library used for the other source configurations described in Section 5.4. The flux-to-dose conversion

factors were also the same used for the other source calculations, the ANSI/ANS 6.1.1-1977 standard. See Section 5.5.4 for a listing of the inputs for SAS1 and SOURCES4C.

The results for the Pu/Be source analysis are given in Table 5-15. The full-density results under conservative conditions show that the doses from the Pu/Be sources described herein are well below those of the other contents considered in Sections 5.2 through 5.4. The maximum total doses for the Pu/Be sources shown in Table 5-15 are 28, 41, and 88 times less than the limiting cases shown in Table 5-1 for NCT surface, NCT 1-m, and HAC 1-m locations respectively. The plutonium metal used in the Pu/Be sources also has a natural component of radiation; however, the Pu mass limit of 200 g for the Pu/Be sources is a factor of 6 lower in mass than the metal-only limits. The conservatisms built into this Pu/Be source analysis include the following:

1. PAT-1 packaging is ignored.
2. Both sides of a Pu/Be disk are assumed to have contact surface areas.
3. Complete decay of Pu-241 to Am-241 is assumed.
4. The minimum source-to-detector distance is used for the surface and 1-m dose locations. The center of the source is assumed to contact the innermost package boundary.
5. No α barrier is included in the calculations, although one is physically present in the sources to be shipped.
6. Comparisons of void source material to full-density sources in the shielding analysis indicate that doses for full-density material are higher due to source multiplication. Comparison of α - and δ -phase Pu also indicated that higher densities produced higher dose estimates.
7. In the shielding model, the source containing Pu was assumed to contain 100% Pu-239 to maximize the source subcritical multiplication.

It can therefore be concluded that the addition of Pu/Be sources as allowable contents of the PAT-1 package have no influence on the limiting dose results given in Table 5-1.

Table 5-15. Dose Results for Pu/Be Source Content

| Case description | Detector location for top, bottom, or side geometry | Neutron dose (gamma dose) mrem/h | Total dose, doubled ^a mrem/h |
|----------------------------------|---|----------------------------------|---|
| Full-density, α -phase Pu | surface | 0.838 (0.004) | 1.68 |
| | 1 m | 0.030 (0.0001) | 0.06 |
| Voided source | surface | 0.680 (1e-8) | 1.36 |
| | 1 m | 0.024 (1e-9) | 0.05 |

^a Dose rates for a doubled case are given to account for the possible rearrangement of multiple Pu/Be sources such that both sides of the Pu surface come in contact with the Be material, doubling the radiation emitted. The comparison of doubled doses to regulatory limits effectively allows the summing of contact surface areas from multiple disks without regard to possible restacking. For example, while a single disk would only have a surface area corresponding to the actual contact area between the Pu and Be, two disks could properly align such that there were three contact surfaces, and three disks could properly align such that there were five contact surfaces. By applying a factor of two, only the actual contact areas for individual sources or multiple sources need to be considered.

5.5.4 List of Various Code Inputs

The ORIGEN-S computer code calculates the neutron and gamma source based on the initial loadings of each isotope as specified in Table 5-2. The code then generates the neutron and gamma spectrum in the specified SCALE 27 neutron and 18 gamma group structures for a series of decay times. The case below determines the sources at the following decay times: 0.1, 0.3, 1, 3, 10, 18, 30, 50, 75, and 100 years.

Code Listing 5-1 ORIGEN-S Input

```
'This SCALE input file was generated by
'OrigenArp Version 5.1 October 27, 2006
#origens
0$$ all 71 e t
Decay Case
3$$ 21 1 1 27 a16 2 a33 18 e t
35$$ 0 t
54$$ a8 1 a11 0 e
56$$ a2 10 a6 1 a10 0 a13 6 a14 5 a15 3 a17 2 e
57** 0 a3 1e-05 e
95$$ 0 t
Case 1
0 MTU
60** 0.1 0.3 1 3 10 18 30 50 75 100
61** f0.05
65$$
'Gram-Atoms Grams Curies Watts-All Watts-Gamma
3z 1 0 0 3z 3z 3z 6z
3z 1 0 0 3z 3z 3z 6z
3z 1 0 0 3z 3z 3z 6z
81$$ 2 0 26 1 a7 200 e
82$$ 2 2 2 2 2 2 2 2 2 e
83**
1.0000000e+07 8.0000000e+06 6.5000000e+06 5.0000000e+06 4.0000000e+06
```

```

3.0000000e+06 2.5000000e+06 2.0000000e+06 1.6600000e+06 1.3300000e+06
1.0000000e+06 8.0000000e+05 6.0000000e+05 4.0000000e+05 3.0000000e+05
2.0000000e+05 1.0000000e+05 5.0000000e+04 1.0000000e+04 e
84**
2.0000000e+07 6.4340000e+06 3.0000000e+06 1.8500000e+06
1.4000000e+06 9.0000000e+05 4.0000000e+05 1.0000000e+05 1.7000000e+04
3.0000000e+03 5.5000000e+02 1.0000000e+02 3.0000000e+01 1.0000000e+01
3.0499900e+00 1.7700000e+00 1.2999900e+00 1.1299900e+00 1.0000000e+00
8.0000000e-01 4.0000000e-01 3.2500000e-01 2.2500000e-01 9.9999850e-02
5.0000000e-02 3.0000000e-02 9.999980e-03 1.0000000e-05 e
73$$ 942360 942380 942390 942400 942410 942420
74** 0.00026 52 1300 520 195 130
75$$ 2 2 2 2 2 2
t
56$$ 0 0 a10 1 e t
56$$ 0 0 a10 2 e t
56$$ 0 0 a10 3 e t
56$$ 0 0 a10 4 e t
56$$ 0 0 a10 5 e t
56$$ 0 0 a10 6 e t
56$$ 0 0 a10 7 e t
56$$ 0 0 a10 8 e t
56$$ 0 0 a10 9 e t
56$$ 0 0 a10 10 e t
56$$ f0 t
end
=opus
LIBUNIT=21
TYPARAMS=NUCLIDES
UNITS=WATTS
LIBTYPE=ALL
TIME=YEARS
NPOSITION=1 2 3 4 5 6 7 8 9 10 end
End
=shell
[command to copy file ft71f001 to a local directory]
end

```

The Shielding Analysis Sequence #4 (SAS4) code reads the shielding problem definitions from a single input stream, then proceeds to automatically execute the BONAMI, NITAWL, XSDRNPM, and MORSE-SCG computer codes in sequence. The SCALE driver software reads the single input stream and prepares individual inputs for each of the above codes, automatically executes each code, and then collects all output into a common output file. The source file written by the ORIGEN-S code with the input stream shown in Code Listing 5-1 is copied into the ft30f001 file just prior to execution as described in the first =shell input shown in Code Listing 5-2.

The input options for SAS4 were carefully chosen to ensure accurate dose estimates. The radial calculations along the package side utilize the IDR=0 option with full automated biasing as well as point detectors because the code is fully applicable under these conditions. The axial calculations for the package top and bottom used the IDR=2 option and effectively turned off the automated biasing (note all void materials in the one-dimensional adjoint model). The axial biasing produces inaccurate results for a nonsymmetric axial model because the SAS4 code is designed to bias particles in opposite directions above and below the model axial centerline. The effective removal of the automated biasing allows the underlying MORSE-SCG code to run

without the axial symmetry requirement. The accuracy of these results was tested by comparison to another SCALE module under development that removes these limitations.

Code Listing 5-2 SAS4 Input Stream for NCT Reduced-Density Smeared Cylinder Source (radial side gamma)

```
=shell
[copy ORIGEN-S ft71f001 output file previously saved to file named ft30f001]
end
'Input generated by Espn 5.1 Compiled on 8-07-2006
=sas4      parm=size=1000000
pat-1 pu large cyl 3d case
27n-18couple infhommedium
pu 1 den=0.818 1 300 end
redwood 3 den=0.36 1 300 end
aluminum 4 den=2.6989 1 300 end
ss304 5 den=7.9 1 300 end
copper 6 den=8.94 1 300 end
mgconcrete 7 1 300 end
arbmph13-8mo 7.5 5 0 0 0 24000 12.75 28000 8 13000 1.125 42000 2.25
26000 75.875 2 1 300 end
end comp
izm=6 mhw=2 frd=5.4 end
5.4 6.8 13.97 15.24 28.58 28.73 end
1 2 0.4 3 5 end
xend
ran=000003600621 tim=1200 nst=4000 nmt=12000 nit=900 nco=4 ist=0 ipr=0
iso=0 nod=16 sfa=9.517e+12 igo=4 inb=0 ine=0 mfu=2 isp=6 ipf=0 isd=4
nda=1000 end
det 30 0 0 30 0 2 30 0 4 30 0 6 30 0 8 30 0 10 30 0 15 30 0 20
128.7 0 0 128.7 0 5 128.7 0 10 128.7 0 15 128.7 0 20 128.7 0 25 128.7 0 30
128.7 0 35 end
sxy 1 -5.4 5.4 -5.4 5.4 0 10 100 100 100 100 end
gend
shielding problem
0 0 0 0
rcc 0 0 -5.64 0 0 15.11 5.40
sph 0 0 -3.74 5.72
rcc 0 0 -5.64 0 0 16.71 6.795
sph 0 0 -3.74 7.12
rcc 0 0 -5.64 0 0 16.71 10
rcc 0 0 -10.86 0 0 21.93 6.875
rcc 0 0 -18.25 0 0 7.39 6.875
rcc 0 0 -18.25 0 0 20.32 7.52
rcc 0 0 2.07 0 0 9 8.74
rcc 0 0 -18.25 0 0 36.79 13.97
rcc 0 0 -20.79 0 0 41.87 13.97
rcc 0 0 -30.35 0 0 60.81 13.97
rcc 0 0 -30.35 0 0 60.81 15.24
rcc 0 0 -48.69 0 0 99.13 28.58
rcc 0 0 -48.84 0 0 99.43 28.73
sph 0 0 0 300
rcc 0 0 -2.936 0 0 5.872 4.032
rcc 0 0 -2.936 0 0 5.872 4.445
end
src +1
src +2 -3
tbl +3 -1
tbl +4 -2 -5
vod +6 -5 -4 or 6 5 8 -3
wod +7 -6
```

```

cop +8 -7 -6
vod +9 -3
wod +10 -9 -8
alu +11 -10
wod +12 -11
alu +13 -12
wod +14 -13
drm +15 -14
vod +16 -15
exv -16
end
1 1 1 1 1 1 1 1 1 1 1 1 1 1 1
0 0 0 0 0 0 0 0 0 0 0 0 0 0 0
1 1 2 2 1000 1000 6 1000 1000 4 3 4 3 5 1000 0
0

```

End

Code Listing 5-3 SAS4 Input Stream for NCT Reduced-Density Smearred Cylinder Source (radial side neutron)

```

=shell
[copy ORIGEN-S ft71f001 output file previously saved to file named ft30f001]
end
'Input generated by Espn 5.1 Compiled on 8-07-2006
=sas4      parm=size=1000000
pat-1 pu large cyl 3d case
27n-18couple infhommedium
pu 1 den=0.818 1 300 end
redwood 3 den=0.36 1 300 end
aluminum 4 den=2.6989 1 300 end
ss304 5 den=7.9 1 300 end
copper 6 den=8.94 1 300 end
mgconcrete 7 1 300 end
arbmph13-8mo 7.5 5 0 0 0 24000 12.75 28000 8 13000 1.125 42000 2.25
26000 75.875 2 1 300 end
end comp
ity=1 irf=9029 izm=6 mhw=2 frd=5.4 end
5.4 6.8 13.97 15.24 28.58 28.73 end
1 2 0 4 3 5 end
xend
ran=000003600621 tim=1200 nst=4000 nmt=12000 nit=200 nco=4 ist=0 ipr=0
iso=0 nod=16 sfa=1.95e+6 igo=4 inb=0 ine=0 mfu=2 isp=7 ipf=0 isd=4
nda=1000 end
det 30 0 0 30 0 2 30 0 4 30 0 6 30 0 8 30 0 10 30 0 15 30 0 20
128.7 0 0 128.7 0 5 128.7 0 10 128.7 0 15 128.7 0 20 128.7 0 25 128.7 0 30
128.7 0 35 end
sxy 1 -5.4 5.4 -5.4 5.4 0 10 100 100 100 100 end
gend
shielding problem
0 0 0 0
rcc 0 0 -5.64 0 0 15.11 5.40
sph 0 0 -3.74 5.72
rcc 0 0 -5.64 0 0 16.71 6.795
sph 0 0 -3.74 7.12
rcc 0 0 -5.64 0 0 16.71 10
rcc 0 0 -10.86 0 0 21.93 6.875
rcc 0 0 -18.25 0 0 7.39 6.875
rcc 0 0 -18.25 0 0 20.32 7.52
rcc 0 0 2.07 0 0 9 8.74
rcc 0 0 -18.25 0 0 36.79 13.97
rcc 0 0 -20.79 0 0 41.87 13.97

```

```

rcc 0 0 -30.35 0 0 60.81 13.97
rcc 0 0 -30.35 0 0 60.81 15.24
rcc 0 0 -48.69 0 0 99.13 28.58
rcc 0 0 -48.84 0 0 99.43 28.73
sph 0 0 0 300
rcc 0 0 -2.936 0 0 5.872 4.032
rcc 0 0 -2.936 0 0 5.872 4.445
  end
src +1
src +2 -3
tbl +3 -1
tbl +4 -2 -5
vod +6 -5 -4 or 6 5 8 -3
wod +7 -6
cop +8 -7 -6
vod +9 -3
wod +10 -9 -8
alu +11 -10
wod +12 -11
alu +13 -12
wod +14 -13
drm +15 -14
vod +16 -15
exv -16
  end
1 1 1 1 1 1 1 1 1 1 1 1 1 1 1
0 0 0 0 0 0 0 0 0 0 0 0 0 0 0
1 1 2 2 1000 1000 6 1000 1000 4 3 4 3 5 1000 0
0

```

End

Code Listing 5-4 SAS4 Input Stream for NCT Reduced-Density Smear Cylinder Source (axial top neutron)

```

=shell
[copy ORIGEN-S ft71f001 output file previously saved to file named ft30f001]
end
'Input generated by Espn 5.1 Compiled on 8-07-2006
=sas4      parm=size=1000000
pat-1 pu large cyl top 3d case
27n-18couple infhommedium
pu 1 den=0.818 1 300 end
redwood 3 den=0.36 1 300 end
aluminum 4 den=2.6989 1 300 end
ss304 5 den=7.9 1 300 end
copper 6 den=8.94 1 300 end
mgconcrete 7 1 300 end
arbmph13-8mo 7.5 5 0 0 0 24000 12.75 28000 8 13000 1.125 42000 2.25
26000 75.875 2 1 300 end
end comp
idr=2 ity=1 irf=9029 izm=6 mhw=2 frd=5.4 end
9.46 11.06 18.54 21.08 50.44 50.59 end
0 0 0 0 0 0 end
xend
ran=000003600621 tim=1200 nst=4000 nmt=12000 nit=1000 nco=4 ist=0 ipr=0
iso=0 nod=7 sfa=1.95e+6 igo=4 inb=0 ine=0 mfu=2 isp=7 ipf=0 isd=4
nda=1000 end
det 0 0 52 2 0 52 4 0 52 6 0 52
0 0 150.59 5 0 150.59 10 0 150.59 end
sxy 1 -5.4 5.4 -5.4 5.4 0 10 100 100 100 100 end
gend

```

```

shielding problem
0 0 0 0
rcc 0 0 -5.64 0 0 15.11 5.40
sph 0 0 -3.74 5.72
rcc 0 0 -5.64 0 0 16.71 6.795
sph 0 0 -3.74 7.12
rcc 0 0 -5.64 0 0 16.71 10
rcc 0 0 -10.86 0 0 21.93 6.875
rcc 0 0 -18.25 0 0 7.39 6.875
rcc 0 0 -18.25 0 0 20.32 7.52
rcc 0 0 2.07 0 0 9 8.74
rcc 0 0 -18.25 0 0 36.79 13.97
rcc 0 0 -20.79 0 0 41.87 13.97
rcc 0 0 -30.35 0 0 60.81 13.97
rcc 0 0 -30.35 0 0 60.81 15.24
rcc 0 0 -48.69 0 0 99.13 28.58
rcc 0 0 -48.84 0 0 99.43 28.73
sph 0 0 0 300
rcc 0 0 -2.936 0 0 5.872 4.032
rcc 0 0 -2.936 0 0 5.872 4.445
end
src +1
src +2 -3
tbl +3 -1
tbl +4 -2 -5
vod +6 -5 -4 or 6 5 8 -3
wod +7 -6
cop +8 -7 -6
vod +9 -3
wod +10 -9 -8
alu +11 -10
wod +12 -11
alu +13 -12
wod +14 -13
drm +15 -14
vod +16 -15
exv -16
end
1 1 1 1 1 1 1 1 1 1 1 1 1 1 1
0 0 0 0 0 0 0 0 0 0 0 0 0 0 0
1 1 2 2 1000 1000 6 1000 1000 4 3 4 3 5 1000 0
0

end

```

Code Listing 5-5 SAS4 Input Stream for HAC Reduced-Density Smearred Cylinder Source (radial gamma)

```

=shell
[copy ORIGEN-S ft71f001 output file previously saved to file named ft30f001]
end
'Input generated by Espn 5.1 Compiled on 8-07-2006
=sas4      parm=size=1000000
pat-1 pu large cyl 3d case
27n-18couple infhommedium
pu 1 den=0.818 1 300 end
redwood 3 den=0.36 1 300 end
aluminum 4 den=2.6989 1 300 end
ss304 5 den=7.9 1 300 end
copper 6 den=8.94 1 300 end
mgconcrete 7 1 300 end
arbmph13-8mo 7.5 5 0 0 0 24000 12.75 28000 8 13000 1.125 42000 2.25

```

```

26000 75.875 2 1 300 end
end comp
izm=6 mhw=2 frd=5.4 end
5.4 6.8 13.97 15.24 28.58 28.73 end
1 2 0 0 0 0 end
xend
ran=000003600621 tim=1200 nst=4000 nmt=12000 nit=900 nco=4 ist=0 ipr=0
iso=0 nod=10 sfa=9.517e+12 igo=4 inb=0 ine=0 mfu=2 isp=6 ipf=0 isd=4
nda=1000 end
det 106.8 0 0 106.8 0 5 106.8 0 10 106.8 0 15 106.8 0 20 106.8 0 25 106.8 0 30
106.8 0 35 0 0 -110.98 0 0 111.06 end
sxy 1 -5.4 5.4 -5.4 5.4 0 10 100 100 100 100 end
gend
shielding problem
0 0 0 0
rcc 0 0 -5.64 0 0 15.11 5.40
sph 0 0 -3.74 5.72
rcc 0 0 -5.64 0 0 16.71 6.795
sph 0 0 -3.74 7.12
rcc 0 0 -5.64 0 0 16.71 10
rcc 0 0 -10.86 0 0 21.93 6.875
rcc 0 0 -18.25 0 0 7.39 6.875
rcc 0 0 -18.25 0 0 20.32 7.52
rcc 0 0 2.07 0 0 9 8.74
rcc 0 0 -18.25 0 0 36.79 13.97
rcc 0 0 -20.79 0 0 41.87 13.97
rcc 0 0 -30.35 0 0 60.81 13.97
rcc 0 0 -30.35 0 0 60.81 15.24
rcc 0 0 -48.69 0 0 99.13 28.58
rcc 0 0 -48.84 0 0 99.43 28.73
sph 0 0 0 300
rcc 0 0 -2.936 0 0 5.872 4.032
rcc 0 0 -2.936 0 0 5.872 4.445
end
src +1
src +2 -3
tbl +3 -1
tbl +4 -2 -5
vod +6 -5 -4 or 6 5 8 -3
wod +7 -6
cop +8 -7 -6
vod +9 -3
wod +10 -9 -8
alu +11 -10
wod +12 -11
alu +13 -12
wod +14 -13
drm +15 -14
vod +16 -15
exv -16
end
1 1 1 1 1 1 1 1 1 1 1 1 1 1 1 1
0 0 0 0 0 0 0 0 0 0 0 0 0 0 0 0
1 1 2 2 1000 1000 1000 1000 1000 1000 1000 1000 1000 1000 1000 0
0
end

```

The Shielding Analysis Sequence #1 (SAS1) code reads the shielding problem definitions from a single input stream, then proceeds to automatically execute the BONAMI, NITAWL, XSDRNPM, and XSDOSE computer codes in sequence. The SCALE driver software reads the single input stream and prepares individual inputs for each of the above codes, automatically

executes each code, and then collects all output into a common output file. The (α ,n) source description written by the SOURCES4C code with the input stream shown in Code Listing 5-6 is entered by hand into the SAS1 input stream.

Code Listing 5-6 SAS1 Input Stream for Pu/Be spherical source with full density alpha-Pu metal

```
=sas1  parm=nitawl
pube neutron source alpha phase - no void
27n-18couple  infhommedium
plutoniumalp 1 1.0 293 end
end comp
end
last
neutron case
spherical
1 1.34 1 -1 0 0 3304 0
end zone
2.90211e-1 4.11765e-1 2.26912e-1 1.91999e-2 2.54550e-2
2.39615e-2 2.58964e-3 8.56173e-5 3.16844e-6 4.29906e-8
17z 18z
ndetec=2
read xsdose
23.33 123.33
end
```

The SOURCES4C code is designed to predict the (α ,n) source generation for homogenous and interface problems. This analysis uses the interface option to determine the (α ,n) source per unit area of contact between the α generator and a target nucleus. In this case, the α generator is plutonium metal and the target material is Be. The code can output the neutron source in any group structure; in this case, the 27-group structure used in SCALE is specified and the source spectrum from SOURCES4C is used directly in the SAS1 case shown above.

Code Listing 5-7 SOURCES4C Input Stream for Pu-Be Interface Source Problem

```
WPu-Be Interface Problem
2 2 1
2 0 6.50 0.0000001
 94 0.99
 95 0.01
100
5
 942380 0.0005
 942390 0.9238
 942400 0.0648
 942420 0.0010
 952410 0.0099
target is composed of Be
1 0
 4 1.0
-27 20.0 1e-11
20 6.43 3 1.85 1.4 0.9 0.4 0.1 0.017 0.003 0.00055
1e-4 3e-5 1e-5 3.05e-6 1.77e-6 1.3e-6 1.13e-6 1e-6
8e-7 4e-7 3.25e-7 2.25e-7 1e-7 5e-8 3e-8 1e-8
1 4000
 40090 1.0
```

6. CRITICALITY EVALUATION

This section describes the criticality evaluation for incorporating plutonium (Pu) metal as a new payload for the PAT-1 package. The Pu metal is packed in an inner container (*T-Ampoule Assembly*,* Drawing 2A0261, designated the T-Ampoule) that replaces the PC-1 inner container. The T-Ampoule and associated Pu metal content packing configurations are described in Section 1.2.1 and Section 1.2.2 of this addendum, respectively.

This section was written to meet the applicable requirements of 10 CFR Part 71, "*Packaging and Transportation of Radioactive Material*," and to be consistent with the guidance provided in U.S. Nuclear Regulatory Commission, Office of Nuclear Regulatory Research, Regulatory Guide 7.9, Rev. 2, "*Standard Format and Content of Part 71 Applications for Approval of Packages for Radioactive Material*," dated March 2005. The section also considers the recommendations provided in NUREG/CR-5661, ORNL/TM-11936, "*Recommendations for Preparing the Criticality Safety Evaluation of Transportation Packages*," U.S. Nuclear Regulatory Commission, Oak Ridge National Laboratory, March 1997.¹

6.1 Description of Criticality Design

6.1.1 Design Features

The primary feature important for criticality control is the ability of the TB-1 containment vessel to retain the fissile material under normal and hypothetical accident conditions (HAC).

Retention of the fissile material within the approximately 1.5-liter (0.4 gallon) inner volume of the TB-1 limits the quantity of water available for neutron moderation. As discussed in Sections 4.2 and 4.3 of this addendum, containment integrity is maintained for both normal conditions of transport and under hypothetical accident conditions. No credit is taken in the criticality safety analysis for containment integrity of material packages designed to be transported by air.

Credit is taken for some spacing provided by the package in the criticality safety analysis of package arrays for normal conditions of transport and under hypothetical accident conditions. No criticality control credit is taken for the packaging inside the TB-1. Such packaging may include sample holders and containers, structural supports, tantalum foil, plastic bagging, etc. Instead, the criticality analysis for all normal and hypothetical accident conditions considered optimum water moderation to the extent achievable within the TB-1 containment vessel. This approach eliminates the need for controls limiting the quantity of hydrogenous packaging materials (e.g., plastic bagging) that may be used within the TB-1 containment vessel.

The optimum H/Pu ratio cannot be achieved within the TB-1 unless plutonium (Pu) quantities are less than 1300 g (2.87 lb). Note that a plutonium quantity of 1300 g represents a conservative upper bound for analysis and is greater than the payload quantities shown in Table 1-1 of Section 1.2.2.1 of this addendum. Results presented later in this section show that removing Pu and adding water results in significantly lower k_{eff} values.

* Note: The drawing titles are in italics and are used interchangeably with the designated names in this addendum. See Section 1.3.2 in this addendum and Chapter 9 in the SAR² for drawing number, title, and revision.

6.1.2 Summary Table of Criticality Evaluation

Table 6-1 is a summary table of the criticality evaluation.

Table 6-1. Summary Table of Criticality Evaluation Results

| Case | Number of Packages | Internal Moderation ^a | Array size | $k_{eff} \pm \sigma^b$ | Bias ^c (Δk) | Upper Subcritical Limit ^d |
|-----------------|--------------------|----------------------------------|-----------------------------|------------------------|----------------------------------|--------------------------------------|
| <i>cv001</i> | 1 | 0 | 1 ^e | 0.6565 ± 0.0005 | 0 | 0.8893 |
| <i>cv031</i> | 1 | 0.956 | 1 ^e | 0.7076 ± 0.0006 | 0 | 0.9383 |
| <i>fhlsf001</i> | 2646 | 0 | $19 \times 15.5 \times 9^f$ | 0.6509 ± 0.0005 | 0 | 0.8893 |
| <i>fslsf031</i> | 2601 | 0.956 | $17 \times 17 \times 9^g$ | 0.6337 ± 0.0005 | 0 | 0.9396 |
| <i>hexsdry</i> | 1152 | 0.956 | $18 \times 10.7 \times 6^h$ | 0.7027 ± 0.0007 | 0 | 0.9351 |
| <i>hexs100</i> | 1152 | 0.956 | $18 \times 10.7 \times 6^h$ | 0.7154 ± 0.0005 | 0 | 0.9396 |
| <i>sph14</i> | 1 | 0.956 | 1 ⁱ | 0.7147 ± 0.0005 | 0 | 0.9383 |

^a Internal moderation is the specific gravity of the water mixed with the Pu-239.

^b KENO V.a calculated k_{eff} and one standard deviation values.

^c As noted in Section 6.8.2.7, the average k_{eff} value for each validation set was greater than 1.0, resulting in positive biases, which were discarded (i.e., no credit taken for positive bias).

^d From Section 6.8.2.7, Table 6-7.

^e Normal conditions, single package, see Section 6.3.4.1.

^f Normal conditions, close-packed hexagonal-pitched array, see Section 6.3.4.2 and Figure 6-10.

^g Normal conditions, close-packed square-pitched array, see Section 6.3.4.2.

^h HAC, close-packed hexagonal-pitched array. See Section 6.3.4.3 and Figure 6-12.

ⁱ Expanded HAC, single package for air transport. See Section 6.3.4.4.

6.1.3 Criticality Safety Index

From preliminary scoping calculations, it was concluded that an infinite array of damaged packages, as described in Section 6.3.1.3, would not be subcritical under optimum moderation conditions. Consequently, a criticality safety index (CSI) value of zero is unattainable. Per 10 CFR 71.59(b), the smallest allowed CSI above zero is 0.1. Assignment of a 0.1 CSI requires an N value of 500, and that 2500 (= 5 × N) undamaged packages, with nothing between the packages, be subcritical and that 1000 (= 2 × N) damaged packages would be subcritical with optimum interspersed hydrogenous moderation.

The CSI for the package was calculated as prescribed by 10 CFR 71.59. The evaluation in Section 6.5 shows that an array of more than 2500 undamaged packages, with nothing between the packages, is subcritical. Thus the value of “N” identified in 10 CFR 71.59 is 500, calculated as 2500 divided by 5. The evaluation in Section 6.6 shows that an array of greater than 2 times N (or 1000) damaged packages would be subcritical with optimum interspersed hydrogenous moderation. As per 10 CFR 71.59, the CSI value is 0.1, which is calculated as 50 divided by N (N=500).

6.2 Fissile Material Contents

6.2.1 Plutonium Metal – General Form

The fissile material loaded into the package will include up to 1300 g (2.87 lb) of plutonium metal. There are no criticality controls on the form or number of pieces of plutonium metal.

There are no criticality controls on the isotopic composition of the Pu. It is assumed, however, that the Pu-240 content exceeds the Pu-241 content. With this assumption, the fissile material is conservatively modeled as 100% Pu-239. The justification for this assumption is that the presence of Pu-241 content greater than Pu-240 content would require expensive isotopic enrichment, generating only milligrams of Pu enriched in Pu-241. The vast majority of Pu present in the world today meets this isotopic composition assumption. Note that of the Pu nuclides that may be present, Pu-241 has the shortest half-life (14.4 years). It then decays to americium (Am-)241, which is included in the Pu mass. Counting the Am-241 as Pu-239 is conservative because it is a parasitic neutron absorber in well moderated systems and, in unmoderated systems, requiring a larger mass (~ 34 kg [75 lb] Am-241) than Pu-239 (~ 5 kg [11 lb] Pu-239) to achieve criticality.

The Pu may be alloyed with other non-neutron-multiplying metals and may also contain trace impurities, typically small fractions of a percent, both of which are conservatively omitted for the criticality analysis. It is conservative to ignore these impurities, which are frequently parasitic neutron absorbers, because modeling them would either have no effect or would reduce k_{eff} (resulting from neutron absorption and scattering). Modeling the presence of alloyed metals and impurities would decrease the density of the fissile material and thus, decrease the volume available for water inside the TB-1 containment vessel. Replacing water with nonfissile alloys or impurities results in lower k_{eff} values for the limiting cases.

There are no criticality controls for the fissile material dimensions other than that it must fit within the TB-1 containment vessel.

There are no criticality controls for the fissile material density. Consequently, the plutonium metal may have a density up to the maximum theoretical density for alpha phase plutonium metal, which is 19.84 g [0.044 lb] Pu/cm³. The criticality analysis considers the full range of Pu density.

While it is anticipated that the Pu will have very low moisture content, no criticality control for the Pu moisture content is required, because it is considered in the criticality analysis that the containment vessel may be fully flooded with water and the Pu may be mixed with and surrounded by water for all normal conditions of transport and hypothetical accident conditions. The water in the TB-1 vessel is included as a bounding model for packaging that may be in the TB-1.

For use of the general-forms Pu loading limit (1300 g [2.87 lb] Pu maximum), presence of neutron-multiplying materials (e.g., beryllium (Be), normal or depleted uranium) within the TB-1 vessel is not permitted.

6.2.2 Plutonium Metal – Pu/Be Sources

Loading of the TB-1 vessel may include Pu/Be sources, subject to the following limits/restrictions:

- The maximum mass of Pu metal or alloy present is 200 g (0.44 lb), as one or more pieces/parts with no restriction on shape or density. The primary Pu isotope present is Pu-239 and the Pu-240 content must exceed the Pu-241 content.
- The maximum mass of beryllium present is 30 g (0.066 lb) and (except for the Pu) no other neutron multiplying materials (e.g., normal or depleted uranium) are permitted within the TB-1 vessel.

As for the general-form Pu contents, the Nuclear Criticality Safety (NCS) evaluation for the Pu/Be sources assumes that the TB-1 containment vessel contents may include water (up to full flooding) for all normal conditions of transport and hypothetical accident conditions. Thus, the NCS evaluation for Pu/Be source contents assumes a model which bounds packaging material that may be present as part of the Pu/Be source loading. Note that the quantity of Pu/Be evaluated in this section is an upper bound for analysis and is less than that specified in Table 1-1 of Section 1.2.2.1 of this addendum.

6.3 General Considerations

6.3.1 Model Configuration

Of the two permitted loadings for the PAT-1 package (Pu metal in general form or Pu/Be sources), the general-form 1300 g (2.87 lb) Pu metal limit is the limiting case for NCS evaluation purposes. For Pu/Be source loadings, both the Pu and Be are restricted to much smaller mass limits (200 g [0.44 lb] Pu alloy, 30 g [0.066 lb] Be). If the Be is replaced with Pu metal on either a mass or volume basis (for NCS modeling purposes), the resulting NCS models contain far less than the 1300 g (2.87 lb) Pu general-form metal loading limit. Thus, this and subsequent Section 6 sections evaluate the PAT-1 package with 1300 g (2.87 lb) Pu metal as the most reactive, most limiting case for NCS purposes. Section 6.9.6 provides additional justification that the Pu/Be source loading is bounded by considerations for the 1300 g (2.87 lb) general-form Pu metal loading.

Several computational models were used in the criticality analysis. The package models include a detailed model constructed using nominal dimensions, five variations of a simplified model, and two post-testing simplified models used for analysis of HAC. In the base simplified model (Model 1), the steel outer container, redwood, and steel TB-1 containment vessel are modeled. Variations on the base simplified model include:

- Models in which the redwood density was varied $\pm 20\%$ of the nominal redwood density;
- A model in which the redwood is replaced with full density water; and
- A model in which the outer container steel, redwood, and TB-1 steel are all replaced with water.

A detailed model was used to confirm that the simplified models in which the redwood is replaced with water are conservative representations of the PAT-1 package. These models are discussed in Sections 6.3.1.1 and 6.3.1.2. The post-testing simplified models used to analyze damaged package arrays from a hypothetical accident condition are discussed in Section 6.3.1.3.

Except for a few sensitivity calculations, in which water inside the TB-1 but outside a plutonium metal sphere was removed to quantify the reactivity worth of that water, all calculations were performed with the maximum quantity of water that could fit in the TB-1, given the quantity of Pu also present. The maximum quantity of water was included to provide a conservative model for the packaging, some of which may be hydrogenous, within the TB-1. Comparison of cases *sudma* and *sudmb* show that, for this particular model, removing the water in the TB-1 reduced k_{eff} by nearly 10% Δk . The calculations generated to support the criticality analysis show that, due to the limited TB-1 internal volume, the Pu is under moderated in all cases. Other than case *sudma*, all cases included the maximum quantity of water that could fit within the TB-1, given the quantity of plutonium present. Section 6.9.4 includes a list of the cases, excluding the Pu/Be scoping calculations described in Section 6.9.6, used to support the criticality analysis.

6.3.1.1 Detailed Model

A detailed package model was generated using the nominal dimensions and material descriptions provided in the reference drawings.⁴⁻³⁰ Figure 6-1 shows a cutaway view of the detailed model. The load spreader assembly¹⁹ includes a cadmium-plated copper cylinder. The cadmium plating is not modeled. Omitting the cadmium is conservative because it is a strong thermal neutron absorber. Several minor simplifications were made, such as omitting glue, bolts, and other fasteners used to assemble the package.

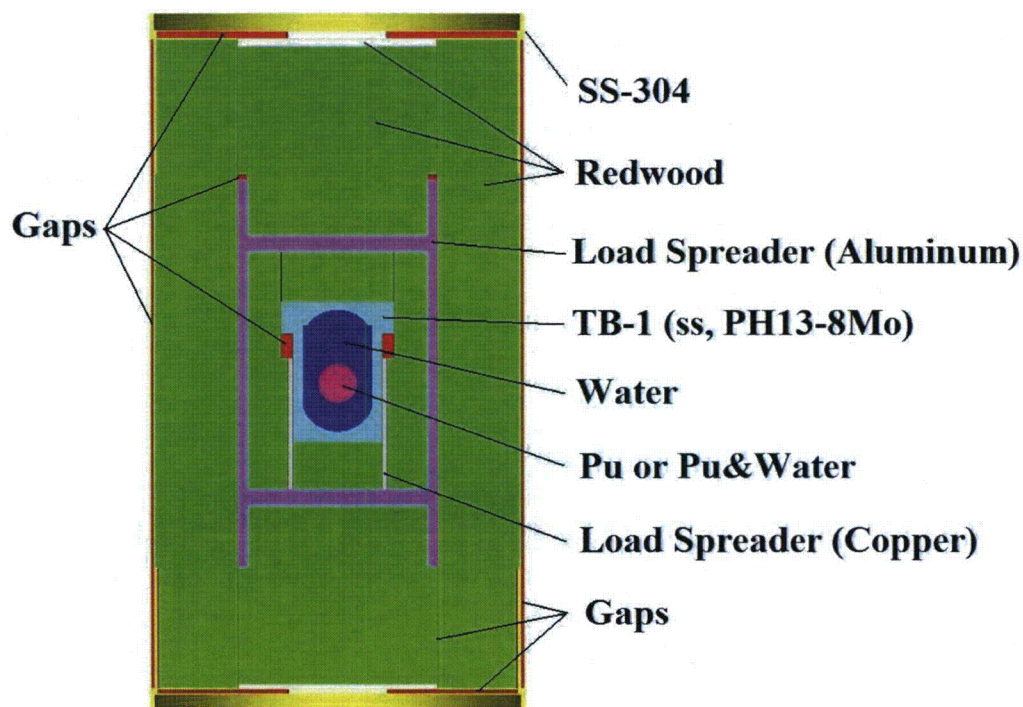


Figure 6-1. Detailed Model of a Single Package

This detailed model was prepared to confirm that the simplified models, which were used to perform most of the parametric studies, are adequately conservative.

6.3.1.2 Simplified Models

The criticality analysis of the single-package normal conditions of transport, single-package hypothetical accident conditions, and normal conditions of transport arrays is based primarily on simplified model calculations. The simplified models were developed using dimensions and materials described in References 4 through 30, and are shown in Figure 6-2. The simplified models were developed as follows:

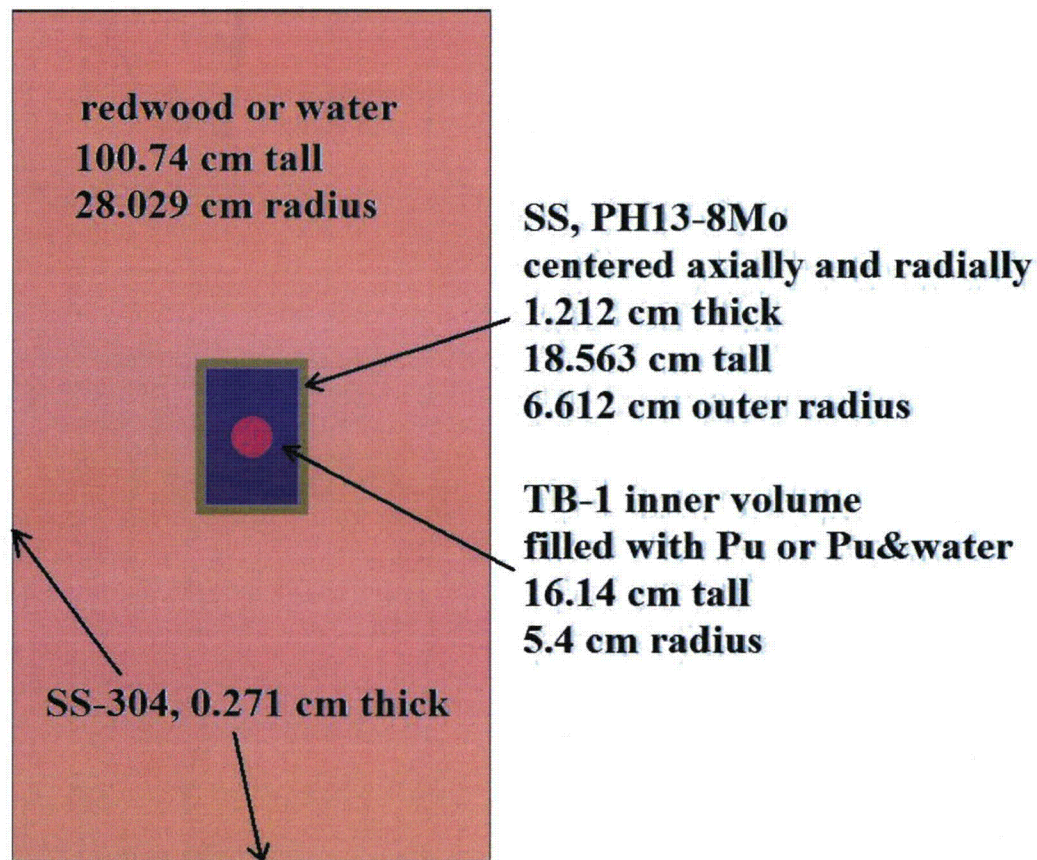


Figure 6-2. Simplified Model of a Single Package

The maximum volume inside the TB-1 containment vessel was calculated to be 1478cm^3 (90.22 in^3). Using the maximum internal volume maximizes the quantity of water that may be present in the fissile material to moderate neutrons. The calculation of this volume is described in Section 45. Use of other containers and supporting structures within the TB-1 are anticipated. If modeled, these other materials would reduce the quantity of water that could be present within the TB-1. As shown in the calculation results and plots presented throughout this section, maximizing the quantity of water mixed with the plutonium within the TB-1 results in a maximum k_{eff} value. The inner volume of the TB-1 was modeled as a cylinder with a radius of 5.400 cm (2.126 in.) and a height of 16.14 cm (6.354 in.). The radius is equivalent to the maximum internal radius for the TB-1, and the height is set so that the maximum internal volume is 1478 cm^3 (90.22 in^3).

The fissile material inside the TB-1 containment vessel is modeled as various mixtures of Pu-239 metal and water. At a density of 19.84 g/cm^3 (0.717 lb/in^3), the 1300 g (2.87 lb) of Pu-239 fills 65.52 cm^3 (3.99 in^3) of the interior volume, leaving 1412 cm^3 (86.16 in^3) of TB-1 internal volume that is modeled as filled with water. The criticality analysis considers various arrangements of the plutonium metal/water mixture surrounded by any unused water. Any of the 1412 cm^3 (86.16 in^3) of water not used in the plutonium metal/water mixture fills the remainder of the TB-1 interior.

The TB-1 containment vessel was modeled as a simple cylinder around the volume described in Figure 6-2. The wall thickness used for the top, bottom, and side was 1.212 cm (0.477 in.). This dimension is the minimum steel thickness identified from the reference drawings and is the minimum distance through the center of the TB-1 lid.

The PAT-1 package includes an internal structure referred to as the load spreader assembly. These components are constructed of aluminum and cadmium-plated copper. In the simplified models, these components and the small gaps between components are replaced with redwood or water, depending on the analysis. See Figure 6-1.

The TB-1 is modeled as surrounded by redwood or water to the minimum outer dimensions of the redwood specified by the reference drawings. The minimum dimensions were used to minimize the center-to-center spacing between drums in array calculations. The TB-1 is surrounded by a cylinder of redwood or water with a radius of 28.029 cm (11.04 in.) and a height of 100.7 cm (39.66 in.).

A review of Reference Drawings⁴⁻³⁰ reveals that the outer steel package is composed of two or more layers of 16-gauge, Type 304 stainless steel. The nominal and minimum thicknesses for 16 gauge steel are 0.15189 cm (0.598 in.) and 0.13538 cm (0.533 in.), respectively.³¹ The last layer of the simplified package model is steel wrapped tightly around the enclosed wood or water region. A steel thickness of 0.271 cm (0.1063 in.) was used in the simplified model. This represents the minimum thickness for two sheets of 16-gauge steel.

For the simplified model used in array calculations, the total package height is 101.28 cm (39.87 in.) and the outer diameter is 56.60 cm (22.28 in.). The drawings describe the package as being approximately 108.58 cm (42.75 in.) tall and the drum body having an outer diameter of approximately 57.15 cm (22.50 in.). The simplified model does not include the top and bottom drum closure rings and does not model the space between the outer covers and the liners on both ends. Omitting these features is conservative because the height and diameter reductions result in more tightly packed arrays, minimizing neutron leakage from arrays.

The conditions of reflection outside the package model vary with the analysis for which the model is being used. For example, full density water reflection is used for the single package analysis. In analysis of arrays for normal conditions of transport, nothing exists between the packages, and the outside of the arrays are reflected with full density water.

For the single-package analysis, calculations performed included a series (Cases *cv001* through *cv038*) in which the outer drum steel and TB-1 steel were replaced with full density water that

extended axially and radially 30 cm (11.81 in.) beyond the Pu and water contained within the TB-1.

For discussion purposes, the simplified model variations used in the analysis are identified as follows.

- Model 1: Base model, redwood modeled at 100% nominal density, TB-1 steel modeled, outer container steel modeled.
- Model 2: Similar to Model 1, except redwood modeled at 80% of nominal density.
- Model 3: Similar to Model 1, except redwood modeled at 120% of nominal density.
- Model 4: Similar to Model 1, except redwood replaced with full density water.
- Model 5: Similar to Model 1, except redwood, TB-1 steel, and outer container steel all replaced with full density water extending axially and radially 30 cm (11.81 in.) beyond the Pu and water contained within the TB-1. This model was used only in the single package analysis.

6.3.1.3 Damaged Container Models

Damaged container models were created for end-impact and side-impact test cases. Dimensions for the end-impact case were taken from Figures 2.18 and 2.30 of NUREG-0361.² Dimensions for the side-impact case were taken from Figure 2.24 of NUREG-0361.²

The model for the end-impact case is basically the normal case simplified model described above, except the outer drum has been shortened from 101.28 cm (39.87 in.) long to 76.2 cm (30 in.) long and the top of the TB-1 containment vessel is located 19.05 cm (7.5 in.) from the top end of the drum. The redwood is modeled with varying densities of water to simulate combustion of the redwood and potential postfire flooding. This model is shown in Figure 6-3.

The model of the side-impact case is a half-cylinder that is 101.28 cm (39.87 in.) long and has an outer diameter of 74.93 cm (29.5 in.). The undamaged TB-1 containment vessel is centered axially and is located immediately adjacent to the center of the flattened side of the drum. The redwood is modeled with varying densities of water to simulate combustion of the redwood and potential postfire flooding. This model is shown in Figure 6-4.

A final damaged container model was created to support evaluation of 10 CFR 71.55, "General requirements for fissile material packages," paragraph (f), which covers fissile material packages transported by air. To meet the requirements of this section, calculations were performed with the TB-1 contents (1300 g [2.87 lb] of Pu-239 and up to 1412 cm³ [86.16 in³] of water) in spheres of varying radii reflected by 20 cm (7.9 in.) of water. The purpose of this model is to show that, provided there is no leakage of water into the TB-1 containment vessel, a single package is subcritical without taking credit for the geometry of the package or the continued presence of any package structural materials. This analysis is discussed in Section 6.7. This model is shown in Figure 6-5.

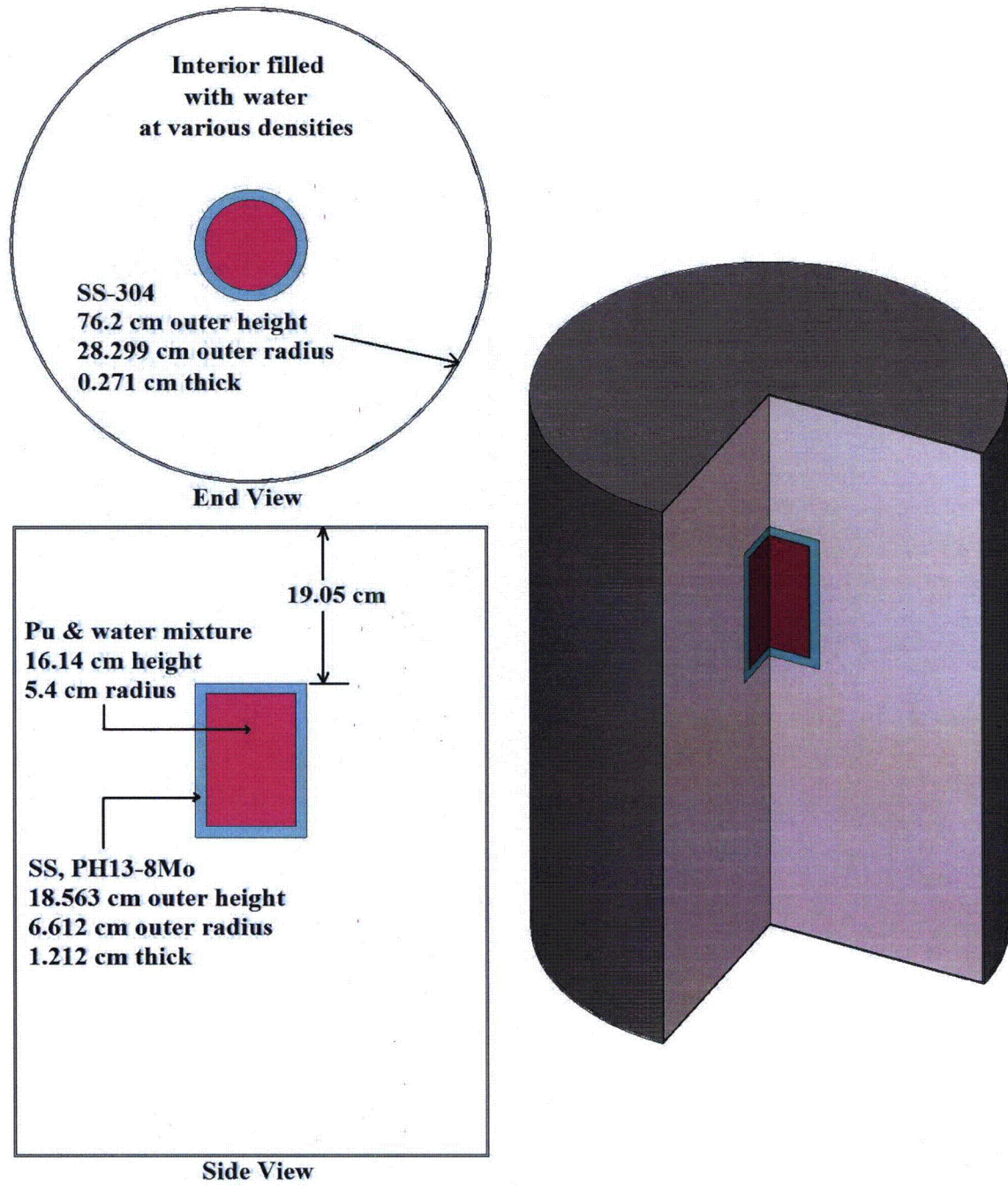


Figure 6-3. End-Impact Damaged Package Model

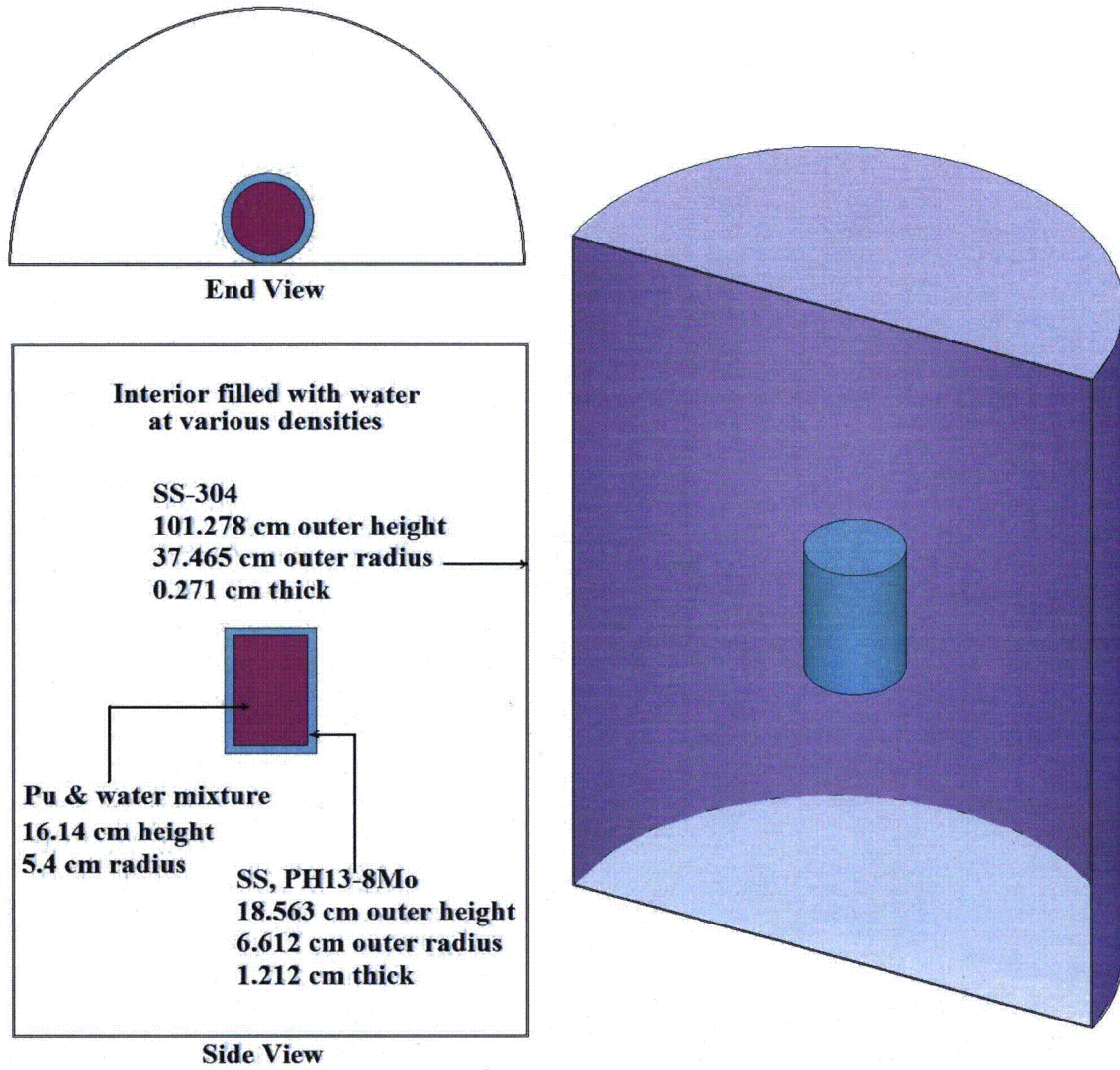


Figure 6-4. Side-Impact Damaged Package Model

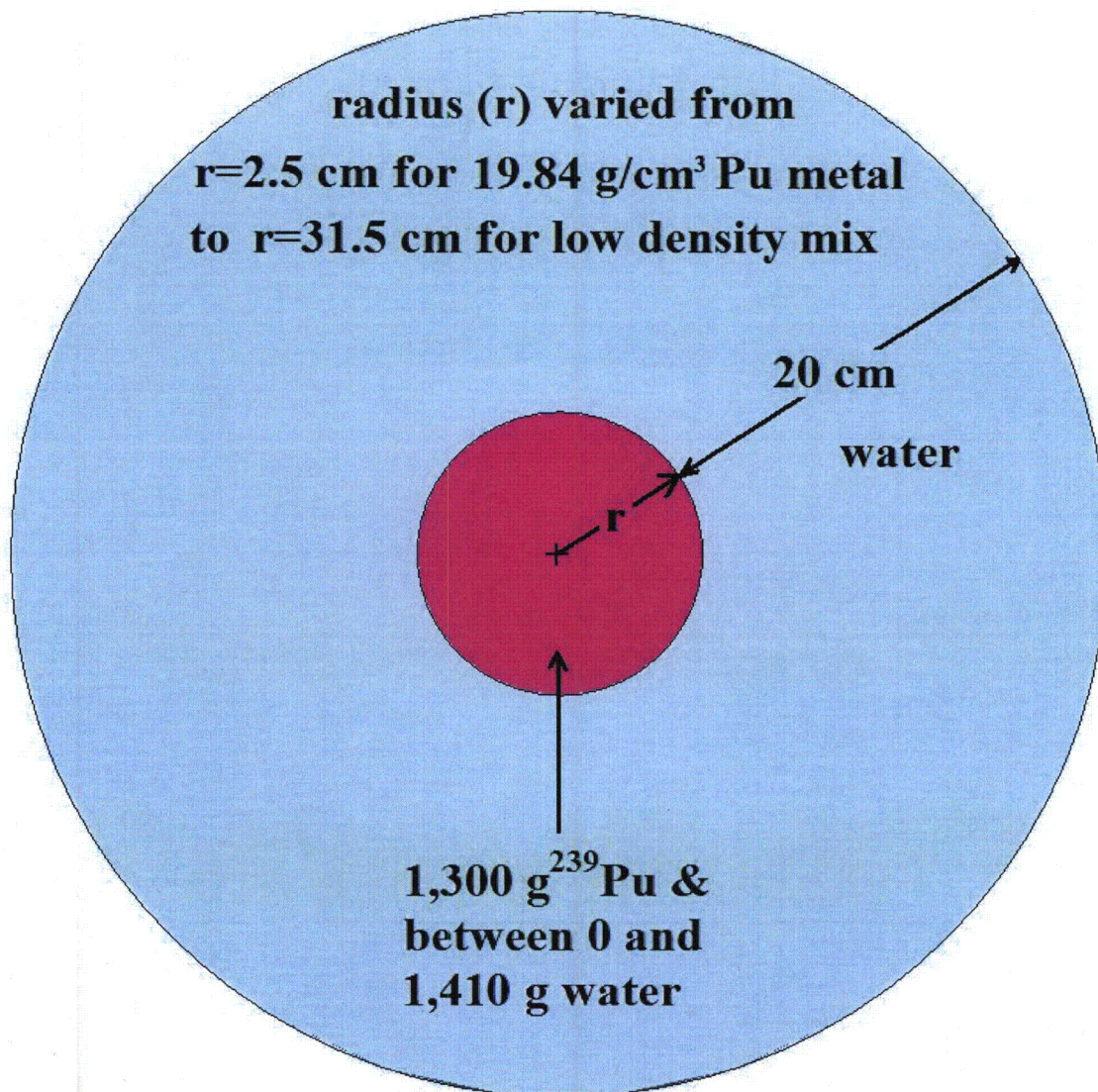


Figure 6-5. HAC Single Package Model for 10 CFR 71.55(f) Analysis

6.3.2 Material Properties

The materials used in the criticality analysis are described in this section. Table 6-2 shows the weight and densities for the materials used in the criticality analysis models.

Table 6-2. Material Specifications

| Material | Density (g/cm ³) | Constituent | Atomic Density (atoms/b-cm) |
|-----------------------------|------------------------------|------------------------------------|-----------------------------|
| Pu-239 metal | 19.84 | Pu-239 metal | 4.9980E-02 |
| Pu-239 and Water Mixture | 1.8331 | | |
| (H/Pu atom ratio = 28.8) | | Pu-239 (0.8794 g/cm ³) | 2.2155E-03 |
| (limiting case composition) | | H (0.9537 g/cm ³ water) | 6.3793E-02 |
| | | O (0.9537 g/cm ³ water) | 3.1896E-02 |

Table 6-2. Material Specifications (Continued)

| Material | Density (g/cm ³) | Constituent | Atomic Density (atoms/b-cm) |
|--|------------------------------|------------------|-----------------------------|
| Full Density Water | 0.9979 | | |
| | | H | 6.6752E-02 |
| | | O | 3.3376E-02 |
| PH13-8Mo Stainless Steel | 7.74 | | |
| | | Fe (75.775 wt %) | 6.3246E-02 |
| | | Cr (12.75 wt %) | 1.1430E-02 |
| | | Ni (8 wt %) | 6.3532E-03 |
| | | Mo (2.25 wt %) | 1.0931E-03 |
| | | Al (1.125 wt %) | 1.9435E-03 |
| | | Mn (0.1 wt %) | 8.4843E-05 |
| Redwood (C ₆ H ₁₀ O ₅) | 0.387 | | |
| (± 20% density considered) | | H | 1.4375E-02 |
| | | C | 8.6253E-03 |
| | | O | 7.1877E-03 |
| Stainless Steel-304 | 7.94 | | |
| | | C (0.08 wt %) | 3.1848E-04 |
| | | Si (1 wt %) | 1.7025E-03 |
| | | P (0.045 wt %) | 6.9468E-05 |
| | | Cr (19 wt %) | 1.7472E-02 |
| | | Mn (2 wt %) | 1.7407E-03 |
| | | Fe (68.375 wt %) | 5.8546E-02 |
| | | Ni (9.5 wt %) | 7.7401E-03 |
| Aluminum | 2.702 | Al | 6.0307E-02 |
| Copper | 8.92 | Cu | 8.4534E-02 |

The criticality analysis of the hypothetical accident conditions evaluates the loss of redwood packaging material during a fire by replacing the redwood and charred redwood with water with densities that vary from zero to full density (see Table 6-2). The only other package materials included in the HAC models are the TB-1 containment vessel and the stainless steel outer drum. The aluminum and copper included in the detailed model described in Section 6.3.1.1 are not included in the HAC models. The TB-1 containment vessel is not significantly affected by the HAC conditions. Changes to the stainless steel outer drum shape and dimensions are modeled, as described in Section 6.3.1.3, consistent with the results of prior HAC testing.

6.3.2.1 Fissile Material

The fissile material is comprised of Pu-239 metal mixed with water at varying concentrations. The default Pu density in the SCALE standard composition library³ is 1.0 g Pu/cm³ (0.036 lb Pu/in.³). Consequently, the desired Pu density is entered as a density multiplier in the

composition input data. The calculations use Pu-239 densities ranging from 19.84 g/cm³ (0.717 lb/in.³) down to 0.00992 g/cm³ (0.000358 lb/in.³).

The default water density in the SCALE standard composition library is 0.99793 g/cm³ (0.036053 lb/in.³) when the 238 group ENDF/B-VI nuclear data library is used. Water with densities ranging from full density to effectively zero density is mixed with the Pu-239 in the TB-1 containment vessel. Within the Pu region, the remaining non-Pu volume fraction is modeled as being filled with water. The water volume fraction in the mixture is, thus calculated as one minus the ratio of the desired Pu-239 density divided by 19.84 g/cm³ (0.717 lb/in.³). For example, if the mixture will have Pu-239 at 1.000 g/cm³ (0.036 lb/in.³), the volume fraction for the water is then calculated to be 0.9496 (= 1.0 - 1.000/19.84). This value is entered in the Mixture 1 composition data as the density multiplier for water.

When the Pu-239 is mixed with the maximum quantity of water, completely filling the interior of the TB-1, the Pu-239 density is:

$$1300 \text{ g Pu-239}/1478 \text{ cm}^3 = 0.8794 \text{ g Pu-239 /cm}^3.$$

In this case, the volume fraction for the water mixed with the Pu-239 is calculated as

$$1.0 - 0.8794/19.84 = 0.9557.$$

For this case, the SCALE inputs would be density multipliers of 0.8794 for Pu-239 and 0.9557 for the intermixed water. These inputs would result in a mixture with a Pu-239 density of 0.8794 g Pu-239/cm³ (0.0318 lb Pu-239/ in.³) and water at 0.9537 g water/cm³ (0.0344 lb water/in.³).

From page 8 of LA-12808, "Nuclear Criticality Safety Guide,"³² "*With the exception of uranium enriched to less than about 6 weight percent (wt%) ²³⁵U, subcritical masses for solutions apply conservatively to other distributions in water at the same hydrogen-to-fissile atomic ratio.*" For Pu-239, the homogeneous metal/water mixture bounds all heterogeneous mixtures. Consequently, except for cases with H/Pu of zero, all cases use a homogeneous plutonium metal and water mixture.

6.3.2.2 Water

The models use water at various densities, from effectively zero density up to full density water. The default water density provided by the SCALE standard composition library when ENDF/B-VI cross sections are used is 0.99793 g/cm³ (0.36053 lb/in.³). Note: that a slightly different value (0.9982 g/cm³ [0.3606 lb/in.³]) is reported in the SCALE 5.1 documentation.³ The difference is due to a slight change in the oxygen atomic weight in the ENDF/B-VI nuclear data evaluation. The SCALE input used for H₂O is a density multiplier on the default density. A density multiplier value of 1.0 translates to a water density of 0.99793 g/cm³ (0.36053 lb/in.³).

6.3.2.3 Stainless Steel PH 13-8 Mo

The TB-1 containment vessel and lid are made of stainless steel alloy PH13-8 Mo. Table 1.041 of the *Aerospace Structural Metals Handbook*³³ describes the composition of PH13-8Mo as shown in the Min. and Max. columns of Table 6-3. Except for hydrogen, the trace constituents

below manganese are absorbers and weak moderators. Even at their maximum values, the presence of these elements has an insignificant effect on k_{eff} . Consequently, trace elements below manganese were omitted.

Table 6-3. Stainless Steel PH 13-8 Mo Composition (wt %)

| Element | Min. | Max. | Modeled |
|------------|-----------|--------|---------|
| Chromium | 12.25 | 13.25 | 12.75 |
| Nickel | 7.5 | 8.5 | 8 |
| Molybdenum | 2 | 2.5 | 2.25 |
| Aluminum | 0.9 | 1.35 | 1.125 |
| Manganese | — | 0.1 | 0.1 |
| Silicon | — | 0.1 | 0 |
| Carbon | — | 0.05 | 0 |
| Nitrogen | — | 0.01 | 0 |
| Phosphorus | — | 0.01 | 0 |
| Sulfur | — | 0.01 | 0 |
| Oxygen | — | 0.005 | 0 |
| Hydrogen | — | 0.0025 | 0 |
| Iron | Remainder | | 75.78 |

PH13-8Mo density information is limited. The analysis reported in Chapter 5 of NUREG-0361² used a value of 7.76 g/cm³ (0.28 lb/in.³). Chapter 6 of the same report used atom densities equivalent to 7.843 g/cm³ (0.283 lb/in.³). Table 2.021 of the *Aerospace Structural Metals Handbook*³³ provides densities for PH13-8Mo stainless steel ranging from 7.74 to 7.76 g/cm³ (0.2796 to 0.2803 lb/in.³). A density of 7.74 g/cm³ (0.2796 lb/in.³) is used in the calculations. The lower 7.74 g/cm³ (0.2796 lb/in.³) value was used to minimize the quantity of steel present in array calculations. The steel is modeled as water in the limiting cases for the single-package analyses.

Sensitivity calculations were performed using two of the side-impact hypothetical accident condition models, and with the steel density varied $\pm 2\%$ of the 7.74 g/cm³ (0.2796 lb/in.³) value. Results from these calculations are presented in Figure 6-6. This figure shows that for PAT-1 models in which the redwood is modeled as full density water, the k_{eff} value of the system is insensitive to the steel density. The figure also shows that for systems where the redwood is missing, such as some of the hypothetical accident cases, k_{eff} value increases slightly with increased steel density. From the sensitivity data, increasing the density from 7.74 to 7.76 increases k_{eff} less than 0.02% Δk .

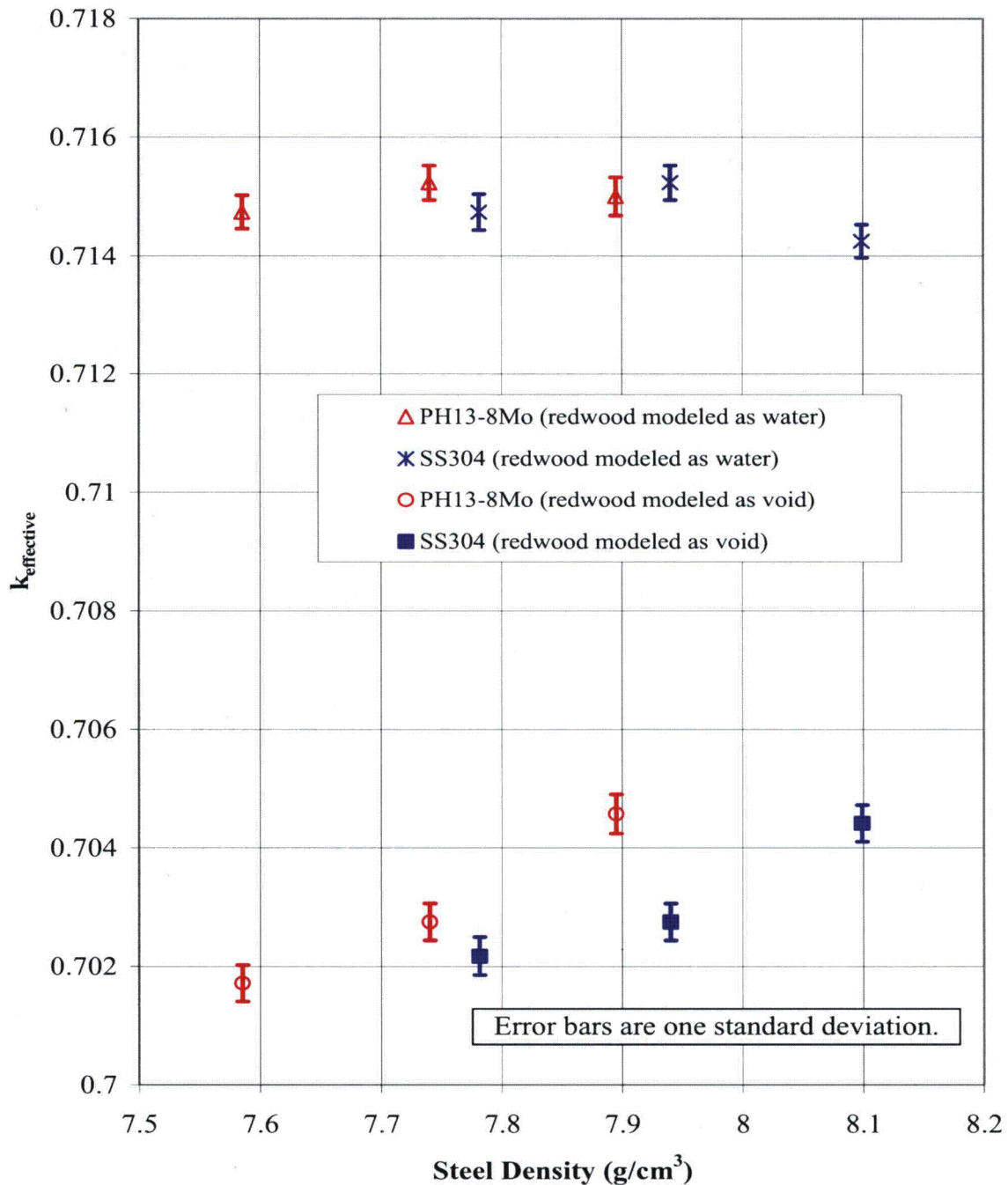


Figure 6-6. Sensitivity of k_{eff} to Steel Density

6.3.2.4 Redwood

Most of the space between the TB-1 containment vessel and the outer steel drum is filled with redwood. The Standard Composition Library³ in SCALE includes a model for redwood with a default density of 0.3868 g/cm³ (0.01397 lb/in.³). An informal review of the literature found redwood densities ranging from 0.34 to 0.45 g/cm³ (0.01228 to 0.01626 lb/in.³), depending on whether the redwood was from new growth or old growth and how much moisture was retained. The models used in the criticality analysis use the SCALE default redwood density. Calculations

were also performed at $\pm 20\%$ of the default density. Results from these calculations are presented in the figures of Section 6.3.4.

6.3.2.5 Aluminum

The detailed model included modeling of the load spreader, which is constructed of aluminum and cadmium-plated copper. The detailed model used aluminum with a density of 2.702 g/cm^3 (0.976 lb/in.^3), which is the maximum theoretical density for aluminum provided in the 74th edition of the CRC Handbook of Chemistry and Physics.³⁴

6.3.2.6 Copper

The detailed model included modeling of the load spreader, which is constructed of aluminum and cadmium-plated copper. The detailed model used copper at a density of 8.92 g/cm^3 (0.32 lb/in.^3), which is the maximum theoretical density for copper provided in the 74th edition of the CRC Handbook of Chemistry and Physics.³⁴ The cadmium plating on the copper was conservatively omitted from the load spreader model. This is conservative because Cd is a strong thermal neutron absorber.

6.3.2.7 Stainless Steel 304

The outer steel drum and liner are constructed of stainless steel-304 (ss304). Except for the sensitivity cases, the models used the standard ss304 provided by the SCALE Standard Composition Library.³ The SCALE ss304 has a density of 7.94 g/cm^3 (0.29 lb/in.^3) and has the following composition: 68.375 wt % iron, 19 wt % chromium, 9.5 wt % nickel, 2 wt % manganese, 1 wt % silicon, 0.08 wt % carbon, and 0.045 wt % phosphorus. This composition is close that provided for ss304 on page 12-161 of the 74th edition of the CRC Handbook of Chemistry and Physics.³⁴ The only difference being that the mid-range value provided in the CRC for nickel is 10.0 wt % rather than the 9.5wt% used in the SCALE ss304. On page 12-160, the CRC Handbook of Chemistry and Physics³⁴ provides a density of 7.9 g/cm^3 (0.286 lb/in.^3) for ss304. Sensitivity cases, $\pm 2\%$ on ss304 density, were run for two of the most limiting cases containing ss304. The results of the sensitivity study are presented in Figure 6-6. These results show that the k_{eff} value is insensitive to the steel density when the redwood is modeled as full density water and that changing the density from 7.94 g/cm^3 (0.29 lb/in.^3) to 7.90 g/cm^3 (0.286 lb/in.^3) reduces system reactivity by about 0.03% Δk when the redwood is modeled as void.

6.3.3 Computer Codes and Cross-Section Libraries

The SCALE 5.1 computer software package³⁵ was used for all analysis and validation calculations. Criticality calculations were performed using the CSAS25³⁶ sequence and the SCALE 238-energy-group ENDF/B-VI nuclear data (SCALE 5.1 library id = v6-238). The CSAS25 sequence used BONAMI for incorporating problem specific unresolved resonance data, CENTRM/PMC for the resolved resonance data, and KENO V.a for k_{eff} calculation. The SCALE 5.1 computer software package is a well-established analysis tool for criticality evaluation of fissile material packages. The SCALE ENDF/B-VI 238-energy-group cross-section library is the most modern nuclear data set publicly distributed with SCALE 5.1.

All calculations were initially performed on the "nuc" cluster of workstations identified as nuc1 through nuc30. The nuc workstations are DEC Alpha workstations running Tru64 UNIX, version 5.1. All k_{eff} calculations for the limiting safety analysis models and validation set critical

experiments were run on the nuc cluster. In connection with the revision of Section 6 to incorporate Pu/Be source limits, some TSUNAMI and direct perturbation cases were run on the “cpile2” cluster, nodes 1 – 6. The first 6 nodes of the cpile2 cluster, nodes 1 – 6, have an AMD Opteron™ Processor 246 running the GNU/Linux 2 operating system. The SCALE 5.1 software used for the PAT-1 work was in a directory tree starting at /projects/ymp/scale5.1/ and is controlled under a quality assurance plan, software quality assurance plans, and requirements consistent with 10 CFR 71, Subpart H, “Quality Assurance.”

Criticality calculations were performed using at least 3,000 neutrons per generation. The number of generations requested was either 1,050 or 3,050, with at least the first 50 generations being discarded. The KENO V.a “sig” input parameter was used to terminate calculations when the standard deviation of the mean k_{eff} value reached a value of 0.0005. The default starting neutron distribution was used. Neutrons were started uniformly in fissile material for the initial generation. All reflectors were modeled explicitly and no albedo or “bias” data were used.

The convergence plots for each of the limiting cases were reviewed to verify convergence. Trend plots of k_{eff} values were reviewed to identify any cases that may not be converged. Cases with poor convergence or that failed the KENO internal normality tests were rerun with a different number of neutrons per generation, effectively changing the random number sequence of the Monte Carlo method calculations.

The validation study used the SCALE 5.1 TSUNAMI^{37,38} sensitivity and uncertainty analysis tools to assess the similarity of the safety analysis cases and the validation study critical experiments. TSUNAMI-3D³⁷ was used to generate a set of nuclide- and reaction-specific k_{eff} sensitivity neutron energy-dependent profiles for each limiting safety analysis case and for each critical experiment used in the validation study. The TSUNAMI-3D calculations were performed using the SCALE ENDF/B-VI 238-energy-group cross-section library.

The TSUNAMI-IP³⁸ module was used to compare the safety analysis cases with critical experiment models. TSUNAMI-IP used the SCALE 5.1 44-group ENDF/B-VI recommended covariance data set (SCALE 5.1 library id = 44groupv6rec). The c_k parameter, average lethargy of fission (EALF), and H/Pu were used to quantify similarity between limiting safety cases and the critical experiments used in the validation. Details are provided in Section 6.8. The 44-neutron-energy-group structure is a subset of the 238-group structure used in the cross-section library that is used for all neutron transport calculations. When the 44-group covariance data is used with the 238-group cross-section library, all of the fine groups within each of the 44 groups use the same 44-group covariance data.

6.3.4 Demonstration of Maximum Reactivity

The purpose of this section is to identify the configuration of maximum reactivity for:

- Section 6.3.4.1 a single package under normal conditions of transport (NCT) and HAC
- Section 6.3.4.2 an array of 5*N undamaged packages under NCT
- Section 6.3.4.3 an array of 2* N damaged packages under HAC

- Section 6.3.4.4 a single package under the expanded HAC specified by 10 CFR 71.55(f)

6.3.4.1 *Single Package Under Normal Conditions of Transport and Hypothetical Accident Conditions*

The purpose of this section is to identify and demonstrate the maximum reactivity configurations for a single package under normal and hypothetical accident conditions. To support this analysis, simplified and detailed models were created and used in parametric studies.

A parametric study was performed using five variations of the simplified model to show the impact on k_{eff} from various modeling approximations. The results of this study are shown in Figure 6-7 and in the list of calculations provided in Section 6.9.4.1 of this addendum.

Three curve segments are plotted for each of the five simplified model variations described as Models 1 through 5 in Section 6.3.1.2. The left-most segments cover the H/Pu range of 0 to 12.1. In this range, the results are for 1300 g (2.87 lb) of Pu or Pu-water in spheres of increasing radii ranging from the minimum 2.50 cm (0.98 in.), for unmoderated maximum theoretical density plutonium metal, to 5.40 cm (2.13 in.), for a sphere that is the maximum size that could fit within the TB-1 containment vessel. The second set of segments cover the H/Pu range from 5.34 through 28.8. In this range, the results are for a 1300 g (2.87 lb) plutonium and water cylinder with an outer radius of 5.40 cm (2.13 in.) and with height varying from 3.58 to 16.14 cm (1.41 to 6.35 in.), which completely fills the interior of the TB-1 containment vessel. The right-most segments curve cover the H/Pu range from 28.8 through 132.2 and show the impact of replacing Pu with water in the TB-1. All simplified model results show one maxima at a H/Pu ratio equal to zero (maximum theoretical density plutonium metal sphere surrounded by water in the TB-1) and another at a H/Pu ratio equal to 28.8, where the 1300 g (2.87 lb) of Pu are spread throughout the TB-1 and mixed with the maximum quantity of water that could fit within the TB-1, considering the presence of 1300 g (2.87 lb) of Pu.

The curves for simplified Models 1, 2, and 3 show the sensitivity of k_{eff} to the density of the redwood. As discussed in Section 6.3.2, the density of the redwood may vary considerably. The black (Model 3) and purple (Model 2) curves show the effect on k_{eff} from the variation of the redwood density by $\pm 20\%$ around the nominal $0.387 \text{ g redwood/cm}^3$ (1.139 lb/in.^3). Model 1 has nominal redwood density. Model 2 has 80% of nominal redwood density. Model 3 has 120% of nominal redwood density. The red curve (Model 4) shows the effect on k_{eff} from the replacement of the redwood with full density water. The blue curve (Model 5) shows the effect on k_{eff} from the replacement of both the redwood and steel with water. It is concluded from this study that the maximum k_{eff} value is generated by the simplified model case *cv031*, in which the redwood and steel were replaced with full density water and the 1300 g (2.87 lb) of Pu is spread throughout the inside of the TB-1 containment vessel and mixed with the maximum quantity of water that could also be present in the TB-1 (i.e., the peak of the Model 5 curve at H/Pu = 28.8).

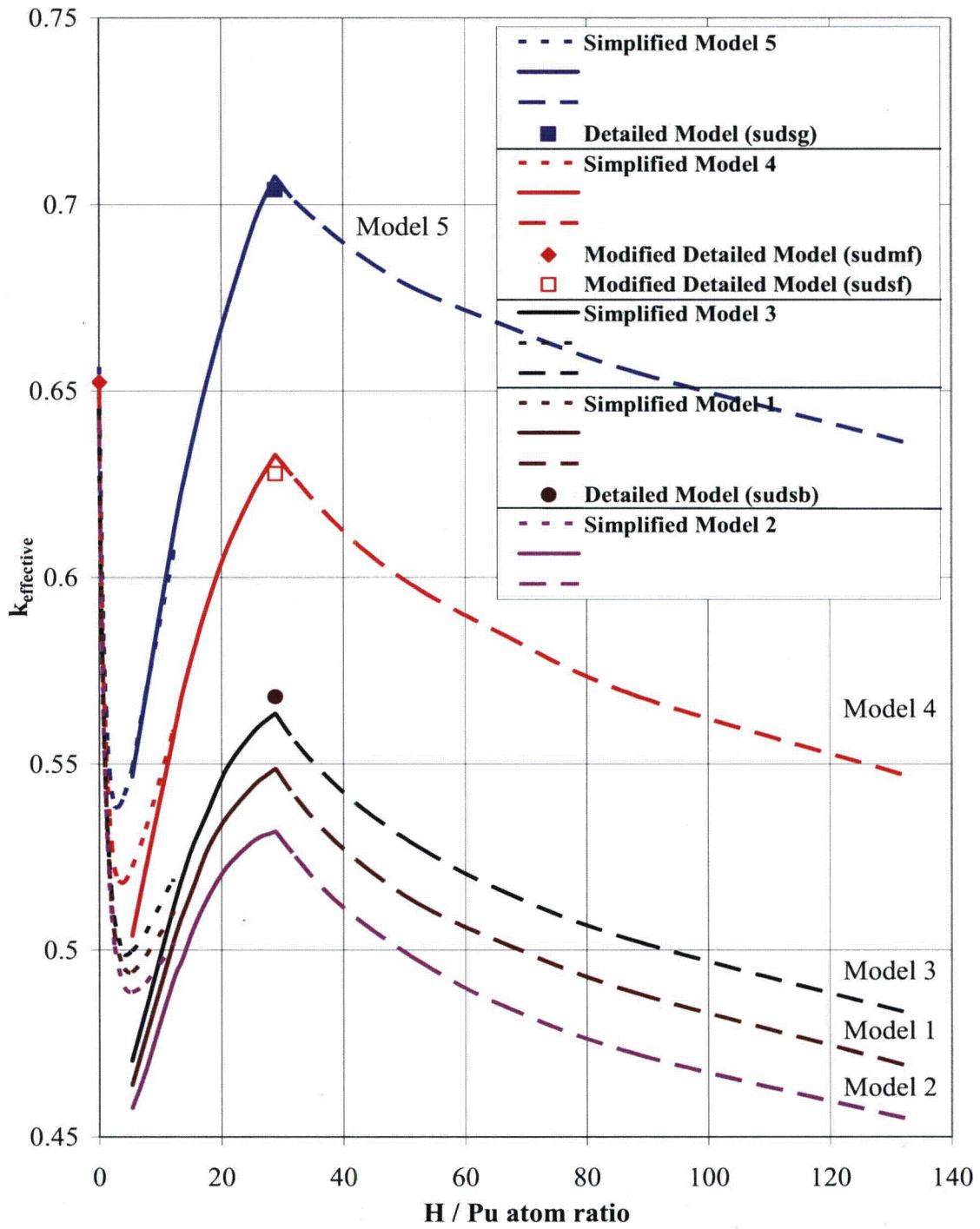


Figure 6-7. Single Package Moderation Study

Impact of Modeling Simplifications

Additional calculations were performed with a detailed model (see Figure 6-1) to show that the simplified model results bound the detailed model results and to show the impact of various modeling approximations.

In the first series of additional detailed model calculations, the package payload is a 1300 g (2.87 lb) plutonium metal sphere ($H/Pu = 0$) in the middle of the TB-1 containment vessel. The results from the first series are presented in Table 6-4. The results from case *sudmf* is plotted in Figure 6-7 as “Modified Detailed Model (*sudmf*).” This modified detailed model yielded a k_{eff} of 0.6523 ± 0.0005 , which is lower than the k_{eff} of 0.6565 ± 0.0005 produced by simplified Model 5 (blue curve in Figure 6-7) with an H/Pu of zero.

Table 6-4. Detailed Model, Plutonium Metal Sphere, Modeling Impact Study

| Case | k_{eff} | σ | Case Description |
|------------------|-----------|----------|--|
| <i>sudma</i> | 0.5525 | 0.0005 | Detailed model with no water in TB-1 or in gaps. Redwood, aluminum, copper, and steel modeled. |
| <i>sudmb</i> | 0.6492 | 0.0005 | Case <i>sudma</i> with TB-1 filled with water |
| <i>sudmwoodm</i> | 0.6486 | 0.0005 | Case <i>sudmb</i> with redwood density decreased 20% |
| <i>sudmwoodp</i> | 0.6500 | 0.0005 | Case <i>sudmb</i> with redwood density increased 20% |
| <i>sudmc</i> | 0.6504 | 0.0005 | Case <i>sudmb</i> with gaps filled with water |
| <i>sudmd</i> | 0.6499 | 0.0005 | Case <i>sudmc</i> with copper changed to water |
| <i>sudme</i> | 0.6489 | 0.0005 | Case <i>sudmd</i> with aluminum changed to water |
| <i>sudmf</i> | 0.6523 | 0.0005 | Case <i>sudme</i> with redwood changed to water |

In a second series of detailed model calculations, the package payload is 1300 g (2.87 lb) Pu mixed with 1412 g (3.113 lb) of water in the TB-1 containment vessel ($H/Pu = 28.8$). The results are presented in Table 6-5. The results from cases *sudsb*, *sudsf*, and *sudsg* are plotted on Figure 6-7 as “Detailed Model *sudsb*,” “Detailed Model *sudsf*,” and “Detailed Model *sudsg*,” respectively. Calculations *sudmf* and *sudsf* produce k_{eff} values that are similar to those from simplified Model 4 in which the redwood, gaps, copper, and aluminum have all been replaced with water. Calculation *sudsg* produce a k_{eff} value (0.7040 ± 0.0005) that is a slightly lower than the peak k_{eff} value (0.7076 ± 0.0006) from the simplified Model 5 at an H/Pu of 28.8.

It is concluded from the results presented in Figure 6-7 that analysis case *cv031*, in which the wood, steel, aluminum, copper, and gaps are modeled as water, yields the maximum k_{eff} value (0.7076 ± 0.0006) for a single package under normal conditions of transport. Furthermore, because this case already includes the maximum quantity of water possible within the TB-1 containment vessel and the maximum flooding of the package outside the TB-1, it also yields the maximum k_{eff} value for a single package under hypothetical accident conditions. Figure 6-7 also shows that removing water from inside the TB-1 containment vessel results in a decreased k_{eff} value and that removing Pu from the TB-1 vessel to make room to add water also results in a decreased k_{eff} value.

A note of interest: is the relationship between the detailed model (with steel, redwood, copper, and aluminum modeled) results and the simplified model (with steel and redwood modeled) results. In Figure 6-7, the brown dot representing detailed model case *sudsb* is significantly higher than the simplified Model 1 result at an H/Pu of 28.8. A similar trend is seen in Figure 6-9 between the detailed model results and the simplified Model 1 results.

Table 6-5. Detailed Model, Plutonium and Water Solution Cylinder, Modeling Impact Study

| Case | k_{eff} | σ | Case Description |
|-----------------|-----------|----------|---|
| <i>sudsb</i> | 0.56797 | 0.0005 | Detailed model with no water in gaps. Redwood, aluminum, copper, and steel modeled. |
| <i>sudswodm</i> | 0.5599 | 0.0005 | Case <i>sudsb</i> with redwood density decreased 20% |
| <i>sudswodp</i> | 0.5761 | 0.0005 | Case <i>sudsb</i> with redwood density increased 20% |
| <i>sudsc</i> | 0.5911 | 0.0005 | Case <i>sudsb</i> with gaps filled with water |
| <i>sudsd</i> | 0.5920 | 0.0005 | Case <i>sudsc</i> with copper changed to water |
| <i>sudse</i> | 0.5932 | 0.0005 | Case <i>sudsd</i> with aluminum changed to water |
| <i>sudsf</i> | 0.6278 | 0.0005 | Case <i>sudse</i> with redwood changed to water |
| <i>sudsg</i> | 0.7040 | 0.0005 | Case <i>sudsf</i> with all steel changed to water |

The results in Table 6-5 show if the copper or aluminum is replaced in the detailed model with water, k_{eff} decreases. This is somewhat counterintuitive. This effect is likely due to the much larger total neutron cross section that hydrogen has and the physical locations of the copper and aluminum components. The additional moderation provided by replacing the copper or aluminum with water at the locations of the copper and aluminum components appears to decrease the fraction of neutrons that can migrate back to the Pu. Figure 6-7 and Figure 6-9 show that the simplified Models 4 and 5, in which the redwood, copper, and aluminum have been replaced with water, yield significantly higher k_{eff} values than simplified Models 1, 2, and 3 and the detailed model. Figure 6-7 also shows the results at an H/Pu of 28.8 for a detailed model in which the redwood, copper, aluminum, and gaps have been changed to water (case *sudsf*) and where the TB-1 steel and outer container steel have been changed to water (case *sudsg*). These modified details yield k_{eff} values that are slightly lower than the simplified model results. It is concluded that simplified Models 4 and 5 provide conservative representations of the PAT-1 package.

6.3.4.2 Array of Packages Under Normal Conditions of Transport

Title 10 CFR 71.59(a)(1) requires that a water reflected array of five times “N” undamaged packages with nothing between the packages would be subcritical. From Section 6.1.3, the value of N is 500, thus it must be shown that 2500 undamaged packages would be subcritical. Calculations were performed with packages in both square and hexagonal pitched arrays with the package contents varied from a 1300 g (2.87 lb) plutonium metal sphere to a 1300 g (2.87 lb) Pu-water mixture spread throughout the interior of the TB-1 containment vessel. Additional calculations were also performed to show that removing Pu to make room for additional water would result in a lower k_{eff} value.

Using a square-pitched array in a $17 \times 17 \times 9$ arrangement, results in a near cuboidal arrangement of 2,601 packages. The space between packages is modeled as void per 10 CFR 71.59(a)(1) and a 30-cm-thick (11.8 in.) layer of water surrounds the array on all sides. Figure 6-8 shows a cutaway view of the array model. The series of calculations were performed on both detailed and simplified models.

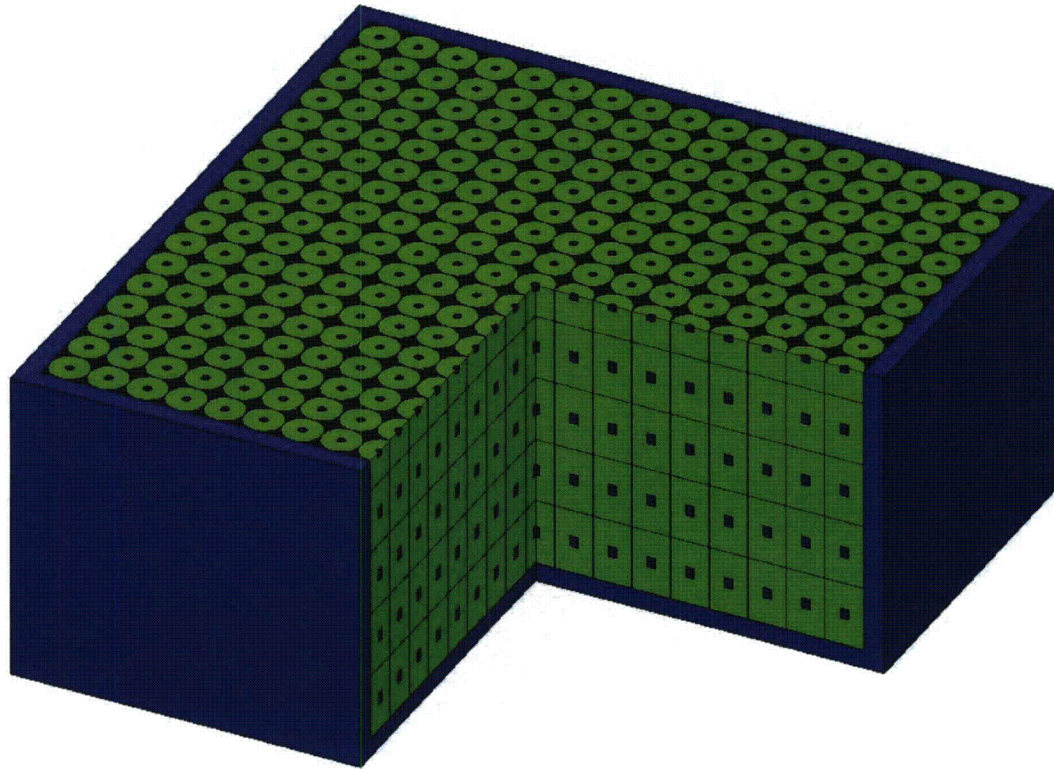


Figure 6-8. Normal Conditions of Transport – Square-Pitched Array

Figure 6-9 and the table in Section 6.9.4.2 show the results of the series of calculations with simplified and detailed models in a square-pitched array. Calculations were performed for H/Pu ratios ranging from zero to 132.2. Three curve segments are plotted for each of four simplified model variations, described as Models 1 through 4 in Section 6.3.1.2, and for an array of detailed models, described in Section 6.3.1.1.

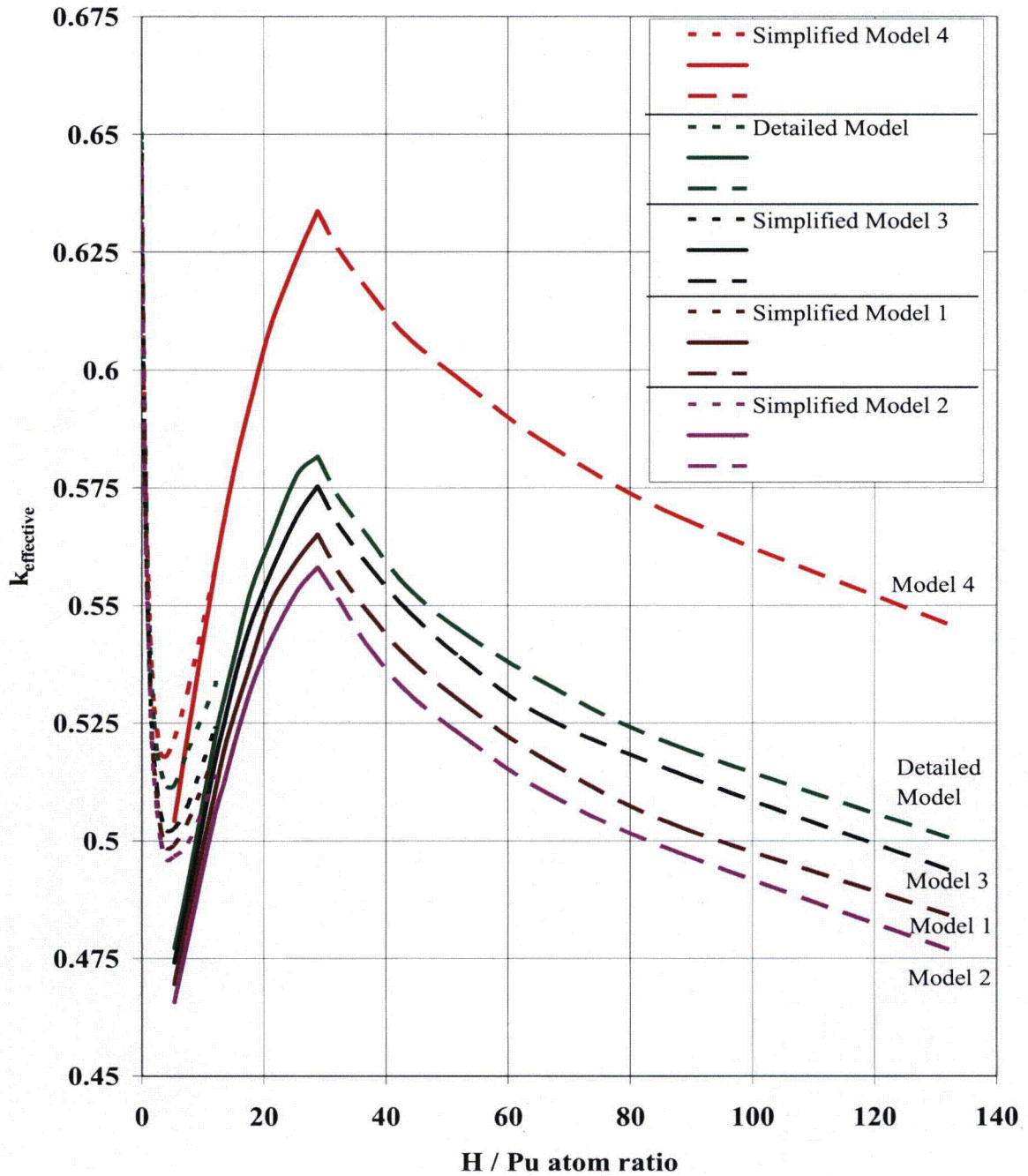


Figure 6-9. Normal Conditions of Transport – Square-Pitched Array Results

The left-most segment for each curve covers the H/Pu range of 0 to 12.1. In this range, the results are for 1300 g (2.87 lb) Pu or Pu-water spheres of increasing radii ranging from the minimum 2.50 cm (0.98 in.), for unmoderated maximum theoretical density plutonium metal, to 5.40 cm, for a sphere that is the maximum size that could fit within the TB-1 containment vessel. The second segment of each curve covers the H/Pu range from 5.34 through 28.8. In this range, the results are for a 1300 g (2.87 lb) Pu-water cylinder with an outer radius of 5.40 cm and with height varying from 3.58 to 16.14 cm (1.41 to 6.35 in.), which completely fills the interior of the TB-1 containment vessel. The right-most segment of each curve covers the H/Pu range from

28.8 through 132.2 and shows the effect on k_{eff} of removing Pu and adding water into the TB-1. The model results all show one maxima at a H/Pu ratio equal to zero and another at a H/Pu ratio equal to 28.8, where the 1300 g (2.87 lb) of Pu are spread throughout the TB-1 and mixed with the maximum quantity of water that could fit within the TB-1 considering the presence of 1,300 g of Pu.

For all models, the highest k_{eff} values were generated with the 1300 g (2.87 lb) plutonium metal sphere in the TB-1 containment vessel with the remainder of the containment vessel filled with water. The detailed model and the simplified model with redwood replaced by water yielded statistically equivalent k_{eff} values (i.e., 0.6505 ± 0.0005 for the detailed model and 0.6504 ± 0.0005 for Simplified Model 4) at the H/Pu of zero. These were the highest k_{eff} values generated for the square-pitched arrays.

The series of calculations were also performed with the simplified model packages in a close-packed hexagonal array. The array model includes 2,646 packages in a near cuboidal shaped array as shown in Figure 6-10.

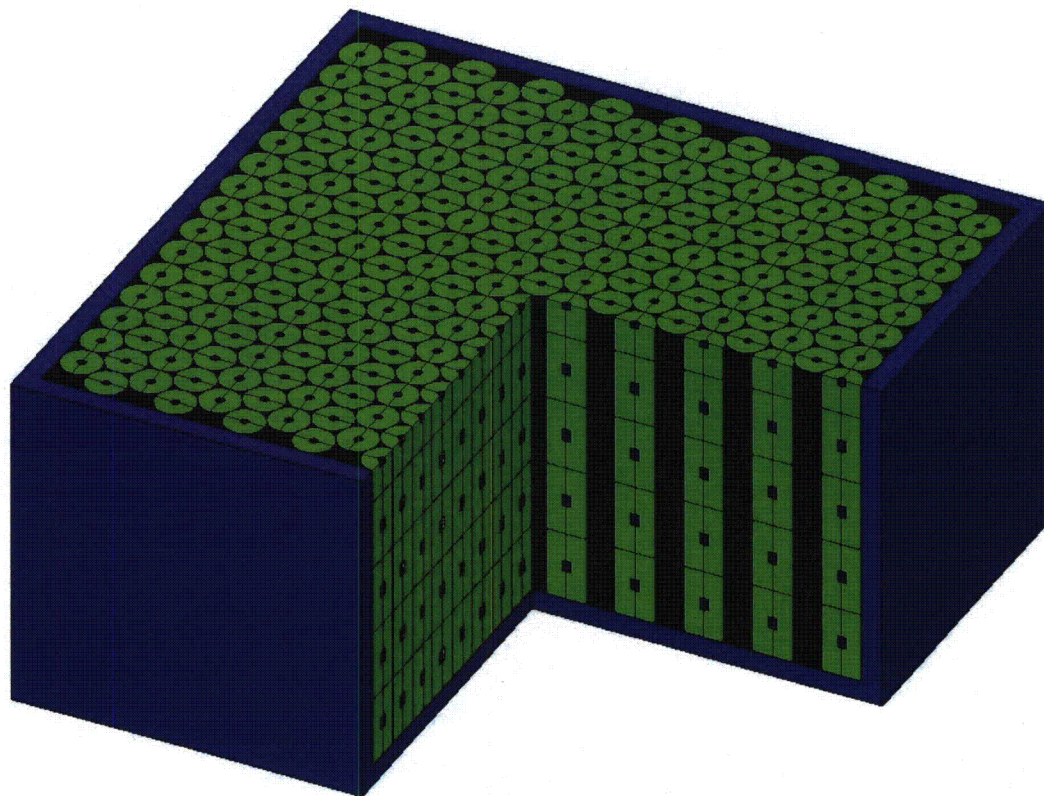


Figure 6-10. Normal Conditions of Transport – Hexagonal-Pitched Array

Figure 6-11 shows the results of series of calculations with simplified models. Calculations were performed for H/Pu ratios ranging from zero to 132.2. Three curve segments are plotted for each of four simplified model variations, described as Models 1 through 4 in Section 6.3.1.2.

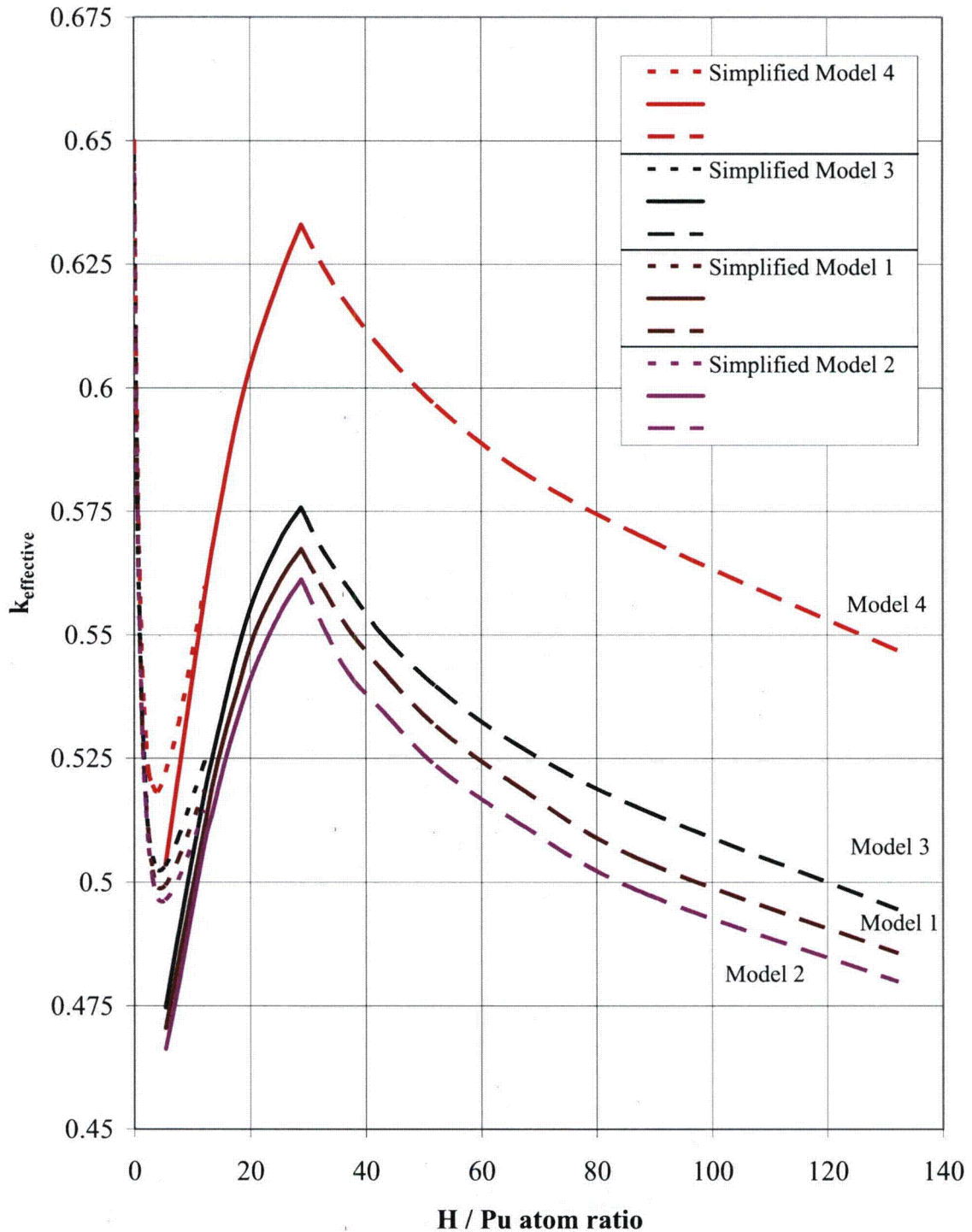


Figure 6-11. Normal Conditions of Transport – Hexagonal-Pitched Array Results

The left-most segment for each curve covers the H/Pu range of 0 to 12.1. In this range, the results are for 1300 g (2.87 lb) Pu or Pu -water spheres of increasing radii ranging from the minimum 2.50 cm (0.98 in.), for unmoderated maximum theoretical density plutonium metal, to 5.40 cm (2.13 in.), for a sphere that is the maximum size that could fit within the TB-1 containment vessel. The second segment of each curve covers the H/Pu range from 5.34 through

28.8. In this range, the results are for a 1300 g (2.87 lb) Pu -water cylinder with an outer radius of 5.40 cm (2.3 in.) and with height varying from 3.58 to 16.14 cm (1.41 to 6.35 in.), which completely fills the interior of the TB-1 containment vessel. The right-most segment of each curve covers the H/Pu range from 28.8 through 132.2 and shows the effect on k_{eff} of removing Pu and adding water into the TB-1. The model results all show one maxima at a H/Pu ratio equal to zero and another at a H/Pu ratio equal to 28.8, where the 1300 g (2.87 lb) of Pu are spread throughout the TB-1 and mixed with the maximum quantity of water that could fit within the TB-1, considering the presence of 1300 g (2.87 lb) of Pu.

For all models, the highest k_{eff} values were generated with the 1300 g (2.87 lb) plutonium metal sphere in the TB-1 containment vessel with the remainder of the containment vessel filled with water. The Simplified Model 4, with redwood replaced by water, and at an H/Pu ratio of zero, yielded the highest k_{eff} value, 0.6509 ± 0.0005 . While this k_{eff} value is slightly higher than the value for the square-pitched array of packages, it is statistically the same. This indicates that, with the redwood zone modeled as full density water, the maximum k_{eff} value is not sensitive to the number or arrangement of the surrounding packages.

The NCT array analysis was performed with redwood at nominal and $\pm 20\%$ density and full density water to ensure that the NCT array model was conservative. The results presented in Figure 6-9 and Figure 6-11 clearly show this is the case for all configurations except the single solid metal Pu sphere. As shown by comparing the results in Section 6.9.4.2, replacing the redwood with water is conservative even for the metal sphere cases. The NCT arrays with full density water replacing the redwood yields a higher array k_{eff} than does the same array with the redwood modeled.

The maximum k_{eff} value for an array under normal conditions of transport is 0.6509 ± 0.0005 for Simplified Model 4 with each package containing a 1300 g (2.87 lb) Pu metal sphere and arranged in hexagonal-pitched arrangement of 2646 packages (Case *fhlsf001*).

6.3.4.3 Array of Packages Under Hypothetical Accident Conditions

Title 10 CFR 71.59(a)(2) requires that a water reflected array of two times "N" damaged packages with optimum interspersed moderation between the packages would be subcritical. From Section 6.1.3, the value of N is 500, thus, it must be shown that 1000 damaged packages would be subcritical. Two different damaged container models described in Section 6.3.1.3 were evaluated: one for an end-impact case (see Figure 6-3) and one for a side-impact case (see Figure 6-4). Calculations were performed with both damaged-container models in various arrangements of varying numbers of packages to identify which damaged container and which arrangement produced the highest k_{eff} values. In all cases, the number of rows, columns, and layers were set to produce a nearly cubic array of packages. The intent of this study is to show which damaged container model in which arrangement of 1000 packages produces the highest k_{eff} value. The results of this study are presented in Figure 6-19. All calculations used in the analysis of package arrays under HACs are listed in the Section 6.9.4.3 table.

Four different array arrangements were considered for the side-impact damaged container model. The most limiting array involved pairs of damaged packages oriented so that their flat sides were together. Pairs of damaged packages were then placed in a hexagonal-pitch array. Figure 6-12

shows an overhead view of one of these arrays. The array is enclosed on three sides by a 30-cm-thick (11.8 in.) water reflector. A reflective boundary condition is used on the other three sides.

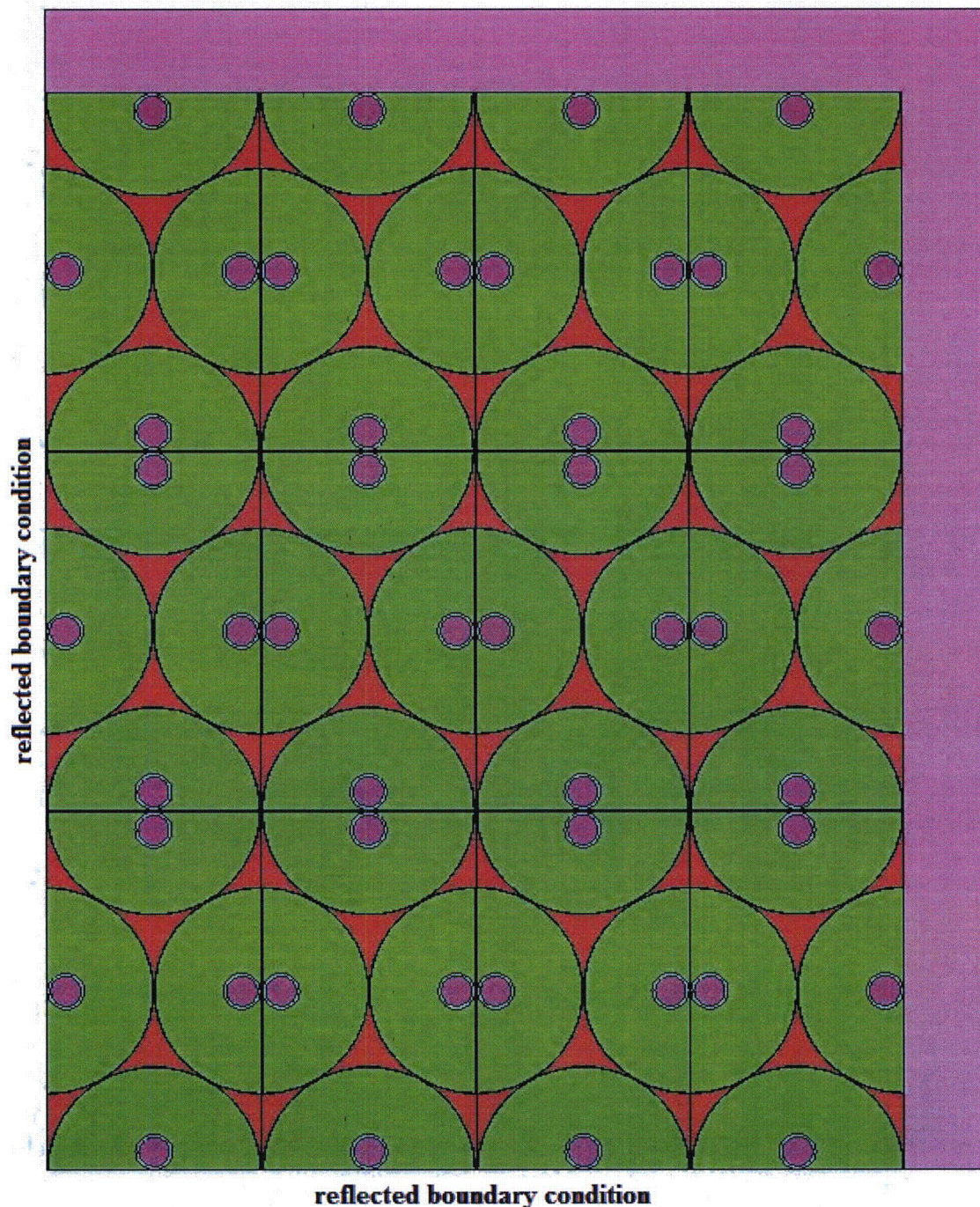


Figure 6-12. Damaged Packages – Side-Impact Hexagonal-Pitch Array, Top View

Calculations were also performed for an array of damaged packages arranged such that each pair of damaged packages was arranged in a square-pitch as shown in Figure 6-13. Figure 6-14 and Figure 6-15 show arrays in which damaged packages were oriented to try to locally increase the fissile material density within the array.

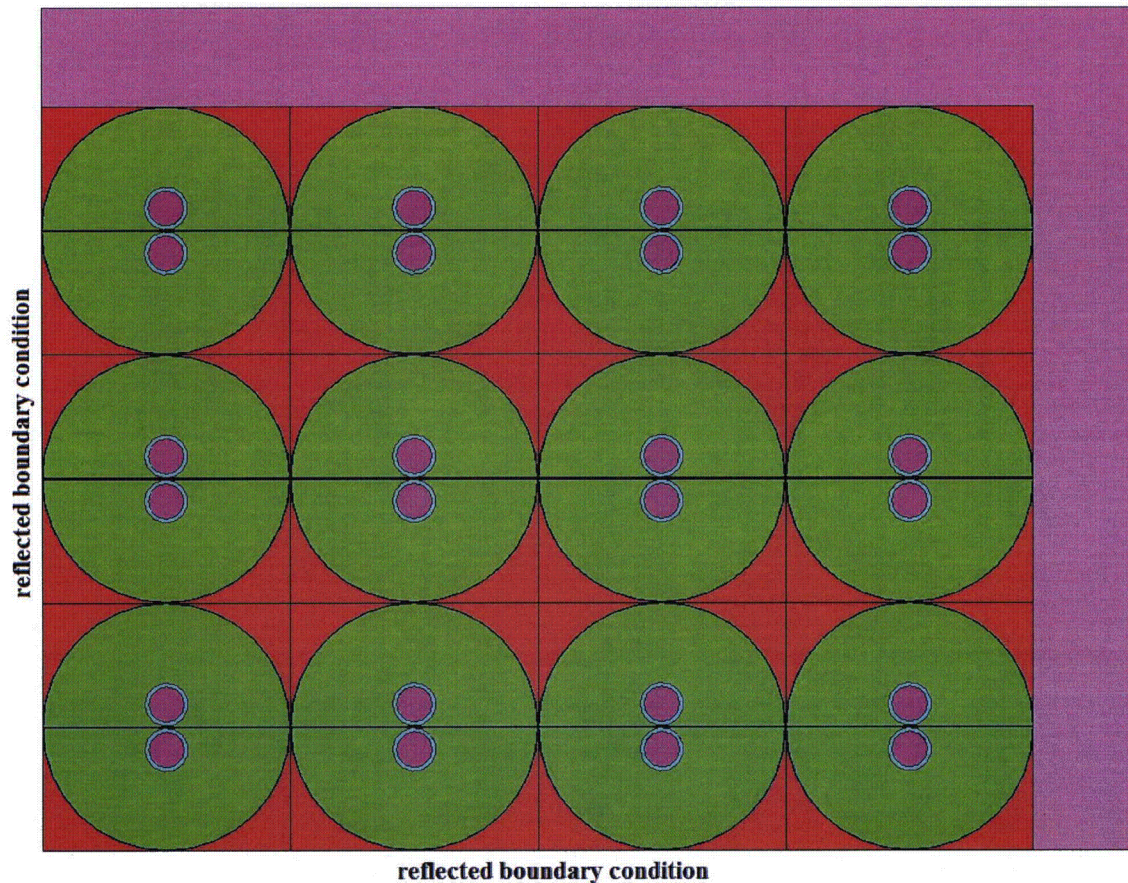


Figure 6-13. Damaged Packages – Side-Impact Square-Pitch Array, Top View

Two types of arrays of end-impact damaged packages were also considered. In both cases, the damaged drums are arranged horizontally in a close-packed hexagonal array. In one type of end-impact damaged package array, each vertical layer is repeated. In the other type, the packages are turned upside-down in alternating layers to minimize the spacing between the fissile material in every other layer. Side views of these two arrangements are provided in Figure 6-17 and Figure 6-18. A top view is shown in Figure 6-18.

Calculations were performed with both damaged-container models in various arrangements of varying numbers of packages to identify which damaged container and which arrangement produced the highest k_{eff} values. In all cases, the number of rows, columns, and layers were set to produce a nearly cubic array of packages. The intent of this study is to show which damaged container model in which arrangement of 1000 packages produces the highest k_{eff} value. The results of this study are presented in Figure 6-19. In this study, the redwood, aluminum, and copper are modeled as void to maximize interaction between units. Based on the study results, it is concluded that the close-packed hexagonal array of side-impact damaged drums yields the highest k_{eff} values for array sizes of 1000 damaged packages.

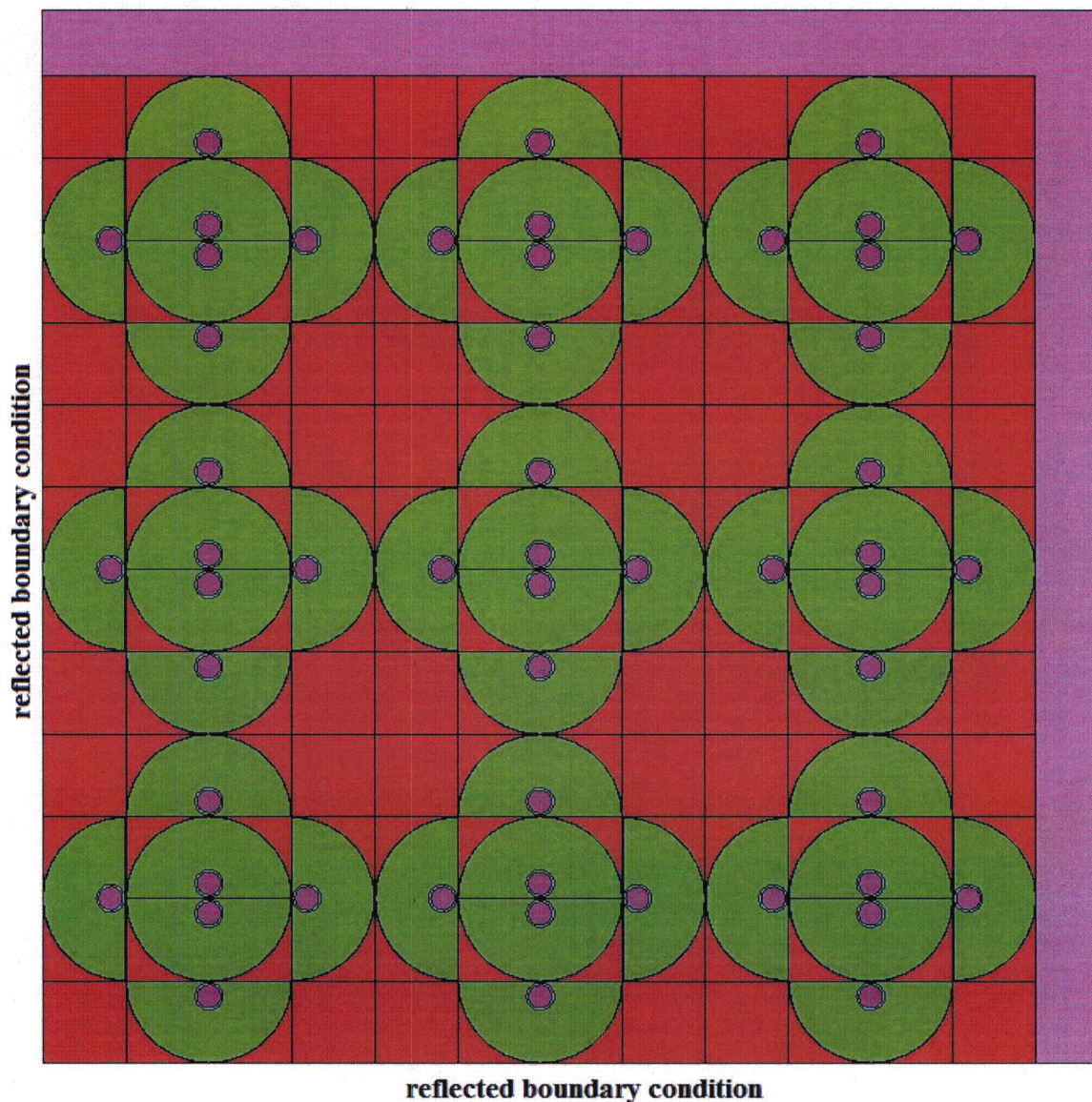


Figure 6-14. Damaged Packages – Side-Impact Nested Arrangement No. 1, Top View

The tests performed on the damaged package included a fire test that resulted in burning and loss of some of the redwood. The criticality analysis considers that some or all of the redwood may be lost and may be replaced with water. This bounds the entire range (0 to 100%) of wood and/or water that could be present following hypothetical accident conditions. A series of calculations were performed to identify the optimum level of moderation in the redwood package zone. Figure 6-20 presents the results of a study identifying the optimum quantity of moderator to place in the charred redwood zone. Calculations were performed for the two combinations of Pu-water in the TB-1 that produced maxima in the normal conditions array calculations. These were with a 1300 g (2.87 lb) Pu sphere inside a flooded TB-1 container and with the 1300 g (2.87 lb) of Pu intimately mixed with the 1412 g of water that could be in the TB-1. Calculations were performed for the side-impact damaged drums in the close-packed hexagonal and square-pitched arrays. Each series of calculations was performed with the redwood zone replaced with water varying from 0% to 100% density.

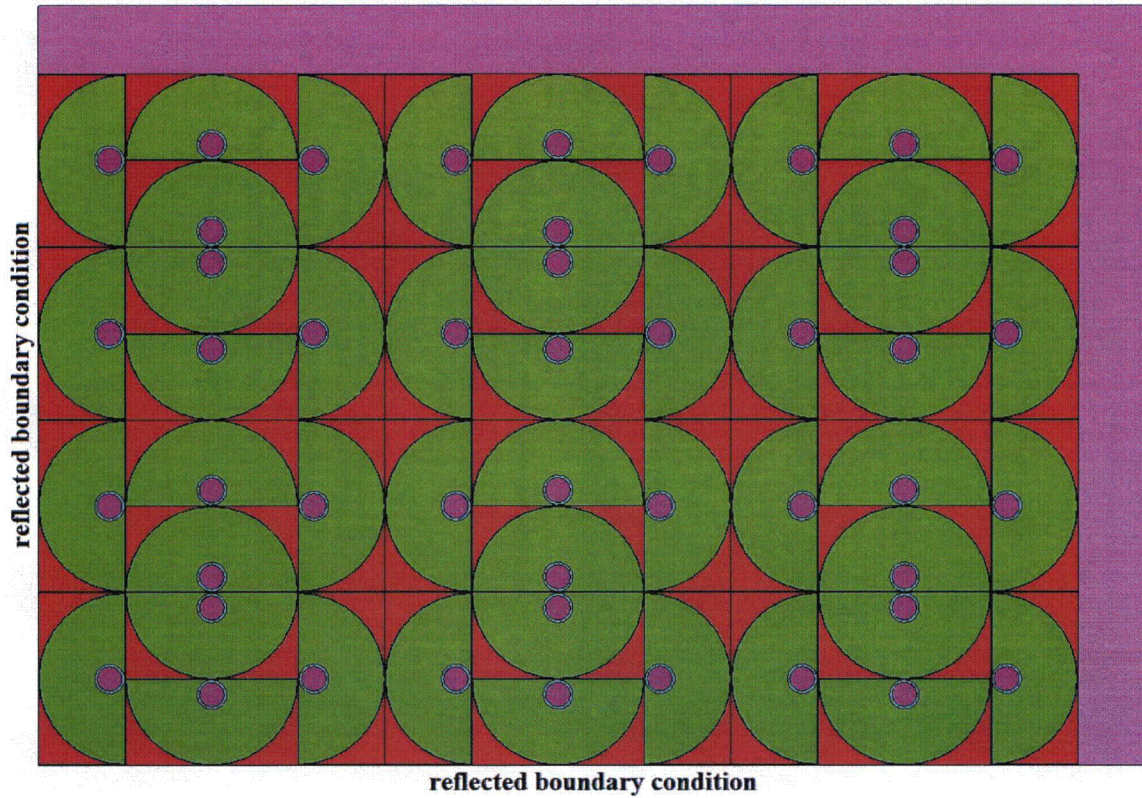


Figure 6-15. Damaged Packages – Side-Impact Nested Arrangement No. 2, Top View

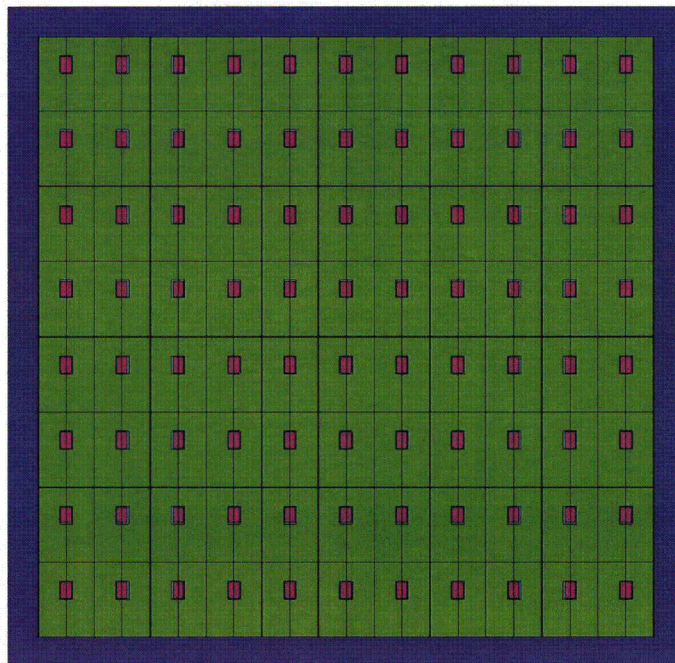


Figure 6-16. Damaged Packages – End-Impact Array, Repeated Layers, Side View

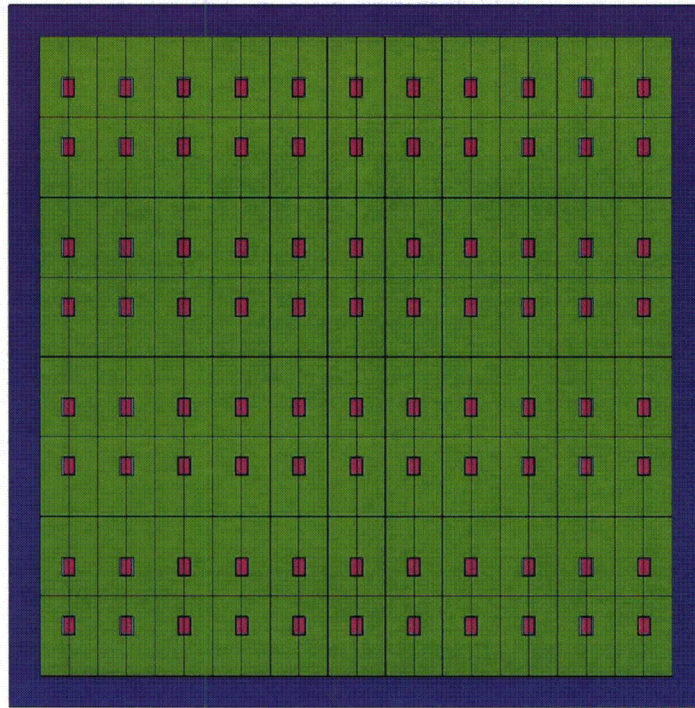


Figure 6-17. Damaged Packages – End-Impact Array, Alternating Layers, Side View

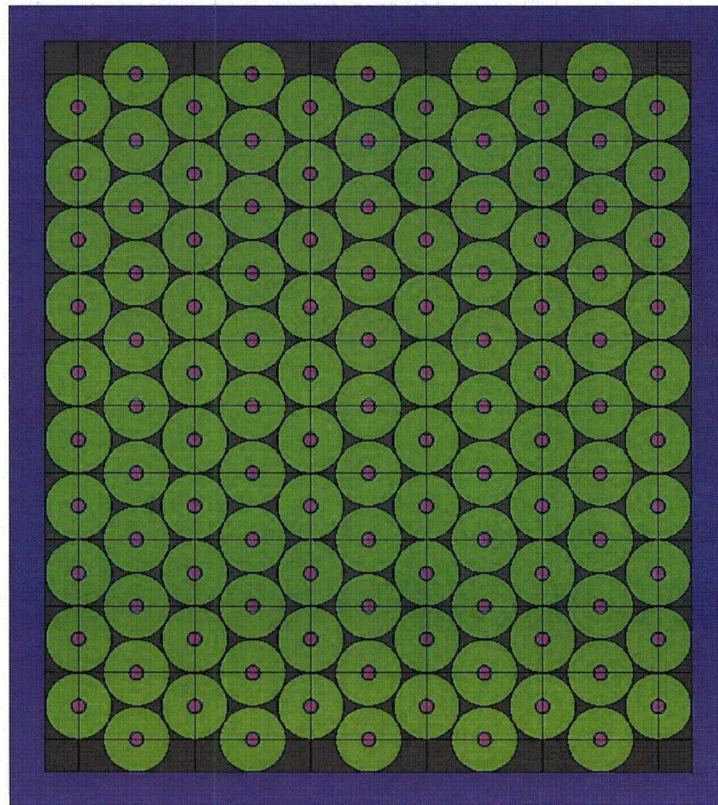


Figure 6-18. Damaged Packages – End-Impact Arrays, Repeated and Alternating Layers, Top View

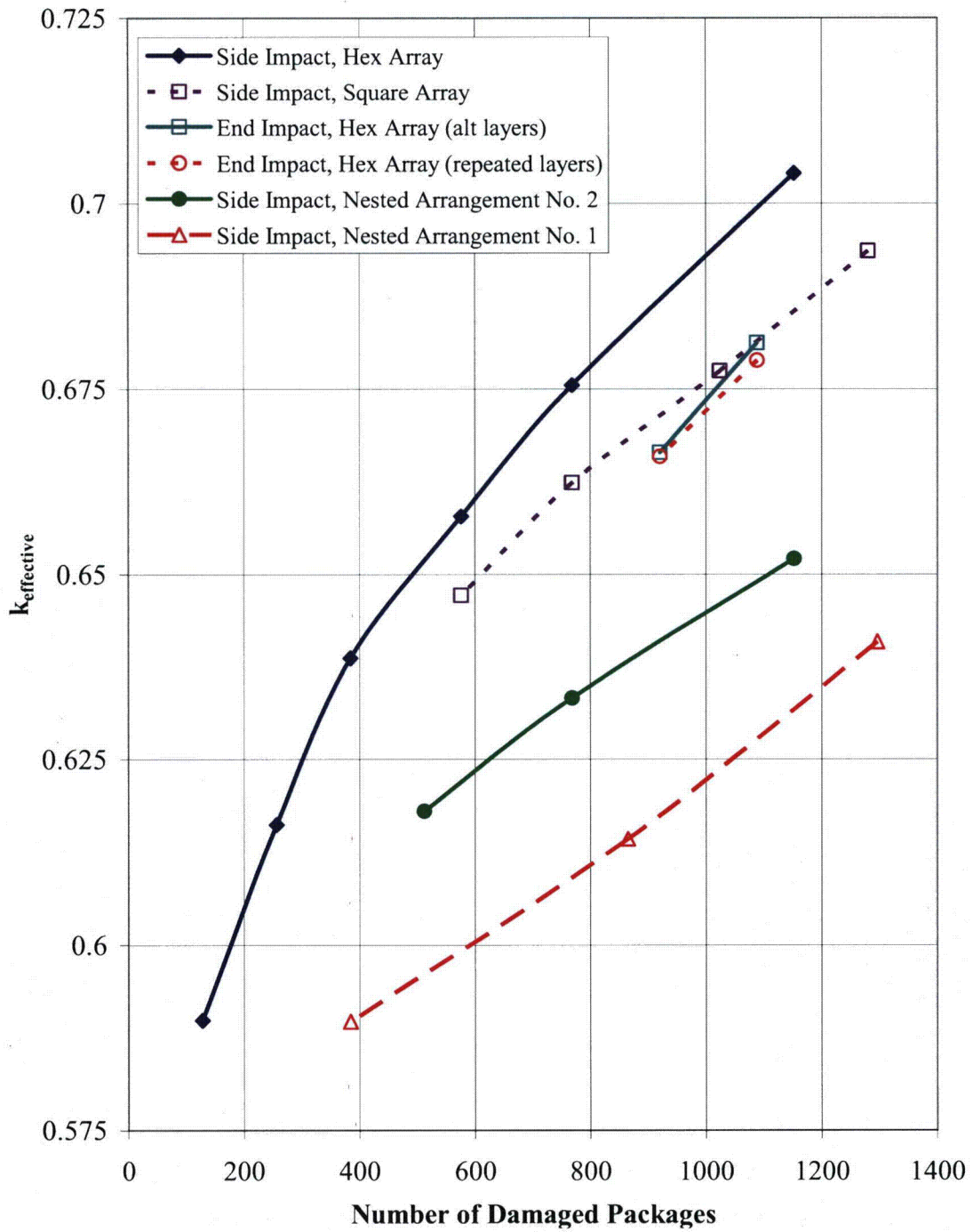


Figure 6-19. Damaged Package Array Study

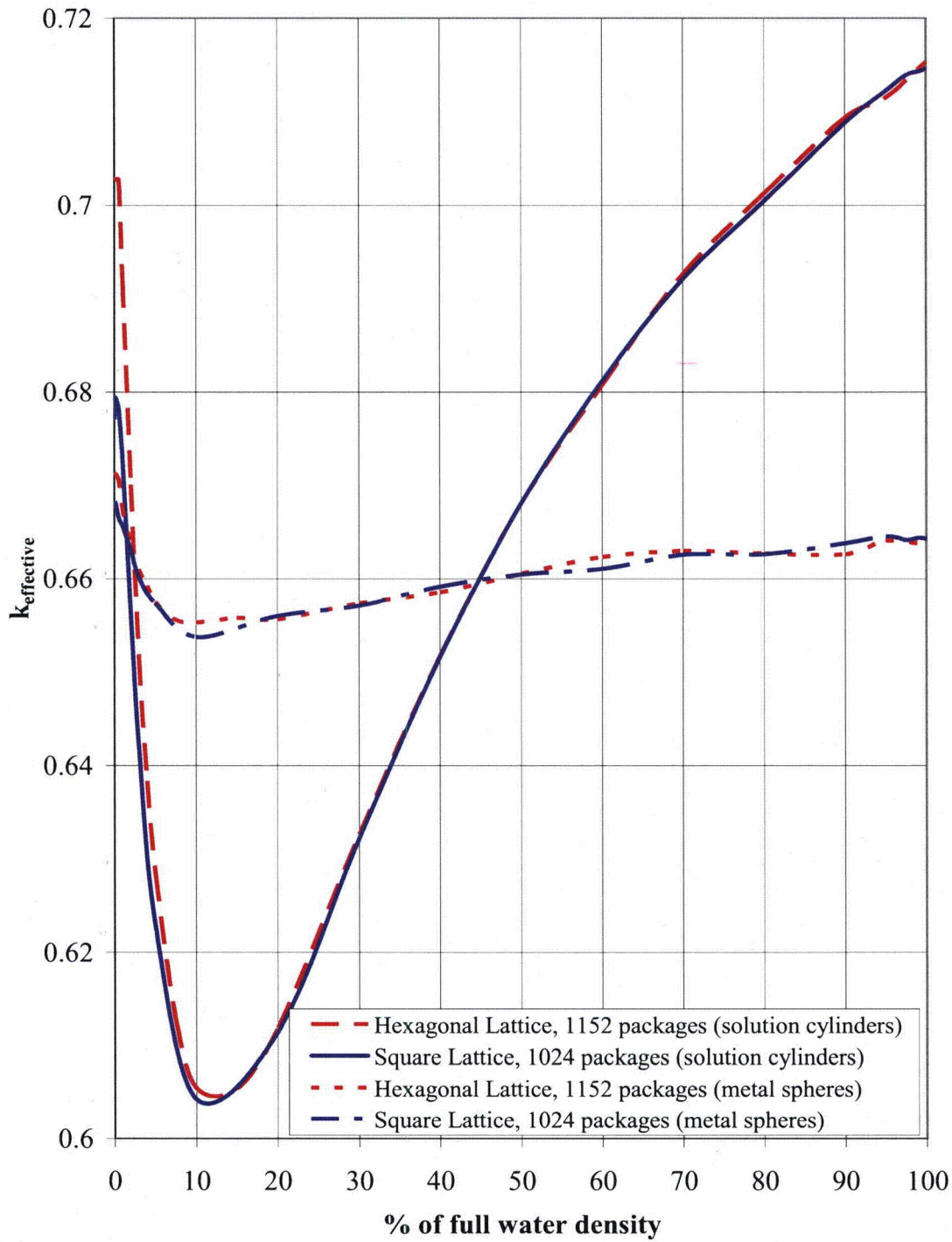


Figure 6-20. Damaged Package Array Internal (redwood zone) Moderation Study

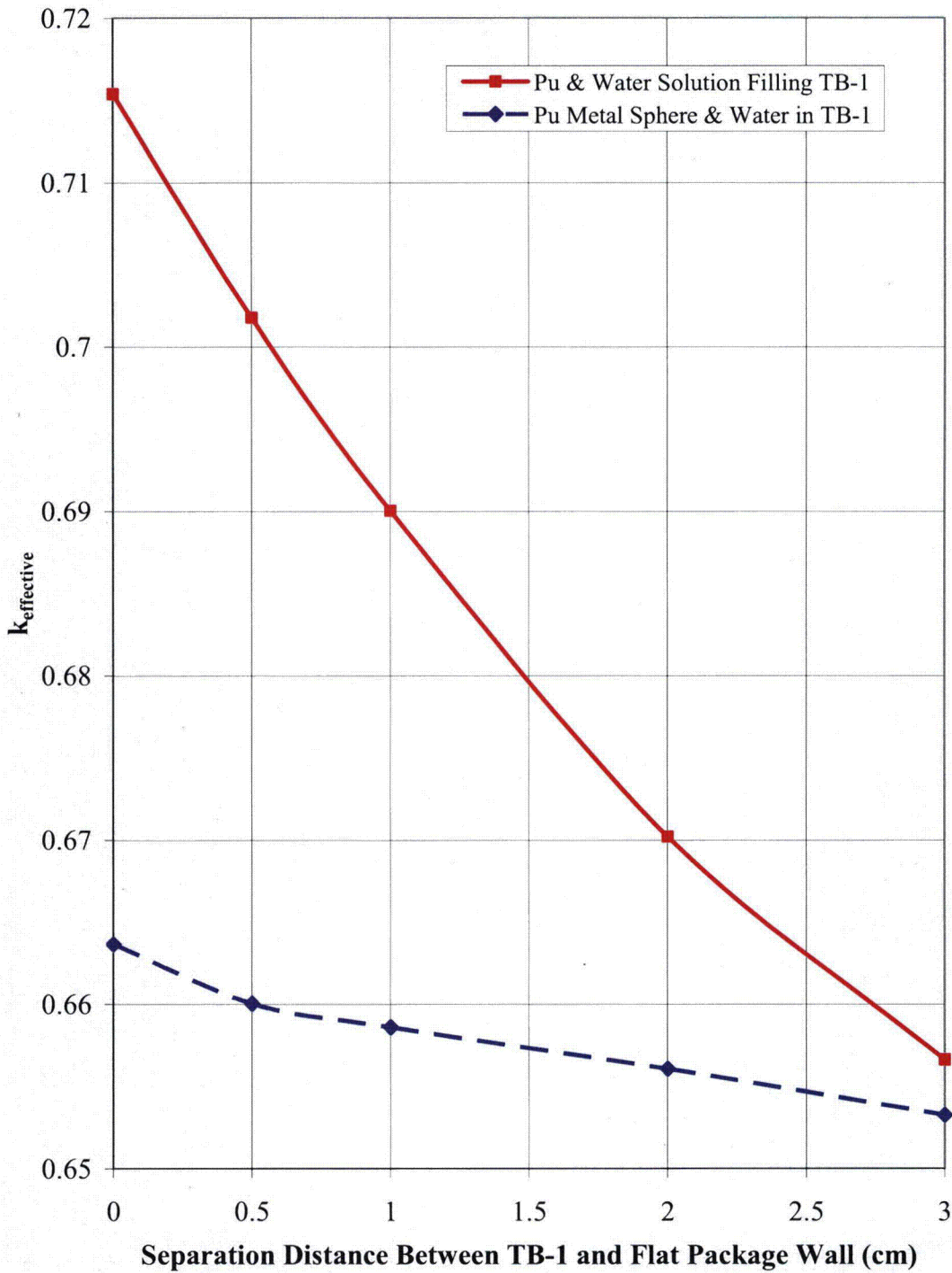


Figure 6-21. Damaged Package TB-1 Location Study

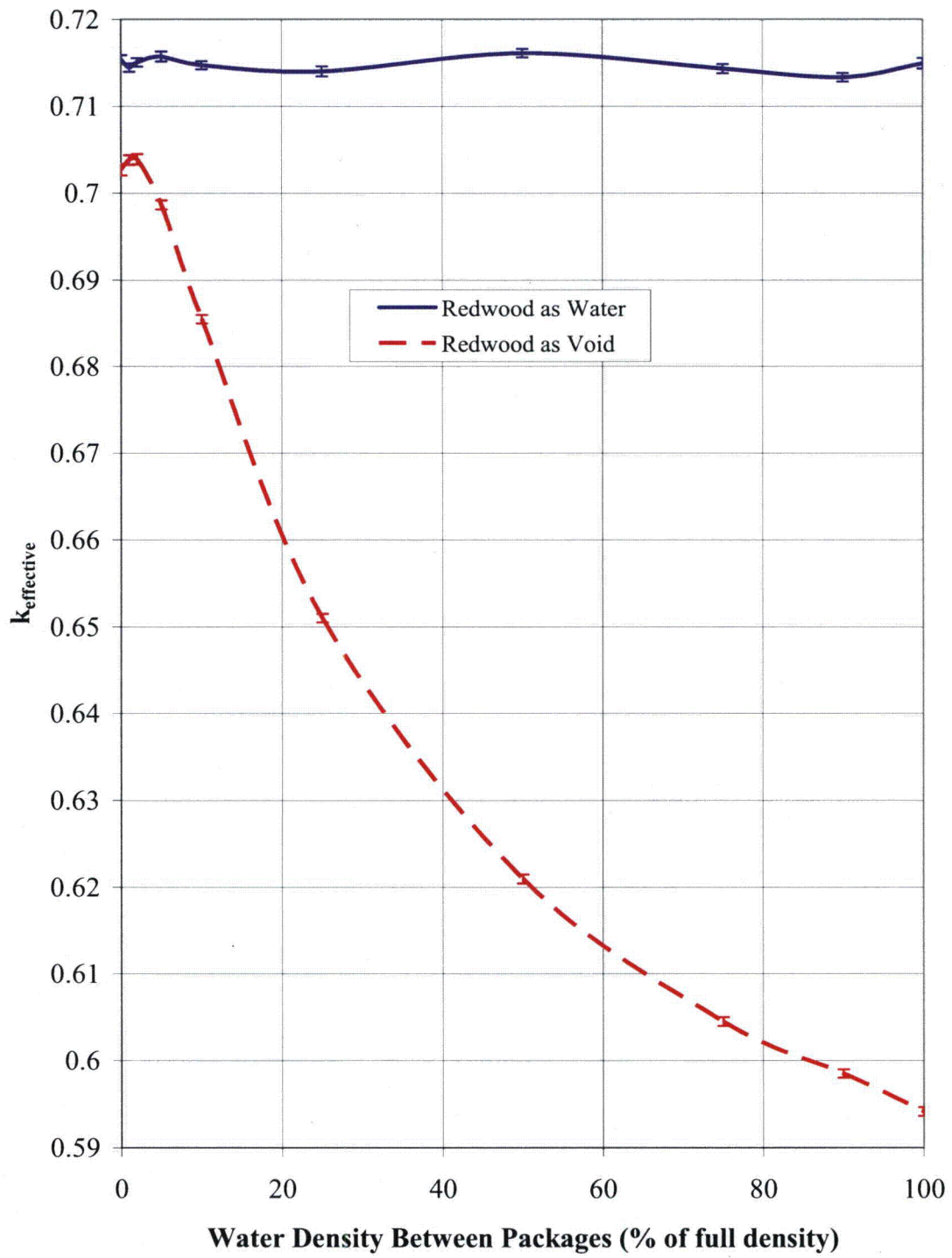


Figure 6-22. Damaged Package External Moderation Study

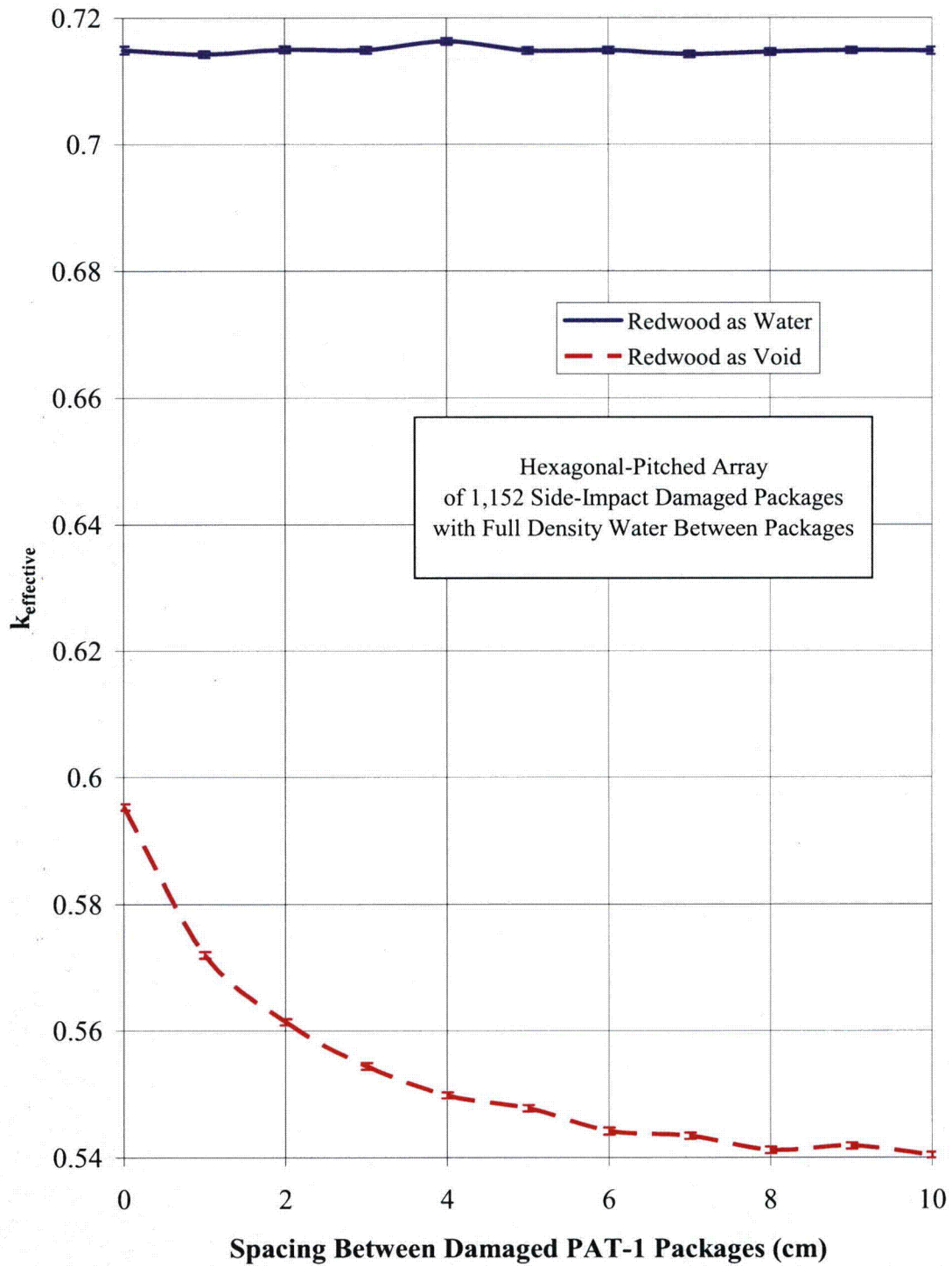


Figure 6-23. Damaged Package External Moderation Study (Package Spacing Varied)

This study shows that the highest k_{eff} value would be obtained with 1300 g (2.87 lb) Pu mixed with 1412 g of water in the TB-1 and with all of the wood replaced with full density water. Because this is the limiting hypothetical accident condition case, an additional study was performed with the side-impact damaged package array to demonstrate that the highest k_{eff} value was obtained with the TB-1 immediately adjacent to the flat side of the package. Figure 6-21 shows the results of calculations in which the TB-1 containment vessel was moved away from the flat side of the package. The redwood zone was modeled as full density water in these calculations. Note: from Figure 6-21 that the highest k_{eff} value is obtained with the TB-1 containment vessel immediately adjacent to the flat side of the package.

Consideration of optimum moderation between packages is also required. Figure 6-22 shows the results of a study in which water with density varying between 0% and 100% was placed between the packages. Figure 6-23 shows the results of a study in which full density water is placed between packages and the distance between packages is varied from 0 to 10 cm (0 to 3.9 in.). Calculations were performed with models for both of the maxima shown in Figure 6-21, namely the redwood modeled as either void or full density water. For the series in which the redwood was modeled as full density water, the water between the drums has no impact on the value of k_{eff} . The minor variation in the curve is due solely to variation introduced by the Mont Carlo method. For the series in which the redwood is modeled as void, adding water between the packages significantly reduces the k_{eff} value.

Considering the discussion provided above, the configuration producing the maximum k_{eff} value for the hypothetical accident conditions is case *hexs100*. This model has 1300 g (2.87 lb) Pu mixed with 1412 g (3.113 lb) of water in the TB-1 containment vessels in 1152 side-impact damaged packages arranged, touching, as shown in Figure 6-12. In this model, the redwood, aluminum, copper, and gaps inside the PAT-1 are modeled as full density water. Optimum moderation between containers was studied and found to have no impact.

6.3.4.4 Single Package Under Expanded Hypothetical Accident Conditions of 10 CFR 71.55(f)

Title 10 CFR 71.55(f) addresses additional requirements applicable to fissile material packages designed to be transported by air. The specifications in 10 CFR 71.55(f) permit use of an assumption that there is no water in-leakage. Considering this assumption, and due to the limited quantity of Pu and hydrogenous packaging that could be present in the TB-1 containment vessel, the analysis in this section shows that criticality cannot be achieved with a single package. Note: that the up to 1412 g (3.113 lb) of water that may be inside the TB-1 vessel is a bounding model for the presence of hydrogenous and other nonneutron multiplying packaging materials. This does not represent water that has leaked into the TB-1.

The criticality analysis considers the remainder of the volume within the TB-1 that is not filled by the Pu may be filled with full density water. This is a bounding model for the packaging materials that could be inside the TB-1. As shown in Section 45, the internal volume of the TB-1 containment vessel is no greater than 1478 cm³. Because 1300 g (2.87 lb) Pu fills a minimum of 65.6 cm³ (4.003 in.³), there could be up to 1412 cm³ (90.19 in.³) of water in the TB-1. Because the package will have, at most, 1300 g (2.87 lb) Pu, a simple conservative analysis approach is used to show that a single damaged package remains subcritical. A series of calculations was performed where the 1300 g (2.87 lb) of Pu were mixed with from 0 to 1412 g (0 to 3.113 lb) of water. The radius of the Pu-water mixture sphere was varied from 2.5 cm

(0.98 in.) for a plutonium metal sphere, to 7.07 cm (2.78 in.) for the smallest sphere that can contain 1300 g (2.87 lb) Pu and 1412 g (3.113 lb) of water, and beyond. As required by 10 CFR 71.55(f)(1), the sphere is reflected by 20 cm (7.8 in.) of water.

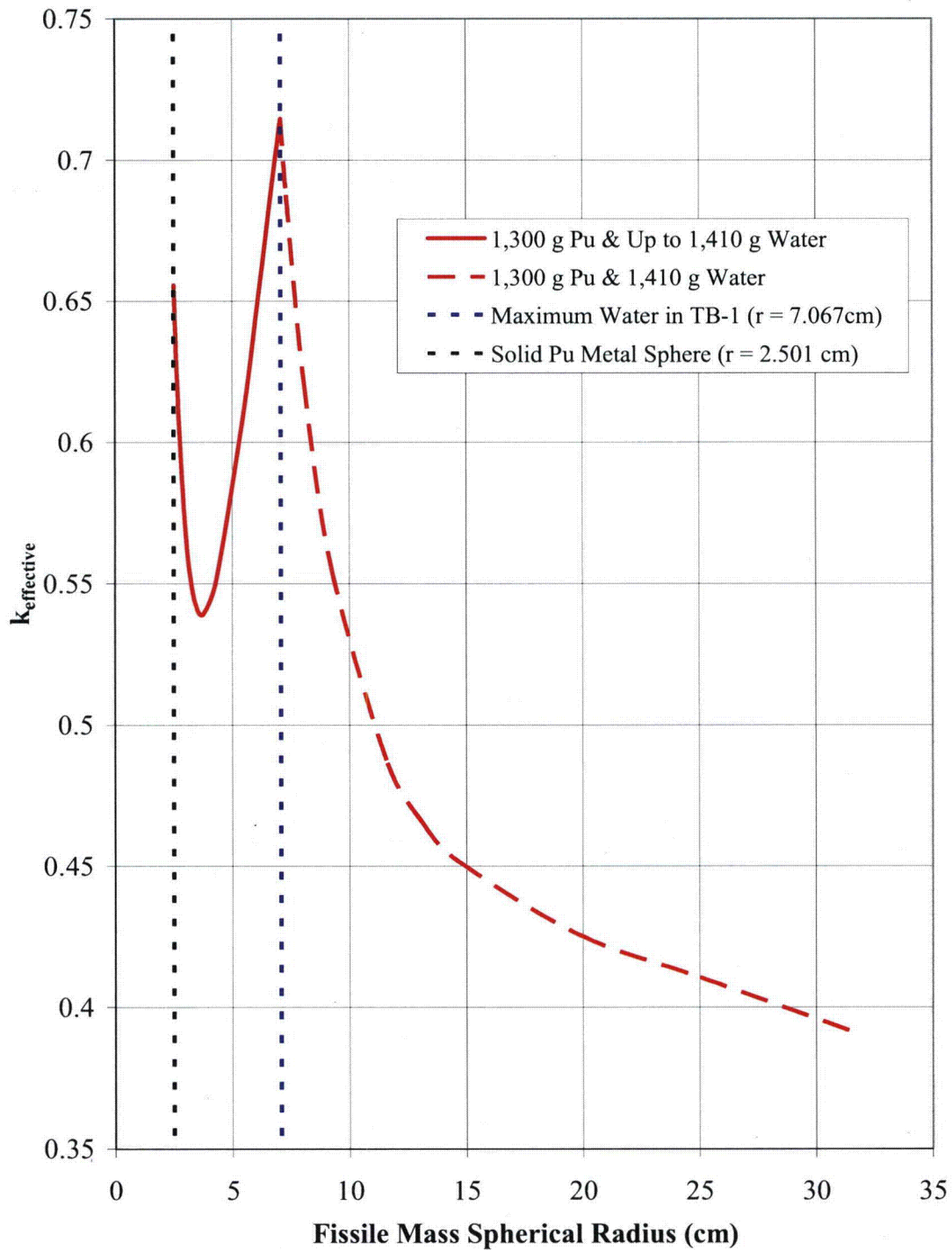


Figure 6-24. Single Package HAC for Air Transport

The results of this study are presented in Figure 6-24. The maximum k_{eff} value of 0.7147 ± 0.0005 was generated by case *sph14*. This analytical approach takes no credit for the dimensions or presence of any structural materials. Consequently, the results of the various tests specified by 10 CFR 71.55(f) do not affect the analysis. The analysis reported in this section takes no credit for the continued presence of any package materials or any package dimensions. The analysis documented in this section is different from the analysis that was presented in Section 6.3.4.1, because this analysis takes credit for the maximum internal diameter of the TB-1 containment vessel.

6.4 Single Package Evaluation

6.4.1 Configuration

The purpose of this section is to demonstrate that a single package is subcritical under both normal conditions of transport and HAC, as specified in 10 CFR 71.55(b) and 10 CFR 71.55(d)(2)-(d)(4). The limiting configuration for these conditions was demonstrated in Section 6.3.4.1.

From Section 1.2.1 of Reference 2, the PAT-1 container is 108 cm (42.52 in.) long and has a diameter of 62.2 cm (24.49 in.). From Section 6.3.1.2, the simplified model is 101.28 cm long and has a diameter of 56.6 cm (22.28 in.). The criteria specified in 10 CFR 71.55(d)(4)(i) and (ii)—consideration of a 5% reduction in volume and spacing—are met because the evaluation model has a diameter that is 9% smaller than the actual package and is 6% shorter than the actual package. The volume of the simplified model is 22% smaller than the actual package. Consequently, criticality safety has been evaluated with a 5% reduction in packaging volume and a 5% reduction in the effective spacing between fissile contents and the outer surface of the packaging. The criteria specified in 10 CFR 71.55(d)(4)(iii) is met because there are no apertures in the outer surface of the packaging large enough to permit entry of a 10 cm (4 in.) cube.

The bounding model adopted for the single package evaluation is the simplified model described in Section 6.3.1 with the wood and outer steel container replaced with water. As demonstrated in Section 6.3.4.1, the case *cv031* yielded the highest k_{eff} value. In this calculation, 1300 g (2.87 lb) of Pu-239 was spread throughout the internal volume of the TB-1 containment vessel and mixed homogeneously with 1412 g (3.113 lb) of water. This model was reflected by 30 cm (11.8 in.) of full density water.

This model is bounding for both the single package normal conditions of transport and hypothetical accident conditions, because the TB-1 containment vessel already holds as much water as it can. No further in-leakage is possible. In the bounding case, the redwood, load spreader, gaps, and outer steel drum are modeled as full density water. Consequently, no further in-leakage into the package is possible. As seen in Figure 6-7, the model yields a far higher k_{eff} value when the steel and redwood are modeled as full density water than when they are modeled as steel and redwood. As described in NUREG-0361,² the test specified for normal conditions of transport had negligible effect on the package geometry. Additional discussion is provided in Section 6.3.4.1 supporting the concept that this model is the bounding model for both normal conditions of transport and hypothetical accident conditions.

6.4.2 Results

The maximum k_{eff} value of 0.7076 ± 0.0006 was produced by Case *cv031*, in which 1300 g (2.87 lb) of Pu-239 was spread throughout the internal volume of the TB-1 containment vessel and mixed homogeneously with 1412 g (3.113 lb) of water. As determined in Section 6.8.2.5, an upper subcritical limit (USL) of 0.9456 is applicable to this case. Because the calculated k_{eff} value plus two standard deviations is less than the USL, a single package is subcritical under both normal conditions of transport and the single package hypothetical accident conditions.

6.5 Evaluation of Package Arrays under Normal Conditions of Transport

6.5.1 Configuration

The purpose of this section is to demonstrate that 2500 ($5 \times N$, where $N = 500$) packages with nothing between the packages are subcritical. The limiting configuration for these conditions was demonstrated in Section 6.3.4.2.

As shown in Section 6.3.4.2, each package in the selected limiting configuration has a 1300 g (2.87 lb) Pu-239 metal sphere surrounded by 1412 g of water inside the TB-1 containment vessel. The “simplified” model shown in Figure 6-2 was used, with the redwood modeled as full density water. The model has 2646 packages in a $19 \times 15.5 \times 9$ hexagonal-pitched array with 30 cm (11.8 in.) of close-fitting full density water around the outside of the array.

6.5.2 Results

The maximum k_{eff} value of 0.6509 ± 0.0005 was produced by case *fhlsf001*. As determined in Section 6.8.2.3, a USL of 0.8893 is applicable to this case. Because the calculated k_{eff} value plus two standard deviations is less than the USL, an array of 2646 packages is subcritical under normal conditions of transport. Thus a smaller array of 2500 packages is also subcritical under normal conditions of transport.

6.6 Package Arrays under Hypothetical Accident Conditions

6.6.1 Configuration

The purpose of this section is to demonstrate that 1000 ($2 \times N$, where $N = 500$) damaged packages are subcritical. The limiting configuration for these conditions was demonstrated in Section 6.3.4.3.

As was shown in Section 6.3.4.3, each package in the selected limiting configuration has 1300 g (2.87 lb) Pu-239 metal homogeneously mixed with 1412 g (3.113 lb) of water inside the TB-1 containment vessel. The “side impact” model shown in Figure 6-4 was used, with the redwood modeled as full density water. The model has 1152 packages arranged in a near cubic array. Pairs of packages are arranged in a tight-fitting hexagonal array. Figure 6-12 shows how the packages are arranged in each of the six layers. Note: that this model uses a reflective boundary condition along the bottom and left-hand side of the figure such that each of the six layers has four times as many packages than are shown in the figure. As was shown in Section 6.3.4.3, optimum interspersed moderation is achieved with nothing present between the packages. A close-fitting 30-cm-thick (11.8-in.-thick) full-density-water reflector completely encloses the array.

6.6.2 Results

The maximum k_{eff} value of 0.7154 ± 0.0005 was produced by case *hexs100*. As determined in Section 6.8.2.4, a USL of 0.9396 is applicable to this case. Because the calculated k_{eff} value plus two standard deviations is less than the USL, an array of 1152 packages is subcritical under hypothetical accident conditions. Thus, a smaller array of 1000 packages is also subcritical under hypothetical accident conditions.

6.7 Fissile Material Packages for Air Transport

6.7.1 Configuration

The purpose of this section is to demonstrate that a single package, subjected to the additional tests and conditions specified in 10 CFR 71.55(f) for fissile material package designs to be transported by air, would be subcritical. As shown in Section 6.3.4.4, the limiting configuration is a sphere with a radius of 7.067 cm, containing 1300 g (2.87 lb) of Pu-239 mixed homogeneously with 1412 g of water, and reflected by 20 cm of water.

6.7.2 Results

The maximum k_{eff} value of 0.7147 ± 0.0005 was produced by case *sph14*. As determined in Section 6.8.2.5, a USL of 0.9462 is applicable to this case. Because the calculated k_{eff} value plus two standard deviations is less than the USL, a single package, with no water in-leakage, is subcritical without taking any credit for packaging materials and dimensions.

6.8 Benchmark Evaluations

The purpose of the benchmark evaluations is to validate the computational method used to calculate the neutron multiplication factors (e.g., k_{eff} values) for the limiting safety calculations involving plutonium metal and packaging materials that comprise a loaded PAT-1 package and water that is placed in and around the PAT-1 packages for the safety analysis. Validation is completed using the same computational methods to model critical configurations, which are similar to the limiting safety calculations, and performing statistical analyses to determine upper subcritical limits applicable to the safety calculations. The computational method is described in Section 6.3.3.

The process used to validate the computational method for the PAT-1 packages is comprised of the following steps:

1. Identify the limiting application systems and the ranges of parameters and conditions for which the validation will apply.
2. Select critical benchmark configurations for consideration based on similarities in physical characteristics between the limiting application systems and critical benchmark configurations.
3. Identify applicable critical benchmark configurations based on neutronic similarity between the application systems and the selected critical benchmark configurations, as determined by comparing characteristic parameters such as the hydrogen to Pu-239 atom

ratio (H/Pu) and the energy of average lethargy of neutrons causing fission (EALF) and by using the SCALE 5.1 sensitivity/uncertainty computational tools (TSUNAMI).^{37, 38}

4. Use the results from the critical experiment models to determine the USLs that are applicable to the limiting applications using accepted statistical analysis techniques and industry tools. Only critical experiments that have neutronic similarities—that is, similar material compositions, neutron spectra, and leakage—with the application systems are used in the determination of the USLs. As is described in Section 6.8.2, the USLs include bias, bias uncertainty, administrative margin, and any additional margin that may be required by the statistical technique used to derive the USLs.

6.8.1 Applicability of Benchmark Experiments

All critical configurations used in the benchmark evaluation were selected from the *International Handbook of Evaluated Criticality Safety Benchmark Experiments* (IHECSBE) from the Nuclear Energy Agency of the Organization for Economic Co-operation and Development (OECD-NEA).³⁹ The IHECSBE contains evaluations of criticality benchmark experiments that have been peer reviewed by an international group of experts. Each evaluation contains a detailed description of the critical configuration with an extensive analysis of any assumptions and biases resulting from the difference between the actual experimental configuration and its description.

CSAS25/KENO V.a^{35,34, 36} models of a large portion of the critical benchmark configurations in the evaluated experiments contained in the IHECSBE have been created by Oak Ridge National Laboratory (ORNL) staff. TSUNAMI-3D³⁷ was used to perform sensitivity analysis for each of these critical configurations. TSUNAMI-3D uses flux moment data, generated by forward and adjoint Monte Carlo calculations, in a first-order linear perturbation theory method to calculate energy-, nuclide-, reaction-, and mixture-dependent k_{eff} sensitivity data. As part of the PAT-1 validation study, TSUNAMI-IP³⁸ was used to compare the k_{eff} sensitivity data of the safety calculations to the sensitivity data for about 240 Pu-critical experiment configurations. TSUNAMI-IP yields a correlation coefficient, c_k , which is a measure of how similar each critical configuration is to each of the limiting safety applications. The correlation coefficients were used to identify 125 critical configurations that are most similar to the limiting safety applications. These critical configurations include the following: 7 plutonium metal spherical assemblies with and without a reflector; 29 Pu-polystyrene slabs with and without a reflector; and 89 Pu solutions in spheres or cylinders. The 125 critical benchmark configurations, the evaluated experiment they are from, and brief descriptions are listed in Section 6.9.3.

The similarity or applicability of critical configurations to specific criticality analysis cases was assessed by comparing characteristic neutron parameters (EALF, H/Pu, and c_k) for the safety analysis cases with those from the critical configurations. The energy from average lethargy of neutrons causing fission (EALF) values were extracted from the KENO V.a output. The H/Pu ratios were calculated from the composition information for the mixture containing the Pu. Ideally, the sets of validation experiments should have EALF and H/Pu values bounding the analysis cases and have data points near the EALF and H/Pu values for the safety applications. The c_k parameter provides a more detailed neutronic comparison of the safety cases and validation experiments. A c_k of 1 indicates perfect similarity, and a c_k value greater than 0.9 indicates good similarity for validation purposes. More details are provided below on performing similarity analysis using the SCALE 5.1 sensitivity and uncertainty tools.

TSUNAMI-3D calculations were performed for the set of 11 application models that are representative of the limiting normal and hypothetical accident conditions. A brief description of each application is provided below with its acronym.

- *cv001* – The application consists of a single sphere consisting of 1300 g (2.87 lb) of Pu-239 metal centered in a cylinder of water approximately the volume of a PAT-1 package.
- *cv031* – The application consists of a single cylinder containing a Pu-239 metal-water mixture having 1300 g (2.87 lb) of Pu homogeneously mixed with sufficient water to fill the inside volume of a TB-1 container. This Pu-water cylinder is then centered in a cylinder of water approximately the volume of a PAT-1 package.
- *sph14* – The application consists of a single sphere containing a Pu-239 metal-water mixture having 1300 g (2.87 lb) of Pu-239 homogeneously mixed with sufficient water to fill the inside volume of a TB-1 container reflected by 20 cm (7.87 in.) of water.
- *fhlsf001* – The application consists of a roughly cubic-shaped hexagonal-pitch array of 2646 PAT-1 packages, with each position containing the following geometry. The innermost region contains a 1300 g (2.87 lb) Pu-239 metal sphere centered in a water cylinder representing the inside of a TB-1 container. This is centered in a steel cylinder representing the TB-1 container. The space between the TB-1 container and outer PAT-1 container is filled with water. The water is surrounded by a steel cylinder representing a PAT-1 outer container. The space between PAT-1 packages is void and a 30-cm-thick (11.81-in.-thick) water reflector surrounds the array on all sides.
- *fhlsf031* – The application consists of a roughly cubic-shaped hexagonal-pitch array of 2646 PAT-1 packages, with each position containing the following geometry. The innermost region contains a Pu-239 metal-water mixture having 1300 g (2.87 lb) of Pu-239 homogeneously mixed with sufficient water to fill the inside volume of a TB-1 container. This is centered in a steel cylinder representing a TB-1 container. The space between the TB-1 container and outer PAT-1 outer container is filled with water. The water is surrounded by a steel cylinder representing a PAT-1 outer container. The space between PAT-1 packages is void and a 30-cm-thick (11.81-in.-thick) water reflector surrounds the array on all sides.
- *fslsf001* – The application consists of a 17×17×9 square-pitched array of 2601 PAT-1 packages, with each position containing the following geometry. The innermost region contains a 1300 g (2.87 lb) Pu-239 metal sphere centered in a water cylinder representing the inside of a TB-1 container. This is centered in a steel cylinder representing a TB-1 container. The space between the TB-1 container and outer PAT-1 container is filled with water. The water is surrounded by a steel cylinder representing a PAT-1 outer container. The space between PAT-1 packages is void and a 30-cm-thick (11.81-in.-thick) water reflector surrounds the array on all sides.
- *fslsf031* – The application consists of a 17×17×9 square-pitched array of 2601 PAT-1 packages, with each position containing the following geometry. The innermost region

contains a Pu-239 metal/water mixture having 1300 g (2.87 lb) of Pu-239 homogeneously mixed with sufficient water to fill the inside volume of a TB-1 container. This is centered in a steel cylinder representing a TB-1 container. The space between the TB-1 container and outer PAT-1 container is filled with water. The water is surrounded by a steel cylinder representing a PAT-1 outer container. The space between PAT-1 packages is void, and a 30-cm-thick (11.81-in.-thick) water reflector surrounds the array on all sides.

- *hexs100* – A roughly cubic-shaped hexagonal-pitch array representing 1152 damaged PAT-1 packages. Each container holds a Pu-239 metal-water cylinder having 1300 g (2.87 lb) of Pu-239 homogeneously mixed with sufficient water to fill the inside volume of a TB-1 container. This is centered in a steel cylinder representing a TB-1 container. The outer PAT-1 container is a steel hemicylinder, representing a smashed container. The containers are then stacked flat side to flat side and loaded into a hexagonal array with each row rotated 90 degrees. The TB-1 container is located inside and immediately adjacent to the center of the damaged outer drum's flat side. The space between the TB-1 container and the damaged outer PAT-1 container is filled with water. The space between PAT-1 packages is void. A 30-cm-thick (11.81-in.-thick) water reflector surrounds the array on all positive faces (i.e., +x, +y, and +z). The model uses specular reflection on all negative faces.
- *hexsdry* – A roughly cubic-shaped hexagonal-pitch array representing 1152 damaged PAT-1 packages. Each container holds a Pu-239 metal/water cylinder having 1300 g (2.87 lb) of plutonium homogeneously mixed with sufficient water to fill the inside volume of a TB-1 container. This is centered in a steel cylinder representing a TB-1 container. The outer PAT-1 container is a steel hemicylinder, representing a smashed container. The containers are then stacked flat side to flat side and loaded into a hexagonal array with each row rotated 90 degrees. The TB-1 container is located inside and immediately adjacent to the center of the flat side of the damaged outer drum. The space between the TB-1 container and outer PAT-1 container is void. The space between PAT-1 packages is void. A 30-cm-thick (11.81-in.-thick) water reflector surrounds the array on all positive faces. The model uses specular reflection on all negative faces.
- *octs100* – A 4×8×4 square-pitched lattice representing 1024 damaged PAT-1 packages. Each container holds a Pu-239 metal/water cylinder having 1300 g (2.87 lb) of Pu-239 homogeneously mixed with sufficient water to fill the inside volume of a TB-1 container. This is centered in a steel cylinder representing a TB-1 container. The outer PAT-1 container is a hemicylinder, representing a smashed container. The containers are then stacked flat side to flat side and loaded into a square-pitched array. The TB-1 container is located inside and immediately adjacent to the center of the damaged outer drum's flat side. The space between the TB-1 container and outer PAT-1 container is filled with water. The space between PAT-1 packages is void. A 30-cm-thick (11.81-in.-thick) water reflector surrounds the array on all positive faces and specular reflection is used on all negative faces.
- *octsdry* – A 4×8×4 square pitched lattice representing 1024 damaged PAT-1 packages. Each container holds a Pu-239 metal/water cylinder having 1300 g (2.87 lb) of Pu-239 homogeneously mixed with sufficient water to fill the inside volume of a TB-1 container.

This is centered in a steel cylinder representing a TB-1 container. The outer PAT-1 container is a hemicylinder, representing a smashed container. The containers are then stacked flat side to flat side and loaded into a square-pitched array. The TB-1 container is located inside and immediately adjacent to the center of the damaged outer drum's flat side. The space between the TB-1 container and outer PAT-1 container is filled with void. The space between PAT-1 packages is void. A 30-cm-thick (11.81-in.-thick) water reflector surrounds the array on all positive faces and specular reflection is used on all negative faces.

The convergence of each of the CSAS25/KENO V.a and TSUNAMI-3D calculations for the set of 125 critical benchmark configurations and the 11 applications were assessed by reviewing the plot of average k_{eff} by generation run and the plot of average k_{eff} by generation skipped. No trends were observed in these plots that would be indicative of poor convergence. In addition, the frequency distribution plots were examined. These frequency distribution plots show single k_{eff} peaks, which is also an indication of convergence. The k_{eff} results of KENO V.a forward and adjoint calculations, which are used in the S/U (TSUNAMI-3D) analysis, were adequately similar, varying by less than 1% for most cases.

Although each application was examined individually, they were divided into four general groups with the members of each group having very similar neutronic characteristics. A short description of the types of critical benchmark configurations used to validate each group of applications is provided below. Table 6-6 provides a synopsis of each application and the critical benchmark configurations used for their validation.

- Metal Pu Spheres (*cv001*, *fhlsf001*, *fhlsf001*) – These applications contain 1300 g (2.87 lb) plutonium metal spheres surrounded by water. The EALF of these three applications is between 54 and 80 keV. The critical benchmark configurations that best represent these applications are from the Plutonium Metal Fast (PMF) experiments and Plutonium Compound Mixed (PCM) experiments whose EALF values range from 1.76 keV to 1.27 Mev.
- Solution Lattices (*fhlsf031*, *fhlsf031*, *hexs100*, *octs100*) – These applications contain Pu-water solutions surrounded by water in either a hexagonal or rectangular pitched lattice. The lattice is reflected by 30 cm (11.81 in.) of water.
- The EALF of these four applications is between 2.54 and 2.70 eV. The critical benchmark configurations that best represent these applications are primarily from the Plutonium Solution Thermal (PST) experiments and a few PCM experiments whose EALF values range from 0.147 to 6.446 eV.
- Single Solution Units (*cv031*, *sph14*) – These applications contain plutonium-water solutions surrounded by water. The EALF of the two applications is 1.094 and 1.259 eV respectively. The critical benchmark configurations that best represent these applications are from the PST experiments whose EALF values range from 0.112 to 5.405 eV.

Table 6-6. Summary of Similarity Between Benchmark Configurations and Applications

| Application Name | Application | | | Critical Benchmark Configurations | | | |
|------------------|-------------|-----------|------|-----------------------------------|-----------------|----------------|-----------------------|
| | k_{eff} | EALF (eV) | H/Pu | N ^a | EALF (eV) | H/Pu Ratio | c _k Values |
| <i>cv001</i> | 0.6565 | 5.470E4 | 0.0 | 13 | 1.76E3 – 1.27E6 | 0.00 – 0.05 | 0.9158 – 0.9948 |
| <i>fhlsf001</i> | 0.6509 | 8.034E4 | 0.0 | 13 | 1.76E3 – 1.27E6 | 0.00 – 0.05 | 0.9178 – 0.9960 |
| <i>fslsf001</i> | 0.6504 | 7.957E4 | 0.0 | 13 | 1.76E3 – 1.27E6 | 0.00 – 0.05 | 0.9176 – 0.9958 |
| <i>fhlsf031</i> | 0.6324 | 2.682 | 28.8 | 60 | 0.147 – 6.446 | 15.46 – 220.19 | 0.8933 – 0.9362 |
| <i>fslsf031</i> | 0.6337 | 2.692 | 28.8 | 60 | 0.147 – 6.446 | 15.46 – 220.19 | 0.8903 – 0.9334 |
| <i>hexs100</i> | 0.7154 | 2.544 | 28.8 | 60 | 0.147 – 6.446 | 15.46 – 220.19 | 0.8979 – 0.9517 |
| <i>octs100</i> | 0.7147 | 2.531 | 28.8 | 60 | 0.147 – 6.446 | 15.46 – 220.19 | 0.8974 – 0.9505 |
| <i>cv031</i> | 0.7076 | 1.091 | 28.8 | 95 | 0.112 – 5.405 | 15.46 – 258.46 | 0.9018 – 0.9604 |
| <i>sph14</i> | 0.7147 | 1.255 | 28.8 | 95 | 0.112 – 5.405 | 15.46 – 258.46 | 0.9088 – 0.9588 |
| <i>hexsdry</i> | 0.7027 | 4.845 | 28.8 | 33 | 0.254 – 37.727 | 15.46 – 131.30 | 0.9059 – 0.9741 |
| <i>octsdry</i> | 0.6772 | 5.020 | 28.8 | 33 | 0.254 – 37.727 | 15.46 – 131.30 | 0.9025 – 0.9706 |

^a Number of critical configurations in validation set.

- Dry Lattices (*hexsdry*, *octsdry*) – These applications contain plutonium-water solutions with no surrounding hydrogenous material. The array, however, is surrounded by 30 cm of water. The EALF is 4.864 and 5.042 eV respectively. The critical benchmark configurations that best represent these applications are primarily from the PCM experiments and a few PST experiments whose EALF values range from 0.254 to 37.727 eV.

TSUNAMI-3D was used to calculate the sensitivity profiles used in the assessment of the similarity of the safety analysis models and the critical experiment models. When using TSUNAMI-3D the analyst selects from several analysis approaches depending upon the nature and complexity of the problem. The analyst verifies that a correct analytical approach was used by performing direct perturbation calculations. These calculations involve running additional k_{eff} calculations with the densities of selected nuclides or mixtures varied to show effect of these changes on system k_{eff} . The direct perturbation results are then compared with the TSUNAMI sensitivity analysis results, confirming that an appropriate analytical approach was used. Generally, it is not necessary to perform direct perturbation calculations for all nuclides in a problem. Typically, direct perturbations calculations are performed for the primary fissile nuclide and the primary neutron moderator. It is not necessary to perform direct perturbation calculations for every nuclide mixed in with the primary fissile nuclide or mixed in with the primary moderator because checking those two nuclides ensures that the forward and adjoint neutron transport solutions used in the TSUNAMI calculation are adequately converged and the problem has enough spatial resolution to adequately capture local variations. Additional direct

perturbation calculations may also be performed for other key model features, such as neutron poison panels in a spent fuel storage rack.

To verify the TSUNAMI-3D sensitivity analysis, a representative sample of the critical benchmark configuration set was selected for direct perturbation analysis. The 15 critical benchmark configurations in this sample were analyzed by increasing and decreasing the Pu-239 concentration and, where possible, the hydrogen concentration such that the resulting k_{eff} values span approximately 10 standard deviations. The sensitivities from the direct perturbation results were then compared to the sensitivities produced by TSUNAMI-3D. For the critical benchmark configurations, the direct perturbation sensitivities compare to the TSUNAMI sensitivities within approximately 2 standard deviations in all but one case as shown in Section 6.9.3. Thus, the direct perturbation results confirm that the TSUNAMI-3D calculations were performed properly.

The TSUNAMI-3D sensitivity analyses for each of the 11 applications were also verified using direct perturbation analysis. The applications were analyzed by increasing and decreasing the Pu-239 concentration and water concentration such that the resulting k_{eff} values span approximately 10 standard deviations. The sensitivities from the direct perturbation results were then compared to the sensitivities produced by TSUNAMI-3D. For the set of 11 applications, the direct perturbation sensitivities compare to the TSUNAMI sensitivities within 2 standard deviations for all cases as shown in Table 6-10 in Section 6.9.3. Thus, the direct perturbation results confirm that the TSUNAMI-3D calculations were performed properly.

The similarity of the critical benchmark configurations to each application was evaluated by comparing the EALF values and H/Pu ratios of the critical experiments to the values from the applications. The application EALF and H/Pu values are similar to the values from the critical configurations. Similarity was also evaluated by examining the c_k values produced when comparing the available critical benchmark configurations to each application using TSUNAMI-IP.³⁸ The value of the TSUNAMI global integral index, c_k , measures the correlation of sensitivity and nuclear data uncertainty between systems. Systems that have highly correlated sensitivities and nuclear data uncertainties should exhibit similar calculation biases, because the sensitivity is a measure of system response to data variation or data errors. A c_k value of 1.0 indicates that the experiment and application are identical in terms of sensitivity and uncertainty data. Critical benchmark configurations, with correlation coefficient (c_k) values greater than 0.8, are considered marginally applicable.⁴⁴ Critical configurations, with c_k values greater than 0.9, are considered applicable to the validation of the application.

The applications were sorted into groups based on their similarity in nuclear parameters and sensitivities to the critical benchmark configurations. A set of critical benchmark configurations having the highest c_k values was selected for each application to be included in the validation. The EALF and H/Pu ratios of the critical benchmark configurations with the highest c_k values were then checked to see if they encompassed the application. The goal was to have as many as possible critical benchmark configurations in the validation for each application that had c_k values greater than 0.9. The set of critical benchmark configurations were then collected for each group. Section 6.9.3 contains lists of the critical benchmark configurations that have the highest c_k values of all the available Pu configurations relative to the applications.

Comparison of the EALF values, H/Pu ratios, and c_k values indicate that the critical configurations in the validation sets for the applications are similar to the associated applications as indicated primarily by the high c_k values.

Table 6-6 summarizes of the nuclear parameters of the applications and critical benchmark configurations used for each validation. Note that the validation sets for 5 of the 1 applications included fewer than 50 critical configurations. This is acceptable because the Distribution-Free Tolerance Limit Method used for the USL calculation in these sets is designed to be used with as few as 10 data points.

6.8.2 Bias Determination

This section describes the methods used to determine an USL for the applications evaluated in this report based on the critical benchmark configurations chosen as representative of the applications. Bias and bias uncertainty over the area of applicability of critical experiments are determined using the guidance in ANSI/ANS 8.1-1998, ANSI/ANS 8.17-2004, and ANSI/ANS 8.24-2007. The accuracy of the computational method and cross section data is established by evaluating critical experiments. Computational bias is the difference between calculated and experimental results. The uncertainty in bias is an allowance for uncertainties in the experiment conditions, the lack of accuracy and precision in the calculational method, and, if necessary, the extension of the area of applicability.

Generally, the bias and bias uncertainty are expected to be functions of various physical or neutronic parameters that can be determined using trending analyses. This technique can be applied to establish bias and bias uncertainty because k_{eff} values often exhibit an increasing or decreasing trend as a function of parameters such as fissile material concentration, hydrogen-to-fissile material ratio, EALF, sensitivity coefficient, etc., that can be distinguished from random behavior.

Statistical techniques exist for evaluating the bias and bias uncertainty, and for establishing limits that can reliably be used to predict subcriticality, such as tolerance band, single-sided tolerance limit, and distribution-free tolerance limit (nonparametric) methods.^{40,41,42,43} These methods use bias and the bias uncertainty in combination with additional considerations (e.g., administrative margins, where applicable) to establish a critical limit (CL) (single value or a function, depending on the method applied) above which a desired fraction of the true population of k_{eff} values calculated for critical systems is expected to lie, with a prescribed confidence and within the area of applicability. The parametric methods typically require that the k_{eff} values for the applicable critical experiments form a normal distribution. When the k_{eff} values for the critical experiments are not normally distributed about a mean value, a nonparametric statistical treatment (i.e., distribution-free methods) should be used.⁴³

The level of subcriticality required to maintain safety is calculated based on Section 5.1 of ANSI/ANS 8.17. For an application or system to be considered subcritical, the calculated multiplication factor for the system, k_s , must be less than or equal to an established maximum allowable multiplication factor based on benchmark calculations and uncertainty terms, as shown in Equation 6-1.

$$k_s \leq k_c - \Delta k_s - \Delta k_c - \Delta k_m \quad (\text{Eq. 6-1})$$

where

- k_s = multiplication factor k_{eff} for the application or system for which subcriticality must be maintained;
- k_c = the mean value of k_{eff} resulting from the calculation of benchmark criticality experiments using a specific calculational method and data;
- Δk_s = uncertainty in the value of k_s ;
- Δk_c = uncertainty in the value of k_c ;
- Δk_m = an additional margin to ensure subcriticality.

The value of Δk_m is often referred to as the administrative margin and assigned an arbitrary limit of 0.05. This value is set in Method 1 and calculated in Method 2 of USLSTATS.⁴⁰

If calculational bias, β , is defined as $\beta = k_c - 1.0$, then the uncertainty in the calculational bias is identical to the uncertainty in k_c , (i.e., $\Delta\beta = \Delta k_c$). The bias is defined as negative if $k_c \leq 1$ and positive if $k_c \geq 1$. By convention, a positive bias is never allowed; if $k_c \geq 1$, then k_c is set equal to 1.0.

The values of k_c and β may not be constant, but instead may vary over some parameter (e.g., EALF, H/Pu, correlation coefficient, etc.). In this case $k_c(x)$ and $\beta(x)$ are determined using a least squares fit over the calculated k_{eff} values as a function of the parameters of interest, x . Positive biases are not considered by setting $k_c(x) = 1.0$ wherever it is greater than 1.0.

Based on the criteria for subcriticality set forth in ANSI/ANS-8.17 and what is above, a USL can be determined using a set of critical experiment benchmarks. The USL is determined such that there is a high degree of confidence that a calculated result is subcritical; i.e., an application or system is considered subcritical with a high degree of certainty if a calculated k_{eff} plus calculational uncertainties lies at or below this limit ($k_s + \Delta k_s < USL$). Thus, the USL is the magnitude of the sum of the biases, uncertainties, and administrative and/or statistical margins applied to a set of critical benchmarks, such that with a high degree of confidence:

$$USL = 1.0 - \Delta k_m + \beta(x) - \Delta\beta(x). \quad (\text{Eq. 6-2})$$

Only the distribution-free tolerance method and the confidence band with administrative margin were used and are described in Sections 6.8.2.1 and 6.8.2.2, respectively. Derivation of USLs for each of the application groups is discussed in Sections 6.8.2.3 through 6.8.2.6. The results are summarized in Section 6.8.2.7.

6.8.2.1 Distribution-Free Tolerance Limit Method

The distribution-free tolerance limit method⁴³ is typically used to calculate a lower band threshold limit (LBTL) when the k_{eff} values for the critical experiments do not pass tests for normality.⁴³ This method involves sorting all k_{eff} values for the applicable critical experiments in ascending order and determining the degree of confidence for the fraction of the true population that lies above the smallest observed value. The percent confidence that a fraction of the population of k_{eff} values calculated for critical systems is above the lowest observed value can be determined using the following equation:

$$\beta = 1 - \sum_{j=0}^{m-1} \frac{n!}{j!(n-1)!} (1-q)^j q^{(n-j)}, \quad (\text{Eq. 6-3})$$

where

- n = sample size (number of k_{eff} values),
- m = rank order of the smallest k_{eff} value, and
- q = the desired population fraction above the smallest k_{eff} value (normally 0.95).

For a desired population fraction of 0.95 and a rank order of 1 (the lowest data sample), Equation 6-3 reduces to

$$\beta = 1 - q^n = 1 - 0.95^n \quad (\text{Eq. 6-4})$$

The nonparametric margin is determined by first calculating β using Equation 6-4. The nonparametric margin is then determined using Table 2.2 in Reference 43. The single-valued *LBTL* function for nonparametric data analysis is then determined as follows:

$$LBTL = \text{smallest } k_{eff} - \text{uncertainty for smallest } k_{eff} - \text{nonparametric margin.} \quad (\text{Eq. 6-5})$$

Note that the confidence value determined by Equations 6-3 and 6-4 increases with increasing sample size and the nonparametric margin, in Equation 6-5, is used to account for small sample size.

6.8.2.2 USL Method 1: Confidence Band with Administrative Margin

The USLSTATS code, documented in Section 4 and Appendix C of Reference 40, Method 1 applies a statistical calculation of the bias and its uncertainty plus an administrative margin to a linear fit of the critical experimental benchmark data. The approach to this method is to first calculate a linear fit of the critical experiments, $k_c(x)$. To remove any positive bias, $k_c(x)$ is reset such that $k_c(x) = 1.0$ anywhere $k_c(x) > 1.0$. A confidence band for a single additional calculation is then determined. The width of this band is determined statistically based on the existing data and a specified level of confidence; the greater the standard deviation in the data or the larger the confidence desired, the larger the band width. This confidence band, W , accounts for uncertainties in the experiments, cross sections, and calculational method, and is therefore a statistical basis of $\Delta\beta$, the uncertainty in the value of β . W is defined for a confidence level of $(1 - \gamma)$ using the relation

$$W = \max \{w(x) \mid x_{\min}, x_{\max}\} \quad (\text{Eq. 6-6})$$

where

$$w(x) = t_{1-\gamma} s_p \left[1 + \frac{1}{n} + \frac{(x - \bar{x})^2}{\sum_{i=1,n} (x_i - \bar{x})^2} \right]^{\frac{1}{2}} \quad (\text{Eq. 6-7})$$

and

- n = the number of critical calculations used in establishing $k_c(x)$,
- $t_{1-\gamma}$ = the Student-t distribution statistic for $1-\gamma$ and $n-2$ degrees of freedom
- S_p = the pooled standard deviation for the set of criticality calculations, and
- x = the mean value of parameter x in the set of calculations.

Typically, W is determined at the 95% confidence level. For transport and storage packages, an administrative margin, Δk_m , 0.05 Δk is typically used.

Using the above formulas, the USL Method 1 is defined as

$$USL_1(x) = 1 - \Delta k_m - W + \beta(x). \quad (\text{Eq. 6-8})$$

With one exception, the USLSTATS inputs are described in Appendix C of Reference 40. The exception is that the first word in the title must be “tsunami” when the trending parameter is c_k . Without this input, USLSTATS will not permit extrapolation of the USLs. When “tsunami” is included as the first word on the first line, USLSTATS will extrapolate to a c_k value of 1.0. The other input parameters used were as follows:

- P = 0.999 = proportion of population falling above the lower tolerance level
- $1 - \gamma$ = 0.95 = confidence on fit
- α = 0.95 = confidence on proportion P
- x_{\min} = 0 = minimum value of trending parameter
- x_{\max} = 1.0 = maximum value of trending parameter
- σ_{sample} = -1 = estimated average standard deviation of all input values of k_{eff}
a “-1” value directs USLSTATS to use third column of experiment-specific input
- Δk_m = 0.05 = administrative margin used to ensure subcriticality

The remainder of the input is provided as three pieces of data for each critical configuration on individual lines. The first input is the value of the trending parameter. The second input is the calculated k_{eff} value divided by the expected k_{eff} value. The expected value is taken from the IHECSBE³⁹ and includes biases for simplifications used in describing the critical configuration. These expected and calculated k_{eff} values are provided in Section 6.9.3. The third parameter is the uncertainty in the calculated k_{eff} values. A USLSTATS input deck for application *cv031* is included in Section 6.9.5.5.

6.8.2.3 Metal Sphere Applications

The METAL SPHERE applications consist of three cases: *cv001*, *fhlsf001*, and *fslsf001*. A set of 13 selected, critical benchmark configurations are well correlated to the three applications from a neutronic perspective as represented by the range of c_k values calculated using TSUNAMI. The c_k values for the *cv001* application range from 0.916 to 0.995, the *fhlsf001* application range from 0.918 to 0.996, and the *fslsf001* application range from 0.918 to 0.996. Values above 0.9 indicate a high correlation between cases. The EALF and the H/Pu ratio of the three applications are contained within the range of these values from the set of critical benchmark configurations used in the validation. The EALF values of the three applications are 5.470e4, 8.034e4, and 7.957e4 eV; whereas the range of EALF values for the set of critical

benchmark configurations is 1.76e3 to 1.27e6 eV. The H/Pu ratios of the three applications are 0.0 where as the range of H/Pu ratios for the critical benchmarks ranges from 0.0 to 0.05. Both the H/Pu ratio and EALF for the three applications are bounded by the selected cases that have c_k values above 0.9.

The normality of the distribution of the k_{eff} values for the group of critical benchmark configurations used to validate the METAL SPHERE applications was checked using the Shapiro-Wilk Test.⁴³ This test was used because of the small number of samples in this group—only 13 critical benchmark configurations. The Chi-Squared (χ^2) Test implemented in USLSTATS requires a minimum of 25 samples. The test calculated $W = 0.8546$, which is less than the value from Table A.5 of Reference 43, which for $\alpha = 0.05$ and $n = 13$ is $W_t = 0.866$. This indicates the sample distribution test is not normally distributed. As is shown in Figure 6-25, the distribution has two peaks. For the samples to pass a normality test, the calculated W must be greater than the W test value from Table A.5 of Reference 43 for a given α and n .

Because the data is not normally distributed, the distribution-free tolerance limit method is used. The nonparametric margin is determined using Equation 6-3. Given a population (n) of 13 and a desired population fraction (q) of 0.95 the degree of confidence is calculated to be 48.6%. From Table 2.2 of Reference 43, a nonparametric margin of 0.05 needs to be included in the calculation of the USL. The resulting USL is 0.8893, which is calculated as follows:

$$\text{USL} = \text{lowest } k_{eff} \text{ value} - \text{combined Monte Carlo and experimental uncertainty} - \text{administrative margin} - \text{nonparametric margin}$$

$$\text{USL} = 0.9916 - (0.0005^2 + 0.0022^2)^{0.5} - 0.05 - 0.05 = 0.8893$$

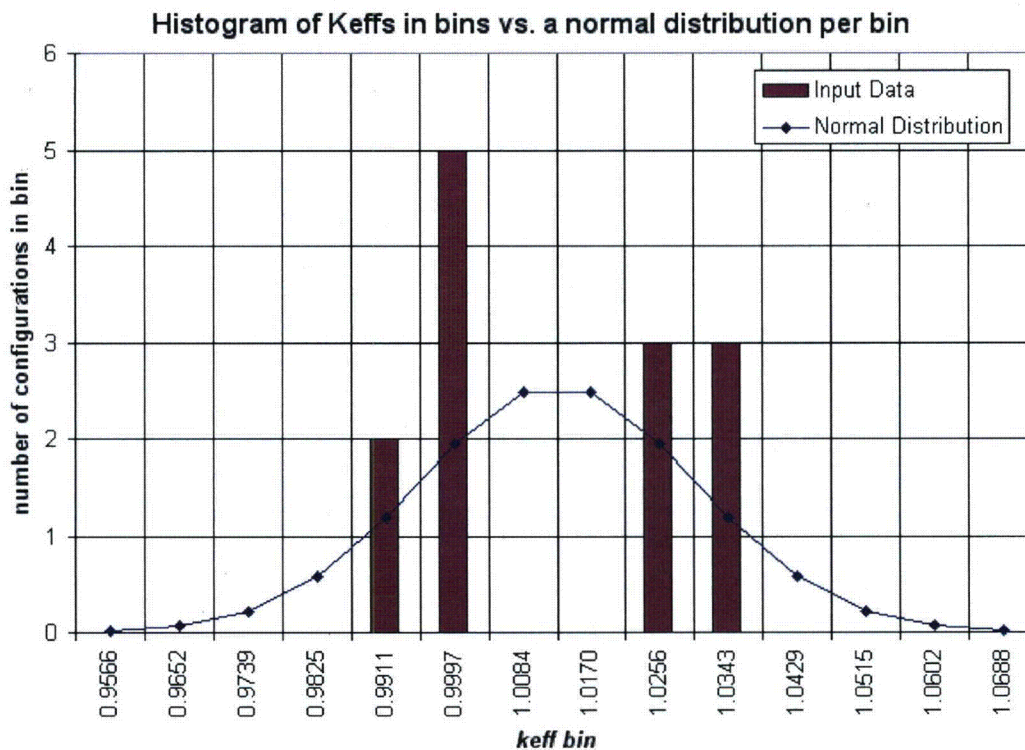


Figure 6-25. Pu Metal Sphere Critical Benchmark Histogram

6.8.2.4 Solution Lattice Applications

The SOLUTION LATTICE applications include four cases: *fhlsf031*, *fslsf031*, *hexs100*, and *octs100*. A set of 60 selected critical benchmark configurations are well correlated to the four applications from a neutronic perspective as represented by the range of c_k values calculated using TSUNAMI. The c_k values for the *fhlsf031* application range from 0.893 to 0.936, the *fslsf031* application range from 0.890 to 0.933, the *hexs100* application range from 0.898 to 0.952 and the *octs100* application range from 0.897 to 0.950. Values above 0.9 indicate a high correlation between cases. The EALF and the H/Pu ratio of the four applications are contained within the range of these values from the set of critical benchmark configurations used in the validation. The EALF values of the four applications are 2.682, 2.692, 2.544, and 2.531 eV; whereas the range of EALF values for the benchmark configurations is 0.147 to 6.446 eV. The H/Pu ratios of the four applications are 28.8 where as the range of H/Pu ratios for the benchmark configurations is 15.46 to 220.19. Both the H/Pu ratio and EALF for the four applications are bounded by the selected cases that have c_k values of approximately 0.9 or above.

The normality of the k_{eff} values for the group of critical benchmark configuration used to validate the SOLUTION LATTICE applications was checked using the χ^2 test. The test determined that the samples are not normally distributed. A visual inspection of the k_{eff} distribution, shown in Figure 6-26, shows a pronounced single peak with a long tail on the side with increasing k_{eff} and a very short tail on the side with decreasing k_{eff} .

Because the data is not normally distributed, the USL is determined using the distribution-free tolerance limit method described in Section 6.8.2.1. A nonparametric margin is determined using Equation 6-3. Given a population (n) of 60 and a desired population fraction (q) of 0.95, the degree of confidence is calculated to be 95.4%. From Table 2.2 of Reference 43, no additional nonparametric margin is needed to obtain a 95% confidence for 95% of the population. The resulting USL is 0.9396, which is calculated as follows:

$$\begin{aligned} \text{USL} &= \text{lowest } k_{eff} \text{ value-combined Monte Carlo and experimental uncertainty-} \\ &\quad \text{administrative margin-nonparametric margin} \\ \text{USL} &= 0.9956 - (0.0005^2 + 0.0060^2)^{0.5} - 0.05 - 0.0 = 0.9396 \end{aligned}$$

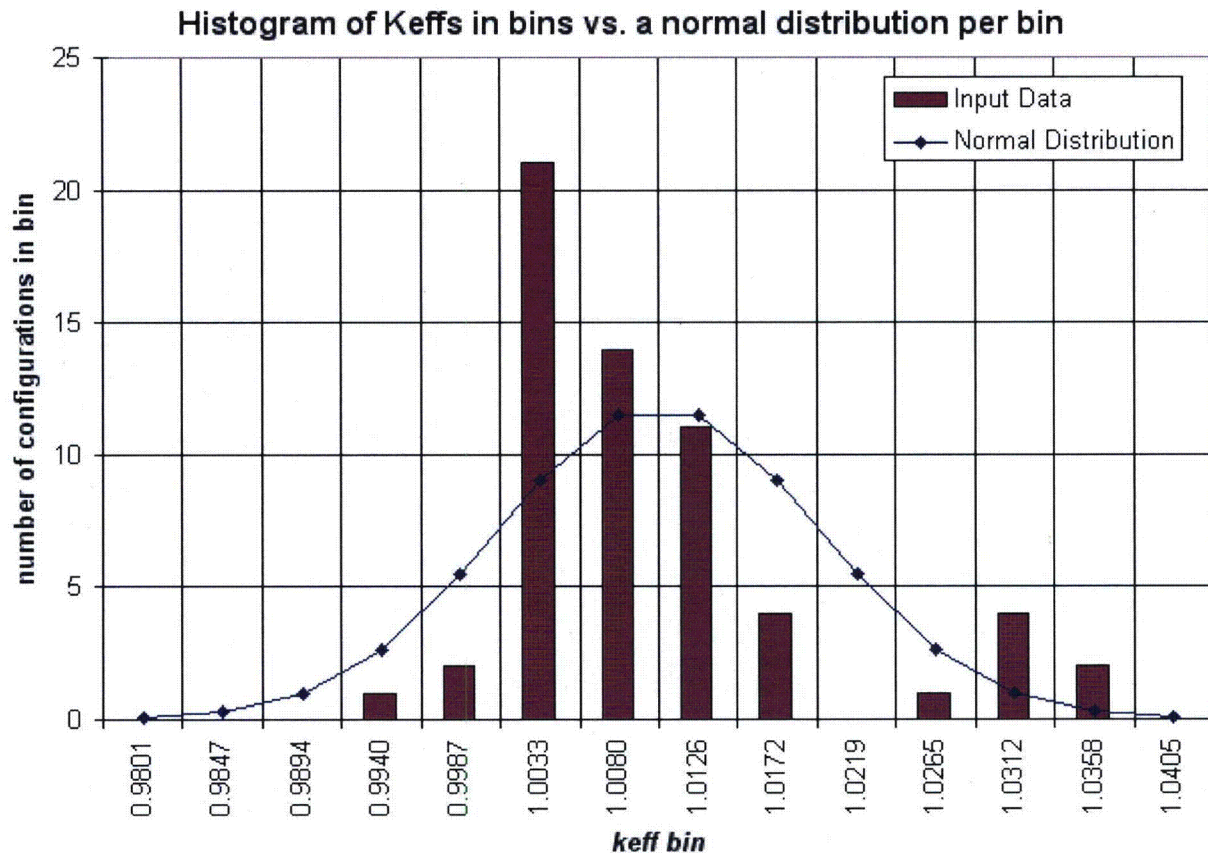


Figure 6-26. Solution Lattice Critical Benchmark Histogram

6.8.2.5 Single Unit Solution Applications

The SINGLE UNIT SOLUTION applications consist of two cases: *cv031* and *sph14*. A set of 95 selected critical benchmark configurations are well-correlated to the two applications from a neutronic perspective as represented by the range of c_k values calculated using TSUNAMI. The c_k values for the *cv031* application range from 0.902 to 0.961 and for the *sph14* application from 0.909 to 0.959. Values above 0.9 indicate a high correlation between cases. The EALF and the H/Pu ratio of the two applications are contained within the range of these values from the set of critical benchmark configurations used in the validation. The EALF values of the two applications are 1.091 and 1.255 eV; whereas the range of EALF values for the benchmark configurations is 0.112 to 5.405 eV. The H/Pu ratios of the two applications are 28.8 where as the range of H/Pu ratios for the benchmark configurations is 15.46 to 258.46. Both the H/Pu ratio and EALF for the two applications are bounded by the selected cases that have c_k values above 0.9 for both applications.

The normality of the k_{eff} values for the group of critical benchmark configuration used to validate the SOLUTION LATTICE applications was checked using the χ^2 test. The test determined that the 95 samples are not normally distributed. A visual inspection of the k_{eff} distribution, shown in Figure 6-27, shows a pronounced single peak with a long tail on the side, and increasing k_{eff} and a very short tail on the side with decreasing k_{eff} .

Histogram of Keffs in bins vs. a normal distribution bin

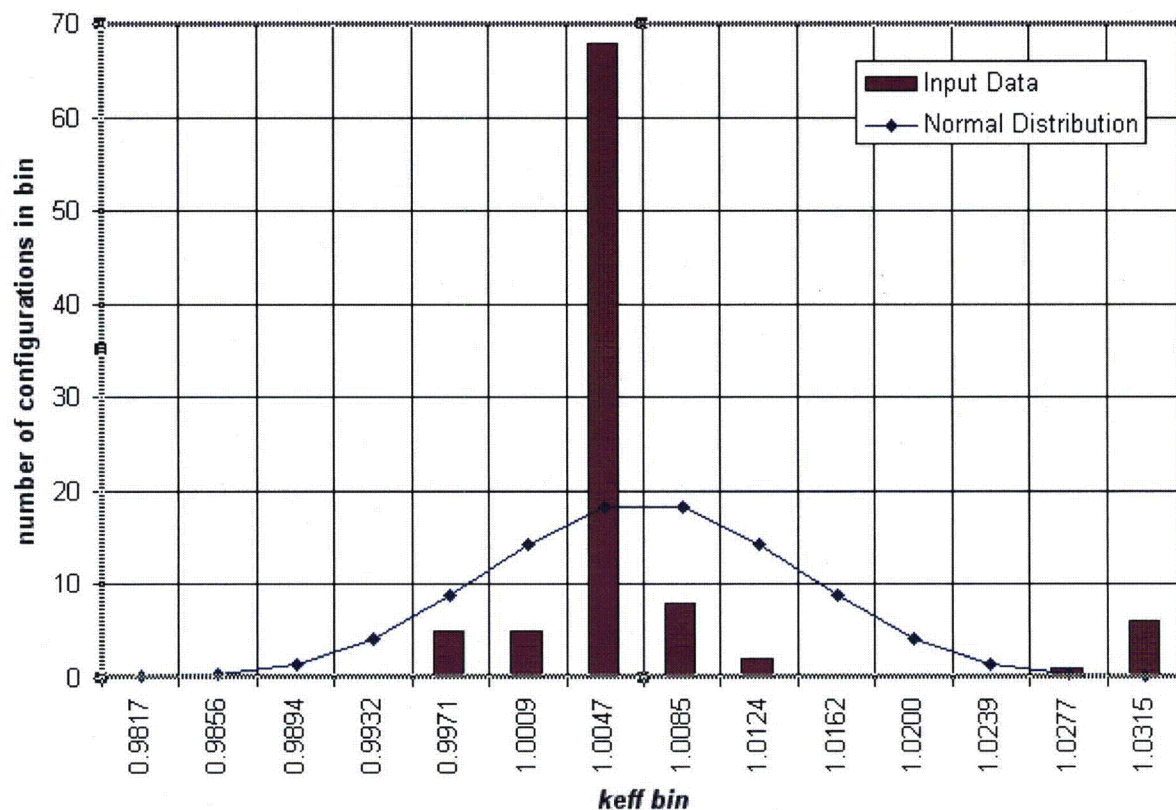


Figure 6-27. Single Unit Solution Critical Benchmark Histogram

Because the data is not normally distributed, the USL is determined using the distribution-free tolerance limit method described in Section 6.8.2.1. A nonparametric margin is determined using Equation 6-3. Given a population (n) of 95 and a desired population fraction (q) of 0.95 the degree of confidence is calculated to be 99.2%. From Table 2.2 of Reference 43, no additional nonparametric margin is needed to obtain a 95% confidence for 95% of the population. The resulting USL is 0.9383, which is calculated as follows:

$$\text{USL} = \text{lowest } k_{\text{eff}} \text{ value} - \text{combined Monte Carlo and experimental uncertainty} - \text{administrative margin} - \text{nonparametric margin}$$

$$\text{USL} = 0.9956 - (0.0005^2 + 0.0073^2)^{0.5} - 0.05 - 0.0 = 0.9383$$

6.8.2.6 Dry Lattice Applications

The DRY LATTICE applications consist of two cases: *hexsdry* and *octsdry*. A set of 33 selected critical benchmark configurations are well-correlated to the two applications from a neutronic perspective as represented by the range of c_k values calculated using TSUNAMI. The c_k values for the *hexsdry* application range from 0.906 to 0.974 and for the *octsdry* application from 0.903 to 0.971. Values above 0.9 indicate a high correlation between cases. In addition, the EALF and the H/Pu ratio of the selected benchmark applications span the range of these values from the set

of critical benchmark configurations used in the validation. The EALF values of the two applications are 4.864 and 5.042 eV, whereas the range of EALF values for the benchmark configurations is 0.254 to 37.727 eV. The H/Pu ratios of the two applications are 28.8, whereas the range of H/Pu ratios for the benchmark configurations is 15.46 to 131.3. Both the H/Pu ratio and EALF for the two applications are bounded by the selected cases that have c_k values above 0.9 for both applications.

The normality of the k_{eff} values for the group of critical benchmark configurations used to validate the DRY LATTICE applications was checked using the χ^2 test. The test determined that the 33 samples are not normally distributed with some bins not containing the required 5 values. The normality was then checked using the Shapiro-Wilk test.⁴³ The Shapiro-Wilk test is a more mathematically rigorous test of normality than the χ^2 test. The Shapiro-Wilk test calculated $W=0.941546$, which is greater than the value from Table A.5 of Reference 43, which for $\alpha = 0.05$ and $n = 33$ is $W_t = 0.931$. A visual inspection of the k_{eff} distribution in Figure 6-28 shows a peak in the center with approximately equal tails on each side. This indicates the sample distribution is normally distributed.

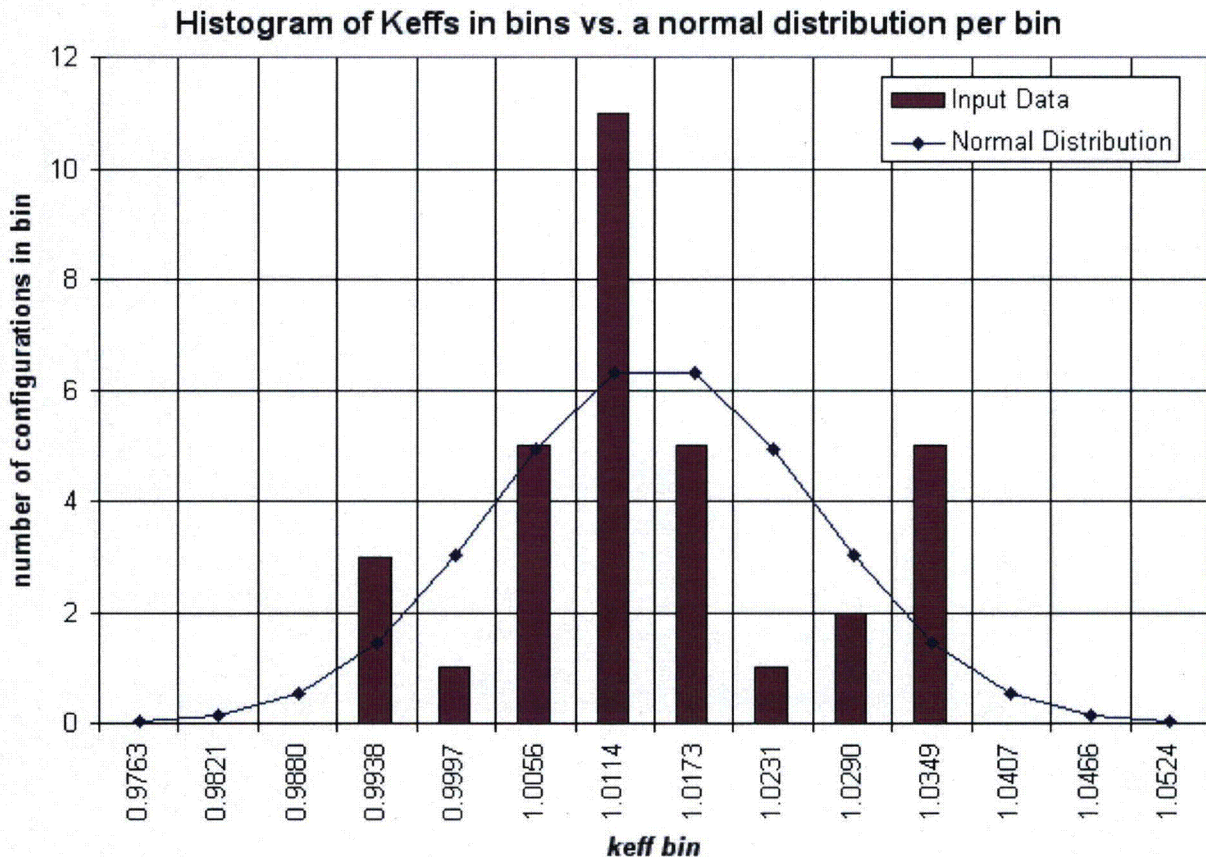


Figure 6-28. Dry Lattice Critical Benchmark Histogram

Trending was done using the c_k values of the critical benchmark configurations for each of the dry lattice applications using the USLSTATS code distributed with SCALE 5.1. This version of USLSTATS permits extrapolation of the USL-1 to a c_k value of 1.0, which is the c_k of the application. The inputs used for USLSTATS are described in Section 6.8.2.2.

USLSTATS is used to calculate an upper subcritical limit for each application using the set of critical benchmark configurations and c_k values as the trending parameter. Figure 6-29 and Figure 6-30 show the results of the USLSTATS analysis for *hexsdry* and *octsdry*. The c_k values have a positive slope as c_k approach 1.0. The linear fit of k_{eff} is above 1.0 throughout the range. Credit is not taken for the positive bias. Based on the analysis, the USL can be established as $USL = 0.9351$ for *hexsdry* and $USL = 0.9352$ for *octsdry*.

6.8.2.7 Results Summary

Based on the above data, an USL and bias can be determined for each application. An administrative margin of 0.05 is used for all applications. The USL and bias was determined using nonparametric methods for 9 of the 11 applications because the k_{eff} values of the applicable critical benchmark configurations did not fit a normal distribution. For these nine applications, a nonparametric margin was determined using the number of benchmark configurations to validate the application and a desired population fraction of 0.95 above the minimum k_{eff} . The USL is then determined by subtracting the administrative margin, the nonparametric margin, and 2 standard deviations from the minimum k_{eff} value.

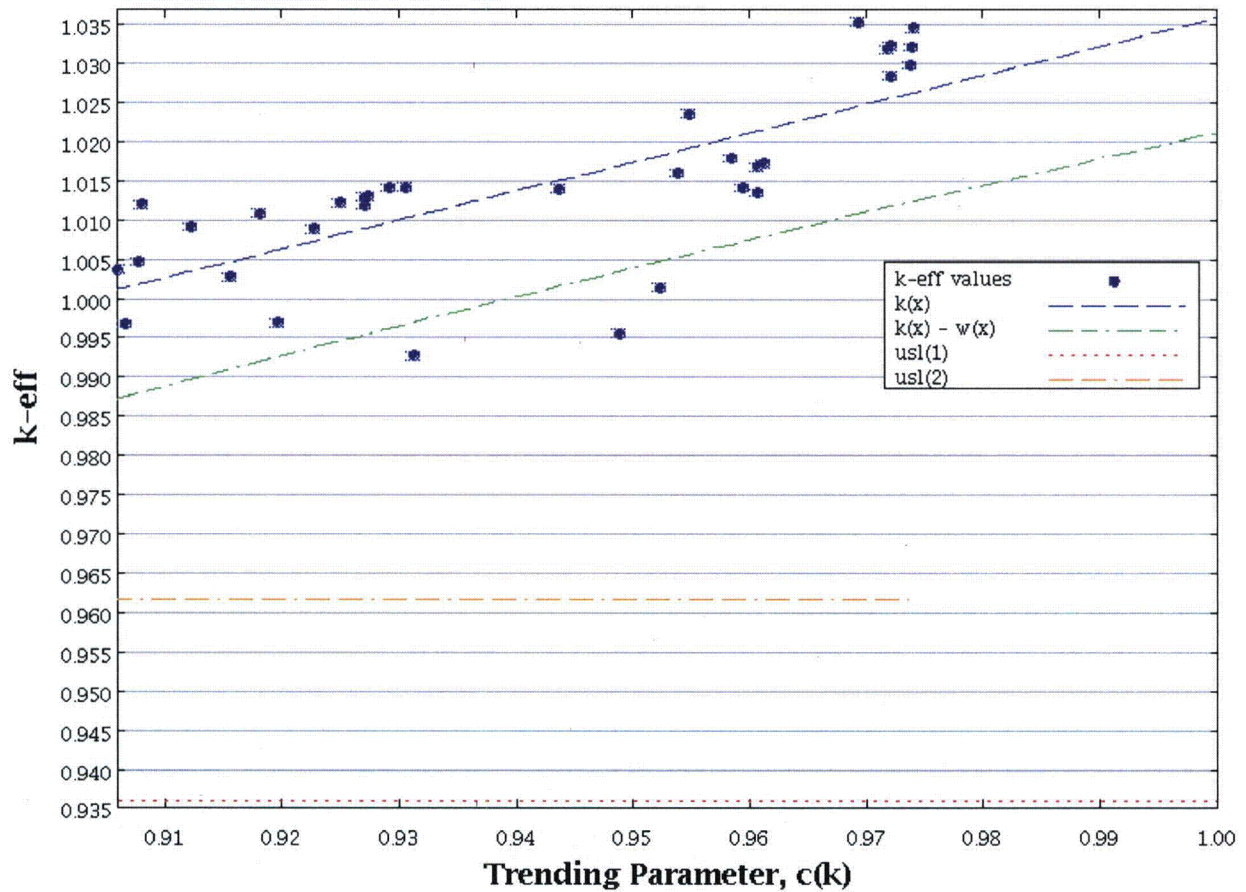


Figure 6-29. USLSTATS Plot for HEXSDRY Application of c_k vs. k_{eff}

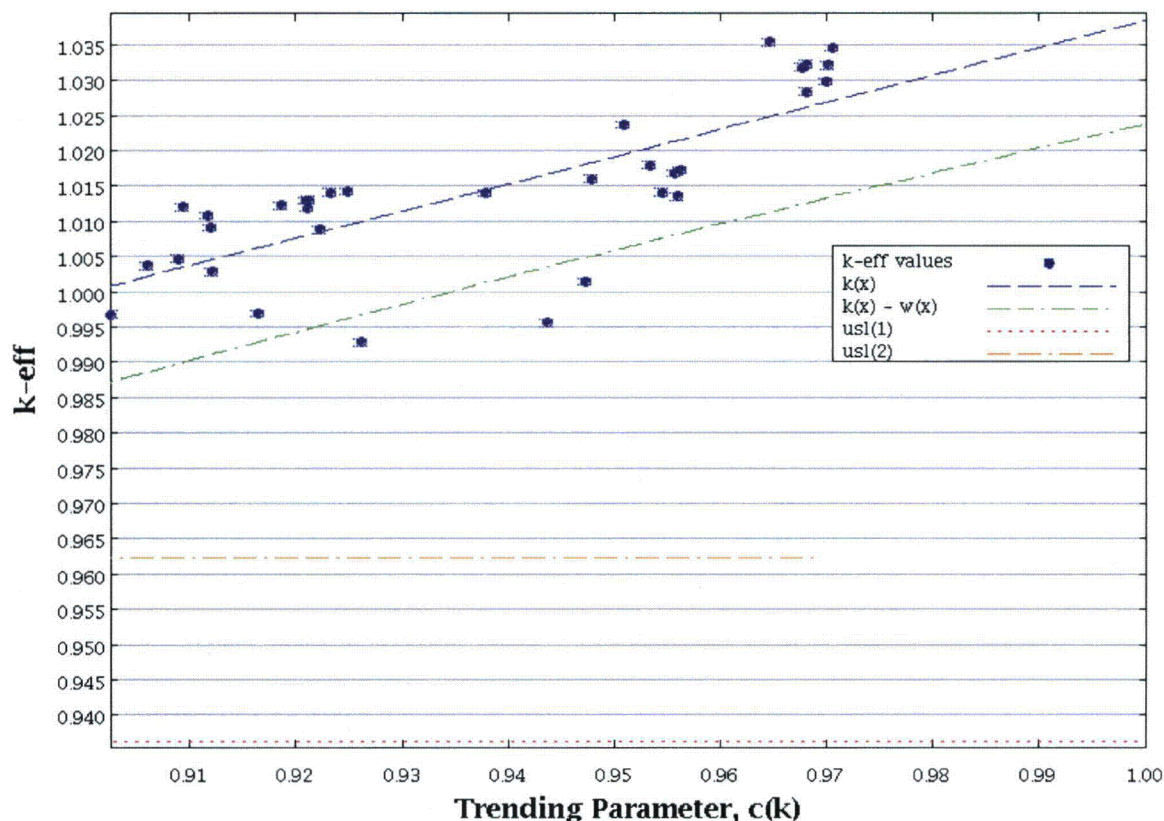


Figure 6-30. USLSTATS Plot for OCTSDRY Application of c_k vs. k_{eff}

Table 6-7. USL and Bias Data Summary

| Application Name | Method Used | NPM | Minimum k_{eff} | USL | Bias |
|------------------|---------------|------|-------------------|--------|------|
| <i>cv001</i> | Nonparametric | 0.05 | 0.9916 | 0.8893 | 0 |
| <i>fhlsf001</i> | Nonparametric | 0.05 | 0.9916 | 0.8893 | 0 |
| <i>fslsf001</i> | Nonparametric | 0.05 | 0.9916 | 0.8893 | 0 |
| <i>fhlsf031</i> | Nonparametric | 0.0 | 0.9956 | 0.9396 | 0 |
| <i>fslsf031</i> | Nonparametric | 0.0 | 0.9956 | 0.9396 | 0 |
| <i>hexs100</i> | Nonparametric | 0.0 | 0.9956 | 0.9396 | 0 |
| <i>octs100</i> | Nonparametric | 0.0 | 0.9956 | 0.9396 | 0 |
| <i>cv031</i> | Nonparametric | 0.0 | 0.9958 | 0.9383 | 0 |
| <i>sph14</i> | Nonparametric | 0.0 | 0.9958 | 0.9383 | 0 |
| <i>hexsdry</i> | USLSTATS | N/A | N/A | 0.9351 | 0 |
| <i>octsdry</i> | USLSTATS | N/A | N/A | 0.9352 | 0 |

All cases use an administrative margin of 0.05.

USL for nonparametric cases = $\min k_{eff} - [(\sigma_{exp})^2 + (\sigma_{MC})^2]^{0.5} - 0.05 - \text{NPM}$.

USL for parametric cases is USL Method 1 is determined using USLSTATS.

All cases are run to a $\sigma = 0.0005$.

Positive biases (average calculated k_{eff} value > 1) are discarded.

For the two applications where the critical configuration k_{eff} values tested as a normal distribution, the USL was calculated using USLSTATS. The method used in USLSTATS is described in Section 6.8.2.1. An administrative margin of 0.05 was included in the calculations. The reported USL is USL Method 1, which is the confidence band with administrative margin. The bias for the *hexsdry* and *octsdry* applications is zero because the fits of k_{eff} for the critical configurations were above 1.0 throughout their ranges. No credit is taken for such positive biases.

6.9 Appendices

Consistent with the guidance from the U.S. Nuclear Regulatory Commission, Office of Nuclear Regulatory Research, Regulatory Guide 7.9, Rev. 2, “*Standard Format and Content of Part 71 Applications for Approval of Packages for Radioactive Material*,” March 2005, this section includes supplemental information.

6.9.1 References

1. United States. Nuclear Regulatory Commission. NUREG/CR-5661, ORNL/TM-11936. Dyer, H. R. and C. V. Parks. “Recommendations for Preparing the Criticality Safety Evaluation of Transportation Packages,” Oak Ridge National Laboratory, March 1997.
2. United States. Nuclear Regulatory Commission. NUREG-0361. “Safety Analysis Report for the Plutonium Air Transportable Package, Model PAT-1.” Washington, D.C. 1978..
3. Petrie, L. M., P. B. Fox, and K. Lucius, “Standard Composition Library,” Vol. III, Sect. M8 in *SCALE: A Modular Code System for Performing Standardized Computer Analyses for Licensing Evaluations*, ORNL/TM-2005/39, Version 5.1, Vols. I–III, November 2006. Available from Radiation Safety Information Computational Center at Oak Ridge National Laboratory as CCC-732.
4. Drawing 1001, Issue A, “PAT-1 ASSEMBLY.” May 9, 1978.
5. Drawing 1002, Issue A, “OVERPACK, AO.” May 9, 1978.
6. Drawing 1003, Issue A, “CONTAINER SUBASSEMBLY.” May 9, 1978.
7. Drawing 1004, Issue B, “DRUM.” July 11, 1990.
8. Drawing 1005, Issue A, “COVER, MODIFIED.” May 9, 1978.
9. Drawing 1006, Issue A, “RING, CLAMP, MODIFIED.” May 9, 1978.
10. Drawing 1007, Issue A, “COVER,LINER.” May 8, 1978.
11. Drawing 1008, Issue A, “CYLINDER, WOOD.” May 8, 1978.
12. Drawing 1009, Issue B, “CYLINDER, WOOD.” July 9, 1990.
13. Drawing 1010, Issue A, “PLUG, WOOD, FIXED.” May 9, 1978.
14. Drawing 1011, Issue A, “CYLINDER, WOOD.” May 8, 1978.

15. Drawing 1012, Issue A, "PLUG, WOOD, FIXED." May 8, 1978.
16. Drawing 1013, Issue B, "PLUG, WOOD, REMOVABLE." July 5, 1990.
17. Drawing 1014, Issue A, "PLUG, WOOD, REMOVABLE." May 9, 1978.
18. Drawing 1015, Issue A, "SPACER, TOP." May 9, 1978.
19. Drawing 1016, Issue B, "LOAD SPREADER ASSEMBLY." July 9, 1990.
20. Drawing 1017, Issue B, "CONTAINMENT VESSEL." July 19, 1990.
21. Drawing 1018, Issue B, "BOLD, SOCKET, HEAD SPECIAL .500-20." July 10, 1990.
22. Drawing 1019, Issue B, "GASKET COPPER." July 10, 1990.
23. Drawing 1020, Issue B, "LID, TB." July 18, 1990.
24. Drawing 1021, Issue A, "FORGING, TB LID." May 9, 1978.
25. Drawing 1022, Issue B, "BODY, TB." July 16, 1990.
26. Drawing 1023, Issue A, "FORGING, TB BODY." May 9, 1978.
27. Drawing 1024, Issue B, "CAN ASSEMBLY." June 1, 1978.
28. Drawing 1025, Issue A, "CYLINDER, LINER." May 9, 1978.
29. Drawing 1026, Issue A, "PAD, INSULATION." May 9, 1978.
30. Drawing 1027, Issue A, "PAD INSULATION." May 9, 1978.
31. No current standard specifies the minimum thickness for 16-gauge steel. The value used was cited as the minimum thickness for 16-gauge steel used in DOT 17C and 17H drums. These standards are ANSI/ASC MH2-1985(3.4), "American National Standard for 55-Gallon (208-Liter) Tight-Head Steel (Double-Seam Chime) Drums (DOT-17C) and ANS MH2-1991 (3.8), "American National Standard for 55-Gallon (208-Liter) Full-Removable-Head Steel (Round-Seam Chime) Drums (DOT-17H, UFC-Rule 40, NMFC-Item260). Considering their past use in similar applications, the specified 16 gauge minimum steel thickness is a reasonable value for the minimum steel thickness.
32. Los Alamos National Laboratory, ed. Pruvost, N. L. and Paxton, H. C.: *Nuclear Criticality Safety Guide*. LA-12808 (UC-714), September 1996.
33. Brown, Jr., W. F. and S. J. Setlak, *Aerospace Structural Metals Handbook, 37th Edition*, CINDAS/USAF CRDA Handbooks Operation, Purdue University, West Lafayette, IN. 2001.
34. *Handbook of Chemistry and Physics, 74th Edition*. CRC Press, Inc. Boca Raton, FL. 1993.
[Page 4-83]

35. *SCALE: A Modular Code System for Performing Standardized Computer Analyses for Licensing Evaluations*, ORNL/TM-2005/39, Version 5.1, Vols. I–III, November 2006. Available from Radiation Safety Information Computational Center at Oak Ridge National Laboratory as CCC-732.
36. Goluoglu, S., N. F. Landers, L. M. Petrie, and D. F. Hollenbach, “CSAS: Control Module for Enhanced Criticality Safety Analysis Sequences,” Vol. I, Sect. C4 in *SCALE: A Modular Code System for Performing Standardized Computer Analyses for Licensing Evaluations*, ORNL/TM-2005/39, Version 5.1, Vols. I–III, November 2006. Available from Radiation Safety Information Computational Center at Oak Ridge National Laboratory as CCC-732.
37. Rearden, B. T., “TSUNAMI-3D: Control Module for Three-Dimensional Cross-Section Sensitivity and Uncertainty Analysis for Criticality,” Vol. I, Sect. C9 in *SCALE: A Modular Code System for Performing Standardized Computer Analyses for Licensing Evaluations*, ORNL/TM-2005/39, Version 5.1, Vols. I–III, November 2006. Available from Radiation Safety Information Computational Center at Oak Ridge National Laboratory as CCC-732.
38. Rearden, B. T., “TSUNAMI Utility Modules,” Vol. III, Sect. M18.1 in *SCALE: A Modular Code System for Performing Standardized Computer Analyses for Licensing Evaluations*, ORNL/TM-2005/39, Version 5.1, Vols. I–III, November 2006. Available from Radiation Safety Information Computational Center at Oak Ridge National Laboratory as CCC-732.
39. *International Handbook of Evaluated Criticality Safety Benchmark Experiments*. NEA/NSC/DOC(95)03, NEA Nuclear Science Committee. September 2007.
40. United States. Nuclear Regulatory Commission. NUREG/CR-6361 (ORNL/TM-13211). Lichtenwalter, J. J., S. M. Bowman, M. D. DeHart, and C. M. Hopper. “Criticality Benchmark Guide for Light-Water-Reactor Fuel in Transportation and Storage Packages.” Oak Ridge National Laboratory. March 1997.
41. Bowden, D. C. and F. A. Graybill, “Confidence Bands of Uniform and Proportional Width for Linear Models,” *Am. Stat. Assoc. J.*, 61, 182. March 1966.
42. Johnson, N. L., Ed., “Query” *Technometrics*, 10, 207–209. February 1968.
43. United States. Nuclear Regulatory Commission. NUREG/CR-6698. “Guide for Validation of Nuclear Criticality Safety Calculational Methodology.” Washington D.C.: January 2001.
44. Broadhead, B. L., B. T. Rearden, C. M. Hopper, J. J. Wagschal, and C. V. Parks, “Sensitivity and Uncertainty-Based Criticality Safety Validation Techniques,” *Nuc. Sci. Eng.* 146, 340–366. 2004.
45. Oberg, E., F. D. Jones, H. L. Horton, and H. H. Ryffel, “Machinery’s Handbook, 24th Edition.” Industrial Press Inc.: New York. 1992.

6.9.2 TB-1 Containment Vessel Inner Volume

A key parameter of the criticality analysis is the maximum quantity of water that could be present within the TB-1 containment vessel. Since this component has a rather complicated internal shape, the calculation of its internal volume is presented in this section.

The TB-1 containment vessel is shown in Drawing 1017.²⁰ The volume can be divided into three sub-volumes. Most of the volume is in the straight right-circular cylinder that extends from the bottom spherical section up to the bottom edge of the lid. As indicated in Drawing 1022,²⁵ the bottom is a spherical section. As indicated in Drawing 1020,²³ the recess in the lid is also a spherical section.

Equations and figure provided in the Machinery's Handbook [Reference 45, page 66] for calculating volumes of spherical segments are reproduced in Figure 6-31.

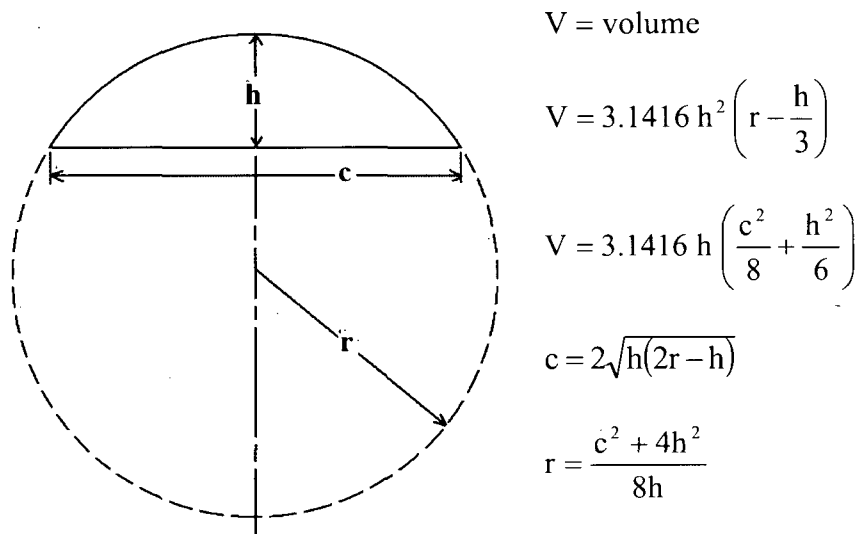


Figure 6-31. Spherical Segment Volume Calculations

The volume in the bottom of the TB-1 can be calculated using information from Drawing 1022.²⁵

$$h = 25 + 0.005 - 5.450 + 4.700 = 1.505''$$

$$c = 4.250 + 0.0022 = 4.2522''$$

$$V_{\text{bottom}} = 3.1416 * 1.505 * (4.2522^2 / 8 + 1.505^2 / 6) = 12.471 \text{ in}^3$$

The volume of the central cylinder can be calculated using information from Drawings 1020²³ and 1022.²⁵

$$V = \pi * r^2 * L$$

$$r = (4.250 + 0.0022) / 2 = 2.1261''$$

$$L = 5.450 + 0.010 - 0.437 + 0.010 - 0.047 + 0.002 + 0.080 + 0.002$$

$$L = 5.070''$$

$$V_{\text{middle}} = \pi * 2.1261^2 * 5.070 = 71.999 \text{ in}^3$$

The volume in the lid is calculated using information from Drawing 1020:²³

$$h = 0.437 + 0.01 + 0.513 + 0.01 = 0.970''$$

$$r = 2.25 + 0.02 = 2.27''$$

$$V_{\text{top}} = 3.1416 * 0.97^2 * (2.27 - 0.97/3) = 5.754 \text{ in}^3$$

The total volume is then the sum of the partial volumes:

$$V = 12.471 + 71.999 + 5.754 = 90.22 \text{ in}^3 = 1478 \text{ cm}^3$$

Thus the maximum internal volume of the TB-1 containment vessel is 1478 cm³. The Pu, any packaging, and other internal containment and support structures must fit within this volume.

6.9.3 Applicability of Benchmark Experiments

Table 6-8 lists all of the validation cases used in this evaluation. There are 125 cases considered in this validation. All cases contain plutonium as the primary fissile material and are either fast metal, intermediate spectrum Pu/Polystyrene blocks or thermal solution cases. The standard deviation for all the calculated k_{eff} values is 0.0005.

Table 6-8. List of Validation Critical Configurations

| IHECSBE Identifier | Case | Description | Benchmark | | Calculated | |
|--------------------|------|-------------------------------------|------------------|-------------|------------------|----------|
| | | | k_{eff} | $\pm\sigma$ | k_{eff} | EALF |
| pcm*001 | 1 | PuO ₂ –Polystyrene Slab | 0.9986 | 0.0041 | 1.02438 | 9.73E+05 |
| | 3 | | 0.9990 | 0.0047 | 1.02356 | 30.518 |
| | 4 | | 1.0000 | 0.0033 | 0.99275 | 37.727 |
| | 5 | | 0.9989 | 0.0053 | 1.01403 | 1.468 |
| pcm002 | 1 | Plexiglas Reflected | 0.9990 | 0.0046 | 1.03757 | 4.56E+03 |
| | 2 | PuO ₂ –Polystyrene Slabs | 0.9990 | 0.0046 | 1.03641 | 3.98E+03 |
| | 3 | | 0.9990 | 0.0046 | 1.03179 | 3.26E+03 |
| | 4 | | 0.9990 | 0.0046 | 1.02547 | 2.42E+03 |
| | 5 | | 0.9990 | 0.0046 | 1.02328 | 1.76E+03 |
| | 10 | | 1.0000 | 0.0044 | 1.03534 | 4.026 |
| | 11 | | 1.0000 | 0.0044 | 1.03184 | 4.405 |
| | 12 | | 1.0000 | 0.0044 | 1.03209 | 4.970 |
| | 13 | | 1.0000 | 0.0044 | 1.02982 | 5.262 |
| | 14 | | 1.0000 | 0.0044 | 1.03451 | 5.405 |
| | 15 | | 1.0000 | 0.0044 | 1.03220 | 5.366 |
| | 16 | | 1.0000 | 0.0044 | 1.02841 | 4.998 |
| | 17 | | 0.9988 | 0.0044 | 1.01596 | 4.762 |
| | 18 | | 0.9988 | 0.0044 | 1.01408 | 5.998 |
| | 19 | | 0.9988 | 0.0044 | 1.01680 | 6.268 |
| | 20 | | 0.9988 | 0.0044 | 1.01355 | 6.446 |
| | 21 | | 0.9988 | 0.0044 | 1.01719 | 6.400 |

Table 6-8. List of Validation Critical Configurations

| IHECSBE Identifier | Case | Description | Benchmark | | Calculated | |
|--------------------|--------|---|-----------|-------------|------------|----------|
| | | | k_{eff} | $\pm\sigma$ | k_{eff} | EALF |
| | 22 | | 0.9988 | 0.0044 | 1.01789 | 6.241 |
| | 23 | | 1.0000 | 0.0046 | 1.01077 | 0.663 |
| | 24 | | 1.0000 | 0.0046 | 1.01215 | 0.673 |
| | 25 | | 1.0000 | 0.0046 | 1.01189 | 0.684 |
| | 26 | | 1.0000 | 0.0046 | 1.01298 | 0.689 |
| | 27 | | 1.0000 | 0.0046 | 1.01294 | 0.700 |
| | 28 | | 1.0000 | 0.0046 | 1.01412 | 0.703 |
| | 29 | | 1.0000 | 0.0046 | 1.01424 | 0.708 |
| pmf*002 | 1 | Bare Pu metal sphere | 1.0000 | 0.0020 | 0.99666 | 1.27E+06 |
| pmf011 | 1 | H ₂ O reflected Pu metal sphere | 1.0000 | 0.0010 | 0.99746 | 8.37E+04 |
| pmf022 | 1 | Bare Pu metal spherical ass. | 1.0000 | 0.0021 | 0.99409 | 1.23E+06 |
| pmf024 | 1 | Poly Refl Spherical Assembly | 1.0000 | 0.0020 | 0.99872 | 6.31E+05 |
| pmf027 | 1 | Poly Refl Spherical Assembly | 1.0000 | 0.0022 | 1.00215 | 7.02E+04 |
| pmf029 | 1 | Bare Pu Spherical Assembly | 1.0000 | 0.0022 | 0.99155 | 1.26E+06 |
| pmf031 | 1 | Poly Refl Spherical Assembly | 1.0000 | 0.0021 | 1.00215 | 1.85E+05 |
| pst*001 | 4 | Water Reflected filled 29.21 cm (11.5in.) Pu Nitrate solution spheres | 1.0000 | 0.0050 | 1.00433 | 0.147 |
| | 5 | | 1.0000 | 0.0050 | 1.00819 | 0.155 |
| | 6 | | 1.0000 | 0.0050 | 1.00882 | 0.337 |
| pst007 | 2 | Water reflected partially filled 29.21 cm (11.5in.) Pu Nitrate sol. Spheres | 1.0000 | 0.0047 | 1.00909 | 0.267 |
| | 3 | | 1.0000 | 0.0047 | 1.00375 | 0.254 |
| | 8 | | 1.0000 | 0.0047 | 0.99874 | 0.112 |
| pst014 | 3 | Interacting 30 cm (11.81 in.) diameter cylinders of Pu Nitrate solution (115.1 g Pu/l [0.9605 lb/gal]) in air | 0.9980 | 0.0032 | 1.00489 | 0.162 |
| | 4 | | 0.9980 | 0.0032 | 1.00520 | 0.162 |
| | 6 | | 0.9980 | 0.0032 | 1.00533 | 0.162 |
| | 8 | | 0.9980 | 0.0032 | 1.00292 | 0.163 |
| | 9 | | 0.9980 | 0.0032 | 1.00336 | 0.162 |
| | 10 | | 0.9980 | 0.0032 | 1.00470 | 0.162 |
| | 11 | | 0.9980 | 0.0032 | 1.00475 | 0.162 |
| | 12 | | 0.9980 | 0.0032 | 1.00440 | 0.162 |
| | 14 | | 0.9980 | 0.0043 | 1.00461 | 0.163 |
| | 16 | | 0.9980 | 0.0043 | 1.00416 | 0.162 |
| | 17 | | 0.9980 | 0.0043 | 1.00372 | 0.162 |
| | 20 | | 0.9980 | 0.0043 | 1.00455 | 0.162 |
| | 22 | | 0.9980 | 0.0043 | 1.00405 | 0.162 |
| | 23 | | 0.9980 | 0.0043 | 1.00358 | 0.162 |
| 25 | 0.9980 | 0.0043 | 1.00367 | 0.163 | | |
| 26 | 0.9980 | 0.0043 | 1.00279 | 0.162 | | |

Table 6-8. List of Validation Critical Configurations

| IHECSBE Identifier | Case | Description | Benchmark | | Calculated | |
|--------------------|------|--|-----------|-------------|------------|-------|
| | | | k_{eff} | $\pm\sigma$ | k_{eff} | EALF |
| | 27 | | 0.9980 | 0.0043 | 1.00479 | 0.162 |
| | 28 | | 0.9980 | 0.0043 | 1.00403 | 0.162 |
| | 29 | | 0.9980 | 0.0043 | 1.00392 | 0.162 |
| | 30 | | 0.9980 | 0.0043 | 1.00519 | 0.163 |
| | 31 | | 0.9980 | 0.0043 | 1.00260 | 0.163 |
| | 32 | | 0.9980 | 0.0043 | 1.00296 | 0.163 |
| | 33 | | 0.9980 | 0.0043 | 1.00340 | 0.163 |
| | 34 | | 0.9980 | 0.0043 | 1.00408 | 0.162 |
| | 35 | | 0.9980 | 0.0043 | 1.00533 | 0.162 |
| pst015 | 1 | Interacting 30 cm (11.81 in.) diameter cylinders of Pu Nitrate solution (152.5 g Pu/l [1.273 lb/gal]) in air | 0.9980 | 0.0038 | 1.00653 | 0.230 |
| | 2 | | 0.9980 | 0.0038 | 1.00642 | 0.229 |
| | 3 | | 0.9980 | 0.0038 | 1.00535 | 0.229 |
| | 4 | | 0.9980 | 0.0038 | 1.00597 | 0.229 |
| | 5 | | 0.9980 | 0.0038 | 1.00658 | 0.228 |
| | 6 | | 0.9980 | 0.0038 | 1.00733 | 0.228 |
| | 7 | | 0.9971 | 0.0047 | 1.00753 | 0.230 |
| | 8 | | 0.9971 | 0.0047 | 1.00520 | 0.230 |
| | 9 | | 0.9971 | 0.0047 | 1.00625 | 0.229 |
| | 10 | | 0.9971 | 0.0047 | 1.00457 | 0.228 |
| | 11 | | 0.9971 | 0.0047 | 1.00329 | 0.231 |
| | 12 | | 0.9971 | 0.0047 | 1.00475 | 0.230 |
| | 13 | | 0.9971 | 0.0047 | 1.00501 | 0.229 |
| | 14 | | 0.9971 | 0.0047 | 1.00636 | 0.228 |
| | 15 | | 0.9971 | 0.0047 | 1.00765 | 0.231 |
| | 16 | | 0.9971 | 0.0047 | 1.00520 | 0.230 |
| | 17 | | 0.9971 | 0.0047 | 1.00472 | 0.229 |
| pst016 | 1 | Interacting 30 cm (11.81 in.) and 25.6 cm (10.01 in.) diameter cylinders of Pu Nitrate solution (152.5 and 115.1 g Pu/l [1.273 and 0.9605 lb/gal]) and nitric acid (2N) in air | 0.9980 | 0.0043 | 1.00555 | 0.230 |
| | 2 | | 0.9980 | 0.0043 | 1.00501 | 0.229 |
| | 3 | | 0.9980 | 0.0043 | 1.00672 | 0.229 |
| | 4 | | 0.9980 | 0.0043 | 1.00696 | 0.228 |
| | 5 | | 0.9969 | 0.0038 | 1.00372 | 0.163 |
| | 6 | | 0.9969 | 0.0038 | 1.00502 | 0.162 |
| | 7 | | 0.9969 | 0.0038 | 1.00582 | 0.162 |
| | 8 | | 0.9969 | 0.0038 | 1.00492 | 0.162 |
| | 9 | | 0.9963 | 0.0033 | 1.00541 | 0.161 |
| | 10 | | 0.9963 | 0.0033 | 1.00564 | 0.161 |
| | 11 | | 0.9963 | 0.0033 | 1.00658 | 0.162 |
| pst017 | 1 | Interacting 30 cm (11.81 in.) and | 0.9969 | 0.0038 | 1.00379 | 0.162 |

Table 6-8. List of Validation Critical Configurations

| IHECSBE Identifier | Case | Description | Benchmark | | Calculated | |
|--------------------|--------|--|-----------|----------------------------|------------|--------|
| | | | k_{eff} | $\pm\sigma$ | k_{eff} | EALF |
| | 2 | 25.6cm (10.01 in.) diameter cylinders of Pu Nitrate solution (115.1 g Pu/l [0.9605 lb/gal]) in air I | 0.9969 | 0.0038 | 1.00490 | 0.162 |
| | 3 | | 0.9969 | 0.0038 | 1.00346 | 0.162 |
| | 4 | | 0.9969 | 0.0038 | 1.00499 | 0.162 |
| | 5 | | 0.9969 | 0.0038 | 1.00452 | 0.162 |
| | 6 | | 0.9969 | 0.0038 | 1.00461 | 0.162 |
| | 7 | | 0.9969 | 0.0038 | 1.00422 | 0.162 |
| | 8 | | 0.9969 | 0.0038 | 1.00485 | 0.162 |
| | 9 | | 0.9969 | 0.0038 | 1.00389 | 0.162 |
| | 10 | | 0.9969 | 0.0038 | 1.00441 | 0.162 |
| | 11 | | 0.9969 | 0.0038 | 1.00387 | 0.162 |
| | 12 | | 0.9969 | 0.0038 | 1.00536 | 0.162 |
| | 13 | | 0.9969 | 0.0038 | 1.00454 | 0.162 |
| | 14 | | 0.9969 | 0.0038 | 1.00545 | 0.162 |
| | 15 | | 0.9969 | 0.0038 | 1.00497 | 0.162 |
| | 16 | | 0.9969 | 0.0038 | 1.00506 | 0.162 |
| | 17 | | 0.9969 | 0.0038 | 1.00568 | 0.162 |
| | 18 | | 0.9969 | 0.0038 | 1.00465 | 0.162 |
| | pst020 | | 9 | Pu Nitrate solution sphere | 1.0000 | 0.0059 |
| pst021 | 3 | Pu Nitrate solution sphere | 1.0000 | 0.0065 | 1.01198 | 0.302 |
| | 8 | | 1.0000 | 0.0065 | 1.00474 | 0.302 |
| pst024 | 3 | Polyethylene reflected Pu Nitrate solution slab | 1.0000 | 0.0062 | 1.00277 | 0.444 |
| | 6 | | 1.0000 | 0.0077 | 1.00136 | 1.607 |
| | 16 | | 1.0000 | 0.0053 | 1.00457 | 0.287 |
| pst025 | 22 | Water reflected Pu Nitrate solution slab | 1.0000 | 0.0044 | 0.99944 | 0.240 |
| | 31 | | 1.0000 | 0.0048 | 0.99675 | 0.353 |
| | 42 | | 1.0000 | 0.0060 | 0.99558 | 1.142 |
| pst026 | 12 | Unreflected Pu Nitrate solution slab | 1.0000 | 0.0047 | 1.00047 | 0.239 |
| | 16 | | 1.0000 | 0.0044 | 0.99735 | 0.312 |
| | 19 | | 1.0000 | 0.0049 | 0.99688 | 0.503 |

All k_{eff} values were calculated with a standard deviation of 0.0005.

Table 6-9. Comparison of Tsunami Sensitivities and Direct Perturbation Sensitivities for a Representative Selection of Benchmark Critical Configurations

| Case | Perturbed Material | Direct Perturbation | | TSUNAMI | | Number Std. Dev. Apart |
|-----------|--------------------|---------------------|--------|-------------|--------|------------------------|
| | | Sensitivity | Sigma | Sensitivity | Sigma | |
| pcm001c01 | H | 0.0020 | 0.0007 | 0.0014 | 0.0001 | 0.94 |
| | Pu-239 | 0.6016 | 0.0846 | 0.6410 | 0.0017 | 0.47 |
| pcm001c05 | H | 0.4158 | 0.0374 | 0.2956 | 0.0092 | 2.67 |
| | Pu-239 | 0.1326 | 0.0171 | 0.1126 | 0.0008 | 1.17 |
| pcm002c01 | H | 0.0002 | 0.0007 | 0.0015 | 0.0001 | 1.88 |
| | Pu-239 | 0.3442 | 0.0477 | 0.3856 | 0.0092 | 0.85 |
| pcm002c20 | H | 0.2592 | 0.0311 | 0.2390 | 0.0056 | 0.64 |
| | Pu-239 | 0.1804 | 0.0244 | 0.1813 | 0.0009 | 0.04 |
| pcm002c24 | H | 0.2673 | 0.0139 | 0.2715 | 0.0048 | 0.28 |
| | Pu-239 | 0.1128 | 0.0059 | 0.1061 | 0.0006 | 1.14 |
| pmf002c01 | H | N/A | N/A | N/A | N/A | N/A |
| | Pu-239 | 0.6986 | 0.0869 | 0.6881 | 0.0016 | 0.12 |
| pmf011c01 | H | N/A | N/A | N/A | N/A | N/A |
| | Pu-239 | 0.6529 | 0.0868 | 0.6501 | 0.0014 | 0.03 |
| pmf024c01 | H | N/A | N/A | N/A | N/A | N/A |
| | Pu-239 | 0.7585 | 0.0867 | 0.7754 | 0.0015 | 0.20 |
| pst001c05 | H | 0.4075 | 0.0573 | 0.4840 | 0.0074 | 1.32 |
| | Pu-239 | 0.0742 | 0.0104 | 0.0751 | 0.0004 | 0.08 |
| pst014c03 | H | 0.5493 | 0.0690 | 0.6034 | 0.0047 | 0.78 |
| | Pu-239 | 0.0801 | 0.0108 | 0.07996 | 0.0005 | 0.01 |
| pst015c01 | H | 0.5613 | 0.0688 | 0.5996 | 0.0039 | 0.55 |
| | Pu-239 | 0.0613 | 0.0098 | 0.0708 | 0.0004 | 0.96 |
| pst024c03 | H | 0.4644 | 0.0494 | 0.3894 | 0.0093 | 1.49 |
| | Pu-239 | 0.0863 | 0.0133 | 0.0974 | 0.0009 | 0.83 |
| pst024c06 | H | 0.3395 | 0.0433 | 0.3483 | 0.0090 | 0.20 |
| | Pu-239 | 0.1151 | 0.0165 | 0.1214 | 0.0008 | 0.38 |
| pst024c16 | H | 0.3605 | 0.0493 | 0.4074 | 0.0106 | 0.93 |
| | Pu-239 | 0.1159 | 0.0138 | 0.1021 | 0.0010 | 1.00 |
| pst025c31 | H | 0.3530 | 0.0435 | 0.3452 | 0.0061 | 0.18 |
| | Pu-239 | 0.0920 | 0.0129 | 0.0953 | 0.0007 | 0.26 |

pcm = PU-COMP-MIXED

pmf = PU-MET-FAST

pst = PU-SOL-THERM

Table 6-10. Comparison of Direct Perturbation Sensitivities and Tsunami Sensitivities for the 11 Representative Applications

| Case | Perturbed Material | Direct Perturbation | | TSUNAMI | | Number Std. Dev. Apart |
|-----------------|--------------------|---------------------|--------|-------------|--------|------------------------|
| | | Sensitivity | Sigma | Sensitivity | Sigma | |
| <i>cv001</i> | Pu-239 | 0.6857 | 0.1051 | 0.8527 | 0.1390 | 0.96 |
| | H ₂ O | 0.1539 | 0.0215 | 0.1977 | 0.0654 | 0.64 |
| <i>cv031</i> | Pu-239 | 0.0970 | 0.0173 | 0.0944 | 0.0306 | 0.07 |
| | H ₂ O | 0.8443 | 0.0999 | 0.9643 | 0.3201 | 0.36 |
| <i>fhlsf001</i> | Pu-239 | 0.7719 | 0.1032 | 0.7434 | 0.0017 | 0.28 |
| | H ₂ O | 0.1778 | 0.0059 | 0.1382 | 0.0234 | 1.63 |
| <i>fhlsf031</i> | Pu-239 | 0.1204 | 0.0272 | 0.1451 | 0.0057 | 0.89 |
| | H ₂ O | 0.8882 | 0.1089 | 0.6675 | 0.0781 | 1.65 |
| <i>fslsf001</i> | Pu-239 | 0.7183 | 0.1060 | 0.7418 | 0.0018 | 0.22 |
| | H ₂ O | 0.1836 | 0.0212 | 0.1441 | 0.0226 | 1.28 |
| <i>fslsf031</i> | Pu-239 | 0.1590 | 0.0272 | 0.1304 | 0.0020 | 1.05 |
| | H ₂ O | 0.7623 | 0.1117 | 0.6070 | 0.0297 | 1.34 |
| <i>hexs100</i> | Pu-239 | 0.1329 | 0.0247 | 0.1302 | 0.0013 | 0.11 |
| | H ₂ O | 0.8358 | 0.0940 | 0.5574 | 0.1259 | 1.77 |
| <i>hexsdry</i> | Pu-239 | 0.2105 | 0.0805 | 0.1524 | 0.0006 | 0.72 |
| | H ₂ O | 0.7135 | 0.0654 | 0.7153 | 0.0060 | 0.03 |
| <i>octs100</i> | Pu-239 | 0.1469 | 0.0235 | 0.1368 | 0.0025 | 0.43 |
| | H ₂ O | 0.5071 | 0.0965 | 0.5577 | 0.0357 | 0.49 |
| <i>octsdry</i> | Pu-239 | 0.0944 | 0.0835 | 0.1549 | 0.0006 | 0.72 |
| | H ₂ O | 0.8289 | 0.0644 | 0.7584 | 0.0065 | 1.09 |
| <i>sph14</i> | Pu-239 | 0.1633 | 0.0241 | 0.1212 | 0.0120 | 1.56 |
| | H ₂ O | 0.9150 | 0.0963 | 0.6715 | 0.1178 | 1.60 |

Table 6-11. Comparison of METAL SPHERE Applications to Critical Benchmarks

| IHECSBE Identifier | Case | <i>cv001</i> c_k | <i>fhlsf001</i> c_k | <i>fslsf001</i> c_k | EALF (eV) | H/Pu | k_{eff} |
|--------------------|------|-----------------------|--------------------------|-----------------------|-----------|------|-----------|
| pcm001 | 1 | 0.9686 | 0.9684 | 0.9682 | 9.73E+05 | 0.05 | 1.02438 |
| pcm002 | 1 | 0.9427 | 0.9440 | 0.9439 | 4.56E+03 | 0.05 | 1.03757 |
| | 2 | 0.9390 | 0.9404 | 0.9402 | 3.98E+03 | 0.05 | 1.03641 |
| | 3 | 0.9345 | 0.9361 | 0.9359 | 3.26E+03 | 0.05 | 1.03179 |
| | 4 | 0.9260 | 0.9277 | 0.9275 | 2.42E+03 | 0.05 | 1.02547 |
| | 5 | 0.9158 | 0.9178 | 0.9176 | 1.76E+03 | 0.05 | 1.02328 |

Table 6-11. Comparison of METAL SPHERE Applications to Critical Benchmarks

| IHECSBE Identifier | Case | <i>cv001</i> c_k | <i>fhlsf001</i> c_k | <i>fslsf001</i> c_k | EALF (eV) | H/Pu | k_{eff} |
|--------------------|------|-----------------------|--------------------------|-----------------------|-----------|------|-----------|
| pmf002 | 1 | 0.9699 | 0.9714 | 0.9709 | 1.27E+06 | 0.00 | 0.99666 |
| pmf011 | 1 | 0.9948 | 0.9960 | 0.9958 | 8.37E+04 | 0.00 | 0.99746 |
| pmf022 | 1 | 0.9856 | 0.9871 | 0.9866 | 1.23E+06 | 0.00 | 0.99409 |
| pmf024 | 1 | 0.9917 | 0.9930 | 0.9927 | 6.31E+05 | 0.00 | 0.99872 |
| pmf027 | 1 | 0.9916 | 0.9930 | 0.9928 | 7.02E+04 | 0.00 | 1.00215 |
| pmf029 | 1 | 0.9822 | 0.9837 | 0.9832 | 1.26E+06 | 0.02 | 0.99155 |
| pmf031 | 1 | 0.9915 | 0.9929 | 0.9926 | 1.85E+05 | 0.02 | 1.00215 |

All k_{eff} values were calculated with a standard deviation of 0.0005.

For all applications H/ Pu = 0.0

EALF values for the above applications is as follows:

Case cv001: 5.449E+04 eV

Case fhlsf001: 7.872E+04 eV

Case fslsf001: 7.976E+04 eV

Table 6-12. Comparison of SOLUTION LATTICE Applications to Critical Benchmarks

| IHECSBE Identifier | Case | <i>fhlsf031</i> c_k | <i>fslsf031</i> c_k | <i>hexs100</i> c_k | <i>octs100</i> c_k | EALF (eV) | H/Pu Ratio | k_{eff} |
|--------------------|--------|--------------------------|--------------------------|-------------------------|-------------------------|-----------|------------|-----------|
| pcm001 | 5 | 0.9102 | 0.9078 | 0.9324 | 0.9307 | 1.468 | 65.37 | 1.01403 |
| pcm002 | 10 | 0.9296 | 0.9262 | 0.9471 | 0.9457 | 4.026 | 15.46 | 1.03534 |
| | 11 | 0.9328 | 0.9297 | 0.9494 | 0.9480 | 4.405 | 15.46 | 1.03184 |
| | 12 | 0.9362 | 0.9334 | 0.9517 | 0.9505 | 4.970 | 15.46 | 1.03209 |
| | 13 | 0.9345 | 0.9317 | 0.9499 | 0.9487 | 5.262 | 15.46 | 1.02982 |
| | 14 | 0.9353 | 0.9325 | 0.9500 | 0.9489 | 5.405 | 15.46 | 1.03451 |
| | 15 | 0.9307 | 0.9276 | 0.9465 | 0.9452 | 5.366 | 15.46 | 1.03220 |
| | 16 | 0.9315 | 0.9286 | 0.9478 | 0.9465 | 4.998 | 15.46 | 1.02841 |
| | 17 | 0.9101 | 0.9069 | 0.9311 | 0.9297 | 4.762 | 16.40 | 1.01596 |
| | 18 | 0.9140 | 0.9100 | 0.9318 | 0.9306 | 5.998 | 16.40 | 1.01408 |
| | 19 | 0.9180 | 0.9150 | 0.9365 | 0.9353 | 6.268 | 16.40 | 1.01680 |
| | 20 | 0.9148 | 0.9109 | 0.9318 | 0.9307 | 6.446 | 16.40 | 1.01355 |
| | 21 | 0.9187 | 0.9157 | 0.9369 | 0.9358 | 6.400 | 16.40 | 1.01719 |
| | 22 | 0.9111 | 0.9071 | 0.9292 | 0.9280 | 6.241 | 16.40 | 1.01789 |
| | 23 | 0.8933 | 0.8903 | 0.9159 | 0.9141 | 0.663 | 65.37 | 1.01077 |
| | 24 | 0.8979 | 0.8940 | 0.9196 | 0.9178 | 0.673 | 65.37 | 1.01215 |
| | 25 | 0.9007 | 0.8970 | 0.9220 | 0.9202 | 0.684 | 65.37 | 1.01189 |
| 26 | 0.9007 | 0.8969 | 0.9220 | 0.9202 | 0.689 | 65.37 | 1.01298 | |

Table 6-12. Comparison of SOLUTION LATTICE Applications to Critical Benchmarks

| IHECSBE Identifier | Case | <i>fhlsf031</i> c_k | <i>fslsf031</i> c_k | <i>hexs100</i> c_k | <i>octs100</i> c_k | EALF (eV) | H/Pu Ratio | k_{eff} |
|---------------------------|-------------|---|---|--|--|----------------------|-----------------------|-----------------------------|
| | 27 | 0.8996 | 0.8957 | 0.9211 | 0.9194 | 0.700 | 65.37 | 1.01294 |
| | 28 | 0.9024 | 0.8987 | 0.9236 | 0.9218 | 0.703 | 65.37 | 1.01412 |
| | 29 | 0.9043 | 0.9008 | 0.9252 | 0.9235 | 0.708 | 65.37 | 1.01424 |
| pst001 | 4 | 0.8973 | 0.8953 | 0.9000 | 0.8994 | 0.147 | 190.43 | 1.00433 |
| | 5 | 0.8999 | 0.8978 | 0.9030 | 0.9024 | 0.155 | 180.16 | 1.00819 |
| | 6 | 0.9340 | 0.9319 | 0.9409 | 0.9400 | 0.337 | 91.19 | 1.00882 |
| pst007 | 2 | 0.9262 | 0.9234 | 0.9318 | 0.9309 | 0.267 | 109.55 | 1.00909 |
| | 3 | 0.9235 | 0.9216 | 0.9290 | 0.9282 | 0.254 | 113.97 | 1.00375 |
| pst014 | 11 | 0.8985 | 0.8985 | 0.9024 | 0.9017 | 0.162 | 220.19 | 1.00475 |
| pst015 | 1 | 0.9100 | 0.9069 | 0.9141 | 0.9132 | 0.230 | 162.67 | 1.00653 |
| | 2 | 0.9107 | 0.9077 | 0.9143 | 0.9135 | 0.229 | 162.67 | 1.00642 |
| | 3 | 0.9115 | 0.9085 | 0.9146 | 0.9138 | 0.229 | 162.67 | 1.00535 |
| | 4 | 0.9119 | 0.9090 | 0.9148 | 0.9140 | 0.229 | 162.67 | 1.00597 |
| | 5 | 0.9118 | 0.9089 | 0.9147 | 0.9139 | 0.228 | 162.67 | 1.00658 |
| | 6 | 0.9126 | 0.9097 | 0.9151 | 0.9144 | 0.228 | 162.67 | 1.00733 |
| | 7 | 0.9084 | 0.9055 | 0.9145 | 0.9135 | 0.230 | 162.67 | 1.00753 |
| | 8 | 0.9097 | 0.9066 | 0.9141 | 0.9132 | 0.230 | 162.67 | 1.00520 |
| | 9 | 0.9113 | 0.9083 | 0.9146 | 0.9138 | 0.229 | 162.67 | 1.00625 |
| | 10 | 0.9126 | 0.9097 | 0.9152 | 0.9144 | 0.228 | 162.67 | 1.00457 |
| | 11 | 0.9095 | 0.9065 | 0.9145 | 0.9136 | 0.231 | 162.67 | 1.00329 |
| | 12 | 0.9107 | 0.9077 | 0.9145 | 0.9137 | 0.230 | 162.67 | 1.00475 |
| | 13 | 0.9117 | 0.9087 | 0.9148 | 0.9140 | 0.229 | 162.67 | 1.00501 |
| | 14 | 0.9124 | 0.9095 | 0.9151 | 0.9143 | 0.228 | 162.67 | 1.00636 |
| | 15 | 0.9071 | 0.9042 | 0.9140 | 0.9130 | 0.231 | 162.67 | 1.00765 |
| | 16 | 0.9096 | 0.9066 | 0.9143 | 0.9134 | 0.230 | 162.67 | 1.00520 |
| | 17 | 0.9112 | 0.9082 | 0.9146 | 0.9138 | 0.229 | 162.67 | 1.00472 |
| pst016 | 1 | 0.9112 | 0.9081 | 0.9145 | 0.9137 | 0.230 | 162.66 | 1.00555 |
| | 2 | 0.9125 | 0.9096 | 0.9150 | 0.9143 | 0.229 | 162.66 | 1.00501 |
| | 3 | 0.9126 | 0.9097 | 0.9151 | 0.9143 | 0.229 | 162.66 | 1.00672 |
| | 4 | 0.9127 | 0.9099 | 0.9151 | 0.9144 | 0.228 | 162.66 | 1.00696 |
| | 8 | 0.8989 | 0.8989 | 0.9025 | 0.9019 | 0.162 | 220.20 | 1.00492 |
| pst017 | 1 | 0.8977 | 0.8948 | 0.8980 | 0.8974 | 0.162 | 220.19 | 1.00379 |
| | 2 | 0.8985 | 0.8962 | 0.8998 | 0.8992 | 0.162 | 220.19 | 1.00490 |
| | 5 | 0.8973 | 0.8944 | 0.8979 | 0.8974 | 0.162 | 220.19 | 1.00452 |
| | 7 | 0.8974 | 0.8947 | 0.8987 | 0.8981 | 0.162 | 220.19 | 1.00422 |
| pst021 | 3 | 0.9233 | 0.9203 | 0.9258 | 0.9251 | 0.302 | 131.30 | 1.01198 |

Table 6-12. Comparison of SOLUTION LATTICE Applications to Critical Benchmarks

| IHECSBE Identifier | Case | <i>fhlsf031</i> c_k | <i>fslsf031</i> c_k | <i>hexs100</i> c_k | <i>octs100</i> c_k | EALF (eV) | H/Pu Ratio | k_{eff} |
|--------------------|------|--------------------------|--------------------------|-------------------------|-------------------------|-----------|------------|-----------|
| | 8 | 0.9234 | 0.9204 | 0.9258 | 0.9251 | 0.302 | 131.30 | 1.00474 |
| pst024 | 3 | 0.9065 | 0.9025 | 0.9213 | 0.9198 | 0.444 | 115.40 | 1.00277 |
| | 6 | 0.9190 | 0.9141 | 0.9376 | 0.9360 | 1.607 | 59.25 | 1.00136 |
| pst025 | 31 | 0.9034 | 0.8987 | 0.9187 | 0.9172 | 0.353 | 115.40 | 0.99675 |
| | 42 | 0.9233 | 0.9179 | 0.9412 | 0.9398 | 1.142 | 59.25 | 0.99558 |
| pst026 | 19 | 0.9090 | 0.9050 | 0.9232 | 0.9217 | 0.503 | 115.40 | 0.99688 |

All k_{eff} values were calculated with a standard deviation of 0.0005.

For all applications H/ Pu = 28.79

EALF values for the above applications is as follows:

Case fhlsf031: 2.693 eV

Case fslsf031: 2.695 eV

Case hexs100: 2.548 eV

Case octs100: 2.547 eV

Table 6-13. Comparison of SINGLE UNIT SOLUTION Applications to Critical Benchmarks

| IHECSBE | Case | <i>cv031</i> c_k | <i>sph14</i> c_k | EALF (eV) | H / Pu | k_{eff} |
|---------|------|-----------------------|-----------------------|-----------|--------|-----------|
| pcm002 | 10 | 0.9067 | 0.9282 | 4.026 | 15.46 | 1.03534 |
| | 11 | 0.9091 | 0.9309 | 4.405 | 15.46 | 1.03184 |
| | 12 | 0.9118 | 0.9339 | 4.970 | 15.46 | 1.03209 |
| | 13 | 0.9081 | 0.9308 | 5.262 | 15.46 | 1.02982 |
| | 14 | 0.9083 | 0.9311 | 5.405 | 15.46 | 1.03451 |
| | 15 | 0.9025 | 0.9257 | 5.366 | 15.46 | 1.03220 |
| | 16 | 0.9046 | 0.9276 | 4.998 | 15.46 | 1.02841 |
| | 29 | 0.9018 | 0.9168 | 0.708 | 65.37 | 1.01424 |
| pst001 | 4 | 0.9388 | 0.9314 | 0.147 | 190.43 | 1.00433 |
| | 5 | 0.9401 | 0.9333 | 0.155 | 180.16 | 1.00819 |
| | 6 | 0.9583 | 0.9588 | 0.337 | 91.19 | 1.00882 |
| pst007 | 2 | 0.9558 | 0.9530 | 0.267 | 109.55 | 1.00909 |
| | 3 | 0.9534 | 0.9515 | 0.254 | 113.97 | 1.00375 |
| | 8 | 0.9292 | 0.9194 | 0.112 | 258.46 | 0.99874 |
| pst014 | 3 | 0.9438 | 0.9340 | 0.162 | 220.19 | 1.00489 |
| | 4 | 0.9446 | 0.9346 | 0.162 | 220.19 | 1.00520 |
| | 6 | 0.9451 | 0.9351 | 0.162 | 220.19 | 1.00533 |
| | 8 | 0.9411 | 0.9320 | 0.163 | 220.19 | 1.00292 |

Table 6-13. Comparison of SINGLE UNIT SOLUTION Applications to Critical Benchmarks

| IHECSBE | Case | <i>cv031</i> c_k | <i>sph14</i> c_k | EALF (eV) | H / Pu | k_{eff} |
|---------|------|-----------------------|-----------------------|--------------|--------|-----------|
| | 9 | 0.9432 | 0.9335 | 0.162 | 220.19 | 1.00336 |
| | 10 | 0.9440 | 0.9342 | 0.162 | 220.19 | 1.00470 |
| | 11 | 0.9380 | 0.9351 | 0.162 | 220.19 | 1.00475 |
| | 12 | 0.9453 | 0.9352 | 0.162 | 220.19 | 1.00440 |
| | 14 | 0.9411 | 0.9320 | 0.163 | 220.19 | 1.00461 |
| | 16 | 0.9447 | 0.9348 | 0.162 | 220.19 | 1.00416 |
| | 17 | 0.9450 | 0.9351 | 0.162 | 220.19 | 1.00372 |
| | 20 | 0.9435 | 0.9338 | 0.162 | 220.19 | 1.00455 |
| | 22 | 0.9449 | 0.9349 | 0.162 | 220.19 | 1.00405 |
| | 23 | 0.9454 | 0.9353 | 0.162 | 220.19 | 1.00358 |
| | 25 | 0.9397 | 0.9310 | 0.163 | 220.19 | 1.00367 |
| | 26 | 0.9428 | 0.9333 | 0.162 | 220.19 | 1.00279 |
| | 27 | 0.9448 | 0.9349 | 0.162 | 220.19 | 1.00479 |
| | 28 | 0.9447 | 0.9347 | 0.162 | 220.19 | 1.00403 |
| | 29 | 0.9452 | 0.9352 | 0.162 | 220.19 | 1.00392 |
| | 30 | 0.9381 | 0.9298 | 0.163 | 220.19 | 1.00519 |
| | 31 | 0.9399 | 0.9313 | 0.163 | 220.19 | 1.00260 |
| | 32 | 0.9412 | 0.9320 | 0.163 | 220.19 | 1.00296 |
| | 33 | 0.9421 | 0.9328 | 0.163 | 220.19 | 1.00340 |
| | 34 | 0.9432 | 0.9336 | 0.162 | 220.19 | 1.00408 |
| | 35 | 0.9435 | 0.9338 | 0.162 | 220.19 | 1.00533 |
| pst015 | 1 | 0.9494 | 0.9432 | 0.230 | 162.67 | 1.00653 |
| | 2 | 0.9506 | 0.9442 | 0.229 | 162.67 | 1.00642 |
| | 3 | 0.9518 | 0.9451 | 0.229 | 162.67 | 1.00535 |
| | 4 | 0.9523 | 0.9456 | 0.229 | 162.67 | 1.00597 |
| | 5 | 0.9522 | 0.9456 | 0.228 | 162.67 | 1.00658 |
| | 6 | 0.9533 | 0.9465 | 0.228 | 162.67 | 1.00733 |
| | 7 | 0.9444 | 0.9403 | 0.230 | 162.67 | 1.00753 |
| | 8 | 0.9487 | 0.9428 | 0.230 | 162.67 | 1.00520 |
| | 9 | 0.9513 | 0.9448 | 0.229 | 162.67 | 1.00625 |
| | 10 | 0.9532 | 0.9464 | 0.228 | 162.67 | 1.00457 |
| | 11 | 0.9471 | 0.9420 | 0.231 | 162.67 | 1.00329 |
| | 12 | 0.9502 | 0.9440 | 0.230 | 162.67 | 1.00475 |
| | 13 | 0.9518 | 0.9453 | 0.229 | 162.67 | 1.00501 |
| | 14 | 0.9530 | 0.9462 | 0.228 | 162.67 | 1.00636 |

Table 6-13. Comparison of SINGLE UNIT SOLUTION Applications to Critical Benchmarks

| IHECSBE | Case | <i>cv031</i> c_k | <i>sph14</i> c_k | EALF (eV) | H / Pu | k_{eff} |
|---------|------|-----------------------|-----------------------|--------------|--------|-----------|
| | 15 | 0.9423 | 0.9387 | 0.231 | 162.67 | 1.00765 |
| | 16 | 0.9481 | 0.9425 | 0.230 | 162.67 | 1.00520 |
| | 17 | 0.9511 | 0.9447 | 0.229 | 162.67 | 1.00472 |
| pst016 | 1 | 0.9511 | 0.9446 | 0.230 | 162.66 | 1.00555 |
| | 2 | 0.9532 | 0.9463 | 0.229 | 162.66 | 1.00501 |
| | 3 | 0.9533 | 0.9465 | 0.229 | 162.66 | 1.00672 |
| | 4 | 0.9535 | 0.9466 | 0.228 | 162.66 | 1.00696 |
| | 5 | 0.9431 | 0.9334 | 0.163 | 220.20 | 1.00372 |
| | 6 | 0.9443 | 0.9344 | 0.162 | 220.20 | 1.00502 |
| | 7 | 0.9456 | 0.9355 | 0.162 | 220.20 | 1.00582 |
| | 8 | 0.9387 | 0.9357 | 0.162 | 220.20 | 1.00492 |
| | 9 | 0.9453 | 0.9352 | 0.161 | 220.20 | 1.00541 |
| | 10 | 0.9457 | 0.9356 | 0.161 | 220.20 | 1.00564 |
| | 11 | 0.9456 | 0.9355 | 0.162 | 220.20 | 1.00658 |
| pst017 | 1 | 0.9460 | 0.9358 | 0.162 | 220.19 | 1.00379 |
| | 2 | 0.9446 | 0.9362 | 0.162 | 220.19 | 1.00490 |
| | 3 | 0.9457 | 0.9356 | 0.162 | 220.19 | 1.00346 |
| | 4 | 0.9451 | 0.9352 | 0.162 | 220.19 | 1.00499 |
| | 5 | 0.9453 | 0.9354 | 0.162 | 220.19 | 1.00452 |
| | 6 | 0.9456 | 0.9355 | 0.162 | 220.19 | 1.00461 |
| | 7 | 0.9442 | 0.9351 | 0.162 | 220.19 | 1.00422 |
| | 8 | 0.9452 | 0.9352 | 0.162 | 220.19 | 1.00485 |
| | 9 | 0.9454 | 0.9353 | 0.162 | 220.19 | 1.00389 |
| | 10 | 0.9448 | 0.9348 | 0.162 | 220.19 | 1.00441 |
| | 11 | 0.9458 | 0.9357 | 0.162 | 220.19 | 1.00387 |
| | 12 | 0.9453 | 0.9352 | 0.162 | 220.19 | 1.00536 |
| | 13 | 0.9450 | 0.9350 | 0.162 | 220.19 | 1.00454 |
| | 14 | 0.9446 | 0.9347 | 0.162 | 220.19 | 1.00545 |
| | 15 | 0.9453 | 0.9352 | 0.162 | 220.19 | 1.00497 |
| | 16 | 0.9453 | 0.9352 | 0.162 | 220.19 | 1.00506 |
| | 17 | 0.9455 | 0.9354 | 0.162 | 220.19 | 1.00568 |
| | 18 | 0.9453 | 0.9352 | 0.162 | 220.19 | 1.00465 |
| pst021 | 3 | 0.9601 | 0.9546 | 0.302 | 131.30 | 1.01198 |
| | 8 | 0.9604 | 0.9548 | 0.302 | 131.30 | 1.00474 |
| pst024 | 3 | 0.9205 | 0.9260 | 0.444 | 115.40 | 1.00277 |

Table 6-13. Comparison of SINGLE UNIT SOLUTION Applications to Critical Benchmarks

| IHECSBE | Case | <i>cv031</i> c_k | <i>sph14</i> c_k | EALF (eV) | H / Pu | k_{eff} |
|---------|------|-----------------------|-----------------------|--------------|--------|-----------|
| | 6 | 0.9085 | 0.9240 | 1.607 | 59.25 | 1.00136 |
| | 16 | 0.9068 | 0.9088 | 0.287 | 161.28 | 1.00457 |
| pst025 | 31 | 0.9127 | 0.9165 | 0.353 | 115.40 | 0.99675 |
| | 42 | 0.9119 | 0.9251 | 1.142 | 59.25 | 0.99558 |
| pst026 | 12 | 0.9157 | 0.9147 | 0.239 | 189.80 | 1.00047 |
| | 16 | 0.9074 | 0.9099 | 0.312 | 161.28 | 0.99735 |
| | 19 | 0.9240 | 0.9297 | 0.503 | 115.40 | 0.99688 |

All k_{eff} values were calculated with a standard deviation of 0.0005.

For all applications H/ Pu = 28.79

EALF values for the above applications is as follows:

Case cv031: 1.094 eV

Case sph14: 1.259 eV

Table 6-14. Comparison of DRY LATTICE Applications to Critical Benchmarks

| IHECSBE Identifier | Case | <i>Hexsdry</i> c_k | <i>Octsdry</i> c_k | EALF (eV) | H / Pu | k_{eff} |
|--------------------|--------|-------------------------|-------------------------|--------------|---------|-----------|
| pcm001 | 3 | 0.9549 | 0.9509 | 30.518 | 15.46 | 1.02356 |
| | 4 | 0.9313 | 0.9262 | 37.727 | 16.40 | 0.99275 |
| | 5 | 0.9437 | 0.9378 | 1.468 | 65.37 | 1.01403 |
| pcm002 | 10 | 0.9693 | 0.9646 | 4.026 | 15.46 | 1.03534 |
| | 11 | 0.9718 | 0.9676 | 4.405 | 15.46 | 1.03184 |
| | 12 | 0.9739 | 0.9701 | 4.970 | 15.46 | 1.03209 |
| | 13 | 0.9738 | 0.9700 | 5.262 | 15.46 | 1.02982 |
| | 14 | 0.9741 | 0.9706 | 5.405 | 15.46 | 1.03451 |
| | 15 | 0.9721 | 0.9681 | 5.366 | 15.46 | 1.03220 |
| | 16 | 0.9722 | 0.9681 | 4.998 | 15.46 | 1.02841 |
| | 17 | 0.9538 | 0.9479 | 4.762 | 16.40 | 1.01596 |
| | 18 | 0.9594 | 0.9545 | 5.998 | 16.40 | 1.01408 |
| | 19 | 0.9607 | 0.9557 | 6.268 | 16.40 | 1.01680 |
| | 20 | 0.9607 | 0.9560 | 6.446 | 16.40 | 1.01355 |
| | 21 | 0.9612 | 0.9563 | 6.400 | 16.40 | 1.01719 |
| | 22 | 0.9584 | 0.9534 | 6.241 | 16.40 | 1.01789 |
| | 23 | 0.9181 | 0.9117 | 0.663 | 65.37 | 1.01077 |
| | 24 | 0.9249 | 0.9187 | 0.673 | 65.37 | 1.01215 |
| | 25 | 0.9270 | 0.9211 | 0.684 | 65.37 | 1.01189 |
| | 26 | 0.9273 | 0.9213 | 0.689 | 65.37 | 1.01298 |
| 27 | 0.9271 | 0.9210 | 0.700 | 65.37 | 1.01294 | |
| 28 | 0.9292 | 0.9233 | 0.703 | 65.37 | 1.01412 | |
| 29 | 0.9306 | 0.9248 | 0.708 | 65.37 | 1.01424 | |
| pst001 | 6 | 0.9227 | 0.9223 | 0.337 | 91.19 | 1.00882 |
| pst007 | 2 | 0.9122 | 0.9120 | 0.267 | 109.55 | 1.00909 |
| | 3 | 0.9059 | 0.9060 | 0.254 | 113.97 | 1.00375 |
| pst021 | 3 | 0.9081 | 0.9093 | 0.302 | 131.30 | 1.01198 |
| | 8 | 0.9078 | 0.9090 | 0.302 | 131.30 | 1.00474 |
| pst024 | 3 | 0.9156 | 0.9121 | 0.444 | 115.40 | 1.00277 |
| | 6 | 0.9523 | 0.9473 | 1.607 | 59.25 | 1.00136 |
| pst025 | 31 | 0.9067 | 0.9025 | 0.353 | 115.40 | 0.99675 |
| | 42 | 0.9488 | 0.9437 | 1.142 | 59.25 | 0.99558 |
| pst026 | 19 | 0.9196 | 0.9164 | 0.503 | 115.40 | 0.99688 |

All k_{eff} values were calculated with a standard deviation of 0.0005.

For all applications H/ Pu = 28.79

EALF values for the applications are as follows: Case *hexsdry*: 4.864 eV

Case *octsdry*: 5.042 eV

6.9.4 Calculation Results

6.9.4.1 *Calculations Supporting Single Package Analysis*

Table 6-15 lists calculations performed to support the standard single package analysis for normal conditions of transport and hypothetical accident conditions.

Table 6-15. Tabulation of Calculations Supporting the Standard Single Package Analysis for Normal Conditions of Transport and Hypothetical Accident Conditions

| Case Name | k_{eff} | σ | Model Type | Description | H/Pu | Case location |
|--------------------------|-----------|----------|------------|---|-------|----------------------------------|
| <i>Sudma</i> | 0.55252 | 0.00049 | detailed | Pu metal sphere, no water in TB-1 | 0 | /pat1/apps/normsp/detailed/met/ |
| <i>sudmb</i> | 0.64919 | 0.00049 | detailed | Pu metal sphere reflected by water in TB-1 | 0 | /pat1/apps/normsp/detailed/met/ |
| <i>sudmwoodm</i> | 0.64857 | 0.00050 | detailed | sudmb with 80% of redwood density | 0 | /pat1/apps/normsp/detailed/met/ |
| <i>sudmwoodp</i> | 0.65003 | 0.00049 | detailed | sudmb with 120% of redwood density | 0 | /pat1/apps/normsp/detailed/met/ |
| <i>sudmc</i> | 0.65037 | 0.00049 | detailed | sudmb with gaps filled with water | 0 | /pat1/apps/normsp/detailed/met/ |
| <i>sudmd</i> | 0.64988 | 0.00049 | detailed | sudmc with copper changed to water | 0 | /pat1/apps/normsp/detailed/met/ |
| <i>sudme</i> | 0.64889 | 0.00050 | detailed | sudmd with aluminum changed to water | 0 | /pat1/apps/normsp/detailed/met/ |
| <i>sudmf</i> | 0.65231 | 0.00050 | detailed | sudme with redwood changed to water | 0 | /pat1/apps/normsp/detailed/met/ |
| <i>sudsb</i> | 0.56797 | 0.00051 | detailed | Pu-water in TB-1 | 28.8 | /pat1/apps/normsp/detailed/soln/ |
| <i>sudswoodm</i> | 0.55988 | 0.00053 | detailed | sudsb with 80% of redwood density | 28.8 | /pat1/apps/normsp/detailed/soln/ |
| <i>sudswoodp</i> | 0.57611 | 0.00049 | detailed | sudsb with 120% of redwood density | 28.8 | /pat1/apps/normsp/detailed/soln/ |
| <i>sudsc</i> | 0.59112 | 0.00050 | detailed | sudsb with gaps filled with water | 28.8 | /pat1/apps/normsp/detailed/soln/ |
| <i>sudsd</i> | 0.59200 | 0.00050 | detailed | sudsc with copper changed to water | 28.8 | /pat1/apps/normsp/detailed/soln/ |
| <i>sudse</i> | 0.59316 | 0.00049 | detailed | sudsd with aluminum changed to water | 28.8 | /pat1/apps/normsp/detailed/soln/ |
| <i>sudsf</i> | 0.62781 | 0.00052 | detailed | sudse with redwood changed to water | 28.8 | /pat1/apps/normsp/detailed/soln/ |
| <i>sudsg</i> | 0.70400 | 0.00050 | detailed | sudsf with steel changed to water | 28.8 | /pat1/apps/normsp/detailed/soln/ |
| <i>cv001^a</i> | 0.65648 | 0.00046 | simplified | redwood and outer steel drum modeled as water | 0 | /pat1/apps/normsp/simple/cv/ |
| <i>cv002</i> | 0.65418 | 0.00049 | simplified | redwood and outer steel drum modeled as water | 0.013 | /pat1/apps/normsp/simple/cv/ |
| <i>cv003</i> | 0.65184 | 0.00048 | simplified | redwood and outer steel drum modeled as water | 0.027 | /pat1/apps/normsp/simple/cv/ |
| <i>cv004</i> | 0.64541 | 0.00049 | simplified | redwood and outer steel drum modeled as water | 0.070 | /pat1/apps/normsp/simple/cv/ |
| <i>cv005</i> | 0.63449 | 0.00050 | simplified | redwood and outer steel drum modeled as water | 0.15 | /pat1/apps/normsp/simple/cv/ |
| <i>cv006</i> | 0.62351 | 0.00049 | simplified | redwood and outer steel drum modeled as water | 0.24 | /pat1/apps/normsp/simple/cv/ |
| <i>cv007</i> | 0.61203 | 0.00049 | simplified | redwood and outer steel drum modeled as water | 0.33 | /pat1/apps/normsp/simple/cv/ |
| <i>cv008</i> | 0.60147 | 0.00050 | simplified | redwood and outer steel drum modeled as water | 0.45 | /pat1/apps/normsp/simple/cv/ |

Table 6-15. Tabulation of Calculations Supporting the Standard Single Package Analysis for Normal Conditions of Transport and Hypothetical Accident Conditions

| Case Name | k_{eff} | σ | Model Type | Description | H/Pu | Case location |
|--------------------|-----------|----------|------------|---|------|------------------------------|
| cv009 | 0.59098 | 0.00049 | simplified | redwood and outer steel drum modeled as water | 0.57 | /pat1/apps/normsp/simple/cv/ |
| cv010 | 0.58139 | 0.00045 | simplified | redwood and outer steel drum modeled as water | 0.72 | /pat1/apps/normsp/simple/cv/ |
| cv011 | 0.57148 | 0.00049 | simplified | redwood and outer steel drum modeled as water | 0.89 | /pat1/apps/normsp/simple/cv/ |
| cv012 | 0.56435 | 0.00049 | simplified | redwood and outer steel drum modeled as water | 1.09 | /pat1/apps/normsp/simple/cv/ |
| cv013 | 0.55469 | 0.00050 | simplified | redwood and outer steel drum modeled as water | 1.34 | /pat1/apps/normsp/simple/cv/ |
| cv014 | 0.54769 | 0.00050 | simplified | redwood and outer steel drum modeled as water | 1.63 | /pat1/apps/normsp/simple/cv/ |
| cv015 | 0.54270 | 0.00050 | simplified | redwood and outer steel drum modeled as water | 2.00 | /pat1/apps/normsp/simple/cv/ |
| cv016 | 0.53871 | 0.00050 | simplified | redwood and outer steel drum modeled as water | 2.48 | /pat1/apps/normsp/simple/cv/ |
| cv017 | 0.53848 | 0.00049 | simplified | redwood and outer steel drum modeled as water | 3.12 | /pat1/apps/normsp/simple/cv/ |
| cv018 | 0.54156 | 0.00050 | simplified | redwood and outer steel drum modeled as water | 4.01 | /pat1/apps/normsp/simple/cv/ |
| cv019 | 0.54894 | 0.00049 | simplified | redwood and outer steel drum modeled as water | 5.34 | /pat1/apps/normsp/simple/cv/ |
| cv020 | 0.56885 | 0.00049 | simplified | redwood and outer steel drum modeled as water | 7.57 | /pat1/apps/normsp/simple/cv/ |
| cv021 | 0.60586 | 0.00050 | simplified | redwood and outer steel drum modeled as water | 12.0 | /pat1/apps/normsp/simple/cv/ |
| cv022 | 0.60740 | 0.00054 | simplified | redwood and outer steel drum modeled as water | 12.1 | /pat1/apps/normsp/simple/cv/ |
| cv023 | 0.54664 | 0.00049 | simplified | redwood and outer steel drum modeled as water | 5.34 | /pat1/apps/normsp/simple/cv/ |
| cv024 | 0.56835 | 0.00050 | simplified | redwood and outer steel drum modeled as water | 7.57 | /pat1/apps/normsp/simple/cv/ |
| cv025 | 0.61086 | 0.00050 | simplified | redwood and outer steel drum modeled as water | 12.0 | /pat1/apps/normsp/simple/cv/ |
| cv026 | 0.62366 | 0.00049 | simplified | redwood and outer steel drum modeled as water | 13.5 | /pat1/apps/normsp/simple/cv/ |
| cv027 | 0.63709 | 0.00049 | simplified | redwood and outer steel drum modeled as water | 15.4 | /pat1/apps/normsp/simple/cv/ |
| cv028 | 0.65343 | 0.00049 | simplified | redwood and outer steel drum modeled as water | 17.7 | /pat1/apps/normsp/simple/cv/ |
| cv029 | 0.67196 | 0.00053 | simplified | redwood and outer steel drum modeled as water | 20.9 | /pat1/apps/normsp/simple/cv/ |
| cv030 | 0.69513 | 0.00057 | simplified | redwood and outer steel drum modeled as water | 25.4 | /pat1/apps/normsp/simple/cv/ |
| cv031 ^a | 0.70756 | 0.00055 | simplified | redwood and outer steel drum modeled as water | 28.8 | /pat1/apps/normsp/simple/cv/ |
| cv032 | 0.70106 | 0.00054 | simplified | redwood and outer steel drum modeled as water | 32.0 | /pat1/apps/normsp/simple/cv/ |

Table 6-15. Tabulation of Calculations Supporting the Standard Single Package Analysis for Normal Conditions of Transport and Hypothetical Accident Conditions

| Case Name | k_{eff} | σ | Model Type | Description | H/Pu | Case location |
|-----------|-----------|----------|------------|---|-------|----------------------------------|
| cv033 | 0.69423 | 0.00050 | simplified | redwood and outer steel drum modeled as water | 36.8 | /pat1/apps/normsp/simple/cv/ |
| cv034 | 0.68607 | 0.00051 | simplified | redwood and outer steel drum modeled as water | 43.2 | /pat1/apps/normsp/simple/cv/ |
| cv035 | 0.67715 | 0.00051 | simplified | redwood and outer steel drum modeled as water | 52.1 | /pat1/apps/normsp/simple/cv/ |
| cv036 | 0.66815 | 0.00052 | simplified | redwood and outer steel drum modeled as water | 65.4 | /pat1/apps/normsp/simple/cv/ |
| cv037 | 0.65515 | 0.00050 | simplified | redwood and outer steel drum modeled as water | 87.7 | /pat1/apps/normsp/simple/cv/ |
| cv038 | 0.63611 | 0.00053 | simplified | redwood and outer steel drum modeled as water | 132.2 | /pat1/apps/normsp/simple/cv/ |
| sp001 | 0.64320 | 0.00049 | simplified | nominal redwood & steel modeled | 0 | /pat1/apps/normsp/simple/rdwood/ |
| sp002 | 0.64219 | 0.00049 | simplified | nominal redwood & steel modeled | 0.013 | /pat1/apps/normsp/simple/rdwood/ |
| sp003 | 0.63869 | 0.00050 | simplified | nominal redwood & steel modeled | 0.027 | /pat1/apps/normsp/simple/rdwood/ |
| sp004 | 0.63183 | 0.00049 | simplified | nominal redwood & steel modeled | 0.070 | /pat1/apps/normsp/simple/rdwood/ |
| sp005 | 0.62057 | 0.00049 | simplified | nominal redwood & steel modeled | 0.15 | /pat1/apps/normsp/simple/rdwood/ |
| sp006 | 0.60807 | 0.00049 | simplified | nominal redwood & steel modeled | 0.24 | /pat1/apps/normsp/simple/rdwood/ |
| sp007 | 0.59672 | 0.00049 | simplified | nominal redwood & steel modeled | 0.33 | /pat1/apps/normsp/simple/rdwood/ |
| sp008 | 0.58466 | 0.00049 | simplified | nominal redwood & steel modeled | 0.45 | /pat1/apps/normsp/simple/rdwood/ |
| sp009 | 0.57386 | 0.00049 | simplified | nominal redwood & steel modeled | 0.57 | /pat1/apps/normsp/simple/rdwood/ |
| sp010 | 0.56209 | 0.00048 | simplified | nominal redwood & steel modeled | 0.72 | /pat1/apps/normsp/simple/rdwood/ |
| sp011 | 0.55118 | 0.00049 | simplified | nominal redwood & steel modeled | 0.89 | /pat1/apps/normsp/simple/rdwood/ |
| sp012 | 0.54046 | 0.00049 | simplified | nominal redwood & steel modeled | 1.09 | /pat1/apps/normsp/simple/rdwood/ |
| sp013 | 0.53048 | 0.00049 | simplified | nominal redwood & steel modeled | 1.34 | /pat1/apps/normsp/simple/rdwood/ |
| sp014 | 0.52122 | 0.00050 | simplified | nominal redwood & steel modeled | 1.63 | /pat1/apps/normsp/simple/rdwood/ |
| sp015 | 0.51185 | 0.00049 | simplified | nominal redwood & steel modeled | 2.00 | /pat1/apps/normsp/simple/rdwood/ |
| sp016 | 0.50434 | 0.00050 | simplified | nominal redwood & steel modeled | 2.48 | /pat1/apps/normsp/simple/rdwood/ |
| sp017 | 0.49909 | 0.00050 | simplified | nominal redwood & steel modeled | 3.12 | /pat1/apps/normsp/simple/rdwood/ |
| sp018 | 0.49516 | 0.00049 | simplified | nominal redwood & steel modeled | 4.01 | /pat1/apps/normsp/simple/rdwood/ |

Table 6-15. Tabulation of Calculations Supporting the Standard Single Package Analysis for Normal Conditions of Transport and Hypothetical Accident Conditions

| Case Name | k_{eff} | σ | Model Type | Description | H/Pu | Case location |
|-----------|-----------|----------|------------|---------------------------------|-------|---------------------------------------|
| sp019 | 0.49425 | 0.00047 | simplified | nominal redwood & steel modeled | 5.34 | /pat1/apps/normsp/simple/rdwood/ |
| sp020 | 0.49848 | 0.00049 | simplified | nominal redwood & steel modeled | 7.57 | /pat1/apps/normsp/simple/rdwood/ |
| sp021 | 0.51005 | 0.00050 | simplified | nominal redwood & steel modeled | 12.0 | /pat1/apps/normsp/simple/rdwood/ |
| sp022 | 0.51044 | 0.00049 | simplified | nominal redwood & steel modeled | 12.1 | /pat1/apps/normsp/simple/rdwood/ |
| sp023 | 0.46393 | 0.00049 | simplified | nominal redwood & steel modeled | 5.34 | /pat1/apps/normsp/simple/rdwood/ |
| sp024 | 0.47663 | 0.00049 | simplified | nominal redwood & steel modeled | 7.57 | /pat1/apps/normsp/simple/rdwood/ |
| sp025 | 0.50178 | 0.00049 | simplified | nominal redwood & steel modeled | 12.0 | /pat1/apps/normsp/simple/rdwood/ |
| sp026 | 0.50911 | 0.00049 | simplified | nominal redwood & steel modeled | 13.5 | /pat1/apps/normsp/simple/rdwood/ |
| sp027 | 0.51691 | 0.00050 | simplified | nominal redwood & steel modeled | 15.4 | /pat1/apps/normsp/simple/rdwood/ |
| sp028 | 0.52725 | 0.00049 | simplified | nominal redwood & steel modeled | 17.7 | /pat1/apps/normsp/simple/rdwood/ |
| sp029 | 0.53595 | 0.00047 | simplified | nominal redwood & steel modeled | 20.9 | /pat1/apps/normsp/simple/rdwood/ |
| sp030 | 0.54436 | 0.00049 | simplified | nominal redwood & steel modeled | 25.4 | /pat1/apps/normsp/simple/rdwood/ |
| sp031 | 0.54872 | 0.00053 | simplified | nominal redwood & steel modeled | 28.8 | /pat1/apps/normsp/simple/rdwood/ |
| sp032 | 0.54122 | 0.00053 | simplified | nominal redwood & steel modeled | 32.0 | /pat1/apps/normsp/simple/rdwood/ |
| sp033 | 0.53213 | 0.00049 | simplified | nominal redwood & steel modeled | 36.8 | /pat1/apps/normsp/simple/rdwood/ |
| sp034 | 0.52280 | 0.00049 | simplified | nominal redwood & steel modeled | 43.2 | /pat1/apps/normsp/simple/rdwood/ |
| sp035 | 0.51265 | 0.00054 | simplified | nominal redwood & steel modeled | 52.1 | /pat1/apps/normsp/simple/rdwood/ |
| sp036 | 0.50240 | 0.00049 | simplified | nominal redwood & steel modeled | 65.4 | /pat1/apps/normsp/simple/rdwood/ |
| sp037 | 0.48877 | 0.00050 | simplified | nominal redwood & steel modeled | 87.7 | /pat1/apps/normsp/simple/rdwood/ |
| sp038 | 0.46921 | 0.00049 | simplified | nominal redwood & steel modeled | 132.2 | /pat1/apps/normsp/simple/rdwood/ |
| rwh001 | 0.64527 | 0.00049 | simplified | 120% redwood density | 0 | /pat1/apps/normsp/simple/rdwood+/ |
| rwh002 | 0.64286 | 0.00050 | simplified | 120% redwood density | 0.013 | /pat1/apps/normsp/simple/rdwood+/ |
| rwh003 | 0.64097 | 0.00050 | simplified | 120% redwood density | 0.027 | /pat1/apps/normsp/simple/rdwood+/ |
| rwh004 | 0.63332 | 0.00050 | simplified | 120% redwood density | 0.070 | /pat1/apps/normsp/simple/rdwood+/ |

Table 6-15. Tabulation of Calculations Supporting the Standard Single Package Analysis for Normal Conditions of Transport and Hypothetical Accident Conditions

| Case Name | k_{eff} | σ | Model Type | Description | H/Pu | Case location |
|---------------|-----------|----------|------------|----------------------|-------|---------------------------------------|
| <i>rwh029</i> | 0.54898 | 0.00049 | simplified | 120% redwood density | 20.9 | /pat1/apps/normsp/simple/rdwood+/ |
| <i>rwh030</i> | 0.55880 | 0.00048 | simplified | 120% redwood density | 25.4 | /pat1/apps/normsp/simple/rdwood+/ |
| <i>rwh031</i> | 0.56354 | 0.00049 | simplified | 120% redwood density | 28.8 | /pat1/apps/normsp/simple/rdwood+/ |
| <i>rwh032</i> | 0.55604 | 0.00049 | simplified | 120% redwood density | 32.0 | /pat1/apps/normsp/simple/rdwood+/ |
| <i>rwh033</i> | 0.54737 | 0.00050 | simplified | 120% redwood density | 36.8 | /pat1/apps/normsp/simple/rdwood+/ |
| <i>rwh034</i> | 0.53800 | 0.00049 | simplified | 120% redwood density | 43.2 | /pat1/apps/normsp/simple/rdwood+/ |
| <i>rwh035</i> | 0.52800 | 0.00049 | simplified | 120% redwood density | 52.1 | /pat1/apps/normsp/simple/rdwood+/ |
| <i>rwh036</i> | 0.51637 | 0.00051 | simplified | 120% redwood density | 65.4 | /pat1/apps/normsp/simple/rdwood+/ |
| <i>rwh037</i> | 0.50261 | 0.00049 | simplified | 120% redwood density | 87.7 | /pat1/apps/normsp/simple/rdwood+/ |
| <i>rwh038</i> | 0.48353 | 0.00048 | simplified | 120% redwood density | 132.2 | /pat1/apps/normsp/simple/rdwood+/ |
| <i>rwl001</i> | 0.64199 | 0.00050 | simplified | 80% redwood density | 0 | /pat1/apps/normsp/simple/rdwood-/ |
| <i>rwl002</i> | 0.64025 | 0.00050 | simplified | 80% redwood density | 0.013 | /pat1/apps/normsp/simple/rdwood-/ |
| <i>rwl003</i> | 0.63708 | 0.00050 | simplified | 80% redwood density | 0.027 | /pat1/apps/normsp/simple/rdwood-/ |
| <i>rwl004</i> | 0.63111 | 0.00050 | simplified | 80% redwood density | 0.070 | /pat1/apps/normsp/simple/rdwood-/ |
| <i>rwl005</i> | 0.61906 | 0.00049 | simplified | 80% redwood density | 0.15 | /pat1/apps/normsp/simple/rdwood-/ |
| <i>rwl006</i> | 0.60665 | 0.00049 | simplified | 80% redwood density | 0.24 | /pat1/apps/normsp/simple/rdwood-/ |
| <i>rwl007</i> | 0.59477 | 0.00050 | simplified | 80% redwood density | 0.33 | /pat1/apps/normsp/simple/rdwood-/ |
| <i>rwl008</i> | 0.58214 | 0.00049 | simplified | 80% redwood density | 0.45 | /pat1/apps/normsp/simple/rdwood-/ |
| <i>rwl009</i> | 0.57065 | 0.00050 | simplified | 80% redwood density | 0.57 | /pat1/apps/normsp/simple/rdwood-/ |
| <i>rwl010</i> | 0.55970 | 0.00050 | simplified | 80% redwood density | 0.72 | /pat1/apps/normsp/simple/rdwood-/ |
| <i>rwl011</i> | 0.54871 | 0.00050 | simplified | 80% redwood density | 0.89 | /pat1/apps/normsp/simple/rdwood-/ |
| <i>rwl012</i> | 0.53773 | 0.00048 | simplified | 80% redwood density | 1.09 | /pat1/apps/normsp/simple/rdwood-/ |
| <i>rwl013</i> | 0.52837 | 0.00050 | simplified | 80% redwood density | 1.34 | /pat1/apps/normsp/simple/rdwood-/ |
| <i>rwl014</i> | 0.51804 | 0.00050 | simplified | 80% redwood density | 1.63 | /pat1/apps/normsp/simple/rdwood-/ |

Table 6-15. Tabulation of Calculations Supporting the Standard Single Package Analysis for Normal Conditions of Transport and Hypothetical Accident Conditions

| Case Name | k_{eff} | σ | Model Type | Description | H/Pu | Case location |
|---------------|-----------|----------|------------|---------------------|-------|-----------------------------------|
| <i>rw1015</i> | 0.50939 | 0.00049 | simplified | 80% redwood density | 2.00 | /pat1/apps/normsp/simple/rdwood-/ |
| <i>rw1016</i> | 0.50098 | 0.00049 | simplified | 80% redwood density | 2.48 | /pat1/apps/normsp/simple/rdwood-/ |
| <i>rw1017</i> | 0.49512 | 0.00050 | simplified | 80% redwood density | 3.12 | /pat1/apps/normsp/simple/rdwood-/ |
| <i>rw1018</i> | 0.49014 | 0.00049 | simplified | 80% redwood density | 4.01 | /pat1/apps/normsp/simple/rdwood-/ |
| <i>rw1019</i> | 0.48891 | 0.00049 | simplified | 80% redwood density | 5.34 | /pat1/apps/normsp/simple/rdwood-/ |
| <i>rw1020</i> | 0.49139 | 0.00050 | simplified | 80% redwood density | 7.57 | /pat1/apps/normsp/simple/rdwood-/ |
| <i>rw1021</i> | 0.50138 | 0.00052 | simplified | 80% redwood density | 12.0 | /pat1/apps/normsp/simple/rdwood-/ |
| <i>rw1022</i> | 0.50208 | 0.00050 | simplified | 80% redwood density | 12.1 | /pat1/apps/normsp/simple/rdwood-/ |
| <i>rw1023</i> | 0.45772 | 0.00049 | simplified | 80% redwood density | 5.34 | /pat1/apps/normsp/simple/rdwood-/ |
| <i>rw1024</i> | 0.46789 | 0.00049 | simplified | 80% redwood density | 7.57 | /pat1/apps/normsp/simple/rdwood-/ |
| <i>rw1025</i> | 0.49183 | 0.00050 | simplified | 80% redwood density | 12.0 | /pat1/apps/normsp/simple/rdwood-/ |
| <i>rw1026</i> | 0.49746 | 0.00049 | simplified | 80% redwood density | 13.5 | /pat1/apps/normsp/simple/rdwood-/ |
| <i>rw1027</i> | 0.50572 | 0.00050 | simplified | 80% redwood density | 15.4 | /pat1/apps/normsp/simple/rdwood-/ |
| <i>rw1028</i> | 0.51415 | 0.00050 | simplified | 80% redwood density | 17.7 | /pat1/apps/normsp/simple/rdwood-/ |
| <i>rw1029</i> | 0.52251 | 0.00049 | simplified | 80% redwood density | 20.9 | /pat1/apps/normsp/simple/rdwood-/ |
| <i>rw1030</i> | 0.52951 | 0.00050 | simplified | 80% redwood density | 25.4 | /pat1/apps/normsp/simple/rdwood-/ |
| <i>rw1031</i> | 0.53188 | 0.00050 | simplified | 80% redwood density | 28.8 | /pat1/apps/normsp/simple/rdwood-/ |
| <i>rw1032</i> | 0.52522 | 0.00057 | simplified | 80% redwood density | 32.0 | /pat1/apps/normsp/simple/rdwood-/ |
| <i>rw1033</i> | 0.51621 | 0.00049 | simplified | 80% redwood density | 36.8 | /pat1/apps/normsp/simple/rdwood-/ |
| <i>rw1034</i> | 0.50720 | 0.00052 | simplified | 80% redwood density | 43.2 | /pat1/apps/normsp/simple/rdwood-/ |
| <i>rw1035</i> | 0.49733 | 0.00049 | simplified | 80% redwood density | 52.1 | /pat1/apps/normsp/simple/rdwood-/ |
| <i>rw1036</i> | 0.48574 | 0.00053 | simplified | 80% redwood density | 65.4 | /pat1/apps/normsp/simple/rdwood-/ |
| <i>rw1037</i> | 0.47230 | 0.00049 | simplified | 80% redwood density | 87.7 | /pat1/apps/normsp/simple/rdwood-/ |
| <i>rw1038</i> | 0.45497 | 0.00049 | simplified | 80% redwood density | 132.2 | /pat1/apps/normsp/simple/rdwood-/ |

Table 6-15. Tabulation of Calculations Supporting the Standard Single Package Analysis for Normal Conditions of Transport and Hypothetical Accident Conditions

| Case Name | k_{eff} | σ | Model Type | Description | H/Pu | Case location |
|-----------|-----------|----------|------------|--------------------------|-------|-----------------------------------|
| spw001 | 0.65033 | 0.00050 | simplified | redwood modeled as water | 0 | /pat1/apps/normsp/simple/h2owood/ |
| spw002 | 0.64843 | 0.00049 | simplified | redwood modeled as water | 0.013 | /pat1/apps/normsp/simple/h2owood/ |
| spw003 | 0.64700 | 0.00049 | simplified | redwood modeled as water | 0.027 | /pat1/apps/normsp/simple/h2owood/ |
| spw004 | 0.63908 | 0.00049 | simplified | redwood modeled as water | 0.070 | /pat1/apps/normsp/simple/h2owood/ |
| spw005 | 0.62742 | 0.00050 | simplified | redwood modeled as water | 0.15 | /pat1/apps/normsp/simple/h2owood/ |
| spw006 | 0.61727 | 0.00049 | simplified | redwood modeled as water | 0.24 | /pat1/apps/normsp/simple/h2owood/ |
| spw007 | 0.60483 | 0.00049 | simplified | redwood modeled as water | 0.33 | /pat1/apps/normsp/simple/h2owood/ |
| spw008 | 0.59386 | 0.00050 | simplified | redwood modeled as water | 0.45 | /pat1/apps/normsp/simple/h2owood/ |
| spw009 | 0.58271 | 0.00049 | simplified | redwood modeled as water | 0.57 | /pat1/apps/normsp/simple/h2owood/ |
| spw010 | 0.57190 | 0.00049 | simplified | redwood modeled as water | 0.72 | /pat1/apps/normsp/simple/h2owood/ |
| spw011 | 0.56188 | 0.00049 | simplified | redwood modeled as water | 0.89 | /pat1/apps/normsp/simple/h2owood/ |
| spw012 | 0.55272 | 0.00049 | simplified | redwood modeled as water | 1.09 | /pat1/apps/normsp/simple/h2owood/ |
| spw013 | 0.54391 | 0.00049 | simplified | redwood modeled as water | 1.34 | /pat1/apps/normsp/simple/h2owood/ |
| spw014 | 0.53537 | 0.00049 | simplified | redwood modeled as water | 1.63 | /pat1/apps/normsp/simple/h2owood/ |
| spw015 | 0.52825 | 0.00049 | simplified | redwood modeled as water | 2.00 | /pat1/apps/normsp/simple/h2owood/ |
| spw016 | 0.52190 | 0.00050 | simplified | redwood modeled as water | 2.48 | /pat1/apps/normsp/simple/h2owood/ |
| spw017 | 0.51869 | 0.00050 | simplified | redwood modeled as water | 3.12 | /pat1/apps/normsp/simple/h2owood/ |
| spw018 | 0.51825 | 0.00049 | simplified | redwood modeled as water | 4.01 | /pat1/apps/normsp/simple/h2owood/ |
| spw019 | 0.52240 | 0.00049 | simplified | redwood modeled as water | 5.34 | /pat1/apps/normsp/simple/h2owood/ |
| spw020 | 0.53256 | 0.00050 | simplified | redwood modeled as water | 7.57 | /pat1/apps/normsp/simple/h2owood/ |
| spw021 | 0.55865 | 0.00050 | simplified | redwood modeled as water | 12.0 | /pat1/apps/normsp/simple/h2owood/ |
| spw022 | 0.55901 | 0.00049 | simplified | redwood modeled as water | 12.1 | /pat1/apps/normsp/simple/h2owood/ |
| spw023 | 0.50382 | 0.00049 | simplified | redwood modeled as water | 5.34 | /pat1/apps/normsp/simple/h2owood/ |
| spw024 | 0.52217 | 0.00046 | simplified | redwood modeled as water | 7.57 | /pat1/apps/normsp/simple/h2owood/ |

Table 6-15. Tabulation of Calculations Supporting the Standard Single Package Analysis for Normal Conditions of Transport and Hypothetical Accident Conditions

| Case Name | k_{eff} | σ | Model Type | Description | H/Pu | Case location |
|---------------|-----------|----------|------------|--------------------------|-------|-----------------------------------|
| <i>spw025</i> | 0.55687 | 0.00049 | simplified | redwood modeled as water | 12.0 | /pat1/apps/normsp/simple/h2owood/ |
| <i>spw026</i> | 0.56847 | 0.00050 | simplified | redwood modeled as water | 13.5 | /pat1/apps/normsp/simple/h2owood/ |
| <i>spw027</i> | 0.57991 | 0.00050 | simplified | redwood modeled as water | 15.4 | /pat1/apps/normsp/simple/h2owood/ |
| <i>spw028</i> | 0.59315 | 0.00049 | simplified | redwood modeled as water | 17.7 | /pat1/apps/normsp/simple/h2owood/ |
| <i>spw029</i> | 0.60796 | 0.00049 | simplified | redwood modeled as water | 20.9 | /pat1/apps/normsp/simple/h2owood/ |
| <i>spw030</i> | 0.62351 | 0.00049 | simplified | redwood modeled as water | 25.4 | /pat1/apps/normsp/simple/h2owood/ |
| <i>spw031</i> | 0.63291 | 0.00050 | simplified | redwood modeled as water | 28.8 | /pat1/apps/normsp/simple/h2owood/ |
| <i>spw032</i> | 0.62643 | 0.00050 | simplified | redwood modeled as water | 32.0 | /pat1/apps/normsp/simple/h2owood/ |
| <i>spw033</i> | 0.61758 | 0.00050 | simplified | redwood modeled as water | 36.8 | /pat1/apps/normsp/simple/h2owood/ |
| <i>spw034</i> | 0.60761 | 0.00049 | simplified | redwood modeled as water | 43.2 | /pat1/apps/normsp/simple/h2owood/ |
| <i>spw035</i> | 0.59709 | 0.00051 | simplified | redwood modeled as water | 52.1 | /pat1/apps/normsp/simple/h2owood/ |
| <i>spw036</i> | 0.58537 | 0.00051 | simplified | redwood modeled as water | 65.4 | /pat1/apps/normsp/simple/h2owood/ |
| <i>spw037</i> | 0.56841 | 0.00050 | simplified | redwood modeled as water | 87.7 | /pat1/apps/normsp/simple/h2owood/ |
| <i>spw038</i> | 0.54692 | 0.00051 | simplified | redwood modeled as water | 132.2 | /pat1/apps/normsp/simple/h2owood/ |

^a Limiting cases listed in Table 6-1.

6.9.4.2 *Calculations Supporting Normal Conditions of Transport Array Analysis*

Table 6-16 lists calculations performed to support the analysis of arrays of undamaged packages.

Note that some case names were used multiple times. Refer to the case description and file location to differentiate cases.

Table 6-16. Tabulation of Calculations Supporting the Analysis of Arrays of Undamaged Packages

| Case Name | k_{eff} | σ | Package Model Type | Array Type | Description | H/Pu | Location |
|-----------------|-----------|----------|--------------------|------------|---------------------|-------|------------------------------------|
| <i>fsl</i> d001 | 0.65045 | 0.00049 | detailed | square | Base detailed model | 0 | /pat1/apps/normarray/detail/fsl/d/ |
| <i>fsl</i> d002 | 0.64841 | 0.00050 | detailed | square | Base detailed model | 0.013 | /pat1/apps/normarray/detail/fsl/d/ |
| <i>fsl</i> d003 | 0.64611 | 0.00050 | detailed | square | Base detailed model | 0.027 | /pat1/apps/normarray/detail/fsl/d/ |
| <i>fsl</i> d004 | 0.63833 | 0.00049 | detailed | square | Base detailed model | 0.070 | /pat1/apps/normarray/detail/fsl/d/ |
| <i>fsl</i> d005 | 0.62772 | 0.00050 | detailed | square | Base detailed model | 0.15 | /pat1/apps/normarray/detail/fsl/d/ |
| <i>fsl</i> d006 | 0.61627 | 0.00050 | detailed | square | Base detailed model | 0.24 | /pat1/apps/normarray/detail/fsl/d/ |
| <i>fsl</i> d007 | 0.60399 | 0.00049 | detailed | square | Base detailed model | 0.33 | /pat1/apps/normarray/detail/fsl/d/ |
| <i>fsl</i> d008 | 0.59302 | 0.00049 | detailed | square | Base detailed model | 0.45 | /pat1/apps/normarray/detail/fsl/d/ |
| <i>fsl</i> d009 | 0.58156 | 0.00049 | detailed | square | Base detailed model | 0.57 | /pat1/apps/normarray/detail/fsl/d/ |
| <i>fsl</i> d010 | 0.57146 | 0.00046 | detailed | square | Base detailed model | 0.72 | /pat1/apps/normarray/detail/fsl/d/ |
| <i>fsl</i> d011 | 0.55968 | 0.00048 | detailed | square | Base detailed model | 0.89 | /pat1/apps/normarray/detail/fsl/d/ |
| <i>fsl</i> d012 | 0.55046 | 0.00048 | detailed | square | Base detailed model | 1.09 | /pat1/apps/normarray/detail/fsl/d/ |
| <i>fsl</i> d013 | 0.54098 | 0.00050 | detailed | square | Base detailed model | 1.34 | /pat1/apps/normarray/detail/fsl/d/ |
| <i>fsl</i> d014 | 0.53212 | 0.00049 | detailed | square | Base detailed model | 1.63 | /pat1/apps/normarray/detail/fsl/d/ |
| <i>fsl</i> d015 | 0.52530 | 0.00050 | detailed | square | Base detailed model | 2.00 | /pat1/apps/normarray/detail/fsl/d/ |
| <i>fsl</i> d016 | 0.51857 | 0.00050 | detailed | square | Base detailed model | 2.48 | /pat1/apps/normarray/detail/fsl/d/ |
| <i>fsl</i> d017 | 0.51468 | 0.00046 | detailed | square | Base detailed model | 3.12 | /pat1/apps/normarray/detail/fsl/d/ |
| <i>fsl</i> d018 | 0.51149 | 0.00050 | detailed | square | Base detailed model | 4.01 | /pat1/apps/normarray/detail/fsl/d/ |
| <i>fsl</i> d019 | 0.51174 | 0.00050 | detailed | square | Base detailed model | 5.34 | /pat1/apps/normarray/detail/fsl/d/ |
| <i>fsl</i> d020 | 0.51919 | 0.00050 | detailed | square | Base detailed model | 7.57 | /pat1/apps/normarray/detail/fsl/d/ |
| <i>fsl</i> d021 | 0.53283 | 0.00049 | detailed | square | Base detailed model | 12.0 | /pat1/apps/normarray/detail/fsl/d/ |
| <i>fsl</i> d022 | 0.53398 | 0.00050 | detailed | square | Base detailed model | 12.1 | /pat1/apps/normarray/detail/fsl/d/ |
| <i>fsl</i> d023 | 0.47720 | 0.00049 | detailed | square | Base detailed model | 5.34 | /pat1/apps/normarray/detail/fsl/d/ |
| <i>fsl</i> d024 | 0.49116 | 0.00050 | detailed | square | Base detailed model | 7.57 | /pat1/apps/normarray/detail/fsl/d/ |
| <i>fsl</i> d025 | 0.52185 | 0.00050 | detailed | square | Base detailed model | 12.0 | /pat1/apps/normarray/detail/fsl/d/ |
| <i>fsl</i> d026 | 0.53042 | 0.00049 | detailed | square | Base detailed model | 13.5 | /pat1/apps/normarray/detail/fsl/d/ |

Table 6-16. Tabulation of Calculations Supporting the Analysis of Arrays of Undamaged Packages

| Case Name | k_{eff} | σ | Package Model Type | Array Type | Description | H/Pu | Location |
|-----------------|-----------|----------|--------------------|------------|-------------------------------------|-------|-----------------------------------|
| <i>fsld027</i> | 0.54015 | 0.00049 | detailed | square | Base detailed model | 15.4 | /pat1/apps/normarray/detail/fsld/ |
| <i>fsld028</i> | 0.55270 | 0.00049 | detailed | square | Base detailed model | 17.7 | /pat1/apps/normarray/detail/fsld/ |
| <i>fsld029</i> | 0.56357 | 0.00049 | detailed | square | Base detailed model | 20.9 | /pat1/apps/normarray/detail/fsld/ |
| <i>fsld030</i> | 0.57757 | 0.00051 | detailed | square | Base detailed model | 25.4 | /pat1/apps/normarray/detail/fsld/ |
| <i>fsld031</i> | 0.58160 | 0.00049 | detailed | square | Base detailed model | 28.8 | /pat1/apps/normarray/detail/fsld/ |
| <i>fsld032</i> | 0.57339 | 0.00053 | detailed | square | Base detailed model | 32.0 | /pat1/apps/normarray/detail/fsld/ |
| <i>fsld033</i> | 0.56487 | 0.00061 | detailed | square | Base detailed model | 36.8 | /pat1/apps/normarray/detail/fsld/ |
| <i>fsld034</i> | 0.55433 | 0.00050 | detailed | square | Base detailed model | 43.2 | /pat1/apps/normarray/detail/fsld/ |
| <i>fsld035</i> | 0.54470 | 0.00049 | detailed | square | Base detailed model | 52.1 | /pat1/apps/normarray/detail/fsld/ |
| <i>fsld036</i> | 0.53388 | 0.00053 | detailed | square | Base detailed model | 65.4 | /pat1/apps/normarray/detail/fsld/ |
| <i>fsld037</i> | 0.51999 | 0.00053 | detailed | square | Base detailed model | 87.7 | /pat1/apps/normarray/detail/fsld/ |
| <i>fsld038</i> | 0.50063 | 0.00050 | detailed | square | Base detailed model | 132.2 | /pat1/apps/normarray/detail/fsld/ |
| <i>fsld001a</i> | 0.65125 | 0.00049 | detailed | square | base detailed model, Gap -> redwood | 0.0 | /pat1/apps/normarray/detail/swap/ |
| <i>fsld001b</i> | 0.64857 | 0.00049 | detailed | square | fsld001a with copper -> redwood | 0.0 | /pat1/apps/normarray/detail/swap/ |
| <i>fsld001c</i> | 0.64787 | 0.00050 | detailed | square | fsld001b with aluminum -> redwood | 0.0 | /pat1/apps/normarray/detail/swap/ |
| <i>fsld001d</i> | 0.65266 | 0.00048 | detailed | square | fsld001c with redwood -> water | 0.0 | /pat1/apps/normarray/detail/swap/ |
| <i>fsld031a</i> | 0.58653 | 0.00050 | detailed | square | base detailed model, Gap -> redwood | 28.8 | /pat1/apps/normarray/detail/swap/ |
| <i>fsld031b</i> | 0.57760 | 0.00053 | detailed | square | fsld031a with copper -> redwood | 28.8 | /pat1/apps/normarray/detail/swap/ |
| <i>fsld031c</i> | 0.57512 | 0.00056 | detailed | square | fsld031b with aluminum -> redwood | 28.8 | /pat1/apps/normarray/detail/swap/ |
| <i>fsld031d</i> | 0.62750 | 0.00050 | detailed | square | fsld031c with redwood -> water | 28.8 | /pat1/apps/normarray/detail/swap/ |
| <i>fslw001</i> | 0.64556 | 0.00050 | simplified | square | base simplified model | 0 | /pat1/apps/normarray/square/wood/ |
| <i>fslw002</i> | 0.64345 | 0.00049 | simplified | square | base simplified model | 0.013 | /pat1/apps/normarray/square/wood/ |
| <i>fslw003</i> | 0.64008 | 0.00050 | simplified | square | base simplified model | 0.027 | /pat1/apps/normarray/square/wood/ |
| <i>fslw004</i> | 0.63367 | 0.00050 | simplified | square | base simplified model | 0.070 | /pat1/apps/normarray/square/wood/ |
| <i>fslw005</i> | 0.62197 | 0.00049 | simplified | square | base simplified model | 0.15 | /pat1/apps/normarray/square/wood/ |
| <i>fslw006</i> | 0.60997 | 0.00049 | simplified | square | base simplified model | 0.24 | /pat1/apps/normarray/square/wood/ |

Table 6-16. Tabulation of Calculations Supporting the Analysis of Arrays of Undamaged Packages

| Case Name | k_{eff} | σ | Package Model Type | Array Type | Description | H/Pu | Location |
|----------------|-----------|----------|--------------------|------------|-----------------------|------|-----------------------------------|
| <i>fslw007</i> | 0.59731 | 0.00050 | simplified | square | base simplified model | 0.33 | /pat1/apps/normarray/square/wood/ |
| <i>fslw008</i> | 0.58659 | 0.00050 | simplified | square | base simplified model | 0.45 | /pat1/apps/normarray/square/wood/ |
| <i>fslw009</i> | 0.57517 | 0.00050 | simplified | square | base simplified model | 0.57 | /pat1/apps/normarray/square/wood/ |
| <i>fslw010</i> | 0.56406 | 0.00050 | simplified | square | base simplified model | 0.72 | /pat1/apps/normarray/square/wood/ |
| <i>fslw011</i> | 0.55274 | 0.00050 | simplified | square | base simplified model | 0.89 | /pat1/apps/normarray/square/wood/ |
| <i>fslw012</i> | 0.54323 | 0.00048 | simplified | square | base simplified model | 1.09 | /pat1/apps/normarray/square/wood/ |
| <i>fslw013</i> | 0.53268 | 0.00050 | simplified | square | base simplified model | 1.34 | /pat1/apps/normarray/square/wood/ |
| <i>fslw014</i> | 0.52321 | 0.00049 | simplified | square | base simplified model | 1.63 | /pat1/apps/normarray/square/wood/ |
| <i>fslw015</i> | 0.51526 | 0.00049 | simplified | square | base simplified model | 2.00 | /pat1/apps/normarray/square/wood/ |
| <i>fslw016</i> | 0.50857 | 0.00050 | simplified | square | base simplified model | 2.48 | /pat1/apps/normarray/square/wood/ |
| <i>fslw017</i> | 0.50236 | 0.00050 | simplified | square | base simplified model | 3.12 | /pat1/apps/normarray/square/wood/ |
| <i>fslw018</i> | 0.49835 | 0.00050 | simplified | square | base simplified model | 4.01 | /pat1/apps/normarray/square/wood/ |
| <i>fslw019</i> | 0.49909 | 0.00046 | simplified | square | base simplified model | 5.34 | /pat1/apps/normarray/square/wood/ |
| <i>fslw020</i> | 0.50414 | 0.00049 | simplified | square | base simplified model | 7.57 | /pat1/apps/normarray/square/wood/ |
| <i>fslw021</i> | 0.51817 | 0.00049 | simplified | square | base simplified model | 12.0 | /pat1/apps/normarray/square/wood/ |
| <i>fslw022</i> | 0.51808 | 0.00049 | simplified | square | base simplified model | 12.1 | /pat1/apps/normarray/square/wood/ |
| <i>fslw023</i> | 0.46952 | 0.00050 | simplified | square | base simplified model | 5.34 | /pat1/apps/normarray/square/wood/ |
| <i>fslw024</i> | 0.48411 | 0.00050 | simplified | square | base simplified model | 7.57 | /pat1/apps/normarray/square/wood/ |
| <i>fslw025</i> | 0.51041 | 0.00050 | simplified | square | base simplified model | 12.0 | /pat1/apps/normarray/square/wood/ |
| <i>fslw026</i> | 0.51930 | 0.00049 | simplified | square | base simplified model | 13.5 | /pat1/apps/normarray/square/wood/ |
| <i>fslw027</i> | 0.52770 | 0.00050 | simplified | square | base simplified model | 15.4 | /pat1/apps/normarray/square/wood/ |
| <i>fslw028</i> | 0.53726 | 0.00049 | simplified | square | base simplified model | 17.7 | /pat1/apps/normarray/square/wood/ |
| <i>fslw029</i> | 0.55000 | 0.00051 | simplified | square | base simplified model | 20.9 | /pat1/apps/normarray/square/wood/ |
| <i>fslw030</i> | 0.55945 | 0.00049 | simplified | square | base simplified model | 25.4 | /pat1/apps/normarray/square/wood/ |
| <i>fslw031</i> | 0.56510 | 0.00052 | simplified | square | base simplified model | 28.8 | /pat1/apps/normarray/square/wood/ |
| <i>fslw032</i> | 0.55740 | 0.00051 | simplified | square | base simplified model | 32.0 | /pat1/apps/normarray/square/wood/ |

Table 6-16. Tabulation of Calculations Supporting the Analysis of Arrays of Undamaged Packages

| Case Name | k_{eff} | σ | Package Model Type | Array Type | Description | H/Pu | Location |
|-----------------|-----------|----------|--------------------|------------|-----------------------|-------|------------------------------------|
| <i>fslw033</i> | 0.54891 | 0.00051 | simplified | square | base simplified model | 36.8 | /pat1/apps/normarray/square/wood/ |
| <i>fslw034</i> | 0.53927 | 0.00050 | simplified | square | base simplified model | 43.2 | /pat1/apps/normarray/square/wood/ |
| <i>fslw035</i> | 0.52975 | 0.00050 | simplified | square | base simplified model | 52.1 | /pat1/apps/normarray/square/wood/ |
| <i>fslw036</i> | 0.51761 | 0.00050 | simplified | square | base simplified model | 65.4 | /pat1/apps/normarray/square/wood/ |
| <i>fslw037</i> | 0.50314 | 0.00049 | simplified | square | base simplified model | 87.7 | /pat1/apps/normarray/square/wood/ |
| <i>fslw038</i> | 0.48423 | 0.00051 | simplified | square | base simplified model | 132.2 | /pat1/apps/normarray/square/wood/ |
| <i>fslw+001</i> | 0.64568 | 0.00050 | simplified | square | 120% redwood density | 0 | /pat1/apps/normarray/square/wood+/ |
| <i>fslw+002</i> | 0.64401 | 0.00050 | simplified | square | 120% redwood density | 0.013 | /pat1/apps/normarray/square/wood+/ |
| <i>fslw+003</i> | 0.64154 | 0.00050 | simplified | square | 120% redwood density | 0.027 | /pat1/apps/normarray/square/wood+/ |
| <i>fslw+004</i> | 0.63415 | 0.00049 | simplified | square | 120% redwood density | 0.070 | /pat1/apps/normarray/square/wood+/ |
| <i>fslw+005</i> | 0.62300 | 0.00050 | simplified | square | 120% redwood density | 0.15 | /pat1/apps/normarray/square/wood+/ |
| <i>fslw+006</i> | 0.61131 | 0.00049 | simplified | square | 120% redwood density | 0.24 | /pat1/apps/normarray/square/wood+/ |
| <i>fslw+007</i> | 0.59906 | 0.00049 | simplified | square | 120% redwood density | 0.33 | /pat1/apps/normarray/square/wood+/ |
| <i>fslw+008</i> | 0.58795 | 0.00049 | simplified | square | 120% redwood density | 0.45 | /pat1/apps/normarray/square/wood+/ |
| <i>fslw+009</i> | 0.57705 | 0.00049 | simplified | square | 120% redwood density | 0.57 | /pat1/apps/normarray/square/wood+/ |
| <i>fslw+010</i> | 0.56459 | 0.00049 | simplified | square | 120% redwood density | 0.72 | /pat1/apps/normarray/square/wood+/ |
| <i>fslw+011</i> | 0.55413 | 0.00048 | simplified | square | 120% redwood density | 0.89 | /pat1/apps/normarray/square/wood+/ |
| <i>fslw+012</i> | 0.54491 | 0.00045 | simplified | square | 120% redwood density | 1.09 | /pat1/apps/normarray/square/wood+/ |
| <i>fslw+013</i> | 0.53489 | 0.00050 | simplified | square | 120% redwood density | 1.34 | /pat1/apps/normarray/square/wood+/ |
| <i>fslw+014</i> | 0.52548 | 0.00048 | simplified | square | 120% redwood density | 1.63 | /pat1/apps/normarray/square/wood+/ |
| <i>fslw+015</i> | 0.51717 | 0.00050 | simplified | square | 120% redwood density | 2.00 | /pat1/apps/normarray/square/wood+/ |
| <i>fslw+016</i> | 0.51105 | 0.00049 | simplified | square | 120% redwood density | 2.48 | /pat1/apps/normarray/square/wood+/ |
| <i>fslw+017</i> | 0.50560 | 0.00050 | simplified | square | 120% redwood density | 3.12 | /pat1/apps/normarray/square/wood+/ |
| <i>fslw+018</i> | 0.50222 | 0.00047 | simplified | square | 120% redwood density | 4.01 | /pat1/apps/normarray/square/wood+/ |
| <i>fslw+019</i> | 0.50263 | 0.00049 | simplified | square | 120% redwood density | 5.34 | /pat1/apps/normarray/square/wood+/ |
| <i>fslw+020</i> | 0.50756 | 0.00050 | simplified | square | 120% redwood density | 7.57 | /pat1/apps/normarray/square/wood+/ |

Table 6-16. Tabulation of Calculations Supporting the Analysis of Arrays of Undamaged Packages

| Case Name | k_{eff} | σ | Package Model Type | Array Type | Description | H/Pu | Location |
|-----------------|-----------|----------|--------------------|------------|----------------------|-------|---|
| <i>fslw+021</i> | 0.52384 | 0.00050 | simplified | square | 120% redwood density | 12.0 | /pat1/apps/normarray/square/wood+/ . |
| <i>fslw+022</i> | 0.52420 | 0.00048 | simplified | square | 120% redwood density | 12.1 | /pat1/apps/normarray/square/wood+/ . |
| <i>fslw+023</i> | 0.47407 | 0.00050 | simplified | square | 120% redwood density | 5.34 | /pat1/apps/normarray/square/wood+/ . |
| <i>fslw+024</i> | 0.48817 | 0.00050 | simplified | square | 120% redwood density | 7.57 | /pat1/apps/normarray/square/wood+/ . |
| <i>fslw+025</i> | 0.51666 | 0.00049 | simplified | square | 120% redwood density | 12.0 | /pat1/apps/normarray/square/wood+/ . |
| <i>fslw+026</i> | 0.52504 | 0.00049 | simplified | square | 120% redwood density | 13.5 | /pat1/apps/normarray/square/wood+/ . |
| <i>fslw+027</i> | 0.53514 | 0.00049 | simplified | square | 120% redwood density | 15.4 | /pat1/apps/normarray/square/wood+/ . |
| <i>fslw+028</i> | 0.54560 | 0.00050 | simplified | square | 120% redwood density | 17.7 | /pat1/apps/normarray/square/wood+/ . |
| <i>fslw+029</i> | 0.55633 | 0.00049 | simplified | square | 120% redwood density | 20.9 | /pat1/apps/normarray/square/wood+/ . |
| <i>fslw+030</i> | 0.56867 | 0.00050 | simplified | square | 120% redwood density | 25.4 | /pat1/apps/normarray/square/wood+/ . |
| <i>fslw+031</i> | 0.57535 | 0.00050 | simplified | square | 120% redwood density | 28.8 | /pat1/apps/normarray/square/wood+/ . |
| <i>fslw+032</i> | 0.56751 | 0.00050 | simplified | square | 120% redwood density | 32.0 | /pat1/apps/normarray/square/wood+/ . |
| <i>fslw+033</i> | 0.55898 | 0.00049 | simplified | square | 120% redwood density | 36.8 | /pat1/apps/normarray/square/wood+/ . |
| <i>fslw+034</i> | 0.54947 | 0.00050 | simplified | square | 120% redwood density | 43.2 | /pat1/apps/normarray/square/wood+/ . |
| <i>fslw+035</i> | 0.53894 | 0.00052 | simplified | square | 120% redwood density | 52.1 | /pat1/apps/normarray/square/wood+/ . |
| <i>fslw+036</i> | 0.52669 | 0.00050 | simplified | square | 120% redwood density | 65.4 | /pat1/apps/normarray/square/wood+/ . |
| <i>fslw+037</i> | 0.51434 | 0.00049 | simplified | square | 120% redwood density | 87.7 | /pat1/apps/normarray/square/wood+/ . |
| <i>fslw+038</i> | 0.49369 | 0.00050 | simplified | square | 120% redwood density | 132.2 | /pat1/apps/normarray/square/wood+/ . |
| <i>fslw-001</i> | 0.64322 | 0.00049 | simplified | square | 80% redwood density | 0 | /pat1/apps/normarray/square/wood-/ . |
| <i>fslw-002</i> | 0.64209 | 0.00049 | simplified | square | 80% redwood density | 0.013 | /pat1/apps/normarray/square/wood-/ . |
| <i>fslw-003</i> | 0.63918 | 0.00049 | simplified | square | 80% redwood density | 0.027 | /pat1/apps/normarray/square/wood-/ . |
| <i>fslw-004</i> | 0.63135 | 0.00049 | simplified | square | 80% redwood density | 0.070 | /pat1/apps/normarray/square/wood-/ . |
| <i>fslw-005</i> | 0.62016 | 0.00049 | simplified | square | 80% redwood density | 0.15 | /pat1/apps/normarray/square/wood-/ . |
| <i>fslw-006</i> | 0.60936 | 0.00051 | simplified | square | 80% redwood density | 0.24 | /pat1/apps/normarray/square/wood-/ . |
| <i>fslw-007</i> | 0.59841 | 0.00050 | simplified | square | 80% redwood density | 0.33 | /pat1/apps/normarray/square/wood-/ . |
| <i>fslw-008</i> | 0.58495 | 0.00049 | simplified | square | 80% redwood density | 0.45 | /pat1/apps/normarray/square/wood-/ . |

Table 6-16. Tabulation of Calculations Supporting the Analysis of Arrays of Undamaged Packages

| Case Name | k_{eff} | σ | Package Model Type | Array Type | Description | H/Pu | Location |
|-----------------|-----------|----------|--------------------|------------|---------------------|------|------------------------------------|
| <i>fslw-009</i> | 0.57363 | 0.00049 | simplified | square | 80% redwood density | 0.57 | /pat1/apps/normarray/square/wood-/ |
| <i>fslw-010</i> | 0.56234 | 0.00047 | simplified | square | 80% redwood density | 0.72 | /pat1/apps/normarray/square/wood-/ |
| <i>fslw-011</i> | 0.55087 | 0.00049 | simplified | square | 80% redwood density | 0.89 | /pat1/apps/normarray/square/wood-/ |
| <i>fslw-012</i> | 0.54208 | 0.00049 | simplified | square | 80% redwood density | 1.09 | /pat1/apps/normarray/square/wood-/ |
| <i>fslw-013</i> | 0.53233 | 0.00047 | simplified | square | 80% redwood density | 1.34 | /pat1/apps/normarray/square/wood-/ |
| <i>fslw-014</i> | 0.52107 | 0.00049 | simplified | square | 80% redwood density | 1.63 | /pat1/apps/normarray/square/wood-/ |
| <i>fslw-015</i> | 0.51317 | 0.00048 | simplified | square | 80% redwood density | 2.00 | /pat1/apps/normarray/square/wood-/ |
| <i>fslw-016</i> | 0.50645 | 0.00049 | simplified | square | 80% redwood density | 2.48 | /pat1/apps/normarray/square/wood-/ |
| <i>fslw-017</i> | 0.49987 | 0.00049 | simplified | square | 80% redwood density | 3.12 | /pat1/apps/normarray/square/wood-/ |
| <i>fslw-018</i> | 0.49590 | 0.00049 | simplified | square | 80% redwood density | 4.01 | /pat1/apps/normarray/square/wood-/ |
| <i>fslw-019</i> | 0.49662 | 0.00049 | simplified | square | 80% redwood density | 5.34 | /pat1/apps/normarray/square/wood-/ |
| <i>fslw-020</i> | 0.49943 | 0.00049 | simplified | square | 80% redwood density | 7.57 | /pat1/apps/normarray/square/wood-/ |
| <i>fslw-021</i> | 0.51299 | 0.00049 | simplified | square | 80% redwood density | 12.0 | /pat1/apps/normarray/square/wood-/ |
| <i>fslw-022</i> | 0.51393 | 0.00049 | simplified | square | 80% redwood density | 12.1 | /pat1/apps/normarray/square/wood-/ |
| <i>fslw-023</i> | 0.46574 | 0.00049 | simplified | square | 80% redwood density | 5.34 | /pat1/apps/normarray/square/wood-/ |
| <i>fslw-024</i> | 0.47934 | 0.00049 | simplified | square | 80% redwood density | 7.57 | /pat1/apps/normarray/square/wood-/ |
| <i>fslw-025</i> | 0.50573 | 0.00049 | simplified | square | 80% redwood density | 12.0 | /pat1/apps/normarray/square/wood-/ |
| <i>fslw-026</i> | 0.51249 | 0.00049 | simplified | square | 80% redwood density | 13.5 | /pat1/apps/normarray/square/wood-/ |
| <i>fslw-027</i> | 0.52155 | 0.00050 | simplified | square | 80% redwood density | 15.4 | /pat1/apps/normarray/square/wood-/ |
| <i>fslw-028</i> | 0.53176 | 0.00049 | simplified | square | 80% redwood density | 17.7 | /pat1/apps/normarray/square/wood-/ |
| <i>fslw-029</i> | 0.54201 | 0.00051 | simplified | square | 80% redwood density | 20.9 | /pat1/apps/normarray/square/wood-/ |
| <i>fslw-030</i> | 0.55290 | 0.00050 | simplified | square | 80% redwood density | 25.4 | /pat1/apps/normarray/square/wood-/ |
| <i>fslw-031</i> | 0.55812 | 0.00050 | simplified | square | 80% redwood density | 28.8 | /pat1/apps/normarray/square/wood-/ |
| <i>fslw-032</i> | 0.55161 | 0.00050 | simplified | square | 80% redwood density | 32.0 | /pat1/apps/normarray/square/wood-/ |
| <i>fslw-033</i> | 0.54153 | 0.00051 | simplified | square | 80% redwood density | 36.8 | /pat1/apps/normarray/square/wood-/ |
| <i>fslw-034</i> | 0.53183 | 0.00051 | simplified | square | 80% redwood density | 43.2 | /pat1/apps/normarray/square/wood-/ |

Table 6-16. Tabulation of Calculations Supporting the Analysis of Arrays of Undamaged Packages

| Case Name | k_{eff} | σ | Package Model Type | Array Type | Description | H/Pu | Location |
|-----------------|-----------|----------|--------------------|------------|---------------------------------|-------|------------------------------------|
| <i>fwlw-035</i> | 0.52267 | 0.00049 | simplified | square | 80% redwood density | 52.1 | /pat1/apps/normarray/square/wood-/ |
| <i>fwlw-036</i> | 0.51073 | 0.00050 | simplified | square | 80% redwood density | 65.4 | /pat1/apps/normarray/square/wood-/ |
| <i>fwlw-037</i> | 0.49751 | 0.00050 | simplified | square | 80% redwood density | 87.7 | /pat1/apps/normarray/square/wood-/ |
| <i>fwlw-038</i> | 0.47683 | 0.00050 | simplified | square | 80% redwood density | 132.2 | /pat1/apps/normarray/square/wood-/ |
| <i>fwlsf001</i> | 0.65043 | 0.00049 | simplified | square | redwood -> water, steel modeled | 0 | /pat1/apps/normarray/square/water/ |
| <i>fwlsf002</i> | 0.64824 | 0.00049 | simplified | square | redwood -> water, steel modeled | 0.013 | /pat1/apps/normarray/square/water/ |
| <i>fwlsf003</i> | 0.64602 | 0.00050 | simplified | square | redwood -> water, steel modeled | 0.027 | /pat1/apps/normarray/square/water/ |
| <i>fwlsf004</i> | 0.63965 | 0.00049 | simplified | square | redwood -> water, steel modeled | 0.070 | /pat1/apps/normarray/square/water/ |
| <i>fwlsf005</i> | 0.62794 | 0.00050 | simplified | square | redwood -> water, steel modeled | 0.15 | /pat1/apps/normarray/square/water/ |
| <i>fwlsf006</i> | 0.61670 | 0.00050 | simplified | square | redwood -> water, steel modeled | 0.24 | /pat1/apps/normarray/square/water/ |
| <i>fwlsf007</i> | 0.60480 | 0.00050 | simplified | square | redwood -> water, steel modeled | 0.33 | /pat1/apps/normarray/square/water/ |
| <i>fwlsf008</i> | 0.59330 | 0.00049 | simplified | square | redwood -> water, steel modeled | 0.45 | /pat1/apps/normarray/square/water/ |
| <i>fwlsf009</i> | 0.58317 | 0.00049 | simplified | square | redwood -> water, steel modeled | 0.57 | /pat1/apps/normarray/square/water/ |
| <i>fwlsf010</i> | 0.57226 | 0.00050 | simplified | square | redwood -> water, steel modeled | 0.72 | /pat1/apps/normarray/square/water/ |
| <i>fwlsf011</i> | 0.56133 | 0.00050 | simplified | square | redwood -> water, steel modeled | 0.89 | /pat1/apps/normarray/square/water/ |
| <i>fwlsf012</i> | 0.55309 | 0.00050 | simplified | square | redwood -> water, steel modeled | 1.09 | /pat1/apps/normarray/square/water/ |
| <i>fwlsf013</i> | 0.54294 | 0.00050 | simplified | square | redwood -> water, steel modeled | 1.34 | /pat1/apps/normarray/square/water/ |
| <i>fwlsf014</i> | 0.53598 | 0.00050 | simplified | square | redwood -> water, steel modeled | 1.63 | /pat1/apps/normarray/square/water/ |
| <i>fwlsf015</i> | 0.52848 | 0.00050 | simplified | square | redwood -> water, steel modeled | 2.00 | /pat1/apps/normarray/square/water/ |
| <i>fwlsf016</i> | 0.52345 | 0.00049 | simplified | square | redwood -> water, steel modeled | 2.48 | /pat1/apps/normarray/square/water/ |
| <i>fwlsf017</i> | 0.51828 | 0.00050 | simplified | square | redwood -> water, steel modeled | 3.12 | /pat1/apps/normarray/square/water/ |
| <i>fwlsf018</i> | 0.51784 | 0.00049 | simplified | square | redwood -> water, steel modeled | 4.01 | /pat1/apps/normarray/square/water/ |
| <i>fwlsf019</i> | 0.52162 | 0.00049 | simplified | square | redwood -> water, steel modeled | 5.34 | /pat1/apps/normarray/square/water/ |
| <i>fwlsf020</i> | 0.53219 | 0.00050 | simplified | square | redwood -> water, steel modeled | 7.57 | /pat1/apps/normarray/square/water/ |
| <i>fwlsf021</i> | 0.55776 | 0.00049 | simplified | square | redwood -> water, steel modeled | 12.0 | /pat1/apps/normarray/square/water/ |
| <i>fwlsf022</i> | 0.56011 | 0.00050 | simplified | square | redwood -> water, steel modeled | 12.1 | /pat1/apps/normarray/square/water/ |

Table 6-16. Tabulation of Calculations Supporting the Analysis of Arrays of Undamaged Packages

| Case Name | k_{eff} | σ | Package Model Type | Array Type | Description | H/Pu | Location |
|-----------------------------|-----------|----------|--------------------|------------|---------------------------------|-------|------------------------------------|
| <i>fslsf023</i> | 0.50415 | 0.00050 | simplified | square | redwood -> water, steel modeled | 5.34 | /pat1/apps/normarray/square/water/ |
| <i>fslsf024</i> | 0.52298 | 0.00050 | simplified | square | redwood -> water, steel modeled | 7.57 | /pat1/apps/normarray/square/water/ |
| <i>fslsf025</i> | 0.55762 | 0.00049 | simplified | square | redwood -> water, steel modeled | 12.0 | /pat1/apps/normarray/square/water/ |
| <i>fslsf026</i> | 0.56821 | 0.00050 | simplified | square | redwood -> water, steel modeled | 13.5 | /pat1/apps/normarray/square/water/ |
| <i>fslsf027</i> | 0.58015 | 0.00049 | simplified | square | redwood -> water, steel modeled | 15.4 | /pat1/apps/normarray/square/water/ |
| <i>fslsf028</i> | 0.59283 | 0.00050 | simplified | square | redwood -> water, steel modeled | 17.7 | /pat1/apps/normarray/square/water/ |
| <i>fslsf029</i> | 0.60854 | 0.00053 | simplified | square | redwood -> water, steel modeled | 20.9 | /pat1/apps/normarray/square/water/ |
| <i>fslsf030</i> | 0.62355 | 0.00049 | simplified | square | redwood -> water, steel modeled | 25.4 | /pat1/apps/normarray/square/water/ |
| <i>fslsf031^a</i> | 0.63371 | 0.00050 | simplified | square | redwood -> water, steel modeled | 28.8 | /pat1/apps/normarray/square/water/ |
| <i>fslsf032</i> | 0.62580 | 0.00050 | simplified | square | redwood -> water, steel modeled | 32.0 | /pat1/apps/normarray/square/water/ |
| <i>fslsf033</i> | 0.61719 | 0.00049 | simplified | square | redwood -> water, steel modeled | 36.8 | /pat1/apps/normarray/square/water/ |
| <i>fslsf034</i> | 0.60732 | 0.00050 | simplified | square | redwood -> water, steel modeled | 43.2 | /pat1/apps/normarray/square/water/ |
| <i>fslsf035</i> | 0.59799 | 0.00055 | simplified | square | redwood -> water, steel modeled | 52.1 | /pat1/apps/normarray/square/water/ |
| <i>fslsf036</i> | 0.58499 | 0.00050 | simplified | square | redwood -> water, steel modeled | 65.4 | /pat1/apps/normarray/square/water/ |
| <i>fslsf037</i> | 0.56893 | 0.00053 | simplified | square | redwood -> water, steel modeled | 87.7 | /pat1/apps/normarray/square/water/ |
| <i>fslsf038</i> | 0.54583 | 0.00050 | simplified | square | redwood -> water, steel modeled | 132.2 | /pat1/apps/normarray/square/water/ |
| <i>fhlsf001</i> | 0.64477 | 0.00046 | simplified | hexagonal | base simplified model | 0 | /pat1/apps/normarray/hex/wood/ |
| <i>fhlsf002</i> | 0.64302 | 0.00050 | simplified | hexagonal | base simplified model | 0.013 | /pat1/apps/normarray/hex/wood/ |
| <i>fhlsf003</i> | 0.64060 | 0.00049 | simplified | hexagonal | base simplified model | 0.027 | /pat1/apps/normarray/hex/wood/ |
| <i>fhlsf004</i> | 0.63350 | 0.00049 | simplified | hexagonal | base simplified model | 0.070 | /pat1/apps/normarray/hex/wood/ |
| <i>fhlsf005</i> | 0.62093 | 0.00049 | simplified | hexagonal | base simplified model | 0.15 | /pat1/apps/normarray/hex/wood/ |
| <i>fhlsf006</i> | 0.61030 | 0.00050 | simplified | hexagonal | base simplified model | 0.24 | /pat1/apps/normarray/hex/wood/ |
| <i>fhlsf007</i> | 0.59855 | 0.00050 | simplified | hexagonal | base simplified model | 0.33 | /pat1/apps/normarray/hex/wood/ |
| <i>fhlsf008</i> | 0.58671 | 0.00049 | simplified | hexagonal | base simplified model | 0.45 | /pat1/apps/normarray/hex/wood/ |
| <i>fhlsf009</i> | 0.57560 | 0.00049 | simplified | hexagonal | base simplified model | 0.57 | /pat1/apps/normarray/hex/wood/ |
| <i>fhlsf010</i> | 0.56323 | 0.00049 | simplified | hexagonal | base simplified model | 0.72 | /pat1/apps/normarray/hex/wood/ |

Table 6-16. Tabulation of Calculations Supporting the Analysis of Arrays of Undamaged Packages

| Case Name | k_{eff} | σ | Package Model Type | Array Type | Description | H/Pu | Location |
|-----------|-----------|----------|--------------------|------------|-----------------------|------|--------------------------------|
| fhlsf011 | 0.55382 | 0.00049 | simplified | hexagonal | base simplified model | 0.89 | /pat1/apps/normarray/hex/wood/ |
| fhlsf012 | 0.54309 | 0.00050 | simplified | hexagonal | base simplified model | 1.09 | /pat1/apps/normarray/hex/wood/ |
| fhlsf013 | 0.53321 | 0.00049 | simplified | hexagonal | base simplified model | 1.34 | /pat1/apps/normarray/hex/wood/ |
| fhlsf014 | 0.52341 | 0.00046 | simplified | hexagonal | base simplified model | 1.63 | /pat1/apps/normarray/hex/wood/ |
| fhlsf015 | 0.51540 | 0.00049 | simplified | hexagonal | base simplified model | 2.00 | /pat1/apps/normarray/hex/wood/ |
| fhlsf016 | 0.50797 | 0.00049 | simplified | hexagonal | base simplified model | 2.48 | /pat1/apps/normarray/hex/wood/ |
| fhlsf017 | 0.50226 | 0.00050 | simplified | hexagonal | base simplified model | 3.12 | /pat1/apps/normarray/hex/wood/ |
| fhlsf018 | 0.49941 | 0.00049 | simplified | hexagonal | base simplified model | 4.01 | /pat1/apps/normarray/hex/wood/ |
| fhlsf019 | 0.49842 | 0.00050 | simplified | hexagonal | base simplified model | 5.34 | /pat1/apps/normarray/hex/wood/ |
| fhlsf020 | 0.50482 | 0.00049 | simplified | hexagonal | base simplified model | 7.57 | /pat1/apps/normarray/hex/wood/ |
| fhlsf021 | 0.51877 | 0.00049 | simplified | hexagonal | base simplified model | 12.0 | /pat1/apps/normarray/hex/wood/ |
| fhlsf022 | 0.51934 | 0.00050 | simplified | hexagonal | base simplified model | 12.1 | /pat1/apps/normarray/hex/wood/ |
| fhlsf023 | 0.46992 | 0.00049 | simplified | hexagonal | base simplified model | 5.34 | /pat1/apps/normarray/hex/wood/ |
| fhlsf024 | 0.48301 | 0.00050 | simplified | hexagonal | base simplified model | 7.57 | /pat1/apps/normarray/hex/wood/ |
| fhlsf025 | 0.51101 | 0.00050 | simplified | hexagonal | base simplified model | 12.0 | /pat1/apps/normarray/hex/wood/ |
| fhlsf026 | 0.51898 | 0.00047 | simplified | hexagonal | base simplified model | 13.5 | /pat1/apps/normarray/hex/wood/ |
| fhlsf027 | 0.52944 | 0.00049 | simplified | hexagonal | base simplified model | 15.4 | /pat1/apps/normarray/hex/wood/ |
| fhlsf028 | 0.53935 | 0.00049 | simplified | hexagonal | base simplified model | 17.7 | /pat1/apps/normarray/hex/wood/ |
| fhlsf029 | 0.55131 | 0.00049 | simplified | hexagonal | base simplified model | 20.9 | /pat1/apps/normarray/hex/wood/ |
| fhlsf030 | 0.56197 | 0.00049 | simplified | hexagonal | base simplified model | 25.4 | /pat1/apps/normarray/hex/wood/ |
| fhlsf031 | 0.56731 | 0.00049 | simplified | hexagonal | base simplified model | 28.8 | /pat1/apps/normarray/hex/wood/ |
| fhlsf032 | 0.55967 | 0.00050 | simplified | hexagonal | base simplified model | 32.0 | /pat1/apps/normarray/hex/wood/ |
| fhlsf033 | 0.55178 | 0.00049 | simplified | hexagonal | base simplified model | 36.8 | /pat1/apps/normarray/hex/wood/ |
| fhlsf034 | 0.54092 | 0.00050 | simplified | hexagonal | base simplified model | 43.2 | /pat1/apps/normarray/hex/wood/ |
| fhlsf035 | 0.53123 | 0.00049 | simplified | hexagonal | base simplified model | 52.1 | /pat1/apps/normarray/hex/wood/ |
| fhlsf036 | 0.51910 | 0.00050 | simplified | hexagonal | base simplified model | 65.4 | /pat1/apps/normarray/hex/wood/ |

Table 6-16. Tabulation of Calculations Supporting the Analysis of Arrays of Undamaged Packages

| Case Name | k_{eff} | σ | Package Model Type | Array Type | Description | H/Pu | Location |
|-------------------|-----------|----------|--------------------|------------|-----------------------|-------|---------------------------------|
| <i>fhlsf037</i> | 0.50549 | 0.00050 | simplified | hexagonal | base simplified model | 87.7 | /pat1/apps/normarray/hex/wood/ |
| <i>fhlsf038</i> | 0.48705 | 0.00049 | simplified | hexagonal | base simplified model | 132.2 | /pat1/apps/normarray/hex/wood/ |
| <i>fhlsf001</i> | 0.64580 | 0.00050 | simplified | hexagonal | 120% redwood density | 0 | /pat1/apps/normarray/hex/woodp/ |
| <i>fhlsf002</i> | 0.64354 | 0.00049 | simplified | hexagonal | 120% redwood density | 0.013 | /pat1/apps/normarray/hex/woodp/ |
| <i>fhlsf003</i> | 0.64179 | 0.00049 | simplified | hexagonal | 120% redwood density | 0.027 | /pat1/apps/normarray/hex/woodp/ |
| <i>fhlsf004</i> | 0.63556 | 0.00050 | simplified | hexagonal | 120% redwood density | 0.070 | /pat1/apps/normarray/hex/woodp/ |
| <i>fhlsf005</i> | 0.62339 | 0.00049 | simplified | hexagonal | 120% redwood density | 0.15 | /pat1/apps/normarray/hex/woodp/ |
| <i>fhlsf006</i> | 0.61212 | 0.00049 | simplified | hexagonal | 120% redwood density | 0.24 | /pat1/apps/normarray/hex/woodp/ |
| <i>fhlsf007</i> | 0.59963 | 0.00050 | simplified | hexagonal | 120% redwood density | 0.33 | /pat1/apps/normarray/hex/woodp/ |
| <i>fhlsf008</i> | 0.58871 | 0.00048 | simplified | hexagonal | 120% redwood density | 0.45 | /pat1/apps/normarray/hex/woodp/ |
| <i>fhlsf009</i> | 0.57679 | 0.00050 | simplified | hexagonal | 120% redwood density | 0.57 | /pat1/apps/normarray/hex/woodp/ |
| <i>fhlsf010</i> | 0.56523 | 0.00050 | simplified | hexagonal | 120% redwood density | 0.72 | /pat1/apps/normarray/hex/woodp/ |
| <i>fhlsf011</i> | 0.55469 | 0.00050 | simplified | hexagonal | 120% redwood density | 0.89 | /pat1/apps/normarray/hex/woodp/ |
| <i>fhlsf012</i> | 0.54377 | 0.00049 | simplified | hexagonal | 120% redwood density | 1.09 | /pat1/apps/normarray/hex/woodp/ |
| <i>fhlsf013</i> | 0.53468 | 0.00049 | simplified | hexagonal | 120% redwood density | 1.34 | /pat1/apps/normarray/hex/woodp/ |
| <i>fhlsf014</i> | 0.52574 | 0.00049 | simplified | hexagonal | 120% redwood density | 1.63 | /pat1/apps/normarray/hex/woodp/ |
| <i>fhlsf015</i> | 0.51752 | 0.00050 | simplified | hexagonal | 120% redwood density | 2.00 | /pat1/apps/normarray/hex/woodp/ |
| <i>fhlsf016</i> | 0.51053 | 0.00050 | simplified | hexagonal | 120% redwood density | 2.48 | /pat1/apps/normarray/hex/woodp/ |
| <i>fhlsf017r1</i> | 0.50524 | 0.00049 | simplified | hexagonal | 120% redwood density | 3.12 | /pat1/apps/normarray/hex/woodp/ |
| <i>fhlsf018</i> | 0.50272 | 0.00050 | simplified | hexagonal | 120% redwood density | 4.01 | /pat1/apps/normarray/hex/woodp/ |
| <i>fhlsf019</i> | 0.50388 | 0.00050 | simplified | hexagonal | 120% redwood density | 5.34 | /pat1/apps/normarray/hex/woodp/ |
| <i>fhlsf020</i> | 0.50898 | 0.00048 | simplified | hexagonal | 120% redwood density | 7.57 | /pat1/apps/normarray/hex/woodp/ |
| <i>fhlsf021</i> | 0.52383 | 0.00049 | simplified | hexagonal | 120% redwood density | 12.0 | /pat1/apps/normarray/hex/woodp/ |
| <i>fhlsf022</i> | 0.52515 | 0.00050 | simplified | hexagonal | 120% redwood density | 12.1 | /pat1/apps/normarray/hex/woodp/ |
| <i>fhlsf023</i> | 0.47521 | 0.00049 | simplified | hexagonal | 120% redwood density | 5.34 | /pat1/apps/normarray/hex/woodp/ |
| <i>fhlsf024</i> | 0.48937 | 0.00050 | simplified | hexagonal | 120% redwood density | 7.57 | /pat1/apps/normarray/hex/woodp/ |

Table 6-16. Tabulation of Calculations Supporting the Analysis of Arrays of Undamaged Packages

| Case Name | k_{eff} | σ | Package Model Type | Array Type | Description | H/Pu | Location |
|-----------|-----------|----------|--------------------|------------|----------------------|-------|---------------------------------|
| fhlsf025 | 0.51784 | 0.00050 | simplified | hexagonal | 120% redwood density | 12.0 | /pat1/apps/normarray/hex/woodp/ |
| fhlsf026 | 0.52630 | 0.00050 | simplified | hexagonal | 120% redwood density | 13.5 | /pat1/apps/normarray/hex/woodp/ |
| fhlsf027 | 0.53525 | 0.00049 | simplified | hexagonal | 120% redwood density | 15.4 | /pat1/apps/normarray/hex/woodp/ |
| fhlsf028 | 0.54683 | 0.00049 | simplified | hexagonal | 120% redwood density | 17.7 | /pat1/apps/normarray/hex/woodp/ |
| fhlsf029 | 0.55869 | 0.00050 | simplified | hexagonal | 120% redwood density | 20.9 | /pat1/apps/normarray/hex/woodp/ |
| fhlsf030 | 0.56901 | 0.00049 | simplified | hexagonal | 120% redwood density | 25.4 | /pat1/apps/normarray/hex/woodp/ |
| fhlsf031 | 0.57554 | 0.00049 | simplified | hexagonal | 120% redwood density | 28.8 | /pat1/apps/normarray/hex/woodp/ |
| fhlsf032 | 0.56919 | 0.00049 | simplified | hexagonal | 120% redwood density | 32.0 | /pat1/apps/normarray/hex/woodp/ |
| fhlsf033 | 0.55945 | 0.00049 | simplified | hexagonal | 120% redwood density | 36.8 | /pat1/apps/normarray/hex/woodp/ |
| fhlsf034 | 0.55105 | 0.00050 | simplified | hexagonal | 120% redwood density | 43.2 | /pat1/apps/normarray/hex/woodp/ |
| fhlsf035 | 0.54102 | 0.00049 | simplified | hexagonal | 120% redwood density | 52.1 | /pat1/apps/normarray/hex/woodp/ |
| fhlsf036 | 0.52769 | 0.00050 | simplified | hexagonal | 120% redwood density | 65.4 | /pat1/apps/normarray/hex/woodp/ |
| fhlsf037 | 0.51388 | 0.00049 | simplified | hexagonal | 120% redwood density | 87.7 | /pat1/apps/normarray/hex/woodp/ |
| fhlsf038 | 0.49489 | 0.00048 | simplified | hexagonal | 120% redwood density | 132.2 | /pat1/apps/normarray/hex/woodp/ |
| fhlsf001 | 0.64316 | 0.00050 | simplified | hexagonal | 80% redwood density | 0 | /pat1/apps/normarray/hex/woodm/ |
| fhlsf002 | 0.64231 | 0.00050 | simplified | hexagonal | 80% redwood density | 0.013 | /pat1/apps/normarray/hex/woodm/ |
| fhlsf003 | 0.63914 | 0.00049 | simplified | hexagonal | 80% redwood density | 0.027 | /pat1/apps/normarray/hex/woodm/ |
| fhlsf004 | 0.63221 | 0.00049 | simplified | hexagonal | 80% redwood density | 0.070 | /pat1/apps/normarray/hex/woodm/ |
| fhlsf005 | 0.62042 | 0.00048 | simplified | hexagonal | 80% redwood density | 0.15 | /pat1/apps/normarray/hex/woodm/ |
| fhlsf006 | 0.60825 | 0.00049 | simplified | hexagonal | 80% redwood density | 0.24 | /pat1/apps/normarray/hex/woodm/ |
| fhlsf007 | 0.59688 | 0.00050 | simplified | hexagonal | 80% redwood density | 0.33 | /pat1/apps/normarray/hex/woodm/ |
| fhlsf008 | 0.58585 | 0.00049 | simplified | hexagonal | 80% redwood density | 0.45 | /pat1/apps/normarray/hex/woodm/ |
| fhlsf009 | 0.57398 | 0.00049 | simplified | hexagonal | 80% redwood density | 0.57 | /pat1/apps/normarray/hex/woodm/ |
| fhlsf010 | 0.56363 | 0.00050 | simplified | hexagonal | 80% redwood density | 0.72 | /pat1/apps/normarray/hex/woodm/ |
| fhlsf011 | 0.55205 | 0.00049 | simplified | hexagonal | 80% redwood density | 0.89 | /pat1/apps/normarray/hex/woodm/ |
| fhlsf012 | 0.54133 | 0.00050 | simplified | hexagonal | 80% redwood density | 1.09 | /pat1/apps/normarray/hex/woodm/ |

Table 6-16. Tabulation of Calculations Supporting the Analysis of Arrays of Undamaged Packages

| Case Name | k_{eff} | σ | Package Model Type | Array Type | Description | H/Pu | Location |
|-----------|-----------|----------|--------------------|------------|---------------------|-------|---------------------------------|
| fhlsf013 | 0.53164 | 0.00050 | simplified | hexagonal | 80% redwood density | 1.34 | /pat1/apps/normarray/hex/woodm/ |
| fhlsf014 | 0.52125 | 0.00048 | simplified | hexagonal | 80% redwood density | 1.63 | /pat1/apps/normarray/hex/woodm/ |
| fhlsf015 | 0.51309 | 0.00049 | simplified | hexagonal | 80% redwood density | 2.00 | /pat1/apps/normarray/hex/woodm/ |
| fhlsf016 | 0.50720 | 0.00050 | simplified | hexagonal | 80% redwood density | 2.48 | /pat1/apps/normarray/hex/woodm/ |
| fhlsf017 | 0.50025 | 0.00050 | simplified | hexagonal | 80% redwood density | 3.12 | /pat1/apps/normarray/hex/woodm/ |
| fhlsf018 | 0.49739 | 0.00049 | simplified | hexagonal | 80% redwood density | 4.01 | /pat1/apps/normarray/hex/woodm/ |
| fhlsf019 | 0.49650 | 0.00049 | simplified | hexagonal | 80% redwood density | 5.34 | /pat1/apps/normarray/hex/woodm/ |
| fhlsf020 | 0.50184 | 0.00048 | simplified | hexagonal | 80% redwood density | 7.57 | /pat1/apps/normarray/hex/woodm/ |
| fhlsf021 | 0.51472 | 0.00049 | simplified | hexagonal | 80% redwood density | 12.0 | /pat1/apps/normarray/hex/woodm/ |
| fhlsf022 | 0.51465 | 0.00049 | simplified | hexagonal | 80% redwood density | 12.1 | /pat1/apps/normarray/hex/woodm/ |
| fhlsf023 | 0.46681 | 0.00050 | simplified | hexagonal | 80% redwood density | 5.34 | /pat1/apps/normarray/hex/woodm/ |
| fhlsf024 | 0.47993 | 0.00048 | simplified | hexagonal | 80% redwood density | 7.57 | /pat1/apps/normarray/hex/woodm/ |
| fhlsf025 | 0.50549 | 0.00049 | simplified | hexagonal | 80% redwood density | 12.0 | /pat1/apps/normarray/hex/woodm/ |
| fhlsf026 | 0.51495 | 0.00050 | simplified | hexagonal | 80% redwood density | 13.5 | /pat1/apps/normarray/hex/woodm/ |
| fhlsf027 | 0.52304 | 0.00049 | simplified | hexagonal | 80% redwood density | 15.4 | /pat1/apps/normarray/hex/woodm/ |
| fhlsf028 | 0.53359 | 0.00050 | simplified | hexagonal | 80% redwood density | 17.7 | /pat1/apps/normarray/hex/woodm/ |
| fhlsf029 | 0.54539 | 0.00050 | simplified | hexagonal | 80% redwood density | 20.9 | /pat1/apps/normarray/hex/woodm/ |
| fhlsf030 | 0.55441 | 0.00050 | simplified | hexagonal | 80% redwood density | 25.4 | /pat1/apps/normarray/hex/woodm/ |
| fhlsf031 | 0.56076 | 0.00048 | simplified | hexagonal | 80% redwood density | 28.8 | /pat1/apps/normarray/hex/woodm/ |
| fhlsf032 | 0.55336 | 0.00048 | simplified | hexagonal | 80% redwood density | 32.0 | /pat1/apps/normarray/hex/woodm/ |
| fhlsf033 | 0.54346 | 0.00050 | simplified | hexagonal | 80% redwood density | 36.8 | /pat1/apps/normarray/hex/woodm/ |
| fhlsf034 | 0.53431 | 0.00049 | simplified | hexagonal | 80% redwood density | 43.2 | /pat1/apps/normarray/hex/woodm/ |
| fhlsf035 | 0.52422 | 0.00049 | simplified | hexagonal | 80% redwood density | 52.1 | /pat1/apps/normarray/hex/woodm/ |
| fhlsf036 | 0.51261 | 0.00049 | simplified | hexagonal | 80% redwood density | 65.4 | /pat1/apps/normarray/hex/woodm/ |
| fhlsf037 | 0.49912 | 0.00050 | simplified | hexagonal | 80% redwood density | 87.7 | /pat1/apps/normarray/hex/woodm/ |
| fhlsf038 | 0.47869 | 0.00050 | simplified | hexagonal | 80% redwood density | 132.2 | /pat1/apps/normarray/hex/woodm/ |

Table 6-16. Tabulation of Calculations Supporting the Analysis of Arrays of Undamaged Packages

| Case Name | k_{eff} | σ | Package Model Type | Array Type | Description | H/Pu | Location |
|-----------------------|-----------|----------|--------------------|------------|---------------------------------|-------|---------------------------------|
| fhlsf001 ^a | 0.65094 | 0.00049 | simplified | hexagonal | redwood -> water, steel modeled | 0 | /pat1/apps/normarray/hex/water/ |
| fhlsf002 | 0.64849 | 0.00049 | simplified | hexagonal | redwood -> water, steel modeled | 0.013 | /pat1/apps/normarray/hex/water/ |
| fhlsf003 | 0.64581 | 0.00047 | simplified | hexagonal | redwood -> water, steel modeled | 0.027 | /pat1/apps/normarray/hex/water/ |
| fhlsf004 | 0.63992 | 0.00050 | simplified | hexagonal | redwood -> water, steel modeled | 0.070 | /pat1/apps/normarray/hex/water/ |
| fhlsf005 | 0.62683 | 0.00049 | simplified | hexagonal | redwood -> water, steel modeled | 0.15 | /pat1/apps/normarray/hex/water/ |
| fhlsf006 | 0.61620 | 0.00049 | simplified | hexagonal | redwood -> water, steel modeled | 0.24 | /pat1/apps/normarray/hex/water/ |
| fhlsf007 | 0.60544 | 0.00049 | simplified | hexagonal | redwood -> water, steel modeled | 0.33 | /pat1/apps/normarray/hex/water/ |
| fhlsf008 | 0.59378 | 0.00050 | simplified | hexagonal | redwood -> water, steel modeled | 0.45 | /pat1/apps/normarray/hex/water/ |
| fhlsf009 | 0.58304 | 0.00049 | simplified | hexagonal | redwood -> water, steel modeled | 0.57 | /pat1/apps/normarray/hex/water/ |
| fhlsf010 | 0.57217 | 0.00050 | simplified | hexagonal | redwood -> water, steel modeled | 0.72 | /pat1/apps/normarray/hex/water/ |
| fhlsf011 | 0.56250 | 0.00050 | simplified | hexagonal | redwood -> water, steel modeled | 0.89 | /pat1/apps/normarray/hex/water/ |
| fhlsf012 | 0.55238 | 0.00050 | simplified | hexagonal | redwood -> water, steel modeled | 1.09 | /pat1/apps/normarray/hex/water/ |
| fhlsf013 | 0.54361 | 0.00049 | simplified | hexagonal | redwood -> water, steel modeled | 1.34 | /pat1/apps/normarray/hex/water/ |
| fhlsf014 | 0.53538 | 0.00049 | simplified | hexagonal | redwood -> water, steel modeled | 1.63 | /pat1/apps/normarray/hex/water/ |
| fhlsf015 | 0.52817 | 0.00050 | simplified | hexagonal | redwood -> water, steel modeled | 2.00 | /pat1/apps/normarray/hex/water/ |
| fhlsf016 | 0.52190 | 0.00049 | simplified | hexagonal | redwood -> water, steel modeled | 2.48 | /pat1/apps/normarray/hex/water/ |
| fhlsf017 | 0.51867 | 0.00050 | simplified | hexagonal | redwood -> water, steel modeled | 3.12 | /pat1/apps/normarray/hex/water/ |
| fhlsf018 | 0.51768 | 0.00049 | simplified | hexagonal | redwood -> water, steel modeled | 4.01 | /pat1/apps/normarray/hex/water/ |
| fhlsf019 | 0.52126 | 0.00050 | simplified | hexagonal | redwood -> water, steel modeled | 5.34 | /pat1/apps/normarray/hex/water/ |
| fhlsf020 | 0.53261 | 0.00049 | simplified | hexagonal | redwood -> water, steel modeled | 7.57 | /pat1/apps/normarray/hex/water/ |
| fhlsf021 | 0.55883 | 0.00050 | simplified | hexagonal | redwood -> water, steel modeled | 12.0 | /pat1/apps/normarray/hex/water/ |
| fhlsf022 | 0.55958 | 0.00050 | simplified | hexagonal | redwood -> water, steel modeled | 12.1 | /pat1/apps/normarray/hex/water/ |
| fhlsf023 | 0.50296 | 0.00049 | simplified | hexagonal | redwood -> water, steel modeled | 5.34 | /pat1/apps/normarray/hex/water/ |
| fhlsf024 | 0.52189 | 0.00049 | simplified | hexagonal | redwood -> water, steel modeled | 7.57 | /pat1/apps/normarray/hex/water/ |
| fhlsf025 | 0.55819 | 0.00050 | simplified | hexagonal | redwood -> water, steel modeled | 12.0 | /pat1/apps/normarray/hex/water/ |
| fhlsf026 | 0.56757 | 0.00050 | simplified | hexagonal | redwood -> water, steel modeled | 13.5 | /pat1/apps/normarray/hex/water/ |

Table 6-16. Tabulation of Calculations Supporting the Analysis of Arrays of Undamaged Packages

| Case Name | k_{eff} | σ | Package Model Type | Array Type | Description | H/Pu | Location |
|-----------------|-----------|----------|--------------------|------------|---------------------------------|-------|---------------------------------|
| <i>fhlsf027</i> | 0.57968 | 0.00049 | simplified | hexagonal | redwood -> water, steel modeled | 15.4 | /pat1/apps/normarray/hex/water/ |
| <i>fhlsf028</i> | 0.59359 | 0.00049 | simplified | hexagonal | redwood -> water, steel modeled | 17.7 | /pat1/apps/normarray/hex/water/ |
| <i>fhlsf029</i> | 0.60825 | 0.00049 | simplified | hexagonal | redwood -> water, steel modeled | 20.9 | /pat1/apps/normarray/hex/water/ |
| <i>fhlsf030</i> | 0.62311 | 0.00049 | simplified | hexagonal | redwood -> water, steel modeled | 25.4 | /pat1/apps/normarray/hex/water/ |
| <i>fhlsf031</i> | 0.63235 | 0.00050 | simplified | hexagonal | redwood -> water, steel modeled | 28.8 | /pat1/apps/normarray/hex/water/ |
| <i>fhlsf032</i> | 0.62619 | 0.00049 | simplified | hexagonal | redwood -> water, steel modeled | 32.0 | /pat1/apps/normarray/hex/water/ |
| <i>fhlsf033</i> | 0.61657 | 0.00050 | simplified | hexagonal | redwood -> water, steel modeled | 36.8 | /pat1/apps/normarray/hex/water/ |
| <i>fhlsf034</i> | 0.60778 | 0.00050 | simplified | hexagonal | redwood -> water, steel modeled | 43.2 | /pat1/apps/normarray/hex/water/ |
| <i>fhlsf035</i> | 0.59750 | 0.00049 | simplified | hexagonal | redwood -> water, steel modeled | 52.1 | /pat1/apps/normarray/hex/water/ |
| <i>fhlsf036</i> | 0.58477 | 0.00049 | simplified | hexagonal | redwood -> water, steel modeled | 65.4 | /pat1/apps/normarray/hex/water/ |
| <i>fhlsf037</i> | 0.56890 | 0.00050 | simplified | hexagonal | redwood -> water, steel modeled | 87.7 | /pat1/apps/normarray/hex/water/ |
| <i>fhlsf038</i> | 0.54643 | 0.00049 | simplified | hexagonal | redwood -> water, steel modeled | 132.2 | /pat1/apps/normarray/hex/water/ |

^a Limiting cases listed in Table 6-1.

6.9.4.3 Calculations Supporting Hypothetical Accident Conditions Array Analysis

Table 6-17 lists calculations performed to support the analysis of damaged package arrays.

Table 6-17. Tabulation of Calculations Supporting the Analysis of Arrays of Damaged Packages

| Case Name | k_{eff} | σ | Package Model Type | H/Pu | Water Density Fraction in Wood Zone | Array Type | Number of Packages | Description | Locations |
|------------------|-----------|----------|--------------------|------|-------------------------------------|------------|--------------------|--|---------------------------------|
| <i>enda1088</i> | 0.67887 | 0.00049 | end | 28.8 | 0 | hex | 1088 | identical repeated layers | /pat1/apps/hacarray/arraystudy/ |
| <i>enda1088m</i> | 0.65085 | 0.00050 | end | 0 | 0 | hex | 1088 | enda1088 with Pu metal spheres | /pat1/apps/hacarray/arraystudy/ |
| <i>enda920</i> | 0.66587 | 0.00049 | end | 28.8 | 0 | hex | 920 | identical repeated layers | /pat1/apps/hacarray/arraystudy/ |
| <i>endb1088</i> | 0.68125 | 0.00049 | end | 28.8 | 0 | hex | 1088 | alternating layers, bringing pairs of TB-1s closer | /pat1/apps/hacarray/arraystudy/ |
| <i>endb920</i> | 0.66644 | 0.00049 | end | 28.8 | 0 | hex | 920 | alternating layers, bringing pairs of TB-1s closer | /pat1/apps/hacarray/arraystudy/ |
| <i>hex0</i> | 0.70411 | 0.00056 | side | 28.8 | 0 | hex | 1152 | varying number of packages with air between | /pat1/apps/hacarray/arraystudy/ |
| <i>hex0a</i> | 0.65776 | 0.00054 | side | 28.8 | 0 | hex | 576 | varying number of packages with air between | /pat1/apps/hacarray/arraystudy/ |
| <i>hex0b</i> | 0.67551 | 0.00054 | side | 28.8 | 0 | hex | 768 | varying number of packages with air between | /pat1/apps/hacarray/arraystudy/ |
| <i>hex0c</i> | 0.63864 | 0.00053 | side | 28.8 | 0 | hex | 384 | varying number of packages with air between | /pat1/apps/hacarray/arraystudy/ |
| <i>hex0d</i> | 0.61622 | 0.00056 | side | 28.8 | 0 | hex | 256 | varying number of packages with air between | /pat1/apps/hacarray/arraystudy/ |
| <i>hex0e</i> | 0.58981 | 0.00059 | side | 28.8 | 0 | hex | 128 | varying number of packages with air between | /pat1/apps/hacarray/arraystudy/ |
| <i>hex0met</i> | 0.67138 | 0.00049 | side | 0 | 0 | hex | 1152 | hex0 with Pu metal spheres | /pat1/apps/hacarray/arraystudy/ |
| <i>hex100</i> | 0.71538 | 0.00050 | side | 28.8 | 1 | hex | 1152 | varying number of packages with water between | /pat1/apps/hacarray/arraystudy/ |
| <i>hex100a</i> | 0.71524 | 0.00051 | side | 28.8 | 1 | hex | 576 | varying number of packages with water between | /pat1/apps/hacarray/arraystudy/ |
| <i>hex100b</i> | 0.71456 | 0.00049 | side | 28.8 | 1 | hex | 768 | varying number of packages with water between | /pat1/apps/hacarray/arraystudy/ |
| <i>hex100c</i> | 0.71449 | 0.00056 | side | 28.8 | 1 | hex | 384 | varying number of packages with water between | /pat1/apps/hacarray/arraystudy/ |
| <i>hex100d</i> | 0.71498 | 0.00049 | side | 28.8 | 1 | hex | 256 | varying number of packages with water between | /pat1/apps/hacarray/arraystudy/ |
| <i>hex100e</i> | 0.71481 | 0.00056 | side | 28.8 | 1 | hex | 128 | varying number of packages with water between | /pat1/apps/hacarray/arraystudy/ |
| <i>hex100met</i> | 0.66365 | 0.00049 | side | 0 | 1 | hex | 1152 | hex100 with Pu metal spheres | /pat1/apps/hacarray/arraystudy/ |
| <i>nest1a</i> | 0.58966 | 0.00051 | side | 28.8 | 0 | nest-1 | 384 | varying number of packages with air between | /pat1/apps/hacarray/arraystudy/ |
| <i>nest1b</i> | 0.61431 | 0.00053 | side | 28.8 | 0 | nest-1 | 864 | varying number of packages with air between | /pat1/apps/hacarray/arraystudy/ |
| <i>nest1c</i> | 0.64080 | 0.00053 | side | 28.8 | 0 | nest-1 | 1296 | varying number of packages with air between | /pat1/apps/hacarray/arraystudy/ |
| <i>nest1met</i> | 0.66557 | 0.00049 | side | 0 | 0 | nest-1 | 384 | nest1a with Pu metal spheres | /pat1/apps/hacarray/arraystudy/ |
| <i>nest1metc</i> | 0.66991 | 0.00050 | side | 0 | 0 | nest-1 | 1296 | nest1c with Pu metal spheres | /pat1/apps/hacarray/arraystudy/ |
| <i>nest2a</i> | 0.61807 | 0.00053 | side | 28.8 | 0 | nest-2 | 512 | varying number of packages with air between | /pat1/apps/hacarray/arraystudy/ |
| <i>nest2b</i> | 0.65206 | 0.00050 | side | 28.8 | 0 | nest-2 | 1152 | varying number of packages with air between | /pat1/apps/hacarray/arraystudy/ |
| <i>nest2c</i> | 0.63333 | 0.00050 | side | 28.8 | 0 | nest-2 | 768 | varying number of packages with air between | /pat1/apps/hacarray/arraystudy/ |
| <i>nest2met</i> | 0.66594 | 0.00051 | side | 0 | 0 | nest-2 | 512 | nest2a with Pu metal spheres | /pat1/apps/hacarray/arraystudy/ |

Table 6-17. Tabulation of Calculations Supporting the Analysis of Arrays of Damaged Packages

| Case Name | k_{eff} | σ | Package Model Type | H/Pu | Water Density Fraction in Wood Zone | Array Type | Number of Packages | Description | Locations |
|----------------------------|-----------|----------|--------------------|------|-------------------------------------|------------|--------------------|---|---|
| <i>nest2metb</i> | 0.67004 | 0.00050 | side | 0 | 0 | nest-2 | 1152 | nest2b with Pu metal spheres | /pat1/apps/hacarray/arraystudy/ |
| <i>octa</i> | 0.67746 | 0.00052 | side | 28.8 | 0 | square | 1024 | varying number of packages with air between | /pat1/apps/hacarray/arraystudy/ |
| <i>octb</i> | 0.66231 | 0.00049 | side | 28.8 | 0 | square | 768 | varying number of packages with air between | /pat1/apps/hacarray/arraystudy/ |
| <i>octc</i> | 0.64717 | 0.00049 | side | 28.8 | 0 | square | 576 | varying number of packages with air between | /pat1/apps/hacarray/arraystudy/ |
| <i>octd</i> | 0.69364 | 0.00053 | side | 28.8 | 0 | square | 1280 | varying number of packages with air between | /pat1/apps/hacarray/arraystudy/ |
| <i>octmet</i> | 0.67989 | 0.00050 | side | 0 | 0 | square | 1024 | octa with Pu metal spheres | /pat1/apps/hacarray/arraystudy/ |
| <i>hexsdry^a</i> | 0.70268 | 0.00065 | side | 28.8 | 0 | hex | 1152 | Varying water density in redwood zone | /pat1/apps/hacarray/sideimpact/hexstudy/hexsol/ |
| <i>hexs0005</i> | 0.70279 | 0.00053 | side | 28.8 | 0.005 | hex | 1152 | Varying water density in redwood zone | /pat1/apps/hacarray/sideimpact/hexstudy/hexsol/ |
| <i>hexs001</i> | 0.69192 | 0.00055 | side | 28.8 | 0.01 | hex | 1152 | Varying water density in redwood zone | /pat1/apps/hacarray/sideimpact/hexstudy/hexsol/ |
| <i>hexs002</i> | 0.67005 | 0.00055 | side | 28.8 | 0.02 | hex | 1152 | Varying water density in redwood zone | /pat1/apps/hacarray/sideimpact/hexstudy/hexsol/ |
| <i>hexs003</i> | 0.65145 | 0.00049 | side | 28.8 | 0.03 | hex | 1152 | Varying water density in redwood zone | /pat1/apps/hacarray/sideimpact/hexstudy/hexsol/ |
| <i>hexs004</i> | 0.63834 | 0.00052 | side | 28.8 | 0.04 | hex | 1152 | Varying water density in redwood zone | /pat1/apps/hacarray/sideimpact/hexstudy/hexsol/ |
| <i>hexs005</i> | 0.62834 | 0.00050 | side | 28.8 | 0.05 | hex | 1152 | Varying water density in redwood zone | /pat1/apps/hacarray/sideimpact/hexstudy/hexsol/ |
| <i>hexs0075</i> | 0.61259 | 0.00052 | side | 28.8 | 0.075 | hex | 1152 | Varying water density in redwood zone | /pat1/apps/hacarray/sideimpact/hexstudy/hexsol/ |
| <i>hexs010</i> | 0.60541 | 0.00049 | side | 28.8 | 0.1 | hex | 1152 | Varying water density in redwood zone | /pat1/apps/hacarray/sideimpact/hexstudy/hexsol/ |
| <i>hexs015</i> | 0.60543 | 0.00050 | side | 28.8 | 0.15 | hex | 1152 | Varying water density in redwood zone | /pat1/apps/hacarray/sideimpact/hexstudy/hexsol/ |
| <i>hexs020</i> | 0.61187 | 0.00052 | side | 28.8 | 0.2 | hex | 1152 | Varying water density in redwood zone | /pat1/apps/hacarray/sideimpact/hexstudy/hexsol/ |
| <i>hexs030</i> | 0.63261 | 0.00050 | side | 28.8 | 0.3 | hex | 1152 | Varying water density in redwood zone | /pat1/apps/hacarray/sideimpact/hexstudy/hexsol/ |
| <i>hexs040</i> | 0.65171 | 0.00055 | side | 28.8 | 0.4 | hex | 1152 | Varying water density in redwood zone | /pat1/apps/hacarray/sideimpact/hexstudy/hexsol/ |
| <i>hexs050</i> | 0.66806 | 0.00050 | side | 28.8 | 0.5 | hex | 1152 | Varying water density in redwood zone | /pat1/apps/hacarray/sideimpact/hexstudy/hexsol/ |
| <i>hexs060</i> | 0.68073 | 0.00050 | side | 28.8 | 0.6 | hex | 1152 | Varying water density in redwood zone | /pat1/apps/hacarray/sideimpact/hexstudy/hexsol/ |
| <i>hexs070</i> | 0.69265 | 0.00054 | side | 28.8 | 0.7 | hex | 1152 | Varying water density in redwood zone | /pat1/apps/hacarray/sideimpact/hexstudy/hexsol/ |
| <i>hexs080</i> | 0.70127 | 0.00049 | side | 28.8 | 0.8 | hex | 1152 | Varying water density in redwood zone | /pat1/apps/hacarray/sideimpact/hexstudy/hexsol/ |
| <i>hexs090</i> | 0.70936 | 0.00053 | side | 28.8 | 0.9 | hex | 1152 | Varying water density in redwood zone | /pat1/apps/hacarray/sideimpact/hexstudy/hexsol/ |
| <i>hexs095</i> | 0.71150 | 0.00049 | side | 28.8 | 0.95 | hex | 1152 | Varying water density in redwood zone | /pat1/apps/hacarray/sideimpact/hexstudy/hexsol/ |
| <i>hexs100^a</i> | 0.71538 | 0.00050 | side | 28.8 | 1 | hex | 1152 | Varying water density in redwood zone | /pat1/apps/hacarray/sideimpact/hexstudy/hexsol/ |
| <i>hexs100_1</i> | 0.69003 | 0.00051 | side | 28.8 | 1 | hex | 1152 | TB-1s moved 1 cm from flat side of package | /pat1/apps/hacarray/sideimpact/hexstudy/hexsol/ |
| <i>hexs100_2</i> | 0.67021 | 0.00050 | side | 28.8 | 1 | hex | 1152 | TB-1s moved 2 cm from flat side of package | /pat1/apps/hacarray/sideimpact/hexstudy/hexsol/ |

Table 6-17. Tabulation of Calculations Supporting the Analysis of Arrays of Damaged Packages

| Case Name | k_{eff} | σ | Package Model Type | H/Pu | Water Density Fraction in Wood Zone | Array Type | Number of Packages | Description | Locations |
|------------|-----------|----------|--------------------|------|-------------------------------------|------------|--------------------|--|--|
| hexs100_3 | 0.65663 | 0.00049 | side | 28.8 | 1 | hex | 1152 | TB-1s moved 3 cm from flat side of package | /pat1/apps/hacarray/sideimpact/hexstudy/hexsol/ |
| hexs100_p5 | 0.70177 | 0.00054 | side | 28.8 | 1 | hex | 1152 | TB-1s moved 0.5 cm from flat side of package | /pat1/apps/hacarray/sideimpact/hexstudy/hexsol/ |
| hexs100 | 0.71523 | 0.00029 | side | 28.8 | 1 | hex | 1152 | Rerun for tighter convergence for sens study | /pat1/apps/hacarray/sideimpact/hexstudy/hexsol/sens_study/ |
| Hexsdry | 0.70274 | 0.00031 | side | 28.8 | 0 | hex | 1152 | Rerun for tighter convergence for sens study | /pat1/apps/hacarray/sideimpact/hexstudy/hexsol/sens_study/ |
| ph13m2 | 0.70171 | 0.00031 | side | 28.8 | 0 | hex | 1152 | hexsdry with TB-1 steel at 98% density | /pat1/apps/hacarray/sideimpact/hexstudy/hexsol/sens_study/dry/ |
| ph13p2 | 0.70457 | 0.00033 | side | 28.8 | 0 | hex | 1152 | hexsdry with TB-1 steel at 102% density | /pat1/apps/hacarray/sideimpact/hexstudy/hexsol/sens_study/dry/ |
| ss304m2 | 0.70217 | 0.00032 | side | 28.8 | 0 | hex | 1152 | hexsdry with drum steel at 98% density | /pat1/apps/hacarray/sideimpact/hexstudy/hexsol/sens_study/dry/ |
| ss304p2 | 0.70441 | 0.00031 | side | 28.8 | 0 | hex | 1152 | hexsdry with drum steel at 102% density | /pat1/apps/hacarray/sideimpact/hexstudy/hexsol/sens_study/dry/ |
| ph13m2 | 0.71474 | 0.00028 | side | 28.8 | 1 | hex | 1152 | hexs100 with TB-1 steel at 98% density | /pat1/apps/hacarray/sideimpact/hexstudy/hexsol/sens_study/wet/ |
| ph13p2 | 0.71500 | 0.00032 | side | 28.8 | 1 | hex | 1152 | hexs100 with TB-1 steel at 102% density | /pat1/apps/hacarray/sideimpact/hexstudy/hexsol/sens_study/wet/ |
| ss304m2 | 0.71474 | 0.00030 | side | 28.8 | 1 | hex | 1152 | hexs100 with drum steel at 98% density | /pat1/apps/hacarray/sideimpact/hexstudy/hexsol/sens_study/wet/ |
| ss304p2 | 0.71425 | 0.00028 | side | 28.8 | 1 | hex | 1152 | hexs100 with drum steel at 102% density | /pat1/apps/hacarray/sideimpact/hexstudy/hexsol/sens_study/wet/ |
| Hexmdry | 0.67134 | 0.00049 | side | 0 | 0 | hex | 1152 | Varying water density in redwood zone | /pat1/apps/hacarray/sideimpact/hexstudy/hexmet/ |
| hexm0005 | 0.67054 | 0.00049 | side | 0 | 0.005 | hex | 1152 | Varying water density in redwood zone | /pat1/apps/hacarray/sideimpact/hexstudy/hexmet/ |
| hexm001 | 0.66744 | 0.00050 | side | 0 | 0.01 | hex | 1152 | Varying water density in redwood zone | /pat1/apps/hacarray/sideimpact/hexstudy/hexmet/ |
| hexm002 | 0.66340 | 0.00049 | side | 0 | 0.02 | hex | 1152 | Varying water density in redwood zone | /pat1/apps/hacarray/sideimpact/hexstudy/hexmet/ |
| hexm003 | 0.66093 | 0.00049 | side | 0 | 0.03 | hex | 1152 | Varying water density in redwood zone | /pat1/apps/hacarray/sideimpact/hexstudy/hexmet/ |
| hexm004 | 0.65925 | 0.00050 | side | 0 | 0.04 | hex | 1152 | Varying water density in redwood zone | /pat1/apps/hacarray/sideimpact/hexstudy/hexmet/ |
| hexm005 | 0.65746 | 0.00050 | side | 0 | 0.05 | hex | 1152 | Varying water density in redwood zone | /pat1/apps/hacarray/sideimpact/hexstudy/hexmet/ |
| hexm0075 | 0.65555 | 0.00049 | side | 0 | 0.075 | hex | 1152 | Varying water density in redwood zone | /pat1/apps/hacarray/sideimpact/hexstudy/hexmet/ |
| hexm010 | 0.65528 | 0.00049 | side | 0 | 0.1 | hex | 1152 | Varying water density in redwood zone | /pat1/apps/hacarray/sideimpact/hexstudy/hexmet/ |

Table 6-17. Tabulation of Calculations Supporting the Analysis of Arrays of Damaged Packages

| Case Name | k_{eff} | σ | Package Model Type | H/Pu | Water Density Fraction in Wood Zone | Array Type | Number of Packages | Description | Locations |
|-------------|-----------|----------|--------------------|------|-------------------------------------|------------|--------------------|--|---|
| hexm015 | 0.65577 | 0.00049 | side | 0 | 0.15 | hex | 1152 | Varying water density in redwood zone | /pat1/apps/hacarray/sideimpact/hexstudy/hexmet/ |
| hexm020 | 0.65561 | 0.00048 | side | 0 | 0.2 | hex | 1152 | Varying water density in redwood zone | /pat1/apps/hacarray/sideimpact/hexstudy/hexmet/ |
| hexm030 | 0.65735 | 0.00049 | side | 0 | 0.3 | hex | 1152 | Varying water density in redwood zone | /pat1/apps/hacarray/sideimpact/hexstudy/hexmet/ |
| hexm040 | 0.65854 | 0.00050 | side | 0 | 0.4 | hex | 1152 | Varying water density in redwood zone | /pat1/apps/hacarray/sideimpact/hexstudy/hexmet/ |
| hexm050 | 0.66053 | 0.00049 | side | 0 | 0.5 | hex | 1152 | Varying water density in redwood zone | /pat1/apps/hacarray/sideimpact/hexstudy/hexmet/ |
| hexm060 | 0.66232 | 0.00049 | side | 0 | 0.6 | hex | 1152 | Varying water density in redwood zone | /pat1/apps/hacarray/sideimpact/hexstudy/hexmet/ |
| hexm070 | 0.66298 | 0.00050 | side | 0 | 0.7 | hex | 1152 | Varying water density in redwood zone | /pat1/apps/hacarray/sideimpact/hexstudy/hexmet/ |
| hexm080 | 0.66268 | 0.00049 | side | 0 | 0.8 | hex | 1152 | Varying water density in redwood zone | /pat1/apps/hacarray/sideimpact/hexstudy/hexmet/ |
| hexm090 | 0.66261 | 0.00049 | side | 0 | 0.9 | hex | 1152 | Varying water density in redwood zone | /pat1/apps/hacarray/sideimpact/hexstudy/hexmet/ |
| hexm095 | 0.66402 | 0.00050 | side | 0 | 0.95 | hex | 1152 | Varying water density in redwood zone | /pat1/apps/hacarray/sideimpact/hexstudy/hexmet/ |
| hexm100 | 0.66365 | 0.00049 | side | 0 | 1 | hex | 1152 | Varying water density in redwood zone | /pat1/apps/hacarray/sideimpact/hexstudy/hexmet/ |
| hexm100_1 | 0.65861 | 0.00050 | side | 0 | 1 | hex | 1152 | TB-1s moved 1 cm from flat side of package | /pat1/apps/hacarray/sideimpact/hexstudy/hexmet/ |
| hexm100_2 | 0.65607 | 0.00049 | side | 0 | 1 | hex | 1152 | TB-1s moved 2 cm from flat side of package | /pat1/apps/hacarray/sideimpact/hexstudy/hexmet/ |
| hexm100_3 | 0.65325 | 0.00050 | side | 0 | 1 | hex | 1152 | TB-1s moved 3 cm from flat side of package | /pat1/apps/hacarray/sideimpact/hexstudy/hexmet/ |
| hexm100_p5 | 0.66003 | 0.00049 | side | 0 | 1 | hex | 1152 | TB-1s moved 0.5 cm from flat side of package | /pat1/apps/hacarray/sideimpact/hexstudy/hexmet/ |
| hexs100i01 | 0.71442 | 0.00049 | side | 28.8 | 1 | hex | 1152 | 1% water density between packages | /pat1/apps/hacarray/sideimpact/hexstudy/inter/ |
| hexs100i02 | 0.71503 | 0.00050 | side | 28.8 | 1 | hex | 1152 | 2% water density between packages | /pat1/apps/hacarray/sideimpact/hexstudy/inter/ |
| hexs100i05 | 0.71569 | 0.00058 | side | 28.8 | 1 | hex | 1152 | 5% water density between packages | /pat1/apps/hacarray/sideimpact/hexstudy/inter/ |
| hexs100i10 | 0.71469 | 0.00049 | side | 28.8 | 1 | hex | 1152 | 10% water density between packages | /pat1/apps/hacarray/sideimpact/hexstudy/inter/ |
| hexs100i25 | 0.71398 | 0.00057 | side | 28.8 | 1 | hex | 1152 | 25% water density between packages | /pat1/apps/hacarray/sideimpact/hexstudy/inter/ |
| hexs100i50 | 0.71610 | 0.00050 | side | 28.8 | 1 | hex | 1152 | 50% water density between packages | /pat1/apps/hacarray/sideimpact/hexstudy/inter/ |
| hexs100i75 | 0.71429 | 0.00053 | side | 28.8 | 1 | hex | 1152 | 75% water density between packages | /pat1/apps/hacarray/sideimpact/hexstudy/inter/ |
| hexs100i90 | 0.71330 | 0.00050 | side | 28.8 | 1 | hex | 1152 | 90% water density between packages | /pat1/apps/hacarray/sideimpact/hexstudy/inter/ |
| hexs100i100 | 0.71491 | 0.00062 | side | 28.8 | 1 | hex | 1152 | 100% water density between packages | /pat1/apps/hacarray/sideimpact/hexstudy/inter/ |
| hexsdryi01 | 0.70379 | 0.00056 | side | 28.8 | 0 | hex | 1152 | 1% water density between packages | /pat1/apps/hacarray/sideimpact/hexstudy/inter/ |
| hexsdryi02 | 0.70389 | 0.00060 | side | 28.8 | 0 | hex | 1152 | 2% water density between packages | /pat1/apps/hacarray/sideimpact/hexstudy/inter/ |
| hexsdryi05 | 0.69864 | 0.00052 | side | 28.8 | 0 | hex | 1152 | 5% water density between packages | /pat1/apps/hacarray/sideimpact/hexstudy/inter/ |
| hexsdryi10 | 0.68545 | 0.00050 | side | 28.8 | 0 | hex | 1152 | 10% water density between packages | /pat1/apps/hacarray/sideimpact/hexstudy/inter/ |

Table 6-17. Tabulation of Calculations Supporting the Analysis of Arrays of Damaged Packages

| Case Name | k_{eff} | σ | Package Model Type | H/Pu | Water Density Fraction in Wood Zone | Array Type | Number of Packages | Description | Locations |
|-------------|-----------|----------|--------------------|------|-------------------------------------|------------|--------------------|---------------------------------------|--|
| hexsdryi25 | 0.65098 | 0.00049 | side | 28.8 | 0 | hex | 1152 | 25% water density between packages | /pat1/apps/hacarray/sideimpact/hexstudy/inter/ |
| hexsdryi50 | 0.62096 | 0.00053 | side | 28.8 | 0 | hex | 1152 | 50% water density between packages | /pat1/apps/hacarray/sideimpact/hexstudy/inter/ |
| hexsdryi75 | 0.60452 | 0.00050 | side | 28.8 | 0 | hex | 1152 | 75% water density between packages | /pat1/apps/hacarray/sideimpact/hexstudy/inter/ |
| hexsdryi90 | 0.59848 | 0.00050 | side | 28.8 | 0 | hex | 1152 | 90% water density between packages | /pat1/apps/hacarray/sideimpact/hexstudy/inter/ |
| hexsdryi100 | 0.59412 | 0.00050 | side | 28.8 | 0 | hex | 1152 | 100% water density between packages | /pat1/apps/hacarray/sideimpact/hexstudy/inter/ |
| octmdry | 0.66773 | 0.00049 | side | 0 | 0 | square | 1024 | Varying water density in redwood zone | /pat1/apps/hacarray/sideimpact/octstudy/metal/ |
| octm0001 | 0.66815 | 0.00050 | side | 0 | 0.001 | square | 1024 | Varying water density in redwood zone | /pat1/apps/hacarray/sideimpact/octstudy/metal/ |
| octm0005 | 0.66646 | 0.00048 | side | 0 | 0.005 | square | 1024 | Varying water density in redwood zone | /pat1/apps/hacarray/sideimpact/octstudy/metal/ |
| octm001 | 0.66552 | 0.00049 | side | 0 | 0.01 | square | 1024 | Varying water density in redwood zone | /pat1/apps/hacarray/sideimpact/octstudy/metal/ |
| octm002 | 0.66298 | 0.00051 | side | 0 | 0.02 | square | 1024 | Varying water density in redwood zone | /pat1/apps/hacarray/sideimpact/octstudy/metal/ |
| octm003 | 0.66009 | 0.00050 | side | 0 | 0.03 | square | 1024 | Varying water density in redwood zone | /pat1/apps/hacarray/sideimpact/octstudy/metal/ |
| octm005 | 0.65731 | 0.00049 | side | 0 | 0.05 | square | 1024 | Varying water density in redwood zone | /pat1/apps/hacarray/sideimpact/octstudy/metal/ |
| octm010 | 0.65370 | 0.00049 | side | 0 | 0.1 | square | 1024 | Varying water density in redwood zone | /pat1/apps/hacarray/sideimpact/octstudy/metal/ |
| octm020 | 0.65596 | 0.00049 | side | 0 | 0.2 | square | 1024 | Varying water density in redwood zone | /pat1/apps/hacarray/sideimpact/octstudy/metal/ |
| octm030 | 0.65707 | 0.00049 | side | 0 | 0.3 | square | 1024 | Varying water density in redwood zone | /pat1/apps/hacarray/sideimpact/octstudy/metal/ |
| octm040 | 0.65914 | 0.00050 | side | 0 | 0.4 | square | 1024 | Varying water density in redwood zone | /pat1/apps/hacarray/sideimpact/octstudy/metal/ |
| octm050 | 0.66046 | 0.00049 | side | 0 | 0.5 | square | 1024 | Varying water density in redwood zone | /pat1/apps/hacarray/sideimpact/octstudy/metal/ |
| octm060 | 0.66105 | 0.00049 | side | 0 | 0.6 | square | 1024 | Varying water density in redwood zone | /pat1/apps/hacarray/sideimpact/octstudy/metal/ |
| octm070 | 0.66256 | 0.00049 | side | 0 | 0.7 | square | 1024 | Varying water density in redwood zone | /pat1/apps/hacarray/sideimpact/octstudy/metal/ |
| octm080 | 0.66262 | 0.00049 | side | 0 | 0.8 | square | 1024 | Varying water density in redwood zone | /pat1/apps/hacarray/sideimpact/octstudy/metal/ |
| octm090 | 0.66378 | 0.00049 | side | 0 | 0.9 | square | 1024 | Varying water density in redwood zone | /pat1/apps/hacarray/sideimpact/octstudy/metal/ |
| octm095 | 0.66449 | 0.00049 | side | 0 | 0.95 | square | 1024 | Varying water density in redwood zone | /pat1/apps/hacarray/sideimpact/octstudy/metal/ |
| octm0975 | 0.66410 | 0.00048 | side | 0 | 0.975 | square | 1024 | Varying water density in redwood zone | /pat1/apps/hacarray/sideimpact/octstudy/metal/ |
| octm099 | 0.66435 | 0.00050 | side | 0 | 0.99 | square | 1024 | Varying water density in redwood zone | /pat1/apps/hacarray/sideimpact/octstudy/metal/ |
| octm100 | 0.66424 | 0.00049 | side | 0 | 1 | square | 1024 | Varying water density in redwood zone | /pat1/apps/hacarray/sideimpact/octstudy/metal/ |
| octsdry | 0.67719 | 0.00057 | side | 28.8 | 0 | square | 1024 | Varying water density in redwood zone | /pat1/apps/hacarray/sideimpact/octstudy/soln/ |
| octs0001 | 0.67944 | 0.00049 | side | 28.8 | 0.001 | square | 1024 | Varying water density in redwood zone | /pat1/apps/hacarray/sideimpact/octstudy/soln/ |
| octs0005 | 0.67808 | 0.00055 | side | 28.8 | 0.005 | square | 1024 | Varying water density in redwood zone | /pat1/apps/hacarray/sideimpact/octstudy/soln/ |

Table 6-17. Tabulation of Calculations Supporting the Analysis of Arrays of Damaged Packages

| Case Name | k_{eff} | σ | Package Model Type | H/Pu | Water Density Fraction in Wood Zone | Array Type | Number of Packages | Description | Locations |
|-----------------|-----------|----------|--------------------|------|-------------------------------------|------------|--------------------|---------------------------------------|---|
| <i>octs001</i> | 0.67270 | 0.00059 | side | 28.8 | 0.01 | square | 1024 | Varying water density in redwood zone | /pat1/apps/hacarray/sideimpact/octstudy/soln/ |
| <i>octs002</i> | 0.65588 | 0.00053 | side | 28.8 | 0.02 | square | 1024 | Varying water density in redwood zone | /pat1/apps/hacarray/sideimpact/octstudy/soln/ |
| <i>octs003</i> | 0.64169 | 0.00049 | side | 28.8 | 0.03 | square | 1024 | Varying water density in redwood zone | /pat1/apps/hacarray/sideimpact/octstudy/soln/ |
| <i>octs005</i> | 0.62271 | 0.00056 | side | 28.8 | 0.05 | square | 1024 | Varying water density in redwood zone | /pat1/apps/hacarray/sideimpact/octstudy/soln/ |
| <i>octs010</i> | 0.60422 | 0.00050 | side | 28.8 | 0.1 | square | 1024 | Varying water density in redwood zone | /pat1/apps/hacarray/sideimpact/octstudy/soln/ |
| <i>octs020</i> | 0.61144 | 0.00055 | side | 28.8 | 0.2 | square | 1024 | Varying water density in redwood zone | /pat1/apps/hacarray/sideimpact/octstudy/soln/ |
| <i>octs030</i> | 0.63223 | 0.00053 | side | 28.8 | 0.3 | square | 1024 | Varying water density in redwood zone | /pat1/apps/hacarray/sideimpact/octstudy/soln/ |
| <i>octs040</i> | 0.65161 | 0.00053 | side | 28.8 | 0.4 | square | 1024 | Varying water density in redwood zone | /pat1/apps/hacarray/sideimpact/octstudy/soln/ |
| <i>octs050</i> | 0.66810 | 0.00063 | side | 28.8 | 0.5 | square | 1024 | Varying water density in redwood zone | /pat1/apps/hacarray/sideimpact/octstudy/soln/ |
| <i>octs060</i> | 0.68116 | 0.00050 | side | 28.8 | 0.6 | square | 1024 | Varying water density in redwood zone | /pat1/apps/hacarray/sideimpact/octstudy/soln/ |
| <i>octs070</i> | 0.69215 | 0.00050 | side | 28.8 | 0.7 | square | 1024 | Varying water density in redwood zone | /pat1/apps/hacarray/sideimpact/octstudy/soln/ |
| <i>octs080</i> | 0.70046 | 0.00059 | side | 28.8 | 0.8 | square | 1024 | Varying water density in redwood zone | /pat1/apps/hacarray/sideimpact/octstudy/soln/ |
| <i>octs090</i> | 0.70881 | 0.00053 | side | 28.8 | 0.9 | square | 1024 | Varying water density in redwood zone | /pat1/apps/hacarray/sideimpact/octstudy/soln/ |
| <i>octs095</i> | 0.71225 | 0.00050 | side | 28.8 | 0.95 | square | 1024 | Varying water density in redwood zone | /pat1/apps/hacarray/sideimpact/octstudy/soln/ |
| <i>octs0975</i> | 0.71395 | 0.00048 | side | 28.8 | 0.975 | square | 1024 | Varying water density in redwood zone | /pat1/apps/hacarray/sideimpact/octstudy/soln/ |
| <i>octs099</i> | 0.71434 | 0.00057 | side | 28.8 | 0.99 | square | 1024 | Varying water density in redwood zone | /pat1/apps/hacarray/sideimpact/octstudy/soln/ |
| <i>octs100</i> | 0.71466 | 0.00051 | side | 28.8 | 1 | square | 1024 | Varying water density in redwood zone | /pat1/apps/hacarray/sideimpact/octstudy/soln/ |

^a Limiting cases listed in Table 6-1.

6.9.4.4 Calculations Supporting Single Package Air Transport Analysis

Table 6-18 lists calculations performed to support the analysis of a single package of fissile material intended for air transport.

Table 6-18. Tabulation of Calculations Supporting the Analysis of a Single Package of Fissile Material Intended for Air Transport

| Case Name | k_{eff} | σ | g Pu | g H ₂ O | Fissile Radius | H/Pu | Location |
|--------------------|-----------|----------|------|--------------------|----------------|-------|-------------------|
| sph01 | 0.65568 | 0.00050 | 1300 | 0 | 2.501 | 0 | /pat1/apps/hacsp/ |
| sph02 | 0.64479 | 0.00050 | 1300 | 3 | 2.544 | 0.07 | /pat1/apps/hacsp/ |
| sph03 | 0.63394 | 0.00050 | 1300 | 7 | 2.590 | 0.15 | /pat1/apps/hacsp/ |
| sph04 | 0.61194 | 0.00049 | 1300 | 16 | 2.694 | 0.33 | /pat1/apps/hacsp/ |
| sph05 | 0.59142 | 0.00049 | 1300 | 28 | 2.817 | 0.57 | /pat1/apps/hacsp/ |
| sph06 | 0.57162 | 0.00050 | 1300 | 44 | 2.965 | 0.89 | /pat1/apps/hacsp/ |
| sph07 | 0.55477 | 0.00050 | 1300 | 65 | 3.151 | 1.33 | /pat1/apps/hacsp/ |
| sph08 | 0.54322 | 0.00049 | 1300 | 98 | 3.394 | 2.00 | /pat1/apps/hacsp/ |
| sph09 | 0.53893 | 0.00049 | 1300 | 153 | 3.736 | 3.11 | /pat1/apps/hacsp/ |
| sph10 | 0.55022 | 0.00050 | 1300 | 262 | 4.277 | 5.34 | /pat1/apps/hacsp/ |
| sph11 | 0.60548 | 0.00050 | 1300 | 588 | 5.388 | 12.01 | /pat1/apps/hacsp/ |
| sph12 | 0.64898 | 0.00049 | 1300 | 869 | 6.068 | 17.74 | /pat1/apps/hacsp/ |
| sph13 | 0.69693 | 0.00051 | 1300 | 1242 | 6.789 | 25.36 | /pat1/apps/hacsp/ |
| sph14 ^a | 0.71468 | 0.00050 | 1300 | 1412 | 7.067 | 28.78 | /pat1/apps/hacsp/ |
| sph15 | 0.68744 | 0.00055 | 1300 | 1412 | 7.313 | 28.78 | /pat1/apps/hacsp/ |
| sph16 | 0.62157 | 0.00049 | 1300 | 1412 | 8.049 | 28.78 | /pat1/apps/hacsp/ |
| sph17 | 0.55564 | 0.00049 | 1300 | 1412 | 9.214 | 28.78 | /pat1/apps/hacsp/ |
| sph18 | 0.48650 | 0.00049 | 1300 | 1412 | 11.608 | 28.78 | /pat1/apps/hacsp/ |
| sph19 | 0.46577 | 0.00049 | 1300 | 1412 | 13.074 | 28.78 | /pat1/apps/hacsp/ |
| sph20 | 0.45167 | 0.00050 | 1300 | 1412 | 14.626 | 28.78 | /pat1/apps/hacsp/ |
| sph21 | 0.42551 | 0.00050 | 1300 | 1412 | 19.850 | 28.78 | /pat1/apps/hacsp/ |
| sph22 | 0.41048 | 0.00049 | 1300 | 1412 | 25.010 | 28.78 | /pat1/apps/hacsp/ |
| sph23 | 0.39143 | 0.00049 | 1300 | 1412 | 31.510 | 28.78 | /pat1/apps/hacsp/ |

^a Limiting case listed in Table 6-1.

6.9.5 Sample inputs

This section contains the *csas25* input decks used for the limiting cases shown in Table 6-1 in Section 6.1.2.

6.9.5.1 Input File For *cv031.inp*

```
=csas25
pat1, single package, case cv031.inp
v6-238
read composition
'4.4327% of MTD Pu = 19.84 g/cm3
pu-239      1 0.879448 300  end
h2o         1 0.955673 300  end
'
h2o         2 1.0 300  end
end composition
read celldata
  multiregion spherical left_bdy=reflected right_bdy=vacuum end
    1          5.4
    2          35.4
  end zone
end celldata
read parameter
  npg=3000
  gen=1050
  nsk=50
  sig=0.0005
  htm=no
end parameter
read geometry
unit 1
com='fuel/moderator region, pu metal/water, sphere'
  cylinder 1 1 5.4 2p8.0680
  cylinder 2 1 35.4 2p38.07
end geometry
end data
end
```

6.9.5.2 Input File for *fslsf001.inp*

```
=csas25
pat1, 17x17x9 square pitched array, void between drums, water in drum
v6-238
read composition
' 100% of MTD Pu = 19.84 g/cm3
pu-239      1 19.84      300  end
h2o         1 1e-9       300  end
'
' water in TB-1, but outside fuel (rho=0.9982 g/cm3)
h2o         2 1.0        300  end
'
' PH13-8Mo for TB-1 containment vessel
fe          3 0 6.3246E-02 300 end
cr          3 0 1.1430E-02 300 end
ni          3 0 6.3532E-03 300 end
mo          3 0 1.0931E-03 300 end
al          3 0 1.9435E-03 300 end
mn          3 0 8.4843E-05 300 end
'
'replace Redwood with full density water
h2o         4 1.0        300  end
'
' ss304 for drum body (rho= 7.94 g/cm3)
ss304       5 1.0 300 end
end composition
read celldata
  multiregion spherical left_bdy=reflected right_bdy=vacuum end
    1          2.501
    2          5.4
    3          6.612
    4          28.0289
    5          28.299
    0          29.000
  end zone
end celldata
read parameter
  npg=3000
  gen=1050
  nsk=50
  sig=0.0005
  htm=no
end parameter
read geometry
unit 1
com='fuel/moderator region, pu metal, sphere + x dir'
sphere      1 1      2.501
cylinder    2 1      5.4      2p8.07
cylinder    3 1      6.612     2p9.2815
cylinder    4 1     28.0289 2p50.368
cylinder    5 1     28.299  2p50.639
cuboid      0 1     4p28.3   2p50.639
global unit 2
array 1 0.0 0.0 0.0
replicate 2 1 6*30.0 1
```

```
end geometry
read array
  ara=1  nux=17  nuy=17  nuz=9  fill  f1  end fill
end array
read mixt
  eps=1.0
end mixt
end data
end
```

6.9.5.3 Input File for hexs100.inp

```
=csas25
pat1, damaged, hex arrangement
v6-238
read composition
pu-239      1 0.879448 300 end
h2o        1 0.955673 300 end
'
' PH13-8Mo for TB-1 containment vessel
fe         3 0 6.3246E-02 300 end
cr         3 0 1.1430E-02 300 end
ni         3 0 6.3532E-03 300 end
mo         3 0 1.0931E-03 300 end
al         3 0 1.9435E-03 300 end
mn         3 0 8.4843E-05 300 end
'
' water for flooding drum (rho=0.9982 g/cm3)
h2o        4 1.0      300 end
'
' ss304 for drum body (rho= 7.94 g/cm3)
ss304      5 1.0 300 end
'
' water between drum (rho=0.9982 g/cm3)
h2o        6 0.00001 300 end
'
' water reflector around array
' vf = 1 -> rho=0.9982 g/cm3
h2o        7 1.0 300 end
'
end composition
read celldata
  multiregion spherical left_bdy=reflected right_bdy=reflected end
    1      5.4
    3      6.612
    4     37.194
    5     37.465
    6      38
  end zone
end celldata
read parameter
  npg=3000
  gen=1050
  nsk=50
  sig=0.0005
  htm=no
end parameter
read geometry
unit 1
com='fuel/moderator region, pu metal, sphere'
cylinder  1 1      5.4      2p8.07      origin 0 6.613
cylinder  3 1      6.612     2p9.2815     origin 0 6.613
zhemicyl+y 4 1     37.194    2p50.368
zhemicyl+y 5 1     37.465    2p50.639
unit 2
```

```
com='fuel/moderator region, pu metal, sphere'
cylinder 1 1 5.4 2p8.07 origin 6.613 0
cylinder 3 1 6.612 2p9.2815 origin 6.613 0
zhemicyl+x 4 1 37.194 2p50.368
zhemicyl+x 5 1 37.465 2p50.639
unit 3
com='fuel/moderator region, pu metal, sphere'
cylinder 1 1 5.4 2p8.07 origin 0 -6.613
cylinder 3 1 6.612 2p9.2815 origin 0 -6.613
zhemicyl-y 4 1 37.194 2p50.368
zhemicyl-y 5 1 37.465 2p50.639
unit 4
com='fuel/moderator region, pu metal, sphere'
cylinder 1 1 5.4 2p8.07 origin -6.613 0
cylinder 3 1 6.612 2p9.2815 origin -6.613 0
zhemicyl-x 4 1 37.194 2p50.368
zhemicyl-x 5 1 37.465 2p50.639
unit 5
com='drum steel on flat side of drum on long side'
cuboid 5 1 0.2708 0 2p37.465 2p50.639
unit 6
com='drum steel on flat side of drum on short side'
cuboid 5 1 2p37.465 0.2708 0 2p50.639
unit 7
com='fuel/moderator region, pu metal, sphere'
cuboid 6 1 2p37.737 2p65.1622 2p50.639
hole 1 0 -64.8914 0
hole 6 0 -65.1622 0
hole 2 -37.466 0 0
hole 5 -37.737 0 0
hole 3 0 64.8914 0
hole 6 0 64.8914 0
hole 4 37.466 0 0
hole 5 37.466 0 0
global unit 8
com='array of hemicylinder drums'
array 1 0 0 0
reflector 7 1 30 0 30 0 30 0 1
end geometry
read array
ara=1 nux=4 nuy=3 nuz=3
fill 36*7 end fill
end array
read bound
+fc=vacuum -fc=mirror
end bound
end data
end
```

6.9.5.4 Input File for sph14.inp

```
=csas25
pat1, single package for 10CFR71.55(f) analysis
v6-238
read composition
' 4.4327% of MTD Pu = .879448 g/cm3
pu-239      1 .879448      300      end
h2o         1 .9557        300      end
'
' water outside Pu/water mix
' vf =1.0 -> rho=0.9982 g/cm3
h2o         2 1.0          300      end
'
end composition
read celldata
  multiregion spherical left_bdy=reflected right_bdy=vacuum end
  1          7.0667
  2          27.0667
  end zone
end celldata
read parameter
npg=3000
gen=1050
nsk=50
sig=0.0005
htm=no
end parameter
read geometry
unit 1
com='pu metal/water sphere and 20 cm water reflector'
  sphere    1 1      7.0667
  reflector 2 1    20.0    1
end geometry
end data
end
```

6.9.5.5 USLSTATS Input File for Application cv031

tsunami, c(k) vs. keff trend for cv031

0.999 0.950 0.950 0.0 1.0 -1 0.05

0.9659 1.00882 0.0005

0.9602 1.00909 0.0005

0.9604 1.00375 0.0005

0.9454 1.00734 0.0005

0.9481 1.00676 0.0005

0.9455 1.00641 0.0005

0.9454 1.00573 0.0005

0.9456 1.00559 0.0005

0.9455 1.00593 0.0005

0.9513 1.00855 0.0005

0.9521 1.00844 0.0005

0.9531 1.00736 0.0005

0.9536 1.00799 0.0005

0.9535 1.00860 0.0005

0.9545 1.00935 0.0005

0.9490 1.01046 0.0005

0.9509 1.00812 0.0005

0.9528 1.00918 0.0005

0.9543 1.00749 0.0005

0.9503 1.00621 0.0005

0.9521 1.00767 0.0005

0.9533 1.00793 0.0005

0.9542 1.00929 0.0005

0.9474 1.01058 0.0005

0.9507 1.00812 0.0005

0.9528 1.00764 0.0005

0.9525 1.00757 0.0005

0.9542 1.00702 0.0005

0.9544 1.00874 0.0005

0.9546 1.00898 0.0005

0.9458 1.00895 0.0005

0.9486 1.00804 0.0005

0.9455 1.00914 0.0005

0.9458 1.00937 0.0005

0.9458 1.01032 0.0005

0.9461 1.00691 0.0005

0.9472 1.00802 0.0005

0.9458 1.00658 0.0005

0.9455 1.00812 0.0005

0.9457 1.00764 0.0005

0.9458 1.00773 0.0005

0.9458 1.00734 0.0005

0.9455 1.00797 0.0005

0.9456 1.00701 0.0005

0.9459 1.00699 0.0005

0.9455 1.00849 0.0005

0.9453 1.00766 0.0005

0.9455 1.00810 0.0005

0.9455 1.00819 0.0005

0.9457 1.00881 0.0005

0.9455 1.00777 0.0005

0.9601 1.01198 0.0005

0.9603 1.00474 0.0005

6.9.6 Considerations for Pu/Be Sources

6.9.6.1 Background: The Need for Pu/Be Source Evaluation

Following completion of work for the revision of Section 6, NCS evaluation of an additional loading of the PAT-1 package was requested. The proposed additional loading includes Pu/Be source items, with the total desired inventory of the sources per PAT-1 package consisting of less than 200 g (0.441 lb) Pu alloy and less than 30 g (0.066 lb) Be metal. Other than the Pu and Be, the proposed loading includes no other neutron-multiplying materials.

Be has several unique properties for interaction with neutrons. It is a neutron-multiplying media; when subjected to high-energy neutrons (such as those from Pu-239 fission), Be can multiply neutrons via ($n, 2n$) nuclear reactions. In solid form (e.g., as metal parts), Be can be a more effective neutron reflector than water, for either moderated or unmoderated fissile materials.

The preceding sections and analyses of Section 6 do not evaluate presence of Be as an allowable component or material for co-loading with the general-purpose Pu metal loading limit (1300 g [2.87 lb]). If the 1300 g (2.87 lb) Pu limit were to be reevaluated with significant quantities of Be, the reevaluation effort would be substantial and the existing conclusions (e.g., assigned CI value) might require change.

As an alternative approach, it was recognized that if very low loading limits (for both Pu and Be) were accepted as a second (separate) authorized PAT-1 loading, the NCS evaluation work performed for the 1300 g (2.87 lb) general-form Pu metal loading could be demonstrated as clearly bounding the proposed Pu/Be source loading.

6.9.6.2 Basic Comparison Argument for Pu/Be Sources

The basic reason why the proposed Pu/Be source loading limit is bounded by the 1300 g (2.87lb) Pu loading evaluation is that the:

- Permitted Pu loading for the sources is very small (relative to the evaluated 1300 g [2.87 lb] Pu metal loading); and
- Quantity of Be permitted in the source loading (30 g [0.66 lb]) is sufficiently limited to the extent that the beryllium cannot offset the reactivity effect associated with the significant reduction in Pu mass loading.

A simple observation reveals that the impact of the Be presence should be no greater than that resulting from replacement of the Be mass with an equal mass of Pu-239. Using a “mass replacement” basis, it may be asserted that the PAT-1 Pu/Be source loading (200 g [0.441 lb] maximum of Pu alloy plus (30 g [0.066 lb] maximum of Be) is no more reactive than a loading of 230 g (0.507 lb) Pu-239.

The comparison could be done on a more conservative “volume replacement” basis. If theoretical densities of 1.85 g/cm^3 (0.067 lb/in.^3) for the Be [Reference 2, page 4-43] and 19.84 g/cm^3 (0.7167 lb/in.^3) for the Pu [Reference 2, page 4-83] are assumed, and the 30 g (0.066 lb) of Be is replaced by an equal volume of Pu-239 metal (322 g [0.71 lb] Pu-239), the

resulting idealized package loading (522 g [1.15 lb] Pu-239) remains well below the evaluated general-purpose loading limit of 1300 g (2.87 lb) Pu. If the 200 g (0.441 lb) Pu-239 contained in the sources is considered as the initial (primary) loading constituent, the reactivity effect of adding 30 g (0.066 lb) Be cannot plausibly exceed the reactivity effect due to addition of over 10 times that mass (322 g [0.71 lb]) of Pu-239.

This conclusion that a loading of 200 g (0.441 lb) Pu-239 plus 30 g (0.066 lb) Be is bounded by NCS evaluation of a loading of 1300 g (2.87 lb) Pu-239 holds true for all normal and accident condition models evaluated in Section 6.

6.9.6.3 Supporting Scoping Calculations - Computational Method

For informational purposes only: scoping calculations were performed to augment the comparison argument of Section 6.9.6.2. All inputs and outputs for these calculations are located in the directory tree /pat1/apps/Pu/Be.

The calculations were performed using a quality-assurance-controlled version of SCALE 5.1 similar to that described in Section 6.3.3. The scoping calculations were performed on a cluster of 36 workstations referred to as the *cpile2* cluster and identified as node1 through node36; these workstations all utilized LINUX operating systems. The SCALE 5.1 software used for the scoping calculations was in a directory tree starting at /projects/ymp/scale5.1/ and is under a quality assurance plan, software quality assurance plans, and requirements based on 10 CFR 71 Subpart H.

Although there is no difference in the source SCALE software or data used for other Section 6 calculations and these scoping calculations, the scoping calculations were executed on a different set of workstations, using a different operating system. Thus, as a preliminary action, the benchmark validation set in Table 6-8 was reexecuted on the noted LINUX workstations. For the 125-experiment set, the average of all prior-computed k_{eff} values (as shown in Table 6-8 for the UNIX workstations) is 1.00792; the average of all reexecuted cases (using the LINUX workstations) is 1.00795. This indicates a negligible difference between calculations performed on the LINUX and UNIX computing platforms.

6.9.6.4 Scoping Calculations - Single Packages

Table 6-19 provides scoping calculation results for variant models based on cases *cv001* and *cv031*. The single-package scoping results support that a significant reduction in the neutron multiplication factor is expected from a reduced container loading from 1300 g (2.87 lb) Pu-239 to 200 g Pu-239, and that the inclusion of 30 g (0.066 lb) Be (with the 200 g [0.441 lb] Pu-239 loading) is a negligible positive reactivity effect. These results also support that modeling of the 30 g (0.066 lb) of Be as 30 g (0.066 lb) of Pu-239 is conservative, and that modeling of the 30 g (0.066 lb) of Be as 322 g (0.71 lb) Pu-239 on a volume replacement basis is highly conservative.

Table 6-19. Scoping Calculation Results for Single Packages

| Case | $k_{eff} \pm \sigma^a$ | Notes |
|---------------------------|------------------------|--|
| <i>cv001</i> ^b | 0.65648 ± 0.00046 | Prior UNIX result (see Table 6-1 and Table 6-15): Loading of a 1300 g (2.87 lb) Pu-239 metal sphere in the TB-1 vessel. The remaining TB-1 volume is filled with H ₂ O in this case, and in all <i>cv001</i> variants listed below. |
| <i>cv001-v0</i> | 0.65686 ± 0.00050 | Current result; rerun of <i>cv001</i> on LINUX workstations. |
| <i>cv001-v1</i> | 0.25956 ± 0.00050 | Loading of <i>cv001</i> changed to a homogeneous (metal alloy) sphere containing 200 g (0.441 lb) Pu-239 and 30 g (0.066 lb) Be, Be: Pu-239 = 4.0. |
| <i>cv001-v2</i> | 0.36315 ± 0.00048 | Loading of <i>cv001</i> changed to 200 g (0.441 lb) Pu-239 metal sphere surrounded by a 30 g (0.066 lb) Be metal shell. |
| <i>cv001-v3</i> | 0.35350 ± 0.00050 | Loading of <i>cv001-v2</i> changed to 200 g (0.441 lb) Pu-239 metal sphere. (The Be volume is modeled as H ₂ O.) |
| <i>cv001-v4</i> | 0.37073 ± 0.00048 | Loading of <i>cv001-v2</i> changed to 230 g (0.507 lb) Pu-239 metal sphere. (The Be mass is modeled as Pu-239 metal.) |
| <i>cv001-v5</i> | 0.48962 ± 0.00045 | Loading of <i>cv001-v2</i> changed to 522 g (1.151 lb) Pu-239 metal sphere. (The Be volume is modeled as Pu-239 metal.) |
| <i>cv031</i> ^b | 0.70756 ± 0.00055 | Prior UNIX result (see Table 6-1 and Table 6-15): The TB-1 vessel is loaded with a homogeneous metal-water mixture containing 1300 g (2.87 lb) Pu-239 metal, and adequate H ₂ O so as to completely fill the TB-1 volume. H: Pu-239 = 28.8. |
| <i>cv031-v0</i> | 0.70817 ± 0.00051 | Current result; rerun of <i>cv031</i> on LINUX workstations. |
| <i>cv031-v1</i> | 0.61285 ± 0.00054 | Loading of <i>cv031</i> changed to a homogeneous mixture of 200 g (0.441 lb) Pu-239 metal, 30 g (0.066 lb) Be metal, and adequate H ₂ O so as to completely fill the TB-1 vessel. H: Pu-239 = 192.4, Be: Pu-239 = 4.0. |
| <i>cv031-v2</i> | 0.61382 ± 0.00055 | Loading of <i>cv031-v1</i> changed to a homogeneous mixture of 200 g (0.441 lb) Pu-239 metal and adequate H ₂ O so as to completely fill the TB-1 vessel. H: Pu-239 = 194.5. (Be volume modeled as H ₂ O.) |
| <i>cv031-v3</i> | 0.62322 ± 0.00051 | Loading of <i>cv031-v1</i> changed to a homogeneous mixture of 230 g (0.507 lb) Pu-239 metal and H ₂ O. (Be mass modeled as Pu-239.) |
| <i>cv031-v4</i> | 0.66172 ± 0.00054 | Loading of <i>cv031-v1</i> changed to a homogeneous mixture of 522 g (1.151 lb) Pu-239 metal and H ₂ O. (Be volume modeled as Pu-239.) |

^a KENO V.a calculated k_{eff} and standard deviation values.

^b For *cv001* and *cv031* and variant models, the interior of the TB-1 vessel is fully occupied by the payload material (Pu-239, and Be if modeled), with all remaining volume within the TB-1 vessel volume occupied by H₂O. Structural materials of the TB-1 vessel and the PAT-1 container are not modeled. Instead, the TB-1 payload is centered within a cylinder of water; the water cylinder has the approximate outer dimensions of the PAT-1 container.

6.9.6.5 Scoping Calculations - Normal Condition of Transport Arrays

Table 6-20 provides scoping calculation results for variant models based on cases *fhlsf001* and *fhlsf031*. The conclusions are the same as for Table 6-19 single-package results. The computed neutron multiplication constant is significantly reduced by lowering the per-package payload from 1300 g (2.87 lb) Pu-239 to 200 g (0.441 lb) Pu-239, the effect of adding 30 g (0.066 lb) Be

to the 200 g (0.441 lb) Pu-239 loading appears insignificant, and modeling the Be as Pu-239 on mass-replacement or volume-replacement bases is conservative.

Table 6-20. Scoping Calculation Results for Normal Conditions of Transport Arrays

| Case | $k_{eff} \pm \sigma^a$ | Notes |
|-----------------------------|------------------------|---|
| <i>fhlsf001^b</i> | 0.65094 ± 0.00049 | Prior UNIX result (see Table 6-1 and Table 6-16): Each TB-1 vessel is loaded with a 1300 g (2.87 lb) Pu-239 metal sphere. The remaining TB-1 volume is filled with H ₂ O in this case, and in all <i>fhlsf001</i> variants listed below. |
| <i>fhlsf001-v0</i> | 0.65081 ± 0.00050 | Current result; rerun of <i>fhlsf001</i> on LINUX workstations. |
| <i>fhlsf001-v1</i> | 0.25262 ± 0.00047 | Loading of <i>fhlsf001</i> changed to a homogeneous (metal alloy) sphere containing 200 g (0.441 lb) Pu-239 and 30 g (0.066 lb) Be. |
| <i>fhlsf001-v2</i> | 0.35924 ± 0.00049 | Loading of <i>fhlsf001</i> changed to 200 g (0.441 lb) Pu-239 metal sphere surrounded by a 30 g (0.066 lb) Be metal shell. |
| <i>fhlsf001-v3</i> | 0.35163 ± 0.00050 | Loading of <i>fhlsf001-v2</i> changed to 200 g (0.441 lb) Pu-239 metal sphere. (Be volume modeled as H ₂ O.) |
| <i>fhlsf001-v4</i> | 0.36844 ± 0.00049 | Loading of <i>fhlsf001-v2</i> changed to 230 g (0.507 lb) Pu-239 metal sphere. (Be mass modeled as Pu-239.) |
| <i>fhlsf001-v5</i> | 0.48541 ± 0.00050 | Loading of <i>fhlsf001-v2</i> changed to 522 g (1.151 lb) Pu-239 metal sphere. (Be volume modeled as Pu-239.) |
| <i>fslsf031^c</i> | 0.63371 ± 0.00050 | Prior UNIX result (see Table 6-1 and Table 6-16): Each TB-1 vessel is loaded with a homogeneous metal-water mixture containing 1300 g (2.87 lb) Pu-239 metal, with adequate H ₂ O so as to completely fill the TB-1 volume. |
| <i>fslsf031-v0</i> | 0.63336 ± 0.00050 | Current result; rerun of <i>fslsf031</i> on LINUX workstations. |
| <i>fslsf031-v1</i> | 0.52070 ± 0.00050 | Loading of <i>fslsf031</i> changed to a homogeneous mixture of 200 g (0.441 lb) Pu-239 metal, 30 g (0.066 lb) Be metal, and H ₂ O. |
| <i>fslsf031-v2</i> | 0.52248 ± 0.00059 | Loading of <i>fslsf031-v1</i> changed to a homogeneous mixture of 200 g (0.441 lb) Pu-239 metal and H ₂ O. (Be volume modeled as H ₂ O.) |
| <i>fslsf031-v3</i> | 0.53184 ± 0.00050 | Loading of <i>fslsf031-v1</i> changed to a homogeneous mixture of 230 g (0.507 lb) Pu-239 metal and H ₂ O. (Be mass modeled as Pu-239.) |
| <i>fslsf031-v4</i> | 0.57872 ± 0.00050 | Loading of <i>fslsf031-v1</i> changed to a homogeneous mixture of 522 g (1.151 lb) Pu-239 metal and H ₂ O. (Be volume modeled as Pu-239.) |

^a KENO V.a calculated k_{eff} and standard deviation values.

^b Close-packed hexagonal-pitch array of 2646 undamaged packages, redwood modeled as H₂O (see Figure 6-2 and Figure 6-10).

^c Close-packed square-pitch array of 2601 undamaged packages, redwood modeled as H₂O (see Figure 6-2 and Figure 6-8).

6.9.6.6 Scoping Calculations - Hypothetical Accident Condition Arrays

Table 6-21 provides scoping calculation results for hypothetical accident condition arrays. These results further support the conclusions of Sections 6.9.5.4 and 6.9.6.5.

Table 6-21. Scoping Calculation Results for Hypothetical Accident Condition Arrays

| Case | $k_{eff} \pm \sigma^a$ | Notes |
|-------------------------------|------------------------|---|
| <i>hexs100^b</i> | 0.71538 ± 0.00050 | Prior UNIX result (see Table 6-1 and Table 6-17): Each TB-1 vessel is loaded with a homogeneous metal-water mixture containing 1300 g (2.87 lb) Pu-239 metal, with adequate H ₂ O so as to completely fill the TB-1 volume. |
| <i>hexs100-v0</i> | 0.71491 ± 0.00051 | Current result; rerun of <i>hexs100</i> on LINUX workstations. |
| <i>hexs100-v1</i> | 0.59043 ± 0.00050 | Loading of <i>hexs100</i> changed to a homogeneous mixture of 200 g (0.441 lb) Pu-239 metal, 30 g (0.066 lb) Be metal, and H ₂ O. |
| <i>hexs100-v2</i> | 0.59173 ± 0.00051 | Loading of <i>hexs100-v1</i> changed to a homogeneous mixture of 200 g (0.441 lb) Pu-239 metal and H ₂ O. (Be volume modeled as H ₂ O.) |
| <i>hexs100-v3^c</i> | 0.60218 ± 0.00049 | Loading of <i>hexs100-v1</i> changed to a homogeneous mixture of 230 g (0.507 lb) Pu-239 metal and H ₂ O. (Be mass modeled as Pu-239.) |
| <i>hexs100-v3a</i> | 0.57171 ± 0.00049 | Same as <i>hexs100-v3</i> , except that the H ₂ O density in the TB-1 vessel is reduced by 5%. |
| <i>hexs100-v4</i> | 0.65593 ± 0.00054 | Loading of <i>hexs100-v1</i> changed to a homogeneous mixture of 522 g (1.151 lb) Pu-239 metal and H ₂ O. (Be volume modeled as Pu-239.) |
| <i>hexs100-v4a</i> | 0.62931 ± 0.00049 | Same as <i>hexs100-v4</i> , except that the H ₂ O density in the TB-1 vessel is reduced by 5%. |
| <i>hexsdry^c</i> | 0.70268 ± 0.00065 | Prior UNIX result (see Table 6-1 and Table 6-17): Each TB-1 vessel is loaded with a homogeneous metal-water mixture containing 1300 g (2.87 lb) Pu-239 metal, with adequate H ₂ O so as to completely fill the TB-1 volume. |
| <i>hexsdry-v0</i> | 0.70344 ± 0.00054 | Current result; rerun of <i>hexsdry</i> on LINUX workstations. |
| <i>hexsdry-v1</i> | 0.58264 ± 0.00051 | Each TB-1 vessel contains a homogeneous metal-water mixture containing 200 g (0.441 lb) Pu-239. A 30 g (0.066 lb) uniform-thickness shell of Be metal lines the interior surface of the TB-1 vessel. All TB-1 volume is filled with either Be metal or the Pu-239-H ₂ O mixture. |
| <i>hexsdry-v2</i> | 0.57995 ± 0.00055 | Loading of <i>hexsdry</i> changed to a homogeneous mixture of 200 g (0.441 lb) Pu-239 metal, 30 g Be metal, and H ₂ O. |
| <i>hexsdry-v3</i> | 0.58414 ± 0.00052 | Loading of <i>hexsdry-v2</i> changed to a homogeneous mixture of 200 g (0.441 lb) Pu-239 metal and H ₂ O. (Be volume modeled as H ₂ O.) |
| <i>hexsdry-v4</i> | 0.59441 ± 0.00048 | Loading of <i>hexsdry-v2</i> changed to a homogeneous mixture of 230 g (0.507 lb) Pu-239 metal and H ₂ O. (Be mass modeled as Pu-239.) |
| <i>hexsdry-v4a</i> | 0.56395 ± 0.00052 | Same as <i>hexsdry-v4</i> , except that the H ₂ O density in the TB-1 vessel is reduced by 5%. |
| <i>hexsdry-v5</i> | 0.64122 ± 0.00055 | Loading of <i>hexsdry-v2</i> changed to a homogeneous mixture of 522 g (1.151 lb) Pu-239 metal and H ₂ O. (Be volume modeled as Pu-239.) |
| <i>hexsdry-v5a</i> | 0.61907 ± 0.00055 | Same as <i>hexsdry-v5</i> , except that the H ₂ O density in the TB-1 vessel is reduced by 5%. |

^a KENO V.a calculated k_{eff} and standard deviation values.

^b Close-packed array of 1152 damaged (side-impact model) packages (see Figure 6-4 and Figure 6-12). The redwood is modeled as full-density water.

^c Close-packed array of 1152 damaged (side-impact model) packages (see Figure 6-4 and Figure 6-12). The redwood is modeled as void.

The results of cases *hexs100-v3a*, *hexs100-v4a*, *hexsdry-v4a*, and *hexsdry-v5a* all confirm that although the modeled Pu mass (as a homogeneous Pu-239-H₂O mixture) for the Pu/Be cases is significantly less than the general-purpose 1300 g (2.87 lb) Pu load limit, the metal-water mixtures remain under moderated. For each of these four cases, a slight reduction in H₂O content modeled within the TB-1 vessel resulted in a significant reduction in the computed k_{eff} value. A similar effect would be expected for other PAT-1 NCS models, where the TB-1 payload is modeled as a homogeneous mixture of Pu metal and water.

6.9.6.7 Scoping Calculations - Single Package, Air Transport Provision

Table 6-22 provides scoping calculation results for single packages under the air transport accident provision. These results are consistent with conclusions of Sections 6.9.6.4 through 6.9.6.6.

Table 6-22. Scoping Calculation Results for Single Package, Air Transport Accident Provision

| Case | $k_{eff} \pm \sigma^a$ | Notes |
|---------------------------|------------------------|--|
| <i>sph14</i> ^b | 0.71468 ± 0.00050 | Prior UNIX result (see Table 6-1 and Table 6-18): The payload is modeled as a homogeneous metal-water mixture containing 1300 g (2.87 lb) Pu-239. |
| <i>sph14-v0</i> | 0.71540 ± 0.00050 | Current result; rerun of <i>sph14</i> on LINUX workstations. |
| <i>sph14-v1</i> | 0.62441 ± 0.00056 | The central sphere of <i>sph14</i> is modeled as two regions: a central sphere contains 200 g (0.441 lb) Pu-239 as a homogeneous metal-water mixture; and an enclosing Be metal shell of mass 30 g (0.066 lb). |
| <i>sph14-v2</i> | 0.62282 ± 0.00051 | The fuel sphere of <i>sph14</i> is changed to a homogeneous mixture of 200 g (0.441 lb) Pu-239 metal, 30 g (0.066 lb) Be metal, and H ₂ O. |
| <i>sph14-v3</i> | 0.62457 ± 0.00050 | The fuel sphere of <i>sph14-v2</i> is changed to a homogeneous mixture of 200 g (0.441 lb) Pu-239 metal and H ₂ O. (Be volume modeled as H ₂ O.) |
| <i>sph14-v4</i> | 0.63287 ± 0.00054 | The fuel sphere of <i>sph14-v2</i> is changed to a homogeneous mixture of 230 g (0.507 lb) Pu-239 metal and H ₂ O. (Be mass modeled as Pu-239.) |
| <i>sph14-v5</i> | 0.67065 ± 0.00051 | The fuel sphere of <i>sph14-v2</i> is changed to a homogeneous mixture of 522 g (1.151 lb) Pu-239 metal and H ₂ O. (Be volume modeled as Pu-239.) |

^a KENO V.a calculated k_{eff} and standard deviation values.

^b The mixture volume (or mixture volume plus Be shell volume for case *sph14-v1*) equals the internal volume of the TB-1 containment vessel. The containment vessel and remaining structural materials of the PAT-1 container are not explicitly modeled. Instead, the payload volume (1300 g (2.87 lb) Pu-239 as a metal-water mixture) is modeled as a sphere, surrounded by a water reflector providing a reflector thickness of 20 cm (7.87 in.). In all variant cases, a 20 cm-(7.87 in.) thickness of close-fitting water reflector is maintained.

6.9.6.8 Additional Scoping Calculations – Hypothetical Accident Condition Arrays (*hexmdry*)

In Sections 6.9.6.4 through 6.9.6.7, each limiting-case result in Table 6-1 (see Section 6.1.2) was considered with reduced Pu loadings (200 g [0.441 lb] Pu-239) and various modeling changes to account for the impact of 30 g (0.066 lb) Be.

For all array cases from Table 6-1, water was a dominant factor in controlling neutron moderation and secondary influences on package-to-package interaction. Even for case *hexsdry*, where the only PAT-1 structural materials in the model were the TB-1 vessel and outer drum

steels, water within the fully flooded TB-1 vessel remained a significant neutron moderator. Thus, the potential effects of beryllium to enhance package-to-package interaction effects (in the *hexdry* scoping calculations of Section 6.9.6.6) are masked by the presence of significant water moderation.

Case *hexmdry* (of Table 6-17) presents the same damaged-container and array models as case *hexdry*. Case *hexmdry* contains a payload of Pu-239 metal, as was selected as the basis model for Table 6-23 scoping calculations. The purpose of this final set of calculations is to more closely inspect for potential neutron moderating and reflecting effects of the beryllium, for array conditions where the Be surrounds the Pu-239 mass in each package and no H₂O moderator is present outside the TB-1 containment vessel.

The results of Table 6-23 indicate that the effect of the small mass of Be per package (30 g [0.066 lb]) is small compared to the effects of partial or full water flooding internal to the TB-1 vessels.

Table 6-23. Additional Scoping Calculation Results for Hypothetical Accident Condition Arrays

| Case | $k_{eff} \pm \sigma^a$ | Notes |
|-----------------------------|------------------------|---|
| <i>hexmdry</i> ^b | 0.67134 ± 0.00049 | Prior UNIX result (see Figure 6-17): Each TB-1 vessel is loaded with a 1300 g (2.87 lb) Pu-239 metal sphere, with the remaining volume within the TB-1 vessel being filled with H ₂ O. |
| <i>hexmdry-v0</i> | 0.67183 ± 0.00050 | Current result; rerun of <i>hexmdry</i> on LINUX workstations. |
| <i>hexmdry-v1</i> | 0.57556 ± 0.00023 | Same loading as <i>hexmdry</i> (1300 g (2.87 lb) Pu-239 metal sphere), all H ₂ O is removed from the TB-1 vessel (the only water in the model is the 30 cm (11.81 in.) thick external array reflector). |
| <i>hexmdry-v2</i> | 0.17899 ± 0.00010 | Similar to <i>hexmdry-v1</i> , except that the loading per TB-1 vessel has been changed to a homogeneous sphere of Pu-Be metal/alloy, containing 200 g (0.441 lb) Pu-239 and 30 g (0.066 lb) Be. |
| <i>hexmdry-v3.x</i> | 0.30226 ± 0.00049 | Similar to <i>hexmdry-v1</i> , except that the loading per TB-1 vessel has been changed to a 200 g (0.441 lb) sphere of Pu-239 metal. The k_{eff} increased from case <i>hexmdry-v2</i> due to the increased Pu density resulting from removal of the Be. |
| <i>hexmdry-v3.0</i> | 0.31515 ± 0.00049 | Similar to <i>hexmdry-v1</i> , except that the loading per TB-1 vessel has been changed to a 200 g (0.441 lb) sphere of Pu-239 metal surrounded by a close-fitting 30 g (0.066 lb) shell of Be metal. |
| <i>hexmdry-v3.10</i> | 0.32548 ± 0.00049 | Same loading as <i>hexmdry-v3.0</i> , a 1.0 cm thick shell of H ₂ O surrounds the Be/Pu-239. |
| <i>hexmdry-v3.20</i> | 0.33928 ± 0.00048 | Same loading as <i>hexmdry-v3.0</i> , a 2.0 cm thick shell of H ₂ O surrounds the Be/Pu-239. |
| <i>hexmdry-v3.30</i> | 0.35326 ± 0.00050 | Same loading as <i>hexmdry-v3.0</i> , a 3.0 cm thick shell of H ₂ O surrounds the Be/Pu-239. |
| <i>hexmdry-v3.f</i> | 0.36606 ± 0.00048 | Same loading as <i>hexmdry-v3.0</i> , the remainder of the TB-1 vessel is completely filled with H ₂ O. |

^a KENO V.a calculated k_{eff} and standard deviation values.

^b Close-packed array of 1152 damaged (side-impact model) packages (see Figure 6-4 and Figure 6-12). The redwood is modeled as void.

7. PACKAGE OPERATIONS

This section describes the operations used to load and unload the plutonium metal contents as described in Section 1.2.2 of this addendum. The section includes loading and unloading procedures for the configurations depicted in Figures 1-3 through 1-6; loading the *T-Ampoule Assembly*^A (designated T-Ampoule) and *Ring, Filler* (designated Ring Filler) in the TB-1 *Containment Vessel* (designated TB-1); loading the TB-1 in the AQ-1 overpack, preparing the package for shipment; and returning or storing the empty packaging.

The PAT-1 package shall be operated in accordance with applicable Nuclear Regulatory Commission (NRC), U.S. Department of Transportation, and other federal, state, and local regulations to protect the health and safety of the public, workers, and the environment. Furthermore, the PAT-1 shall be operated according to a National Nuclear Security Administration (NNSA) approved quality assurance (QA) plan and U.S. Department of Energy (DOE) Order 461.1A¹ requirements.

Specific criteria for operating the PAT-1 package with the plutonium metal content are presented in this section. The package user shall develop detailed site-specific operating procedures based on these criteria and on the NRC-issued certificate of compliance (CoC). Therefore, the operating procedures shall be written in accordance with 10 CFR 71,² Subparts A, G, and H. Operational radiation exposures for package operations shall be maintained to as low as reasonably achievable (ALARA), as required by the “Standards for Protection against Radiation” in 10 CFR 20.1101(b).³

7.1 Package Loading

The package user shall:

1. Be authorized to acquire, package, transport, or transfer radioactive, fissile, or special nuclear material;
2. Possess a copy of the current NRC PAT-1 CoC, SAR,⁴ and this SAR Addendum;
3. Comply with all requirements and restrictions specified in the NRC PAT-1 CoC, SAR,⁴ and this SAR Addendum;
4. Be a NRC or DOE, EM-60 registered user; and
5. Perform all PAT-1 operations under a NNSA-approved, site-specific, 10 CFR 71² Subpart H-compliant, QA plan.

A cutaway illustration of a PAT-1 package loaded and assembled for shipment is shown in Figure 7-1. The individual part names called out in the procedures are identified in *italics* and drawing number are provided in the tables for clarity. Prior to loading the PAT-1 package, verify that the requirements specified in Section 8.0 have been met for the *Overpack, AQ*

^A The title of the drawing is shown in italics and is used interchangeably with the designated name in this addendum. The drawing number and title information is shown in Section 1.3.2 and Table 7-1, 7-2, 7-3, and 7-4 in this addendum and in Chapter 9 of the SAR.⁴ Drawing titles and numbers are used to provide clarity of discussion when specifying components for the procedures.

(designated AQ-1), TB-1, *Ring, Filler, T-Ampoule Assembly, Inner Cradle*, and *Sample Container-1 (SC-1) Assembly* (designated SC-1) and *Sample Container-2 (SC-2) Assembly* (designated SC-2). This addendum describes the loading-related preparations, tests, and inspections of the T-Ampoule. It includes inspections performed prior to loading the package, to verify that it is not damaged and radiation and surface contamination levels are within allowable limits.

Assembled PAT-1

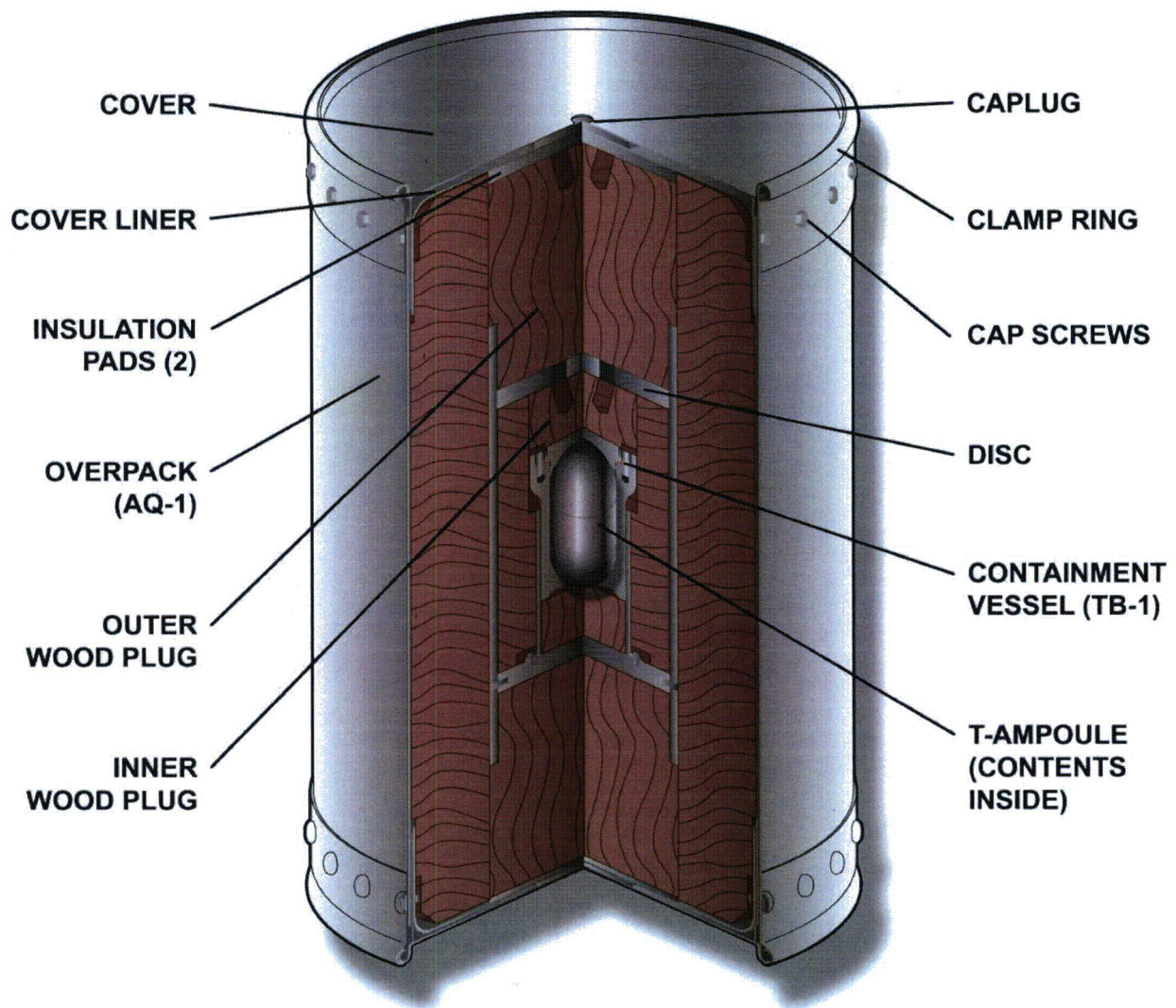


Figure 7-1. Assembled PAT-1 Showing AQ-1, TB-1, and T-Ampoule

7.1.1 Preparation for Loading

The TB-1 *Containment Vessel* (1017) is loaded while outside the *Overpack, AQ* (1002). See Section 1.2.2 of this addendum and the current CoC for the plutonium metal and composite contents.

Detailed, written operating procedures shall be prepared by the user to include, at a minimum, the process steps listed below before the plutonium metal content is placed into the PAT-1 package. These steps, initiated by the operating personnel and their supervisor, ensure that:

- (a) All applicable documents have been reviewed by operating personnel and are available for further review, if necessary.
- (b) The radioactive materials proposed for shipment are authorized by the CoC, and the use of the package complies with the conditions of the CoC.
- (c) The package has been properly maintained and is in an unimpaired condition. All required refurbishment and periodic maintenance shall have been performed and documented within the schedule requirements of the CoC, SAR, SAR Addendum, and maintenance program.
- (d) The TB-1 components are visually inspected for defects to include visible damage to the circular knife-edge on both the body and lid. Small nicks (0.079 cm [1/32 in.]) in the knife-edge may be hand-filed to restore contour and verified leak tight using the leakage rate test of 10^{-7} std cm³/s as described in Section 8.3.1 of the PAT-1 SAR.⁴ Larger nicks are not repairable and any leakage rate test of the TB-1 is no longer valid. If the container fails the leakage rate test, it must be scrapped and replaced with a new TB-1.
- (e) The used TB-1 *Gasket, Copper* (1019) is replaced with a new undamaged *Gasket, Copper* in usable condition prior to each shipment of a loaded TB-1.
- (f) The *O-ring* for TB-1 *Containment Vessel* (1017) is inspected for damage prior to each shipment, and replaced if necessary. The TB-1 *O-ring* is replaced after every third use for radioactive material shipment or annually, whichever occurs first.
- (g) A valid leak-test label must be present on the TB-1 *Containment Vessel* to ensure that the required acceptance, leakage rate test and the annual leakage rate test have been performed.
- (h) The *T-Ampoule Assembly* is inspected for any visible damage and replaced if necessary. Per 10 CFR 71.87(b), superficial surface marks are permitted, provided that they fall within part tolerance. The threads and *O-ring* for T-Ampoule groove in the *T-Ampoule Assembly* are inspected for damage. If damage is noted and the container fails a user defined 10^{-3} cm³ air/sec assembly leakage rate test, the container must be scrapped and replaced with a new *T-Ampoule Assembly*.
- (i) The *T-Ampoule Assembly O-ring* is inspected and replaced, if necessary. The *O-ring* is replaced annually or when damage is discovered.
- (j) Verification of a successful *T-Ampoule Assembly* required acceptance, leakage, rate test.

- (k) The *Ring, Filler* is inspected for damage and replaced if necessary. Per 10 CFR 71.87(b), superficial surface marks are permitted if they fall within the tolerance of the part. A *Ring, Filler* that no longer fits properly on top of the *T-Ampoule Assembly* (form and function not met) is scrapped and replaced.
- (l) The *Inner Cradle* for the *Sample Container-1 (SC-1) Assembly* or *Sample Container-2 (SC-2) Assembly* shipping configuration is inspected to ensure that it is appropriate for the planned configuration and free of damage. The *Inner Cradle*, once installed, is not expected to wear, and no periodic tests are required. The sample containers must slip freely into and out of the cradle. If tightness is noted during sample container installation, the distance between the legs of the cradle is measured to check for proper gap (7.692 ± 0.005 cm [3.030 ± 0.002 in.]). If tightness is noted, the *Inner Cradle* components should be inspected for damage. If no damage is located, the parts may be hand adjusted for proper fit.
- (m) The *Sample Container-1 (SC-1) Assembly* or *Sample Container-2 (SC-2) Assembly* are inspected for any visible damage and replaced, if necessary. If the threads are damaged on the sample containers and closure is not possible, the containers are scrapped.
- (n) The package's interior, nonfixed, surface contamination levels cannot significantly contaminate the contents. Nonfixed, surface contamination requirements are specified in 10 CFR 20.1906,³ 10 CFR 71.87(i),² and 49 CFR 173.443,⁵ for alpha-, beta-, and gamma-emitting radionuclides.
- (o) All closure fasteners are either furnished with the packaging or are certified replacements and acceptable for use.
- (p) All required package parts necessary equipment are available and ready for use.
- (q) The weight of the plutonium metal and the overall assembly weight of the sample container and *T-Ampoule Assembly* are recorded prior to shipment. The TB-1 contents weight (*Ring, Filler* [2A0262] and *T-Ampoule Assembly* and its contents) shall not exceed 2.1 kg (4.7 lb).

The user may replace the packaging parts listed in Table 7-1 during loading. The certification of all replacement parts must be traceable and recorded by the user. The replacement parts shall be recorded in the QA records with applicable identification information, date of replacement, disposition of the old part, and the name of the individual who performed the replacement, along with the name and signature of the individual who made the entry in the QA records. Records of replacement actions and certifications of completed actions shall be sent to SNL for records management and archiving.

There are two types of facilities that may be used depending on the loading or unloading operation:

- Glove boxes or glove bags, which are used to load and unload the plutonium metal contents into the SC-1 or SC-2 or T-Ampoule. These work spaces have a standard glove box line atmosphere: nitrogen or argon or helium or combination with an oxygen content not exceeding 0.5% and a water content not exceeding 20 parts per million.
- Open front hoods and downdraft rooms to load or unload SC-1 or SC-2 sample containers with plutonium metal contents into or out of the T-Ampoule. These work spaces do not provide an inert atmosphere. They are open work areas in a standard air atmosphere. Air flow in these work spaces are controlled to draw any potential contamination away from the operators and is exhausted through HEPA filters.

Both work space environments will be used as follows:

- Any sample container (*SC-1* or *SC-2*) or *T-Ampoule Assembly* directly loaded with plutonium will be processed (loaded) in either the glove box or glove bag work space. This will provide the inert atmosphere for the plutonium metal.
- Sample containers *SC-1* or *SC-2* (previously loaded in the glove box or glove bag with an inert atmosphere) will exit the glove box/glove bag and be decontaminated in either the open front hood or downdraft room. The decontaminated sample containers will then be placed into a *T-Ampoule Assembly* (previously prepared with the applicable *Inner Cradle*).

Pending facility requirements, the loading of the *T-Ampoule Assembly* with the decontaminated sample containers (*SC-1* or *SC-2*) may or may not be performed in open front hoods or downdraft rooms.

7.1.2 Loading of Contents

The operating procedures for the PAT-1 packaging with *T-Ampoule Assembly* configuration and plutonium metal content shall be specific regarding the handling of all packaging components and clearly state safety aspects or activities such as personnel protection (radiation, chemical, physical); surface contamination or radiation surveys; nuclear criticality safety; and environment temperature.

Table 7-1. Replacement Parts for the PAT-1 Packaging with *T-Ampoule Assembly*

| Part Name (ID) | Part Description | Part Material | Drawing/Specification ^a |
|---|-----------------------------------|--|------------------------------------|
| <i>Gasket, Copper</i> | Copper seal for TB-1 | Copper, half hard 110 ETP per QQ-C-576 ⁶ | 1019 |
| <i>O-ring, Viton®</i> , for TB-1 | V747-75-242 | Viton® | 1017, Item 5 |
| <i>Ring, Filler</i> | Filler between T-Ampoule and TB-1 | Ti-6Al-4V Grade 5 | 2A0262 |
| <i>T-Ampoule Assembly</i> | Lid and Body of T-Ampoule | Ti-6Al-4V Grade 5 | 2A0261 |
| <i>O-ring, Viton®</i> , for T-Ampoule | V-0747 M83248-1-241 O-ring | AMS-R-83248/1, Viton®, Parker Compound V0747-75 or approved equivalent | 2A0261, Item 3 |
| <i>Sample Container-1 (SC-1) Assembly</i> | Lid and Body of SC-1 | Ti-6Al-4V Grade 5 | 2A0268 |
| <i>Sample Container-2 (SC-2) Assembly</i> | Lid and Body of SC-2 | Ti-6Al-4V Grade 5 | 2A0265 |
| <i>O-ring, Viton®</i> , for SC-1 and SC-2 | V-0747 M83248-1-147 O-ring | AMS-R83248/1, Viton®, Parker Compound V0747-75 or approved equivalent | 2A0268, Item 3 2A0265, Item 3 |
| <i>Inner Cradle</i> | Titanium Cradle for SC-1 or SC-2 | Ti-6Al-4V Grade 5 | 2A0385 |

^a Drawings are provided in Appendix I.3.2.

7.1.2.1 Loading the *T-Ampoule Assembly*

The *T-Ampoule Assembly* has three basic loading configurations (see Section 1.2 for description):

- Plutonium metal hollow cylinder (831 and 731 gram weights)
- *Sample Container-1* in the *Inner Cradle* (3 of these containers)
- *Sample Container-2* in the *Inner Cradle* (2 of these containers)

The process for loading the plutonium metal, hollow cylinder or sample containers into the *T-Ampoule Assembly* is expected to proceed under the following conditions:

- The *T-Ampoule Assembly* (2A0261) loading operation with a plutonium metal hollow cylinder is performed in a glove box or glove bag with less than ambient atmospheric air pressure, with adequate exhaust filtration, and with appropriate control of surface cleanliness per established requirements for the glove box or glove bag being used.

- The sample container (*SC-1* or *SC-2*) loading operation with plutonium metal is performed in a glove box or glove bag with less than ambient atmospheric air pressure with adequate exhaust filtration, and with appropriate control of surface cleanliness for requirements established for the glove box or glove bag being used. The sample containers with plutonium metal content may be loaded into the *T-Ampoule Assembly* in the glove box or glove bag or in an open front hood or downdraft room.
- If sample containers are used, the *Inner Cradle* (2A0385) is already installed into the *T-Ampoule Assembly*.
- Appropriate processing, handling, and contamination control is implemented to maintain an uncontaminated (\leq free release limits) *T-Ampoule Assembly* exterior.
- The *T-Ampoule Assembly* shall be serialized, identified, and marked as necessary to identify its contents, and visually inspected to ensure proper assembly and freedom from significant defects. Data is recorded as appropriate.

Steps for loading the *T-Ampoule Assembly*:

1. Visually inspect the parts and materials listed in Table 7-1 for major imperfections,* damage, and cleanliness and ensure that they are ready for loading the specified content.
2. Follow specific content-loading instructions:
 - Plutonium metal hollow cylinder – See Section 7.1.2.1.1
 - *Sample Container-1 (SC-1)* or *Sample Container-2 (SC-2) Assemblies* – See Section 1
3. Visually inspect the *O-ring*, *Viton*[®], Parker Compound installed in the *Body, T-Ampoule* (2A0259) to ensure that it is properly lubricated and in place.
4. Engage and tighten the *Lid, T-Ampoule* (2A0260) with strap wrenches until the lid and body flange are fully seated.

Note: Because the *T-Ampoule Assembly* is designed with a bore seal, a specified torque is not required for proper closure of the *T-Ampoule Assembly*.

5. Verify that the weight of the *T-Ampoule Assembly* with its contents does not exceed 2035 g.

Note: This total weight does not include the weight of the *Ring, Filler*.

6. Clean and inspect the exterior of the *T-Ampoule Assembly* using standard health physics, swipe tests for plutonium contamination.

* Major imperfections are flaws, imperfections, or faults that will or may compromise the intended functionality of the assembly.

7. Implement appropriate processing, handling, and contamination control to maintain an uncontaminated (i.e., \leq free release limits) *T-Ampoule Assembly* exterior.

Note: The *T-Ampoule Assembly* is not a containment boundary. Thus, any leakage rate test requirements are user defined.

Table 7-2. Parts List for T-Ampoule Loading

| Quantity (each) | Item | Drawing/Specification |
|--|--|--|
| 1 | <i>T-Ampoule Assembly</i> | 2A0261 |
| | <i>Body, T-Ampoule</i> | 2A0259 |
| | <i>Lid, T-Ampoule</i> | 2A0260 |
| 1 | <i>O-ring, Viton[®], Parker Compound, for T-Ampoule, AS568B-241 (2-241)</i> | 2A0261, Item 3 |
| As required for hollow metal cylinder or samples shipped in SC-1 or SC-2. Sample Containers (see below) | Tantalum Foil | 0.001- to 0.009-in. thickness, minimum purity ranges - 99.75% (3N5), 99.98% (3N8) to 99.99% (4N) |
| As required for supplemental packing of hollow metal cylinder or samples shipped in SC-1 or SC-2 (see below) | Copper Foam | ERG Duocel Open Celled Copper Foam, 10% density, Alloy C10100 oxygen-free electronic grade copper conforming to ASTM F68 Class II or better. |
| Lubricant for T-Ampoule, SC-1 and SC-2 | Silicone Grease | Dow Corning High Vacuum Grease or equal |
| For sample shipments, either SC-1 or SC-2 sample containers are used. | | |
| 1 | <i>Inner Cradle</i> | 2A0385 |
| 3 | <i>Sample Container-1 (SC-1) Assembly</i> | 2A0268 |
| | <i>O-ring, Viton[®], Parker Compound, for SC-1, AS568B-147 (2-147)</i> | 2A0268, Item 3 |
| | <i>Lid, Sample Container-1 (SC-1)</i> | 2A0267 |
| | <i>Body, Sample Container-1 (SC-2)</i> | 2A0264 |
| 2 | <i>Sample Container-2 (SC-2) Assembly</i> | 2A0265 |
| | <i>O-ring, Viton[®], Parker Compound, for SC-2, AS568B-147 (2-147)</i> | 2A0265, Item 3 |
| | <i>Lid, Sample Container-2 (SC-2)</i> | 2A0269 |
| | <i>Body, Sample Container-2 (SC-2)</i> | 2A0266 |

7.1.2.1.1 Loading the Plutonium Metal, Hollow Cylinder

The plutonium metal, hollow cylinder described in Section 1.2 is may be wrapped with tantalum foil or not wrapped based on operational determination and loaded in the *T-Ampoule Assembly*. The plutonium metal hollow cylinder is then packed in the *T-Ampoule Assembly* with crushed tantalum foil. There are no positioning requirements for the plutonium metal, hollow cylinder.

The process for loading the plutonium metal hollow cylinder should proceed under the following conditions:

- The plutonium metal hollow cylinder loading operation is performed in a glove box with less than ambient atmospheric air pressure, with adequate exhaust filtration, and with appropriate control of surface cleanliness per established requirements for the glove box or glove bag being used.
- The plutonium metal hollow cylinder may be serialized, identified, and marked as necessary for data recording purposes, per site requirements.
- The plutonium metal hollow cylinder is ready for loading in the glove box or glove bag.
- Tools needed:
 - Strap wrenches – optional
 - User-supplied suction device
 - User-specified gripping tool such as tongs
 - Scale – 1% accuracy

Steps for loading the plutonium metal hollow cylinder into the *T-Ampoule Assembly*:

1. Visually inspect the parts and materials listed in Table 7-2 for major imperfections, damage, and cleanliness, and ensure that they are ready for loading the specified content.
 - Major imperfections of the metal components are cracks, pinholes, dents, deformed threads, and scratches (>0.001 in. deep).
 - Major imperfections of the O-ring are any indication of marring or chafing (i.e., scuff marks), or the O-ring does not have a round cross section.
2. In the glove box, weigh the plutonium metal hollow cylinder and record the weight.
3. Determine whether the plutonium metal hollow cylinder will be wrapped in tantalum foil or not. If the determination is to wrap the cylinder in foil, go to Step 3.a. If the determination is to leave the cylinder unwrapped, go to Step 4.
- 3.a. Wrap the plutonium metal hollow cylinder in tantalum foil and tuck in the foil ends.
4. Determine whether the plutonium metal hollow cylinder will be packed in the T-Ampoule using crushed tantalum foil, copper foam or no supplemental packing material. If the determination is to pack the hollow cylinder using crushed tantalum foil, go to Step 4.a. If the determination is to pack the hollow cylinder using copper foam, go to Step 4.b. Otherwise go to Step 5.
- 4.a. Add crushed tantalum foil to the open *Body, T-Ampoule*.

- 4.b. Place copper foam in the open *Body, T-Ampoule*.
5. Place the plutonium metal hollow cylinder into the *Body, T-Ampoule*. Add additional crushed tantalum foil as necessary to the sides and top based on operational determination.
6. Install the *Lid, T-Ampoule* and complete loading of the *T-Ampoule Assembly* according to the instructions in Section 7.1.2.1.
7. Weigh the loaded *T-Ampoule Assembly* with contents.
8. Record the weight of the loaded *T-Ampoule Assembly* with contents.

Caution: The maximum weight of the *T-Ampoule Assembly* with contents and *Ring, Filler* shall not exceed 2.1 kg (4.7 lb).

7.1.2.1.2 Loading the Sample Containers (*SC-1 [3 each] or SC-2 [2 each]*)

The plutonium metal sample contents, either bare or wrapped with tantalum foil, as described in Section 1.2 are packed in the sample containers. The sample containers are positioned and held in place, inside the *T-Ampoule Assembly* using an *Inner Cradle*, as depicted in Figures 1-3 and 1-4. Sample containers (*SC-1* and *SC-2*) shall not be comingled in the same *T-Ampoule Assembly*.

The process for loading plutonium (Pu) samples into the sample containers should proceed under the following conditions:

- The sample container loading operation is performed in a glove box or glove bag with less than ambient atmospheric air pressure, with adequate exhaust filtration, and with appropriate control of surface cleanliness per established requirements for the glove box or glove bag being used.
- The plutonium metal samples are properly prepared and ready for loading in the glove box or glove bag.
- The cradle is installed in the *T-Ampoule Assembly* per Section 7.1.2.1.3.
- The sample containers have been inspected and the O-rings properly lubricated and in place.
- Tools needed:
 - Strap wrenches – optional
 - User-supplied suction device
 - User-specified gripping tool such as tongs
 - Scale – 1% accuracy

Steps for loading the sample containers:

1. Visually inspect the parts and materials listed in Table 7-2 for major imperfections, damage, and cleanliness to ensure that they are ready for loading the specified content.
 - Major imperfections of the metal components are cracks, pinholes, dents, deformed threads, and scratches (>0.001 in. deep).
 - Major imperfections of the O-ring are any indication of marring or chafing (i.e., scuff marks), or the O-ring does not have a round cross section.
2. Verify that the *Inner Cradle* components (2A0385) are properly installed in the *T-Ampoule Assembly* (see Section 7.1.2.1.3) and that the *T-Ampoule Assembly* is ready for loading.
3. In the glove box or glove bag, weigh and record the plutonium metal.
4. Determine whether the plutonium metal contents will be wrapped in tantalum foil or not. If the determination is to wrap the contents in foil, go to Step 4.a. If the determination is to leave the contents unwrapped, go to Step 5.
 - 4.a. Wrap the contents in tantalum foil.
5. Determine whether the plutonium metal contents will be packed in the sample container (*SC-1*, 2A0268 or *SC-2*, 2A0265) using crushed tantalum foil, copper foam, or no supplemental packing material. If the determination is to pack the contents using crushed tantalum foil, go to Step 5.a. If the determination is to pack the plutonium metal contents in copper foam, go to Step 5.b. Otherwise, go to Step 6.
 - 5.a. Add crushed tantalum foil to the open *Body, Sample Container-1*, 2A0264 or *Body, Sample Container 2*, 2A0266.
 - 5.b. Place copper foam in the open *Body, Sample Container-1*, 2A0264 or *Body, Sample Container 2*, 2A0266.
6. Place the plutonium metal contents into the *Body, Sample Container-1*, 2A0264 or *Body Sample Container-2*, 2A0266.
7. Visually inspect the *O-ring*, Parker Compound, for *SC-1*, 2A0268, Item 3 or *SC-2*, 2A0265, Item 3 to ensure that it is properly lubricated and in place.
8. Engage and tighten by hand the *Lid, Sample Container (SC-1, 2A0267 or SC-2, 2A0269)* until the lid and body flange are fully seated. Hand tightening until seated is only required for proper closure of the *SC-1* or *SC-2*.
9. Weigh the sample container and record the weight.

Note: The maximum weight of the *T-Ampoule Assembly* with contents and *Ring, Filler* should not exceed 2.1 kg (4.7 lb).

10. Lift the sample container with a user-supplied suction pickup and place into the *Inner Cradle*.
11. Install the Spacer (2A0385-040 [2 each] for *SC-1* or 2A0385-045 [1 each] for *SC-2*) between the *SC-1s* and *SC-2s* as depicted in Figure 1-4 for the *SC-1s* or in Figure 1-3 for the *SC-2s* in this addendum with a user-specified gripping tool such as tongs. Visually center the Spacer within the *Inner Cradle*.
12. Repeat Steps 3 through 8 (only to Step 7 for the *SC-2* configuration) until sample containers are in place.

Note: Loading facility personnel have the option of preloading and weighing the *SC-1s* and *SC-2s* (Steps 3-6) and loading by repeating Steps 7 and 8.

13. Install the *Lid, T-Ampoule* and complete loading of the *T-Ampoule Assembly* per Section 7.1.2.1.

7.1.2.1.3 Installation and Removal of the Inner Cradle

7.1.2.1.3.1 Installation of the Inner Cradle

For shipment of *SC-1* or *SC-2* sample containers, an *Inner Cradle* is used to maintain position for normal conditions of transport (NCT). The minimum requirements for cradle installation are presented below; the user site shall prepare detailed installation instructions. Review Drawing 2A0385 (*Inner Cradle*) for assembly view and parts listing. The cradle components are installed as follows:

1. Position *Body, T-Ampoule* (2A0259) so that it is upright. Install Dish in Body (2A0385-020) in *Body, T-Ampoule*. The dish is not indexed.
2. Install four flat Leg(s) (2A0385-010) into slots in the Dish in Body. Position the legs so they are flush against the *Body, T-Ampoule* wall sides.
3. Install the Lock Ring (2A0385-030) so that it locks into the slots at the top of the leg. The correct assembly of the dish and legs will have the flat legs flush against the *Body, T-Ampoule* wall sides equidistant from each other.
4. Position *Lid, T-Ampoule* (2A0260) so that it is upright. Install the Dish in Lid (2A0383-025) in the *Lid, T-Ampoule*. The dish is not indexed.
5. Install four flat Leg(s) (2A0385-015) into slots in the upper dish. Position legs so that they are flush against the *Lid, T-Ampoule* wall sides.
6. Install Lock Ring (2A0385-030) so that it locks into the slots at the top of the leg. The correct assembly of the dish and legs will have the flat legs flush against the *Lid, T-Ampoule* wall sides equidistant from each other.
7. Measure distance (7.692 ± 0.005 cm [3.030 ± 0.002 in.]) shown in Drawing 2A0385 of this addendum) between two opposite legs to verify proper gap.

8. Verify that the Spacer(s) (2A0385-040 [2 each] for SC-1 or 2A0385-045 [1 each] for SC-2) are available for sample container loading operations identified in Section 7.1.2.1.2, Step 11 of this addendum.
9. The installation of the Spacer(s) is a step in the *SC-1* and *SC-2* loading procedures.

7.1.2.1.3.2 Removal of the Inner Cradle

Steps for removing the cradle components from the T-Ampoule:

1. Position *Body, T-Ampoule* (2A02659) so that it is upright. Remove Lock Ring from Leg(s).
2. Remove four flat Leg(s).
3. Remove Dish in Body from *Body, T-Ampoule*.
4. Position *Lid, T-Ampoule* (2A0260) so that it is upright. Remove Lock Ring from Leg(s).
5. Remove four Leg(s).
6. Remove Dish in Lid from *Lid, T-Ampoule*.
7. Inspect parts for damage and place all removed parts into labeled container for storage.
8. Verify that the Spacer(s) (2A0385-040 [2] for SC-1 or 2A0385-045 [1] for SC-2) are included with the stored items.

Note: The removal of the Spacer(s) is a step in the SC-1 and SC-2 unloading procedures.

7.1.2.2 Loading the T-Ampoule Assembly into the TB-1 Containment Vessel (1017)

The parts and materials required for loading the *T-Ampoule Assembly* into the TB-1 are listed in Table 7-3.

Table 7-3. Parts List for Loading the T-Ampoule into the TB-1

| Quantity | Item | Drawing/Specification |
|----------|---|-----------------------|
| 1 each | <i>TB-1 Shipping Vessel Assembly</i> ^a | 2A0263 |
| 1 each | <i>Body, TB</i> | 1022 |
| 1 each | <i>Lid, TB</i> | 1020 |
| 1 each | <i>Gasket, Copper</i> | 1019 |
| 1 each | <i>O-ring, Viton®</i> , Parker No. V747-75-242 | 1017, Item 5 |
| 12 each | <i>Bolt, Socket, Head, Special 0.500-20</i> | 1018 |
| 1 each | <i>Lifting, Sling (with Grommets installed)</i> | 1017 |

Table 7-3. Parts List for Loading the T-Ampoule into the TB-1 (Continued)

| Quantity | Item | Drawing/Specification |
|-------------|---|---|
| 1 each | <i>T-Ampoule Assembly</i> loaded with contents from Section 7.1.2 | 2A0261 |
| 3 each | Screw, Cap, Hex Head, 0.250-28 × 0.750 in. long | 1017, Item 7, MS90726-6 |
| 3 each | Washer | 1017, Item 8, MS27183-10 |
| 1 each | <i>Ring, Filler</i> | 2A0262 |
| As Required | Silicone grease | General Electric G-624 (MIL-S-8660) ⁷ or Dow Corning DC-4 (MIL-S-8660) |
| As Required | Labels, Nuclear Material | |
| As Required | Labels, Identification | |

^aThis part results from the assembly sequence. See drawing 2A0263 for assembly.

Steps for loading the *T-Ampoule Assembly* into the TB-1 *Containment Vessel*:

1. Visually inspect the components of the TB-1 *Containment Vessel* (see Table 7-3) for defects, damage, cleanliness, and for correct part numbers.

Note: See Section 7.1.1(d) for minor repairs to the knife-edge seal.
2. Use the inspection results in Step 1 and take the necessary steps to ensure that the TB-1 *Containment Vessel* components are in conditions necessary to ensure that the resultant package meets the requirements specified in 10 CFR 71.87.
3. Perform radiation contamination swipes to verify that nonfixed contamination levels are ALARA and within the specified limits prior to loading into the TB-1.
4. Place the loaded *T-Ampoule Assembly* into the *Body, TB* (1022).
5. Place and match the *Filler, Ring* into the *T-Ampoule Assembly* curved surface.

7.1.2.3 Closing the TB-1 *Containment Vessel*

Steps for closing the TB-1:

1. Install an unused *Gasket, Copper* into the seal groove at the top of the *Body, TB*.

Note: This is a single-use seal.

2. Coat the elastomeric *O-ring, Viton*[®] with Silicone Grease (see Table 7-3) and install it into the groove in *Lid, TB* (1020).

Note: The O-ring for the TB-1 *Containment Vessel* is replaced after every third use for radioactive material transport or annually, whichever occurs first.

3. Insert the *Lid, TB* into the *Body, TB*, taking care not to damage the O-ring.
4. Install the 12 Bolt, Socket, Head, Special 0.500-20 (1018), finger tight, through the *Lid, TB* into the *Body, TB*.
5. Tighten the 12 lid bolts, in two steps, in the following sequence: 1-7, 4-10, 2-8, 11-5, 3-9, 12-6. Tighten all bolts to 68 N·m (50 ft-lb) in the first step and to 102 N·m (75 ft-lb) in the second step.

Note: Do not use an impact wrench.

6. Attach the *Lifting, Sling* (1017) to the *Lid, TB* using the three Screw, Cap, Hex Head (0.250-28 × 0.750 in.) (1017) and Washers (1017).

Note: The *Lifting, Sling* remains with the TB-1 during loading into and unloading from the *Overpack, AQ*.

7. Perform a preshipment leakage rate test as specified in Section 8.2.3 of the SAR.⁴ The TB-1 *Containment Vessel* (assembled *Lid, TB*, and *Body, TB*) is assembled in accordance with the steps above and a leakage test shall be completed on the TB-1 *Containment Vessel* with its radioactive contents. This test shall indicate leakages less than 10^{-3} std atm cm³/sec. An acceptable test would be one in which the TB-1 is placed in a closely fitting chamber, a vacuum is rapidly drawn, and any subsequent rise in chamber pressure is correlated with leakage rate.

7.1.2.4 Loading the TB-1 Shipping Vessel Assembly into the Overpack, AQ

The parts and materials required for loading the *TB-1 Shipping Vessel Assembly* into the *Overpack, AQ* are listed in Table 7-4. These parts are visually inspected for major imperfections, damage, cleanliness, and the presence of the correct part number.

- Major imperfections of the metal components are cracks, pinholes, dents, deformed threads, and scratches (>0.001 in. deep).
- Major imperfections of the O-ring are any indication of marring or chafing (i.e., scuff marks), or the O-ring does not have a round cross section.

Use these inspection results and take the necessary steps to ensure that the TB-1 Containment Vessel components are in conditions necessary to ensure that the resultant package meets the requirements specified in 10 CFR 71.87.

The tool list for this procedure includes the following:

- Calibrated hand tools with a tolerance of ±5% for package assembly.

Table 7-4. Parts List for Loading the TB-1 Containment Vessel into the AQ-1 Overpack

| Quantity | Item | Drawing Number |
|-------------|--|--------------------------|
| 1 each | <i>TB-1 Shipping Vessel Assembly</i> | 2A0263 |
| 1 each | <i>Overpack, AQ</i> | 1002 |
| 1 each | <i>Container Subassembly</i> | 1003 |
| 1 each | <i>Plug, Removable</i> | 1014 |
| 1 each | <i>Disc, Removable</i> | 1002, Item 10 |
| 1 each | <i>Plug, Removable</i> | 1013 |
| 1 each | <i>Cover, Liner</i> | 1007 |
| 1 each | <i>Ring, Clamp, Modified</i> with 4 in. 304 SST 0.625-11 hex head bolt and 0.625-11 SST hex locking nut supplied as part of drum (Drawing 1004) | 1006 |
| 1 each | <i>Cover, Modified</i> | 1005 |
| 23 each | Screw Cap, Hexagon Head | 1002 Item 10, MS90726-60 |
| 1 each | <i>Pad, Installation</i> | 1027 |
| 1 each | <i>Pad, Installation</i> | 1026 |
| As required | Security wire and seal [This is a tamper indicating device (TID).] | |

Steps for loading the *TB-1 Shipping Vessel Assembly* (2A0263) into the *Overpack, AQ* (1002):

1. Perform the required contamination swipes to verify that nonfixed contamination levels are ALARA and within the limits specified in 49 CFR 173.443⁵ prior to loading *TB-1 Shipping Vessel Assembly* into the *Overpack, AQ*.
2. Set the *Container Subassembly* (1003) of the *Overpack, AQ* upright prior to loading the *TB-1 Shipping Vessel Assembly*.
3. Visually inspect the removable components of the *Overpack, AQ* (see Table 7-4) for defects, damage, cleanliness, and correct part number.
4. Load the *TB-1 Shipping Vessel Assembly* into the *Overpack, AQ-1* assembly using the Lifting, Sling and ensuring that the *TB-1 Shipping Vessel Assembly* is fully seated. This operation is performed manually because the total weight of the TB-1 is less than 22.7 kg (50 lb). A small hoist (453.6 kg [1000 lb] capacity) may be used to lift the TB-1; however, it is not necessary.

Note: The Lifting, Sling remains with the TB-1 during loading into and unloading from the *Overpack, AQ*.

5. Place the smaller inner wooden plug (*Plug, Removable* 1014) on top of the *TB-1 Shipping Vessel Assembly*, aligning the notches in the plug to clear the Sling, Lifting cap screws in the TB-1.
6. Insert, in order, the (1) aluminum disk (*Disc, Removable* (1002)), (2) outer wooden plug (*Plug, Removable* 1013), and (3) the inner larger insulation pad (*Pad, Installation* (1026)), which is centered.
7. Insert, in order, (1) the *Cover, Liner* (1007), (2) the outer smaller insulation pad (*Pad, Installation* [1027]), which is centered, (3) the *Cover, Modified* (1005), and (4) the *Ring, Clamp, Modified* (1006).

Note: During installation, align the index marks on the *Cover, Liner*, the *Cover, Modified*, and the *Ring, Clamp, Modified*, with the index mark on the *Overpack, AQ-1*. A tapered pin is used to line up the holes with the index marks.

8. Install the 23 screw caps, Hexagon Head (MS90726-60) (1002), finger tight, through the assembled clamp ring and covers. Start by installing one hexagon head screw into the hole by the index mark, and tighten until finger tight. Install the remaining hexagon head screws one-by-one: one to left of the first screw, then one to the right of the first screw, working back and forth toward the gap in the clamp ring. Use a tapered pin to help line up these holes.

Note: If some of the screws are faulty and will not screw in, replace them with new certified hexagon head screws.

9. Tighten the 23 hexagon head screws to 20.3 N·m (15 ft-lb).

CAUTION: Impact wrenches should not be used. For Steps, 8-10, use calibrated hand tools with a tolerance of $\pm 5\%$ for closure of the package.

10. Install the 4-in.-long hexagon head screw in the clamp ring and tighten to 68 N·m (50 ft-lb).

Note: Impact wrenches should not be used.

11. Install the locking nut on the 4-in.-long screw. Hold a wrench on the screw to keep it from turning, and torque the nut to 41 N·m (30 ft-lb).

A security wire and seal (tamper indicating device [TID]) are installed through the holes provided in the clamp ring lugs.

7.1.3 Preparation for Transport

7.1.3.1 PAT-1 Package Handling

Based on the proposed maximum weight of 1300 g (2.87 lb) plutonium metal, the Criticality Safety Index (CSI) is 0.1.

The PAT-1 package is handled using hoists or forklifts and a strap or specially made drum handling equipment to lift and rotate the package. Operating procedures shall include requirements for safe handling of the package and requirements to limit clamping pressures on the forklift drum handling equipment to prevent damage to the *PAT-1 Assembly* (1001).

7.1.3.2 *PAT-1 Package Decontamination*

The PAT-1 package may be placed in areas subject to contamination. If the package becomes contaminated, each user shall prepare procedures to decontaminate packages. The procedures should consider, at a minimum, the following:

- Exterior of the package is stainless steel.
- Package vent holes are sealed with plastic plugs.
- Labels and markings on the package must be legible.
- Cleaning solution must be checked for radioactive contamination after use.

7.1.3.3 *Requirements Prior to Transport of PAT-1 Package*

Prepare the PAT-1 for transport as follows:

1. The onsite movement of this package to storage or to a staging area will be performed in accordance with approved facility procedures.
2. The procedure for loading the PAT-1 package onto the shipping skid is presented below:
 - a. Skid – The PAT-1 is loaded on a PAT-1 wooden skid for transportation and handling. ASTM D 3953⁸ describes proper strapping of the PAT-1 to the wooden skid. All wooden items (wood crates, shipping containers, dunnage, and pallets) are to conform to the appropriate U.S., United Nations (UN), and European Union (EU) legislation regarding *bursaphelenchus xylophilus*, commonly known as the pine wood nematode, and is to be marked appropriately. The containers are typically marked with the letters “HT,” which means heat treatment and is described on the following website:
http://www.aphis.usda.gov/import_export/plants/plant_exports/wpm/wpm_heat_treatment.shtml). General information discusses the requirement for the wood and is located at the following website:
http://www.aphis.usda.gov/import_export/plants/plant_exports/wpm/index.shtml. Procurement documentation for the heat-treated wood shall be retained by SNL. The PAT-1 is steel-banded to the skid that is provided with the AQ-1 overpack for transportation and handling.
 - b. Lifting Equipment – An overhead hoist of the required capacity with a nylon strap may be used to load the PAT-1 package onto the PAT-1 skid. If a suitable overhead hoist is unavailable, a forklift may be used with a nylon strap attached to the tines. Alternately, a forklift equipped with nonmarring side grippers or a forklift drum lifter/rotator designed for the 24 ½ in. diameter of the PAT-1 with

226.8 kg (500 lb) capacity (with safety factor) can be used. Gripping pressure over a 1 ft² area on each side is not to exceed 40 psi (5760 lb). The gripper equipment must meet the requirements of 29 CFR 1910.178.⁹

- c. Handling – The PAT-1 is easily hoisted or lowered with a nylon strap attached to midpoint of the upright or horizontal PAT-1, either by the hoist or forklift. For loading onto the skid, the PAT-1 is positioned over the skid and slowly lowered.
- d. Transport – The skid mounted PAT-1 may be moved, after being properly secured, with a forklift from one location to another or loaded onto a truck for transport to an aircraft loading facility.

The shipper shall ensure that the quality control requirements of 49 CFR 173.475⁵ and the routine determination requirements of 10 CFR 71.87² have been satisfied prior to each shipment. The detailed operating procedures of 10 CFR 71.87(f) shall provide evidence that these requirements are met and shall include, at a minimum, the process steps listed below for preparing the PAT-1 for transport:

1. Verify that the package is proper for the content shipped and verified with the appropriate records by the user prior to content loading per 10 CFR 71.87(a).
2. Verify that the package is in an unimpaired physical condition per 10 CFR 71.87(b).
3. Ensure that the package closure devices are properly installed, secured, and free of defects per 10 CFR 71.87(c).
4. Ensure that the containment vessel has been properly loaded and requirements for shipment have been followed, witnessed, checked, and noted in the QA log.
5. Ensure the internal pressure of the containment system does not exceed the design pressure during transportation per 10 CFR 71.85(b); there are no pressure relief devices per 10 CFR 71(e) in the package.
6. Perform surveys for nonfixed surface contamination. The surveys shall be performed in accordance with user facility procedures. The survey shall use criteria derived from the surface radioactivity guidance of 10 CFR 20.1906,³ 10 CFR 71.87(i),² 49 CFR 173.443,⁵ or the user's site-specific criteria, whichever is the most stringent. Surface contamination on any part of the package must not exceed the limits specified in 49 CFR 173.443, Table 9.⁵
7. Perform radiation measurements. Emanations must not exceed the limits prescribed in 49 CFR 173.441.⁵ Measuring equipment used for surveys must be calibrated and of sufficient accuracy. The radiation (gamma, neutron) emanating from the package shall be measured before the package is released for transport per 10 CFR 71.47 and 71.87(j).² The radiation dose rate is measured at the surface to ensure that it does not exceed the expected or allowable dose rate. It is also measured at 1 meter from the package to determine the package's transportation index (TI).

8. Mark and label the outside of the package in conformance with 49 CFR 172,¹⁰ Sections D and E, 49 CFR 172.310, 172.400, and 172.403 (classified information shall not be revealed).
9. Verify that the package has been properly leak tested and results are noted in the QA log.
10. Ensure all lifting and handling equipment is available and certified for use.
11. Load the PAT-1 on the skid and check strapping for transport.
12. Ensure all loading records for shipment are prepared and maintained.

7.1.3.4 Securing Package to Transport Vehicle

The PAT-1 package shall be secured against movement within the transport vehicle under conditions normally incident to transportation per 49 CFR 177.834¹¹ and 177.842(d). Detailed securing procedures shall be prepared by the shipper and include these requirements as a minimum. The loading and unloading procedures shall include measures to ensure that:

1. DOE/OST package tie down requirements are met.
2. Only an approved, DOE/OST conveyance is used.
3. All reasonable precautions are, employed to prevent motion of the vehicle during loading and unloading.
4. No tampering of packages occurs during transportation.
5. No transport vehicle is loaded or unloaded unless a qualified person, as established according to the loading or unloading procedure, is in attendance, at all times.

7.2 Package Unloading

7.2.1 Receipt of Package from Carrier

Upon receipt of the PAT-1 package from the transport carrier, the following steps must be completed:

1. The consignor (hereafter referred to as the shipper) shall provide any special instructions to the consignee (hereafter referred to as the receiver) to safely open the package per 10 CFR 71.89, including special tools and precautions for handling or unloading. These instructions shall include special actions in the event the tamper indicating device (TID) is not intact, surface contamination is too high, or radiation surveys are too high.
2. The receiver shall accept the package by surveying the conveyance and package surface for contamination and external radiation levels. The receiver's procedures shall clearly indicate that contamination and radiation surveys and inspections shall be conducted upon receipt of the package. The receiver shall, at a minimum, include the following in their procedures in accordance with 10 CFR 71.111:

- Surveying of the conveyance and package for radioactive contamination and radiation levels.
 - Examining the packaging for surface damage that may have occurred during shipping or handling.
 - Examining the TID to ensure the package has not been tampered with during transport. Reporting when a TID is not intact.
 - Ensuring that all lifting and handling equipment is available and certified for use.
3. All users shall include provisions for reporting safety concerns associated with the packaging or its use. The user shall notify the NRC in accordance with 10 CFR 20.2202, and DOE in accordance with DOE Order 231.1A and 10 CFR 20.2202. Although 10 CFR 20.2202 provides a graduated reporting period based on the severity of the incident, DOE Order 231.1A delineates specific reporting periods in accordance with the category of the occurrence. Incidents that require notification include:
- Removable radioactive surface contamination in excess of the limits specified in 10 CFR 71.87; and
 - External radiation levels in excess of the limits specified in 10 CFR 71.47.
4. At a minimum, the user shall maintain the records outlined below for the radiation protection program and the dosimetry records of all monitored individuals:
- ALARA plans and programs and their implementation
 - Individual occupational dose records
 - Monitoring and area control records
 - Monitoring method records
 - Training records of site employees, radiation workers, and radiation safety personnel
 - Records of exposure (provided to all workers)

7.2.2 Removal of Contents

This section describes the operations for unloading the contents from the PAT-1 package.

Should the TID be damaged or not intact, verify that there is no leakage of contents. Notify the shipper and the carrier about the TID. Do not proceed until the cause of damage has been determined.

The operational steps include:

1. Remove the PAT-1 from the skid, if not already performed.
2. Inspect for tampering and remove the security wire and seal.
3. Remove the 23 Screw, Cap, and Hexagon Head at the top of the package.
4. Remove the 4-in.-long hex head screw and associated lock nut from the *Ring, Clamp Modified* (1006).
5. Remove the *Ring, Clamp Modified*.
6. Remove the *Cover, Modified* (1005).
7. Remove the outer, smaller insulation pad (*Pad, Insulation* [1027]).
8. Remove the *Cover, Liner* (1007).
9. Remove the inner, larger insulation pad (*Pad, Insulation* [1026]).
10. Remove the outer wood plug (*Plug, Removable* [1013]).
11. Remove the aluminum disc (*Disc, Removable* [1002, Item 10]).
12. Remove the inner smaller wood plug (*Plug, Removable* [1014]).
13. Lift the *TB-1 Shipping Vessel Assembly* (2A0263) out of the *Overpack, AQ* (1002) using the TB-1 lifting sling.

Note: The Lifting Sling remains attached to the TB-1 during loading and unloading into the *Overpack, AQ-1*.

14. Remove the lifting sling from the *TB-1 Shipping Vessel Assembly*.

CAUTION: Pressure relief action may accompany removal of the TB-1 vessel lid. Use the following step to safely release this pressure.

1. Loosen the TB-1 closure bolts incrementally until any pressure is relieved.

7.2.2.1 *Opening the TB-1 and Removing the T-Ampoule Assembly from the TB-1*

See discussion in Section 7.1.1 of this addendum for facility requirements for unloading a filled *T-Ampoule Assembly*.

Steps for opening the *TB-1* and unloading the *T-Ampoule Assembly*:

1. Remove the 12 Bolt, Socket, Head (1018) that secures the *Lid, TB* (1020) to the *Body, TB* (1022).

2. Remove the *Lid, TB* from the *Body, TB*. This can be done by reinstalling the 3 screws (1017, Item 7, used for the lifting sling) and turning them evenly until the lid releases.
3. Remove *Ring, Filler* (2A0262).
4. Remove the *T-Ampoule Assembly* (2A0261) with contents from the *TB-1*. Unloading of the filled T-Ampoule is performed based on user facility requirements.
5. Reassemble the TB-1, install in the *Overpack, AQ* (1002) and place the PAT-1 package in safe storage.

7.2.2.2 *Opening the T-Ampoule Assembly in a Controlled Atmosphere*

The receiving facility will develop the necessary detailed procedures for opening the T-Ampoule loaded with a plutonium hollow cylinder or sample containers.

7.2.2.2.1 Unloading a T-Ampoule Assembly with Plutonium Metal Hollow Cylinder

The process for unloading the *T-Ampoule Assembly* with plutonium metal hollow cylinders should proceed under the following conditions.

- Unloading the *T-Ampoule Assembly* with plutonium hollow metal cylinder is performed in a glove box with less than atmospheric air pressure, with adequate exhaust filtration, and with appropriate control of surface cleanliness for requirements established for the glove box or glove bag being used.
- Radiation monitoring personnel to check for contamination.
- Tools needed:
 - Strap wrenches
 - User-specified gripping tool such as tongs

Steps for unloading the plutonium metal hollow cylinder from the *T-Ampoule Assembly*:

1. Monitor for contamination before opening the *T-Ampoule Assembly* and when readied for storage.
2. Loosen *Lid, T-Ampoule* and *Body, T-Ampoule* with strap wrenches.
3. Place *T-Ampoule Assembly* upright with *Lid, T-Ampoule* at the top.

Optional: The *T-Ampoule Assembly* may be placed horizontal for unloading plutonium metal hollow cylinders.

4. Remove the *Lid, T-Ampoule* by hand.
5. Remove plutonium metal hollow cylinder with user specified gripping tool and packing material, if used.

6. Replace *Lid, T-Ampoule* by hand.
7. Clean and inspect the exterior of the T-Ampoule Assembly using standard health physics, swipe tests for plutonium contamination.
8. Place *T-Ampoule Assembly* in storage.

7.2.2.2.2 Unloading a T-Ampoule Assembly with Sample Containers

The process for unloading the *T-Ampoule Assembly* with sample containers *SC-1* or *SC-2* should proceed under the following conditions.

- Unloading the *T-Ampoule Assembly* with *Sample Containers* is performed in a glove box or glove bag with less than atmospheric air pressure, with adequate exhaust filtration, and with appropriate control of surface cleanliness for requirements established for the glove box or glove bag being used.
- Radiation monitoring personnel to check for contamination.
- Tools needed:
 - Strap wrenches
 - User specified gripping tool such as tongs
 - User supplied suction device

Steps for unloading the *Sample Containers* from the *T-Ampoule Assembly*:

1. Monitor for contamination before opening the *T-Ampoule Assembly* and when readied for storage.
2. Loosen *Lid, T-Ampoule* and *Body, T-Ampoule* with strap wrenches.
3. Place *T-Ampoule Assembly* upright with *Lid, T-Ampoule* at the top.
4. Remove the *Lid, T-Ampoule* by hand.
5. Remove *Sample Containers* with user supplied suction device or user specified gripping tool. Remove the *Spacer(s)* between the *Sample Containers*.
6. Loosen *Lid, Sample Container* for *SC-1* or *SC-2* by hand or with strap wrenches.
7. Remove contents and packing from the *Sample Container(s)*.
8. Replace *Lid, Sample Container* for *SC-1* or *SC-2* by hand.
9. Place empty assembled *Sample Containers* and *Spacers* in *Body, T-Ampoule* using a user supplied suction device or user specified gripping tool.
10. Replace *Lid, T-Ampoule* by hand.

11. Clean and inspect the exterior of the *T-Ampoule Assembly* using standard health physics, swipe tests for plutonium contamination.
12. Place *T-Ampoule Assembly* in storage.

7.3 Preparation of Empty Package for Transport

If the empty PAT-1 package is to be transported, the following procedure shall be employed. Note that the empty PAT-1 package may be shipped without a *T-Ampoule Assembly*. Section 7.3.1 applies when the PAT-1 is shipped with an empty *T-Ampoule Assembly*. Section 7.3.2 applies when the PAT-1 is shipped without a T-Ampoule.

Note: When storing or preparing an empty TB-1 vessel for return shipment, care should be taken to avoid damaging the knife-edges (which engage the copper gasket) on the lid and body of the vessel.

7.3.1 Transporting the PAT-1 Package with an Empty T-Ampoule

1. Ensure that the contents have been removed from the *T-Ampoule Assembly* (2A0261) and that the *T-Ampoule Assembly* is free of contamination.
2. Tighten (hand tight) the *T-Ampoule Assembly* with the existing O-ring.
3. Place the *T-Ampoule Assembly* within the *Body TB* (1022).
4. Place Lid, TB (1020) with previously installed copper seal and O-ring on the body and tighten the 12 cap screws to 34 N·m (25 ft·lb) in the following sequence: 1-7, 4-10, 2-8, 11-5, 3-9, 12-6.

Note: Prepare a template with the numbering sequence in a clockwise orientation. Arbitrarily define one hole in the TB-1 as "1" and tighten according to the sequence.

5. Visually inspect the *Overpack, AQ* (1002) for damage, defects, and cleanliness.
6. Attach the lifting sling on the TB-1 using the three cap screws (0.250-28UNF) and washers.
7. Using the lifting sling, place the TB-1 in the *Overpack, AQ* and make sure it is seated.
8. Place the inner wood plug (smaller, [1014]) on top of the TB-1 and align the notches in the plug to clear the lifting screws in the TB-1.
9. Insert, in order, (1) the aluminum disk (1002, Item 10), (2) the outer wood plug (1013), and (3) the inner insulation pad (larger, [1026]).
10. Insert, in order, (1) the cover liner (1007), (2) the outer insulation pad (smaller, 1027), cover (1005), and (3) clamp ring (1006) with the index mark aligned to the index mark on the *Overpack, AQ* (1002).

11. Install the 23 hexagon head bolts through the assembled clamp ring, cover, and cover liner and finger tighten.
12. Tighten the 23 hexagon head bolts to 20 N·m (15 ft-lb).
13. Install the 4-in.-long hexagon head bolt in the clamp ring and tighten to 68 N·m (50 ft-lb).
14. Install the locking nut on the 4-in.-long bolt and tighten to 41 N·m (30 ft-lb).

7.3.2 Transporting an Empty PAT-1 package without a T-Ampoule

1. Place *Lid, TB* (1020) with previously installed copper seal and O-ring on body and tighten the 12 cap screws to 34 N·m (25 ft-lb).
2. Visually inspect the *Overpack, AQ* (1002) for damage, defects, and cleanliness.
3. Attach the lifting sling on the TB-1 lid using the three cap screws (0.250-28UNF) and washers.
4. Place the TB-1 in the *Overpack, AQ* using the lifting sling, and make sure it is seated.
5. Place the inner wood plug (smaller, [1014]) on top of the TB-1 and align the notches in the plug to clear the lifting screws in the TB-1.
6. Insert, in order, (1) the aluminum disk (1002, Item 10), (2) the outer wood plug (1013), and (3) the inner insulation pad (larger, [1026]).
7. Insert, in order, (1) the cover liner (1007), (2) the outer insulation pad (smaller, [1027]), (3) the cover (1005), and (4) the clamp ring (1106) with the index mark aligned with the index mark on the *Overpack, AQ*.
8. Install the 23 hexagon head bolts through the assembled clamp ring, the cover, and the cover liner and finger tighten.
9. Tighten the 23 hexagon head bolts to 20 N·m (15 ft-lb).
10. Install the 4-in.-long hexagon head bolt in the clamp ring and tighten to 68 N·m (50 ft-lb).
11. Install the locking nut on the 4-in.-long bolt and tighten to 41 N·m (30 ft-lb).
12. If the package is transported off-site, ensure compliance with 49 CFR 173.443 Table 9, Surface Contamination (at each of the required stages of the packing process), and 49 CFR 172 Sections D & E (49 CFR 172.310, .400 and .403), Marking and Labeling.

The package is now ready for empty transport or storage.

7.4 Other Operations

Through special arrangement with the transport carrier, the shipper shall ensure observance of the operational controls for each air shipment of plutonium, as specified in the package Certificate of Compliance (CoC).

7.5 Appendix

7.5.1 References

1. United States. Dept. of Energy. DOE Order 461.1A, "Packaging and Transfer or Transportation of Materials of National Security Interest." October 2, 1996.
2. United States. Nuclear Regulatory Commission. Code of Federal Regulations, 10 CFR 71. "Packaging and Transportation of Radioactive Material." January 1, 2009.
3. United States. Nuclear Regulatory Commission. Code of Federal Regulations, 10 CFR 20. "Standards for Protection Against Radiation." January 1, 2009.
4. United States. Nuclear Regulatory Commission. NUREG-0361. "Safety Analysis Report for the Plutonium Air Transportable Package, Model PAT-1." Washington, D.C. 1978.
5. United States. Dept. of Transportation. Code of Federal Regulations, 49 CFR 173. "Shippers – General Requirements for Shipments and Packaging." October 1, 2008.
6. QQ-C-576, Federal Specification Copper Flat Products with Slit, Slit and Edge-Rolled, Sheared, Sawed or Machined Edges (Plate, Bar, Sheet, and Strip). July 12, 1961.
7. MIL-S-8660C, Military Specification Silicone Compound, NATO Code Number S-736. September 22, 1983.
8. ASTM D 3953 – 07a. "Standard Specification for Strapping, Flat Steel, and Seals," ASTM International. West Conshohocken, PA. October 1, 2007.
9. United States. Occupational Safety and Health Administration, Labor. Code of Federal Regulations, 29 CFR 1910.178. "Powered Industrial Trucks.." July 1, 2008.
10. United States. Dept. of Transportation. Code of Federal Regulations, 49 CFR 172. "Hazardous Materials Table, Special Provisions, Hazardous Materials Communications, Emergency Response Information, and Training Requirements." October 1, 2008.
11. United States. Dept. of Transportation. Code of Federal Regulations. 49 CFR 177. "Carriage by Public Highway." October 1, 2008.

8. ACCEPTANCE TESTS AND MAINTENANCE PROGRAM

The acceptance tests and maintenance program for the PAT-1 package *Overpack, AQ* (designated AQ-1) and TB-1 *Containment Vessel*^A (designated TB-1) are described in the SAR¹ (NUREG-0361, Chapter 8). This section describes the acceptance tests and maintenance program for the *Ring, Filler* (Drawing 2A0262, designated Ring Filler); *T-Ampoule Assembly* (Drawing 2A0261, designated T-Ampoule); *Sample Container-1 (SC-1) Assembly* (Drawing 2A0268, designated SC-1); *Sample Container-2 (SC-2) Assembly* (Drawing 2A0265, designated SC-2); and *Inner Cradle* (Drawing 2A0385, designated Inner Cradle). Minimum acceptance requirements for fabricating, procuring, and maintaining these components are presented in this section. Detailed procedures shall be developed based on criteria contained herein and on the Certificate of Compliance (CoC)². The fabrication specifications for these components are listed on the fabrication drawings in Section 1.3.2 and Section 1.3.3 of this addendum, respectively.

8.1 Acceptance Tests

This section describes the acceptance tests for the *Ring, Filler*, the *T-Ampoule Assembly*, the *Sample Container-1 (SC-1) Assembly*, the *Sample Container-2 (SC-2) Assembly*, the *Inner Cradle*, and procured components. Note that SC-1 or SC-2 is used as the short form of the long drawing name. For this section, these items are grouped as "T-Ampoule components" and are described in Table 8-1.

Table 8-1. T-Ampoule Components

| Item | Description | Material | Drawing No. ^a |
|---|--|--|----------------------------------|
| <i>Ring, Filler</i> | Filler between T-Ampoule and TB-1 | Ti-6Al-4V Grade 5 | 2A0262 |
| <i>T-Ampoule Assembly</i> | Lid and Body of T-Ampoule | Ti-6Al-4V Grade 5 | 2A0261 |
| <i>O-ring, Viton</i> [®] , for T-Ampoule | V-0747 M83248-1-241 O-ring | AMS-R-83248/1, <i>Viton</i> [®] , Parker Compound V0747-75 or approved equivalent | 2A0261, Item 3 |
| <i>Sample Container-1 (SC-1) Assembly</i> | Lid and Body of SC-1 | Ti-6Al-4V Grade 5 | 2A0268 |
| <i>Sample Container-2 (SC-2) Assembly</i> | Lid and Body of SC-2 | Ti-6Al-4V Grade 5 | 2A0265 |
| <i>O-ring, Viton</i> [®] , for SC-1 and SC-2 | V-0747 M83248-1-147 O-ring | AMS-R83248/1, <i>Viton</i> [®] , Parker Compound V0747-75 or approved equivalent | 2A0268, Item 3 2A0265, Item 3 |
| <i>Inner Cradle</i> | Supports SC-1 and SC-2 Sample Containers | Ti-6Al-4V Grade 5 | 2A0385 |

^a A specification on materials is provided in Section 1.3.3, PAT-1040 *Titanium and O-ring Materials and Component Fabrication Specification* in this addendum.

^A The title of the drawing is shown in italics and is used interchangeably with the designated name in this addendum. The drawing number and title information are shown in Section 1.3.2 and Table 9-3 in this addendum and in Chapter 9 of the SAR.¹ Drawing titles are used to ensure clarity when specifying components.

The package custodian shall determine that the T-Ampoule components listed above have been fabricated in accordance with the approved design and the drawings in Section 1.3.2 of this addendum and inspected for cracks, pinholes, uncontrolled voids, or other defects that could significantly reduce its effectiveness per Title 10, Code of Federal Regulations, Section 71.85 [10 CFR 71.85(c) and (a)].³

Requirements are derived from the packaging drawings and specifications and shall be considered as minimum requirements. This information shall be present in the package custodian's fabrication records.

The minimum acceptance inspection and test requirements for the T-Ampoule components are specified in Table 8-2. These requirements must be met prior to the first use of these components per 10 CFR 71.85.

8.1.1 Visual Inspections and Measurements

Visual inspections with the unaided eye of all pertinent features on the T-Ampoule components shall be performed during fabrication. The inspections include markings, surface conditions, and measurements (i.e., toleranced dimensions, positioning, edge breaks, surface finish).

Measurements will be performed by qualified personnel and with calibrated equipment. There is no welding on these components. The required inspections are described in Table 8-2. Failure to meet the acceptance criteria is cause for rejection of the component.

8.1.1.1 Surface Condition

The metal surfaces of the T-Ampoule components shall be visually inspected for penetrations, dents, and corrosion. Any penetrations, dents, and corrosion found, is cause for rejection of the component. The surfaces must be in accordance with the dimensional requirements from the drawings. Per 10 CFR 71.85(a), superficial markings on the surface (scuff marks) are permitted only if they are within the dimensional tolerances for the component.

8.1.2 Weld Examinations

Not applicable: There are no welds in the T-Ampoule components.

8.1.3 Structural and Pressure Tests

Mechanical property tensile tests are required for the T-Ampoule components. The T-Ampoule component vessels listed are not containment boundaries for normal conditions of transport (NCT) and hypothetical accident conditions (HAC), and no credit is taken for pressure retention.

Table 8-2. Acceptance Tests for T-Ampoule Components

Note: The referenced sections and PAT-1040 specification are found in this addendum.

| Component | Visual Inspections and Measurements | Structural and Pressure Tests | Leakage Tests^c | Component and Material Tests | Miscellaneous Tests |
|---|---|--|----------------------------------|---|---|
| <i>Ring, Filler</i> | Visual Inspection and Measurement ^b (Section 8.1.1) Marking (PAT-1040) Surface Condition ^d (Section 8.1.1.1 and PAT-1040) | No Structural or Pressure Tests Required | Not Applicable (NA) | Material Certification ^a (PAT-1040) COC ^e (PAT-1040) CMTRs (Sections 8.1.3.1 and 8.1.5.3); and PAT-1040 | |
| <i>T-Ampoule Assembly</i> | Visual Inspection and Measurement ^b (Section 8.1.1) Marking (PAT-1040) Surface Condition ^d (Section 8.1.1.1 and PAT-1040) | No Structural or Pressure Tests Required | User Defined | Material Certification ^a (PAT-1040) COC ^e (PAT-1040) CMTRs (Sections 8.1.3.1 and 8.1.5.3); and PAT-1040 | Fit and Function (Section 8.1.8) Measurement (Section 8.1.8) |
| <i>O-ring, Viton[®], for T-Ampoule</i> | Visual Inspection (Section 8.1.5.1 and PAT-1040) | NA | NA | Material Certification (PAT-1040) COC (PAT-1040) | |
| <i>Sample Container-1 (SC-1) Assembly</i> | Visual Inspection and Measurement ^b (Section 8.1.1, Section 8.1.1.1, and Section 8.1.8) Surface Conditions and Marking (PAT-1040) | No Structural or Pressure Tests Required | User Defined | Material Certification ^a (PAT-1040) COC ^e (PAT-1040) CMTRs (Sections 8.1.3.1 and 8.1.5.3); and PAT-1040 | Fit and Function (Section 8.1.8) |

Table 8-2. Acceptance Tests for T-Ampoule Components (Continued)

| Component | Visual Inspections and Measurements | Structural and Pressure Tests | Leakage Tests^c | Component and Material Tests | Miscellaneous Tests |
|---|---|--|----------------------------------|---|----------------------------------|
| <i>Sample Container-2 (SC-2) Assembly</i> | Visual Inspection and Measurement ^b (Section 8.1.1, Section 8.1.1.1, and Section 8.1.8) Surface Conditions and Marking (PAT-1040) | No Structural or Pressure Tests Required | User Defined | Material Certification ^a (PAT-1040) COC ^e (PAT-1040) CMTRs (Sections 8.1.3.1 and 8.1.5.3); and PAT-1040 | Fit and Function (Section 8.1.8) |
| <i>O-ring, Viton[®], for SC-1 and SC-2</i> | Visual Inspection (Section 8.1.5.1 and PAT-1040) Marking (Section 8.1.5.1) Packing (Section 8.1.5.1) | NA | NA | Material Certification (PAT-1040) COC (PAT-1040) | |
| <i>Inner Cradle</i> | Visual Inspection and Measurement ^b (Section 8.1.1 and Section 8.1.8) Marking (PAT-1040) Surface Condition ^d (Section 8.1.1.1 and PAT-1040) | No Structural or Pressure Tests Required | NA | Material Certification ^a (PAT-1040) COC ^e (PAT-1040) CMTRs (Sections 8.1.3.1 and 8.1.5.3); and PAT-1040 | Fit and Function (Section 8.1.8) |

^a Material certification – Certified quantitative data (physical, mechanical, chemical, and/or visual) in the form of Certified Material Test Reports (CMTRs) demonstrating compliance with the drawing/specification requirements; in particular, stress-strain curves for Ti-6Al-4V Grade 5 material. If applicable, heat treatment information is included in the CMTR.

^b Measurement – Dimensional inspections; critical dimensions are noted on the drawings.

^c Leak Test – The vessels listed here are not containment boundaries for normal conditions of transport (NCT) and hypothetical accident conditions (HAC). Leakage rate tests are to demonstrate retention of glovebox atmosphere that is required as part of laboratory support operations to minimize metal contents degradation; the leakage rate acceptance requirements are user defined.

^d Damage – The components shall be inspected to ascertain that there are no cracks, pinholes, uncontrolled voids, or other defects that could significantly reduce the effectiveness of the packaging (10 CFR 71.85(a)).

^e COC (Certificate of Conformance) – A document signed or otherwise authenticated by an authorized individual certifying the degree to which items or services meet specified requirements

8.1.3.1 Mechanical Property Tests

Material mechanical property tests shall be performed on Ti-6Al-4V Grade 5 material for T-Ampoule components to assure that higher strength requirements specified in Section 2, *Structural Evaluation*, of this addendum are met for the ASTM B-348, Grade 5 and ASTM B-265, Grade 5 material. The minimum strength requirements specified in this addendum are higher than the minimum strengths specified in the ASTM standards and are 0.2% yield strength (965 MPa [140 ksi]), ultimate tensile strength (1034 MPa [150 ksi]), elongation at tensile failure (10%), and reduction in area at failure (20%). Acceptance criteria are provided in the appropriate material national standards referenced in the specification entitled PAT-1040, *Titanium and O-Ring Materials and Component Fabrication Specification*, in Section 1.3.3.1 and in the drawings in Section 1.3.2 of this addendum. Failure to meet the acceptance criteria is cause for rejection of the component.

8.1.3.2 Pressure Tests

The *T-Ampoule Assembly*, *Sample Container-1 (SC-1) Assembly*, and *Sample Container-2 (SC-2) Assembly* are not containment vessels and pressure tests are not required for acceptance or maintenance. In accordance with 71.85(b), any new TB-1 *Containment Vessel* shall be pressure-tested in accordance with the regulation.

8.1.4 Leakage Tests

The *T-Ampoule Assembly* is not a containment boundary for NCT and HAC. It serves as a eutectic prevention barrier. The user will define leakage rate test requirements for the *T-Ampoule Assembly*, *Sample Container-1 (SC-1) Assembly*, and *Sample Container-2 (SC-2) Assembly* for laboratory support operations.

8.1.5 Component and Material Tests

8.1.5.1 O-Ring Tests

O-rings for the *T-Ampoule Assembly*, *Sample Container-1 (SC-1) Assembly*, and *Sample Container-2 (SC-2) Assembly* shall be visually inspected. The O-ring surfaces shall be smooth, nonporous, and free of skin defects. O-rings that do not meet these requirements shall be rejected.

Each O-ring shall be packaged separately to provide traceability. Each O-ring package shall be marked with an O-ring identification number, lot number, cure date, and compound number. These material identification numbers shall be assigned uniquely to each lot and to each size of O-ring. The identifications shall be adequate to trace O-rings to their raw material master batch. Improper packaging, marking, or lack of proper documentation COC is cause for rejection. The shelf life of the O-rings is unlimited per Society of Aerospace Engineers (SAE) issued Aerospace Recommended Practice (ARP) 5316.⁴ The shelf life requirement for O-rings of ARP 5316 shall be applied to all organizations handling the O-rings for this package.

8.1.5.2 Titanium Material Property Tests

Material mechanical property tensile tests shall be performed on Ti-6Al-4V Grade 5 material for T-Ampoule components to assure that higher strength requirements specified in Section 2 and PAT-1040 *Titanium and O-Ring Materials and Component Fabrication Specification* of this

addendum are met for the ASTM B-348 Grade 5 and ASTM B-265 Grade 5 material. The minimum strengths are 0.2% yield strength (965 MPa (140 ksi)), ultimate tensile strength (1034 MPa (150 ksi)), elongation at tensile failure (10%), and reduction in area at failure (20%). Acceptance criteria are provided in the appropriate material national standards referenced in the PAT-1040 specification in Section 1.3.3 and in the drawings in Section 1.3.2 of this addendum. Failure to meet the acceptance criteria is cause for rejection of the material.

8.1.5.3 Chemical Tests

Tests shall be performed to determine the chemical properties of the T-Ampoule component materials and provided in the Certified Material Test Report (CMTR) as specified in the PAT-1040 *Titanium and O-Ring Materials and Component Fabrication Specification* in Section 1.3.3 and in the drawings in Section 1.3.2 of this addendum. Material that cannot be traced to the mill or heat-treatment lot shall be rejected.

8.1.6 Shielding Tests

No shielding tests are required for the T-Ampoule components. No credit is taken in Section 5 of this addendum for internal shielding within the TB-1.

8.1.7 Thermal Tests

A thermal test is not required for the *T-Ampoule Assembly*, since the maximum heat generation of the payload is the same as that in the SAR.¹

8.1.8 Miscellaneous Tests

The *Inner Cradle* in the *T-Ampoule Assembly* shall be assembled and checked for function and fit with the *SC-1* or *SC-2*. The clearance gap between the two flat legs of the *Inner Cradle* is 7.692 ± 0.005 cm (3.030 ± 0.002 in.) and is shown in Drawing Number 2A0385 in this addendum. The *Inner Cradle* Assembly may be hand-smoothed for proper fit and function. Individual components of the *Inner Cradle* will be rejected if fit and function are not met.

8.2 Maintenance Program

When the package is being packed or unpacked, the T-Ampoule components shall be examined to ensure that all components are present and functional. A record of the examination results will be generated and must include the identification and serial numbers of the component examined, the names of the personnel who performed the packing/unpacking and examination, and the date of the activity.

Maintenance on the metal T-Ampoule components shall be performed annually and shall include visual inspection. A record of the maintenance action(s) will be generated. The record must identify maintenance performed, the component(s) on which the maintenance was performed, and the names of the personnel who performed the maintenance.

The TB-1 periodic test and maintenance requirements are referenced in Section 8.3 of the SAR.¹ Section 8.3.1 of the SAR¹ describes the requirements for the TB-1 *Containment Vessel* and Section 8.3.2 describes the replacement of gaskets on the TB-1.

8.2.1 Structural and Pressure Tests

No structural or pressure tests are required for maintenance of the T-Ampoule components.

8.2.2 Leakage Tests

The *T-Ampoule Assembly* is not a containment boundary for NCT and HAC. The user will define leakage rate test requirements for the *T-Ampoule Assembly*, *Sample Container-1 (SC-1) Assembly*, and *Sample Container-2 (SC-2) Assembly* for laboratory support operations.

8.2.3 Component and Material Tests

During loading operations, the O-rings for the *T-Ampoule Assembly*, *Sample Container-1 (SC-1) Assembly*, and *Sample Container-2 (SC-2) Assembly* will be inspected for cracks, gouges, or other damage. If any damage is detected, the O-ring must be replaced. The O-rings will be replaced annually.

8.2.4 Thermal Tests

Since the maximum heat generation of the payload is the same as that in the SAR,¹ a thermal test is not applicable for the *T-Ampoule Assembly*.

8.2.5 Miscellaneous Tests

If installation of *Sample Container-1 (SC-1) Assembly* or *Sample Container-2 (SC-2) Assembly* in the *Inner Cradle* becomes difficult after repeated loading and unloading, the *Inner Cradle* must be inspected for damage and for proper clearance between the *Inner Cradle* legs and *SC-1* or *SC-2* sample containers. If damage to the *Inner Cradle* component(s) is discovered, the damaged component(s) will be replaced and the test in Section 8.1.8 of this addendum performed.

The test described in Section 8.1.8 of this addendum is performed annually to ensure that the *Sample Container-1 (SC-1) Assembly* and *Sample Container-2 (SC-2) Assembly* fit and function properly within the *Inner Cradle* of the *T-Ampoule Assembly*. If tightness is observed, inspection and repair as described in Section 8.1.8 shall be performed.

8.3 *Appendix*

8.3.1 References

1. United States. Nuclear Regulatory Commission. NUREG-0361. "Safety Analysis Report for the Plutonium Air Transportable Package, Model PAT-1." Washington, D.C. 1978.
2. United States. Nuclear Regulatory Commission. "Certificate of Compliance for Radioactive Material Packages," Certificate Number 0361, Revision Number 9, Docket Number 71-0361, Package Identification Number USA/0361/B(U)F-96. March 4, 2009.
3. United States. Nuclear Regulatory Commission. Code of Federal Regulations. 10 CFR 71. "Packaging and Transportation of Radioactive Material." January 1, 2009..
4. Society of Aerospace Engineers (SAE). "ARP 5316 Elastomer Shelf Life Recommendation." Aerospace Recommended Practice (ARP) 5316, 1998.
http://www.oringsusa.com/html/shelf_life.html.

9. QUALITY ASSURANCE

This section supplements Chapter 9, *Specifications and Drawings*, of the *Safety Analysis Report for the Plutonium Air Transportable Package, Model PAT-1*, NUREG-0361,¹ and defines the quality assurance (QA) requirements and methods of compliance for requirements associated with the PAT-1 package.

In the late 1970s, Sandia National Laboratories (SNL) developed the PAT-1 under a contract with the Nuclear Regulatory Commission (NRC). The PAT-1 was designed to meet the requirements specified in NUREG-0360, *Qualification Criteria to Certify a Package for Air Transport of Plutonium*.² The QA chapter of SAND76-0587 (NUREG/CR-0030)³ defined the PAT-1 design, procurement, fabrication, testing, and recommended package-user QA requirements. The Department of Energy (DOE) Bendix, Kansas City Plant manufactured 24 PAT-1 packaging systems. SNL used 18 of these 24 packaging systems to perform certification qualification testing, and the remaining packaging systems were made available for use.

The current QA requirements for packaging and transportation of radioactive material are prescribed in Title 10 Code of Federal Regulations Part 71 (10 CFR 71)⁴ Subpart H, *Quality Assurance*, as supplemented by DOE orders for DOE organizations/activities. The NRC guidance for establishing QA programs (QAPs) for packaging used in the transport of radioactive material is provided in Regulatory Guide 7.10 (RG 7.10), *Establishing Quality Assurance Programs for Packaging Used in Transport of Radioactive Material*, Revision 2.⁵ Each of the requirements specified in Subpart H apply to the PAT-1 activities within the scope of this addendum. While not every Subpart H requirement may be applicable to every activity from design through use of the packaging system (based on the nature of the activity), across all of those activities, each of the Subpart H requirements is applicable at least once. PAT-1 activities shall be performed under QAPs that meet all of the applicable 10 CFR 71 Subpart H and DOE/NNSA QA requirements. National Nuclear Security Administration (NNSA) users of the PAT-1 package must establish and maintain a 10 CFR 71 Subpart H-compliant QAP before designation as an authorized user of the PAT-1 package.

For SNL PAT-1 activities, the 10 CFR 71, *Packaging and Transportation of Radioactive Material – Quality Assurance Program Plan*⁶ is the applicable QA program plan.

9.1 Organization

SNL is responsible for maintaining PAT-1 QA requirements, developing new QA requirements and/or specifications based on 10 CFR 71 Subpart H requirements, if necessary, and revising the Safety Analysis Report (SAR) QA requirements, if necessary. The NNSA Service Center, Packaging Certification Division is responsible for ensuring NNSA organizations that perform PAT-1 activities establish, maintain, and comply with applicable QA requirements. All SNL PAT-1 activities are conducted under the NNSA-approved SNL corporate QAP, the *Sandia National Laboratories 10 CFR 71, Subpart H Quality Assurance Program Plan (QAPP), AS-PT-PD-04*⁶ and associated Quality Assurance Implementing Procedures (QAIPs). The program is implemented using a graded approach, as dictated by the importance to safety of the activity being performed.

The responsible organizations are staffed by technically competent personnel with freedom to make appropriate objective judgments, recommendations, and decisions consistent with delegated authority. The level of authority and independence delegated to the QA function were provided in organization charts that were available when the original set of packages was fabricated.

In this addendum, SNL is the design organization and package custodian and has support from Oak Ridge National Laboratory (ORNL) and Los Alamos National Laboratory (LANL). ORNL provides shielding and criticality analyses for the plutonium metal contents described in Sections 5 and 6 of this addendum. LANL consults with shippers and provides recommendations for the design of the inner packing and proposed plutonium metal contents. LANL also provides technical data on eutectics prevention and estimates of gas generation from volatilization of elastomers at high temperature, in the form of LANL-issued reports or documents.

SNL prepared a Subpart H QAPP that was approved by the DOE/NNSA Packaging Certification Division in 2007.⁶ Applicable portions of that plan were extended to ORNL for the shielding and criticality analyses and audits were conducted to ensure compliance.

The SNL Management System Improvement Department provides QA support for the PAT-1 Recertification Project.

See Figure 9-1 for a diagram of the organizational relationships for the PAT-1 Recertification Project.

The users of the PAT-1 package for plutonium metals are contractor organizations within the DOE.

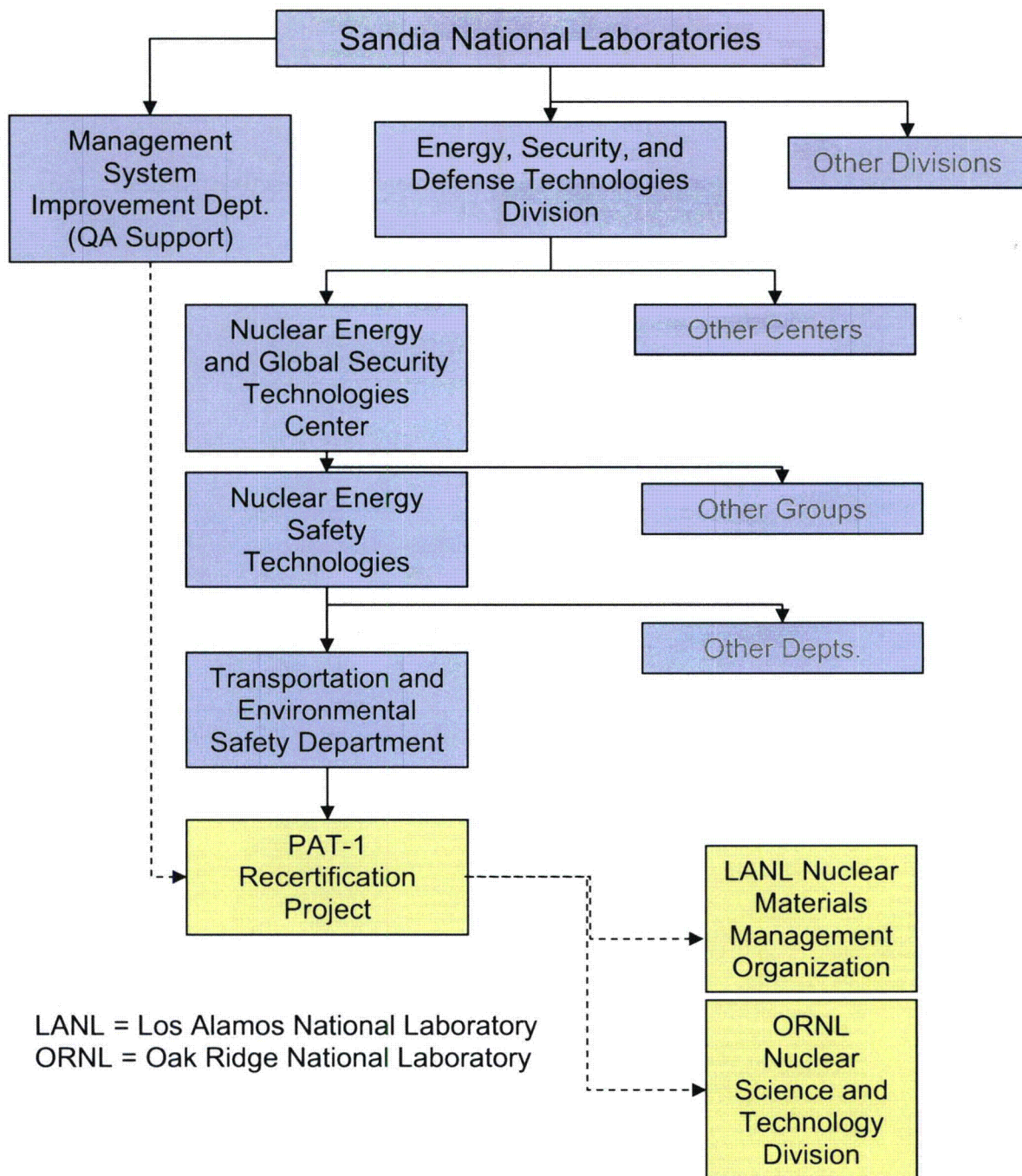


Figure 9-1. Organization Chart for PAT-1 Recertification

9.2 Quality Assurance Program

9.2.1 General

The SNL QAPP is implemented through the use of SNL corporate procedures, where they exist, or the preparation, review, approval, and use of QAIPs for QA controls that are not implemented in the SNL corporate system. These procedures provide a system of checks and balances to ensure a safe, reliable, quality product. Table 9-1 describes the relationship between the

implementing documents and the sections of Subpart H that they implement. The SNL QAP does not apply to PAT-1 packaging system users who use the PAT-1 packaging system to transport materials. These users must have their own NRC- or NNSA-approved 10 CFR 71 Subpart H QAPs.

Table 9-1. Relationship between QA Implementing Documents and Elements of 10 CFR 71, Subpart H

| Implementing Document ID | Title | Related Element of Subpart H | Description |
|---|--|--|---|
| AS-PT-PD-04 ⁶ | <i>Sandia National Laboratories Title 10 CFR 71, Packaging and Transportation of Radioactive Material Quality Assurance Program Plan</i> | 71.103 Organization | Describes the organizational roles, responsibilities, and relationships for activities and projects subject to 10 CFR 71, Subpart H, including packaging system recertification for the PAT-1 system. |
| AS-PT-PD-04 ⁶ | <i>Sandia National Laboratories Title 10 CFR 71, Packaging and Transportation of Radioactive Material Quality Assurance Program Plan</i> | 71.105 Quality Assurance Program | Describes the SNL QA program for activities and projects subject to 10 CFR 71, Subpart H, in general. |
| 1071H-QAIP 2-2 ⁷ | <i>Project Quality Plan Preparation</i> | | Prescribes controls for preparing a Quality Plan specific to an individual project, e.g., PAT-1 Recertification. |
| 1071H-QAIP 3-1 ⁸ | <i>Design Control</i> | 71.107 Package Design Control | Prescribes design control measures for packaging system items and components. |
| 1071H-QAIP 9-2 ⁹ | <i>Model Validation</i> | | Prescribes control mechanisms applied to validating mathematical models used for analysis. |
| 1071H-QAIP 9-3 ¹⁰ | <i>Analyses and Calculations</i> | | Prescribes controls applied to the conduct of analyses and calculations, including QA controls on software used for those analyses. |
| SNL Corporate Process Requirement 500.2.1 | <i>Procurement Manual</i> | 71.109 Procurement Document Control | Prescribes controls for preparation, content, and processing of procurement documents at SNL to ensure that applicable regulatory requirements, design bases, technical, and quality requirements are included or referenced in those documents. |
| 1071H-QAIP 4-111 | <i>Control of Procurement Documents and Purchased Material, Equipment, and Services</i> | | Prescribes controls for preparation, content, and processing of procurement documents by procuring organizations other than SNL to ensure that applicable regulatory requirements, design bases, technical, and quality requirements are included or referenced in those documents. |

Table 9-1. Relationship between QA Implementing Documents and Elements of 10 CFR 71, Subpart H (Continued)

| Implementing Document ID | Title | Related Element of Subpart H | Description |
|---|---|--|---|
| 1071H-QAIP 5-1 ¹² | <i>Quality Assurance Implementing Procedure Preparation and Content</i> | 71.111 Instructions, Procedures, and Drawings | Prescribes controls specific to the content and processing of documents that establish and implement the QA program. |
| 1071H-QAIP 3-1 ⁸ | <i>Design Control</i> | | Prescribes controls specific to the content and processing of design drawings and specifications. |
| 1071H-QAIP 6-1 ¹³ | <i>Document Review and Approval</i> | 71.113 Document Control | Prescribes tools and documentation for review (“inspection”) and approval of documents. |
| 1071H-QAIP 6-2 ¹⁴ | <i>Document Control</i> | | Prescribes controls for the issuance, use, and revision of documents that, themselves, prescribe processes or specify requirements. |
| SNL Corporate Process Requirement 500.2.1 | <i>Procurement Manual</i> | 71.115 Control of Purchased Material, Equipment, and Services | Prescribes controls to ensure that materials, equipment, or services procured by SNL conform to requirements specified in the procurement documents. |
| 1071H-QAIP 4-1 ¹¹ | <i>Control of Procurement Documents and Purchased Material, Equipment, and Services</i> | | Prescribes controls to ensure that materials, equipment, or services procured by organizations other than SNL conform to requirements specified in the procurement documents. |
| 1071H-QAIP 8-1 ¹⁵ | <i>Identification and Control of Materials, Parts, and Components</i> | 71.117 Identification and Control of Materials, Parts, and Components | Prescribes controls to ensure that only correct and accepted items are used as parts of a packaging system. |
| 1071H-QAIP 9-1 ¹⁶ | <i>Control of Special Processes</i> | 71.119 Control of Special Processes | Prescribes controls to ensure that special processes are conducted in a way that ensures their success. |
| 1071H-QAIP 10-1 ¹⁷ | <i>Inspection and Identification of Item Status</i> | 71.121 Internal Inspection | Prescribes controls applicable to inspection activities focused on items, components, and assemblies. |
| 1071H-QAIP 9-5 ¹⁸ | <i>Technical Products and Deliverable Reports</i> | | Prescribes process for review and approval (“inspection”) of technical product documents. |
| 1071H-QAIP 6-1 ¹³ | <i>Document Review and Approval</i> | | Prescribes tools and documentation for review (“inspection”) and approval of documents. |
| 1071H-QAIP 9-5 ¹⁸ | <i>Technical Products and Deliverable Reports</i> | | Prescribes process for review and approval (“inspection”) of technical product documents. |
| 1071H-QAIP 11-1 ¹⁹ | <i>Control of Data Collection and Testing Activities</i> | 71.123 Test Control | Prescribes controls for testing of items, assemblies, or systems to determine whether they meet specified requirements. |

Table 9-1. Relationship between QA Implementing Documents and Elements of 10 CFR 71, Subpart H (Continued)

| Implementing Document ID | Title | Related Element of Subpart H | Description |
|--|---|---|--|
| SNL Corporate Process Requirement 100.3.1 | <i>Standards and Calibration</i> | 71.125 Control of Measuring and Test Equipment | Prescribes controls applicable to measuring and test equipment used by SNL organizations to ensure validity of data and measurements. |
| 1071H-QAIP 12-1 ²⁰ | <i>Control of Measuring and Test Equipment</i> | | Prescribes controls applicable to measuring and test equipment used by organizations other than SNL to ensure validity of data and measurements. |
| SNL Corporate Process Requirement 500.2.3 | <i>Property/Assets Management User's Manual</i> | 71.127 Handling, Storage, and Shipping Control | Prescribes controls to be applied at SNL to preclude damage or deterioration of items and materials. |
| 1071H-QAIP 13-1 ²¹ | <i>Control of Shipping, Handling, Storage, Preservation, and Cleaning</i> | | Prescribes controls to be applied at locations other than SNL to preclude damage or deterioration of items and materials. |
| 1071H-QAIP 10-1 ¹⁷ | <i>Inspection and Identification of Item Status</i> | 71.129 Inspection, Test, and Operating Status | Prescribes controls to ensure that the status of items with respect to inspections or tests is indicated. |
| 1071H-QAIP 15-1 ²² | <i>Control of Nonconformances and Corrective Action</i> | 71.131 Nonconforming Materials, Parts, or Components | Prescribes controls to ensure that materials, parts, or components that do not meet requirements are not used or installed. |
| SNL Corporate Process Requirement 001.3.11 | <i>Corporate Corrective Action Process</i> | 71.133 Corrective Action | Prescribes controls to ensure that conditions adverse to quality are identified and corrected by SNL. |
| 1071H-QAIP 15-1 ²² | <i>Control of Nonconformances and Corrective Action</i> | | Prescribes controls to ensure that conditions adverse to quality are identified and corrected by organizations other than SNL. |
| SNL Corporate Process Requirement 400.2.20 | <i>Management of Information Throughout its Lifecycle</i> | 71.135 Quality Assurance Records | Prescribes controls for the management of records, including QA records. |
| SNL Corporate Process Requirement 001.3.5 | <i>Audits</i> | 71.137 Audits | Prescribes policy and controls concerning internal and external audits at SNL. |
| SNL Corporate Process Requirement 001.3.10 | <i>Corporate Self-Assessment Process</i> | | Prescribes controls for the performance of internal assessments at SNL. |

A graded approach is used to selectively apply the QA requirements to the PAT-1 packaging components and related services and activities in accordance with 10 CFR 71.105. The purpose of the graded approach is to select the QA controls and appropriate verifications to the various packaging items, services, and activities consistent with the extent of their importance to health and safety.

The SNL QAP is extended to ORNL through an implementation plan and QAIPs for the shielding and criticality analyses performed for this addendum. LANL provides technical data and reports that are approved under their quality program requirements for unlimited release external reports.

9.2.2 QA Levels

The QA chapter of SAND76-0587 (NUREG/CR-0030)³ defines the PAT-1 design, procurement, fabrication, testing, and recommended package user QA requirements for the first 24 PAT-1 packaging systems. At that time, there were no defined quality categories.

The tasks performed in support of the PAT-1 with T-Ampoule configuration and plutonium metal content certification effort, and the packaging components for this configuration, are provided in Tables 9-2 and 9-3, respectively. The tasks and packaging components were classified in accordance with the quality categories defined in RG 7.10, Revision 2,⁵ Appendix A, and SNL *QAPP, AS-PT-PD-04*⁶ based on their importance to safety.

Table 9-4 documents the level of control required for each quality category applicable to the packaging system elements. These defined quality categories consider the impact to safety if the component fails or performs outside of design parameters.

9.2.2.1 Graded Quality Category A Items

These items and tasks are critical to safe operations, and include structures, components, and systems for which a failure or malfunction could directly result in a condition that would adversely affect public health and safety. This includes such conditions as loss of primary containment with subsequent release of radioactive material, loss of shielding, or an unsafe geometry compromising criticality control.

9.2.2.2 Graded Quality Category B Items

These items and tasks have a major impact on safety and includes structures, components, and systems for which a failure or malfunction could indirectly result in a condition that would adversely affect public health and safety. However, an unsafe condition could result only if the primary event occurs in conjunction with a secondary event, or other failure or environmental occurrence.

Table 9-2. Project Tasks and Quality Categories for PAT-1 Addendum

| Project Tasks | Quality Category |
|--|-------------------------|
| 1. Project Management | None |
| 2. SAR Structural Analysis for T-Ampoule and Contents for NCT, HAC, and Pu Air Transport | Category A |
| 3. SAR Criticality and Shielding Analysis for NCT, HAC and Pu Air Transport | Category A |
| 4. Eutectics Evaluation | Category B |
| 5. Leak Testing for T-Ampoule | Category C |
| 6. SAR Amendment Preparation | None |
| 7. Redesign and Drawings for SAR | Category B |
| 8. SAR Amendment Assembly | None |
| 9. SAR Section Review | None |
| 10. Meeting Preparation | None |
| 11. SAR Revision Based on NRC Comments | None |
| 12. Testing for Model Verification and Margin | Category B |
| 13. Update QA Section 9 | None |

Table 9-3. QA Categories for Design and Procurement of T-Ampoule Assembly and Inner Packing

| Component Name | Drawing Number | Quality Category |
|--|-----------------------|-------------------------|
| <i>Ring, Filler</i> | 2A0262 | A |
| <i>T-Ampoule Assembly</i> | 2A0261 | A |
| <i>O-ring, Viton[®] for T-Ampoule</i> | 2A0261, Item 3 | C |
| <i>Inner Cradle</i> | 2A0385 | B |
| <i>Sample Container-1 (SC-1) Assembly</i> | 2A0268 | B |
| <i>Sample Container-2 (SC-2) Assembly</i> | 2A0265 | B |
| <i>O-ring, Viton for SC-1</i> | 2A0268, Item 3 | C |
| <i>O-ring, Viton for SC-2</i> | 2A0265, Item 3 | C |

Table 9-4. Level of QA Control Per QA Element

| QA Element | Level of Assurance Effort | Quality Category | | |
|------------|--|------------------|--------|---|
| | | A | B | C |
| 9.1 | Organization – grading not applicable | — | — | — |
| 9.2 | Quality Assurance Program – grading not applicable | — | — | — |
| 9.3 | Package Design Control <ul style="list-style-type: none"> ▪ All controls applicable ▪ No controls required | X | X | X |
| 9.4 | Procurement Document Control <ul style="list-style-type: none"> ▪ Procurement Documents receive management review ▪ Procurement Documents receive technical review ▪ Procurement Documents receive QA review ▪ No review required | X X X | X X | X |
| 9.5 | Instructions, Procedures, and Drawings – Instructions and procedures (such as QAIPs) are prepared and applied to all quality categories, and design drawings are prepared regardless of the quality category of the subject item. Therefore, grading not applicable for this element. | — | — | — |
| 9.6 | Document Control – Document control is applied to <u>all</u> instructions, procedures, and drawings; quality categories are not applicable to those documents. Therefore, grading is not applicable for this element. | — | — | — |
| 9.7 | Control of Purchased Material, Equipment, and Services <ul style="list-style-type: none"> ▪ All controls applicable ▪ No audit/surveillance of supplier required if supplier is qualified; all other controls applicable ▪ Only receipt inspection to verify procurement document requirements met requirements | X | X | X |
| 9.8 | Identification and Control of Material, Parts, and Components <ul style="list-style-type: none"> ▪ Identification by part ID/drawing number and package S/N ▪ Identification by part ID/drawing number only required | X | X | X |
| 9.9 | Control of Special Processes <ul style="list-style-type: none"> ▪ Performed by qualified persons using qualified procedures and equipment ▪ No controls required | X | X | X |
| 9.10 | Inspection <ul style="list-style-type: none"> ▪ All controls applicable – no grading | X | X | X |
| 9.11 | Test Control – testing may be performed on assembled components sets of various quality categories; therefore, no grading by quality category is appropriate – all controls applicable. | — | — | — |
| 9.12 | Control of Measuring and Test Equipment <ul style="list-style-type: none"> ▪ All controls applicable – no grading | X | X | X |

Table 9-4. Level of QA Control Per QA Element (continued)

| QA Element | Level of Assurance Effort | Quality Category | | |
|------------|--|------------------|---|---|
| | | | | |
| 9.13 | Handling, Storage, and Shipping Control <ul style="list-style-type: none"> ▪ All controls applicable ▪ Instructions, procedures, specifications, or drawings not required to govern handling or storage. | X | X | X |
| 9.14 | Inspection, Test, and Operating Status <ul style="list-style-type: none"> ▪ All controls applicable – no grading | X | X | X |
| 9.15 | Nonconforming Materials, Parts, or Components <ul style="list-style-type: none"> ▪ All controls applicable ▪ Control to ensure item not put in use, dispose without records | X | X | X |
| 9.16 | Corrective Action <ul style="list-style-type: none"> ▪ All controls applicable ▪ Determination of cause of condition and action to preclude recurrence not required | X | X | X |
| 9.17 | QA Records – grading not meaningful – all controls applicable | X | X | X |
| 9.18 | Audits – grading not applicable | — | — | — |

Note: Entries of “grading not applicable” in the above table indicate QAP elements for which a grading scheme for implementing the element is either illogical (i.e., the element is not applied at the individual component level, such as Sections 9.1, 9.2, 9.5, 9.6, 9.11, and 9.18 of this addendum) or where differentiation in the applicability of the element provides no significant value for this project (Sections 9.10, 9.12, 9.14, and 9.17 of this addendum).

9.2.2.3 Graded Quality Category C Items

These items and tasks have only a minor impact on safety, and include structures, components, and systems for which a failure or malfunction would not significantly reduce packaging effectiveness and would be unlikely to create a condition that would adversely affect public health and safety. Examples include dunnage, packaging hardware, security lockwire and seals, etc.

9.3 Package Design Control

Design processes are established and implemented to satisfy the requirements of 10 CFR 71.107. Processes, implemented via procedures, shall ensure that design features of packaging systems are appropriately translated into specifications, drawings, procedures, and instructions. Control measures are established for criticality, shielding, thermal, and structural analyses under both normal and accident condition analyses as defined in applicable Department of Transportation (DOT) and NRC regulations.

The design documents (e.g., drawings and specifications) for Quality Category A and B items (*T-Ampoule Assembly; Ring, Filler; Sample Container-1 (SC-1) Assembly; Sample Container-2 (SC-2) Assembly; and Inner Cradle*) are controlled through inclusion in Section 1 of this addendum, and any changes will be reviewed for approval by the NRC. Changes to Category C

items may be approved by NNSA, provided that the applicant demonstrates and documents that the proposed change does not affect safety.

Procedures are established for control design activities to ensure that the following:

- Design activities will be planned, controlled, and documented.
- Regulatory requirements, design requirements, and appropriate quality standards will be correctly translated into specifications, drawings, and procedures.
- Competent engineering personnel, independent of those who produced the design, perform design verification. Verification may include design reviews, alternate calculations, or verification testing. Verification tests are conducted in accordance with test procedures developed, reviewed, approved, and controlled in accordance with this document.
- Design interface controls will be established and adequate.
- Design, specification, drawing, and procedure changes will be reviewed and approved in the same manner as the original issue. Where a proposed design change potentially affects licensed conditions, the QAP shall ensure that licensing considerations have been reviewed and are complied with or otherwise reconciled by amending the license.
- Design errors and deficiencies will be documented, corrected, and corrective action taken to prevent recurrence.

Materials, parts, equipment, and processes essential to the function of items that are important to safety will be selected and reviewed for suitability of application.

9.4 Procurement Document Control

Procurement/acquisition processes and related document control activities shall be established and implemented to satisfy the requirements of 10 CFR 71.109. Processes, implemented via procedures, shall ensure that appropriate levels of quality are achieved for the procurement of material, equipment, and services.

Implementing procedures shall ensure that procurement documents clearly define applicable technical and QA requirements, including codes, standards, regulatory requirements and commitments, and contractual requirements. These documents serve as the principal documents for the procurement of structures, systems, components, and related services for use in the design, fabrication, maintenance and operation, inspection and testing of storage and/or transportation systems. Procedures shall ensure that purchased material, components, equipment, and services adhere to the applicable requirements. Furthermore:

- The assignment of quality requirements through procurement documents is administered and controlled.
- Procurement activities are performed in accordance with approved procedures delineating requirements for preparation, review, approval, and control of procurement documents.
- Procurement documents shall be reviewed and approved by authorized personnel for consistency with these requirements.

- Revisions to procurement documents are reviewed and approved by the same cognizant groups as the original document.
- Quality requirements are included in quality-related purchase orders as applicable to the scope of the procurement referencing 10 CFR 71, Subpart H or other codes and standards, as appropriate. In particular, procuring organizations that do not, themselves, have an NRC-accepted Subpart H QAP must require subcontractors to have such a QAP or recognized equivalent (e.g., a QAP that meets requirements of ANSI/ASME NQA-1, 1983).²³
- Procurement documents will require vendors to roll-down appropriate QA requirements to sub tier suppliers.
- Audits and/or surveys may be conducted to determine acceptability of proposed vendors based on the quality/performance requirements of the item/activity being purchased. These audits/surveys may be based on one or all of the following criteria: the vendor's capability to comply with the requirements of 10 CFR 71, Subpart H; a review of previous records to establish the past performance of the vendor; and/or a survey of the vendor's facilities and review of the supplier's QAP to assess adequacy and verify implementation of quality controls consistent with the requirements being invoked. Such audits or surveys shall be conducted in accordance with Section 9.18 of this addendum.
- Procurement documents shall specify the right of access to supplier facilities by the procuring entity for performing source surveillance and/or audit activities.
- Periodic surveillance of vendor in-process activities may be performed to verify vendor compliance with the procurement documents. When deemed necessary, the need for surveillance shall be specified in approved procurement documents.
- Procurement documents shall include provisions that suppliers either maintain or supply QA records that provide evidence of conformance to the procurement documents. Additionally, procurement documents shall designate the vendor documents required for submittal to the procuring entity for review and/or approval.

The components procured and fabricated per this addendum include *T-Ampoule Assembly; Ring, Filler; Sample Container-1 (SC-1) Assembly; Sample Container-2 (SC-2) Assembly; Inner Cradle* and *O-rings* for the *T-Ampoule Assembly* and sample containers (*SC-1* and *SC-2*). SNL shall have access to vendor facilities and shall qualify and approve the vendor QAP. The vendor QAP shall describe systems for planning, performing, and assessing work, which ensure materials, systems, results, and personnel meet stated quality objectives. The vendor shall ensure any material suppliers and subcontractors utilized during the performance of the contract meet the vendor's QAP. The vendor QAP shall be submitted to SNL for review and written approval, prior to commencement of any work.

Procurement of consumables and replacement parts will be performed under the SNL Subpart H program in a manner consistent with the quality category assigned to the individual items.

9.5 Instructions, Procedures, and Drawings

As required by 10 CFR 71.111, instructions, procedures, and drawings shall be prepared to prescribe processes or work activities, specify requirements, or establish design. Those

documents shall be used in the performance of the work to which they apply. Processes, implemented via procedures, shall ensure that appropriate levels of quality are achieved in development of those documents.

Implementing procedures shall be established to ensure that methods for complying with each of the applicable criteria of 10 CFR Part 71 for activities affecting quality during design, fabrication, inspection, testing, use, and maintenance are specified in instructions, procedures, and/or drawings.

In addition:

- Instructions, procedures, and drawings shall be developed, reviewed, approved, used, and controlled in accordance with the requirements of approved procedures. These instructions, procedures, and drawings shall include appropriate quantitative and qualitative acceptance criteria.
- Changes to instructions, procedures, and drawings are developed, reviewed, approved, used, and controlled with the same requirements and controls applied to the original documents.
- Compliance with these approved instructions, procedures, and drawings is mandatory.

Specific activities regarding preparation of packaging for use, repair, rework, maintenance, loading contents, unloading contents, and transport must be conducted in accordance with written and approved instructions, procedures, and/or drawings. These documents must identify appropriate inspection and hold points and emphasize characteristics that are important to safety and quality. Transportation package procedures are to be developed and reviewed by technical and quality staff and shall be approved by appropriate levels of management.

9.5.1 Operating Procedures for Preparation and Use of Packaging System

Activities concerning loading and shipping shall be performed in accordance with written operating procedures developed by the user and approved by the package custodian. Packaging first-time usage tests, sequential loading and unloading operations, technical constraints, acceptance limits, and references shall be specified in the procedures.

9.5.2 Operating Procedure Changes

Changes in operating procedures that affect the process must be reviewed and approved in the same manner as the initial issue.

9.6 Document Control

As required by 10 CFR 71.113, documents that prescribe processes or work activities, specify requirements, or establish design shall be controlled to ensure the use of applicable versions of those documents during the performance of activities that affect quality. Controlled documents include, but are not limited to:

- Project Plans
- QAP and QAIPs

- This addendum
- Design specifications
- Design and fabrication drawings
- Design verification test procedures along with the results of these test procedures
- Acceptance and maintenance test plans and test procedures
- Special process specifications and procedures

Documents that prescribe activities affecting quality are to be reviewed and approved for technical adequacy and inclusion of appropriate quality requirements prior to approval and issuance. Changes to documents that prescribe activities affecting quality shall be reviewed and approved by the same organization that performed the initial review and approval or by qualified responsible organizations. Measures are taken to ensure that only current documents are available at the locations where activities affecting quality are performed prior to commencing work.

Package users are responsible for establishing, developing, reviewing, approving, distributing, revising, and retaining their documents. Documents that require control, level of control, personnel responsibilities, and training requirements are to be identified.

Packaging-system-related documents to be controlled include, as a minimum:

- Specifications
- Drawings of packaging and components
- Fabrication records
- Operating procedures
- Maintenance procedures
- Inspection and operational test procedures and resulting data
- Loading and unloading procedures
- Preparation for transport procedures
- Repair procedures

Revisions are processed in the same manner as the original issue and only the latest revisions must be available for use.

Documentation received from the supplier for each package must be filed by package serial number. These documents will be retained at the user facility.

9.7 Control of Purchased Material, Equipment, and Services

As required by 10 CFR 71.115, purchased material, equipment, and services shall be controlled according to applicable procurement requirements. Processes, implemented via procedures, shall

ensure that appropriate levels of quality are achieved. Quality category designations are used to grade the application of QA requirements for procurements.

Control of purchased material, equipment, and services consist of the following activities:

- Implementing procedures shall be established to ensure that purchased material, equipment, and services conform to procurement documents.
- Suppliers are required to provide objective evidence that items or services provided meet the requirements specified in procurement documents. Items shall be properly identified on appropriate records that are available to permit verification of conformance with procurement documents. Any procurement requirements not met by suppliers shall be reported in accordance with Section 9.15, *Nonconforming, Materials, Parts, or Components* of this addendum for control and correction of the condition.
- Performance of source surveillance, test, and shipping and/or receiving inspection activities to verify compliance with approved design and licensing requirements, procurement document requirements, or contract specifications must be performed in accordance with approved procedures.
- For commercial “off-the-shelf” items, where specific quality controls appropriate for nuclear applications cannot be imposed in a practical manner, quality verification shall be performed to verify the acceptability and conformance of an item to procurement document requirements.

9.8 Identification and Control of Material, Parts, and Components

As required by 10 CFR 71.117, activities concerning the identification and control of material, parts, and components of the PAT-1 packaging system to be used for transport of radioactive material shall be controlled. Processes, implemented via procedures, shall ensure that appropriate levels of quality are achieved through the identification and control of those materials, parts, and components.

The requirements for identification and control of material, parts, and components include:

- Implementing procedures shall be established to identify and control materials, parts, and components. These procedures shall ensure identification of items by appropriate means during fabrication, installation, and use of the items, and prevent the inadvertent use of incorrect or defective items.
- Each component, if specified in the drawing, shall be assigned a unique serial number after fabrication or purchase. All documentation associated with subsequent storage, use, maintenance, inspection, acceptance, etc., must refer to the assigned serial number.
- Requirements for identification are established during the preparation of procedures and specifications.
- Methods and location of identification are selected so as not to adversely affect the quality of the item(s) being identified.

- Items with a limited shelf or operating life are controlled to prevent their inappropriate use.
- Control and identification must be maintained either directly on the item or within documents traceable to the item to ensure that only correct and acceptable items are used. When physical identification is not practical, other appropriate means of control must be established, such as bagging, physical separation, or procedural control.

Verification of acceptance status is required prior to use. Items that are not acceptable must be controlled accordingly. Control of nonconforming items is addressed in Section 9.15, *Nonconforming Parts, Materials, or Components*, of this addendum.

Each AQ-1 data plate on the PAT-1 package will be conspicuously and durably marked with information identifying the package owner, model number, unique serial number, and package gross weight, in accordance with 10 CFR 71.85(c) and drawing number 1002.

The *T-Ampoule* will be assigned a unique serial number after fabrication. The vendor shall mark the product, packaging, and accompanying documentation with the item's part number. Laser marking is required on all metal parts (*T-Ampoule Assembly*; *Ring*, *Filler*; *Sample Container-1*; *Sample Container-2*; and *Inner Cradle*) identified in the engineering drawing set. The laser-produced marking will be a contrasting color on the metal surface, without edges or depth.

Replacement parts must be identified by marking, tagging, or labeling to ensure correct application. Items should be marked based on their quality category. Items such as the O-rings for the TB-1 *Containment Vessel*, *T-Ampoule Assembly*, and *Sample Container-1 (SC-1) Assembly* and *Sample Container-2 (SC-2) Assembly* that are too small or that otherwise do not lend themselves to marking must be individually packaged and the package marked with the material certification, size, cure date, and shelf-life, etc., as appropriate. All replacement fasteners for the AQ-1 and TB-1 as described in NUREG-0361 (Drawing No. 1002, 1003, 1004, 1017, and 1018) must be source traceable, certified, and marked (or in marked packaging) to reflect their identity, and segregated from other similar fasteners to prevent misuse or installation of unacceptable fasteners. Items that have limited calendar-life, operating-life cycles (*Gasket Copper*, Drawing No. 1019), or shelf life (such as the TB-1 *Containment Vessel*, *T-Ampoule Assembly*, and sample container (*SC-1* or *SC-2*) *O-rings*) must be controlled (QAIP 8-1, 13-1) to preclude the use of expired items. Processes (see Section 7 of this addendum) shall be in place to replace aging items prior to failure or expiration.

9.9 Control of Special Processes

As required by 10 CFR 71.119, special processes (QAIP 9-1) used to fabricate or inspect the PAT-1 system or components shall be controlled. The requirements for control of special processes include:

- Implementing procedures shall be established to control special processes used in the fabrication and inspection of storage/transport systems. These processes may include welding, nondestructive examination, or other special processes as identified in procurement documents.
- Special processes shall be performed in accordance with approved procedures.

- Personnel who perform special processes will be trained and qualified in accordance with applicable codes, standards, specifications, and/or other specific requirements. Records of qualified procedures and personnel are to be maintained and kept current by the organization that performs the special processes.
- Equipment used in conduct of special processes must be qualified in accordance with applicable codes, standards, and specifications. Qualification records of special process procedures, equipment, and personnel must be maintained.

Welding shall be performed as specified in PAT-1030. Nondestructive examination personnel (e.g., for visual inspection, penetrant inspection, or leak testing, etc.) shall be qualified at the American Society for Nondestructive Testing (ASNT) Level II or III for the examination technique to be employed. Containment vessel and criticality control component structural welds must be examined using the approved nondestructive method cited on the design drawings.

Fabrication of the *T-Ampoule Assembly; Ring, Filler; Sample Container-1 (SC-1) Assembly; Sample Container-2 (SC-2) Assembly; and Inner Cradle* is specified in PAT-1040 *Titanium Material Specification and Fabrication*, Section 1.3.3 of this addendum.

9.10 Internal Inspection

In accordance with 10 CFR 71.121, inspection activities used to ensure that materials, parts, and components of the PAT-1 packaging system for transport of radioactive material shall be controlled. Processes, implemented via procedures, shall ensure that appropriate inspections are performed prior to acceptance or use of the packaging or components.

Requirements for control of inspection activities include:

- Implementing procedures shall be established to ensure that inspection is performed to verify that materials, parts, processes, or other activities affecting quality conform to documented instructions, procedures, specifications, drawings, and/or procurement documents.
- Mandatory hold points, inspection equipment requirements, acceptance criteria, personnel qualification requirements, performance characteristics, variable and/or attribute recording instructions, reference documents, and other requirements are considered and included, as applicable, during inspection and surveillance planning.
- Personnel performing inspection activities shall be trained and qualified in accordance with written, approved procedures.
- Inspections are to be performed by individuals other than those who performed or supervise the subject activities.
- Inspection and process monitoring are both required where either one, by itself, will not provide QA.
- Modifications and/or repairs to and replacement of packaging system components and assemblies are inspected in accordance with the original design and inspection requirements or approved alternatives.

9.10.1 Inspections During Fabrication

Specific inspection criteria are incorporated into the drawings for the PAT-1 packaging. The components fabricated in this addendum include the *T-Ampoule Assembly*; *Ring, Filler*; *Sample Container-1 (SC-1) Assembly*; *Sample Container-2 (SC-2) Assembly*; and *Inner Cradle*.

Inspection requirements for fabrication are divided into two areas of responsibility which document that an accepted package conforms to design criteria. These two areas are

- In-process inspections performed by the fabricator pursuant to fabricator's graded QA requirements under the Manufacturing/Fabrication Plan; and
- Independent surveillance of fabrication activities performed by individuals acting on behalf of the purchaser pursuant to graded QA requirements.

The vendor (fabricator) is required to submit a Manufacturing/Fabrication Plan prior to the start of fabrication for approval by SNL. This plan shall be used as a tool for establishing witness and hold points. A review for compliance with procurement documents is normally performed as part of the surveillance function at the vendor facility. The plan shall define how fabrications and inspections are performed, processes are engaged, and the qualification requirements for personnel.

A full-dimensional inspection of manufactured parts shall be performed and documented to ensure adherence to the dimensions and associated tolerances in the engineering drawings. ASME Y14.5M, Dimensioning and Tolerancing,²⁴ shall serve as the basis standard for the dimensional inspections.

Inspections must be documented and records delivered in individual data packages accompanying the manufactured parts in accordance with the procurement specification. Vendor inspectors shall be suitably experienced and qualified. Inspectors independent of the operation shall carry out acceptance inspections.

Independent surveillance activities will be performed by qualified personnel selected with SNL approval. SNL reserves the right to have its own qualified inspectors and personnel present during fabrication and inspections activities. Notice of at least five working days is required prior to inspection and testing activities by the vendor so SNL may arrange its staff participation. Hold points may be identified in the schedule for coordination of inspection activities.

Upon delivery of the fabricated components to SNL, the parts will be dimensionally and visually inspected by SNL inspectors as follows:

- Visually inspect components and assemblies for damage.
- Verify that purchase order/job order number is marked on parts, packaging, or accompanying documentation.
- Verify that the Certified Material Test Report (CMTR) contains purchase order/job number, vendor name, and address and is signed by an authorized vendor representative.
- Verify that a Certificate of Conformance (COC) is provided for each lot of components.

- Verify that the COC contains SNL purchase order/job order number, vendor name and address, and is signed by an authorized vendor representative.
- Verify vendor QAP was shipped with components.
- Verify dimensional attributes when established for components or assemblies.

9.10.2 Inspections during Initial Acceptance and during Service Life

Independent inspections shall be performed by SNL upon receipt of the PAT-1 packaging prior to first usage and on an annual basis. Post-loading inspections by the user are also performed prior to shipment. Inspection (by qualified independent inspection personnel) must include the following:

- First-Usage/Annual by SNL – Ensure compliance with procurement documents. As discussed in Section 8 of this addendum, Acceptance Tests and Maintenance Operations, perform first-time-usage inspections. Annually, ensure adequate packaging maintenance to ensure that performance is not impaired, as discussed in Section 8 of this addendum.
- Preshipment by User – Verify proper assembly and that leak testing (if applicable) is carried out as specified in Section 7 of this addendum, Package Operations. Verify proper contents, assembly, marking, shipping papers, and implementation of any special instructions to ensure that each loaded package is ready for delivery to the carrier.

9.11 Test Control

In accordance with 10 CFR 71.123, testing activities, including design verification testing, acceptance testing of fabricated components and assemblies, and operational testing of the PAT-1 system by users, shall be controlled. Processes, implemented via procedures, shall ensure that testing activities are completed as specified in design documentation and this addendum.

Requirements for test control include the following:

- Implementing procedures shall be established to ensure that required acceptance, first-use, preshipment, and annual tests as identified in design or procurement documents are performed and appropriately controlled.
- Test personnel shall have appropriate training and shall be qualified for the level of testing they perform. Personnel shall be qualified in accordance with approved, written instructions, procedures, and/or checklists.
- Tests shall be performed by qualified personnel in accordance with approved, written instructions, procedures, and/or checklists. Test procedures must contain or reference the following information, as applicable:
 - Acceptance criteria contained in the applicable test specifications or design and procurement documents.
 - Instructions for performance of tests, including environmental conditions.
 - Test prerequisites, such as test equipment, instrumentation requirements, personnel qualification requirements, fabrication, or operational status of the items to be tested.

- Provisions for data recording and records retention.
- Test results are to be documented and evaluated to ensure that acceptance criteria have been satisfied.
- Tests for modifications, repairs, or replacements of safety-related and important-to-safety structures, systems, or components are to be performed in accordance with the original design and testing requirements or approved alternatives.

Tests are required when it is necessary to demonstrate that an item or process will perform satisfactorily. Test procedures must specify the objectives of the tests, testing methods, required documentation, and acceptance criteria. Tests conducted by vendors at vendor facilities must be specified in procurement documents. Personnel who conduct tests, test equipment, and procedures must be qualified, and records documenting qualification retained.

9.11.1 Acceptance Tests

The fabricator (vendor) must supply to SNL, QA documentation for the fabrication of each PAT-1 packaging system in accordance with applicable drawings, specifications, and/or other written requirements, including the results of acceptance tests specified in Section 8 of this addendum.

SNL, the package custodian, must ensure required tests for packaging pressure, leakage rate, or others are performed prior to first usage.

9.11.2 Maintenance Tests

Annual maintenance testing will be performed by SNL to ensure the PAT-1 packaging performance has not deteriorated with time and usage. The requirements for the annual tests are documented in the Section 8, *Acceptance Tests and Maintenance Program* of this addendum. The results of these tests are shall be documented and maintained with the specific packaging records.

9.11.3 Preshipment Tests

Preshipment tests, as specified in Section 8, *Acceptance Tests and Maintenance Program* of this addendum and shall be performed and documented by the package user.

9.12 Control of Measuring and Test Equipment

In accordance with 10 CFR 71.125, measuring and test equipment used for inspection and testing activities shall be controlled to ensure their usability, accuracy, and precision as follows:

- Implementing procedures shall be established to ensure that tools, gages, instruments, and other measuring and testing equipment (M&TE) are properly controlled, calibrated and adjusted to maintain accuracy within required limits.
- M&TE are calibrated at scheduled intervals against certified standards with known, valid relationships to national standards. If no national standards exist, the basis for calibration shall be documented. Calibration intervals are based on required accuracy, precision, purpose, frequency of use, stability characteristics, and other conditions that could affect measurement.

- Calibrations shall be performed in accordance with approved, written procedures.
- M&TE shall be identified, labeled, or tagged indicating the next required calibration due date, and traceable to calibration records.
- If M&TE is found to be out of calibration, an evaluation shall be performed and documented regarding the validity of inspections or tests performed and the acceptability of items inspected or tested since the previous acceptable calibration. The current status of M&TE is to be recorded and maintained. Any M&TE that is consistently found to be out of calibration shall be repaired or replaced.

Special calibration and control measures for rules, tape measures, levels, and other such devices are not required when normal commercial practices provide adequate accuracy.

9.13 Handling, Storage, and Shipping Control

In accordance with 10 CFR 71.127, the handling, storage, and shipping activities for materials, parts, and components of the PAT-1 packaging system used to transport radioactive material shall be controlled. Processes, implemented via procedures, shall ensure that such handling, shipping, and storage activities provide adequate control.

Requirements for handling, storage, and shipping control include the following:

- Implementing procedures shall be established to ensure that materials, parts, assemblies, spare parts, special tools, and equipment are handled, stored, packaged, and shipped in a manner to prevent damage, loss, loss of identity, or deterioration.
- When necessary, storage procedures address special requirements for environmental protection, such as inert gas atmospheres, moisture control, temperature levels, etc.

Package users shall ensure that PAT-1 system components and assemblies are controlled to prevent damage or loss, protect against damage or deterioration, and provide for adequate safety of personnel involved with handling, storage, and shipment (outgoing and incoming) operations.

Handling, storage, and shipping must be conducted in accordance with written and approved instructions, procedures, specifications, and/or drawings. These documents must identify appropriate information regarding shelf life, environment, temperature, cleaning, handling, and preservation, as applicable, to meet design, regulatory, and/or DOE shipping requirements which include applicable DOT requirements.

9.14 Inspection, Test, and Operating Status

In accordance with 10 CFR 71.129, the inspection, test, and operating status of materials, parts, and components of the PAT-1 packaging system to be used for transport of radioactive material shall be identified and controlled. Processes, implemented via procedures, shall ensure that appropriate inspections and tests occur prior to acceptance or use of the packaging or component, and identify the status of packaging items, components, etc.

Requirements for identifying inspection, test, and operating status include the following:

- Implementing procedures shall be established to ensure that the inspection and test status of materials, items, structures, systems, and components throughout fabrication, installation, operation, and test are clearly indicated by suitable means, (e.g., tags, labels, cards, form sheets, checklists, etc.).
- Bypassing required inspections, tests, or other critical operations is prevented through the use of approved instructions, procedures, or other controls.
- As appropriate, the operating status of nonconforming, inoperative, or malfunctioning components of a storage/transport system (e.g., valves, switches, etc.) is indicated to prevent inadvertent operation. The application and removal of status indicators are performed in accordance with approved instructions and procedures.
- Any nonconforming items are identified and controlled in accordance with Section 9.15 of this addendum.

Package users shall ensure that the status of inspection and test activities is identified on the item or in documents traceable to the item to ensure that proper inspections or tests have been performed and that those items that do not pass inspection are not used. The status of fabrication, inspection, testing, assembly, and refurbishment activities must be identified in documents traceable to the package components.

Measures established in specifications, procedures, and other instructions shall ensure that the following objectives are met:

- Personnel responsible for oversight of packaging inspections can readily ascertain the status of inspections, tests, and/or operating conditions.
- No controlled items are overlooked.
- Inadvertent use or installation of nonconforming items is prevented.
- Documentation is complete.

9.15 Nonconforming Materials, Parts, or Components

In accordance with 10 CFR 71.131, nonconforming materials, parts, and components of the PAT-1 packaging system used for transport of radioactive material shall be controlled. Processes, implemented via procedures, shall ensure that nonconforming conditions are identified and appropriately dispositioned.

The requirements for nonconforming materials, parts, or components include the following:

- Implementing procedures shall be established to control materials, parts, and components that do not conform to requirements and prevent their inadvertent use during fabrication or service.
- Nonconforming items include those items that do not meet specification or drawing requirements. Additionally, nonconforming items include items not fabricated or tested (1) in accordance with approved written procedures, (2) by qualified processes, or (3) by

qualified personnel where use of such procedures, processes, or personnel is required by the fabrication, test, inspection, or QA requirements.

- Nonconforming items are identified and/or segregated to prevent their inadvertent use until properly dispositioned. Nonconforming items are identified by marking, use of tagout procedures, or other methods that do not adversely affect the end use of the item if the nonconforming item can be restored to the applicable QA requirement. The identification shall be legible and easily recognizable. When identification of each nonconforming item is not practical, the container, package, or segregated storage area, as appropriate, is identified.
- Nonconforming conditions are documented and affected organizations are notified. The nonconformance report (NCR) shall include a description of the nonconforming condition. Nonconforming items shall be dispositioned as Use-As-Is, Reject, Repair, or Rework.
- Acceptability of rework or repair of nonconforming materials, parts, and components is verified through reinspection and/or retesting the item to the original requirements or equivalent inspection/testing methods. Inspection requirements for nonconforming items following rework, repair, or modification shall be detailed in the NCR and approved following determination of the disposition.
- The disposition of nonconforming items as Use-As-Is or Repair shall include technical justification and independent verification to assure compliance with design, regulatory, and contractual requirements.
- NCRs are part of the inspection records and are periodically reviewed to identify quality trends. Unsatisfactory quality trends are documented as detailed in Section 9.16 of this addendum. The results of these reviews are to be reported to management.
- NCRs relating to internal activities are issued to management of the affected organization. The appropriate QA Manager shall approve the disposition and perform follow-up activities to assure proper closure.
- Compliance with the evaluation and reporting requirements of 10 CFR 21 related to defects and noncompliance is controlled by approved procedures.

The components procured and fabricated per this addendum include *T-Ampoule Assembly; Ring, Filler; Sample Container-1 (SC-1) Assembly; Sample Container-2 (SC-2) Assembly; Inner Cradle* and *O-rings* for the *T-Ampoule Assembly*, and sample containers (*SC-1 or SC-2*). Nonconforming items are to be reported as outlined in the vendor's approved QAP, with immediate notification to SNL. NCRs shall be compiled to document the details of the nonconformance. Any nonconforming components shall be clearly identified and segregated. NCRs shall be traceable to the actual component(s) affected.

SNL shall perform corrective action(s) per Section 9.16 of this addendum. SNL shall disposition "Use-As-Is" and "Repair" nonconforming items in writing prior to the vendor proceeding with the next activity or step in the fabrication process. A copy of the completed NCR shall be submitted to SNL by the vendor as part of the manufacturing documentation.

9.16 Corrective Action

As required by 10 CFR 71.133, requirements for corrective action shall be established and implemented. Processes, implemented via procedures, shall ensure that issues associated with transportation and packaging activities are identified and corrected.

Corrective action activities shall be controlled. The requirements for corrective action include the following:

- Implementing procedures shall be established to identify and address conditions adverse to quality.
- Significant and/or repetitive failures, unsatisfactory quality trends, malfunctions, and deficiencies with material, components, equipment, and operations are to be promptly identified, documented, and reported to appropriate management.
- The cause of the condition and corrective action necessary to prevent recurrence are identified, implemented, and followed up to verify corrective action is complete and effective.

9.17 Quality Assurance Records

As required by 10 CFR 71.135, QA records shall be controlled. The QA records system will ensure that documented evidence relative to quality-related activities is maintained and available for use by DOE/NNSA and/or regulatory agencies.

Requirements for QA records include the following:

- Implementing procedures shall be established to assure control of quality records.
- Approved procedures identify the types of documents to be retained as QA records, as well as those to be retained by the originating organization. QA records are retained by the design organization (design, fabrication, and acceptance records) or by the user (use, shipment, inspection, in-use testing, and maintenance records). Records are identified, indexed, and stored in accessible locations.
- QA Records are retained for 3 years after the life of the packaging to which they apply per 10 CFR 71.91(d) to furnish evidence of activities affecting the quality of structures, systems, and components that are safety-related or important to safety. These records include records of design, procurement, fabrication, assembly, inspection, and testing. In addition, 10 CFR 71.135 states that the records shall be retained 3 years beyond the date when the last activity for which the quality program was developed.
- Maintenance records shall include the use of operating logs; results of reviews, inspections, tests, and audits; results from monitoring work performance and material analyses; results of maintenance, modification, and repair activities; qualification of personnel, procedures, and equipment; records of calibration of measuring and test equipment; and related instructions, procedures, and drawings.

- Requirements for indexing, record retention period, storage method(s) and location(s), classification, preservation measures, disposition of nonpermanent records, and responsibility for safekeeping are specified in approved procedures.
- Record storage facilities are established to prevent destruction of records by fire, flood, theft, and deterioration due to environmental conditions (such as temperature, humidity, or vermin). As an alternative, two identical sets of records (dual storage) may be maintained at separate locations.

Sufficient records must be maintained by package users to furnish evidence of item quality and activities affecting quality. QA records that must be retained three years after the life of the packaging to which they apply include:

- Appropriate production-related records that are generated throughout the package manufacturing and fabrication process (design organization).
- QA records are retained by the design organization (design, fabrication, procurement, and acceptance records), by the organization designated by the DOE/NNSA to perform maintenance (inspection, maintenance, procurement and acceptance records) and the users (inspection, use, shipment and in-use testing [leakage rate testing, etc.] records).
- Records documenting repair, rework, and replacement (user) shall be maintained for the lifetime of the package.
- Audit reports and corrective actions.
- Records used as a baseline for maintenance (user).
- Records showing evidence of delivery of packages to a carrier and proof that all DOT requirements were satisfied (user).

QA records shall be:

- Legible
- Completed to reflect the work accomplished and relevant results or conclusions
- Signed (including printed or typed name of the signing individual) and dated or otherwise authenticated by authorized personnel.

QA records should be placed in a records storage area as soon as feasible to avoid loss or damage. Individual QA records must be generated and maintained for each package and include the unique package identifier.

Records are to be available for inspection as per applicable DOE requirements.

9.17.1 Subcontractor/Supplier Submittal Requirements Summary

The components procured and fabricated per in this addendum include *T-Ampoule Assembly; Ring, Filler; Sample Container-1 (SC-1) Assembly; Sample Container-2 (SC-2) Assembly; Inner Cradle* and *O-rings* for the *T-Ampoule Assembly* and sample containers (*SC-1* or *SC-2*). The vendor shall provide a minimum of three copies of all required document submittals, accompanied by official vendor document transmittal forms. Prior to shipment of the above

mentioned components, the vendor shall submit a formal construction report to SNL for review and written approval (see Section 1.3.3 of this addendum).

9.18 Audits

In accordance with 10 CFR 71.137, audit requirements shall be established and implemented. Processes, implemented via procedures, shall ensure that activities pertaining to audits and assessments are controlled.

Requirements for audits and assessments are as follows:

- Implementing procedures shall be established to ensure that periodic audits verify compliance with all applicable requirements of the QAP and determine its effectiveness. Areas and activities to be audited, such as design, procurement, fabrication, inspection, and testing of storage/transportation systems, are to be identified as part of the audit plan.
- Vendor QAPs, procedures, and implementation activities may be audited to evaluate and verify that they are adequate and comply with applicable requirements.
- Audits are planned and scheduled in a manner to provide coverage and coordination with ongoing QAP activities commensurate with the status and importance of the activities.
- Audits are performed by trained and qualified personnel not having direct responsibilities in the areas being audited, and are conducted in accordance with written plans and checklists. Audit results are documented and reviewed by management having responsibility for the area audited. Corrective actions and schedules for implementation are established and recorded. Audit reports include an objective evaluation of the quality-related practices, procedures, and instructions for the areas or activities being audited and the effectiveness of implementation.
- Responsible management shall undertake corrective actions as a follow-up to audit reports when appropriate. The responsible management shall evaluate audit results for indications of adverse trends that could affect quality. When results of such assessments so indicate, appropriate corrective action will be implemented.

The components procured and fabricated per this addendum include *T-Ampoule Assembly; Ring, Filler; Sample Container-1; Sample Container-2; Inner Cradle* and *O-rings* for the T-Ampoule and sample containers. SNL reserves the right to audit and assess the vendor and the vendor subcontractors and supplier to verify conformance to the QAP prior to award of the contract, and at any time during the performance of the contract.

9.19 Appendix

9.19.1 References

1. United States. Nuclear Regulatory Commission. NUREG-0361. "Safety Analysis Report for the Plutonium Air Transportable Package, Model PAT-1." Washington, D.C. 1978.
2. United States. Nuclear Regulatory Commission. NUREG-0360. "Qualification Criteria to Certify a Package for Air Transport of Plutonium." Washington, D.C. 1978.

3. United States. Nuclear Regulatory Commission. NUREG/CR-0030. "PARC (Plutonium Accident Resistant Container) Program Research, Design, and Development," (SAND76-0587). Sandia National Laboratories. Albuquerque, New Mexico. Reprinted January 1983.
4. United States. Nuclear Regulatory Commission. Code of Federal Regulations, 10 CFR 71. "Packaging and Transportation of Radioactive Material." January 1, 2009.
5. United States. Nuclear Regulatory Commission. Regulatory Guide 7.10 (RG 7.10). *Establishing Quality Assurance Programs for Packaging Used in Transport of Radioactive Material*, Revision 2. Washington, D.C. March 2005.
6. Sandia National Laboratories. "Title 10 Code of Federal Regulations Part 71 Packaging and Transportation of Radioactive Material – Quality Assurance Program Plan." AS-PT-PD-04. Albuquerque, New Mexico. March 5, 2009.
7. 1071H-QAIP 2-2. "Project Quality Plan." Sandia National Laboratories. Albuquerque, New Mexico.
8. 1071H-QAIP 3-1. "Design Control." Sandia National Laboratories. Albuquerque, New Mexico.
9. 1071H-QAIP 9-2. "Model Validation." Sandia National Laboratories. Albuquerque, New Mexico.
10. 1071H-QAIP 9-3. "Analyses and Calculations," Sandia National Laboratories. Albuquerque, New Mexico.
11. 1071H-QAIP 4-1. "Control of Procurement Documents and Purchased Material, Equipment, and Services," Sandia National Laboratories. Albuquerque, New Mexico.
12. 1071H-QAIP 5-1. "Quality Assurance Implementing Procedure Preparation and Content," Sandia National Laboratories. Albuquerque, New Mexico.
13. 1071H-QAIP 6-1. "Document Review and Approval," Sandia National Laboratories. Albuquerque, New Mexico.
14. 1071H-QAIP 6-2. "Document Control," Sandia National Laboratories. Albuquerque, New Mexico.
15. 1071H-QAIP 8-1. "Identification and Control of Materials, Parts, and Components." Sandia National Laboratories. Albuquerque, New Mexico.
16. 1071H-QAIP 9-1. "Control of Special Processes." Sandia National Laboratories. Albuquerque, New Mexico.
17. 1071H-QAIP 10-1. "Inspection and Identification of Item Status." Sandia National Laboratories. Albuquerque, New Mexico.

18. 1071H-QAIP 9-5. "Technical Products and Deliverable Reports." Sandia National Laboratories. Albuquerque, New Mexico.
19. 1071H-QAIP 11-1. "Control of Data Collection and Testing Activities." Sandia National Laboratories. Albuquerque, New Mexico.
20. 1071H-QAIP 12-1. "Control of Measuring and Test Equipment." Sandia National Laboratories. Albuquerque, New Mexico.
21. 1071H-QAIP 13-1 "Control of Shipping, Handling, Storage, Preservation, and Cleaning." Sandia National Laboratories. Albuquerque, New Mexico.
22. 1071H-QAIP 15-1. "Control of Nonconformances and Corrective Action." Sandia National Laboratories. Albuquerque, New Mexico.
23. American National Standards Institute (ANSI). ANSI/ASME NQA-1-1983. 1983.
24. American Society of Mechanical Engineers. "Dimensioning and Tolerancing." New York: 2009.

DISTRIBUTION

| | | |
|---------------------------|--------------------------------|--|
| 1 | NRC Document Control | |
| 8 and 1 (electronic copy) | NRC | |
| 2 and 1 (electronic copy) | NNSA/PCD | |
| 1 and 1 (electronic copy) | NNSA/Paul Mann | |
| 2 and 1 (electronic copy) | Energy Solutions/Scott Shiraga | 2345 Stevens Dr Suite 240 Richland, WA 99354 |
| 1 and 1 (electronic copy) | MS0718 | David Miller |
| 3 and 3 (electronic copy) | MS0718 | Richard Yoshimura |
| 1 (electronic copy) | MS0899 | Technical Library |